

# **Groundwater of the North-Western Kalahari, Namibia**

*Estimation of Recharge and  
Quantification of the Flow Systems*

Doctorate Thesis  
submitted at the  
Julius-Maximilian University of Würzburg

by

**Christoph Külls**

from

**Bälau/Hzgt. Lauenburg**

**Würzburg 2000**



# **Das Grundwasser am Nord-Westrand der Kalahari, Namibia**

*Abschätzung der Neubildung und  
Quantifizierung der Fließsysteme*

Dissertation zur Erlangung des  
naturwissenschaftlichen Doktorgrades  
der Bayerischen Julius-Maximilians-Universität Würzburg

vorgelegt von

**Christoph Külls**

aus

**Bälau/Hzgt. Lauenburg**

**Würzburg 2000**





eingereicht am:

1. Gutachter der Dissertation: Prof. Dr. P. Udluft
2. Gutachter der Dissertation: Prof. Dr. D. Busche

1. Prüfer: Prof. Dr. P. Udluft
2. Prüfer: Prof. Dr. D. Busche

Tag der mündlichen Prüfung:

Doktorurkunde ausgehändigt am:

---

<b>Table of contents</b> .....	I
<b>Acknowledgements</b> .....	IV
<b>Abstract</b> .....	V
<b>Kurzfassung (German summary)</b> .....	VI
<b>1 Introduction</b> .....	1
1.1 Problem statement .....	2
1.2 Objectives of the study .....	4
1.3 Review of previous work relevant to the study area .....	5
1.3.1 Groundwater recharge on basement outcrops .....	6
1.3.2 Groundwater recharge in the Kalahari .....	8
<b>2 The study area</b> .....	13
2.1 Climate .....	14
2.2 Surface drainage .....	16
2.3 Geology .....	19
<b>3 Methods for the assessment of groundwater flow systems</b> .....	25
3.1 Groundwater recharge in (semi-) arid regions .....	25
3.1.1 Direct recharge processes .....	26
3.1.2 Indirect recharge processes .....	29
3.1.3 A proposed geomorphological model of recharge mechanisms .....	30
3.1.4 Quantitative groundwater recharge estimation .....	32
3.2 Developing conceptual flow models using environmental tracers .....	38
3.2.1 Hydrochemistry .....	38
3.2.2 Stable isotopes $^{18}\text{O}$ and $^2\text{H}$ .....	44
3.2.3 Tritium .....	51
3.2.4 $^{14}\text{C}$ -dating .....	52
3.3 Inverse modelling of groundwater flow using environmental tracers .....	54
3.3.1 Hydrochemical discretization .....	54
3.3.2 Flow model development .....	55
3.3.3 Optimization .....	58

---

<b>4</b>	<b>Developing a quantitative flow model of the Upper Omatako</b> .....	59
4.1	Hydrogeological data of the Upper Omatako basin .....	59
4.1.1	Aquifers, hydraulic gradients and groundwater flow directions .....	60
4.1.2	Distribution of saturated Kalahari sediments .....	62
4.1.3	Thickness of the unsaturated zone .....	67
4.2	Estimating groundwater recharge .....	70
4.2.1	Climatic recharge potential .....	70
4.2.2	Parameter estimation for the soil water balance model .....	71
4.2.3	Water balance modelling - results .....	76
4.3	Groundwater hydrochemistry .....	80
4.3.1	Carbonate chemistry .....	82
4.3.2	Strontium .....	85
4.3.3	Chloride .....	87
4.3.4	Cluster analysis .....	89
4.4	Detailed sampling in the Goblenz area .....	98
4.4.1	Hydrochemistry in the Goblenz area .....	99
4.4.2	Stable isotopes .....	111
4.4.3	Tritium, <sup>13</sup> C and <sup>14</sup> C analyses .....	135
4.5	Mixing-cell modelling .....	139
4.5.1	Synthesis of the conceptual flow model .....	140
4.5.2	Single-cell modelling with hydrochemical groups .....	142
4.5.3	Multi-cell modelling with specific boreholes .....	145
<b>5</b>	<b>Conclusions and recommendations</b> .....	149
5.1	Methodological perspectives .....	149
5.2	Hydrogeotopes .....	149
5.2.1	The mountainous hardrock rim .....	151
5.2.2	The Otavi Mountain Foreland .....	152
5.2.3	The Kalahari basin .....	153
5.3	The groundwater resources at Goblenz .....	155
	<b>References</b> .....	157

## **Appendices**

- A Manual for MIG (21 pages)
- B Tabulated hydrochemical data (23 pages)

## Acknowledgements

First of all, I would like to thank Prof. Dr. Peter Udluft for offering me the opportunity to continue working in the field of dryland water resources, for sharing his hydrogeological experience with me during many discussions and for his liberal mentorship. I also express my gratitude to Dr. Eilon Adar as a mentor and as a friend. During a semester I spent with him and his colleagues at the Water Resources Research Centre in Sde Boker he introduced me to the mixing cell approach. During our field work in Namibia and during several working sessions he encouraged me to complement the various aspects of this integrated study with great energy and personal devotion. Prof. Mebus Geyh has measured the stable and radioactive isotopes at the '*Niedersächsisches Landesamt für Bodenforschung*', Hannover. I am thankful for dedicated critical discussions and for many fruitful comments on stable isotope interpretation and on the accuracy of mixing calculations. I would like to thank Dr. Dieter Ploethner for his readiness to support me on regional hydrogeology and for his technical assistance within the German-Namibian Groundwater Exploration Project. I also am very grateful to Prof. Dr. Busche who took it upon him to review the complete text, improve the English phrasing and the geomorphological terminology. Many thanks go to Arnold Bittner, Ingo Bardenhagen and Greg Cristallis as to other members of the Department of Water Affairs (DWA) for helping me during my field trips. The DWA provided a car and other logistical support during my second field mission in 1998 and let me use meteorological and hydrogeological data. At this point the support and hospitality of many Namibians, especially of farmers in my study area, is acknowledged. Without their willingness to give access to boreholes on their private ground this study would not have been feasible. Without their openness and friendliness it would have been much less pleasant to work in the Kalahari thirstland.

This study has been carried in the framework of an interdisciplinary geoscience graduate program '*Geoscience Research in Africa*' at the University of Würzburg. Within this graduate program the German Science Foundation (DFG) and the State of Bavaria provided a scholarship and travel funds. The study forms part of a series of investigations on '*Regionalisation of groundwater recharge in Namibia*' at the Department of Hydrogeology. Many thanks go to colleagues from this group, namely Heike Klock, Holger Mainardy and Jens Wrabel for discussions at the desk and in the field. The graduate scholarship granted by the Jakob Blaustein International Centre at the Ben Gurion University Beer Sheba, Israel and the hospitality and support during my stay in Sde Boker were most welcome at a critical stage of my PhD. Many thanks to Bärbel Seth for scrutinizing the typescript for errors. Finally, those who haven't outspokenly protested of being deprived of my leisure time are silently acknowledged as well.

## Abstract

A quantitative model of groundwater flows contributing to the Goblenz state water scheme at the north-western fringe of the Kalahari was developed within this study. The investigated area corresponds to the Upper Omatako basin and encompasses an outer mountainous rim and sediments of the Kalahari sand desert in the centre. This study revealed the eminent importance of the mountainous rim for the water balance of the Kalahari, both in terms of surface and ground water. A hydrochemical subdivision of groundwater types in the mountain rim around the Kalahari was derived from cluster analysis of hydrochemical groundwater data. The western and south-western secondary aquifers within rocks of the Damara Sequence, the Otavi Mountain karst aquifers of the Tsumeb and Abenab subgroups as well as the Waterberg Etjo sandstone aquifer represent the major hydrochemical groups. Ca/Mg and Sr/Ca ratios allowed to trace the groundwater flow from the Otavi Mountains towards the Kalahari near Goblenz. The Otavi Mountains and the Waterberg were identified as the main recharge areas showing almost no or only little isotopic enrichment by evaporation. Soil water balance modelling confirmed that direct groundwater recharge in hard-rock environments tends to be much higher than in areas covered with thick Kalahari sediments. According to the water balance model average recharge rates in hard-rock exposures with only thin sand cover are between 0.1 and 2.5 % of mean annual rainfall. Within the Kalahari itself very limited recharge was predicted (< 1 % of mean annual rainfall). In the Upper Omatako basin the highest recharge probability was found in February in the late rainfall season. The water balance model also indicated that surface runoff is produced sporadically, triggering indirect recharge events. Several sinkholes were discovered in the Otavi Foreland to the north of Goblenz forming short-cuts to the groundwater table and preferential recharge zones. Their relevance for the generation of indirect recharge could be demonstrated by stable isotope variations resulting from observed flood events. Within the Kalahari basin several troughs were identified in the pre-Kalahari surface by GIS-based analyses. A map of saturated thickness of Kalahari sediments revealed that these major troughs are partly saturated with groundwater. The main trough, extending from south-west to north-east, is probably connected to the Goblenz state water scheme and represents a major zone of groundwater confluence, receiving groundwater inflows from several recharge areas in the Upper Omatako basin. As a result of the dominance of mountain front recharge the groundwater of the Kalahari carries an isotopic composition of recharge at higher altitudes. The respective percentages of inflow into the Kalahari from different source areas were determined by a mixing-cell approach. According to the mixing model Goblenz receives most of its inflow (70 to 80 %) from a shallow Kalahari aquifer in the Otavi Foreland which is connected to the Otavi Mountains. Another 15 to 10 % of groundwater inflow to the Kalahari at Goblenz derive from the Etjo sandstone aquifer to the south and from inflow of a mixed component. In conclusion, groundwater abstraction at Goblenz will be affected by measures that heavily influence groundwater inflow from the Otavi Mountains, the Waterberg, and the fractured aquifer north of the Waterberg.

## Zusammenfassung (German summary)

Ziel dieser Arbeit ist es, die Herkunft des Grundwassers zu untersuchen, das in der Nähe von Goblenz am Rand der Namibianischen Kalahari (Abbildung 1.1, Seite 3) in den letzten Jahren erschlossen worden ist. Fragen zur Erneuerbarkeit dieser Grundwasserreserven aus direkter und indirekter Neubildung und zur Rolle lateraler, unterirdischer Zuflüsse von unterschiedlichen Herkunftsräumen waren hierfür zu beantworten. Dies erforderte eine kombinierte Anwendung hydro(geo)logischer, hydrochemischer und isotopenhydrologischer Methoden.

Das Arbeitsgebiet in Namibia ist als semi-arid zu bezeichnen und durch ein subtropisches Klimaregime geprägt. Aufgrund der hohen Temperaturen während der Regenzeit verdunstet ein erheblicher Teil der Niederschläge direkt oder durch Transpiration. Daher ist die Kalahari trotz der zum Teil für semi-aride Gebiete vergleichbar hohen Niederschläge von 350 bis über 550 mm/Jahr (Abb. 2.1, S. 13) relativ arm an Oberflächen- und verfügbarem Grundwasser. Ein wesentliches Merkmal des Arbeitsgebietes ist zudem die Dichotomie zwischen dem äußeren Festgesteinsbereich und dem überwiegend mit Sanden bedeckten Kalahari-Becken (Abbildung 2.6, S. 20). Eine Analyse der vorhandenen Klima- und Abflußdaten verdeutlicht die großen Unterschiede in den hydrologischen Eigenschaften dieser Bereiche: Während ein Großteil des oberirdischen Abflusses im äußeren Festgesteinsbereich gebildet wird (5 bis 25 mm/m<sup>2</sup> pro Jahr, Abb. 2.4, S. 17), ist die Abflußbildung innerhalb der Kalahari mit ca. 0.5 bis 1.5 mm/m<sup>2</sup> pro Jahr wesentlich geringer (Tabelle 2.1, S. 19). Der äußere Festgesteinsbereich ist damit als Ursprungsgebiet ephemerer Flüsse das Hauptliefergebiet für Oberflächenwasser. Durch den Omatako-Damm wird ein Großteil dieses Zuflusses inzwischen allerdings abgefangen und der Wasserbilanz der oberen Kalahari entzogen. Die Abflußmengen belaufen sich dabei für die Station ‚Ousema‘ am Westrand der Kalahari auf 0.36 bis 34 Millionen m<sup>3</sup> pro Jahr.

Auch für das Grundwasserfließsystem der Kalahari ist der äußere Festgesteinsbereich bestimmend. Der erstellte regionale Grundwassergleichenplan (Abb. 4.1, S. 61) zeigt ein annähernd zentripetales Fließmuster, das in der Nähe von Goblenz konvergiert, mit einer Hauptentwässerung zur Groß-Kalahari Richtung Osten. Die Neubildungsgebiete liegen in den unterschiedlichen zum Teil verkarsteten Festgesteinsbereichen der Damara Sequenz und des Etjo-Sandsteins (Waterberg). Allerdings konnte auch innerhalb der Kalahari südlich von Goblenz ein begrenztes Grundwasserneubildungsgebiet identifiziert werden. In diesem Bereich haben sich durch die Verkarstung anstehender Kalkkrusten gute Neubildungsbedingungen für das flache Grundwasser entwickelt.

Durch die Kombination digitaler Rasterkarten der Geländehöhe, der Kalahari-Mächtigkeit und der Grundwasserstände konnte eine Karte der Bereiche erstellt werden, in denen die Kalahari mit Grundwasser gesättigt ist (Abb. 4.3, S. 64). Ein Vergleich mit digitalisierten Karten aus früheren geophysikalischen Untersuchungen zeigte eine gute Übereinstimmung

(Abb. 4.4, S. 66). Daraus konnte ein verallgemeinertes Modell der Sättigungsmächtigkeit abgeleitet werden. Aus diesem Modell werden zwei mit Kalahari-Sedimenten verfüllte und gesättigte Rinnen erkennbar. Diese Rinnen sind bevorzugte Fließbahnen für die Grundwasserbewegung vom Festgesteinsrand zum Zentrum des Kalahari-Beckens und stellen zudem Erkundungs- und Erschließungsziele für Grundwasser dar. Die Wassererschließung von Goblenz grenzt an die größere nördliche Rinne. Eine Karte der Mächtigkeit der ungesättigten Zone wurde aus der Verschneidung des digitalen Geländemodells mit einem interpolierten Grundwassergleichenplan errechnet (Abb. 4.6, S. 68). Diese Karte deutet auf ausgedehnte Bereiche geringer Flurabstände im südlichen und nördlichen Teil des Einzugsgebietes Oberer Omatako hin. Diese Informationen wurden zudem als wesentliche Grundlagen für die regionale Interpretation der stabilen Isotope verwendet.

Die Grundwasserneubildung im Oberen Omatako wurde mit mehreren Methoden vergleichend abgeschätzt. Eine klimatische Wasserbilanz aus Tageswerten des Niederschlages ( $N_t$ ) und der gemessenen Pfannenverdunstung ( $V_t$ ) zeigte, daß die Neubildung des Grundwassers im Februar am wahrscheinlichsten ist (Abb. 4.7, S. 71). Nur Niederschlagsereignisse mit hoher Jährlichkeit vermögen dabei auf Tagesbasis die erforderliche Neubildungsbedingung  $N_t > V_t$  zu erfüllen. Daraus ergibt sich, daß Grundwasserneubildung in der Regel nur infolge zeitlicher oder räumlicher Konzentration von Niederschlägen und Abflüssen erfolgen kann und unter Umständen nicht jährlich stattfindet. Eine Erweiterung der klimatischen Wasserbilanz um die Modellierung des Bodenwasserhaushaltes wurde schließlich verwendet, um für den Bereich ‚Grootfontein‘ eine detaillierte Betrachtung der Grundwasserneubildung aufgrund von Tageswerten zu ermöglichen. Das Bodenwasserhaushaltsmodell wurde zunächst mit empirisch erhobenen bodenphysikalischen Kennwerten belegt (Abb. 4.8-4.10, S. 72-73) und dann anhand von Grundwasserständen kalibriert (Abb. 4.11, S. 74). Dabei ergaben sich Neubildungsraten von 0.4 bis 9.6 mm/Jahr oder von 0.1 bis 2.5 % des jeweiligen jährlichen Niederschlages (Tab. 4.1, S. 77; Abb. 4.13, S. 78). Ein Zusammenhang zwischen dem Jahresmittel des Niederschlages und der Neubildungsrate war nicht ausgeprägt, die Häufung hoher Intensitäten täglicher Niederschläge erwies sich aber als ein wesentlicher Faktor für hohe direkte Neubildungsraten. Auch die Bodenwassermodellierung deutete auf eine höhere Wahrscheinlichkeit der Grundwasserneubildung im Februar hin. Die mit der Chloridmethode ermittelte Neubildungsrate lag mit 8.5 bis 14 mm/Jahr für dieses Gebiet höher. Der Unterschied kann sich aus den bei der Chloridmethode zusätzlich berücksichtigten Komponenten des Makroporenflusses, der indirekten Neubildung und aus anderen lateralen Zuflüssen ergeben.

Geländebeobachtungen zeigten jedoch, daß solche Modellergebnisse nur begrenzt verallgemeinerbar oder übertragbar sind. Im Otavi Vorland nördlich von Goblenz wurde eine Reihe von Schlucklöchern entdeckt (Abb. 4.12, S. 75). Diese haben sich unter geringmächtiger Sandbedeckung in Kalkkrusten durch Verkarstung entwickelt und sind durch das Einbrechen der oberen Bodenschicht vereinzelt sichtbar geworden. Zum einen deuten diese Schlucklöcher auf eine Veränderung der Grundwasserstände hin. Die Kalkkrusten, die sich im Quellgebiet unterhalb der Otavi-Berge durch Calcitausfällung entwickelt hatten, sind



durch das Absinken der Grundwasserstände und durch die Aufwehung von Kalahari-Sanden nun lokal verkarstet und wiederum zu Neubildungsgebieten geworden. Solche Schlucklöcher können bevorzugte Fließ- und Überbrückungsbahnen zum Grundwasser darstellen. Die hydrologische Funktion solcher Schlucklöcher läßt sich mit physikalischen Modellen im regionalen Maßstab quantitativ schwer erfassen.

Daher wurden hydrochemische und Isotopen-Methoden zur indirekten Abschätzung des Fließsystems herangezogen. Zunächst wurde eine generelle Charakterisierung der Grundwässer anhand der Hauptelementchemie und mittels der hierarchischen Cluster-Analyse vorgenommen. Hierbei ließen sich fünf wesentliche Hauptgruppen im Arbeitsgebiet erkennen (Abb. 4.15, S. 83): Ca-HCO<sub>3</sub>-Wässer finden sich in den Bereichen der Damara Sequenz, in denen Marmore anstehen und gute Neubildungsbedingungen bieten, Ca-Mg-HCO<sub>3</sub>-Wässer und Mg-Ca-HCO<sub>3</sub>-Wässer sind charakteristisch für den Otavi Karst und das ihm vorgelagerte Otavi Vorland. Das Grundwasser im Etjo-Sandstein des Waterberges zeichnet sich durch eine äußerst geringe Mineralisierung und ein ausgeglichenes Verhältnis von Erdalkalien und Alkalien bei hohen Hydrogenkarbonat-Gehalten aus. In der Kalahari und in tieferen Grundwasser-Stockwerken des Otavi-Vorlandes treten schließlich Grundwässer mit hohen Natrium und Chlorid-Gehalten auf.

Das Ca/Mg-Verhältnis (Abb. 4.16, S. 84) und das Sr/Ca Verhältnis erwiesen sich als ausgezeichnete hydrochemische Indikatoren für die Unterscheidung von Grundwasser aus dem Otavi Karst und aus den sekundären Aquiferen der Damara Sequenz. Anhand von äußerst geringen molaren Sr/Ca Verhältnissen konnte der Abstrom des Grundwassers aus dem Otavi Karst in die Kalahari genau abgegrenzt und verfolgt werden (Abb. 4.17, S. 86). Die Chloridkonzentrationen im Grundwasser wurden im Hinblick auf die Anreicherung im Vergleich zum Niederschlag untersucht. Dabei wurden in den Festgesteinsbereichen Konzentrationen zwischen 25 und 100 mg/l festgestellt, die auf Anreicherungsfaktoren von ca. 25 bis 200 bzw. hindeuten (Abb. 4.18, S. 88). Dies entspricht unter vereinfachten Annahmen Neubildungsraten in der Größenordnung von 2 bis 20 mm/Jahr. In der Kalahari liegen die Konzentrationen von Chlorid mit 250 bis 750 mg/l im Mittel wesentlich höher; diese können in einigen Bereichen 5000 mg/l übersteigen. Eine Umrechnung in Neubildungsraten kann wegen der Konvergenz der Fließbahnen und möglicher geogener Quellen nicht mehr direkt erfolgen, allerdings deuten die hohen Chloridkonzentrationen auf Bereiche mit Verdunstungsverlusten und auf deutlich geringere Neubildungsraten innerhalb der Kalahari hin. Dieses gilt nicht für zwei Bereiche, in denen die Kalahari gering mächtig ist: Im Abstrom dieser Gebiete liegen die Chloridkonzentrationen deutlich niedriger und zeigen lokal erhöhte Neubildung des Grundwassers an (Abb. 4.18 (g + h), S. 88).

Eine weitergehende Charakterisierung der Wasserchemie und der Isotopenzusammensetzung erfolgte anhand von Grundwasserproben im direkten Umfeld von Goblenz (Übersichtskarte in Abb. 4.25, S. 100 und Datenblatt in Tab. 4.2, S. 101-102). Hydrochemische Profile durch das Arbeitsgebiet deuteten Mischungsprozesse zwischen Endgliedern der fünf hydrochemischen Gruppen an. So konnte entlang des Flusses Omambonde Richtung Goblenz der laterale

Zustrom von Grundwasser aus dem Etjo Sandstein von Westen und der Zustrom von dolomitischem Grundwasser qualitativ nachgewiesen werden (Abb. 4.30, S. 107). Ebenso ließen sich hydrochemische Hinweise auf eine Neubildung im Otavi Vorland finden, eventuell verursacht durch Versickerung in den beobachteten Schlucklöchern (Abb. 4.31, S. 108).

Eine Untersuchung der stabilen Isotope  $^{18}\text{O}$  und  $^2\text{H}$  bestätigte die qualitativen Aussagen aus den Untersuchungen zur klimatischen Wasserbilanz: Aufgrund der deutlichen Verschiebung zwischen der mittleren gewichteten Isotopen-Zusammensetzung des Niederschlages und des Grundwassers erfolgt die Neubildung wahrscheinlich durch wenige intensive (und an schweren Isotopen abgereicherte) Niederschläge. Die Darstellung der Grundwasserproben im  $^{18}\text{O}/^{16}\text{O}$ - $^2\text{H}/^1\text{H}$ -Diagramm zeigte erneut einen deutlichen Unterschied zwischen den Grundwasserproben aus den Festgesteinsbereichen und denen aus der Kalahari und dem Otavi Vorland (Übersichtskarte in Abb. 4.38, S. 115 und Datenblatt in Tab. 4.3, S. 116-118). Während eine Anreicherung durch Verdunstungseffekte in den vermuteten Neubildungsgebieten (Otavi Karst, Etjo Sandstein) weitgehend fehlte (Abb. 4.40, S. 120), wiesen die Grundwasserproben aus der Kalahari deutliche Anzeichen von Anreicherung durch Verdunstung auf (Abb. 4.32, S. 122). Wurden die Grundwässer nach hydrochemischen Gruppen getrennt aufgetragen, so ließen sich Verdunstungsgeraden mit einer mittleren Steigung von 4.5 ermitteln, die auf Verdunstung von offenen Wasserflächen hindeutet. Allerdings haben die Grundwässer der Kalahari eine ursprüngliche Isotopenzusammensetzung, die derjenigen von hochgelegenen Niederschlagsgebieten entspricht (> 1750 m ü. NN). Damit ergibt sich ein weiterer Hinweis darauf, daß das Grundwasser der Kalahari entweder durch Sturzfluten gebildet wird, die sich in den höher liegenden Festgesteinsbereichen entwickeln, oder direkt im Randbereich neugebildet wird und der Kalahari unterirdisch zuströmt. Die zeitliche Variabilität der Isotopenzusammensetzung begrenzt die Trennschärfe für regionale Analysen. Nördlich von Goblenz im Bereich der beobachteten Schlucklöcher konnte anhand einer Zeitreihe der Isotopenzusammensetzung die Bedeutung von Sturzfluten für die Grundwasserneubildung direkt nachgewiesen werden (Abb. 4.45, S. 128). Die  $^{14}\text{C}$  und  $^3\text{H}$  Daten bestätigten die Abgrenzung der Neubildungsbereiche.

Die aus den hydrogeologischen, hydrologischen, hydrochemischen und isotopenhydrologischen Teiluntersuchungen gewonnenen Erkenntnisse wurden dann in einem Konzeptmodell des Grundwasserfließsystems Goblenz zusammengetragen (Abb. 4.52, S. 141). Aufgrund dieses Konzeptmodells wurden mit einem inversen hydrochemischen Mischungsansatz die jeweiligen Anteile aus den einzelnen Neubildungsgebieten berechnet (Tab. 4.6, S. 142). Hierzu wurde zunächst über thermodynamische Gleichgewichtsbetrachtungen sichergestellt, daß die Annahme konservativen Verhaltens der für die Berechnung verwendeten Wasserinhaltsstoffe für das nähere Arbeitsgebiet um Goblenz gewährleistet war. Kritische Bereiche wurden als ‚Reaktions-Zonen‘ von den ‚Mischungs-Zonen‘ abgegrenzt und nicht in die mathematische Berechnung einbezogen. Der Etjo-Sandstein als Mischungszelle für den Bereich nördlich von Goblenz stellte für die

Verwendung dieses nicht-reaktiven Mischungsansatzes im Arbeitsgebiet nahezu ideale Voraussetzungen dar. Zur praktischen Umsetzung des mathematischen Ansatzes wurde ein Programm (MIG, „*Mixing Input Generator*“) zur interaktiven Erstellung von Mischungsmodellen geschrieben (Anhang 1). Über ein iteratives Verfahren wurden schließlich die Fließraten ermittelt, welche sowohl die Wasserbilanz und als auch die Massenbilanz aller betrachteten Hauptelemente und Isotopen im Arbeitsgebiet optimal erklären. Durch dieses Verfahren wurde errechnet, daß ca. 70 bis 80 Prozent des Wassers, das in Goblenz gefördert wird, aus den Otavi Bergen stammt. Weitere 15 bis 10 % stammen jeweils aus dem Etjo Sandstein bzw. aus einer Mischkomponente von Grundwässern nördlich des Waterbergs. Detailbetrachtungen der Mischungskomponenten im Otavi Vorland zeigten, daß hier in einigen Bereichen eine Zumischung von geringen Anteilen neugebildeten Grundwassers erfolgt, in anderen Bereichen höher mineralisiertes Tiefenwasser zutritt. Der konservative Mischungsansatz stellt unter günstigen Bedingungen ein geeignetes Mittel zur inversen Berechnung von Fließraten dar. Allerdings sind dazu wie in diesem Falle umfangreiche Voruntersuchungen notwendig.

Goblenz liegt in einem Konvergenzgebiet von Grundwasserströmen aus unterschiedlichen Neubildungsgebieten im Festgesteinsbereich. Für Goblenz ist der laterale Zustrom von Grundwasser aus dem Otavi Karst und dem Waterberg die entscheidende Wasserhaushaltskomponente. Die direkte Neubildung in der Kalahari ist dagegen relativ gering. Allerdings kann eine zusätzliche Neubildung in verkarsteten und kaum oder nur mit geringmächtigen Sanden bedeckten Kalkkrusten eine Rolle spielen.



## 1 Introduction

*'Die Sicherstellung der wasserwirtschaftlichen Versorgung Namibias ist die wichtigste Aufgabe der Verwaltung des Landes und wird bei allen zukünftigen entwicklungspolitischen Maßnahmen eine wichtige Rolle spielen.'* (SCHNEIDER, 1989: 228)

Namibia is the driest of the sub-Saharan countries in Africa. The meteorological conditions are characterized by low and at the same time highly variable amounts of rainfall as well as by high potential evaporation. As a result *within* Namibia there are no perennial streams. Even for a socio-economic system well adapted to the '*slender margin of normality*' typical for such environmental conditions (MOORSOM ET AL., 1995: 13), water supply can be at menace in the advent of droughts. Whether at the scale of water supply schemes for Namibia's capital Windhoek or at the scale of rural communities and single farms - the exploration *and* optimal use of water resources is a prerequisite for achieving sustained economic activity.

Key strategies for non-nomadic societies to cope with scarce water resources are the development of storage and distributing networks (BEAUMONT, 1989; AGNEW & ANDERSON, 1992). While the storage of surface water goes along with high evaporation losses and problems of silting, especially in flat and sparsely vegetated areas as in the Kalahari, groundwater aquifers offer good and natural long-term storage capacities. Mean residence times of groundwater reservoirs are in the order of magnitude of hundreds to tens of thousands of years, providing storage that can damp out inter-annual climatic variability. This line of thinking highlights the importance of groundwater resources for Namibia's economy and people.

However, the use of groundwater resources in Namibia has natural and economic limits. With growing abstraction, especially as groundwater resources are being integrated into larger re-distribution networks, there is an increasing need of knowing the safe yield of aquifer systems. For a sustainable use of groundwater resources important questions arise: Where does the groundwater of a specific aquifer come from? How and at which rate is it being replenished by deep percolation and/or by lateral subsurface inflow? These questions can only be answered based on a sound understanding of the hydrogeological system and an improved notion of how water resources are distributed in space and in time. This principle has been defined in the Namibian legislation, where the identification and evaluation of water sources is explicitly required before boreholes are being sited.

Within this study an approach to the assessment of large and complex groundwater reservoirs is developed. It is applied to the macro-scale Omatako basin at the north-western edge of the Kalahari in Namibia, for which groundwater recharge processes and lateral subsurface flow patterns will be analysed and quantified. The suggested method outlined in the following chapters proceeds from the regional to the local small scale. The advantage of such a procedure is that it can draw the attention to previously unknown processes. This issue is further addressed in Chapter 4. The approach chosen for this study builds on hydrochemical data available in Namibia and on affordable analyses of the stable isotopes of water – it can therefore be applied to other basins with similar conditions and scarce hydrological information. Special emphasis is put on the analysis of recharge processes in order to constrain their timing and spatial distribution.

## 1.1 Problem statement

The apparent scarcity of water resources in the Otjozondjupa region, formerly called Hereroland and located at the north-western fringe of the Namibian Kalahari, has been a major obstacle to the development of this area. Surface water is only available episodically when flash floods flow into the Kalahari basin from the adjacent mountains and surface water accumulates in shallow depressions (pans) for several weeks. Although fresh groundwater resources had been discovered in its north-western part near the town of Goblenz (Figure 1.1) the groundwater exploitation scheme was abandoned after 1989 (DEPARTMENT OF WATER AFFAIRS, 1993 and 1997: 2). In the aftermath of the drought of 1992/93 and due to water shortages, groundwater abstraction from the Goblenz well field has been reconsidered. In the vicinity of the previous production scheme successful new boreholes have been drilled with an estimated total potential of 1 million m<sup>3</sup>. For this belt of newly explored groundwater resources in the Kalahari sediments near Goblenz a detailed evaluation of the potential sources and their rate of replenishment has thus become necessary.

In general, groundwater extraction is sustained by a) *in situ* (Lat., in the same place) *recharge* or b) *allocthonous* (Gr., in/from another place) *recharge with lateral groundwater inflow*. Possible *in situ* recharge mechanisms are direct rainfall infiltration through the Kalahari sediments, river-bed infiltration from ephemeral floods in the Omatako and Omambonde washes, or seepage from ponded water in pans (Figure 1.1). Potential groundwater inflow may take place from the Otavi Mountains to the north, the Waterberg area to the north-west and from the Kalahari basin south of Goblenz. In the analysis the role of pans to the south-east of Goblenz also needs to be considered.

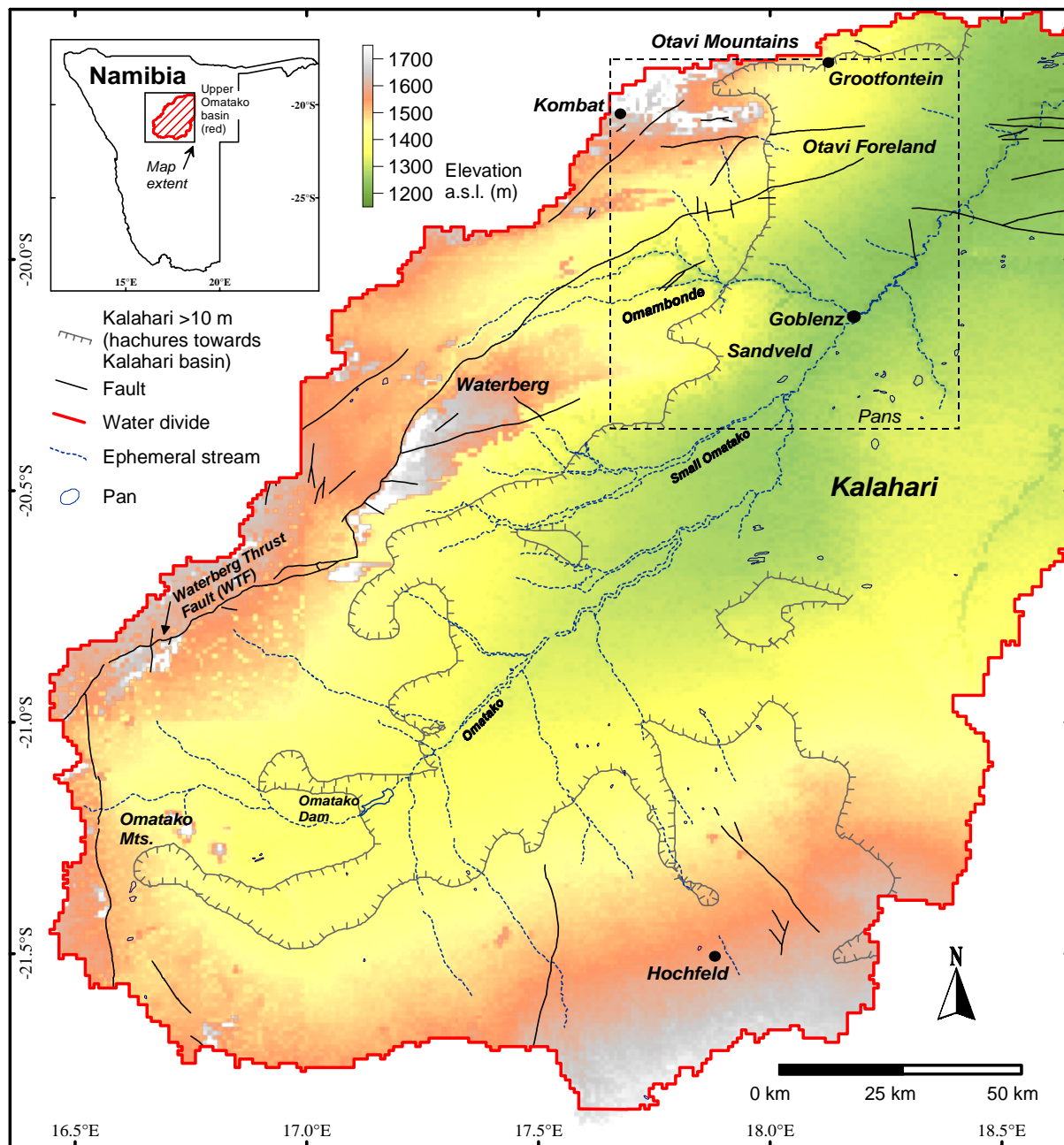


**Figure 1.1** The Upper Omatako basin with location of the Goblenz well-field (●) and target area for investigations (rectangle) in North-east Namibia. Background raster represents elevation above sea level (see legend).

In order to include all possible flow connections, the study area was extended to the natural system boundaries of the Omatako drainage basin, which, in a first approximation, also corresponds to the Omatako groundwater basin. For the analysis of such large basins in semi-arid areas difficulties tend to arise because of *insufficient data for hydrological and hydrogeological models* and because of *scale problems*.

*Lack of data* has been identified as one of the most imminent problems for managing water resources in the world's deserts and semi-deserts (AGNEW & ANDERSON, 1992: 113). In deserts meteorological conditions generally exhibit a high variability. Downpours of rainfall are patchy and highly variable in time – calling for data of high temporal and spatial resolution for adequately representing process heterogeneity (see SEUFFERT ET AL. 1999). This is compounded by the fact that data collection networks are insufficiently dense in the world's dry regions. Therefore the need has been recognized for adequate approaches to water-resources assessment in dry areas (BREDENKAMP ET AL., 1995; SIMMERS ET AL., 1997: 6) that take into account the data limitations and take advantage of the special hydrological conditions in drylands instead. Environmental tracer techniques based on principles of solute transport mechanisms have been introduced for the estimation of groundwater recharge rates. A wealth of studies and handbooks on the application of environmental tracers are available (i. e. VERHAGEN ET AL., 1991; CLARK & FRITZ, 1997; IAEA, 1996), demonstrating their usefulness for deriving flow-paths and elucidating recharge mechanisms.

Still, applications of environmental tracers tend to cluster in two distinct spatial scales: local-scale studies, mainly on vertical tracer transport, and regional-scale applications. While local-scale studies have the advantage of yielding quantitative results for a certain point in space, spatial heterogeneity makes up-scaling difficult and often unreliable (GIESKE ET AL., 1990). On the other hand, regional applications using hydrochemical indicators tend to remain qualitative in nature. Consequently there is a need for bridging this *dilemma of scales* with methods suitable for the quantitative application of environmental tracers to regional scales.

## 1.2 Objectives of the study

The major objectives of this study concern the assessment of the groundwater potential at Goblenz. These are:

- *the development of a conceptual model of groundwater recharge describing the recharge mechanisms, their timing and regional distribution for the Kalahari aquifer at Goblenz*
- *the development of a quantitative model of groundwater flows that contribute to the Kalahari aquifers at Goblenz*
- *the assessment of the role of transmission losses from the Omambonde tributary and the Omatako wash*



---

The quantitative model should identify the sources of groundwater at Goblenz and specify the rate of each individual flow component, such as the potential inflow rates from the Otavi Mountains, from the Waterberg sandstone plateau and from the upper parts of the Omatako basin. Eventually, the results of this study should be translated into recommendations for an appropriate groundwater management at Goblenz and its vicinity.

An objective exceeding the regional context concerns the further development of adequate estimation methods. In the view of earlier remarks concerning the need for quantitative models that take into account regional data constraints, the mixing-cell approach based on hydrochemical data offers a promising tool for the estimation of lateral flow components. Therefore, an additional objective was to *test the validity of the mixing-cell approach in a complex macro-scale, semi-arid groundwater basin*. The Omatako basin presents exceptionally good conditions for testing this technique in a large and variable environment.

### **1.3 Review of previous work relevant to the study area**

A detailed study on the groundwater resources of the Otavi Mountains has been carried out within the German-Namibian Groundwater Exploration Project (BUNDESANSTALT FÜR GEOWISSENSCHAFTEN UND ROHSTOFFE, 1997). A major part of this study was the development of a groundwater model for the Otavi Mountains. A southward boundary flow of  $9.6 \cdot 10^6 \text{ m}^3$  from the Otavi Mountains near Kombat (Figure 1.1) towards the Omatako basin was predicted by numerical groundwater modelling. With a total model area of  $1,825 \text{ km}^2$ , such an outflow corresponds to an average recharge rate of  $5.3 \text{ mm/y}$ . In the context of this study stable isotope,  $^{14}\text{C}$  and  $^3\text{H}$  samples have been taken and available data reviewed (PLOETHNER ET AL., 1997; GEYH & PLOETHNER, 1997).

A series of geophysical surveys have been made for the former Western Hereroland (WORTHINGTON, 1976, 1979; DE BEER & BLUME, 1983, 1985). Using Schlumberger profiles and correlation measurements at boreholes with known stratigraphy, the thickness of aquifer saturation was estimated for the Lower and for the Middle Kalahari. In the study area the upper Kalahari was found to be dry. The major results of these investigations have been summarised in Figure 4.4 and compared to own calculations.

The link between the studies on the recharge areas in the Otavi Mountains and on the water resources in the Kalahari was not well established. An important guideline for this study has been to clarify the hydrogeological and hydrochemical connection between these areas.

For Namibia a paramount value of 1 % groundwater recharge of mean annual rainfall (MAR) has been suggested by HEYNS (1996). This estimate was proposed as a mean figure averaging out the climatic, pedologic and geologic parameters as well as differences in the vegetation cover of Namibia. While a paramount value certainly has merits for educational purposes, and in some locations also as a first-guess estimate, it still lacks verification by empirical or theoretical studies at different scales in Namibia. Due to the high variability of groundwater recharge it cannot replace the individual assessment of groundwater potentials for major groundwater abstraction schemes.

More reliable estimates should take into account not only mean annual rainfall, but also the recharge environment characterized by its topography, geology, soil cover and vegetation. The study area is characterized by the contrast between hard-rock outcrops in the periphery and by the occurrence of Kalahari sediments in the basin centre. As a consequence, in the review on previous groundwater recharge studies, a distinction will be made between areas characterized by exposures of basement rocks or partly consolidated Karoo sediments, the '*hardveld*', on the one hand, and the flat Kalahari environment, the '*sandveld*', on the other hand.

### 1.3.1 Groundwater recharge on basement outcrops

DACHROTH & SONNTAG (1983) carried out studies on groundwater recharge in hard-rock fractured aquifers (quartzite, marble, schist and granite) of central Namibia using a combination of chloride concentrations in the groundwater, isotope methods and physical hydrogeological methods. Their tritium and  $^{14}\text{C}$  data show that groundwater in most areas not covered by Kalahari sediments is recent. A quantitative estimation of groundwater recharge from chloride concentrations in the saturated zone yielded recharge rates between 1.5 and 15 mm/a (0.4 to 4.1 % of a mean annual rainfall of 370 mm at Windhoek).

Within the German-Namibian Groundwater Exploration Project studies on groundwater resources and recharge of the Otavi Mountains in Namibia have been carried out. In this context, a review of previous studies on groundwater recharge in the dolomite karst of the Otavi Mountains and in similar karst environments of Southern Africa has been made (SCHMIDT, 1997a).

Groundwater recharge of different hard-rock environments was investigated by MAINARDY (1999). Local recharge estimates were based on the chloride method and on fracture aperture measurements. Groundwater models were developed for selected areas in order to simulate the response of groundwater levels to different recharge rates. Outcrops of sandstone,

dolomite and marble with small to moderate slopes were found to provide favourable recharge conditions. Recharge rates of 16 to 24 mm/y were determined for a bare, fractured sandstone in the western part of the Waterberg (Figure 1.1). This represents 3.2 to 4.8 % of 450 mm/y mean annual rainfall. Much lower recharge rates of 1 to 8 mm/y or 0.2 to 1.8 % of MAR were derived for quartzite outcrops of the Nossib Group and for meta-sediments belonging to the Damara Sequence.

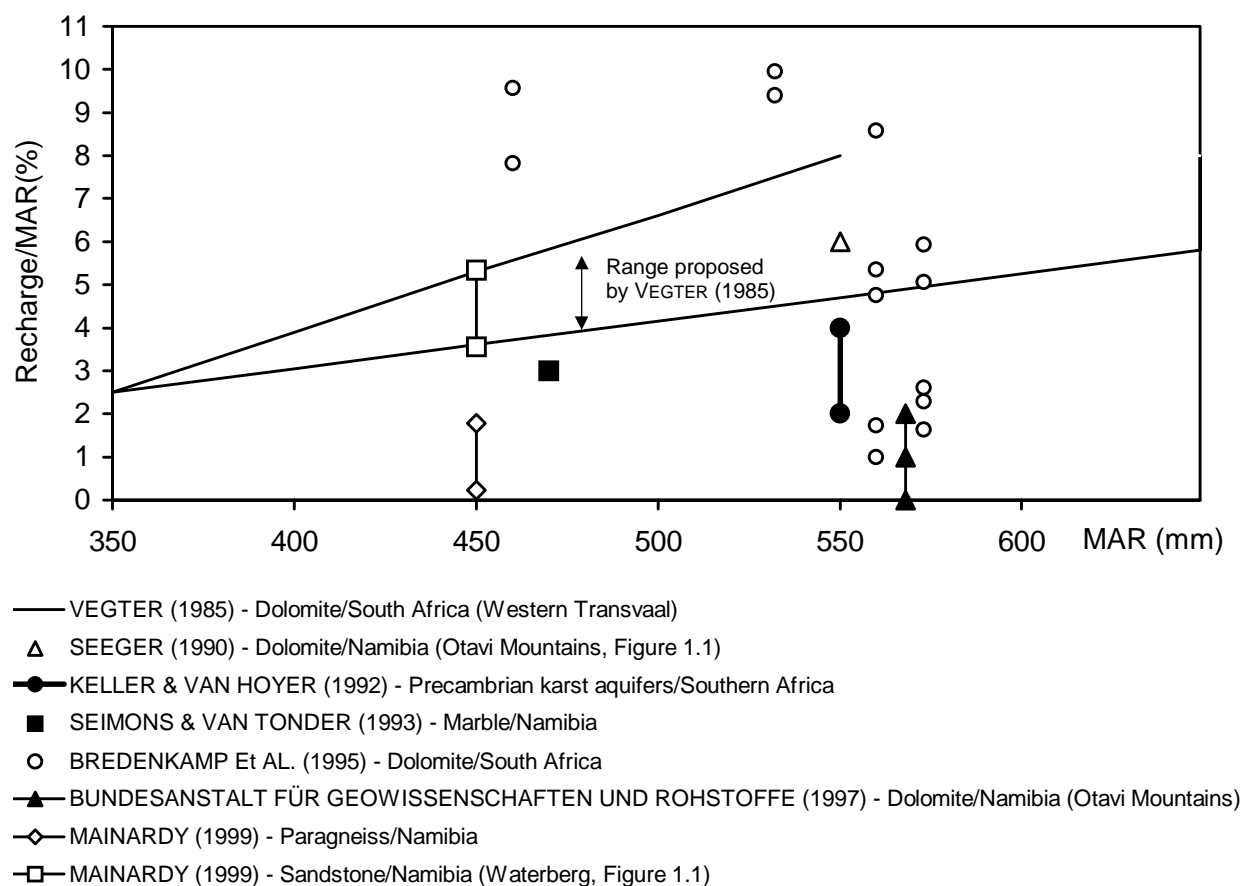


**Figure 1.2** Relationship between mean annual rainfall (MAR) and groundwater recharge (as percentage of MAR) from studies in hard-rock environments of southern Africa (SCHMIDT, 1997a, modified). Location names within the study area are shown in Figure 1.1.

These studies suggest that, within the range of climatic conditions encountered in Namibia, recharge in hard-rock environments ranges from conservative estimates of 1 % up to several percent of mean annual rainfall. Averaged over small areas ( $\sim 1 \text{ km}^2$ ), recharge rates as high as up to 10 % of mean annual rainfall seem to be possible, if favourable recharge conditions are given.

### 1.3.2 Groundwater recharge in the Kalahari

Many early studies on groundwater recharge in the Kalahari have been strongly influenced by what MAZOR (1982) called the '*old theory of Kalahari sand preventing rain recharge*'. This theory originates from statements by PASSARGE (1904) that the occurrence of direct rain recharge would be unlikely in the Kalahari because rainfall would be stored in the Kalahari sands and be evaporated or consumed by vegetation there.

It is interesting to note that PASSARGE limited this statement to *direct* recharge, *not* excluding the existence of recharge from floods or pans. Still, the simplified view that recharge was unlikely in the Kalahari became popular and was reiterated among others by FROMMURZE (1953) and BOOCOCK & VAN STRATEN (1962). FOSTER ET AL. (1982:113) concluded in their studies on recharge in the Kalahari of southern Botswana, that '*diffuse recharge should not be presumed to be occurring where the sand-cover is more than 4 m*'. Their study was based on the interpretation of  $^{14}\text{C}$  and hydrochemical data and used a generalized climatic water-balance approach.

In his pioneering work on the regional distribution of groundwater recharge in the Kalahari of Namibia MARTIN (1961) basically followed this line of thinking, but specified that recharge can occur where *sand cover is thin* or where *shallow calcrete layers are found near the surface*. Calcrete layers were assumed to offer preferred pathways through solution channels and to mechanically prevent roots from abstracting deeper soil water. Notably, in an attempt to define the regions in the Namibian Kalahari where recharge was more likely, MARTIN mapped belts of favourable recharge conditions along the boundaries of Kalahari cover and along some stretches of ephemeral rivers. The application of this way of regionalization to the Omatako basin is shown in Figure 1.3.

The assumption that recharge is reduced to almost nil by a sand cover several metres thick was strongly challenged by MAZOR (1982), based on hydrochemical evidence (MAZOR ET AL., 1980). Especially the discovery of significant amounts of bomb tritium in phreatic Kalahari aquifers (VERHAGEN ET AL., 1975, 1979, 1990) yielded strong evidence for at least local recharge. Indirect recharge mechanisms involving infiltration along root channels, fissures and cracks, or the concentration of runoff in depressions or channels were proposed as likely shortcuts. The fact that in central Namibia groundwater was struck in the marble basement below 120 m of Kalahari sand was seen as supporting evidence for deep percolation by DACHROTH & SONNTAG (1983). Annual recharge of up to 20.8 mm/y (4.6 % of mean annual rainfall), was estimated, using chloride concentrations in the groundwater.

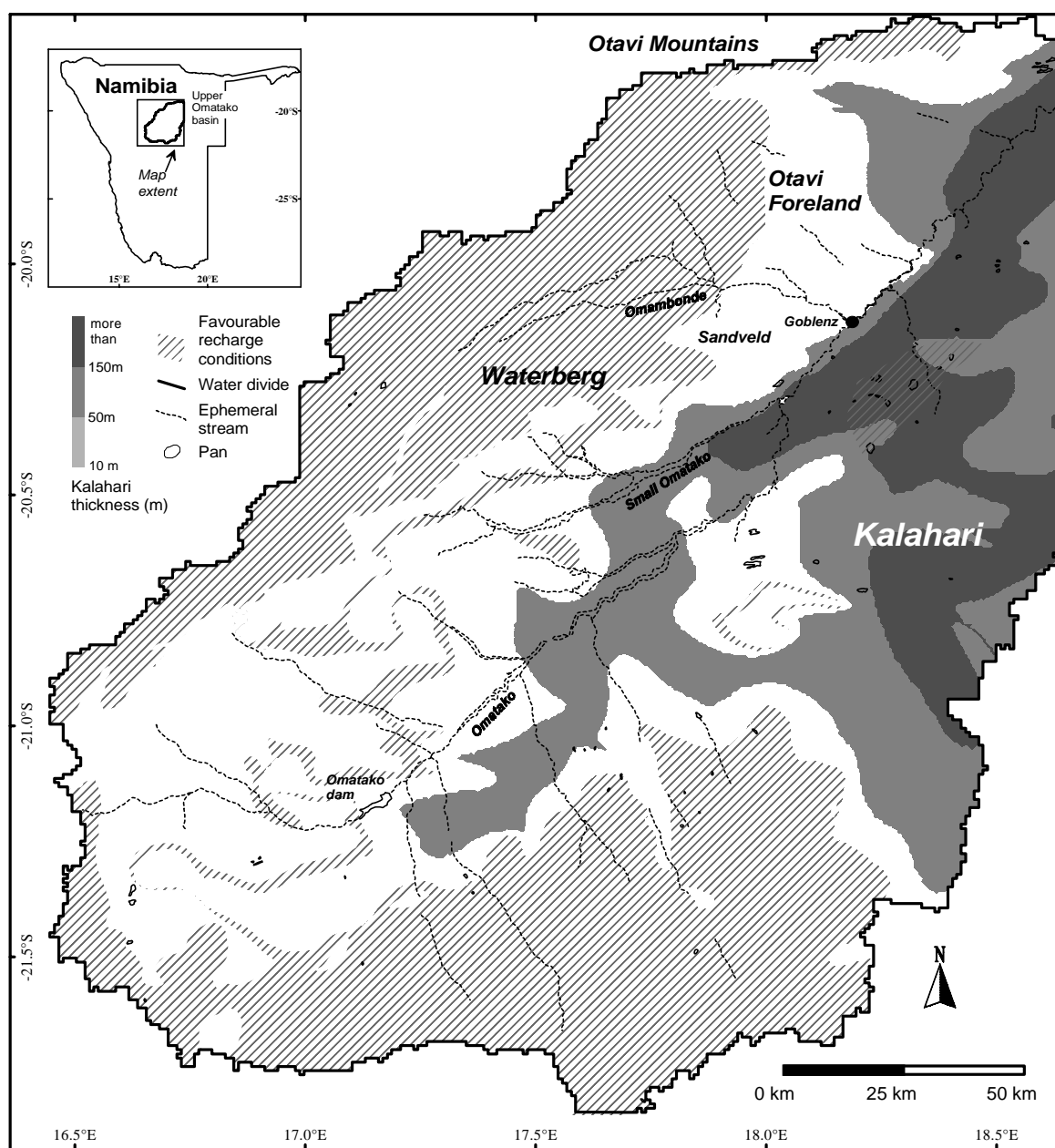


**Figure 1.3** Areas with favourable recharge conditions (marked areas), modified from MARTIN (1961). Good recharge conditions in the Kalahari are restricted to areas with a thin Kalahari cover or where calcrete occurs within the Kalahari formations near the surface. Groundwater levels in these areas are shallow. Grey raster values indicate Kalahari sediment thickness.

However, a careful analysis of the possibility of lateral groundwater inflow is needed before these results can be seen as an indication of deep percolation through thick Kalahari sediments. In areas with a thin Kalahari sand cover of a few metres recharge rates of 4 to 8 mm/y were found by DACHROTH & SONNTAG (1983), corresponding to 0.8 to 1.7 % of 475 mm/y mean annual rainfall in central Namibia.

WRABEL (1999) studied chloride profiles together with chloride concentrations in the saturated zone near Hochfeld (Figure 1.1), located in north-eastern Namibia. The study area is characterized by a flat topography and is mostly covered by a thin veneer of Kalahari sediments overlying sediments and basement rocks of Karoo and Namibian age. In the study area exposures of calcrete exist that may provide favourable recharge conditions. Groundwater recharge rates between 1.4 mm/a and 42 mm/a were derived, corresponding to a range between min. 0.3 % and max. 10.3 % of local mean annual rainfall. Interestingly, the observed chloride concentrations in the groundwater were consistently lower than the equilibrium chloride concentrations in the deeper soil profile. This deviation was interpreted as an indication of bypass flow through macropores and preferred pathways. The fact that this deviation was clearly pronounced in the vicinity of pans or deflation-stripped calcrete supports the assumption by MARTIN (1961) that in such areas recharge conditions are enhanced.

A summary of recharge studies in Namibia, South Africa and Botswana is given in Table 1.1. Comparing the results, it should be noted that Namibia and Botswana receive summer rains, while the southern part of South Africa has a regime with winter rain. A visualization of the data (Figure 1.4) shows a cluster of recharge percentages between 0.1 and 2.6 %, with some exceptionally high values.

**Table 1.1** Recharge rates determined for the Kalahari in Namibia, Botswana and South Africa.

Authors	Country	Method	Rainfall (mm/y)	Recharge (% of MAR)		
				Min.	Mean	Max.
VOGEL ET AL. (1974)	Botswana	tritium	500		2	
DACHROTH & SONNTAG (1983)	Namibia	groundwater chloride	472	0.8		1.7
DE VRIES & HOYER (1988)	Botswana	chloride	550		9.6	
GEHRELS & VAN DER LEE (1990)	Botswana	chloride	586		2.6	
GIESKE (1992)	Botswana	soil chloride	550		2.1	
VERHAGEN (1992)	Botswana	isotopes	450	0.1	0.7	1.3
SAMI & HUGHES (1996)	S. Africa	chloride	483	0.6		1.7
VERHAGEN (1999)	Botswana	equal volume	350	0.9	-	1.4
		equal volume	350	0.8	-	1.7
		isotopes	350	0.3	-	1.1
WRABEL (1999)	Namibia	soil and groundwater chloride	412	0.3	7.1	10.3

The elevated values have been derived from chloride concentrations in groundwater close to exposures of calcrete and probably represent the influence of preferential flow (WRABEL, 1999). Very low chloride concentrations in soil profiles have been reported after intensive rain events (GIESKE ET AL., 1990; WRABEL, 1999). These values do not always reflect steady flow conditions, as required for this estimation method, and can cause an overestimation of mean annual recharge. In addition, due to high lateral variations in the chloride distribution, "*calculation of recharge on the basis of chloride and isotope data along a single vertical profile seems inadvisable*" (GIESKE ET AL., 1990).

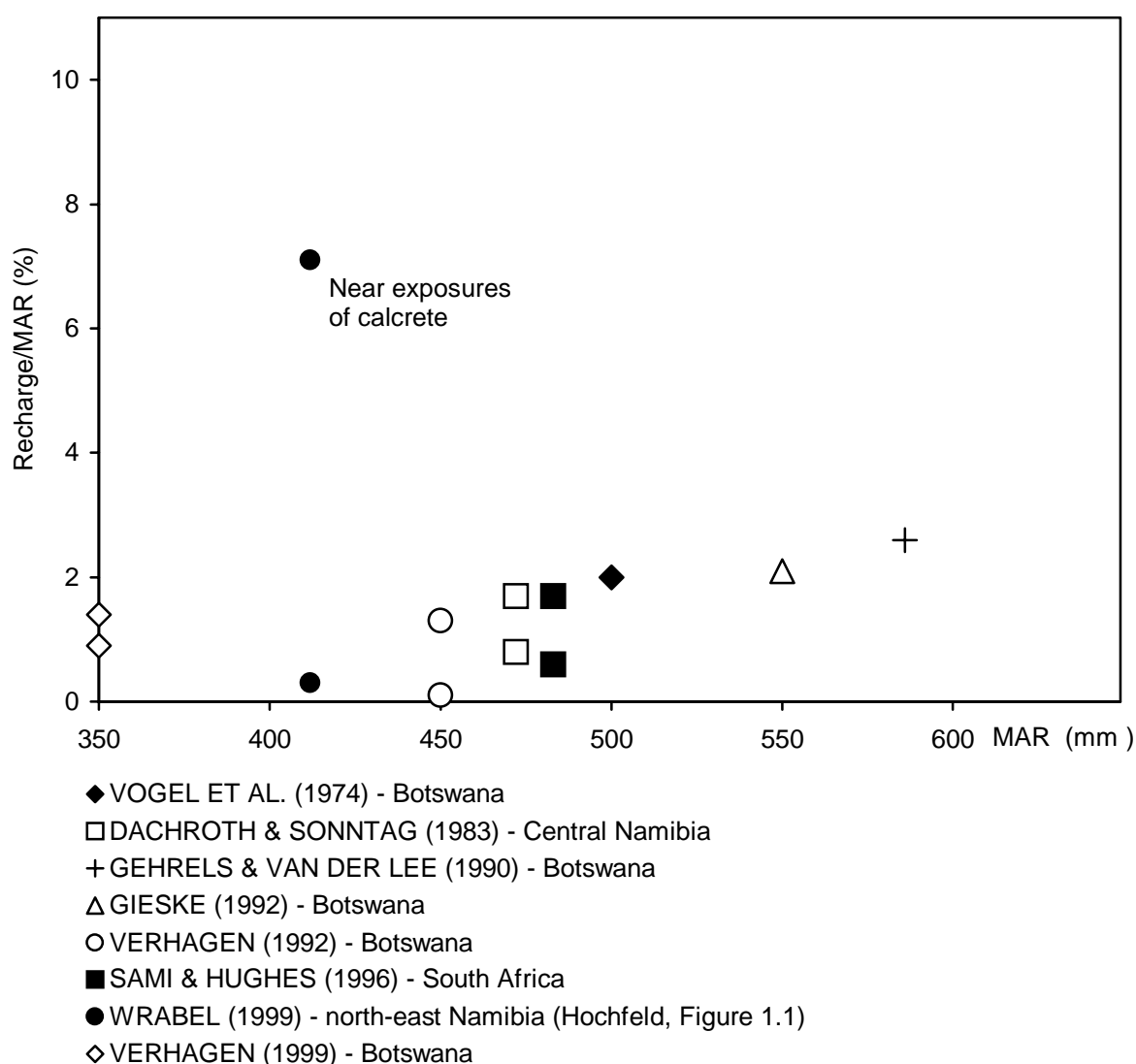


**Figure 1.4** Relationship between mean annual rainfall (MAR) and the percentage of mean annual rainfall becoming recharge from studies in the Kalahari (Namibia, Botswana and South Africa). If two identical symbols are given, they represent minimum and maximum values.

With respect to low chloride concentrations in groundwater it should be carefully analysed whether lateral subsurface inflow from basement outcrops outside the Kalahari may not be the cause, as reported in a study by VERHAGEN (1999). In such a case groundwater chloride will not necessarily indicate high *local* recharge rates through Kalahari sediments.

To summarize, the available data from the Kalahari show that recent groundwater recharge takes place in most locations, even though rates are low, corresponding to 0.1 to 2.6 % of mean annual rainfall. The data also indicate the existence of preferred flow-paths and the possibility of higher recharge in some places such as pans, shallow calcrete or ephemeral rivers. Nevertheless, an independent verification with other methods and an analysis of the spatial extent of increased recharge is necessary before such indications can be used as a basis for water-management practices. After all, the paramount value of HEYNS (1996) is obviously a reasonable guess for regional and general approaches. In the Kalahari, especially in areas with thick sediments and mean annual rainfall below 500 mm/a, groundwater recharge can drop well below 1 % of mean annual rainfall. More favourable recharge conditions are expected where karstified calcrete exposures occur.



## 2 The study area

The study area is located in north-eastern Namibia extending from E 16° 30' to E 18° 30' longitude and from S 21° 40' to S 19° 30' latitude. It covers the area of the endorheic upper Omatako river basin draining into the vast Kalahari sedimentary basin. The climate in the study area is semi-arid.

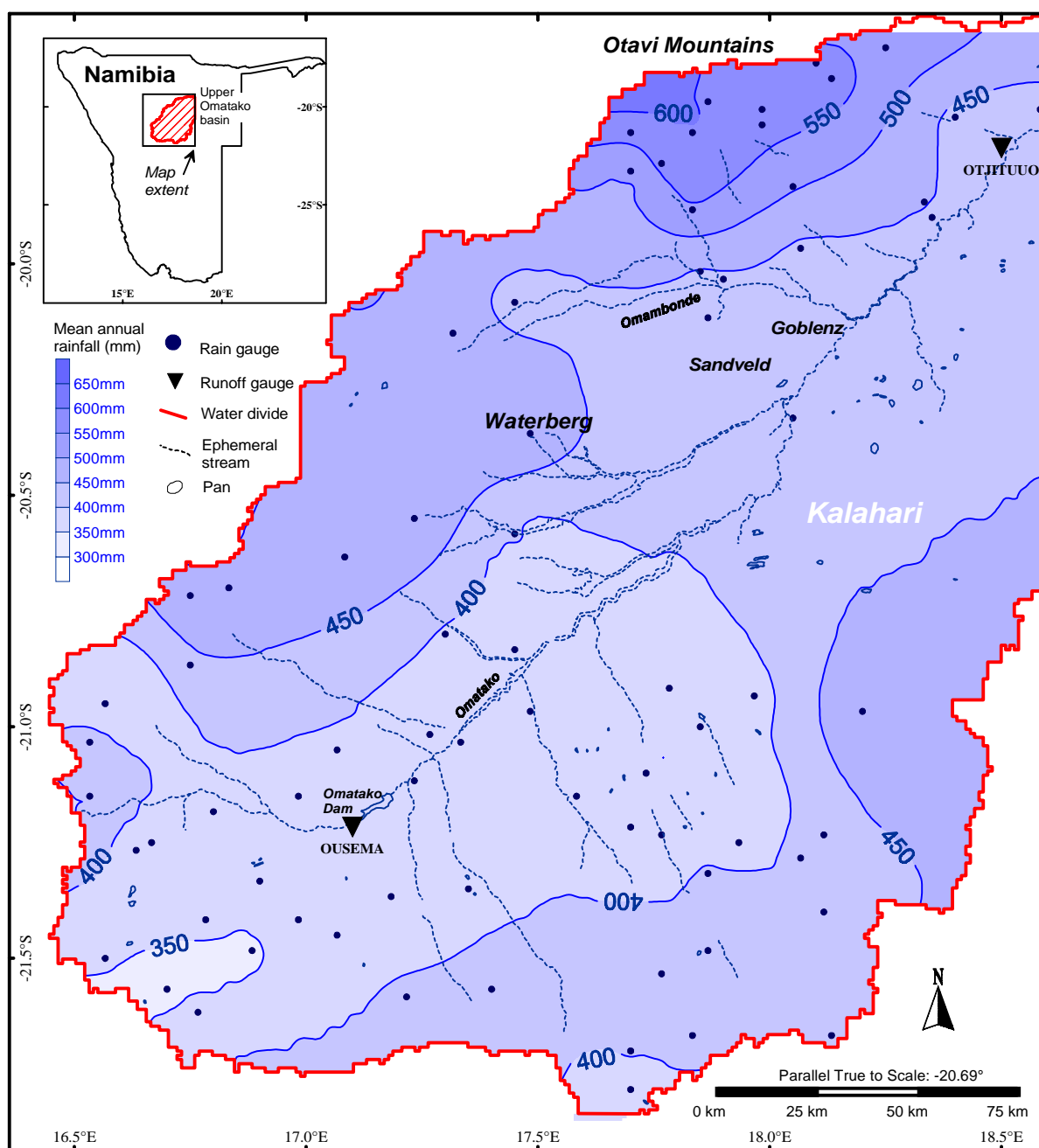


**Figure 2.1** Mean annual rainfall in the Omatako basin (data from DEPARTMENT OF WATER AFFAIRS, 1992a and from Meteorological Survey of Namibia).

## 2.1 Climate

Mean annual rainfall varies between about 400 mm in the central low areas of the basin and 650 mm/year in the Otavi Mountains (Figure 2.1). Due to the location near the Tropic of Capricorn the study area has a subtropical summer rainfall regime. The rainy season starts in October/November and ends in April/May; highest rainfall is observed in February. Figure 2.2 shows the median and the variability of monthly rainfall for the station Omambonde in the study area. On average this station has received 420 mm/year of rainfall between 1949 and 1993. The lower curve represents the 10 % quantile, or monthly rainfall amounts that have been reached in 9 years out of ten. The upper curve shows the 90 % quantile representing extreme monthly rainfall events recorded once during every ten years.

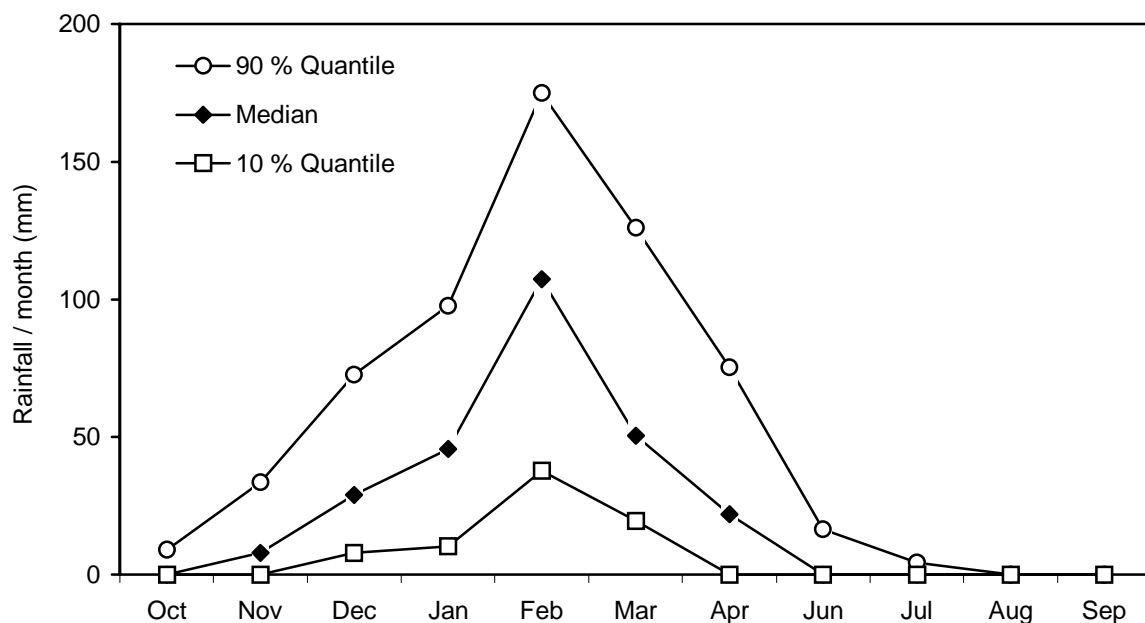


**Figure 2.2** Seasonal variation of monthly rainfall near Omambonde (see Figure 2.1) represented by the median, the 10 % and the 90 % quantile of the time series 1949-1993.

The seasonal rainfall maximum coincides with high temperatures and potential growth of vegetation (as long as a sufficient amount of water is available in the soil storage). As a consequence, the threshold for any rainfall event becoming effective in terms of soil infiltration and groundwater recharge is high. Virga evaporation reduces rainfall already during the initial phase of the events. After any rainfall event high potential evaporation causes an intensive flow of water vapour back to the atmosphere, and water stored in the soil will be consumed to a high degree by plant transpiration. Finally, the soil moisture will drop and actual evaporation of non-irrigated land surfaces will become much lower than potential

evapotranspiration due to soil water deficits during part of the summer and most of the winter season.

The Namibian Weather Bureau and the Hydrology Division of the Department of Water Affairs (DWA) measure pan evaporation, mainly for controlling water losses from reservoirs and dams. Measurements are made on a daily basis or with autographs using Class A and Symons pans. Based on these data an evaporation map of Namibia has been produced by the Hydrology Division of the DEPARTMENT OF WATER AFFAIRS (1988).

For the Omatako basin an annual Class A pan evaporation of approximately 2,800 mm is given in the Namibian evaporation map. Pan evaporation is generally greater than evaporation from larger water bodies. This is due to an '*oasis effect*' and to absorption of energy by water in the pan as well as by the pan itself. Pan coefficients have been introduced in order to reduce such effects (MAIDMENT, 1992). Correcting this value with a recommended pan coefficient of 0.7 for Namibia (DEPARTMENT OF WATER AFFAIRS, 1988), there results an estimated net evaporation of 1,960 mm/year for open water surfaces. The annual amount of evaporation has been disaggregated into monthly evaporation rates (Figure 2.3) using a reference monthly distribution for central Namibia (DEPARTMENT OF WATER AFFAIRS, 1988).

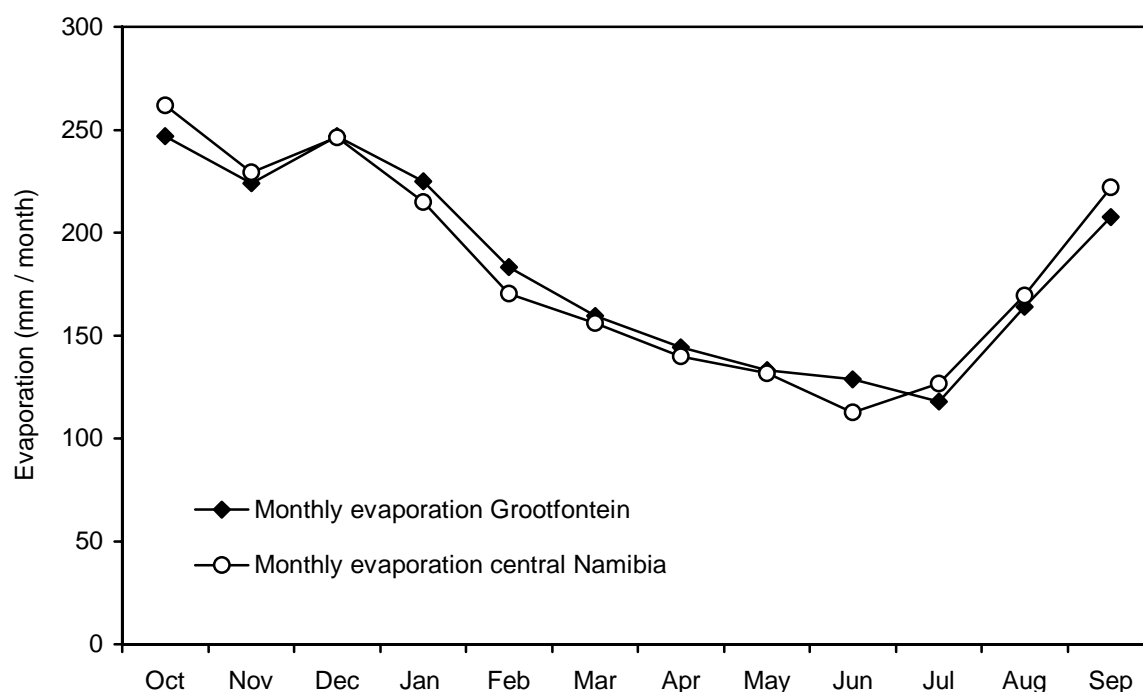


**Figure 2.3** Monthly evaporation rates from Class A pan data corrected with a pan coefficient of 0.7 for the station Grootfontein (Figure 1.1) and for the central region of Namibia.

The evaporation per month varies between 113 and 261 mm. This corresponds to daily evaporation rates between 3.8 and 8.4 mm. The evaporation data indicate regional evaporation rates from open water surfaces and do not reflect local variations in exposure or wind speed.

## 2.2 Surface drainage

The Omatako and all tributaries are ephemeral rivers and are only activated by sporadic generation of surface runoff. In the Omatako basin four hydrometric stations are operated by the Department of Water Affairs. At 'Ousema' (21.22° S, 17.10° E) runoff has been recorded at a weir just upstream of the Omatako dam since March 1961. At this station the catchment has a drainage area of 4,970 km<sup>2</sup>. Just below the Omatako dam the outflow is controlled at the station 'Omatako dam'. The weir 'Rietfontein' (19.74° S, 17.86° E) was set up in March 1993 in order to control the spring flow at Rietfontein. At 'Otjutuuu' runoff has been gauged in an open section between 1970 and 1980 and since 1988. This station is located on the ephemeral Omatako river downstream of Goblenz (at 21.15° S and 17.17° E). The hydrometric data recorded at 'Ousema' and 'Outjituuo' (Figure 2.1) have been analysed. Although the records are short and discontinuous and runoff measurements in semi-arid and arid areas are difficult, the data recorded at both stations shed some light on the hydrological interrelationship between the mountainous rim ('*hardveld*') and the centre of the basin covered mainly by aeolian sediments ('*sandveld*').

### *Runoff from the mountain areas*

At 'Ousema' the Omatako river has a stream length of 103 km and a mean river slope of 2.1 ‰. Mean annual precipitation averaged over the basin up to 'Ousema' amounts to 403 mm/y. The drainage area of the upper station 'Ousema' (4970 km<sup>2</sup>) is characterized by outcrops of intrusive rocks (granites) and paragneisses as well as mudstone and shale (see geological map, Figure 2.6). The discharge measured at 'Ousema' corresponds to unit runoff values (runoff produced per m<sup>2</sup> in mm) of 0.1 to 29 mm/m<sup>2</sup> per year, with a median of about 4 mm/year (Figure 2.4). These values match the unit runoff proposed by DEPARTMENT OF WATER AFFAIRS (1992b): According to the unit runoff map of Namibia 15 to 30 mm/m<sup>2</sup> are produced on granites and gneisses. The Omingonde mudstones and shales, partly covered by a thin cover of Kalahari sand in the lower section, produce an estimated unit runoff of only around 2 mm/m<sup>2</sup>. The significant generation of surface runoff is also reflected by an increased drainage density in the western part of the basin.

The time series exhibits a high variability of discharge, both in terms of measured peak discharge and annual flood volumes. The highest peak discharge measured amounts to 435 m<sup>3</sup>/s, while the median of peak discharges between 1960/61 and 1993/1994 was 62 m<sup>3</sup>/s. The total annual flood volume varied between 0.36 MCM (1 MCM= 1\*10<sup>6</sup> m<sup>3</sup>) and 34 MCM per year - a range of two orders of magnitude.

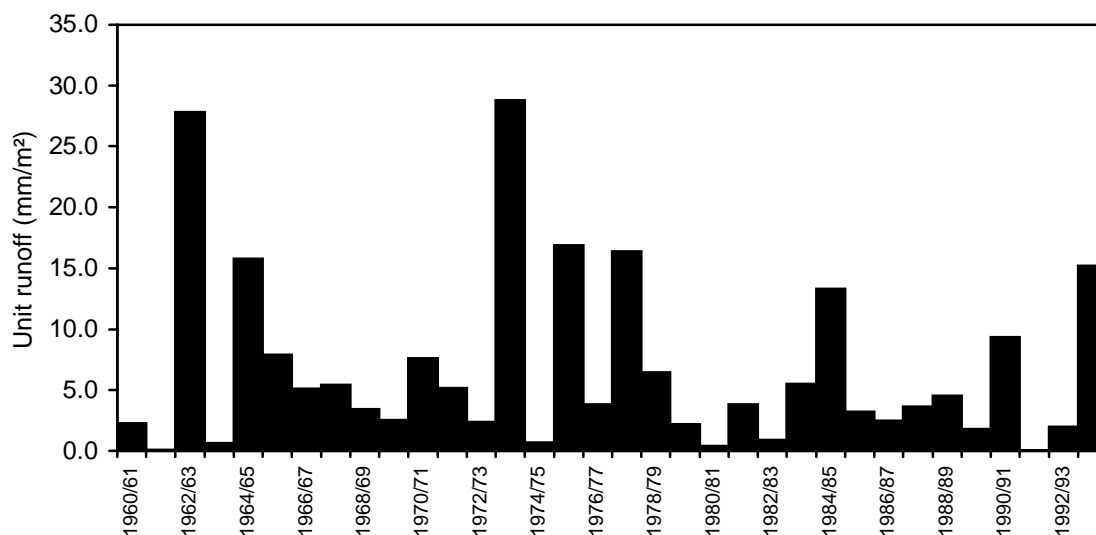


**Figure 2.4** Unit runoff (mm/m<sup>2</sup>) derived from measured discharge (m<sup>3</sup>/s) divided by the catchment area for 'Ousema' station, DWA data.

For estimating the potential of groundwater recharge by transmission losses, an important parameter is the duration during which the channels are inundated. The total time of flooding in the period 1960 to 1994 ranged between 6 and 97 days/year, i.e. up to 3 months, with a median of 32 days/year.

Altogether the 'Ousema' runoff station is typical of the hydrological behaviour of the 'hardveld', characterised by rocky outcrops. In the mountainous parts around the Kalahari basin runoff develops on surfaces of relatively low permeability, forming seasonal flash floods. The hydrological characteristics and in-channel storage cause single or multi-peak floods from several days to a few weeks. In locations where hydrogeological traps exist, i.e. coarse and deep alluvium, good local recharge conditions by transmission losses can be expected. Floods from other ephemeral tributaries of the Omatako not captured by large dams drain into the Kalahari basin, where they fill shallow depressions and are gradually absorbed in dry riverbeds and shallow depressions.

### *Runoff in the Kalahari*

The station 'Otjituuo' is located on the Omatako about 200 km downstream of 'Ousema' (Figure 2.1). The estimated catchment area up to this runoff station is 36,850 km<sup>2</sup>. Most of the

surface drainage recorded at the station 'Ousema' further upstream is intercepted by the Omatako dam. Two major tributaries drain into the Omatako below the Omatako dam from the north-west, the 'Small Omatako' and the 'Omingonde' (confluence at Goblenz). The south-eastern tributaries of the Omatako, located within the Kalahari, are discontinuous and partly obstructed by eolian sand. The time series of runoff data at 'Otjituuo' is short and therefore less representative than the data from 'Ousema' (Figure 2.5).

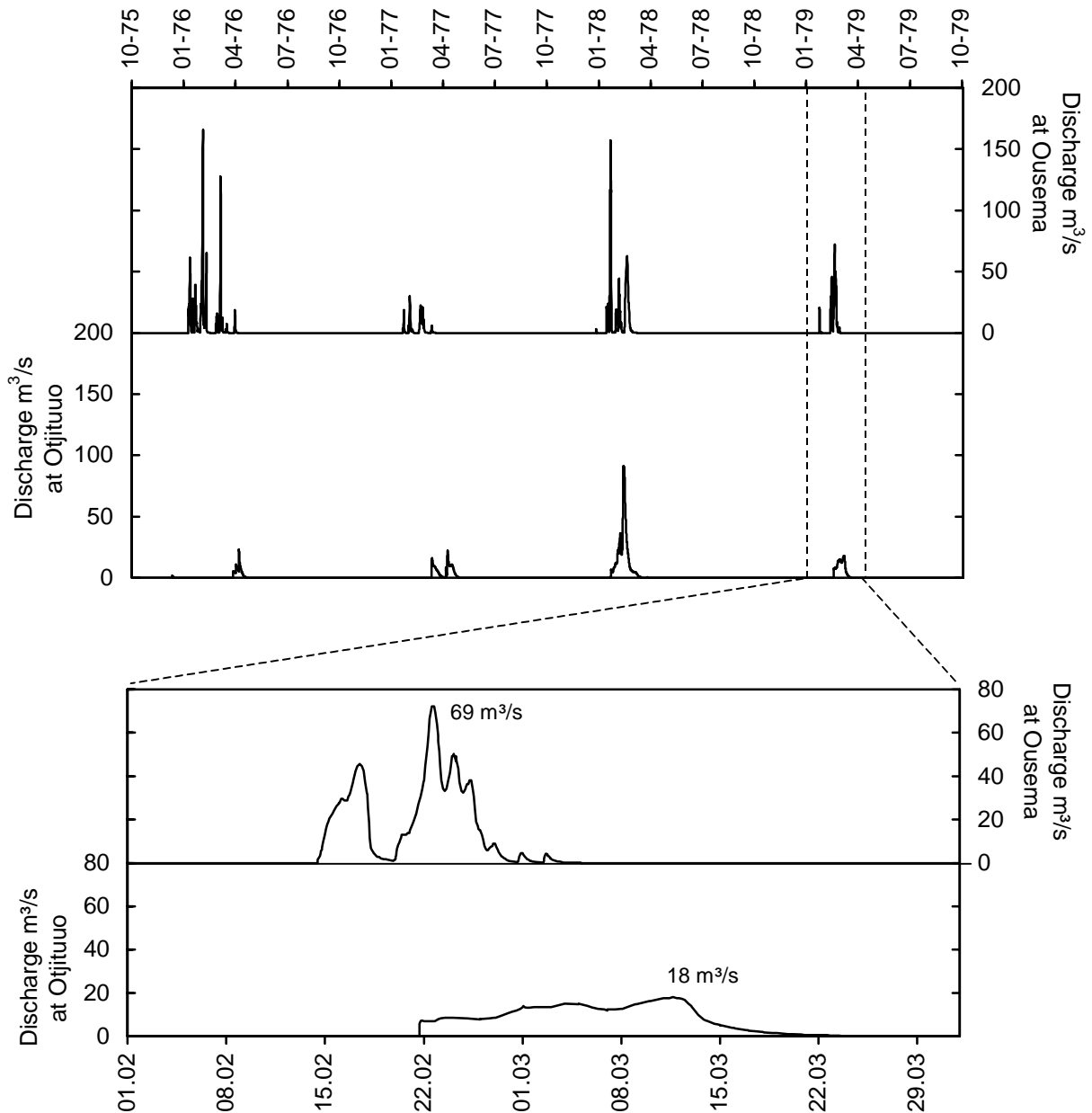


**Figure 2.5** Daily discharge at 'Ousema' (above, right scale) and 'Otjituuo' station (below, left scale) between 1975 and 1979, and in more detail for a single event in February/March 1979, DWA data.

In order to demonstrate the relative response to rainfall events in the Omatako basin at both gauging stations, discharges recorded at 'Otjituuo' (below) have been plotted taking discharge from 'Ousema' as a reference (above). At 'Otjituuo', peak discharges of the events measured between October 1975 and October 1979 range from 20 to 30 m<sup>3</sup>/s (3 events) and were 90 m<sup>3</sup>/s for a major event in 1978. While the event recorded during February/March 1979 had a peak discharge of 69 m<sup>3</sup>/s at 'Ousema', the highest recorded discharge of this event amounts to only 18 m<sup>3</sup>/s at 'Otjituuo'. At the same time the duration of the event had increased to almost one month compared to only 15 days further upstream. The total volume of this flood event decreased from 35.0 MCM at 'Ousema' to 23.2 MCM at 'Otjituuo'. In the Kalahari, the production of surface runoff is limited and an attenuation of channel runoff takes place. The annual flood volumes there, expressed in terms of unit runoff, correspond to only 0.6 to 1.4 mm/m<sup>2</sup>.

**Table 2.1** Runoff data recorded at the Otjituuo gauging station (21.15° S and 17.17° E).

Hydrological year	Volume (m <sup>3</sup> )	Peak (m <sup>3</sup> /s)	Level (m)	Duration (days)	Unit runoff
1975/76	1.2E+07	22	0.83	29	0.6
1976/77	2.5E+07	22	0.81	49	1.3
1977/78	2.8E+07	41	1.26	22	1.4

Nevertheless, a relatively long-lasting flood may considerably contribute to indirect recharge, at least locally. Near the mountain front / Kalahari transition and at river confluences, in particular, transmission losses are a potential recharge factor.

## 2.3 Geology

Paragneisses and granites of the Grootfontein complex are the oldest rocks of the study area (Mokolian, ~1,600 MA). Overlying this complex, the Precambrian Damara Sequence has been deposited in a basin between the Kongo and the Kalahari cratons. The sequence was folded and metamorphosed during the Pan African orogeny, forming the most extended type of pre-Kalahari rocks in the study area. A general overview on the evolution of the Damara Orogen is given in MILLER (1983). Previous work, especially on the Otavi Mountains, has been reviewed in PLOETHNER ET AL. (1997). A Northern, Central and Southern Zone of the Damara Sequence are distinguished. However, only the Northern and the Central one are covered by the study area. They represent various depositional environments and have undergone different degrees of metamorphism. The lowest unit of the Damara Sequence is formed by the basal Nosib Group, mainly composed of quartzite, conglomerate and schist in both the Northern and the Central Zone.

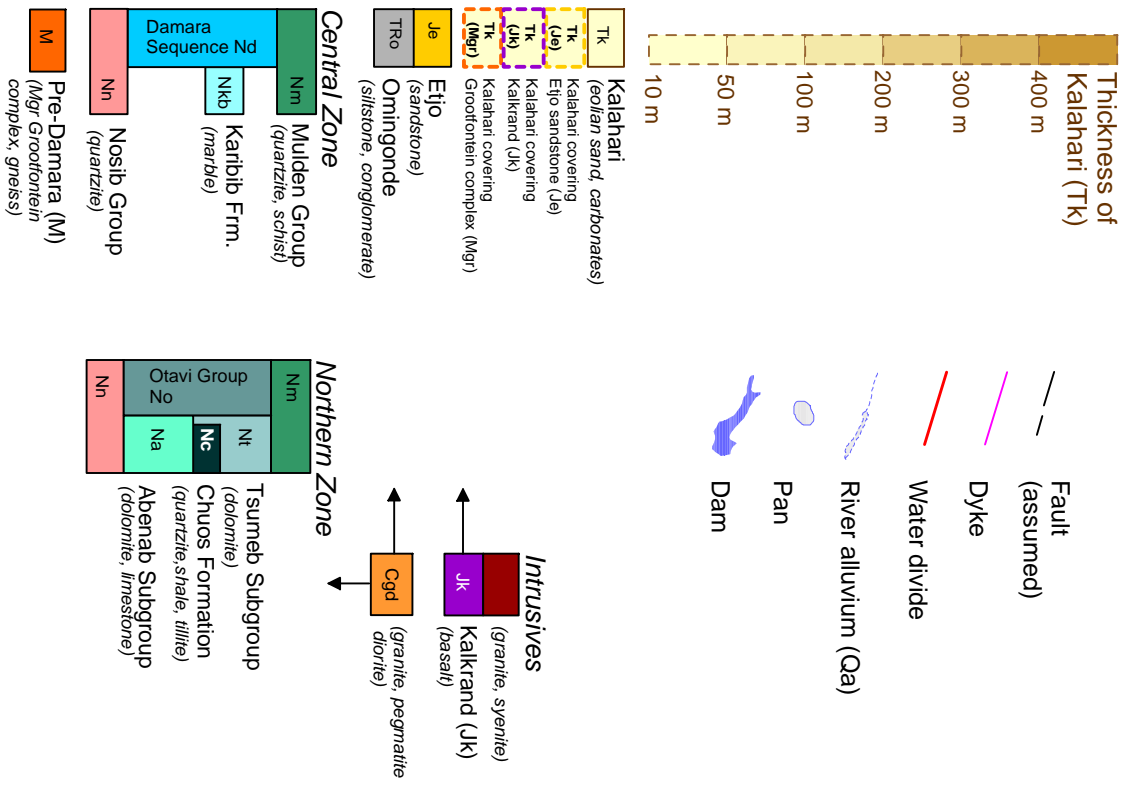
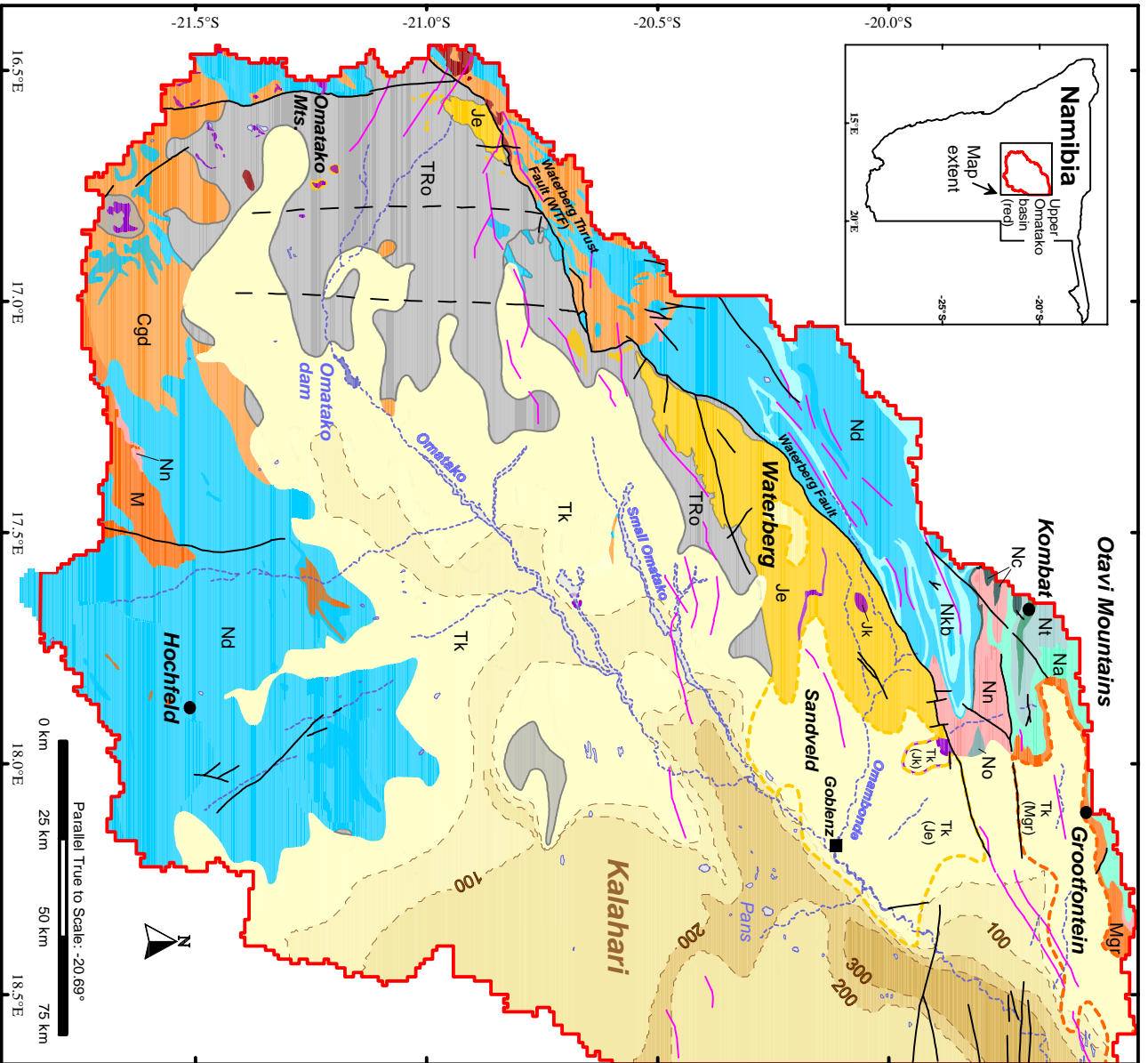


**Figure 2.6** Geological Map of the Upper Omatako basin, Namibia, with isopachs of Kalahari thickness compiled from geological maps of Namibia 1:250,000 (Geological Survey, Namibia). For areas that are relevant for this study, formations beneath the Kalahari are shown: a) Sandveld with Kalahari (Tk) covering Elio sandstone (Je) and Kalkrand basalts (Jk) and b) the Otavi Foreland with Kalahari covering gneisses of the Grootfontein complex (Mg).



---

In the Northern Zone, the Nosib Group is overlain by up to 3000 m of carbonates formed in the platform/shelf environment of the Damara basin (Otavi Group). The Otavi Group has been further subdivided into the Abenab and Tsumeb subgroups, both of them mainly composed of dolomites of different facies. The fractured and partly karstified rocks of the Tsumeb and Abenab subgroups are important aquifers of the study area. The Abenab Subgroup encompasses the Berg Aukas Formation (dolomite, limestone and shale), the Gauss Formation (massive dolomite), and the Auros Formation (dolomite and limestone). The Tsumeb Subgroup is composed of the Chuos, Maieberg, Elandshoek and Hüttenberg formations. The Chuos Formation (tillite, shale and quartzite) acts as an aquitard and separates a lower Otavi karst aquifer complex (Abenab Subgroup) from an upper one (Tsumeb Subgroup).

In the Central Zone, the Swakop Group stratigraphically corresponds to the Otavi Group. The metamorphic rocks of the Swakop Group are further subdivided into the Ugab (Nu) and the Khomas subgroups. Both subgroups mainly consist of marble and schist. In the Ugab Subgroup marbles are dominant. Within the younger Khomas Subgroup, there occur marbles (Karibib Formation) and marbles with schist (Kuiseb Formation). The Mulden Group overlies the middle carbonate units of the Otavi and Swakop groups. In both zones, phyllite and quartzite are dominant, found together with some conglomerates (Northern Zone) and schist (Central Zone). Folding during the Pan-African produced a sequence of synclines/anticlines.

Granites, granodiorites and diorites intruded in the late Namibian and during the Cambrian. These intrusions are frequent in the western and southern part of the Omatako basin. The unfolded Karoo Sequence is separated from the Damara Sequence by an unconformity. Sediments of the lower Karoo Sequence (Ecca Group) have been found in some boreholes in the western part of the Kalahari basin on top of the Damara Sequence. Deposits of thin coal seams have been the target of detailed investigations (GUNTHER, 1983, 1987). Except for their – local – influence on the hydrochemistry of groundwater at the base of the Lower Kalahari, these formations are not relevant in the context of this study. However, extended outcrops of the Omingonde Formation (TRo) have an important impact on the hydrology of the western Omatako basin (Chapter 2.2). The Omingonde Formation contains mudstones, siltstones with some sandstone and occasional lenses of conglomerates.

A prominent feature of the region is a major outcrop of the Etjo Formation: the Waterberg (Figure 2.7a). The Etjo sandstone preserved there crops out in an area south of the Waterberg Fault. Along it, folded rocks of the Damara Sequence, probably initially also overlain by Mesozoic sediments, have been thrust over a southern block (Waterberg Thrust Fault). Due to the contrasting hydraulic properties of the Etjo sandstone and the underlying Omingonde Formation, and due to the good permeability of the Etjo sandstone, it is a fresh groundwater aquifer. Prior to the deposition of sediments belonging to the Karoo Group an intrusion of

basaltic dykes and sills took place. The occurrence of basalt in the Etjo sandstone (Waterberg, Figure 2.7a) is documented from boreholes drilled near the farms Rimini and Hairabib. Dykes have intruded rocks of the Damara Sequence north of the Waterberg.

Tectonic activity has played a crucial role in the deposition and development of the Kalahari Group, especially for the establishment of the initial setting of the sedimentary basin and the creation of local conditions favouring the formation of a thick sediment body. General descriptions of the development of the Kalahari Group are given by JONES (1982), THOMAS (1986), and THOMAS & SHAW (1990, 1992). The Kalahari is often subdivided into three formations: the Tsumkwe Formation, the Eiseb Formation and the Omatako Formation (SACS, 1980).

The Tsumkwe Formation encompasses basal conglomerates of a reddish-brown colour, red clays and marls in the south-western and northern sub-basins as well as sands. The conglomerates are indicative of strong fluvial activity of the early endorheic system, in places angular blocks indicate mass movement induced by fault generated relief (H. KLOCK, pers. communication). Silcretes occur in the basal Kalahari, formed along paleo-perennial rivers; calcretes are likely to be of Late Tertiary to Quaternary age. The Tsumkwe Formation is well developed in the south-west (250 m), as a very fine- to medium-grained sandstone. Hydrogeologically, it has good yields, but the groundwater is of relatively poor quality. The Eiseb Formation displays alternating silcrete and calcrete probably caused by wet and dry cycles. It can be up to 250 m thick and has been further subdivided into a lower (reddish fine-grained sandstone) and an upper unit (calcareous sand, sandstone, limestone facies). The Eiseb Formation is an aquifer and sometimes contains fresh groundwater. Finally, the Omatako Formation is made up of ferricrete and ferruginous (Lat., ferrugineus, containing iron) sandstones. In the study area it does not contain groundwater except for small areas with perched aquifers and some stretches near hard-rock outcrops. The Omatako Formation is overlain by Kalahari Beds of sands and calcrete still being formed in part of the study area (Figure 2.7b). Calcrete development is generally seen as a process of soil formation (BLÜMEL, 1982). In the study area, however, some of the so-called calcretes are up to 30 m thick and correlate with zones of shallow groundwater or drainage lines. They also contain imprints of plants and freshwater fossils. Crete development in groundwater discharge zones has been suggested by JONES (1982), who distinguishes a) calcretes with freshwater fossils occurring adjacent to springs, channels or old lake beds, and b) soft, porous rock or tufa associated with rising groundwater or soil moisture. A typical deposit of pan floors and vegetated floodplains is a grey clay (Figure 2.7c). Surplus water from floods (Figure 2.7d) causes a periodic wetting/drying of the sediments. An enrichment with  $\text{Na}^+$  further reduces the hydraulic conductivity (GANSSEN, 1963).

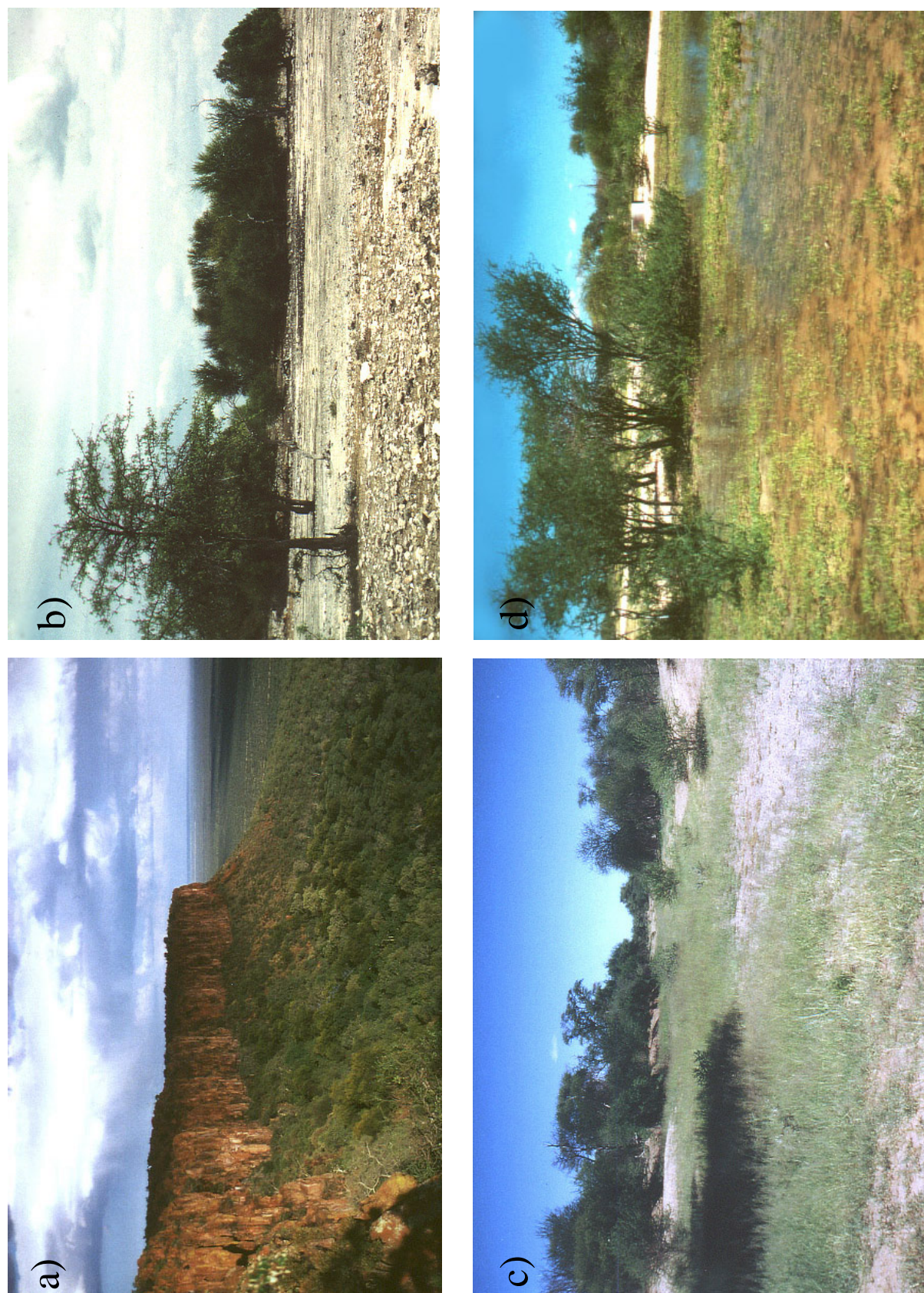


**Figure 2.7** a) View of the Kalahari from the Waterberg plateau with outcrops of Etjo sandstone, b) pan floor without soil cover approximately 5 km north-east of Goblenz, c) valley floor with heavy grey sediments in the Omatako ephemeral river and d) shallow depression (pan) filled with floodwater in the Omatako 8 weeks after the last rainstorm.



### 3 Methods for the assessment of groundwater flow systems

In this chapter methods are described that have been used for assessing the groundwater flow system of the Upper Omatako basin. The first part of this chapter focuses on the characterization of groundwater recharge mechanisms in dry regions and methods for the quantitative estimation of recharge. In the second part, hydrochemical and isotopic methods for the development of conceptual flow models are outlined, whereas in the third part a quantitative hydrochemical approach is introduced for the estimation of lateral groundwater flow. The mixing-cell approach is presented and mathematically described. A technical description of the software that has been programmed for the generation of conceptual mixing models is found in Annex A.

#### 3.1 Groundwater recharge in (semi-) arid regions

Groundwater recharge studies can be made in a more adequate way, if different types of recharge mechanisms are distinguished conceptually and if their relative importance in the climatic realm of the investigation is assessed from the beginning (BALEK, 1988; LERNER ET AL., 1990; SIMMERS ET AL., 1997).

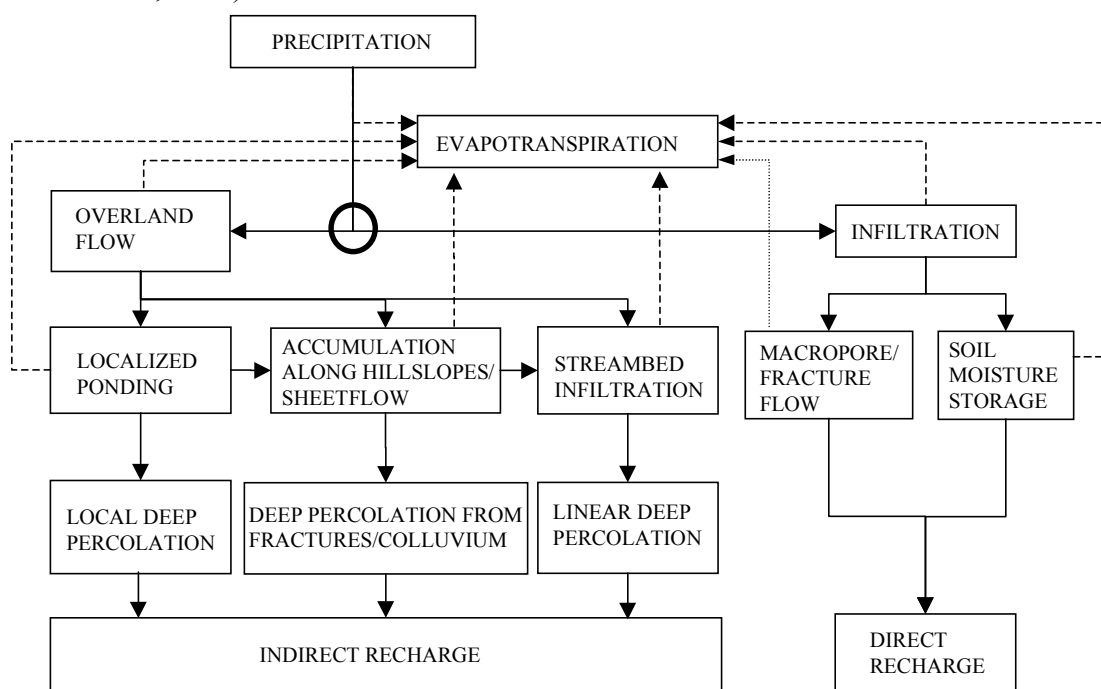


**Figure 3.1** Flow chart of hydrological processes controlling direct and indirect recharge in arid and semi-arid environments (LLOYD, 1986, modified).



A typical feature of dryland hydrology and a major bifurcation (Figure 3.1, bold circle), with respect to the regional distribution of groundwater recharge, is the sporadic development of Hortonian (HORTON, 1940) overland flow. Rainfall dynamics, antecedent moisture conditions, surface and soil properties and the type of vegetation determine the onset and extent of overland flow generation. Special features such as soil crusts, biotic films and cracks may act as additional controls on the infiltration properties of a given soil. Once overland flow has developed, its concentration (i.e. down-slope, along streams, in pans) becomes the driving factor for the spatial distribution of recharge within the river basin. Therefore, a major distinction is made between direct and indirect recharge mechanisms:

- *recharge resulting from rainfall infiltration and from the balance of vertical flow in a soil column, without participation of lateral surface runoff, is referred to as direct or local recharge.*
- *recharge that only occurs after the generation and concentration of surface runoff is termed indirect or localized recharge.*

Indirect or localized recharge is assumed to become more important with increasing aridity, because in more arid environments only localized concentration of runoff and subsequent infiltration can exceed the high thresholds for deep percolation. Therefore, understanding surface processes and the non-linear response of the unsaturated zone to rainfall events are key elements of process-oriented groundwater recharge studies in arid and semi-arid regions.

### **3.1.1 Direct recharge processes**

As long as the soil matrix is not saturated, and as long as the infiltration rate of a soil is not exceeded, all rainfall infiltrates directly. The movement of the liquid water phase in the soil depends mainly on the balance between gravity and the adsorptive and capillary forces. The development of *fingering* in homogeneous soils and the occurrence of *macropores* or *preferred flow-paths* (such as root channels, cracks) in non-homogeneous soils have been observed. These features have been found to be relevant for groundwater recharge, as they create potential bypass connections to the water table.

#### *Relevance of macropores for groundwater recharge*

Macropores provide preferential flow-paths for percolating water, thereby creating efficient shortcuts from the soil to the groundwater table. There is evidence that macropore flow is a

rather common feature and can be extremely important for groundwater recharge studies (BEVEN & GERMANN, 1982). The major processes related to macropore flow in natural soils are demonstrated in Figure 3.2. In general, direct rainfall  $p$  causing direct infiltration  $i$  is not sufficient for filling cracks or macropores. Only the onset of short-distance overland flow  $q_o$  fully activates macropore flow  $q_{mp}$ . The depth of macroporosity depends on the formation process. This can be bioturbation or shrinking of clayey material for example. In general the density or macropores decreases below the root zone. Cracks opened by neo-tectonics may represent an exception.

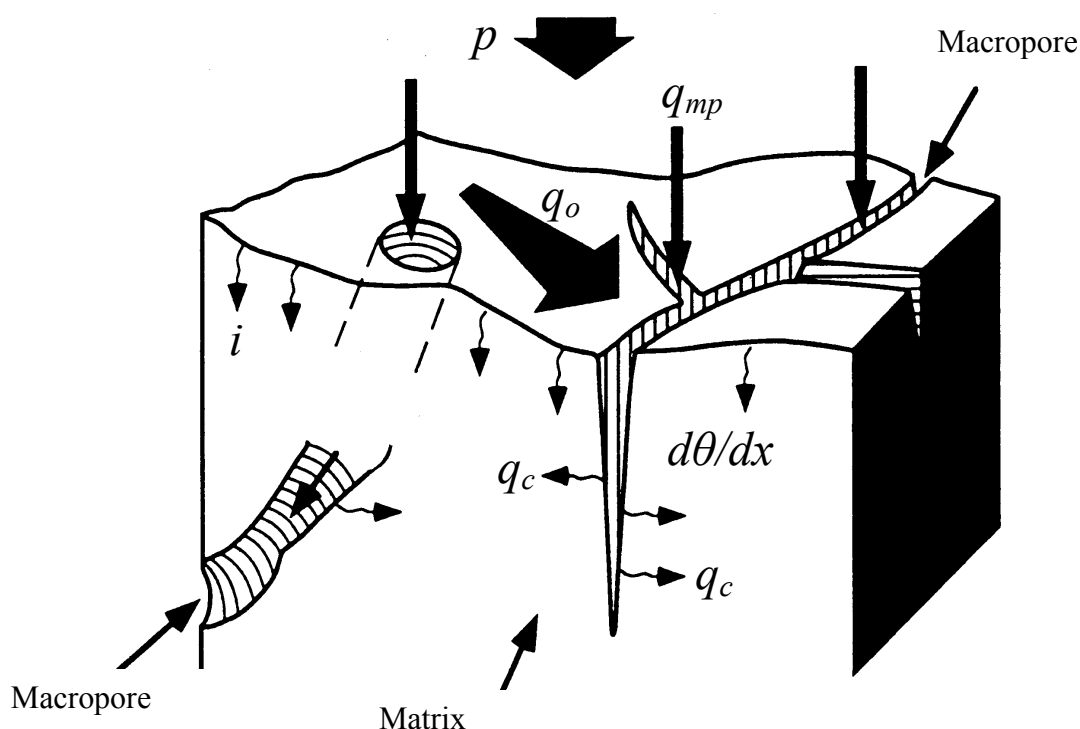


**Figure 3.2** The role of macropores in the infiltration process and its interaction with surface processes (after SIMMERS ET AL., 1997).

Because of higher vertical flow rates in large pores, in the early stages of an infiltration event the water content in the macropores exceeds the moisture content of the surrounding soil matrix. Therefore, once these pores have been activated, a moisture gradient  $d\theta/dx$  will develop between the saturated macropore and the drier soil matrix. This, in turn triggers a lateral capillary flow  $q_c$  into the drier soil matrix and attenuates the propagation of the macropore flow front.

According to the above conceptual model, macropore flow increases after the initiation of ponding, shortly before the generation of widespread surface runoff, and will continue while surface runoff is produced. Macropore flow will be reduced soon after runoff events, when the lateral supply by surface runoff becomes insufficient for supporting macropore flow.

The difference between capillary flow and macropore flow in terms of travel times is dramatic. For macropore flow capillary forces become very small, while friction along the pore-walls becomes the dominant force inhibiting gravity-driven flow. This can be described by Hagen-Poiseuille's law for flow in pipes or tubes (BEAR, 1972):

$$v_{mp} = -\frac{\rho g D^2}{32\mu} * \frac{dh}{dl} \quad (1)$$

where  $v_{mp}$  is the flow velocity for macropore flow,  $\rho$  is the fluid density,  $g$  the gravity acceleration,  $D$  is the (average) pore diameter,  $\mu$  is the fluid dynamic viscosity, and  $dh/dl$  represents the hydraulic gradient. This expression is closely related to the empirical description of groundwater flow for isotropic porous media given by DARCY (1856)  $v_{Darcy} = -K * dh/dl$ , where  $K$  is hydraulic conductivity.

Macropores in otherwise porous media offer an explanation for the discrepant theories about recharge in the Kalahari: Although the retention capacity of thick Kalahari sand retains most of the infiltrating water, fast percolation to great depths is still possible, causing the discovered traces of tritium in groundwater of the Kalahari.

#### *Recharge on fractured hard-rock surfaces*

In a very simplified way fracture flow corresponds to the physical analogue of flow between two plates. According to Poiseuille's law the flow velocity  $v_{fr}$  for laminar parallel flow between smooth walls of unit width is given by:

$$v_{fr} = -\frac{\rho g b^2}{12\mu} * \frac{dh}{dl} \quad (2)$$

where  $\rho$  is fluid density,  $g$  gravity acceleration,  $b$  average fracture aperture and  $\mu$  is fluid dynamic viscosity,  $dh/dl$  represents the hydraulic gradient. In this case the function between flow velocity and aperture is quadratic; hence, with the same potential, water flowing through a fracture of double aperture will have the four-fold flow velocity. Multiplication of flow velocity (Equation 2) with fracture aperture and width yields the flow rate. The increase of flow rate with aperture is cubic. Natural roughness of fracture surface, non-parallel flow patterns and a transition from laminar to non-laminar flow for large apertures and high gradients cause deviations from the simplified model above (UBELL, 1977; HUBER, 1992).



---

Still, fractured hard-rocks with large apertures provide good recharge conditions (MAINARDY, 1999). Recharge potential is highest at the bottom of bare slopes acting as water collectors.

### 3.1.2 Indirect recharge processes

Once the rainfall intensity has exceeded the capacity of direct infiltration mechanisms, and once surface depressions have been filled completely, widespread runoff will develop. Runoff will concentrate along slopes as ‘*sheet flow*’ or in rills, ephemeral rivers will start flowing, and indirect recharge processes will be activated.

#### *Colluvial infiltration and deep percolation at the bottom of hillslopes*

Runoff generated on hard-rock outcrops or steep slopes accumulates along hillslopes and may cause ‘*colluvial infiltration*’ at the bottom of the hillslope, where colluvium often covers the bedrock. The relevance of this process for runoff generation and recharge in the arid Negev has been studied in an experimental basin near Sde Boqer in the Negev desert, Israel. Geomorphological (YAIR & SHACHAK, 1987; YAIR, 1992), hydrological and isotopic evidence for runoff generation processes and their role in initiating indirect recharge has been collected in this experimental basin (DODY ET AL., 1995; ADAR ET AL., 1998; YAKIREVICH ET AL., 1998).

#### *Recharge through large conduits*

As a result of karstification, sinkholes may develop in carbonates, especially when they are covered by soil in which the infiltrating water becomes enriched with carbonic acid. Such a typical soil-carbonate sequence is often found in semi-arid areas as calcrete. Calcrete formation is found in the Otavi Foreland and in part of the Kalahari. With changing climatic and subsequent changes of recharge conditions, a solution of these secondary carbonates may occur.

The formation of large conduits has also been reported from sandstones in the Sahara and was termed ‘*silicate karst*’ (BUSCHE & ERBE, 1987; BUSCHE & SPONHOLZ, 1990). Karst formation in sandstones can result from the selective solution of cementing minerals and/or saprolitic weathering. As will be described in Chapter 4.2.2, sinkholes may form an important shortcut to the groundwater table and enhance recharge conditions significantly.

However, any quantitative estimation is extremely difficult to make, due to the localised and irregular nature of sinkholes and their subterranean passages. Only indirect hydrochemical or isotopic methods can be used as indicators for the location and significance of such '*large conduit recharge*'.

#### *Streambed and pan infiltration*

If also the thresholds of colluvial and large conduit infiltration are exceeded, concentration of runoff in small channels and streambeds will finally occur and produce flash floods. Since these floods run through generally dry river-beds, '*transmission losses*' along ephemeral channels will occur, forming linear recharge sources even in arid areas (ABDULRAZZAK & MOREL-SEYTOUX, 1983; BESBES ET AL. 1978). Sedimentation of fine-grained material and clogging of pores limit the effectiveness of recharge from ephemeral rivers and from pans, as demonstrated by WHEELER ET AL. (1987) and CRERAR ET AL. (1988). Still, transmission losses have been found to cause a systematic reduction of unit runoff with increasing catchment size in semi-arid areas (BOUGHTON & STONE, 1985). In terminal pans or in areas where the drainage network becomes disconnected, local concentration of runoff will take place and cause recharge from depressions.

### **3.1.3 A proposed geomorphological model of recharge mechanisms**

For this study a general conceptual model combining the above direct and indirect recharge sources has been developed (Figure 3.3). It distinguishes four macro-geomorphological environments: *hard-rock exposures* (A), *hillslopes* (B), *ephemeral rivers* (C) and *flat sediment-covered areas* (D) in the Kalahari.

This conceptual model accounts for indirect (A, B, C) and direct recharge processes (D) in flat sand-covered areas typical of the Kalahari environment. Hard-rock outcrops may enhance recharge in situ, if they are fractured or karstified (A, Figure 3.3). Fractures and karst voids enhance percolation. Although plant roots may penetrate into larger fractures the retention capacity for water is limited and water quickly percolates beyond the reach of roots.

The regional analysis presented in Chapter 4 shows that each of these process-regions has further subunits. Hard-rock outcrops, for example, may be either karstified, fractured, fractured and porous, or almost impervious (MAINARDY, 1999). Similarly, the flat Kalahari environment may be further subdivided into dune areas, small pan-catchment systems, or areas with shallow or exposed calcrete (WRABEL, 1999).

Adaptation of the conceptual model to regional conditions and its stepwise refinement will develop in the course of this study.

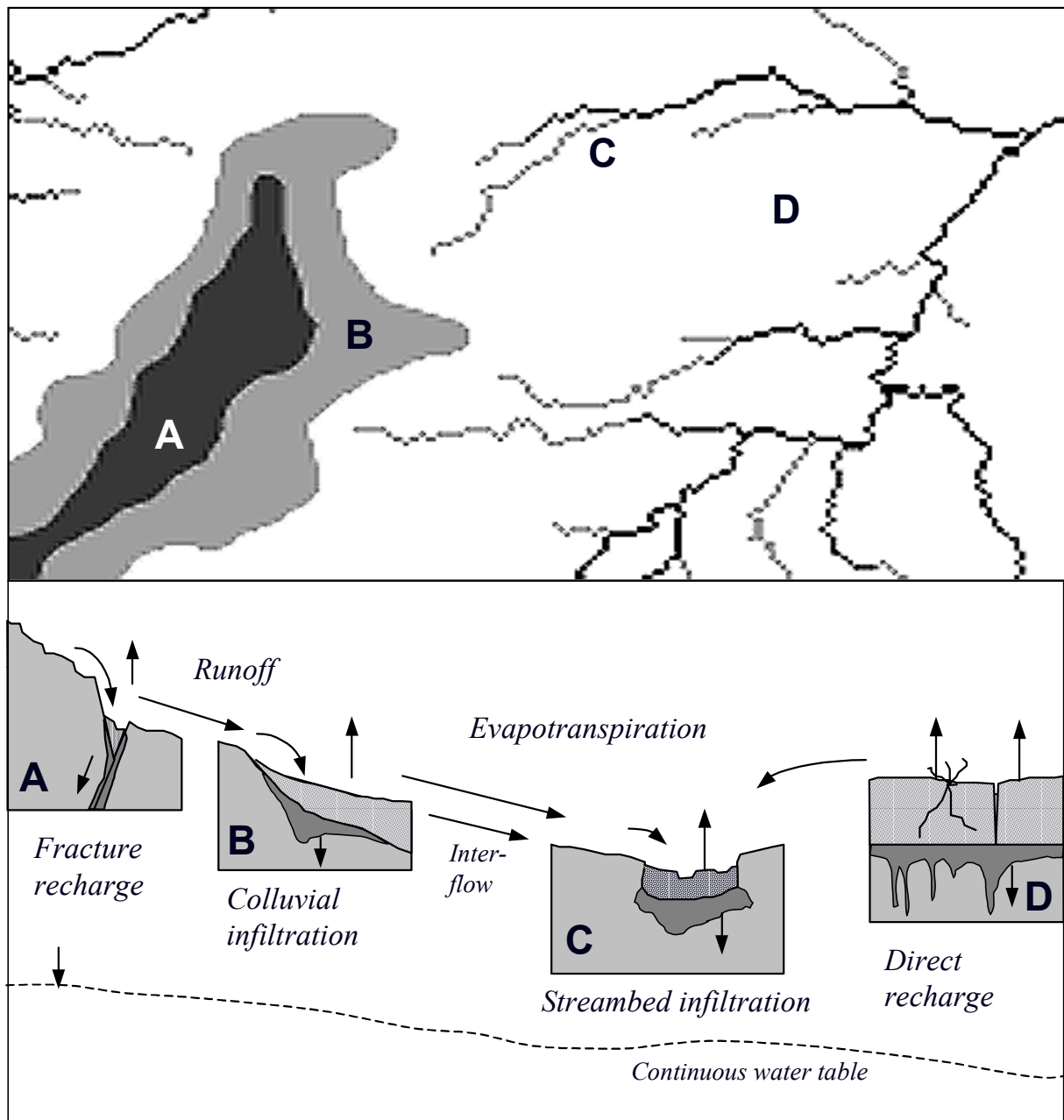


**Figure 3.3** Recharge mechanisms: A, B and C involve prior generation of runoff and a concentration in fissures (A), at the bottom of the hillslope (B) or in ephemeral rivers and pans (C). D is dominated by direct recharge. Arrows indicate flow-paths; the dotted areas represent porous media, dark grey shows the idealized moisture concentration. The influence of fingering and heterogeneity on direct recharge is demonstrated.

### 3.1.4 Quantitative groundwater recharge estimation

Approaches to quantitative groundwater recharge estimation in semi-arid and arid areas are described and discussed in several monographs (SIMMERS, 1987; LERNER ET AL. 1990; ALLISON ET AL., 1994; BREDEKAMP ET AL., 1995; SIMMERS ET AL. 1997). The relative importance of direct and indirect recharge mechanisms is a major criterion for the choice of adequate estimation methods. If direct recharge is the dominant recharge mechanism, numerical or experimental analysis of vertical moisture flow is a suitable approach. Also, water balance methods or the chloride profile method can be applied. However, if indirect recharge mechanisms are dominant, completely different approaches need to be applied. Runoff generation and distribution become important, controlling pan recharge, transmission losses and colluvial infiltration. Preferential recharge areas need to be identified regionally. In this context isotope and hydrochemical indicators as well as inverse methods become helpful tools and have been used for the delineation of favourable recharge areas in complex terrain.

#### *Water balance modelling*

The suitability of daily climatic water balances for the *quantitative* estimation of groundwater recharge in arid and semi-arid areas has been questioned (ALLISON, 1989; GEE & HILLEL, 1988; RUSHTON, 1988). However, more recently, the usefulness of detailed climatic or soil water balances as a supplementary tool for *qualitative* assessments of recharge and for studies on *recharge timing* has been acknowledged (HENDRICKX & WALKER, 1997). Still, some conditions have to be met in order to avoid misleading interpretations derived from climatic water balances:

- *Time resolution must be sufficient. Daily data or even higher temporal resolution are necessary in order to represent processes at the scale of events.*
- *Rare extreme events can be crucial for the replenishment of groundwater in dry areas. Therefore, introducing probability concepts will improve the water balance approach.*

Another difficulty (for the chloride profile method as well, see below) is that in many locations runoff processes cannot be neglected. The generation of runoff on surfaces during storm events, however, is a highly complex process and is difficult to estimate with the data usually available. Any water balance approach requires a definition of a hydrological system for which the individual components of the hydrological cycle are balanced. This may be a vertical soil column, a river reach with defined inlet, and/or a river basin. For the chosen

system, all inflows are integrated and added, net change in storage is accounted for, and all the water losses are subtracted in order to obtain groundwater recharge as the resulting term. In the present study the water balance has been applied for vertical columns only. For a vertical soil column, the discrete form of a water balance formula writes as:

$$R(t) = P(t) - ETP(t) - Q(t) \pm \Delta S \quad (3)$$

with  $R(t)$  as recharge,  $P(t)$  precipitation,  $ETP(t)$  evapotranspiration,  $Q(t)$  runoff and  $\Delta S$  change in water storage. A major problem with this approach in dry climates is that the resulting term  $R(t)$  is very small, compared to precipitation and evapotranspiration on an annual basis. However, this is not so for daily or hourly water balances.

A concept model of hydrological processes that can be used as a basis for computing daily soil water balances is shown in Figure 3.4. This concept follows the systematic description of soil water balance modelling with MODBIL (UDLUFT & ZAGANA, 1994; UDLUFT & KÜLLS, 2000; KÜLLS & UDLUFT, 2000; KÜLLS ET AL., 2000).

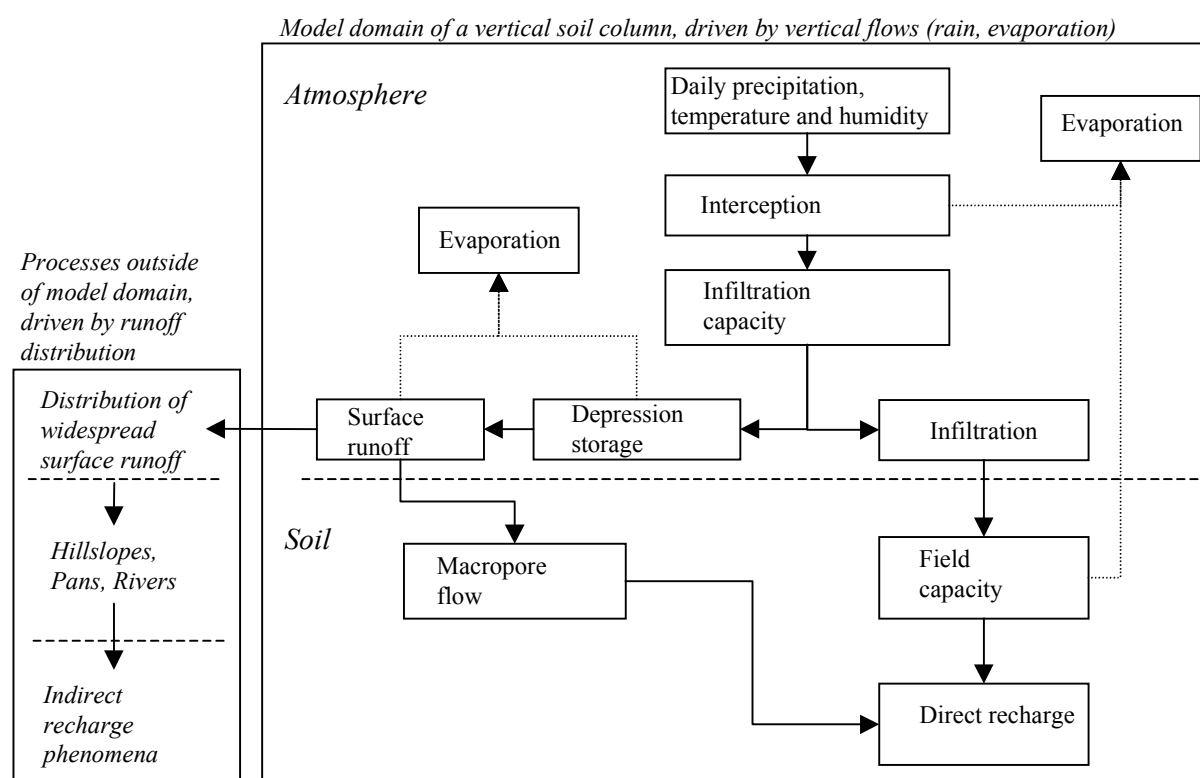


**Figure 3.4** Flow chart representing the water balance model programmed with daily input parameters (rainfall and evaporation in mm), constant parameters (interception, infiltration capacity, field capacity, macropore flow factor), and computed daily data (infiltration, surface runoff, direct recharge).

This model will be used in Chapter 4.2.3 for the computation of daily recharge. Daily rainfall, temperature and relative humidity or pan evaporation are needed as input parameters. Daily rainfall amounts are first reduced by interception on leaves. This interception storage is consumed by actual evaporation (for the calculation of evaporation, see below). Rainfall amounts per day that are larger than interception and do not exceed the infiltration capacity, will infiltrate and are stored up to maximum field capacity within the soil matrix. Runoff is produced a) if the rainfall intensity is larger than the infiltration capacity or b) if the soil moisture storage has reached the maximum value. Before the onset of widespread surface runoff, however, a fixed amount of depression storage has to be accounted for, corresponding to the filling of small surface depressions. Eventually, the activation of surface runoff will also trigger macropore flow. It is assumed that part of the surface runoff will seep through cracks and macropores at a constant rate.

Actual transpiration is deduced from actual soil moisture storage on a daily basis. The actual evapotranspiration is calculated in two steps: First, the potential evaporation is calculated with an empirical (HAUDE, 1954) or with a simplified Penman-Monteith (PRIESTLY & TAYLOR, 1972) formula. For the later method an energy term is directly derived from the latitude of the location and the date. Second, potential evaporation is transformed into actual evaporation depending on soil moisture restrictions. The drier the soil, the smaller the ratio between actual and potential evaporation will become. The soil moisture restriction is expressed by the ratio between actual saturation  $\theta$  and soil moisture at field capacity  $\theta_f$ . Both values are reduced by the amount of immobile soil moisture at the wilting point  $\theta_w$ :

$$f(\theta) = (\theta - \theta_w) / (\theta_f - \theta_w) \quad (4)$$

Recharge is produced when the soil moisture reaches field capacity. Again, the actual percolation rate depends on the soil moisture state. Hydraulic conductivity is calculated as a function of saturated hydraulic conductivity and soil wetness defined by a Van-Genuchten function (VAN GENUCHTEN, 1980).

This model reproduces direct recharge and – in a simplified way – macropore flow as well. The computed runoff leaving the modelled vertical soil column may contribute to widespread surface runoff generation, which may induce indirect recharge by pan recharge or transmission losses. The water balance model has been used to assess direct recharge, groundwater recharge timing and soil moisture dynamics (Chapter 4.2.3). The model was validated using water level fluctuations and groundwater chloride data.

### Validation with groundwater level fluctuations

Groundwater level fluctuations indicate the response of an aquifer to groundwater recharge and can be deconvoluted to recharge time series (BESBES & DE MARSILY, 1984). For a homogeneous, unconfined aquifer the proportionality factor between groundwater level changes and recharge is given by the effective porosity  $p$  of the column affected by groundwater level changes.

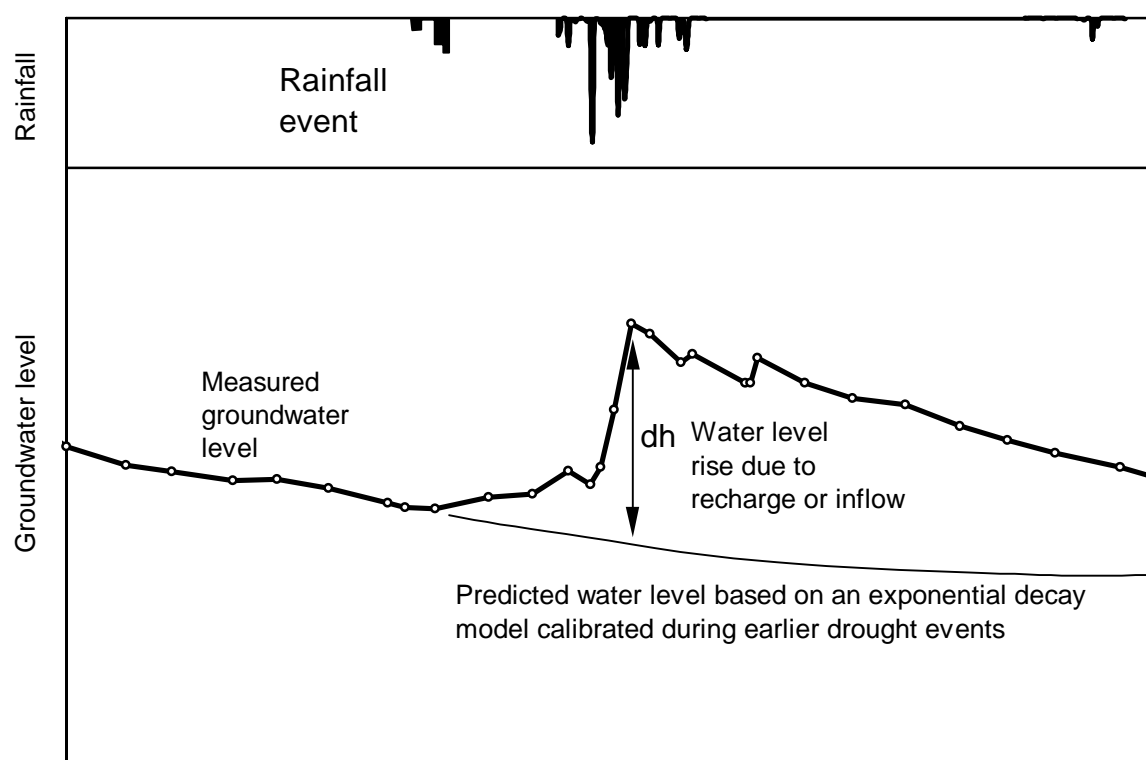


**Figure 3.5** The water level fluctuation method: during periods without recharge (dry seasons) the water level decline is modelled and a predicted water level without recharge is computed. The deviation of the observed water level from this value represents the sum of lateral subsurface inflow and of recharge by percolation.

High seasonal variability of rainfall and distinct recharge events facilitate the isolation of water level rises induced by groundwater recharge. While recharge is characterized by episodic events, natural water losses occur continuously. During periods when the rate of recharge approaches zero, water level decline reflects the net lateral groundwater flow (Figure 3.5). In general, an exponential decay function is used to fit water level declines during such periods without recharge. The application of an exponential decay model requires a base-level at which the recession asymptotically approaches zero. In hydrogeological terms, this may be the level of an outlet (spring) below which the water level will not drop. Therefore,

groundwater levels have to be rescaled to an elevation above a base-level  $h'$ . The drop in water level during no-recharge conditions depends on a decline constant  $y$  and on the time step  $\Delta t$  (UDLUFT & BLASY, 1975):

$$y = -\frac{1}{\Delta t} \ln\left(\frac{h'}{h_0'}\right) \quad \textit{prolonged dry periods} \quad (5)$$

The difference between predicted and actual groundwater levels can then be transformed into groundwater recharge, if the effective porosity is known and is constant for the full range of water level changes:

$$R = p^*(h' - h_0' \exp^{-yt}) \quad (6)$$

It is essential that there exists a linear and invariable function between changes of the groundwater level and groundwater recharge. In this study the analysis of groundwater level changes will be used for calibrating the soil water balance model (see Chapter 4.2.2).

#### *The chloride method*

Chloride is deposited as dry fallout and as a dissolved constituent of rainwater. Both components form the total deposition of chloride, written as mass per  $\text{m}^2$  per year. Most of the chloride deposited is of oceanic origin, deriving from sea spray and advective transport of aerosols. Oceanic chloride is dominant within 300 to 700 km from the coast. However, in the Kalahari, where significant deflation of dust from dry salt pans takes place, continental sources of chloride also become important. Most plants do not take up chloride in significant amounts. Therefore it is concentrated both by direct evaporation from the soil and selective uptake of water by plants. For a simple steady state approach it is assumed that the sum of wet and dry deposition of chloride at the top of a soil profile equals the total mean outflow of chloride from the root zone (ALLISON & HUGHES, 1983; ALLISON ET AL., 1985):

$$\overline{PC} + \overline{D} = \overline{RC_s} \quad (7)$$

where  $\overline{P}$  is mean annual rainfall,  $\overline{C}$  the mean chloride concentration of rainfall, and  $\overline{D}$  is dry deposition. The right hand side of the equation represents the flux of chloride out of the root zone as the product of mean annual recharge  $\overline{R}$  and chloride concentration of the soil water  $\overline{C_s}$ . The average products  $\overline{PC}$  and  $\overline{RC_s}$  can be rewritten as:



$$\begin{aligned}\overline{PC} &= \overline{P} \overline{C} + \overline{\Delta P \Delta C} \approx \overline{P} \overline{C} \\ \overline{RC_s} &= \overline{R} \overline{C_s} + \overline{\Delta R \Delta C_s} \approx \overline{R} \overline{C_s}\end{aligned}\quad (8)$$

In general, it is assumed that the covariances between annual rainfall and annual chloride deposition  $\overline{\Delta P \Delta C}$ , and between recharge and soil-water chloride concentrations  $\overline{\Delta R \Delta C_s}$ , are close to zero which simplifies the equations. Mean annual recharge can then be expressed as a function of mean annual rainfall, mean concentration of chloride in the rainfall, dry deposition, and measured chloride concentrations in the soil water:

$$\overline{R} = \frac{(\overline{P} \overline{C} + \overline{D})}{\overline{C_s}} \quad (9)$$

Under ideal steady state conditions, an increase of chloride concentrations in the soil water within the root zone and a constant chloride concentration profile beneath the root are to be expected. However, bulge-like profiles and other deviations from the theoretical shape have been observed. These may result from:

- *preferred flow paths (see macropore flow above),*
- *changes in the recharge rate due to climatic or environmental changes, or*
- *diffusion*

Only in cases where chloride concentration exceeds 8,000 g/m<sup>3</sup> diffusion will start to play a more important role.

A simplified approach is based on the chloride concentration within the saturated zone. For this approach chloride concentration in the groundwater is used as a substitute value for  $\overline{C_s}$  and the recharge rate is determined accordingly, using Equation (9). Problems will arise in cases of lateral inflow of groundwater at the sampling location, and solution of salt or mixing with deeper groundwater. This method has therefore been used for validation only. A combination of chloride concentrations in the groundwater with soil chloride profiles can be very instructive, as shown by WRABEL (1999). Macropore flow bypassing the soil matrix may dilute the signal from direct infiltration recorded in the soil chloride profile. In such cases, the comparison of chloride profiles in the unsaturated zone and in the groundwater can be used to estimate the percentage of macropore/bypass flow.

## 3.2 Developing conceptual flow models using environmental tracers

The assessment of groundwater flow systems requires information on the aquifer structure, recharge processes and groundwater flow connections in the study area. The validity of estimates will be strongly reduced by neglecting recharge processes (such as indirect recharge along ephemeral rivers) or by having incomplete conceptions of possible groundwater flow connections. In arid and semi-arid areas, where hydrological and hydrogeological data are often scarce, hydrochemical data offer a possibility to develop conceptual models as well as qualitative *and* quantitative estimates of groundwater flow as outlined in the following chapters.

### 3.2.1 Hydrochemistry

In this study hydrochemical data have been applied for:

- *regionalizing groundwater types and relating these types to a specific lithology*
- *tracing different groundwater types and deriving a hydrochemical flow model*
- *delineating recharge areas by hydrochemical indicators*

In the following, notions on equilibrium chemistry and on the hydrochemical evolution of groundwater are introduced that have been applied for this study. Equilibrium chemistry can be used to quantify thermodynamic limits for the concentration of dissolved species in a defined aqueous system. In some cases, the hydrochemical evolution of a certain groundwater type can be identified by inverse methods, yielding information on the recharge environment (lithology) and type (slow soil infiltration or quick infiltration through sinkholes).

The equilibrium concept (Figure 3.6) provides a description of the final state of thermodynamic reactions after an undefined equilibration time  $t_e$ . At any time  $t < t_e$ , reaction kinetics are still relevant for the concentration of different species in the system. The relation between the residence time of a given water volume and the rate of a solution/precipitation reaction determines whether the concentrations are still controlled kinetically (*flow velocity control*) or by equilibrium conditions (*mass balance control*). Further information on mineral-water interface kinetics can be found in HOCELLA & WHITE (1990).

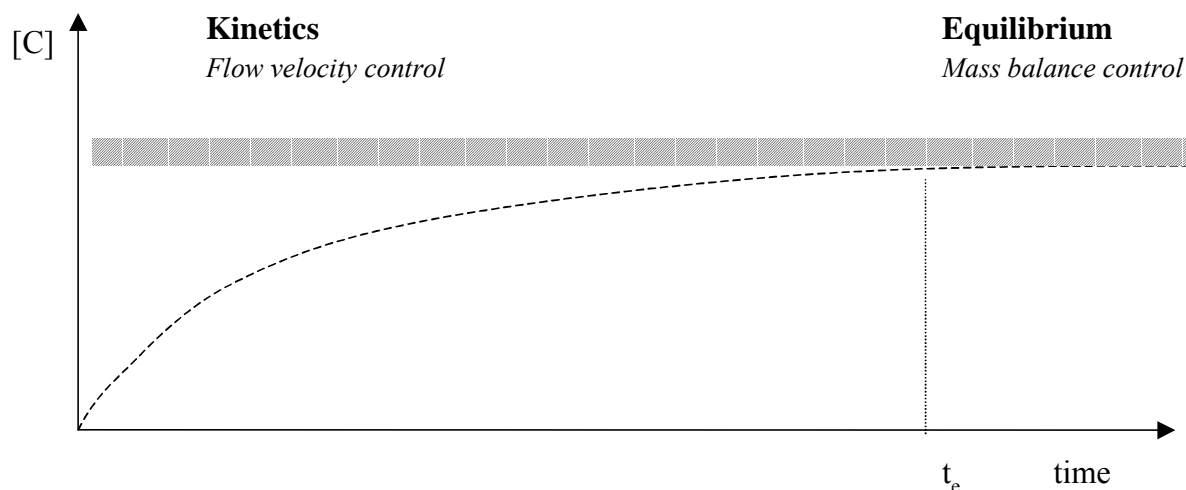


**Figure 3.6** Flow velocity and mass balance control in hydrochemical systems (after APPELO & POSTMA, 1996).

The concept of equilibrium chemistry, reviewed among others by DREVER (1988), APPELO & POSTMA (1996), is based on the chemical law of mass action. This law states that for a reaction between the reactants  $A$ ,  $B$  and the products  $C$ ,  $D$  such as  $aA + bB \leftrightarrow cC + dD$  the distribution of species converges towards an equilibrium state, characterized by the equilibrium constant  $K$

$$K = \frac{[C]^c * [D]^d}{[A]^a * [B]^b} \quad (10)$$

where  $a$ ,  $b$ ,  $c$ ,  $d$  represent the stoichiometric constants of the reaction and where the respective activities are given in brackets. Equilibrium constants can be calculated thermodynamically (STUMM & MORGAN, 1995) and are listed in libraries of computer codes for equilibrium calculations in aquatic solutions such as PHREEQE (PARKHURST ET AL., 1990).

The equilibrium constant depends on the ambient temperature. In general, thermodynamic data are given for standard conditions of 25° C; corrections are made using the Van't Hoff equation (APPELO & POSTMA, 1996: 61). In Namibia, the groundwater temperature is close to 25° C and thermodynamic constants can be used without correction.

Concentrations  $C$  of elements measured in the laboratory need to be converted to activities  $[C]$  before being introduced into mass balance calculus. This is so, because in an aquatic solution the reactivity of ions is reduced by electrostatic interactions (i.e. shielding effects) with other ions. These effects become more important with increasing salinity. Therefore, ion concentrations need to be corrected by a dimensionless activity coefficient  $\gamma$ , hence  $[C] = \gamma C$ .

The activity coefficient  $\gamma$  is a function of the ionic strength  $I$  of the solution, defined as

$$I = 0.5 \sum m_i z_i^2 \quad (11)$$

with  $m_i$  = molar concentration (mol/l) and  $z_i$  = charge of ion. In normal hydrogeological systems (no brines) with low pressures and temperatures, the *Davies* equation can be used, stating that for an ion with charge  $z_i$ , dissolved in a solution with an ionic strength  $I$ , the activity coefficient is:

$$\log \gamma_i = -A z_i^2 \left( \frac{\sqrt{I}}{1 + \sqrt{I}} - 0.3 I \right) \quad (12)$$

$A$  is a temperature factor, corresponding to  $A=0.5085$  for 25°C (typical conditions for groundwater in Namibia).

The application of the mass balance concept is exemplified in a typical carbon dioxide, hydrogenic carbon, carbonate solution cycle of rainwater infiltrating through the soil matrix and reacting in an aquifer. The same concept can be applied to other mineral phases (gypsum) and phase combinations (calcite, dolomite and gypsum) using the hydrochemical modelling software PHREEQE.

### *Solution of gaseous phases*

The content of dissolved CO<sub>2</sub> in the recharge water represents an initial and important control for the hydrochemical evolution of the groundwater. By definition, the activity of gaseous phases corresponds to their partial pressure  $p$ . Rainwater is in equilibrium with the CO<sub>2</sub> partial pressure of the atmosphere, about 10<sup>-3.5</sup> bar. During the infiltration process the rainwater is further enriched with CO<sub>2</sub>.

In the soil zone CO<sub>2</sub> partial pressure is much higher than in the atmosphere due to CO<sub>2</sub> production from decaying organic material and root respiration. The partial pressure of CO<sub>2</sub> in the soil ranges from 10<sup>-3.0</sup> to 10<sup>-1.25</sup>, depending on climatic conditions (mainly temperature) and biotic activity within the soil. A map of soil CO<sub>2</sub> giving an approximate global picture was produced by BROOK ET AL. (1983). According to this global map values of  $p\text{CO}_2 = -3.0$  in the Namib (arid conditions) and  $p\text{CO}_2 = -2.2$  and in the high rainfall areas of the Otavi Mountains are to be expected. In areas with intensive agriculture  $p\text{CO}_2$  may increase.

**Table 3.1** Equilibrium reactions and constants for dissolved CO<sub>2</sub> from STUMM & MORGAN (1995) and APPELO & POSTMA (1996).

H <sub>2</sub> O ↔ H <sup>+</sup> + OH <sup>-</sup>	K <sub>1</sub> = [H <sup>+</sup> ][OH <sup>-</sup> ]	K <sub>1</sub> = 10 <sup>-14.0</sup>	(13)
CO <sub>2(g)</sub> + H <sub>2</sub> O ↔ H <sub>2</sub> CO <sub>3</sub>	K <sub>2</sub> = [H <sub>2</sub> CO <sub>3</sub> ]/[pCO <sub>2</sub> ]	K <sub>2</sub> = 10 <sup>-1.5</sup>	(14)
H <sub>2</sub> CO <sub>3</sub> ↔ H <sup>+</sup> + HCO <sub>3</sub> <sup>-</sup>	K <sub>3</sub> = [H <sup>+</sup> ][HCO <sub>3</sub> <sup>-</sup> ]/[H <sub>2</sub> CO <sub>3</sub> ]	K <sub>3</sub> = 10 <sup>-6.3</sup>	(15)
HCO <sub>3</sub> <sup>-</sup> ↔ H <sup>+</sup> + CO <sub>3</sub> <sup>2-</sup>	K <sub>4</sub> = [H <sup>+</sup> ][CO <sub>3</sub> <sup>2-</sup> ]/[HCO <sub>3</sub> <sup>-</sup> ]	K <sub>4</sub> = 10 <sup>-10.3</sup>	(16)

Gaseous CO<sub>2</sub> reacts with water and forms carbonic acid H<sub>2</sub>CO<sub>3</sub> that dissociates in two steps according to the reactions in Table 3.1. The equilibrium constants (K<sub>1</sub>, K<sub>2</sub>, K<sub>3</sub> and K<sub>4</sub>) are valid for standard conditions of 25°C. For a pH below 10.3 and above 6.3 HCO<sub>3</sub><sup>-</sup> is the dominant species.

### *Solution of minerals*

By definition, the activity of solid phases equals 1. For the solution of a mineral of the general composition A<sub>a</sub>B<sub>b</sub> ↔ a\*A + b\*B the equilibrium constant is called the *solubility product* and writes as

$$K_s = [A]^a * [B]^b \quad (17)$$

The activities [A] and [B] correspond to an equilibrium state with the solid phase A<sub>a</sub>B<sub>b</sub>. Solubility products for common minerals in hydrogeological systems are given in several textbooks; for reference see the appendix of APPELO & POSTMA (1996). In the present study, the equilibrium concept has only been applied to reactions empirically known to be relatively *fast*, compared to groundwater residence times, such as carbonate solution/precipitation or rock salt and gypsum solution/precipitation reactions (see APPELO & POSTMA, 1996: 121-138).

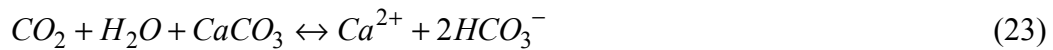
The following equilibrium constants for standard conditions (25°C) have been used for the hydrochemical evaluation in Chapter 4.3 (Table 3.2).

**Table 3.2** Equilibrium reactions and constants for mineral phases APPELO & POSTMA (1996) at 25°C.

Calcite	CaCO <sub>3</sub> ↔ Ca <sup>2+</sup> + CO <sub>3</sub> <sup>2-</sup>	K <sub>c</sub> = 10 <sup>-8.48</sup>	(18)
Magnesite	MgCO <sub>3</sub> ↔ Mg <sup>2+</sup> + CO <sub>3</sub> <sup>2-</sup>	K <sub>m</sub> = 10 <sup>-8.24</sup>	(19)
Dolomite	CaMg(CO <sub>3</sub> ) <sub>2</sub> ↔ Ca <sup>2+</sup> + Mg <sup>2+</sup> + 2CO <sub>3</sub> <sup>2-</sup>	K <sub>d</sub> = 10 <sup>-16.54</sup>	(20)
(disordered)		K <sub>dd</sub> = 10 <sup>-17.09</sup>	(21)
Gypsum	CaSO <sub>4</sub> ↔ Ca <sup>2+</sup> + SO <sub>4</sub> <sup>2-</sup>	K <sub>g</sub> = 10 <sup>-4.58</sup>	(22)

### Open system solution

In the case of calcite solution, the equilibrium concentrations for  $\text{Ca}^{2+}$  and  $\text{HCO}_3^-$  also depend on the recharge conditions. The controlling factors are the partial pressure of  $\text{CO}_2$  in the soil and calcite availability in the root-zone. If the soil is calcite-rich, *open system solution* of calcite, in equilibrium with the soil water and with  $\text{CO}_2$ , will increase  $\text{Ca}^{2+}$  and  $\text{HCO}_3^-$  towards equilibrium concentrations for the open system (STUMM & MORGAN, 1995):



Using the equilibrium constants from Table 3.1 and Table 3.2, the equilibrium concentration of  $\text{Ca}^{2+}$  can be estimated from the partial pressure of  $\text{CO}_2$  by

$$[\text{Ca}^{2+}] = \sqrt[3]{10^{-5.8} p\text{CO}_2 / 4} \quad (24)$$

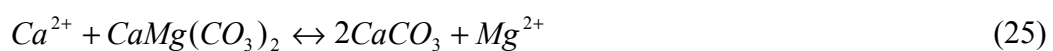
According to Equation (24), open system solution of calcite in the soil produces a  $\text{Ca}^{2+}$  concentration of about 100 mg/l for  $p\text{CO}_2 = 10^{-1.5}$ .

### Closed system solution

*Closed system solution* of calcite prevails when the  $\text{CO}_2$  concentration is fixed and no further supply of  $\text{CO}_2$  takes place during calcite solution. The initial  $\text{CO}_2$  is consumed by calcite solution, and the resulting equilibrium concentrations of  $\text{Ca}^{2+}$  and of  $\text{HCO}_3^-$  are much lower.

In the case of dolomite solution, the expected stoichiometric ratio of  $\text{Ca}^{2+}$  and  $\text{Mg}^{2+}$  is 1.0. Besides the fully crystallised dolomite, however, there also exist so-called magnesian calcites. Magnesian calcites are calcites with extensive  $\text{Mg}^{2+}$  substitution and are less stable than  $\text{CaCO}_3$ .

In the common case of groundwater being in contact both with calcite *and* dolomite, the molar ratio of  $\text{Ca}^{2+}$  and  $\text{Mg}^{2+}$  is determined by the equilibrium reaction (MORSE & MACKENZIE, 1990).



A special case is the co-existence of calcite, dolomite and gypsum causing ‘*dedolomitisation*’. The solution of gypsum releases  $\text{Ca}^{2+}$  and  $\text{SO}_4^{2-}$  according to  $\text{CaSO}_4 \leftrightarrow \text{Ca}^{2+} + \text{SO}_4^{2-}$ . The increased  $\text{Ca}^{2+}$  concentration in the solution causes calcite precipitation (see Table 3.2). Calcite precipitation reduces the  $\text{CO}_3^{2-}$  concentration. As the  $\text{CO}_3^{2-}$  concentration decreases, dolomite becomes subsaturated and can be dissolved. For a given  $\text{CO}_2$  partial pressure the combination of these reactions yields (APPELO & POSTMA, 1996):



As a result, gypsum dissolves and causes the transformation of dolomite into calcite. The groundwater in equilibrium with calcite, dolomite and gypsum has increased  $\text{Ca}^{2+}$ ,  $\text{Mg}^{2+}$  and  $\text{SO}_4^{2-}$  concentrations. The molar  $\text{Ca}^{2+}:\text{Mg}^{2+}$  ratio is about 1.3. At the same time the groundwater has a typical  $\text{Mg}^{2+}:\text{SO}_4^{2-}$  molar ratio of 0.4.

In order to describe the degree of saturation, the solubility product  $K$  of a mineral in aqueous solution is compared to the product of activities  $[A]_{\text{sample}}$  and  $[B]_{\text{sample}}$  actually found in the solution: the *ion activity product*:

$$\text{Ion activity product} = [A]_{\text{sample}}^a * [B]_{\text{sample}}^b \quad (27)$$

The ratio between the ion activity product and solubility product  $K_s$  indicates the saturation state with respect to that mineral. In general, the logarithm of the saturation state is used, called the *saturation index*

$$\text{saturation Index (SI)} = \log\left(\frac{\text{ion activity product}}{K_s}\right) \quad (28)$$

A saturation index of 0 indicates full equilibrium of a solution with respect to a certain mineral phase. Deviations from this equilibrium point to the potential direction of a reaction: Negative values suggest subsaturation or solution of this phase, positive values correspond to super-saturation or possible precipitation. However, the saturation index does not indicate whether the reaction actually takes place and at which rate the reaction proceeds.

The chemical methods described above have been applied for calculating maps of saturation indices (Chapter 4.4.1) and formed the basis for interpreting  $\text{Ca}^{2+}:\text{Mg}^{2+}$  and  $\text{Sr}^{2+}:\text{Ca}^{2+}$  cation ratios (Chapter 4.3.1 and 4.3.2).

### 3.2.2 Stable Isotopes $^{18}\text{O}$ and $^2\text{H}$

In arid and semi-arid areas stable isotopes  $^{18}\text{O}$  and  $^2\text{H}$  have become important investigative tools for hydrogeological studies (VERHAGEN ET AL., 1991). Variations in the isotopic composition of rainfall and groundwater have been mainly used in order to identify the provenance of groundwater, likely mechanisms of groundwater recharge, or recharge conditions such as altitude and degree of evaporative enrichment. In this study stable isotopes have been used for the investigation of recharge processes and recharge environments (Chapter 4.4.2).

Stable isotope ratios are expressed in relation to a common standard. For oxygen,

$$\delta^{18}\text{O}_{\text{sample}} = \frac{(^{18}\text{O}/^{16}\text{O})_{\text{sample}} - (^{18}\text{O}/^{16}\text{O})_{\text{standard}}}{(^{18}\text{O}/^{16}\text{O})_{\text{standard}}} * 1000 \text{‰ } VSMOW \quad (29)$$

The  $\delta^{18}\text{O}$  or  $\delta^2\text{H}$  values are expressed in ‰ difference from the standard *VSMOW*, which is the *Vienna Standard Mean Ocean Water*. Positive values indicate an enrichment of  $^{18}\text{O}$  or  $^2\text{H}$  compared to *VSMOW* whereas negative values signify a depletion of the heavier isotopes in the sample. *VSMOW* was prepared from distilled sea water and, according to BAERTSCHI (1976) and HAGEMAN ET AL. (1970), has the isotopic ratios of

$$\begin{aligned} \left( \frac{^{18}\text{O}}{^{16}\text{O}} \right)_{VSMOW} &= 2005.2 \pm 0.45 * 10^{-6} \\ \left( \frac{^2\text{H}}{^1\text{H}} \right)_{VSMOW} &= 155.76 \pm 0.05 * 10^{-6} \end{aligned} \quad (30)$$

In order to simply express differences between isotopic ratios, regardless of a genetic or thermodynamic link, also the isotopic difference  $\Delta_{A \leftrightarrow B}$  is used, defined as  $\Delta_{A \leftrightarrow B} = \delta_A - \delta_B$ .

#### *Isotope fractionation*

The isotopic composition changes due to fractionation processes. An introductory overview on the basics of fractionation of stable isotopes in hydrogeological systems is given by CLARK & FRITZ (1997). An in-depth physical description of fractionation based on kinetic gas theory, specifically for the stable isotopes of water, has been given by GAT & GONFIANTINI (1981).



### Equilibrium fractionation

According to a model suggested by UREY (1947), equilibrium fractionation arises from the exchange of isotopes between different phases (i.e., water and vapour) or chemical species at equilibrium conditions. For a specific reaction at full equilibrium, the degree of fractionation is expressed by a fractionation factor  $\alpha$ :

$$\alpha_{\text{water} \leftrightarrow \text{vapour}} = \frac{\left( \frac{^{18}\text{O}/^{16}\text{O}}{\text{water}} \right)}{\left( \frac{^{18}\text{O}/^{16}\text{O}}{\text{vapour}} \right)} \text{ or in general terms } \alpha_{A \leftrightarrow B} = \frac{R_A}{R_B} \quad (31)$$

where  $R_A$  and  $R_B$  represent the isotopic ratios of the two phases  $A$  (*water*) and  $B$  (*vapour*). In ‰ notation also the enrichment factor  $\epsilon_{A \leftrightarrow B}$  is used. The enrichment factor is defined as:

$$\epsilon_{A \leftrightarrow B} = \left( \frac{R_A}{R_B} - 1 \right) * 1000 \text{‰} \quad (32)$$

The approximate relation between the enrichment factor  $\epsilon_{A \leftrightarrow B}$  and the fractionation factor  $\alpha_{A \leftrightarrow B}$  in the form  $\epsilon_{A \leftrightarrow B} \approx 10^3 \ln \alpha_{A \leftrightarrow B}$  only holds for small enrichment factors, because of the approximation  $\ln \alpha \approx 1 - \alpha$  when  $\alpha \approx 1$ .

For the stable isotopes of water, ice  $\leftrightarrow$  water  $\leftrightarrow$  vapour phase transitions are of special importance. Fractionation between different phases of water results from differences in the physical properties of water molecules containing different isotopic species of oxygen and hydrogen. As an example, the water vapour pressures of the species  $^1\text{H}_2^{16}\text{O}$  and  $^1\text{H}_2^{18}\text{O}$  differ by about 1 ‰ at 20° C (SZAPIRO & STECKEL, 1967). This difference in physical properties causes a higher diffusion of  $^1\text{H}_2^{16}\text{O}$  into the ambient air as compared to  $^1\text{H}_2^{18}\text{O}$  during the evaporation process. Hence, there results a depletion of the heavier molecules of  $^1\text{H}_2^{18}\text{O}$  in the gaseous phase.

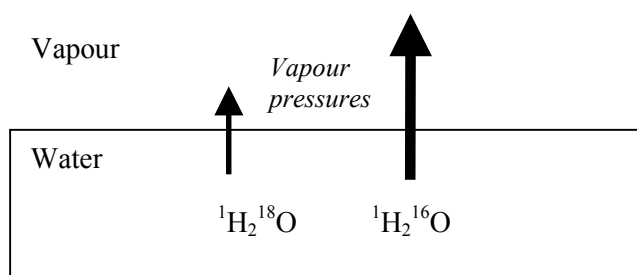


**Figure 3.7** Differences in the vapour pressure for the two isotope species  $^1\text{H}_2^{18}\text{O}$  and  $^1\text{H}_2^{16}\text{O}$  during equilibrium exchange with water vapour.

For  $^{18}\text{O}$  a fractionation factor of  $\alpha^{18}\text{O}_{\text{water}\leftrightarrow\text{vapour}} = 1.0093$  was measured for equilibrium phase transitions between water and vapour at  $25^\circ\text{C}$ . The fractionation factor for  $^2\text{H}$  during the same equilibrium phase transition is as high as  $\alpha^2\text{H}_{\text{water}\leftrightarrow\text{vapour}} = 1.076$  (MAJOUBE, 1971). Isotope equilibrium fractionation is also a function of temperature. SZAPIRO & STECKEL (1967) and MAJOUBE (1971) found that the fractionation factor  $\alpha_{A\leftrightarrow B}$  generally follows an equation of the type  $\ln\alpha_{A\leftrightarrow B} = a/T^2 + b/T + c$ . Tabulated values for a, b and c for the most common thermodynamic reactions in hydrogeological systems are given in CLARK & FRITZ (1997). For water  $\leftrightarrow$  vapour equilibrium exchange, the fractionation is higher at low than at high temperatures.

### Non-equilibrium fractionation

Often, the assumption of isotopic equilibrium is not met and so-called kinetic fractionation processes take place. This may be caused by temperature changes and the removal or addition of the product or reactant. Major non-equilibrium processes in hydrological systems are ‘diffusive fractionation’ and ‘Rayleigh distillation’.

Diffusive fractionation is the fractionation of isotopes caused by diffusion processes. In hydrological systems diffusive fractionation occurs, for example, during the evaporation process when water vapour diffuses into air. The fractionation factor for diffusion of water vapour into dry air can be derived directly from the molecular masses of water and air molecules (for a mean composition of the air) as  $\alpha_{\text{water-vapour}} = 1.0323$ . For the more common case of diffusion of water vapour into air with a relative humidity  $h$  GONFIANTINI (1986) empirically found that fractionation decreases with increasing humidity:

$$\begin{aligned}\Delta\varepsilon_{^{18}\text{O}} &= 14.2 * (1 - h) \text{‰} \\ \Delta\varepsilon_{^2\text{H}} &= 12.5 * (1 - h) \text{‰}\end{aligned}\tag{33a,b}$$

Another important kinetic fractionation process is the Rayleigh distillation. It can be used to describe systems where the reactant is continuously being removed by, for example, rain-out from clouds or evaporation. The distillation equation states that the isotopic ratio  $R$  is a function of the initial ratio  $R_o$ , the fraction of water remaining in the reservoir  $f$ , and the fractionation factor  $\alpha$ .

$$R = R_o f^{(\alpha-1)}\tag{34}$$

For Rayleigh distillation processes, the fractionation strongly increases when the residual water fraction approaches small values.

---

### *The isotopic composition of rainfall*

A review of time series from a global survey of stable isotopes in rainfall (ROZANSKI ET AL, 1993) reveals patterns in their seasonal and geographic distribution. These patterns are the result of the fractionation processes described above that take place in the hydrologic cycle. The so-called ‘*isotope effects*’ are the basis for the interpretation of isotope data in hydrogeological studies.

CRAIG (1961) found that, at a global scale,  $\delta^{18}\text{O}$  and  $\delta^2\text{H}$  in surface waters are characterized by the correlation  $\delta^2\text{H} = 8\delta^{18}\text{O} + 10\text{‰}$  (this equation was established for the SMOW reference, Standard Mean Ocean Water). The equation defines the *global meteoric water line*. At a regional scale deviations from this global correlation exist, and specific regional meteoric water lines have been introduced, for example for the Mediterranean. Meanwhile, a slightly modified relationship based on the data of the IAEA global network of isotopes in precipitation (GNIP) has been proposed by ROZANSKI ET AL. (1993). This revised regression has a slope of  $8.17(\pm 0.07)$  and an intercept of  $11.27(\pm 0.65)\text{‰}$ . It takes into account rainfall data from the IAEA only and is based on the *VSMOW* standard.

For large continents, precipitation becomes more depleted with increasing distance from the coast. Since the vapour is mainly derived from the oceans, water in clouds will become depleted in heavier isotopes with each rainfall event along the trajectory. This phenomenon is termed continental effect. Continental effects are rather relevant for characterizing the general isotopic composition in Namibia. Therefore it will not be discussed in detail. Temperature, altitude and seasonal effects can be used for the interpretation of stable isotope data in the study area.

#### Temperature effect

As mentioned before in the discussion of fractionation processes, fractionation factors depend on temperature. During water  $\leftrightarrow$  vapour phase transitions fractionation is more efficient at low temperatures. The isotopic composition of rainfall in cold environments is more depleted compared to warm environments.

#### Seasonal effect

Often a seasonal fluctuation of the stable isotope ratios is observed as a result of temperature effects, different trajectories of air masses, and varying fractionation processes in the source area of atmospheric moisture.

### Altitude effect

Often values of precipitation more depleted than normal are observed at higher altitudes. This is the combined result of temperature effects and repeated rain-out. Equilibrium fractionation increases with lower temperatures, making fractionation more efficient at higher altitudes. Repeated rain-out during uplift of air masses causes a Rayleigh-type distillation process.

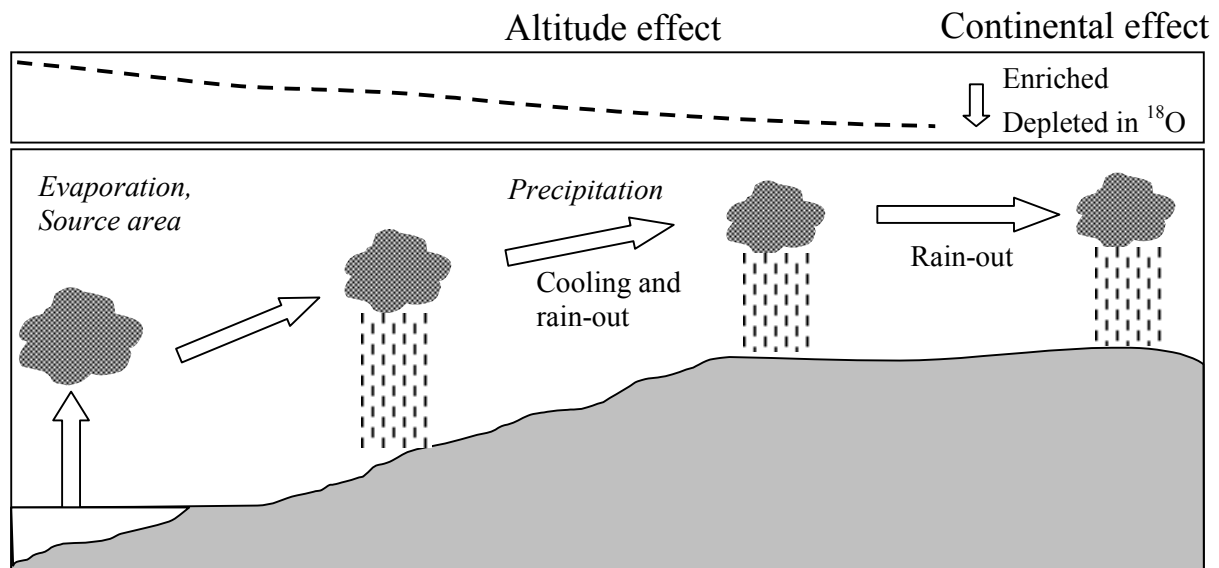


**Figure 3.8** Altitude and continental effects and their impact on the  $^{18}\text{O}/^{16}\text{O}$  ratio in precipitation.

Detailed sequential sampling of rainstorms in the arid Negev Desert, Israel, revealed strong isotopic variations ( $-2\text{‰}$  to  $-9\text{‰}$   $\delta^{18}\text{O}$ ) between different rain spells within hours. Interestingly, a rain spell with low intensity but long duration was more depleted than preceding and following short, intensive spells (DODY ET AL., 1995; ADAR ET AL. 1998). Selective runoff generation and recharge from these spells may bias the isotopic composition of runoff and groundwater.

### *The isotopic composition of groundwater*

The isotopic input of precipitation is modified by fractionation processes during recharge. An excellent review of the isotope effects in the transition from rainfall to groundwater for semi-arid and arid zones was prepared by GAT (1995). In this chapter an overview of evaporation, attenuation of seasonal variations, biases in the average isotopic composition and of mixing is given. The influence of water-rock interactions on the stable isotopes  $^{18}\text{O}$  and  $^2\text{H}$  is only detectable in systems with specific conditions (hydrothermal springs, volcanic volatiles) and will not be dealt with. An introduction is given by HOEFS (1996).

### Evaporation

In semi-arid regions with summer rainfall evaporation may produce isotopic enrichment by two different processes. Evaporation can remove moisture from a soil column by diffusion. Diffusive evaporation from a soil column results in a low-slope evaporation line in a  $\delta^{18}\text{O}$ - $\delta^2\text{H}$  diagram (DINÇER ET AL., 1974; ALLISON ET AL., 1985; GAT, 1995). Evaporation can also take place from surface runoff and from water ponded in small depressions or pans. Evaporation from surface water causes an enrichment in the remaining water with slope 4 to 5 in a  $\delta^{18}\text{O}$ - $\delta^2\text{H}$  diagram. The slope depends on the conditions during evaporation (GONFIANTINI, 1986). It becomes smaller with decreasing relative humidity. Indirect recharge from enriched surface water then carries the isotopic signal to the groundwater. The impact of evaporation on the isotopic composition of runoff in arid area has been demonstrated by DODY ET AL. (1995: 417).

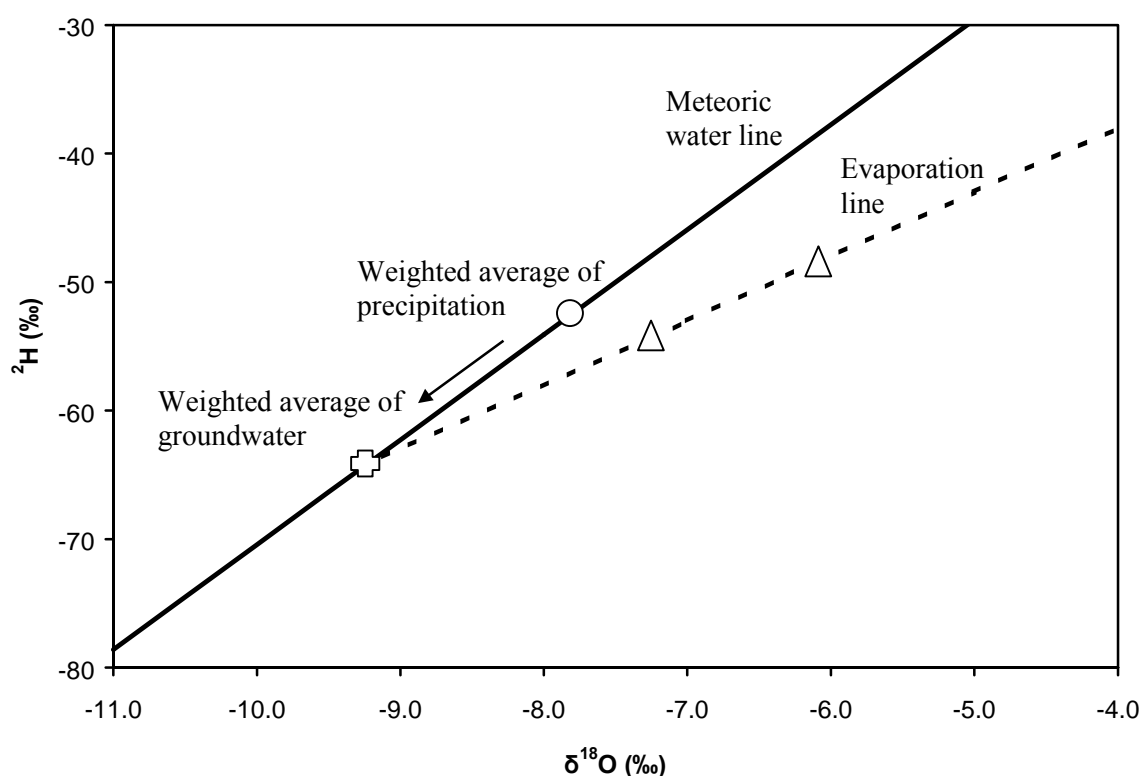


**Figure 3.9** Elements for the interpretation of stable isotope data: the meteoric water line (continuous line), the evaporation line (dashed) along which evaporated samples plot (triangles), the weighted averages in the isotopic composition of precipitation (circle) and of groundwater (cross). The arrow between both averages represents the bias.

### Bias

The weighted averages of the isotopic composition of precipitation and groundwater may differ and be biased. This happens if selective recharge occurs from precipitation events with a specific isotopic composition. Recharge from flash floods has been observed to cause an isotopic depletion of the groundwater, as compared to precipitation under arid conditions in general. This finding has been interpreted to result from selective activation of runoff and

subsequent recharge by very intensive and exceptionally depleted precipitation (LEVIN ET AL., 1980). The effect of a bias between the average composition of precipitation and groundwater samples as well as of evaporation is shown in Figure 3.9. On a secular time scale, a bias between the *actual* average isotopic composition of rainfall and groundwater may indicate that the groundwater was recharged during a period with a different isotopic signal in the precipitation.

### Attenuation

In the unsaturated zone an attenuation of seasonal variations of the isotopic composition of precipitation will take place. This is a result of hydrodynamic dispersion within the soil, where the infiltrating water travels at different velocities through pores with a range of different sizes, and in some cases also through cracks, fissures or macropores. In fine-grained soils the depth at which the seasonal signals is damped out tends to be less than in coarse soils. In fractured or karstified rock, attenuation is expected to be slow and depth of full attenuation relatively large. The depth at which the isotopic signal becomes stable was found to reach 3 to 5 m in fine-grained soils (ZIMMERMANN ET AL., 1967) and up to 9 m in gravel (EICHINGER ET AL., 1984). If the percolating water reaches the water table before the seasonal signal has been attenuated, these fluctuations will also be found in the groundwater. Depth of attenuation is relevant, as it determines whether seasonal fluctuations in the groundwater of the recharge area are to be expected. If seasonal fluctuations are damped out completely, samples can be taken to be representative for the location; otherwise time series sampling needs to be carried out.

### Mixing

The isotopic composition also changes by mixing processes of groundwater types with different isotopic signals. For two-component mixing, the concentration of the mixed component  $C_n$  is given by:

$$C_1 a_1 + C_2 a_2 = C_n \quad (35)$$

where  $a_1$  and  $a_2$  are the fractions of groundwater flow of the components  $C_1$  and  $C_2$  respectively. Because of the mass balance both fractions must give 1, and  $a_2$  can be expressed and replaced by  $1-a_1$ . By substitution both fractions can be calculated:

$$a_1 = \frac{C_n + C_2}{C_1 - C_2} \quad (36)$$

$$a_2 = 1 - a_1$$

Based on the stable isotopes  $^{18}\text{O}$  or  $^2\text{H}$ , mixing can be calculated for two components at most. Of course, this is only possible if the signals  $C_1$  and  $C_2$  are clearly different. In addition,

mixing calculations are only meaningful as long as the tracer is conservative, i.e. as long as no additional fractionation occurs. The mixing approach for several environmental tracers will be introduced in Chapter 3.3.

### 3.2.3 Tritium

The radioactive isotope of hydrogen,  $^3\text{H}$  (tritium), has a half life of 12.43 years. It decays to  $^3\text{He}$  by  $\beta^-$  emission. Tritium levels are given as absolute concentrations in tritium units (TU). One tritium unit is defined as one  $^3\text{H}$  atom per  $10^{18}$  atoms of hydrogen, causing a radioactivity of 0.118 Bq per kg of water.

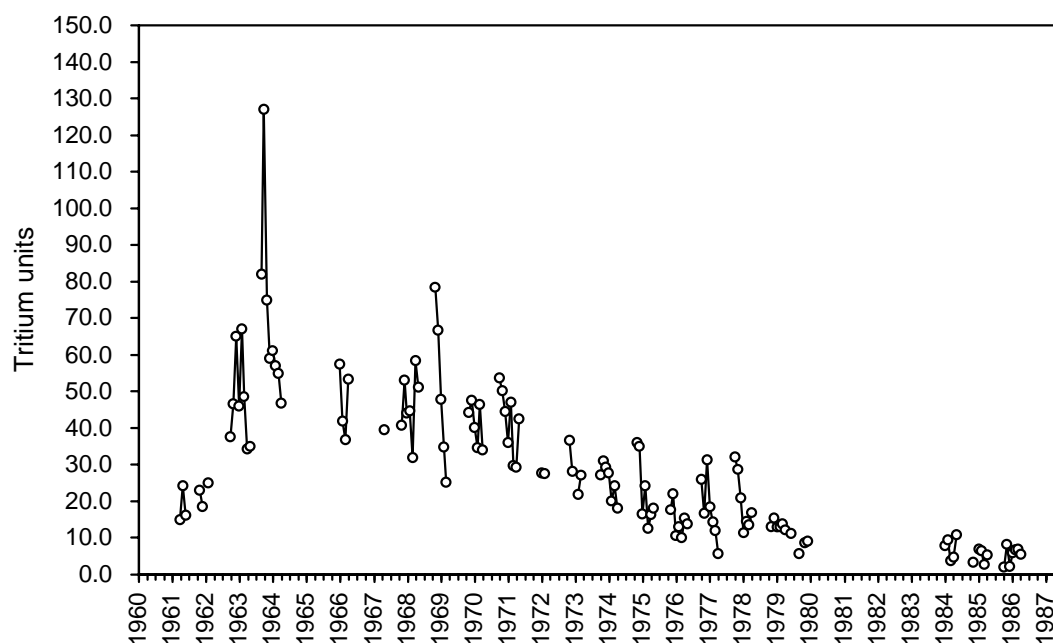


**Figure 3.10** The input function of  $^3\text{H}$  at Windhoek. Data from IAEA, GNIP.

Tritium is measured by liquid scintillation counting of  $\beta^-$  decays. Tritium is produced naturally in the upper atmosphere from nitrogen by neutron impacts of cosmic radiation. It enters the water cycle by precipitation, with a seasonal and spatial variation in tritium fallout. Natural fallout is higher in higher geomagnetic latitudes. For northern mid-latitudes a natural level between 3.4 and 6.6 TU has been reconstructed from wines (KAUFMANN & LIBBY, 1954). Thermonuclear bomb tests, starting in 1951, have overdriven this natural level for several decades (Figure 3.10). Tritium levels in rainfall have exceeded the naturally occurring levels in the environment by several orders of magnitude. However, the impact of  $^3\text{H}$  fallout has been less pronounced in the southern hemisphere as compared to the northern hemisphere due to an asymmetric distribution of tritium emissions from bomb tests and an air mass circulation barrier along the equator. Due to low input levels of tritium in the southern hemisphere, natural attenuation by decay, and mixing

with pre-bomb groundwater tritium levels will only be used for qualitative interpretation in this study. In the study area, tritium levels above ~0.5 TU for enriched samples are interpreted as indicating some mixture with recent recharge.

### 3.2.4 $^{14}\text{C}$ -dating

Radiocarbon is produced in the upper atmosphere through cosmic radiation. Collision of a neutron with nitrogen produces  $^{14}\text{C}$  and a proton.  $^{14}\text{C}$  enters the troposphere as  $\text{CO}_2$  and participates in the hydrologic and biologic carbon cycles. It is radioactive and decays according to:

$$a_t = c * a_0 * e^{-\lambda * t} \quad \Rightarrow \quad t = -\frac{1}{\lambda} * \ln\left(\frac{a_t}{c * a_0}\right) \quad (37)$$

where  $\lambda = 1.2097\text{e-}4$  is the decay constant,  $c$  is a dilution factor (see Equation 38),  $a_t$  the  $^{14}\text{C}$  activity at time  $t$ , and  $a_0$  the initial  $^{14}\text{C}$  activity (GEYH & SCHLEICHER, 1990). The half-life of  $^{14}\text{C}$  is 5730 years. Activities are expressed as percent of the standard ‘*modern carbon*’ abbreviated as ‘*pmC*’. The standard is defined as 95 % of the  $^{14}\text{C}$  activity in 1950 of a NBS oxalic acid standard. It corresponds to the activity of wood grown in 1890 before the combustion of fossil carbon. The actual  $^{14}\text{C}$  in the sample is measured by scintillation counting or with accelerator mass spectrometry. In some hydrogeological systems where groundwater is isolated from input of modern carbon sources containing  $^{14}\text{C}$ , radioactive decay of  $^{14}\text{C}$  in dissolved inorganic and organic carbon compounds may be used for dating. Time  $t$  since groundwater became isolated from the atmosphere and the soil can be derived from the ratio of actual and initial activities  $a_0$  and  $a_t$  according to Equation (37).

Some difficulties arise as for the estimation of the initial activity  $a_0$ . The activity in a living plants is about 100 % pmC. However, the production of  $^{14}\text{C}$  in the upper atmosphere fluctuates with time. Calibration with oak tree dendrochronology (STUIVER & KRA, 1986; STUIVER & REIMER, 1993) and corals (BARD et al., 1990) showed that initial  $^{14}\text{C}$  activity varied by about 10 % during the Holocene. In addition anthropogenic effects have altered the natural regime. Combustion of fossil fuel has diluted the atmosphere with  $^{14}\text{C}$ -free  $\text{CO}_2$ . Nuclear weapons testing and power plants have released artificial  $^{14}\text{C}$  into the atmosphere.

An additional ‘*reservoir effect*’ needs to be taken into account for the application of  $^{14}\text{C}$  to groundwater systems (GEYH, 1995). Soil water equilibrates with soil  $\text{CO}_2$  during infiltration.



$\text{HCO}_3^-$  concentrations increase and solution of available primary or secondary carbonates ensues (MÜNNICH, 1968). The solution of  $^{14}\text{C}$ -free carbon reduces the initial activity of carbon compounds in deep percolation. Several correction methods have been proposed. VOGEL (1970) derived initial activities using statistical analysis of measured activities in the recharge area. For different recharge environments the following average factors were suggested:

0.65-0.75	for karst systems
0.75-0.90	for sediment with fine grained carbonate
0.90-1.00	for crystalline rocks

The  $^{13}\text{C}/^{12}\text{C}$  ratio has been proposed as a parameter for correcting  $^{14}\text{C}$  initial activities (PEARSON, 1965). Ratios of the stable carbon isotopes  $^{13}\text{C}$  and  $^{12}\text{C}$  are compared to the VPDB standard (Vienna Pee Dee Belemnite) and given in  $\delta$ -notation. The correction method takes advantage of the large difference between  $\delta^{13}\text{C}$  values of soil  $\text{CO}_2$  and of marine limestone.  $\text{C}_3$  plants reach  $\sim 23$  ‰ VPDB,  $\text{C}_4$  plant values range from  $\sim -10$  to  $-16$  ‰ (VOGEL, 1993). Marine limestone is often close to zero. The correction is calculated with Equation (38):

$$c_{\text{Carbon-13}} = \frac{\delta^{13}\text{C}_{\text{DIC}} - \delta^{13}\text{C}_{\text{carbonate}}}{\delta^{13}\text{C}_{\text{soil}} - \delta^{13}\text{C}_{\text{carbonate}}} \quad (38)$$

where  $c_{\text{Carbon-13}}$  is the dilution factor,  $\delta^{13}\text{C}_{\text{DIC}}$  is the measured value in the dissolved inorganic carbon of groundwater,  $\delta^{13}\text{C}_{\text{carbonate}}$  that of the carbonate being dissolved, and  $\delta^{13}\text{C}_{\text{soil}}$  stands for the  $\delta^{13}\text{C}$  value of the soil. Equation (38) holds only for closed system dissolution.

Chemical mass balance correction (CMB) is based on the ratio  $c_{\text{CMB}}$  between  $^{14}\text{C}$ -active dissolved inorganic carbon ( $m\text{DIC}_{\text{recharge}}$ ) from soil  $\text{CO}_2$  and the total carbonate content at the time of sampling ( $m\text{DIC}_{\text{final}}$ ). Different means of estimating  $m\text{DIC}_{\text{recharge}}$  and  $m\text{DIC}_{\text{final}}$  exist. The initial carbonate content during recharge can be estimated by assuming pH and  $\text{pCO}_2$  and calculating the equilibrium concentrations of different carbonate species with the equations (13) to (16) in Table 3.1 above. The final carbonate content can either be measured (titrated) or calculated from chemical data as listed in Equation (39).

$$c_{\text{CMB}} = \frac{m\text{DIC}_{\text{recharge}}}{m\text{DIC}_{\text{final}}} \quad \text{with} \quad (39)$$

$$m\text{DIC}_{\text{final}} = m\text{DIC}_{\text{recharge}} + m\text{Ca}^{2+} + m\text{Mg}^{2+} - m\text{SO}_4^{2-} + \frac{1}{2}(m\text{Na}^+ + m\text{K}^+ - m\text{Cl}^-)$$

Finally the general hydrochemical correction by FONTES & GARNIER (1979) is only mentioned. This model combines measured  $\delta^{13}\text{C}$  and major ion concentrations and also accounts for open system dissolution. This approach has not been used due to uncertain estimates of the strongly pH dependent enrichment factor  $\varepsilon^{13}\text{C}_{\text{CO}_2 \leftrightarrow \text{CaCO}_3}$  that is required for this model.

### 3.3 Inverse modelling of groundwater flow using environmental tracers

In dry regions, where direct recharge is small, the estimation of lateral subsurface flow can become a crucial element for the assessment of groundwater resources. Environmental tracers may provide information on lateral inflow of groundwater to an aquifer. In this chapter the mixing-cell approach is outlined, which represents a method for the inverse calculation of groundwater flow from hydrochemical and isotopic data. This approach is an extension of the mixing with two end members described above (Equation 35 and 36). It makes use of the mathematical theory and techniques for optimizing systems of linear equations serving as chemical mass balance constraints.

The hydrogeological flow system is first conceptualized and then translated into a mathematical expression: a set of linear equations. In general, real hydrogeological systems tend to have 'fuzzy' parameters, and measured data are prone to errors. Therefore, optimization methods need to be applied for solving the systems of linear equations describing the flow model structure.

#### 3.3.1 Hydrochemical discretization

It is assumed that the hydrogeological system modelled with a mixing-cell approach can be subdivided into discrete and homogeneous or well-mixed *compartments*. Discrete state compartment models were introduced for the interpretation of  $^{14}\text{C}$  decay ages in terms of residence times (SIMPSON & DUCKSTEIN, 1976; CAMPANA & SIMPSON, 1984). In such models the distribution of environmental tracers is discretized, each compartment having a set of *homogeneous internal properties*. In the case of a hydrogeological system this set of internal properties is represented by a typical hydrochemical (i.e.  $\text{Ca}^{2+}$ ,  $\text{Mg}^{2+}$ ,  $\text{Na}^+$ ,  $\text{K}^+$ ,  $\text{HCO}_3^-$ ,  $\text{SO}_4^{2-}$ ,  $\text{Cl}^-$ ) or isotopic composition. A compartment can be, but is not necessarily, the whole aquifer or a geological water-bearing unit as long as the chemical and isotopic parameters are relatively constant all over the unit.

---

The mixing-cell approach as used in this study is based on conservative tracers. It is assumed that the internal properties of each compartment are not affected by chemical reactions, decay or growth at the spatial and temporal scale of discretization. It is further assumed that each internal property (or chemical composition) has been completely homogenised or mixed, in general by hydrodynamic dispersion.

As suggested by ROSENTHAL ET AL. (1990) and ADAR ET AL. (1992) compartments or cells within the aquifer can be defined by cluster analysis. Cluster analysis is an inductive statistical method by which a number of elements are aggregated into groups of similar properties so as to minimize variance within and maximize distance between groups. It requires a definition of similarity or proximity between elements for defined parameters and an objective aggregation method. Squared euclidian distances have been used as a measure of distance. The individual elements are then aggregated by a criterion of homogeneity within the groups, or by a measure of heterogeneity between them. A common method employed in this study is the Ward method (reference in BROWN, 1998 and BAHRENBERG ET AL., 1992).

### **3.3.2 Flow model development**

The fundamental assumption on which the mixing-cell approach is based, is that internal properties of a given compartment can be expressed as a linear combination of the internal properties of other compartments. In terms of a hydrogeological system this means that water chemistry of a certain homogeneous groundwater region is basically a mixture of a number of inflows from other groundwater regions. In some cases the relative contribution from different inflows can be calculated by inverse methods. This approach was used for identifying and quantifying diffuse groundwater inflow to a river reach of the Amper, Germany, based on major ion hydrochemistry (UDLUFT & SALAMEH, 1976). WOOLHISER ET AL. (1982, 1985) used major ion chemistry in order to quantify inflows into a river reach. They developed a general mathematical description for one cell with  $n$  sources based on mass balance equations for major elements and water. They also introduced optimization techniques for minimizing mass balance errors and thereby solving for the inflow amounts.

#### *Terminology*

Here, it is useful to introduce a distinction used for different types of compartments. A *source* term is any flow component contributing water and mass of dissolved constituents to any cell within the modelled aquifer. A source is used to represent external inputs into the flow system (for example: sources of groundwater recharge or any genuine contribution from outside the

modelled aquifer). It is considered to be a potential end member with a constant chemical and isotopic composition. A source can also be used to simplify part of the modelled system, so that a complex subsystem can be introduced as a source of inflow into the modelled area.

The modelled aquifer is discretized into homogeneous compartments, within which all the parameters considered, such as hydraulic head, isotopic composition and ionic concentration, are assumed to be constant. Mixing and dilution of contributors such as upstream compartments and external sources control the characteristic chemicals and isotopic composition of each compartment. Each well-mixed or homogeneous aquifer section (or compartment) characterized by a unique representative chemical and/or isotopic composition and receiving input fluxes is referred to as a *cell*.

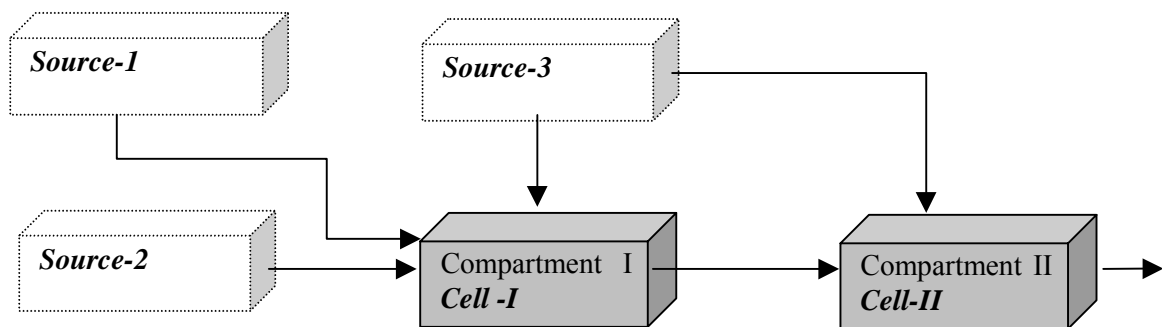


**Figure 3.11** Example of a simple conceptual flow model with two mixing cells and three sources

A cell must have in- and outflow, either as flow into a downstream cell or withdrawal of water by pumping. It may have a number of sources and may contribute water to (a) downstream cell(s). In the above example, cell I receives *inflows* from sources 1, 2 and 3 and contributes to cell II. Cell II receives inflow from source 3 and from cell I.

Any connection between two compartments has a unique flow direction. Flow into and out of cells must follow groundwater gradients. Possible hydraulic connections among cells are defined prior to the optimization process, based on groundwater head gradients; i.e. the direction of the assigned flow vector is not optimized; it cannot be inverted as a result of the optimization.

Resulting from the optimization process a flow rate ( $\geq 0$ ) is attributed to each potential flow connection. Some connections may have an effective flow rate that equals 0. This means that this specific connection does not really exist. However, the model will not assign any flow rates to connections that were not identified or introduced into the model.

### Mathematical description

The following physical and mathematical model is based on ADAR ET AL. (1988) and ADAR & SOREK (1990). A set of balance equations for the flux of water and for the associated flux of solutes is written for each cell  $n$  over a given time period  $dt$ . For a fluid with constant density the mass balance for the cell  $n$  is expressed by the following equation:

$$\sum_{r=1}^R Q_{rn} + \sum_{i=1}^I q_{in} - \sum_{j=1}^J q_{nj} - W_n = S_n \frac{dh_n}{dt} \quad (40)$$

The symbol  $Q_{rn}$  denotes sources contributing to cell  $n$ , and  $q_{in}$  denotes the flux from the  $i^{th}$  compartment or cell into the  $n^{th}$  cell. In the above example for cell  $i$  there are no flows from upstream cells and there are 3 external sources  $r = 1, 2$  and  $3$ . In a similar way,  $q_{nj}$  stands for the outflow from the  $n^{th}$  cell into the  $j^{th}$  one.  $W_n$  accounts for withdrawal of water from cell  $n$ , i.e. for a sink term or pumping rate in the  $n^{th}$  cell. The inflows and outflows are iterated over the number of inflows  $I$  and outflows affecting cells  $J$ .  $S_n$  represents the storage capacity within cell  $n$ , and  $h_n$  denotes the hydraulic head associated with that cell. For a steady flow system Equation (41) is obtained by integrating the terms of Equation (40) over a sufficiently long time interval and by dividing by  $t$ :

$$\sum_{r=1}^R \overline{Q_{rn}} + \sum_{i=1}^I \overline{q_{in}} - \sum_{j=1}^J \overline{q_{nj}} - \overline{W_n} = \epsilon_n \quad (41)$$

This is the average water balance for the specific time interval. The notation is the same as in the previous equation, except that each term represents average flows. An error term  $\epsilon_n$  is introduced in order to account for measurement errors and other deviations from flux and solute balances in cell  $n$ . For quasi-steady state concentrations the mixing-cell concept is applied, based on mass balance expressions for each tracer  $k = 1, 2, \dots, K$  in cell  $n$ :

$$\sum_{r=1}^R \overline{C_{rk} Q_{rn}} + \sum_{i=1}^I \overline{C_{ink} q_{in}} - \overline{C_{nk}} \left( \sum_{j=1}^J \overline{q_{nj}} - \overline{W_n} \right) = \epsilon_{nk} \quad (42)$$

$\overline{C_{rk} Q_{rn}}$  denotes the average flow of the  $k^{th}$  constituent from source  $r$  into cell  $n$ .  $\overline{q_{in}}$  represents the average flow from the  $i^{th}$  cell into the  $n^{th}$  cell having an average concentration  $\overline{C_{ink}}$  of solute  $k$ . In Equation (42)  $\overline{C_{nk}}$  denotes the average concentration of the  $k^{th}$  constituent within

cell  $n$ , and  $\overline{q_{nj}}$  stands for the average outflow from the  $n^{\text{th}}$  into the  $j^{\text{th}}$  cell. Average pumping from the  $n^{\text{th}}$  cell during a specific time interval is expressed by  $\overline{W}_n$ , and  $\varepsilon_{nk}$  is the error associated with mass balance of the  $k^{\text{th}}$  constituent or the deviation from the flow and solute balance in cell  $n$ . By combining the equations into a matrix form for each cell  $n$  we obtain:

$$\underline{\underline{\mathbf{C}}}_n \underline{\underline{X}}_n + \underline{\underline{P}}_n = \underline{\underline{\mathbf{E}}}_n \quad (43)$$

where  $\underline{\underline{\mathbf{C}}}_n$  is a matrix with known concentrations in cell  $n$ ,  $\underline{\underline{X}}_n$  is a vector of the unknown flows through the boundaries of cell  $n$ ,  $\underline{\underline{P}}_n$  is a vector containing elements with known values in cell  $n$  (such as known pumping rates), and  $\underline{\underline{\mathbf{E}}}_n$  is the error vector in cell  $n$ . By assembling the square error terms over all cells we obtain:

$$J = \sum_{n=1}^N (\underline{\underline{\mathbf{E}}}_n^T \underline{\underline{\mathbf{W}}} \underline{\underline{\mathbf{E}}}_n) = \sum_{n=1}^N (\underline{\underline{\mathbf{C}}}_n \underline{\underline{X}}_n + \underline{\underline{P}}_n - \underline{\underline{\mathbf{E}}}_n)^T \underline{\underline{\mathbf{W}}} (\underline{\underline{\mathbf{C}}}_n \underline{\underline{X}}_n + \underline{\underline{P}}_n - \underline{\underline{\mathbf{E}}}_n) \quad (44)$$

where  $^T$  denotes transpose and  $\underline{\underline{\mathbf{W}}}$  represents a diagonal matrix comprised of weighting values of estimated errors. The weighting values are independent of each other and express the degree of confidence in each of the terms building the mass balance for the fluid and the dissolved constituents. The flow rates can now be estimated using measured ion concentrations or isotope ratios by a minimization of the sum of square error  $J$ .

### 3.3.3 Optimization

Resulting from the mathematical optimization a flow rate is attributed to each potential flow connection. Depending on the results obtained by mathematical optimization, the flow model may be slightly changed mainly by modification of the proposed flow pattern and the potential sources. Repeated failures of the model optimization scheme indicate disagreement between the hydrogeological and hydrochemical flow pattern versus the proposed set-up of the model. This implies the need for modification of the proposed compartmental flow pattern and sometimes necessitates a review of hydrogeological system analysis, i.e. the definition of compartments and possible flow connections. The computational optimization scheme is based on the mixing-cell model of ADAR (1984). This model extends the approach for one single mixing-cell (WOOLHISER ET AL., 1982) to multiple cells. A detailed description of the theoretical background is given in ADAR (1996). In order to facilitate the generation of conceptual flow models a new computer program was written that allows the user to construct conceptual mixing models, run and test them interactively. A detailed program description is given in Annex A.

---

## 4 Developing a quantitative flow model of the Upper Omatako

In order to build a detailed hydrogeological model of the groundwater flow system in the Omatako basin, geological, hydrodynamic and hydrochemical information was analysed. A systematic scheme for the integration of these different types of data on the flow system was followed:

- *analysis of hydrogeological data and estimation of groundwater recharge sources,*
- *analysis of hydrochemistry and isotope hydrology,*
- *development of a conceptual flow model,*
- *quantification of this flow model by inverse-mixing modelling.*

Available hydrogeological and hydrodynamic information constraining groundwater flow was reviewed first for identifying major aquifers and hydraulic gradients that control the flow directions (Chapter 4.1). Following the delineation of recharge areas from the distribution of groundwater levels, groundwater recharge was estimated making use of a climatic and a soil water balance approach (Chapter 4.2). Another important aspect, besides quantitative estimation, was the role of specific recharge processes and recharge timing. In Chapter 4.3 the evaluation of available hydrochemical data for the whole Omatako basin will be presented for the analysis of groundwater flow patterns. This overview was complemented and refined with data from two sampling campaigns (Chapter 4.4). Groundwater samples were analysed for major ions, stable isotopes  $^{18}\text{O}$  and  $^2\text{H}$ , and for  $^3\text{H}$  and  $^{14}\text{C}$  dating. Based on the interpretation of hydrochemistry and isotope data a conceptual flow model in agreement with known hydrogeological conditions was developed. Finally, groundwater flow was quantified using a steady state mixing-cell approach (Chapter 4.5).

### 4.1 Hydrogeological data of the Upper Omatako basin

The hydrogeological data used in this Chapter were available at the Department of Water Affairs of Namibia (DWA) but are regionalized and presented here in a hydrogeological synopsis of the Upper Omatako basin for the first time. The combination of different thematic layers was made with a commercial GIS system (© TNT Mips 5.4).

#### 4.1.1 Aquifers, hydraulic gradients and groundwater flow directions

A regional groundwater contour map for the Omatako basin up to longitude E 18° 35' was derived (Figure 4.1) from groundwater level data of the Department of Water Affairs (DWA). Due to a number of obvious inconsistencies in the data, a thorough check for errors became necessary. Each data set showing one of the following inconsistencies was deleted:

- total depth to the water level exceeded the drilled depth
- strike was below the drilled depth
- extreme deviations from adjacent boreholes indicated that depth values may represent *feet* instead of *metres*

These corrections significantly improved the quality of the data set. Due to the lack of information as to exactly which aquifer was tapped by a certain borehole, no general distinction between different aquifers on the vertical scale could be made. It is only for areas where the water level figures obviously clustered at different levels that shallow perched aquifers (S) were entered into the groundwater level map.

The groundwater level map was derived from 4,894 water level readings (shown as dots in the map) by inverse distance interpolation. The groundwater flow is driven by recharge in the horseshoe-shaped mountainous rim of pre-Kalahari outcrops. The highest water levels are found in the Otavi Mountains to the north, along outcrops of the Karibib Formation (marbles belonging to the Damara Sequence) to the north-west, and in extensive basement outcrops (Damara Sequence) to the south. The groundwater flow system is further modified by a groundwater mound in the Waterberg area contributing to a convergence of groundwater flow from the west (Waterberg, Karibib marbles) and north (Otavi Mountains) in the Goblenz area. In the eastern Waterberg area groundwater level data indicate the existence of shallow perched aquifers (S).

A strong scatter in the water level data east of Goblenz indicates the existence of another shallow, possibly perched, aquifer. Numerous pans are found there. Even after the separation of these shallow groundwater levels from the regional groundwater level there is an indication of a groundwater mound in this area. The configuration of the groundwater contour lines around the pans points to increased recharge in this area. The regional flow pattern produces a convergence of groundwater flow near Goblenz. From this convergence zone the groundwater leaves the study area by two divergent flows to the north-east and to the east. This divergent flow pattern follows two pre-Kalahari basement depressions as indicated by the isopach map of Kalahari sediments.



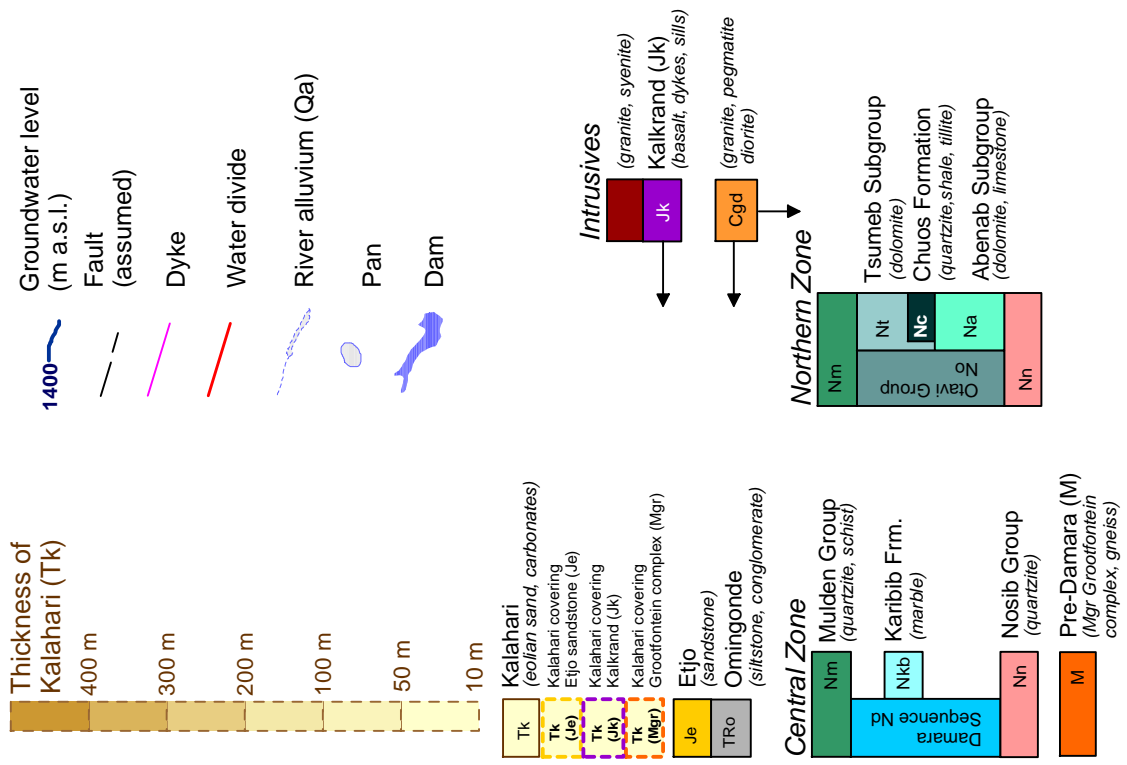
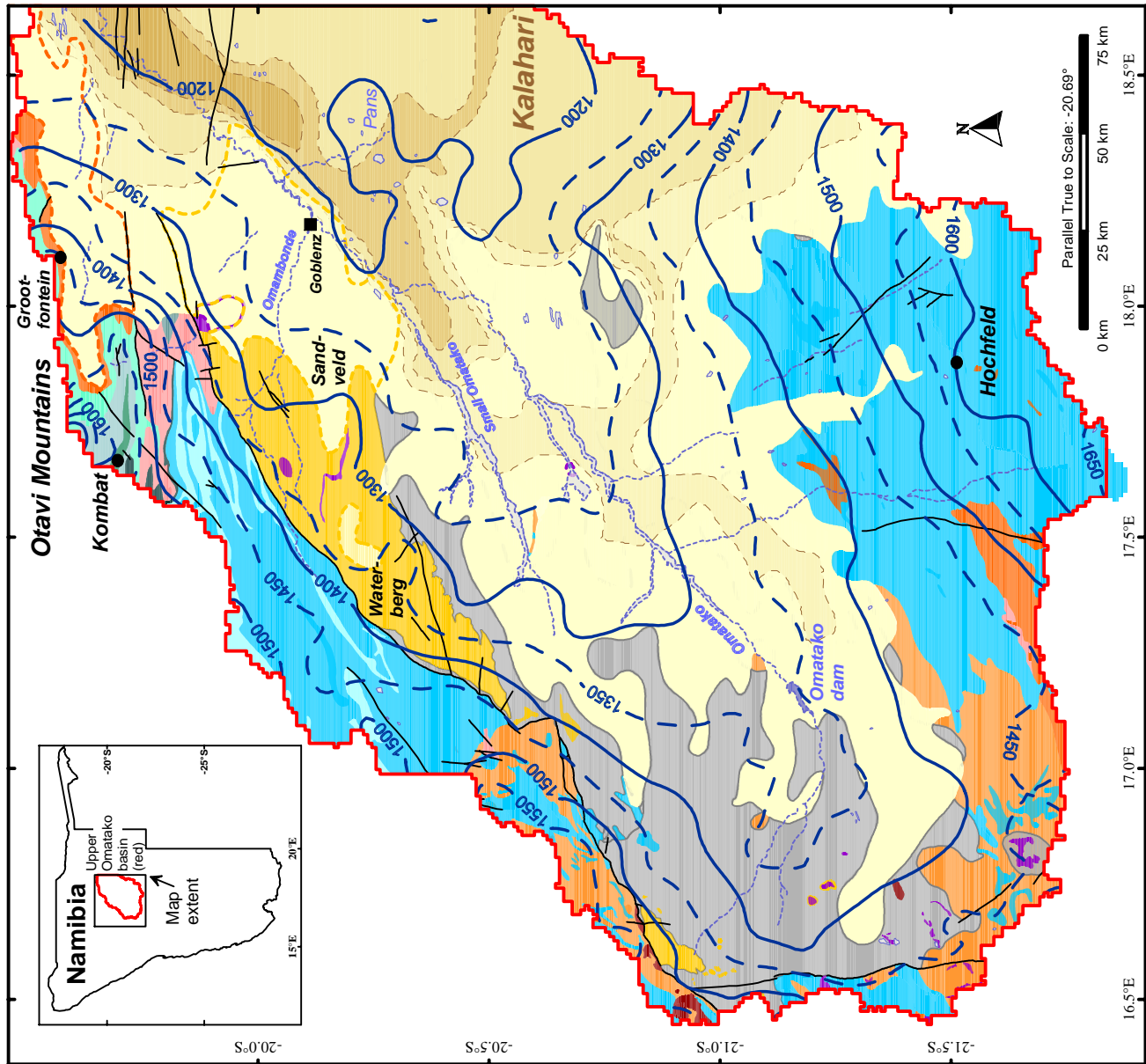


**Figure 4.1**  
Groundwater level contour map of the Upper Omatako basin derived by the method of inverse distance interpolation from DWA borehole reports. Background map of the geology in the Upper Omatako basin, Namibia, with isopachs of Kalahari thickness compiled from geological maps of Namibia 1:250,000 (Geological Survey, Namibia).

#### 4.1.2 Distribution of saturated Kalahari sediments

An approximate map of the saturation of Kalahari sediments has been derived in order to delineate aquifers within the Kalahari and possible flow connections. It was calculated using available information on surface elevation, on the Kalahari thickness, and on groundwater strikes.

In the DWA database the groundwater *strike* is listed as the depth from the earth surface to the first major occurrence of groundwater during drilling. From an existing map of the digital terrain elevation above sea level an absolute level of the groundwater strike was calculated by simple subtraction. The absolute level at which groundwater was struck was then compared to the absolute level of the pre-Kalahari basement. Elevation of the latter was then calculated from the surface elevation minus the Kalahari thickness taken from existing isopach maps.

This calculation was made for grids using the Geographic Information System (GIS) TNT Mips 5.4. The grid of Kalahari saturation was derived by constructing the difference  $A_{ij}-B_{ij}$  (with  $1 \leq i \leq I$  and  $1 \leq j \leq J$ ) between absolute groundwater strike level (Figure 4.2, A) and pre-Kalahari basement elevation (Figure 4.2, B) for each grid cell over the number of columns  $I$  and the number of rows  $J$ . The difference raster  $A-B$  displays saturated thickness as a positive value and distance between basement elevation and first groundwater strike in the basement as a negative value.

The grid of groundwater strike levels (A) was interpolated from the database of groundwater strikes and levels of the DWA. The grid of basement elevation (B) was produced by stripping the Kalahari sediments from the digital terrain elevation model. This was done by reducing topographical elevation by the thickness of Kalahari sediments for each grid cell. The grid of the thickness of Kalahari sediments was obtained from the interpolation of Kalahari isopachs as mapped in 1:250,000 geological maps of the Geological Survey of Namibia. The digital terrain elevation model was taken from the Digital Chart of the World (DCW) providing 30-by-30 arc-second digital elevation data of the U.S. Defence Mapping Agency (DMA).

Elevation of groundwater strikes instead of groundwater levels was used in order to account for confining conditions. There are, in fact, such confining beds of red clays and marls within the Lower Kalahari which may act as confining beds in some locations.

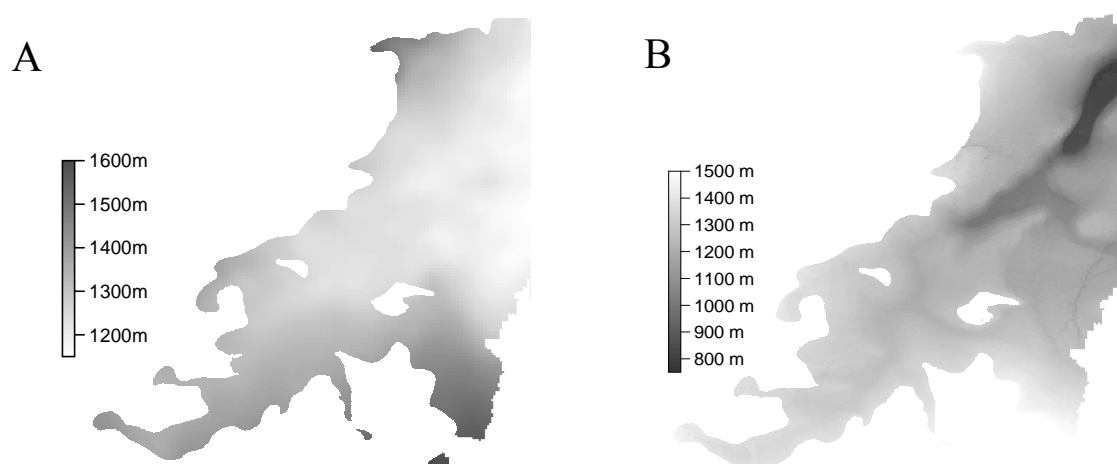


**Figure 4.2** Grid of groundwater strikes (A) and of basement elevation (B) above sea level used for the calculation of the saturated thickness of Kalahari sediments.

As a result the free static water level of a borehole may be found within the Kalahari beds although they are not the corresponding aquifer. In some cases strikes directly indicate the depth to the aquifer top. The use of strikes must be applied with care and should be considered as a proxy. This is due to several problems with strike definition.

In fractured rock the data on strikes will scatter because strike depth also depends on the distribution and inclination of fractures. For the general purpose of this map this is not problematic: In areas where the Kalahari is not saturated and groundwater is struck in the pre-Kalahari basement, the borehole will have to penetrate not only the full Kalahari, but also the additional distance to the first water-bearing fracture zone. Consequently, the depth of strikes tends to be larger than the total depth of the Kalahari, and the separation between saturated and unsaturated areas becomes even sharper.

Problems may arise also for confining conditions. As the confining bed will be saturated up to the static water level, lenses of coarse sediments may cause ‘*little*’ strikes. Therefore, the discussion of accuracy is an important issue. More so as several layers of data are combined, each being subjected to a specific interpolation error. The map of saturated thickness of the Kalahari sediments (Figure 4.3) should be seen as an attempt to visualize relative regional patterns and structures and should only be used in combination with borehole data at the local scale. Data on the degree of accuracy of the digital elevation model are not available, but even if this is high, the accuracy of the derived map is certainly not better than  $\pm 25$  to  $\pm 35$  m. Consequently, a calculated saturation between 10 and 50 m is shown dashed; only for a saturated thickness of more than 50 m full colours are used.

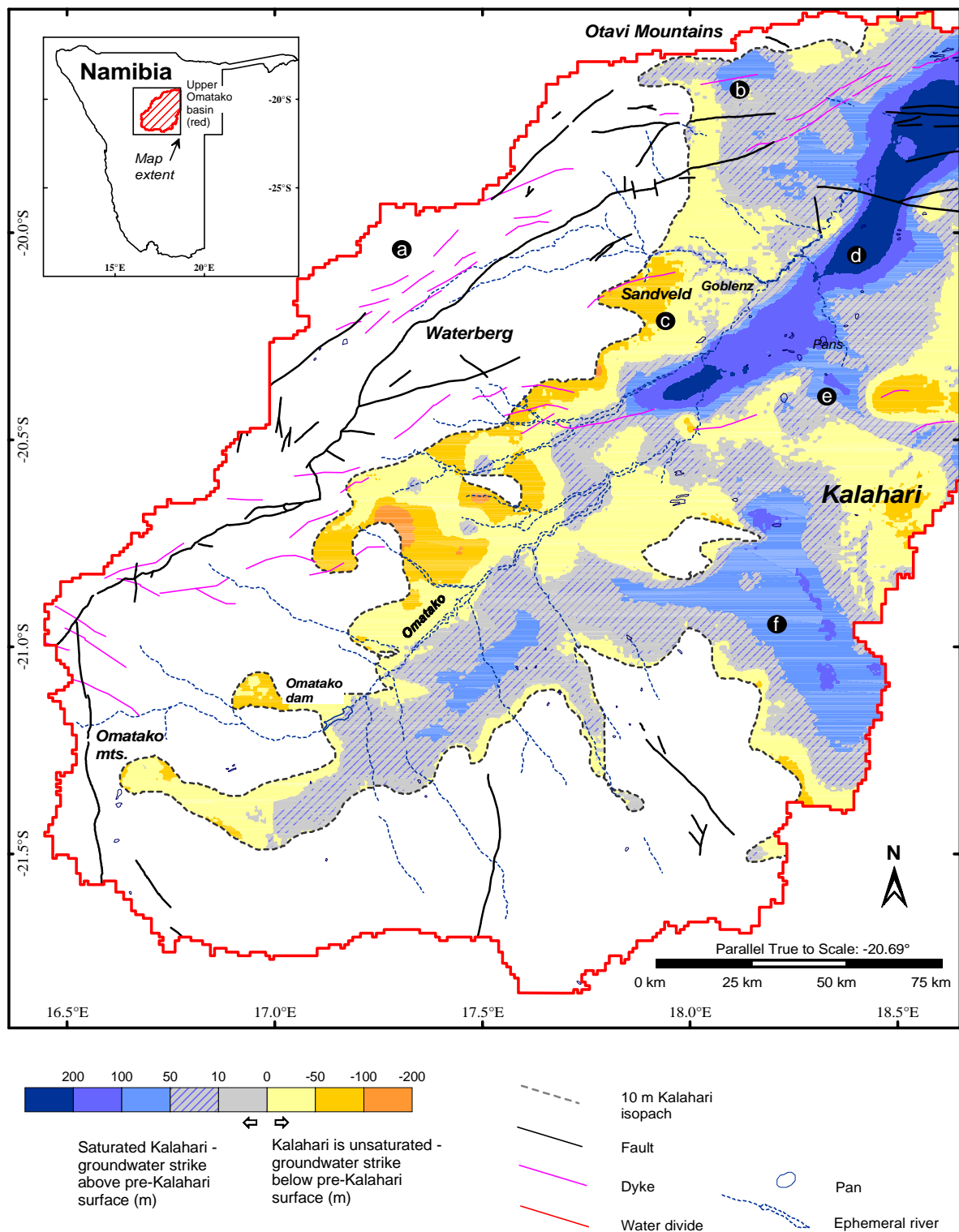


**Figure 4.3** Distribution of saturated Kalahari sediments. Blue indicates areas saturated with groundwater, grey shows areas of limited saturation, and yellow indicates areas that are not saturated. The map represents the difference between a digital model of the pre-Kalahari surface and the interpolated groundwater strike map. Areas not covered by Kalahari sediments are shown in white.

Areas not covered with Kalahari sediments (a) are white. The map shows a major trough with a thickness of saturated Kalahari sediments of more than 200 m in places (d). This trough extends just south of Goblenz from south-west to north-east. It is parallel to the Waterberg Thrust Fault and corresponds to a deep pre-Kalahari depression filled with Kalahari sediments. Recent drilling has shown that this trough has a depth of more than 400 m in some places (pers. communication, H. Grobelaar, Namwater). This major trough is connected to some other minor saturated troughs, corresponding to filled pre-Kalahari depressions (e, f). These minor troughs are important as flow connections between the hard-rock rim and the deep trough near Goblenz. According to the map of saturated thickness, the Kalahari is not saturated in some areas (yellow colours). Especially north-west of the Upper Omatako (c) and upstream of the confluence of the Omatako and the Small Omatako the Kalahari appears to be dry. The same holds true for the westernmost part of the Otavi Mountain Foreland, where the aquifer is found in the Etjo sandstone underlying the Kalahari. In the eastern part of the Otavi Mountain Foreland (b) the Kalahari is saturated conveying groundwater from the Otavi Mountains to the Kalahari. Before the map of saturated thickness of the Kalahari can be used for groundwater prospecting, its data will have to be combined with groundwater quality data.

For validation, the map of saturated thickness was compared to maps of estimated saturated thickness produced during previous geophysical surveys (Figure 4.4) by DE BEER & BLUME (1985). The approximate extent of the Etjo sandstone underlying the Kalahari sediments is marked by a red line. The geophysical survey area is delimited by a green line. For the rest of the Kalahari (grey) no information is available. In general the map of saturated thickness of Kalahari sediments (Figure 4.3) is in good agreement with the previous estimates (Figure 4.4). Both maps show a saturated trough of Kalahari sediments striking south-west to north-east and beginning at 18° E.

However, there are deviations along the western border of the survey area. Obviously high longitudinal conductances there have been attributed to a well developed water-bearing Middle Kalahari Formation by DE BEER & BLUME (1985). In the geological map 1:250,000 this area has been mapped as a succession of Etjo sandstone overlain by Kalahari sediments. Hence, part of the saturated thickness attributed to the Kalahari formations in the geophysical survey probably belongs to the Etjo sandstone. The differences in this area result from a different geological interpretation of the underlying sediments. Due to similar aquifer characteristics, however, they do not affect the recommendations given by DE BEER & BLUME (1985). Although Figure 4.3 is less detailed for the central part near Goblenz it has the advantage of giving a complete overview for the Kalahari in the Upper Omatako basin. It also shows the pre-Kalahari troughs connecting the large depression with its saturated Kalahari sediments south of Goblenz to the hard-rock outcrops around the Kalahari basin.

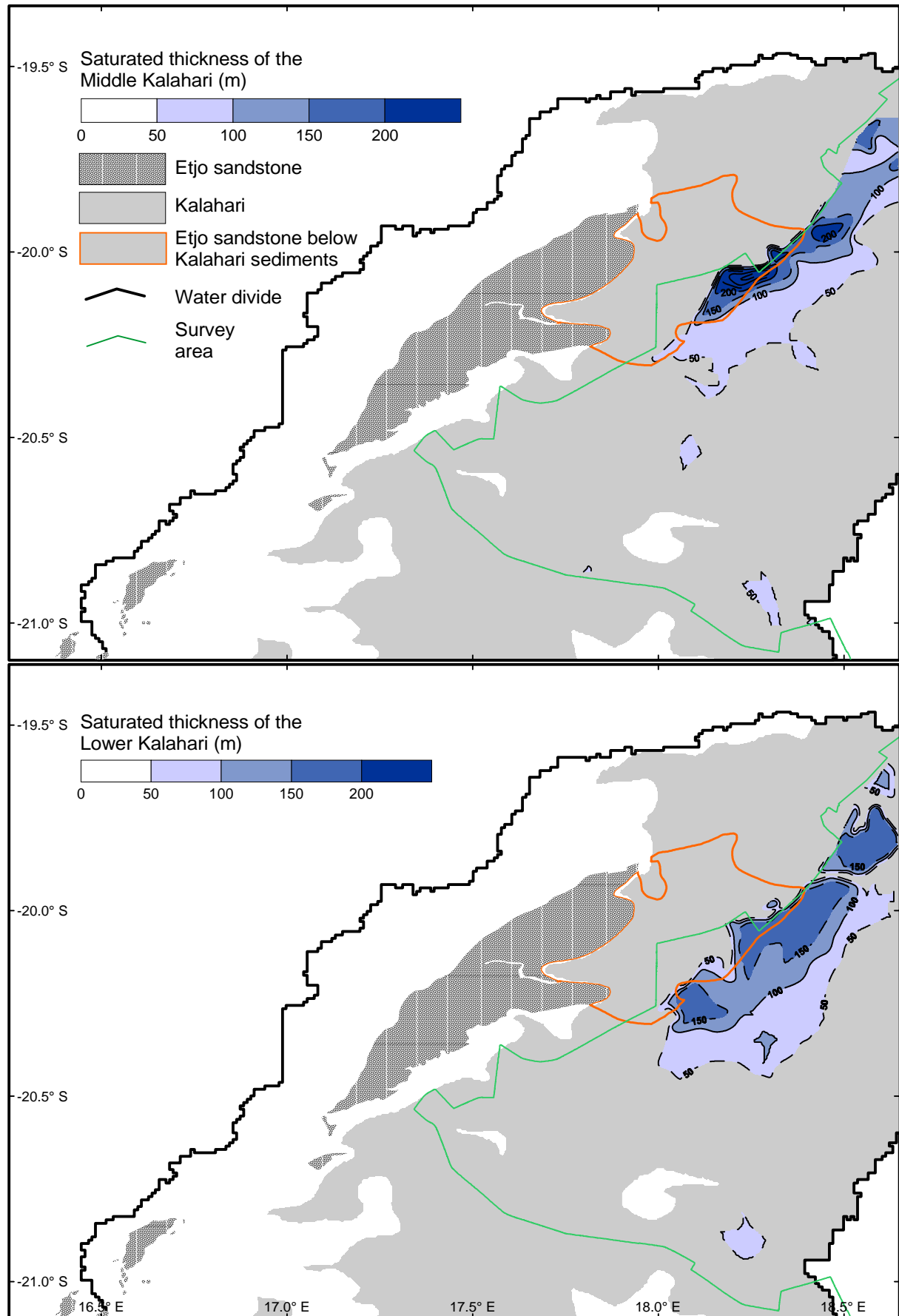


**Figure 4.4** Maps of saturated thickness of Lower and Middle Kalahari from geophysical surveys.

### 4.1.3 Thickness of the unsaturated zone

The depth to the water table respectively the thickness of the unsaturated zone has been calculated from the digital elevation model (Figure 4.5, A) and the groundwater level raster map (Figure 4.5, B). This information is important for the interpretation of stable isotope data, because possible zones with capillary connection to the atmosphere and consequent evaporative enrichment can thus be delimited. Besides, this map has practical applications for groundwater exploration. The map shown in Figure 4.6 was obtained by constructing the difference  $C_{i,j}=A_{i,j}-B_{i,j}$  (with  $1 \leq i \leq I$  and  $1 \leq j \leq J$ ) for each pixel of the map over the number of columns  $I$  and the number of rows  $J$ . Again, the digital elevation model (Figure 4.5, map A) was taken as a subset from the Digital Chart of the World (DCW) already referred to, with a resolution of  $0.9 \times 0.9$  km. The groundwater level raster (Figure 4.5, map B) was interpolated from the database of groundwater level data of the Department of Water Affairs, Windhoek/Namibia, as described above. In order to create compatible grids the map resolution was adjusted (with TNT Mips 5.4) to  $250 \times 250$  m for both maps.

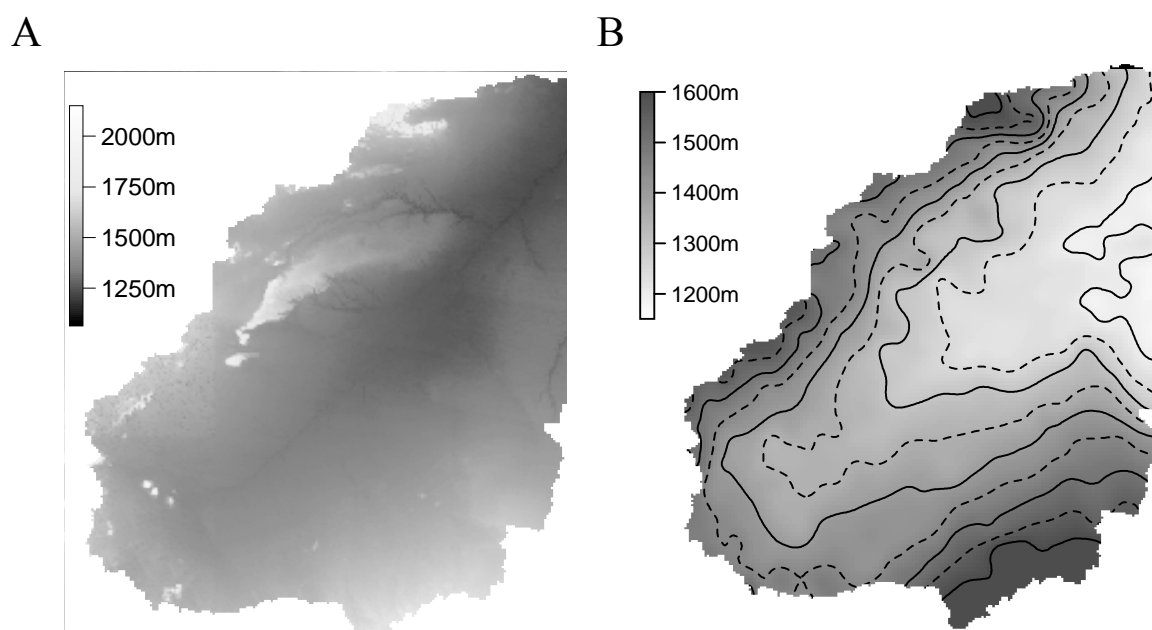


**Figure 4.5** Digital elevation model (A) and groundwater level raster (with 50m and 100m contour lines) (B) used for the calculation of the depth to groundwater table.

The error  $E_c$  associated with each raster element of the combined map C is  $E_c=(E_a^2+E_b^2)^{0.5}$ , where  $E_a$  and  $E_b$  are the errors of elevation and groundwater level at each raster point, respectively. Assuming errors of 25 m for the digital elevation model and 15 m for the groundwater level map, the accuracy of the combined map is not better than  $\pm 29$  m.



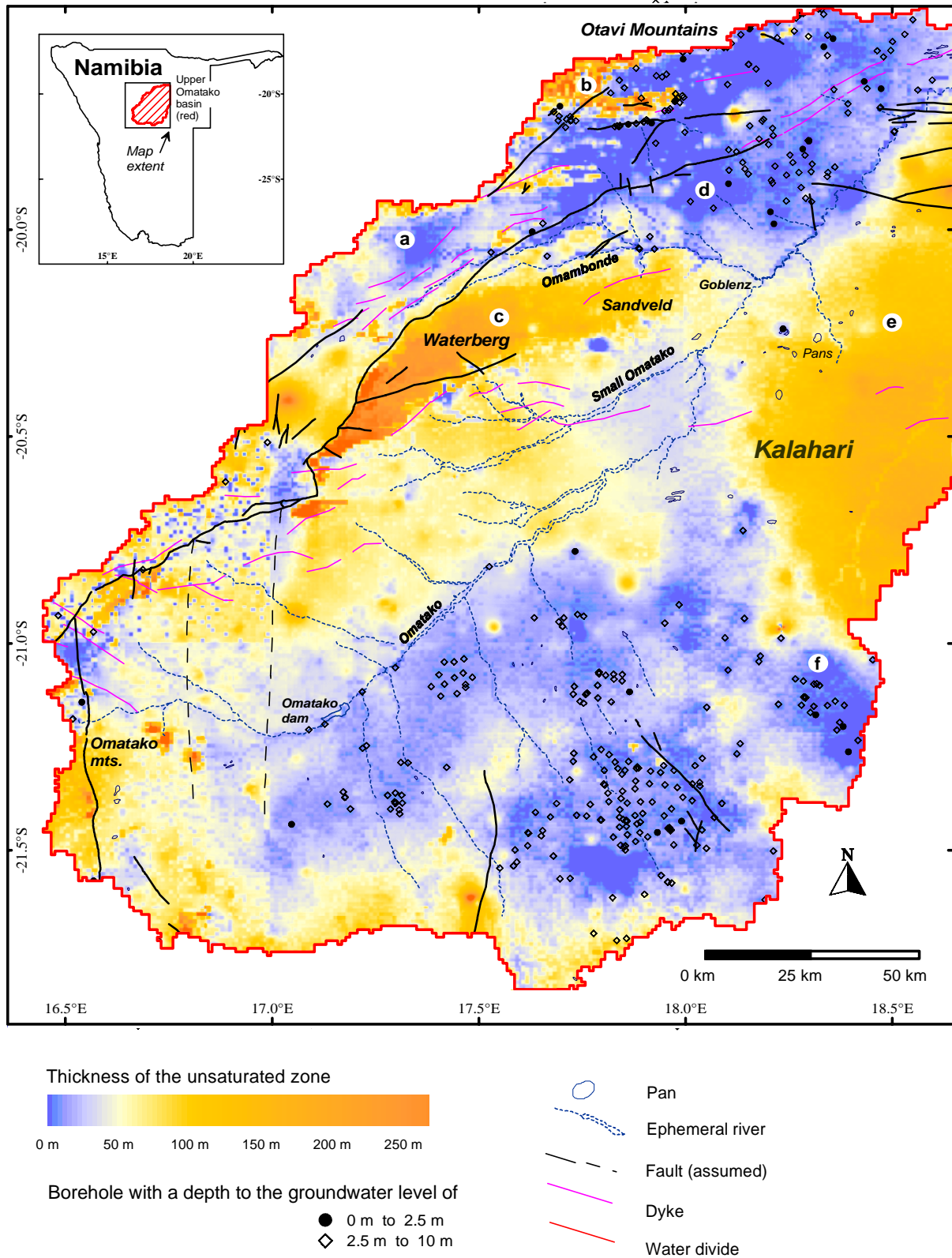


**Figure 4.6** Map of the depth to groundwater table computed from digital elevation data and an interpolated groundwater level grid in the Upper Omatako basin.



Therefore, the map should be used for a regional overview and interpretation only. At the local scale data from the borehole database of the DWA should be consulted. In order to include the point data with much smaller associated measurement errors without obstructing the map with thousands of point symbols, only those boreholes have been marked where depth to the water table was found to be smaller than 10 m (open circles) or smaller than 2.5 m (filled circles). The combination of raster and point data was also used for checking the validity of the derived raster map. A good agreement between the computed raster and the point data is evident in Figure 4.3. The two classes of very shallow (< 2.5 m) and shallow water tables (2.5 to 10 m) stand for two important thresholds: from very shallow groundwater direct evaporation is possible, at least seasonally; from shallow groundwater evapotranspiration losses due to phreatophytes with deep root systems can still occur.

The map (Figure 4.6) shows areas with shallow groundwater in blue and areas with a thick unsaturated zone in yellow. While the northern Omambonde tributaries (a), the Otavi Mountain Foreland (d) and part of the Kalahari to the south (f) are characterized by shallow groundwater levels, thick unsaturated zones are found in parts of the Otavi Mountains (b), at the Waterberg (c) and in the eastern Kalahari (e). Shallow groundwater levels in perched aquifers are found near pans south of Goblenz and along several reaches of ephemeral streams. The map also shows for the Otavi Mountain Foreland (d) that losses by discharge of and evapo(transpi)ration from groundwater can take place at least during periods with elevated water levels. This is important for the interpretation of isotope data in this area and also has implications for the water balance and for estimating groundwater flow into the Kalahari: part of the mountain front recharge from the Otavi Mountains can be '*lost*' in the Otavi Mountain Foreland by evaporation. The following analysis of stable isotopes will further elaborate on this point.

As a first conclusion, synthesis of hydrogeological data for the Upper Omatako basin already reveals some important features of the groundwater system of the Upper Omatako basin:

- A horseshoe-shaped mountainous rim without Kalahari cover directs the groundwater flow system towards the Kalahari basin.
- Within this rim four hydrogeological zones are especially relevant: 1) the Otavi Mountains to the north, 2) the outcrops of metamorphic rocks of the Damara Sequence to the north-west and south, 3) the Etjo sandstones (Waterberg), and 4) the outcrops of granites and Mesozoic sediments (Omingonde) to the west (Figure 2.6).
- An interesting feature is found just south-east of Goblenz where a belt of pans has developed (e). In this area a shallow, probably perched, aquifer is found that can only be sustained by local recharge.

- Goblenz is a convergence zone for the groundwater flow from all of these zones and is thus the key area for the understanding of the hydrogeology of the Upper Omatako basin.
- Of prime importance for the groundwater resources development of the area is the deep trough within the pre-Kalahari surface extending from south-west to north-east and located just south of Goblenz. Refilled with Kalahari sediments, it has a saturated thickness of more than 200 m in some places. The Goblenz wellfield is connected to this extensive aquifer.

## 4.2 Estimating groundwater recharge

Two different methods based on daily water balance calculations have been applied: a statistical method for evaluating the *climatic recharge potential* from daily data, and a full physical water balance model, computing *daily soil water balances* based on soil property data. The main objective was to investigate the timing of recharge processes and their potential as a function of the meteorological conditions, and the influence of soil physical characteristics on groundwater recharge.

### 4.2.1 Climatic recharge potential

Following a frequency analysis as outlined in SIMMERS ET AL. (1997: 61), descriptive statistics have been used in order to visualize the meteorological water balance conditions in the study area based on daily rainfall and evaporation data. The method yields conservative estimates of recharge potentials and helps resolve the seasonal pattern of recharge conditions.

Rainfall records from *Grootfontein* (Figure 1.1) between 01-Oct-1979 and 31-Mar-1985 and class A pan evaporation data from the same location were used. Both daily time series were split into subgroups of data for each calendar month. Each group contains all daily data recorded in a given month during the observation period. The subgroups of monthly rainfall data contain between a minimum of 60 values for April and up to 166 values for January with daily rainfall amounts above 0.1 mm. For both the rainfall and evaporation data, the values within each subgroup were ranked in ascending order. From the ranked data, quantiles of 80 % and 95 % were calculated for each month and for both the rainfall and evaporation records. The 80 % quantile of rainfall in January, for example, represents a value that is larger than 80 % of all the other daily amounts recorded between 01-Oct-1979 and 31-Mar-1985. This corresponds to a value that is reached or exceeded by only 20 % of daily rainfall amounts of this month. The 80 (95) % quantile has a recurrence interval of 5 (20) years.

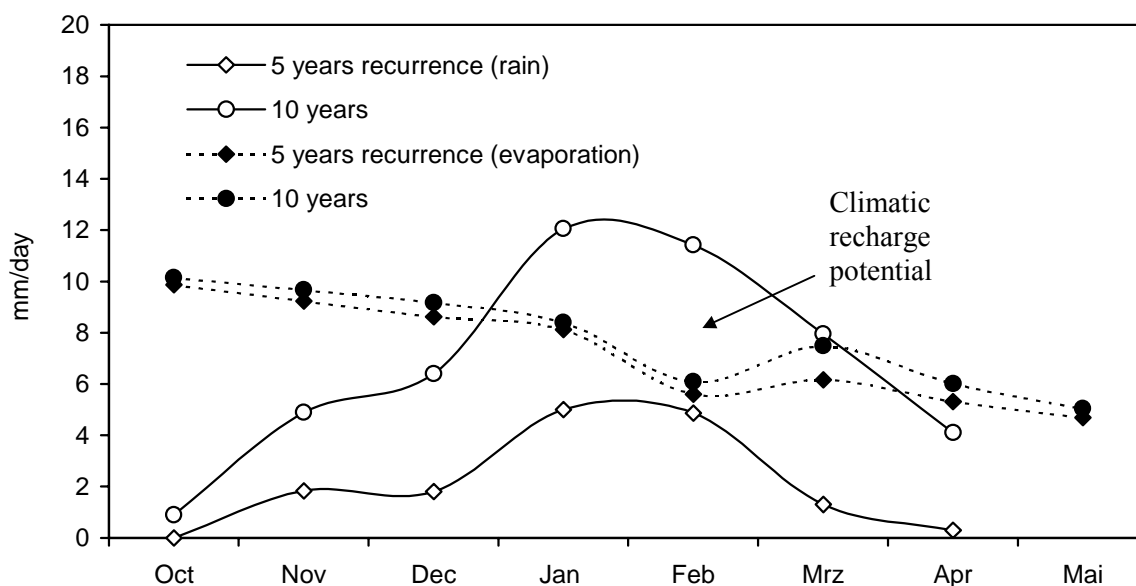


**Figure 4.7** Frequencies of daily water balance components for 'Grootfontein', derived from time series between Oct-79 and Mar-85.

This first analysis does not take into account the correlation between daily rainfall events (series of days with rainfall) and pedological factors or indirect recharge mechanisms. However, these data give a first indication that direct groundwater recharge does not necessarily occur on an annual basis. Even in a relatively 'wet' region of the Omatako basin intensive rainfall events with a recurrence interval of several years are required to produce favourable conditions for direct recharge. Based on considerations of daily water balance, the potential for direct recharge is highest in February, followed by January and March. Even for 10 year recurrence there is no daily recharge potential during the other months of the year.

#### 4.2.2 Parameter estimation for the soil water balance model

More sophisticated soil water balance methods also take into account data on the physical properties of the soil profile and the depth of the root zone. A description of the soil water balance model applied below was given in Chapter 3.1.4. In addition to climatic data the infiltration rate at the soil surface, hydraulic conductivity  $K$  of the soil, effective field capacity of the root zone and bedrock permeability as invariant soil parameters were introduced.

##### *Estimating hydraulic conductivity*

Hydraulic conductivity was estimated for given soil profiles by infiltration tests in the field. They were carried out with a single ring infiltrometre inserted 10 cm deep into the soil.

Cumulative infiltration amounts were measured at time intervals of 5 seconds. Hydraulic conductivity was then determined by inverse modelling of the experimental data according to a procedure outlined in KÜLLS ET AL. (1994). A physical infiltration model is fitted to the infiltration test data. The hydraulic conductivity, the wetting front suction and the volumetric change in soil moisture are determined as independent parameters by a quadratic solution technique, the Newton-Raphson method (MAIDMENT, 1992). This procedure accounts and corrects for the influence of static pressure exerted by the column of infiltrating water as well as for the increased suction at the beginning of the experiment. The infiltration test shown in Figure 4.8 was made south of Grootfontein (Figure 1.1) on a ‘grey sand’. The upper 20 cm of this profile have a greyish colour due to organic material. The infiltration rates are relatively low, only reaching 150 mm after 240 seconds. Inverse modelling yielded a hydraulic conductivity of  $3.3 \times 10^{-5}$  m/s for the Grootfontein ‘grey sand’.

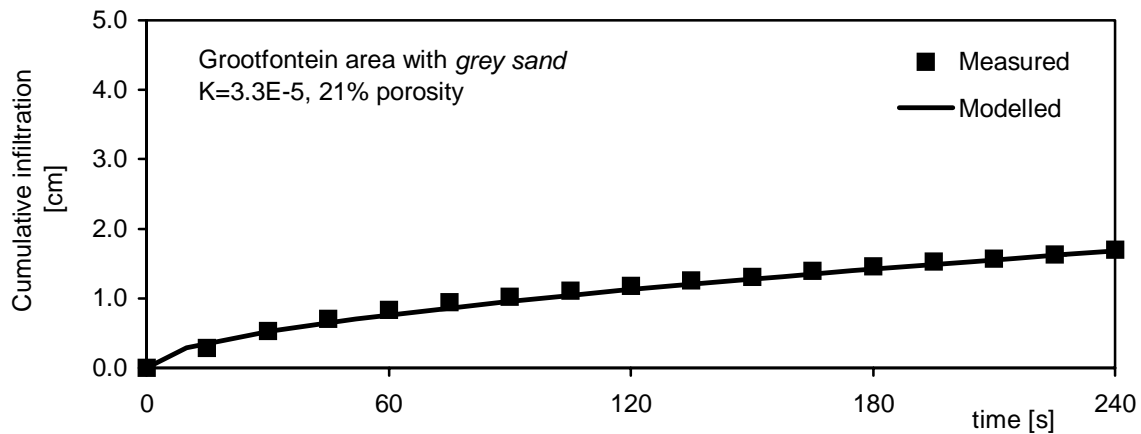


**Figure 4.8** Infiltration test near Grootfontein ‘grey sand’, fitting and parameter estimation.

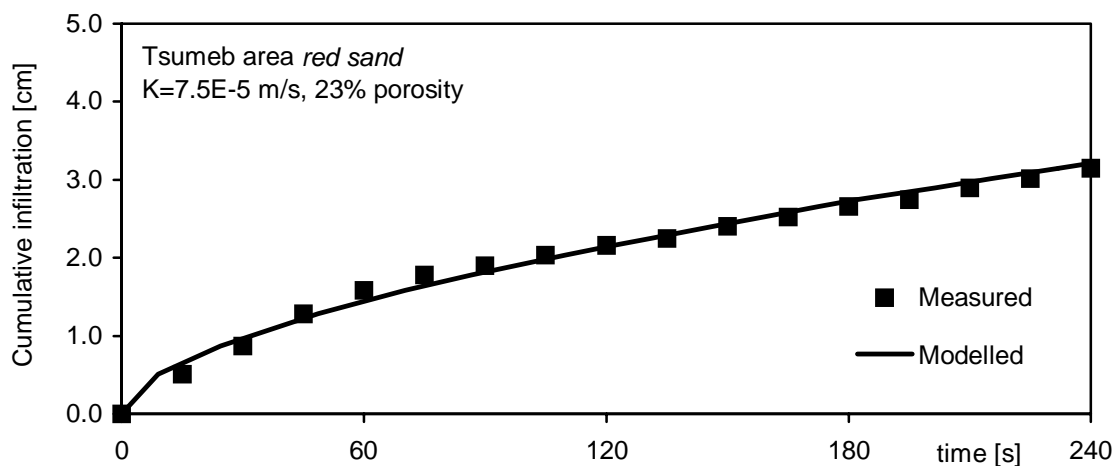


**Figure 4.9** Infiltration test near Tsumeb ‘red sand’, fitting and parameter estimation.

The infiltration tests described in Figure 4.9 were carried out in valley sediments of the Otavi Mountains (Figure 1.1) near Tsumeb. The tests were made on typical ‘red sand’. In this case

the red colour is caused by iron oxides accumulated as the residual fraction of carbonate weathering. The best fit of the infiltration model (line) to the experimental data (filled squares) was obtained for a hydraulic conductivity ( $K$ ) of  $7.5 \times 10^{-5}$  m/s.

The most permeable sediments were found in the Waterberg and Sandveld area. In this area well sorted eolian Kalahari sands cover the Etjo sandstone.

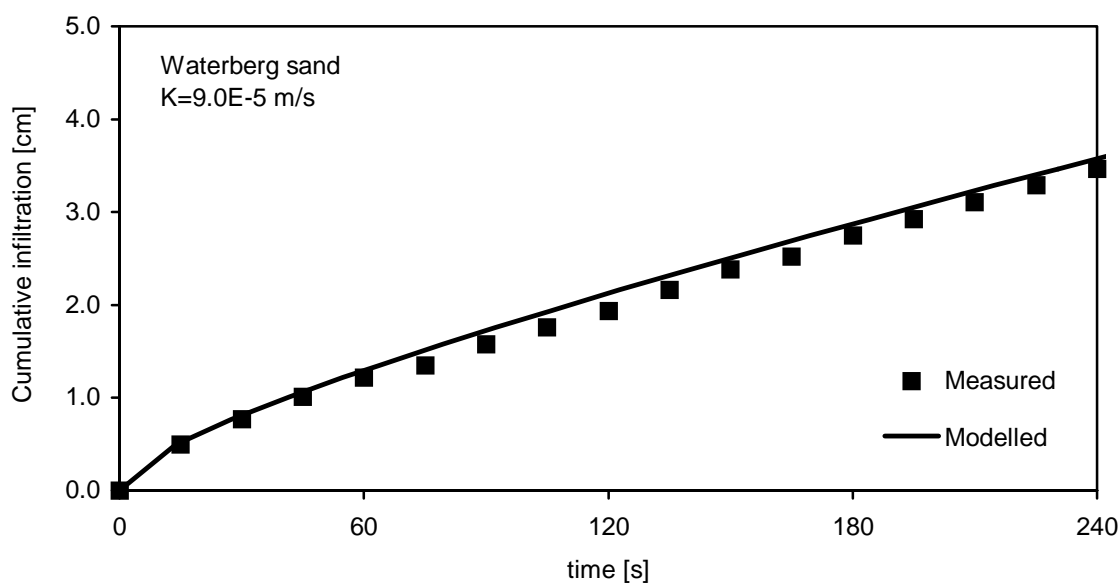


**Figure 4.10** Infiltration at Waterberg covered with Kalahari sand with model fitting and parameter estimation.

From the slope of cumulative infiltration there results a hydraulic conductivity  $K$  of  $9 \times 10^{-5}$  m/s. Infiltration tests were repeated in several locations. A range of  $3$  to  $9 \times 10^{-5}$  m/s was found to be typical for the hydraulic conductivity for the upper metre of Kalahari sediments. The highest values are reached where well-sorted wind-blown sand occurs (Sandveld); medium values were found for accessory iron-oxides (Otavi Mountains, part of the Waterberg), and relatively low hydraulic conductivity was associated with the enrichment of organic material in the upper part of the soil profile (south of Grootfontein).

#### *Estimating field capacity*

Field capacity as a physical parameter of a soil sample can be determined in the laboratory from saturation and de-watering experiments. However, the effective field capacity of a natural soil column depends on additional factors such as depth of the root zone and the horizontal distribution of roots. In Namibia, as in other drylands with patchy vegetation, the spatial pattern of vegetation with its simultaneous existence of grass, bushes and trees, all having different root depths, makes it very difficult to estimate this parameter. Therefore, an

inverse method was used that takes into account measured groundwater levels near the modelled soil profile. The prevailing effective field capacity was estimated by comparing the model results for different field capacity values (35 mm, 45 mm, 55 mm, 65 mm, 75 mm, 85 mm and 95 mm) to observed groundwater level fluctuations. During dry spells without recharge the decay of groundwater levels was modelled as a simple exponential decay. The fitting (Figure 4.11) could only be made for the Grootfontein location, since no other time series of groundwater levels of sufficient resolution (1 month) were available.

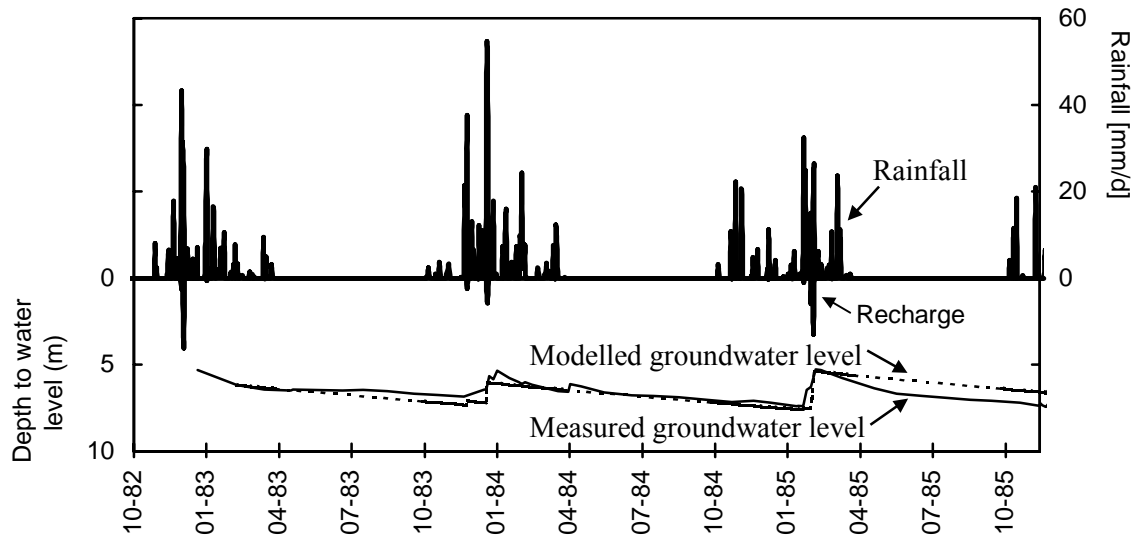


**Figure 4.11** Daily hydrologic water balance model with seasonal variation of calculated recharge and measured daily rainfall data. Modelled groundwater levels are shown dashed, measured water levels solid.

Field capacities of more than 65 mm reduced the recharge to almost zero and did not reproduce fluctuations of the groundwater level as observed. In contrast, field capacities of 55 mm and below produced very high recharge rates and fluctuations of the groundwater level that had not been measured in the field. Low field capacities also produced modelled fluctuations earlier during the rain season, for which no empirical evidence was found in the measured water level record. The effective field capacity of the modelled soil profile could therefore be constrained to a range of 60 - 70 mm. The best fit was obtained for a field capacity of 65 mm.

#### *Spatial heterogeneity of hydraulic parameters*

It is important to stress the heterogeneity of soil physical properties in the field and the problems associated with the scaling of point parameters obtained from field experiments. This is demonstrated with impressive field observations of dissolution features and of variability of riverbed sediments within the study area (Figure 4.12).



**Figure 4.12** a+b) Sinkholes near Schwarzfelde (about 15 km north of Goblenz) in Kalahari sediments, c) sandy and permeable river sediments near the Kalahari fringe d) sediments in the flat valley floor of the Omatoko with carbonate concretions.

Infiltration tests only characterize the soil matrix controlling direct infiltration through the soil. Macropores existing within the soil, especially near bushes and trees, will dramatically alter the hydrological properties. Geomorphologic features may even introduce new flow mechanisms. Sinkholes discovered during field work close to the farm 'Schwarzfelde' (Figure 4.12 a+b), 15 km north of Goblenz in the Otavi Mountain Foreland, may serve as an example. The exact location is given by sample CN029 'Schwarzfelde' in Figure 4.25. The carbonates, 20 to 30 m thick, probably formed in shallow swamps of the discharge area of the Otavi Karst Mountains and not as a result of soil formation. Groundwater levels have dropped to 5 - 25 m below ground. Presently, dissolution of the thick calcrete takes place. Encroaching Kalahari sand has formed a 0.5 - 1 m sandy soil cover on top of the calcareous formation, which sustains a sparse grass and bush vegetation. The biologic activity in the soil during the wet season increases the CO<sub>2</sub> partial pressure in the soil atmosphere. Thus the soil water has become enriched with CO<sub>2</sub> and subsaturated for calcite by the time it comes into contact with the calcareous formation, causing the dissolution of calcite and the formation of sinkholes. The former groundwater discharge area has now become a through-flow and recharge area with sinkholes. Farmers reported widespread flooding in the Otavi Mountain Foreland lasting for several days. Farmers' reports and videos taken during flood events prove that sinkholes act as drains for surface runoff, forming efficient short-cuts and preferential paths to the groundwater table.

Figure 4.12 c+d) shows how variable the material in ephemeral rivers is within short distances. Along reaches with higher gradients and sources of sand, for instance, thick accumulations of sand bars provide high infiltration capacities (Figure 4.12 c, downstream of Omatako dam). Indeed, these bars are often saturated and form perched aquifers for weeks and few months after heavy floods. In flat areas, the ephemeral river sediments contain high percentages of fines and are thus less permeable. In Figure 4.12 d), white carbonate concretions are visible at a depth of 30 to 40 cm in the profile (Omatako ephemeral river 50 km upstream of Goblenz). The carbonate concretions are found at a depth corresponding to a 'zero flux plane': the soil moisture front slows down at this level and the soil water is consumed by vegetation growing on the ephemeral river bed, or evaporated by capillary rise. Groundwater recharge at this profile is therefore very small, unless bypass-flow plays a role.

### 4.2.3 Water balance modelling - results

The water balance model was introduced in Chapter 3.1.4 and is described in UDLUFT & KÜLLS (2000) and KÜLLS & UDLUFT (2000). The soil water balance model was run using the hydraulic conductivity determined in the field by infiltration tests as  $3.3 \times 10^{-5}$  m/s as well as the effective field capacity as derived from model fitting (65 mm). The model computed daily



soil water storage, surface runoff and groundwater recharge for six rain seasons for which complete daily records of meteorological data were available. The results of the model application are summarized in Table 4.1. The detailed daily time series of rainfall in grey (upper x-axis, right y-axis), and computed recharge in black (lower x-axis, left y-axis) are presented in Figure 4.13, together with information on mean annual rainfall, total amount of recharge per season and the percentage of rainfall that actually produced recharge.

**Table 4.1** Sum of precipitation and direct recharge per season and percentage of rainfall producing recharge for six rain seasons at Grootfontein, 'grey sand' profile, 1.1 m thickness, hydraulic conductivity  $K=3.3 \times 10^{-5}$  m/s, effective field capacity 65 mm

Season	Precipitation (mm)	Direct recharge (mm)	%
80/81	364	3.8	1.0
81/82	488	4.8	1.0
82/83	346	2.7	0.8
83/84	497	0.4	0.1
84/85	380	9.6	2.5
85/86	477	5.9	1.2
<b>Average</b>	<b>425</b>	<b>4.5</b>	<b>1.1*</b>

\* Weighted with rainfall amounts

Computed direct recharge varies between 0.4 mm/year and 9.6 mm/year; the weighted average is 4.5 mm/year. The percentage of recharge divided by precipitation varies between 0.1 % and 2.5 %, with a weighted average of 1.1 %. There is no obvious correlation between the total amount of precipitation and the amount of recharge: high recharge rates have been modelled in a season with only 380 mm of rainfall, and very low recharge rates have been modelled for a season with 497 mm of precipitation.

These results show the limitations of assumed simple relationships between mean annual rainfall and groundwater recharge. The paramount value of about 1 % is confirmed for areas with a thin sandy soil cover. For a similar distribution of daily rainfall, recharge rates will drop with increasing soil thickness and higher effective field capacities, and they will probably be higher in areas with less than 1 m of soil cover.

The distribution of daily precipitation is a crucial factor for the generation of groundwater recharge, as shown in Figure 4.13. The soil acts as a reservoir. The soil moisture in the reservoir is consumed by transpiration and direct evaporation. Leakage from the reservoir will increase with higher saturation (a result of the BUCKINGHAM-DARCY equation stating that hydraulic conductivity is a steady monotone function of volumetric soil water content). Therefore, only clusters of rainy days will produce high volumetric soil water contents and high initial percolation rates.

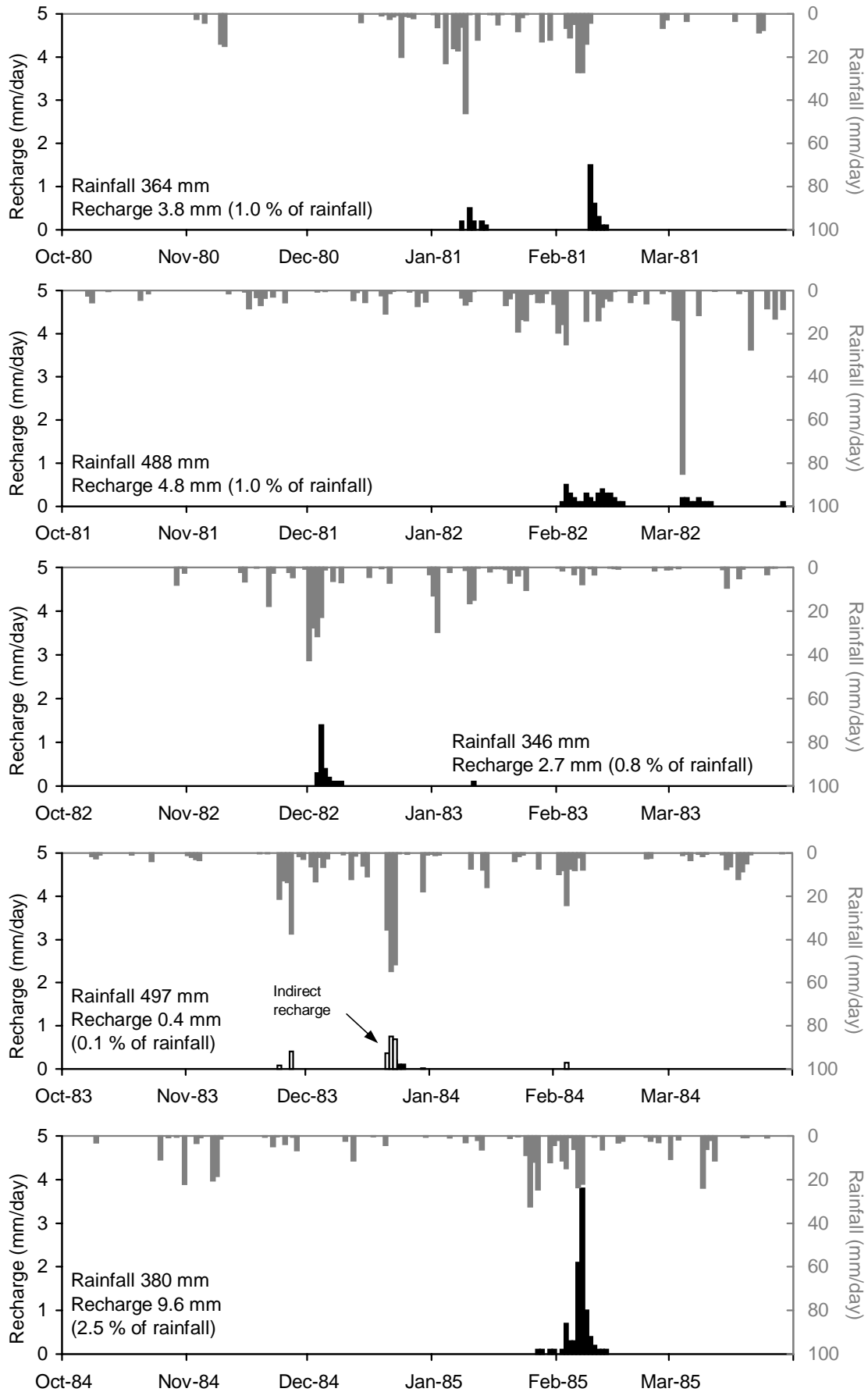


**Figure 4.13** Recharge calculation with a daily water balance model for Grootfontein 'grey sand'

The probability of groundwater recharge during the early rainy season (November to mid-January) seems to be lower than that for the second half of it (mid-January to the end of March). Although the length of the record is not sufficient for a more detailed description of the seasonal distribution of recharge, it has to be noted that in four out of six seasons recharge was modelled for the month of February; in two seasons high recharge rates were observed in the early rainy season; and in two other seasons a second recharge event followed towards the end of the rainy season.

It has been noted earlier that the soil water balance model was applied for estimating *direct* recharge, and that it is not suited for the prediction of indirect recharge resulting from surface runoff in channels and ponding in pans. During the season of '83/'84 two consecutive events with intense precipitation occurred during January. The model predicted the generation of surface runoff because the precipitation rates exceeded the soil infiltration rates. It is very likely that surface runoff triggers indirect flow components (the field evidence presented in the following chapter shows features that are relevant for this aspect). However, without the availability of good hydrological records (discharge time series, flow volumes of ephemeral rivers), and without further process studies modelling of indirect recharge components has to remain speculative. A hypothetical factor of 1 % of surface runoff becoming indirect recharge has been used in order to at least indicate the occurrence of indirect recharge.

#### *Comparison with groundwater chloride data obtained near Grootfontein*

The chloride method described in Chapter 3.1.4 was used for comparison. A wet atmospheric deposition of 0.3 to 0.9 mg/l chloride per litre of precipitation has been determined for central Namibia by MAINARDY (1999), with a weighted mean of 0.5 mg/l. Mean annual rainfall amounts to about 425 mm/y. The groundwater near Grootfontein has a chloride concentration of about 15 to 25 mg/l. Compared to the atmospheric input, chloride in groundwater has been concentrated by a factor of 30 to 50. The recharge rate corresponding to this concentration factor is 2 - 3.3 % of mean annual rainfall, or 8.5 to 14 mm/y.

This value is higher than the percentage of groundwater recharge calculated with the soil water balance model. The difference between these estimates may result from the fact that the soil water balance model only simulates direct infiltration through the soil matrix. The groundwater chloride method integrates over all recharge mechanisms including flash floods and infiltration through fractures or sinkholes. However, in comparison with other data (Chapter 1), the recharge rates obtained from chloride mass balances are high and probably represent local extremes only, rather than average recharge rates.

The aforementioned field observations strongly suggest that indirect recharge plays an important role at least in parts of the Kalahari and in the Otavi Foreland. The most promising approach for identifying and estimating indirect recharge seems to be to look at the saturated zone first and then to infer from chemical and isotopic properties of the groundwater where indirect recharge is likely to take place. The groundwater reflects indirect recharge by fluctuating levels, in some cases also by changing chemical and isotopic properties. Along this line of thinking, a thorough analysis of the hydrochemical parameters will be presented in Chapter 4.3 below.

### 4.3 Groundwater hydrochemistry

In the context of this study the effort has been made to reconstruct an existing and comprehensive hydrochemical database for the Upper Omatako basin. The dataset completely covers the study area and contains 1,531 chemical analyses for major elements and for  $\text{Sr}^{2+}$ ,  $\text{Si}$ ,  $\text{Br}^-$  and  $\text{F}^-$ . The data were initially collected by the Department of Water Affairs (DWA) in the 1980ies, during a sampling programme covering all of Namibia with the aim of producing maps of groundwater quality. Sampling of the majority of productive boreholes in Namibia, an enormous logistic effort over several years, has been documented in regional reports listing and summarizing the hydrochemical analyses and borehole characteristics (HUYSER, 1979a, b). Although a digital database had been created at that time, its content was lost during the administrative and political changes of Namibian independence. The dataset is a unique archive of hydrochemical data with good temporal homogeneity based on identical sampling and analytical procedures. Therefore the data for the Grootfontein and part of the Otjiwarongo districts were re-entered, reorganized and checked. They have been used for the generation of hydrochemical maps presented in this chapter.

The chemical data were checked for errors and inconsistencies. The charge balance was calculated for each analysis; those with an error of more than 5 % were rejected. The full table of data including borehole information on each location and its geology is given in Annex B. The majority of samples had charge balance deviations of 2 to 3 % or less, which is considered to be within the range of analytical error. The concentrations in mg/l for the cations  $\text{Ca}^{2+}$ ,  $\text{Mg}^{2+}$ ,  $\text{Na}^+$ ,  $\text{K}^+$  and  $\text{Sr}^{2+}$  and the anions  $\text{HCO}_3^-$ ,  $\text{SO}_4^{2-}$ ,  $\text{Cl}^-$ ,  $\text{F}^-$  were converted to mmol/l. For an overview, the regional distribution of hydrochemical parameters in the uppermost aquifer is presented in three different maps displaying major controls of the groundwater hydrochemistry:

- Calcium:Magnesium molar ratio (*Carbonate dissolution and precipitation reactions*)
- Strontium concentration (*Different carbonate sources: terrestrial, marine*)
- Chloride concentration (*Concentration by evaporation and - in some cases - indicator of groundwater recharge rate otherwise controlled by the dissolution of salt*)

Each map was generated by geostatistical interpolation from 1,531 analyses. Before interpolation the distance-variance relationship was analysed in the form of semi-variograms in order to check the validity of the kriging model. In all cases point kriging was used with an exponential variogram model.

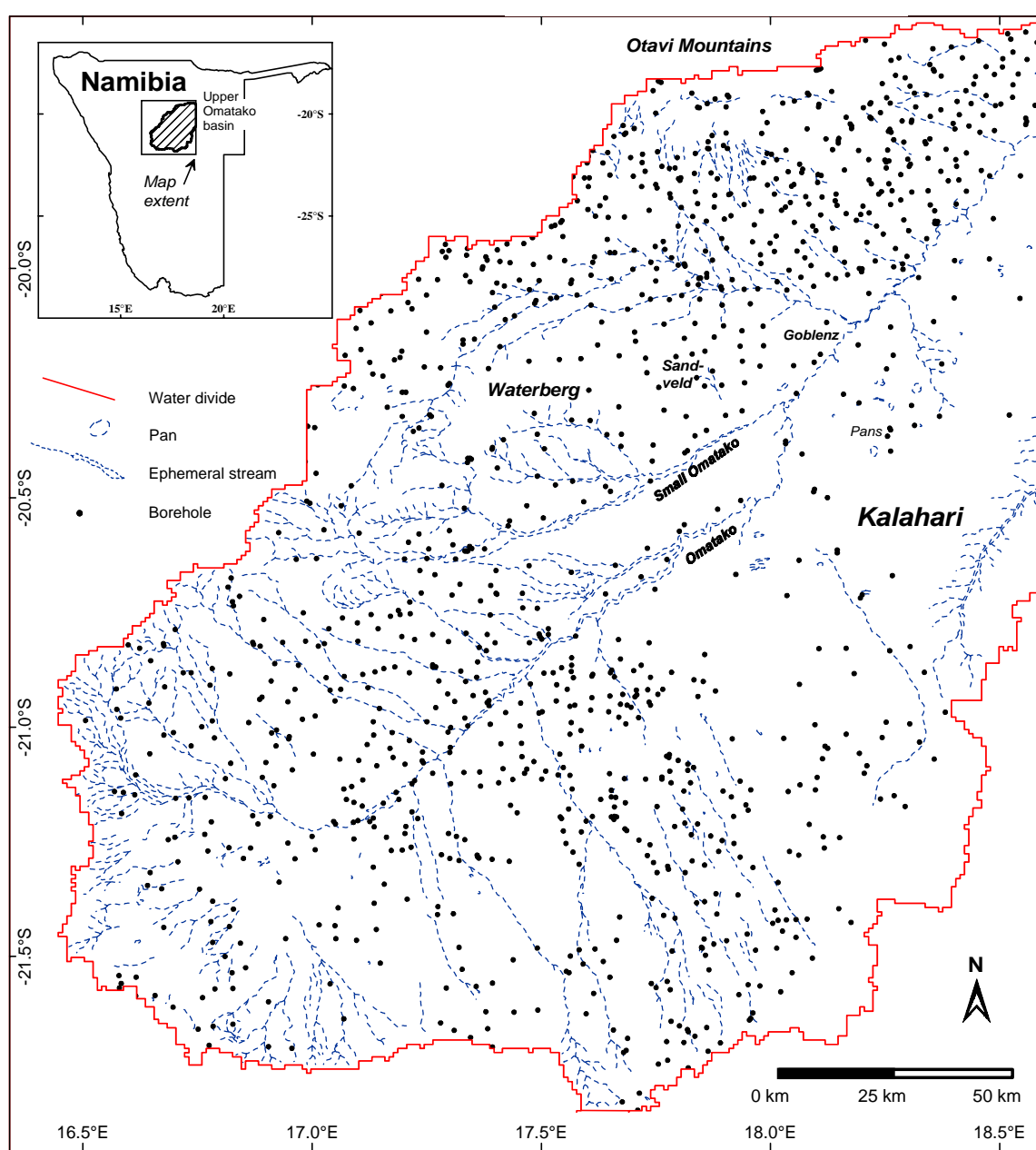


**Figure 4.14** The distribution of data on groundwater chemistry in the Omatako basin: for each point a full chemical analysis for major elements and for  $\text{Sr}^{2+}$ ,  $\text{F}^-$  is available.

### 4.3.1 Carbonate chemistry

In the study area carbonate dissolution and precipitation are an important hydrochemical control for two reasons:

- calcite and dolomite dissolution are relatively '*fast*' as compared to dissolution reactions of silicates,
- secondary carbonate is ubiquitous in soils of semi-arid areas where the activation and re-precipitation of carbonates in seasonal wetting-drying cycles are a typical features.

The major inflow sources to the Goblenz area each have a distinctly different carbonate hydrochemistry. In some outcrops of metamorphic rocks of the Damara Sequence marbles are found; dissolution of calcite has to be expected there. In the Otavi Mountains there is dolomite (Tsumeb Subgroup). The Foreland area south of the Otavi Mountains is characterized by secondary carbonates and conglomerates of Kalahari formations overlying the metamorphic Grootfontein complex. The Etjo sandstones are composed of quartzitic material with iron hydroxide bonds and contain only little carbonate.

A hydrochemical parameter displaying differences in carbonate geochemistry of the host-rock area is the molar  $\text{Ca}^{2+}:\text{Mg}^{2+}$  ratio. For dominant calcite dissolution, the molar ratio is expected to be high and well above 2.5. Dolomite dissolution theoretically results in a stoichiometric molar ratio of 1:1. However, it is more common that calcite and dolomite coexist in the aquifer. In this case, the  $\text{Ca}^{2+}:\text{Mg}^{2+}$  molar ratio is controlled by equilibrium reactions between calcite and dolomite (and site-specific factors such as the typical super-saturation of calcite due to chemical inhibitors). In general, groundwater that is fully equilibrated with calcite and dolomite has a molar ratio of  $\text{Ca}^{2+}:\text{Mg}^{2+}$  that is close to 1.3.

These hydrochemical fingerprints can be recognized in the cation triangle of the Piper diagram (Figure 4.15, lower left). Except for the group with highly mineralized groundwater with elevated  $\text{Cl}$  and  $\text{SO}_4^{2-}$ , all other samples have high percentages of  $\text{HCO}_3^-$ . The major groups each display a distinctly different cation hydrochemistry. Type (a) in Figure 4.15 corresponds to groundwater found in the Karibib marbles belonging to the Damara Sequence north of the Waterberg (Figure 2.6). The dominance of  $\text{Ca}^{2+}$  and of  $\text{HCO}_3^-$  with high  $\text{Ca}^{2+}:\text{Mg}^{2+}$  molar ratios indicates dissolution of calcite from the Karibib Formation. Group (b) has a characteristic  $\text{Ca}^{2+}:\text{Mg}^{2+}$  molar ratio between 1 and 2, with  $\text{HCO}_3^-$  as the dominant anion. This range of ratios corresponds to the stoichiometric dissolution of dolomite and of solid-solution magnesian calcites (see Chapter 3, equations 25 and 26).

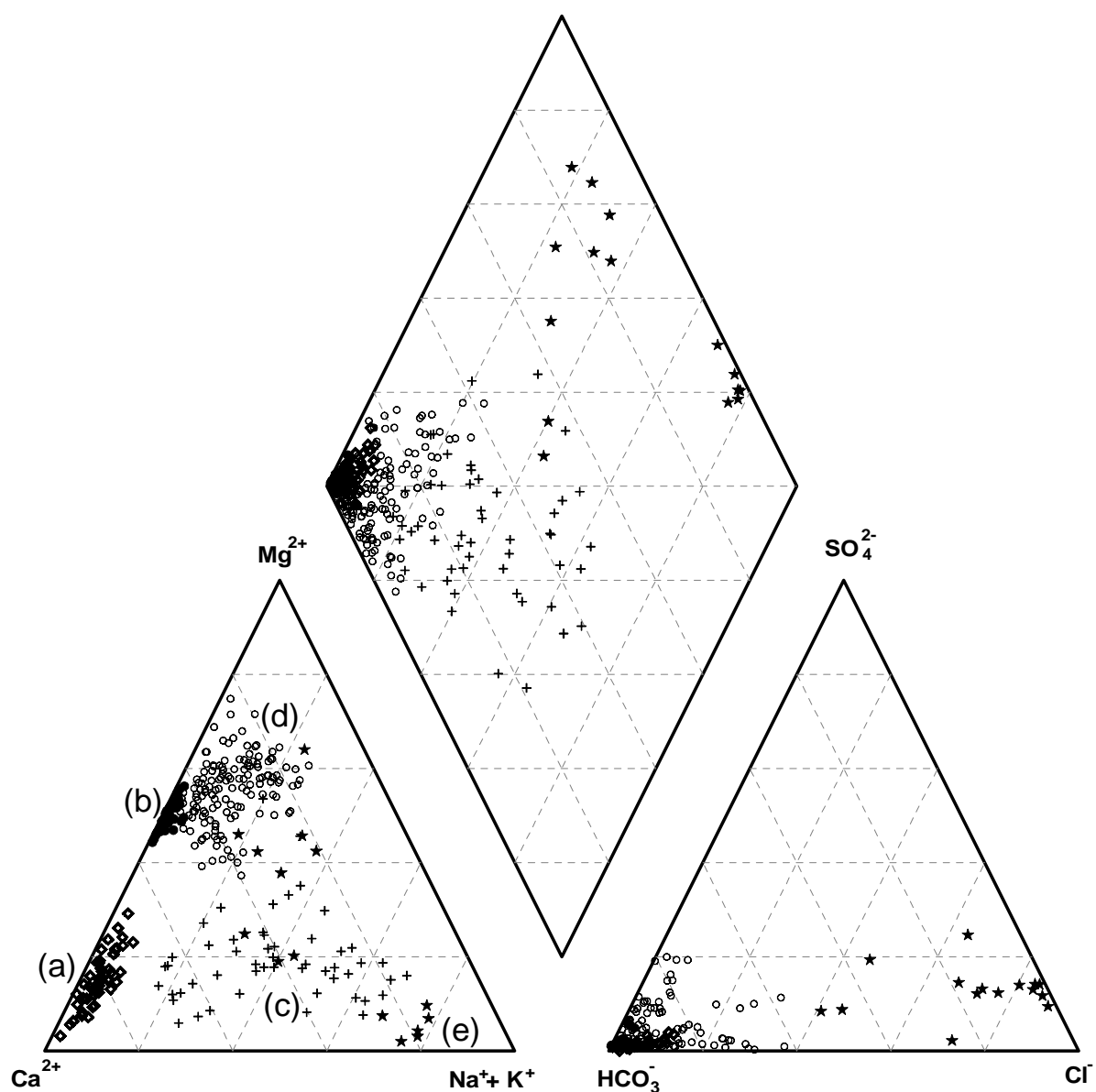


**Figure 4.15** Piper diagram of the samples of the Upper Omatako basin showing the major groundwater types: (a) marbles north of the Waterberg, b) Otavi Mountain dolomite, c) Waterberg Etjo sandstone, d) Otavi Mountain Foreland, and e) Kalahari sediments.

Groundwater forming a very narrow cluster in Figure 4.15 and having an almost balanced molar ratio between 1 and 1.3 occurs in the Otavi Mountains. Its hydrochemistry clearly points to dolomite dissolution. Boreholes with the hydrochemical signature of group (c) in Figure 4.15 (balanced  $\text{Ca}^{2+}:\text{Mg}^{2+}$  molar ratio and 20 to 40 % of  $\text{Na}^+ + \text{K}^+$ ) are located in the Waterberg area. The samples belonging to group (d) were taken in the Otavi Mountain Foreland. Precipitation of calcite is a likely cause for the relative enrichment of  $\text{Mg}^{2+}$  with respect to  $\text{Ca}^{2+}$ . Another factor for elevated  $\text{Mg}^{2+}$  concentrations can be related to the dissolution of  $\text{Mg}^{2+}$ -rich minerals in weathered dykes and gneisses of the Grootfontein metamorphic complex underlying this area.

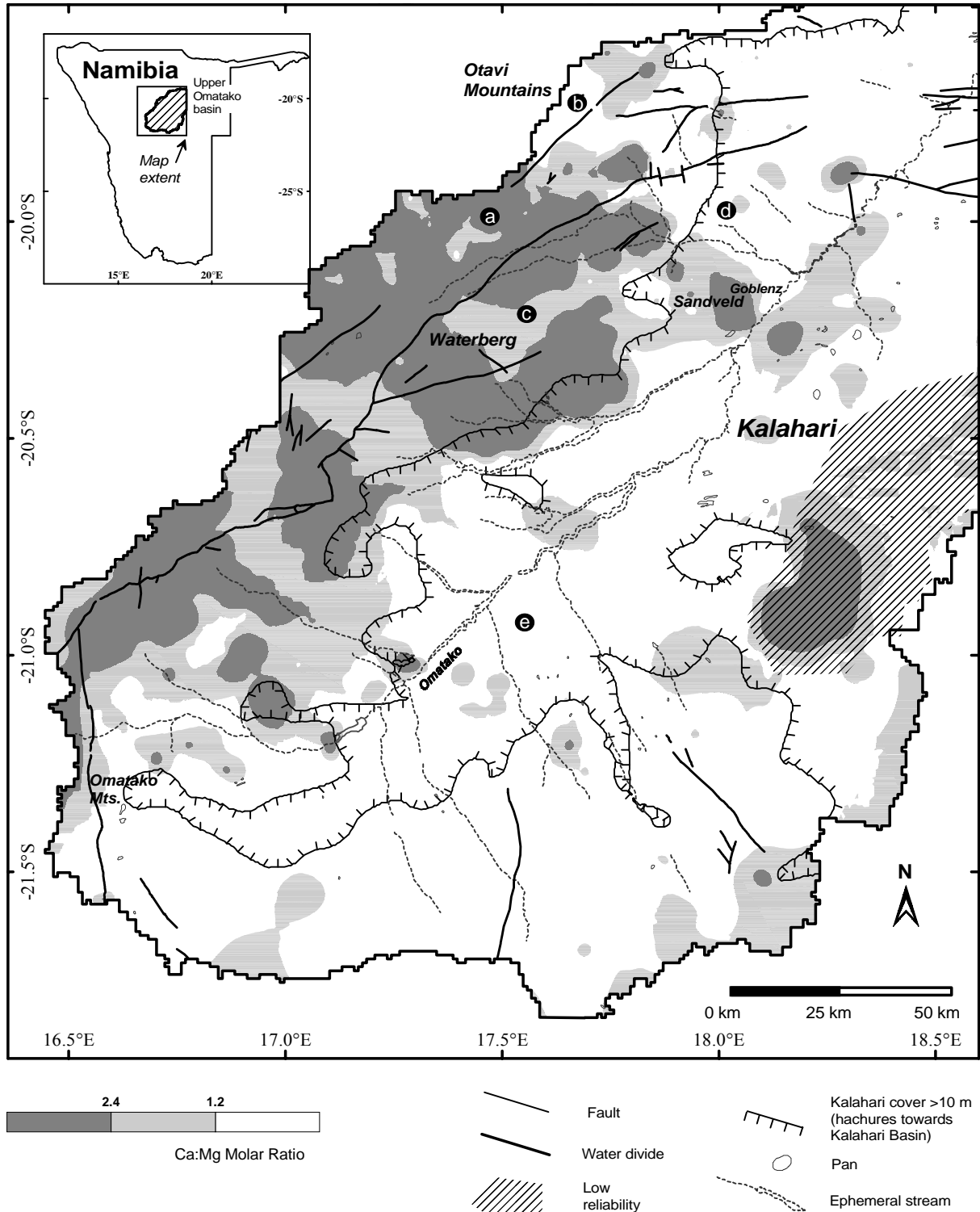


**Figure 4.16** Map of  $\text{Ca}^{2+}:\text{Mg}^{2+}$  molar ratios derived from 1531 analyses in the Upper Omatako basin: (a) Karibib Formation (marbles) north of the Waterberg, (b) Otavi Mountains (dolomite, limestone), (c) Waterberg (Etjo sandstone), (d) Otavi Mountain Foreland and (e) Kalahari sediments.

The more heterogeneous groundwater type (e) that is mainly found in the Kalahari indicates a combination of hydrochemical processes with strong evaporative enrichment. The  $\text{Ca}^{2+}:\text{Mg}^{2+}$



molar ratios have also been displayed as an interpolated raster map (Figure 4.16). This map was produced from the same 1,531 chemical analyses of the Upper Omatako basin by kriging. It shows the extent of the major groups identified above. The  $\text{Ca}^{2+}$ -rich groundwater in the north-western part of the study area, belonging to groups (a) and (c), can be clearly separated from the  $\text{Mg}^{2+}$ -rich groundwater of the Otavi Mountain Foreland (d) and the Kalahari (e). The dolomite area in the Otavi Mountains with a balanced  $\text{Ca}^{2+}:\text{Mg}^{2+}$  molar ratio (b) is relatively small.

It should be noted that the areas of  $\text{Mg}^{2+}$  enrichment in part of the Otavi Foreland area are related to shallow water tables. The same observation was made in the western part of the Kalahari along the uppermost reach of the Omatako and along the Small Omatako. A possible factor is the release and consumption of  $\text{CO}_2$  in pans and river sediments with subsequent precipitation of calcite. Calcite nodules have been found in river sediments in this area at a depth of 50 cm to 120 cm.

South of Goblenz, along the Omatako river, a plume of high  $\text{Ca}^{2+}:\text{Mg}^{2+}$  ratios extends into the Kalahari. The distribution of  $\text{Ca}^{2+}:\text{Mg}^{2+}$  molar ratios suggests that the plume results from the dissolution of calcite in the pan-belt, which is another indicator of groundwater recharge in the area. Further to the south-east there prevails the inflow of  $\text{Mg}^{2+}$ -rich groundwater.

### 4.3.2 Strontium

$\text{Sr}^{2+}$  can substitute  $\text{Ca}^{2+}$  in aragonite and in dolomite. No  $\text{Sr}^{2+}$  substitution takes place in calcite due to different ion radii. Aragonite is unstable in freshwater environments and is gradually transformed into low Mg-calcite as it equilibrates with fresh groundwater (PLUMMER ET AL., 1976). The specific Strontium geochemistry is reflected in the groundwater dissolving these different carbonate species, as long as  $\text{Sr}^{2+}$  and  $\text{Ca}^{2+}$  are not modified by additional sources or dissolution/precipitation reactions involving strontium.

In the study area the  $\text{Sr}^{2+}:\text{Ca}^{2+}$  ratio could be used as an additional criterion for the separation of groundwater from the Otavi Mountain area and of groundwater recharged in the north-western part along exposures of the Karibib Formation. Figure 4.17 shows the logarithm of the  $\text{Sr}^{2+}:\text{Ca}^{2+}$  molar ratio derived from the 1,531 analyses of the Omatako basin. Instead of absolute  $\text{Sr}^{2+}$  concentrations  $\text{Sr}^{2+}:\text{Ca}^{2+}$  ratios were used in order to remove the influence of evaporation. Dark grey areas show groundwater with a very low  $\text{Sr}^{2+}:\text{Ca}^{2+}$  ratio; light grey areas indicate higher  $\text{Sr}^{2+}:\text{Ca}^{2+}$  ratios.

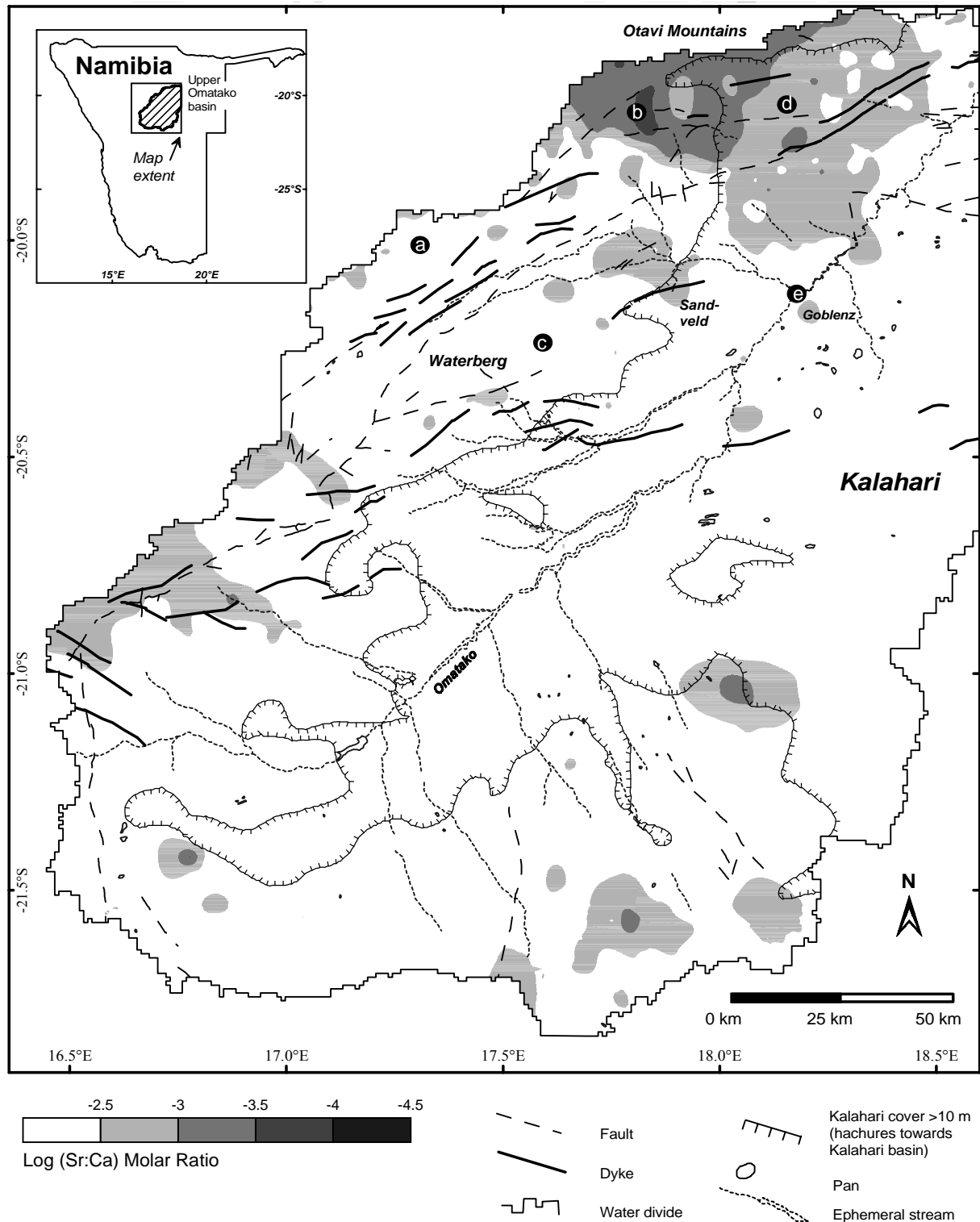


**Figure 4.17** Map of log (Sr<sup>2+</sup>:Ca<sup>2+</sup>) ratios derived from 1,531 analyses of the Upper Omatako basin: (a) Karibib Formation (marbles) north of the Waterberg, b) Otavi Mountains (dolomite, limestone), c) Waterberg (Etjo sandstone), d) Otavi Mountain Foreland, and e) Kalahari sediments.

Comparing areas having low  $\text{Sr}^{2+}:\text{Ca}^{2+}$  ratios with the geological map, there appears a pronounced correlation with the spatial extent of the northern zone of the Damara Sequence. Groundwaters of the Abenab and Tsumeb Subgroups (b) in the Otavi Mountains have particularly low  $\text{Sr}^{2+}:\text{Ca}^{2+}$  ratios ( $< 10^{-3}$ ) and can be well distinguished from groundwater in the Karibib Formation (a) and Etjo sandstone (c). Low  $\text{Sr}^{2+}:\text{Ca}^{2+}$  ratios are still found in the Otavi Foreland (d) between the Otavi Mountains (b) and Goblenz (e).  $\text{Sr}^{2+}:\text{Ca}^{2+}$  ratios provide an excellent fingerprint of outflow from the Otavi Mountains into the Otavi Foreland. In the rest of the study area, differences in  $\text{Sr}^{2+}:\text{Ca}^{2+}$  ratios are not sufficient for a hydrochemical separation.

### 4.3.3 Chloride

Chloride in the groundwater mainly originates from atmospheric input as dry fallout or solute in the precipitation, and from the dissolution of evaporites containing chloride. Only if the dissolution of evaporites can be excluded and if the atmospheric input of chloride at the time of groundwater recharge is known, groundwater chloride can be used for the calculation of concentration factors. The distribution of chloride in the groundwater (Figure 4.18) shows extreme differences in chloride content within the Omatako basin. Relatively low chloride concentrations are typical for the hard-rock outcrops, whereas high chloride concentrations are found in large parts of the Kalahari.

In general, the chloride concentration of groundwater found in aquifers not covered by Kalahari sediments is lower, ranging between 25 and 100 mg/l - with chloride concentrations of less than 25 mg/l in places. Such groundwater with very low chloride concentrations occurs in the outermost northern mountainous rim of the basin (a) and (b) in the Etjo sandstone (c). The groundwater in fractured aquifers of the Damara Sequence in the southern part of the Omatako basin (i) tends to have slightly higher chloride concentrations (around 50 mg/l) than groundwater in similar rocks further north (a).

High chloride concentrations are mainly found where the Lower Kalahari is the only available aquifer (e). There are two possible origins of elevated chloride. It is observed that in several areas high chloride contents correlate with fracture zones. This is the case in the Otavi Foreland and in the Kalahari (south of the Waterberg). The other possible source of chloride is mineralized groundwater formed at earlier times in groundwater discharge zones and still entrapped or being flushed. The groundwater of the Middle Kalahari tapped by boreholes north-east of Goblenz (f) is characterized by good water quality of much lower salinity. Chloride concentrations of groundwater found in the Kalahari south of Goblenz range between 250 and 750 mg/l, with some extreme values ( $> 5000$  mg/l).

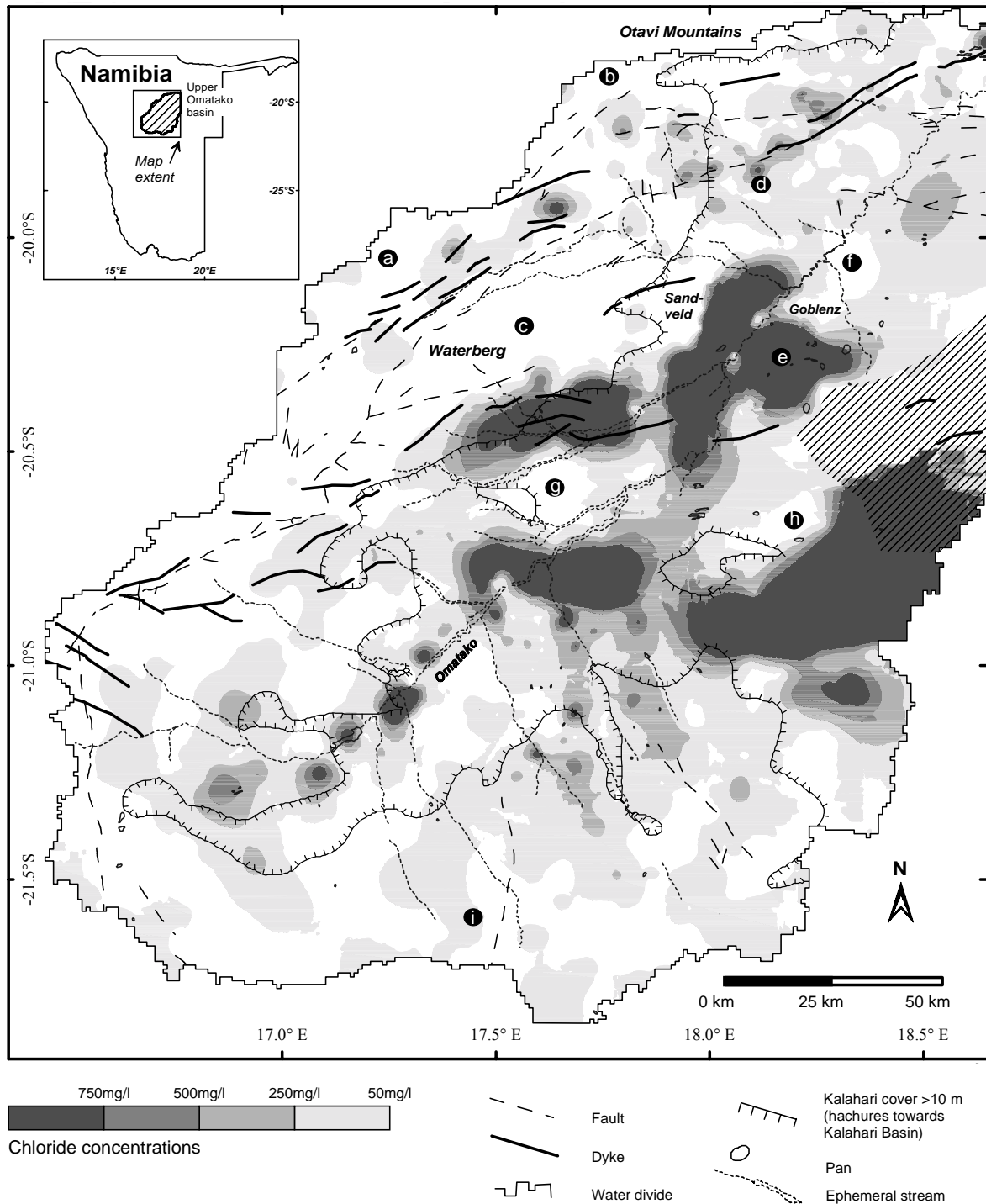


**Figure 4.18** Map of chloride concentrations: a) Karibib Formation (marbles) north of the Waterberg, b) Otavi Mountains (dolomite, limestone), c) Waterberg (Etjo sandstone), d) Otavi Mountain Foreland, e) Lower Kalahari sediments, f) Middle Kalahari, g-h) plume of fresh groundwater, and i) southern mountain rim.

Nevertheless, there are some areas where groundwater of good quality is found within the Kalahari. Two plumes of fresh groundwater can be observed downstream of two isolated basement outcrops within the Kalahari (g) and (h). These plumes indicate groundwater recharge on or around the basement outcrops: evaporation, and as a result, also the concentration of chloride is smaller in these areas than in the surrounding Kalahari.

#### 4.3.4 Cluster analysis

Hierarchical multi-element cluster analysis is used for identifying *unknown* groups within groundwater samples or geochemical data (WILLIAMS, 1982; ADAR ET AL. 1992). Hierarchical cluster analysis was performed for the definition of hydrochemical components to be used in the mixing-cell modelling. It requires a *measure of similarity* between samples and an *aggregation method*. The similarity between samples was calculated as the squared euclidian distance between the  $\text{Ca}^{2+}$ ,  $\text{Mg}^{2+}$ ,  $\text{Na}^+$ ,  $\text{HCO}_3^-$ ,  $\text{SO}_4^{2-}$  and  $\text{Cl}^-$  concentrations in mmol/l. Nitrate concentrations in the groundwater were not included, because they did not show any regular spatial pattern. In the study area nitrate probably reflects local influences (leaching from termite mounds and from manure at watering points) and does not correlate with any lithological groups.  $\text{K}^+$  was not used because of low concentrations and a high correlation with  $\text{Na}^+$ . The different clusters were then aggregated hierarchically in such a way that the variability of chemical concentrations within the cluster was minimized (Ward-method). Further details on the methodology of cluster analysis are given in BROWN (1998) and BAHRENBERG ET AL. (1992).

The hierarchical cluster analysis indicates five major hydrochemical groups. Each of them has a distinct and typical major element composition and a homogeneous degree and type of mineralization (electric conductivity and relative ion distribution). For some major groups even subgroups could be identified. They have the same typical ion distribution as the main group, but also reflect limited influences by additional hydrochemical processes or by mixing with adjoining end member groups.

For each group the major hydrochemical components have been plotted in Piper diagrams in order to show the relative percentages of cations and anions. The cation and anion distribution was interpreted in terms of characteristic dissolution/precipitation processes. In addition, electric conductivity was plotted against bicarbonate concentration in mmol/l in order to visualize the total degree and type of mineralization. The regional distribution of samples belonging to each cluster was mapped together with the extent of the geological formation from which these samples were taken.

##### *Group a - Karibib Formation*

A typical calcium-bicarbonate groundwater was identified in the western part of the study area. This hydrochemical component has typical electric conductivities between 800 and 1000  $\mu\text{S}/\text{cm}$  and contains between 7.5 and 10 mmol/l  $\text{HCO}_3^-$ . The Piper diagram in

Figure 4.19 shows that  $\text{Ca}^{2+}$  is the dominant cation and that the percentage of alkali elements  $\text{Na}^+$  and  $\text{K}^+$  is low. Still,  $\text{Mg}^{2+}$  accounts for up to 40 % of the positive electric charge. The spatial distribution of this hydrochemical component is correlated with the extent of the Karibib Formation  $N_{kb}$  (Damara Sequence) as shown on the map. It is characterized by marble bands forming characteristic outcrops that represent good aquifers in this area. The lithological composition of the source area and the hydrochemical composition of the groundwater belonging to it correspond well. Locally elevated concentrations of  $\text{Mg}^{2+}$  are observed.

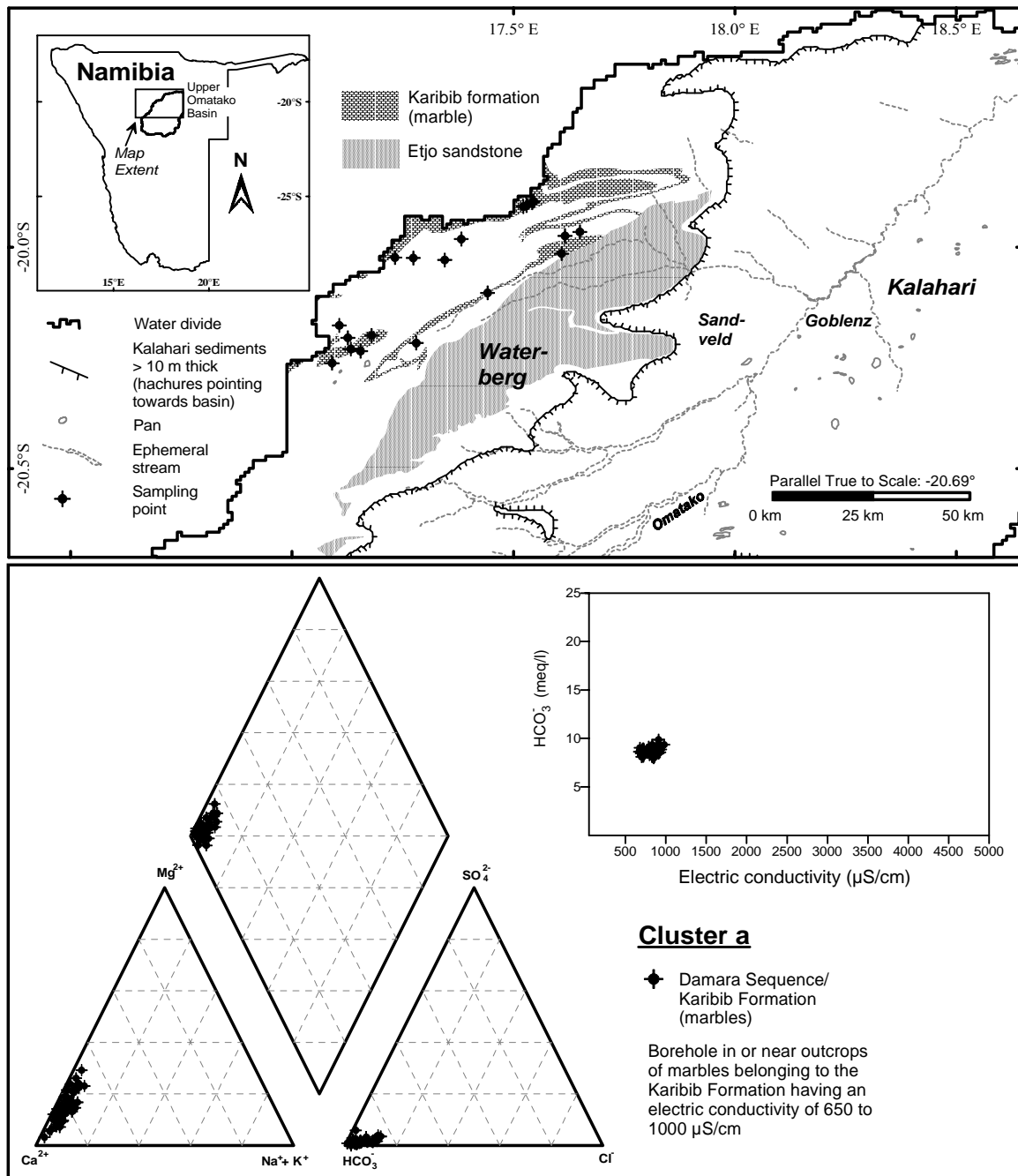
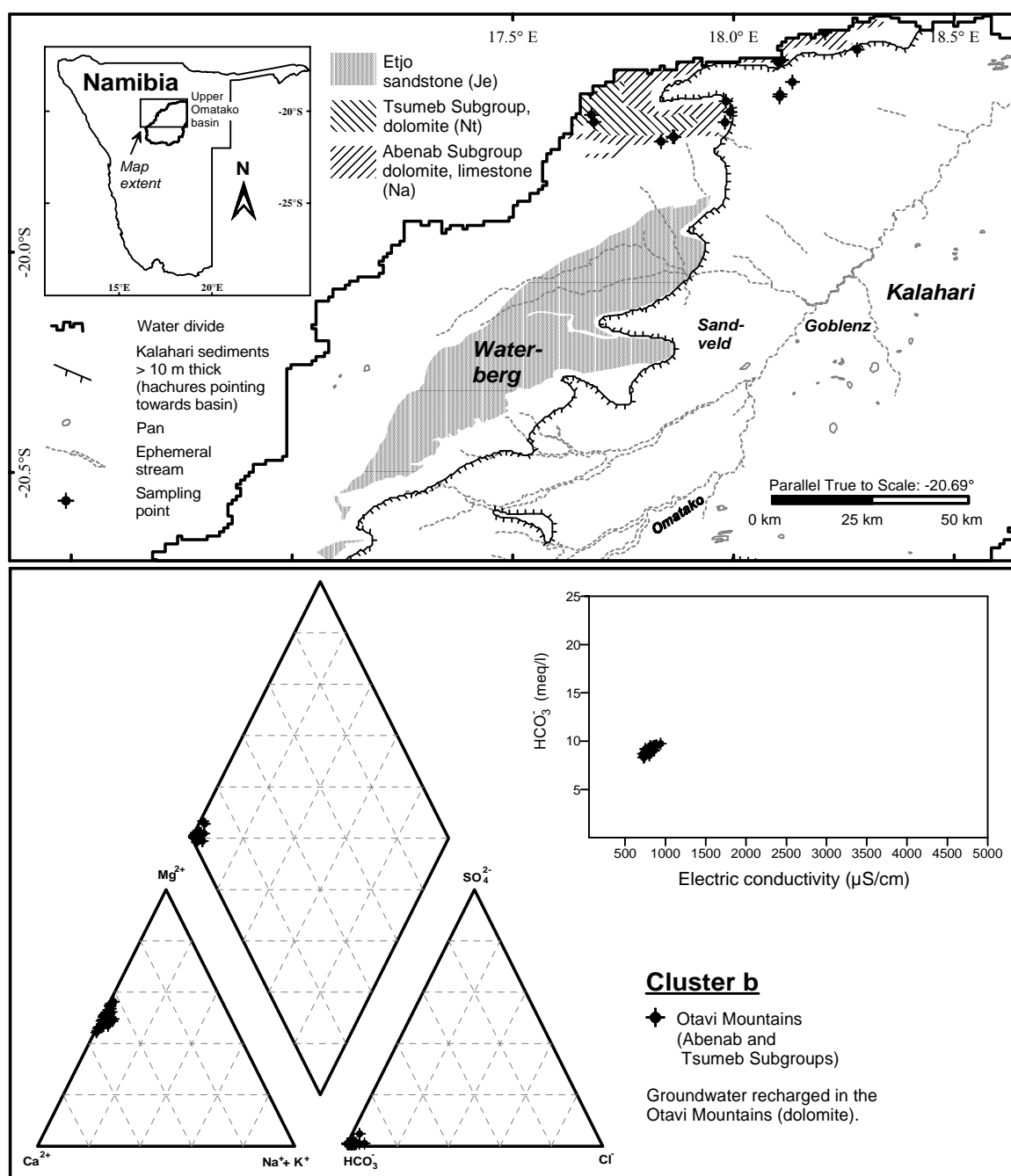


Figure 4.19 Hydrochemical characteristics of cluster a and location of samples.

### Group b - Otavi Mountains

The second major hydrochemical component consists of groundwater with a characteristic Ca:Mg molar ratio of 1 to 1.3, bicarbonate being the major anion. Groundwater samples belonging to this group have sulphate and chloride concentrations below 0.1 and 0.2 mmol/l, respectively (Figure 4.20).



**Figure 4.20** Hydrochemical characteristics of cluster b and location of samples.

The samples of this group were taken from boreholes in the Otavi Mountains. In most cases they are located in outcrops of the Tsumeb and Abenab Subgroup (Damara Sequence, Northern Zone) composed of dolomite and some limestone.

The association of cluster b with the Tsumeb and Abenab Subgroups is supported by the major element chemistry as shown in the Piper diagram (Figure 4.22). The cations are mainly composed of  $\text{Ca}^{2+}$  and  $\text{Mg}^{2+}$ , with a  $\text{Ca}^{2+}:\text{Mg}^{2+}$  ratio between 0.8 and 1.3. This balanced ratio is typical for dolomite dissolution (1.0) or dolomite dissolution in the presence of calcite (1.3). Group b has an electric conductivity ranging between 550 and 950  $\mu\text{S}/\text{cm}$  and  $\text{HCO}_3^-$  concentrations quite similar to group groundwater.

#### *Group c - Waterberg*

The third group c has a very low electric conductivity (25 to 250  $\mu\text{S}/\text{cm}$ ) and can be distinguished from all other hydrochemical groups by its very low total ion concentrations and low concentrations of  $\text{HCO}_3^-$ . The exceptional sample CN041 with 25  $\mu\text{S}/\text{cm}$  (!) was taken at the spring Waterberg No.2. The Piper diagram shows a variable relative cation and anion composition: with the exception of only two samples,  $\text{Ca}^{2+}$  concentrations are higher than the concentrations of  $\text{Mg}^{2+}$  (in meq/l). The sum of alkali cations ( $\text{Na}^+$  and  $\text{K}^+$ ), however, can reach up to 80 %.

The relatively high  $\text{Na}^+$  and  $\text{K}^+$  concentrations correlate with lower  $\text{Ca}^{2+}$  concentrations of some samples and are probably the result of cation exchange with the underlying Omingonde Formation at the aquifer base of the Etjo sandstone.  $\text{Ca}^{2+} - \text{HCO}_3^-$  water is transformed into  $\text{Na}^+ - \text{HCO}_3^-$  water by cation exchange in contact with  $\text{Na}^+$ -rich clays. Group c is also found below the Kalahari cover in the eastern part of the Waterberg (Sandveld), corresponding to the regional flow pattern towards Goblenz. A detailed analysis of the cation composition and of the relationship between electric conductivity and  $\text{HCO}_3^-$  reveals that there are actually two subgroups ( $c_1$  and  $c_2$ ).  $c_1$  has a lower electric conductivity than  $c_2$ , resulting from lower bicarbonate concentrations,  $< 1.5$  meq/l as compared to  $< 2.5$  meq/l.

Both hydrochemical subgroups are clearly associated with the Etjo sandstone aquifer. The Etjo sandstone is a reddish sandstone mainly cemented with iron-oxides. It is fractured and has less than 10 m of Kalahari cover to the west.  $\text{HCO}_3^-$  concentration depends on the partial pressure of  $\text{CO}_2$  in the soil and on the degree of equilibration between soil  $\text{CO}_2$  and infiltration water. Comparably low  $\text{HCO}_3^-$  concentrations indicate fast infiltration through fractures. Different concentrations of  $\text{HCO}_3^-$  in subgroups  $c_1$  and  $c_2$  indicate that there are differences in the recharge environment.



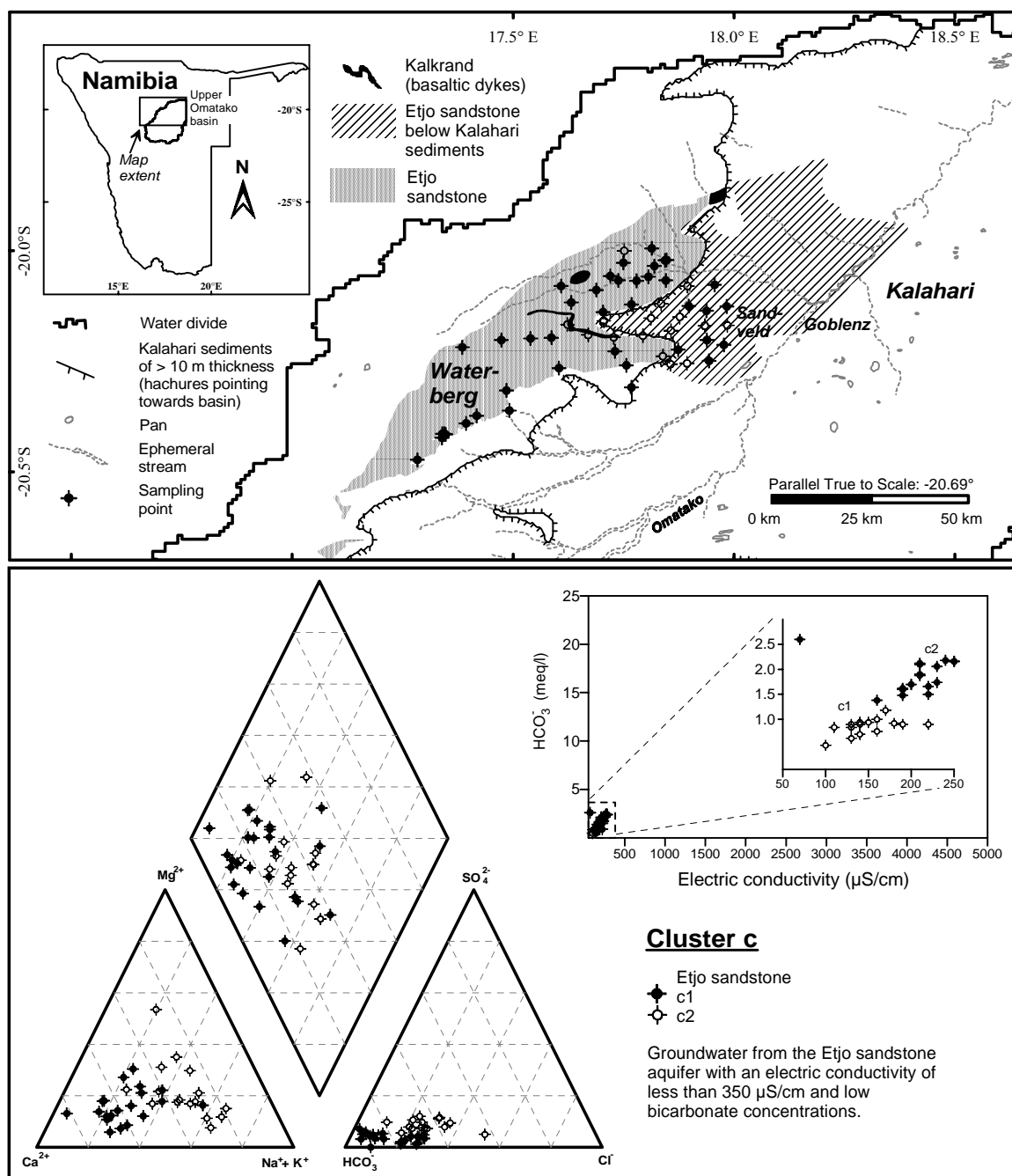


**Figure 4.21** Hydrochemical characteristics of cluster c and location of samples.

C<sub>1</sub> is mainly found downstream of outcrops of Kalkrand basalt (Figure 2.6, Figure 4.21), which could offer preferential flow paths and reduce the equilibration with soil CO<sub>2</sub>.

#### *Group d - Otavi Mountain Foreland*

The fourth major hydrochemical component still carries the fingerprint of dolomite dissolution but has a higher mineralization than group b. Groundwater belonging to this group tends to have higher Mg<sup>2+</sup> concentrations (up to 80 % of all ions in meq/l).

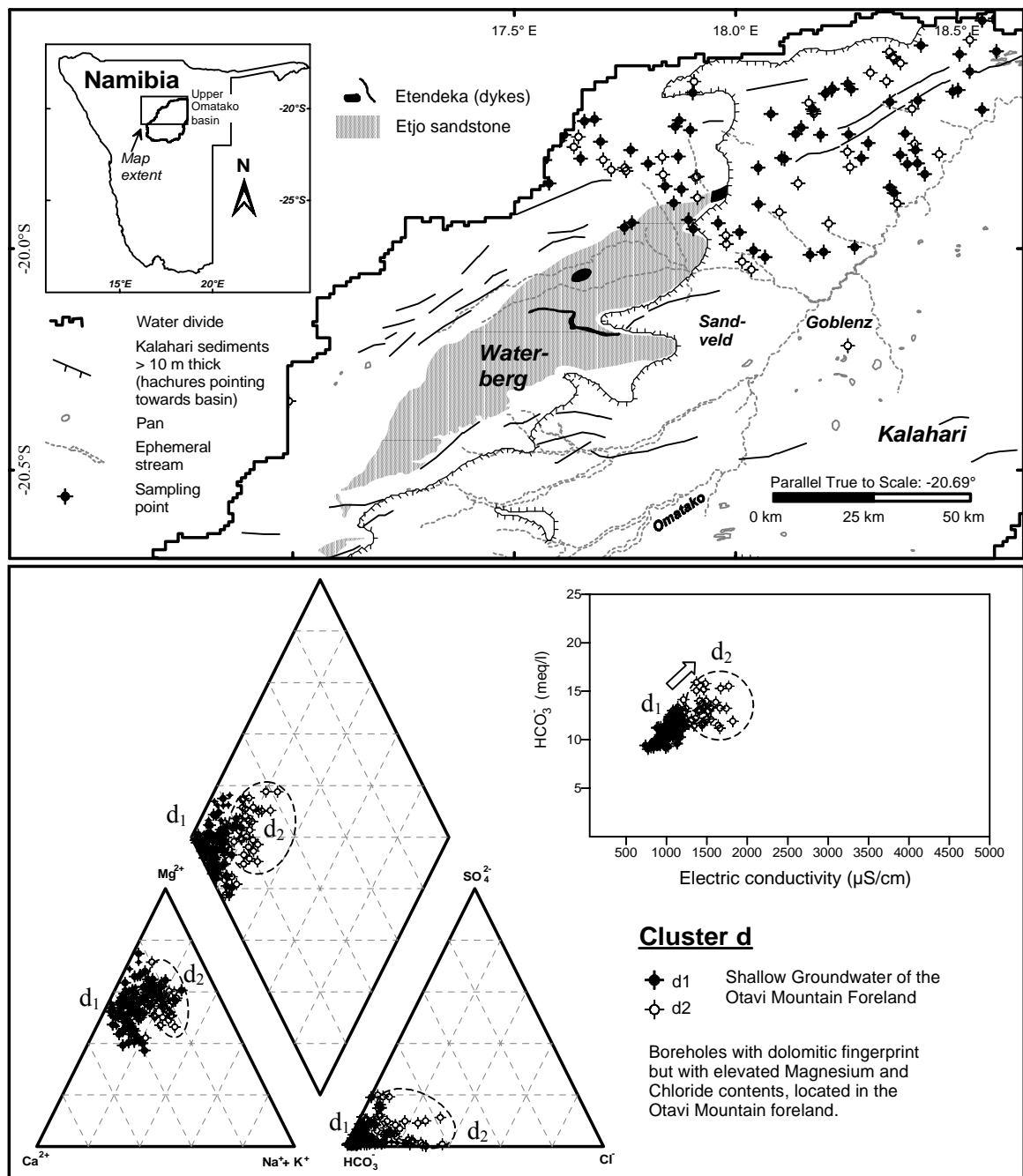


**Figure 4.22** Hydrochemical characteristics of cluster d and location of samples.

This is indicated by a general shift towards the upper part of the cation triangle in the Piper diagram ( $Mg^{2+}$ ). A comparison with group b reveals that the percentages of  $Cl^-$  and of  $SO_4^{2-}$  are also relatively higher. Electric conductivity ranges from 1,000 to 2,000  $\mu S/cm$ , and  $HCO_3^-$  concentrations are between 10 and 15 meq/l. Within group d two subgroups ( $d_1$  and  $d_2$ ) can be distinguished hydrochemically. Subgroup  $d_1$  has lower electric conductivities and  $HCO_3^-$  concentrations than subgroup  $d_2$  and also tends to have lower percentages of  $Mg^{2+}$ ,  $Cl^-$  and  $SO_4^{2-}$ , as shown in the Piper diagram. There is no obvious pattern in the spatial distribution of these two subgroups.

This groundwater type is found in the Otavi Mountain Foreland. There is no clear correlation with a geological unit as for the previous hydrochemical groups. Group d occurs in fractured rocks of the Grootfontein metamorphic complex (Mgr) and in the eastern part of the Etjo sandstone, both covered by Kalahari sediments (Tk/Mgr and Tk/Je). Based on the groundwater level contour map and on the hydrochemical characteristics, this groundwater is considered to be the outflow of the Otavi karst. The higher mineralization, as compared to groundwater type b (found directly within the Otavi karst aquifers), may result from water-rock-interactions, evaporation, or mixing with a more saline end member.

As shown in Figure 4.22, several dykes belonging to the Kalkrand Formation are found in this area. Contact with mafic minerals of weathering products derived from the Kalkrand basalt could be one reason for the elevated  $Mg^{2+}$  concentrations.

Evaporation is likely to take place in a groundwater discharge zone directly south of the Otavi Mountains in the Rietfontein area (for a delineation of this zone see the following chapter on stable isotopes). Also in other parts of the Otavi Mountain Foreland, groundwater levels are very shallow and thus allow evaporation losses causing the concentration of dissolved solids in the groundwater.

The cluster analysis shows that also other more saline hydrochemical end members exist in the Otavi Mountain Foreland. They will be discussed in the following chapter, together with other highly mineralized types of groundwater in the study area.

#### *Group e - highly mineralized groundwater*

Cluster analysis helped identify three highly mineralized groundwater types ( $e_1$ ,  $e_2$ ,  $e_3$ ) lumped together in group e. For all three types electric conductivities are above 2,000  $\mu\text{S}/\text{cm}$  and reach up to almost 20,000  $\mu\text{S}/\text{cm}$  for some samples of the Kalahari.

A sulphate-rich subgroup is found in a well-defined area ( $20.0^\circ \text{S}$ ,  $17.5^\circ \text{E}$ ) within non-differentiated metamorphic rocks of the Damara Sequence. Groundwater belonging to the subgroup  $e_1$  has an electric conductivity of about 2,000  $\mu\text{S}/\text{cm}$  and significantly higher Cl<sup>-</sup> concentrations than the groundwater types a and c in this area. The spatial extent of this group is very well defined (see Figure 4.23, map): north of the Waterberg in fractured rocks belonging to the Damara Sequence. Subgroup  $e_2$  has an electric conductivity of 5,000  $\mu\text{S}/\text{cm}$  and a significant spread in  $\text{HCO}_3^-$  concentrations. The relative cation composition resembles that of group d, but the anion composition is much different: The major anion is chloride with only slightly elevated  $\text{SO}_4^{2-}$  concentrations.

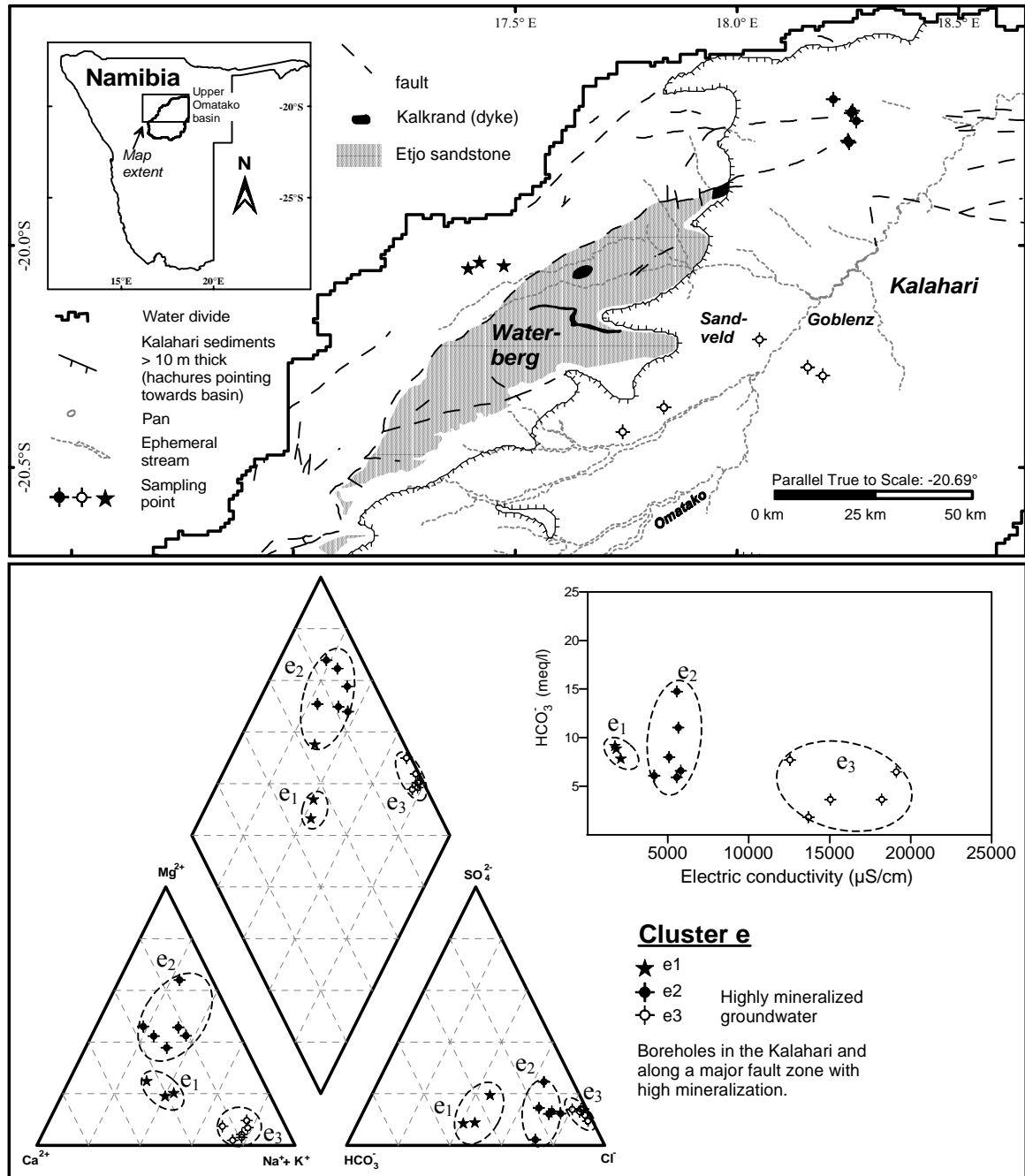


**Figure 4.23** Hydrochemical characteristics of cluster e and location of samples.

Subgroup  $e_2$  is found in the Otavi Mountain Foreland in a well defined area. Both subgroups  $e_1$  and  $e_2$  are located on major fault zones as shown in Figure 4.23 (map). It is therefore assumed that these groups derive from deeper aquifers. Subgroup  $e_3$  represents a highly mineralized  $Na^{+}-Cl^{-}$ -type groundwater with an electric conductivity ranging between 10,000 and 20,000  $\mu S/cm$ . It is known from previous investigations in the study area (DEPARTMENT OF WATER AFFAIRS, 1993) that highly mineralized groundwater exists in the Lower Kalahari, especially west of Goblenz. The average concentrations in meq/l of all major hydrochemical clusters are plotted in Figure 4.23 together with their respective standard deviations.

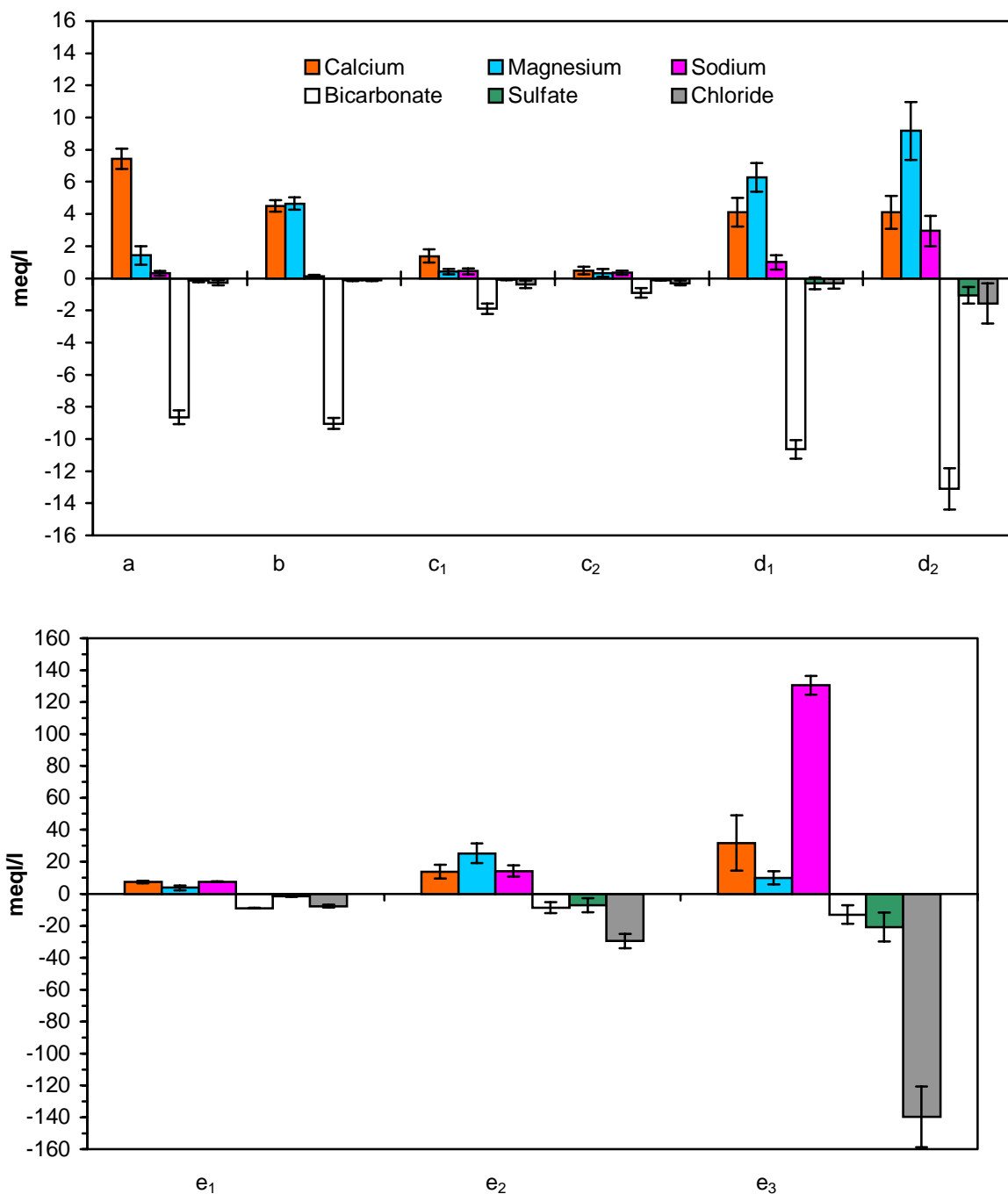


**Figure 4.24** Average concentrations of major hydrochemical groups in the study area in meq/l. Groups a-d<sub>2</sub> and e<sub>1</sub>-e<sub>3</sub> have different scales: the range of e<sub>1</sub>-e<sub>3</sub> is 10 x larger!

Positive values correspond to the charge of cations, negative values to the respective charge of anions. Potassium was not plotted due to very low concentrations, nitrate was omitted due to its extreme variability. The lower graph with groups e<sub>1</sub>, e<sub>2</sub> and e<sub>3</sub> has the tenfold range of concentrations!

Calcite and dolomite dissolution of group a and b can easily be recognised from Ca<sup>2+</sup> and Mg<sup>2+</sup> concentrations. Figure 4.24 also highlights the exceptionally low mineralization of

groups  $c_1$  and  $c_2$ . The difference between  $d_1$  and  $d_2$  is caused by an increase in  $Mg^{2+}$ ,  $SO_4^{2+}$  and  $Cl^-$  from group  $d_1$  to  $d_2$ . It is interesting to note that group  $e_2$  found in the Otavi Foreland has a major ion profile that is similar to the source causing the salinization of  $d_2$ . From Figure 4.24 the suitability of individual tracers and of tracer combinations for mixing-cell calculations (Chapter 4.5) can easily be checked: the variability between groups must be higher for all chosen components than the internal variability.  $Ca^{2+}$  concentrations within  $d_1$  and  $d_2$  vary strongly and will not help to discriminate mixing ratios from these sources.

In conclusion,

- the dominant hydrochemical processes in the study area are fast carbonate dissolution/precipitation reactions. Other mineral phases obviously are of minor importance due to low reaction rates, causing only modifications of the main groups a, b and c.
- Each of the different hydrochemical end members a, b, c and d could be regionalized and linked to hydrogeological units. Three potential source areas have thus been identified: the calcitic groundwater of group a has been linked to the marbles of the Karibib Formation; group b correlates with dolomite formations in the Tsumeb and Abenab subgroups; and, finally, group c with its extremely low mineralization corresponds to the Etjo sandstone aquifer and could be traced even into the Kalahari.
- The fourth group d apparently undergoes evaporation leading to increased ion concentrations. A more detailed study on the effect of evaporation in this area will be presented in the following chapter on stable isotopes.
- North of the Waterberg, in the Otavi Foreland area and in the Kalahari deeper aquifers with more mineralized groundwater need to be included as additional sources into the conceptual flow model.

#### **4.4 Detailed sampling in the Goblenz area**

For a detailed hydrochemical characterization of groundwater in the Goblenz area two sampling campaigns took place in 1997 and 1998. Samples of 1 litre were taken for major ion analysis. Electric conductivity and pH were determined in the field. Temperature correction for electric conductivity was made for 25 °C.

The objective of these sampling campaigns was to study the extent of temporal variations by repeated sampling and to gather more detailed analyses along selected flow-paths. The analytical error for all samples was below  $\pm 3.5\%$ . Major element concentrations were

determined by ion chromatography;  $\text{HCO}_3^-$  was analysed by titration. Saturation indices (abbreviated as s.i.) calculated for calcite and gypsum and the sum of  $\text{CO}_2$  as the sum of all dissolved carbon dioxide species in water are presented in Table 4.2.

#### 4.4.1 Hydrochemistry in the Goblenz area

Although an extensive dataset of hydrochemical analyses already exists (see previous chapter), additional sampling was important for several reasons:

- Changes in time of the hydrochemical composition of groundwater might prevent the application of a steady-state mixing model. Re-sampling was therefore important for checking the validity of steady-state conditions.
- Saturation indices were calculated in order to check the dissolution/precipitation potential of the groundwater with respect to calcite and gypsum. This information is important for the application of the mixing-cell model due to the required conservative tracer behaviour.
- For most of the stable isotope analyses, the hydrochemical composition was determined in order to assign the sample to one of the hydrochemical groups (a), (b), (c), (d) or (e). The combined interpretation of hydrochemistry and stable isotopes allowed to study groundwater with different hydrochemical and isotopic evolution separately.
- For all  $^{14}\text{C}$  samples hydrochemical analysis was made for thermodynamic mass balance calculations (i.e. saturation indices of calcite) as an indicator of possible carbonate dissolution and the resulting addition of  $^{14}\text{C}$  free inorganic carbon.

Figure 4.25 shows the location of boreholes that were sampled for major ions during the sampling campaigns 1997 and 1998. The hydrochemical data, the location names and the coordinates are given in Table 4.2. The outcrops of Etjo sandstone are marked as dark grey areas for orientation. Areas with a cover of Kalahari sediments more than 10 m thick are shown in light grey.

In Figure 4.25, three selected boreholes are highlighted with frames: **CN017**, **CN021** and **CN081**. For these boreholes a comparison of the hydrochemical composition in 1997 (late southern winter, July/August) and in 1998, just after the rainy season, was made.

The map also contains the location of three profiles AG (Waterberg), BG (Otavi Foreland) and EG (Kalahari), along groundwater flow lines towards Goblenz (G). Along these profiles the hydrochemical evolution of groundwater was studied.

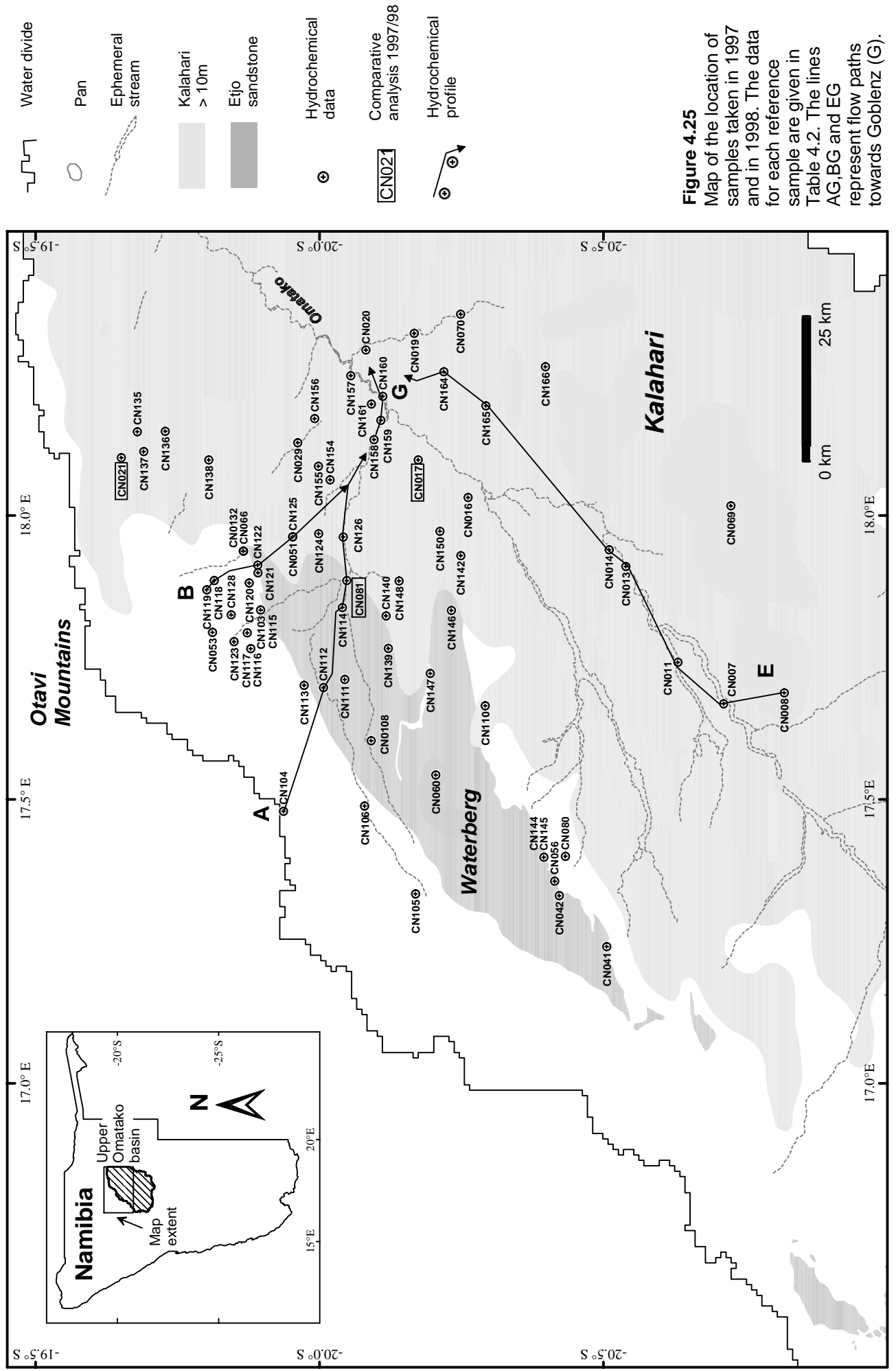


**Figure 4.25**

Map of the location of samples taken in 1997 and in 1998. The data for each reference sample are given in Table 4.2. The lines AG, BG and EG represent flow paths towards Goblenz (G).



**Table 4.2** Hydrochemistry of groundwater samples taken in the vicinity of Goblenz

sample	locality	longitude °E	latitude °S	date	ec µS/cm	pH	Ca <sup>2+</sup>	Mg <sup>2+</sup>	Na <sup>+</sup>	← meq/l			Cl <sup>-</sup>	analytical error (%)	s.i.* calcite	s.i.* gypsum	sCO <sub>2</sub>
										K <sup>+</sup>	HCO <sub>3</sub> <sup>-</sup>	SO <sub>4</sub> <sup>2-</sup>					
CN007	Okahitwa	17.6682	-20.7119	Jun-97	4590	8.4	4.00	1.96	35.49	0.24	7.49	9.73	0.05	22.42	0.8	-0.6	7.5
CN008	Ovitatu	17.6873	-20.8187	Jun-97	2401	7.5	6.08	7.92	11.35	0.49	8.00	6.87	1.19	8.74	0.8	-0.5	8.4
CN011	Omatanga	17.7414	-20.6312	Jun-97	5140	7.3	6.12	4.96	40.45	0.38	7.80	12.68	4.44	23.69	0.3	-0.3	8.4
CN013	Ombujomenje	17.9100	-20.5398	Jun-97	8875	7.2	10.00	13.00	56.55	0.90	8.39	21.81	0.64	51.62	0.4	0.0	9.2
CN014	Okaipe	17.9397	-20.5100	Jun-97	220	7.8	1.64	0.48	0.18	0.18	2.34	0.08	0.01	0.08	0.1	-3.1	2.4
CN016	Ojituwa	18.0315	-20.2618	Jun-97	1280	7.6	1.16	1.64	11.88	0.59	14.51	0.10	0.14	0.54	0.4	-3.4	15.2
CN017	Okambora	18.0978	-20.1738	Jun-97	489	7.6	3.96	1.14	0.19	0.31	5.10	0.06	0.11	0.17	0.6	-3.0	5.3
CN019	Omitjete	18.3208	-20.1671	Jun-97	1079	7.5	4.28	4.40	3.44	0.54	9.01	0.18	0.19	2.99	0.6	-0.7	9.5
CN020	Okomuparara	18.2913	-20.0817	Jun-97	5560	6.7	16.79	18.92	26.97	0.69	20.42	9.16	0.09	34.98	0.6	-0.7	26.6
CN021	Tiefwasser	18.1017	-19.6510	Jun-97	777	7.5	3.56	4.82	0.56	0.02	7.70	0.19	0.33	0.93	0.6	-2.6	8.1
CN029	Schwarzfelde	18.1278	-19.9618	Jun-97	1398	7.1	6.84	6.72	2.06	0.04	9.80	0.65	2.07	2.78	0.5	-1.9	11.1
CN041	Waterberg No2	17.2404	-20.5059	Jun-97	25	6.8	0.12	0.18	0.07	0.06	0.22	0.02	0.04	0.16	-0.3	-4.7	0.3
CN042	Okomumbonde	17.3303	-20.4224	Jun-97	234	7.5	1.70	0.30	0.61	0.08	1.95	0.51	0.03	0.13	-0.2	-2.3	2.1
CN051	Omambondetal Nord	17.9625	-19.9529	Jul-97	862	7.3	3.36	6.81	0.68	0.06	10.70	0.29	0.02	0.11	0.5	-2.5	11.6
CN053	Salzbrunnen Farm	17.7940	-19.8117	Jul-97	1861	6.9	7.90	13.23	3.25	0.16	12.01	10.56	0.25	0.63	0.4	-0.7	14.4
CN056	Waterberg Tief	17.3559	-20.4141	Jul-97	317	6.9	2.06	0.22	0.80	0.12	2.70	0.16	0.20	0.17	-0.5	-2.8	3.3
CN060	Panorama	17.5430	-20.2049	Jul-97	141	6.4	0.53	0.26	0.26	0.21	1.09	0.04	0.04	0.07	0.5	-3.8	1.9
CN066	Hairbib Heiße Quelle	17.9371	-19.8660	Jul-97	4974	6.5	13.54	14.37	30.84	1.85	33.45	4.26	0.00	21.49	0.5	-1.0	49.9
CN069	Ohamuheke	18.0170	-20.7247	Jul-97	1972	6.9	4.98	0.24	13.27	0.07	2.49	2.83	0.01	14.10	0.1	-1.9	3.0
CN070	Otjisepa	18.3545	-20.2484	Jul-97	12540	6.9	18.18	12.59	98.31	1.74	7.71	18.95	0.93	108.32	0.3	-0.5	9.1
CN080	Okatjkona	17.3995	-20.4331	Jul-97	666	7.7	1.90	0.41	3.65	0.12	1.61	0.31	0.18	4.23	-0.1	-2.6	1.7
CN081	Omambonde Ost	17.8856	-20.0478	Jul-97	592	7.9	1.98	1.27	1.65	0.90	5.13	0.36	0.10	0.48	0.6	-2.5	5.3
CN103	Gai Kaisa	17.8335	-19.8963	Mar-98	1263	6.8	5.98	4.48	0.63	0.07	9.73	0.31	0.39	0.19	0.2	-2.2	12.4
CN104	Harubib	17.4791	-19.9363	Mar-98	1506	6.8	9.65	1.36	1.37	0.58	8.88	0.94	0.91	2.56	0.3	-1.5	11.3
CN105	Oase	17.3334	-20.1692	Mar-98	950	6.7	7.94	0.84	0.47	0.04	8.01	0.43	0.49	0.21	0.1	-1.9	10.8
CN106	Gutweide Haus	17.4885	-20.0796	Mar-98	743	6.8	5.71	0.82	0.32	0.10	6.80	0.26	0.23	0.01	0.0	-2.2	8.7
CN108	Rimini Farm	17.6032	-20.0908	Mar-98	188	6.7	0.86	0.22	0.36	0.20	1.44	0.08	0.00	0.13	-0.2	-3.4	2.0
CN110	Bisepan	17.6648	-20.2920	Mar-98	643	7.5	2.90	0.22	2.95	0.05	3.13	2.32	0.20	0.68	0.1	-1.5	3.3
CN111	B.-Bach Wilhelmsfeld	17.7112	-20.0445	Mar-98	197	6.5	0.96	0.35	0.27	0.18	1.54	0.07	0.00	0.11	0.6	-3.4	2.4
CN112	B.-Bach Mittelposten	17.6967	-20.0069	Mar-98	464	7.0	2.97	0.81	0.39	0.14	4.22	0.09	0.16	0.02	-0.2	-2.9	5.0
CN113	Breitenbach Farm	17.7007	-19.9730	Mar-98	941	6.7	6.31	1.79	1.02	0.09	8.92	0.24	0.31	0.22	0.1	-2.3	12.0
CN114	Omambonde West	17.8378	-20.0403	Mar-98	240	6.5	0.87	0.37	0.54	0.32	1.63	0.14	0.24	0.19	-1.6	-3.1	2.6
CN115	Gai Kaisa Farm	17.8324	-19.8967	Mar-98	947	6.8	9.12	2.07	0.42	0.03	10.34	0.26	0.31	0.09	0.4	-2.1	13.1
CN116	Osambusatjuru	17.7656	-19.8789	Mar-98	896	6.8	7.51	2.40	0.18	0.02	10.03	0.20	0.17	0.01	0.3	-2.3	12.7
CN117	Gai Kaisa West	17.7933	-19.8725	Mar-98	932	6.8	8.25	0.98	0.20	0.02	9.19	0.10	0.21	0.12	0.3	-2.5	11.7
CN118	Hochkamp Farm	17.8853	-19.8144	Mar-98	1049	7.0	4.98	6.63	0.24	0.02	10.85	0.11	0.05	0.14	0.3	-2.8	12.7

**Table 4.2 (continued)** Hydrochemistry of groundwater samples taken in the vicinity of Goblenz

sample	locality	longitude °E	latitude °S	date	ec µS/cm	pH	Ca <sup>2+</sup>	Mg <sup>2+</sup>	Na <sup>+</sup>	K <sup>+</sup>	HCO <sub>3</sub> <sup>-</sup>	SO <sub>4</sub> <sup>2-</sup>	NO <sub>3</sub> <sup>-</sup>	Cl <sup>-</sup>	analytical error (%)	s.i.* calcite	s.i.* gypsum	sCO <sub>2</sub>
CN119	Hochkamp No. 14	17.8693	-19.8014	Mar 98	850	7.1	4.45	5.47	0.36	0.02	9.90	0.06	0.05	0.14	0.8	0.4	-3.0	11.2
CN120	Gunuchas Windmotor	17.8812	-19.8760	Mar 98	1099	6.8	5.03	7.20	1.34	0.07	12.42	0.48	0.09	0.14	1.9	0.2	-2.1	15.7
CN121	Gunuchas Haus	17.8989	-19.8919	Mar 98	2082	6.2	11.33	8.81	4.77	0.31	23.37	1.60	0.53	1.13	-2.7	0.1	-1.4	47.3
CN122	Gunuchas E-Pumpe	17.9125	-19.8911	Mar 98	1679	6.5	4.90	11.95	5.38	0.11	15.47	4.53	0.04	1.06	2.9	-0.1	-1.3	23.5
CN123	Gesundbrunnen	17.7778	-19.8495	Mar 98	910	6.6	7.72	3.32	0.27	0.02	10.13	0.24	0.25	0.03	3.1	0.1	-2.2	14.5
CN124	Omambondetal	17.9678	-19.9987	Mar 98	1273	7.0	4.03	9.64	2.56	0.15	13.06	1.98	0.04	0.68	2.0	0.3	-1.6	15.2
CN125	Omambondetal Nord	17.9625	-19.9529	Mar 98	905	7.4	3.27	7.07	0.95	0.06	10.88	0.21	0.07	0.02	0.8	0.6	-2.6	11.6
CN126	Omambondetal Haus	17.9621	-20.0417	Mar 98	552	7.7	2.50	2.42	1.16	0.16	5.54	0.26	0.43	0.10	-0.8	0.5	-2.5	5.7
CN128	Schönhausen	17.8250	-19.8445	Mar 98	1212	7.2	4.31	9.01	1.79	0.06	13.55	0.76	0.08	0.05	2.5	0.5	-2.0	15.0
CN132	Hairabib Haus	17.9371	-19.8659	Mar 98	1508	7.1	4.36	12.10	2.52	0.09	13.98	0.32	0.32	3.80	1.8	0.4	-2.4	15.8
CN135	Kikuyu	18.1475	-19.6794	Mar 98	941	7.1	4.30	6.20	0.93	0.02	10.06	0.02	0.34	0.49	2.4	0.3	-3.4	11.4
CN136	Okamutombe Farm	18.1481	-19.7284	Mar 98	921	7.1	5.03	5.74	0.44	0.01	10.54	0.02	0.15	0.17	1.6	0.4	-3.4	12.0
CN137	Okamutombe Nord	18.1124	-19.6903	Mar 98	1148	7.0	4.88	7.55	1.18	0.04	11.29	0.17	0.69	1.07	1.6	0.3	-2.6	13.2
CN138	Havelberg	18.0978	-19.8050	Mar 98	923	7.0	5.00	5.46	0.88	0.01	10.37	0.07	0.02	0.30	2.6	0.3	-2.9	12.1
CN139	Omega Groote Pos	17.7656	-20.1210	Mar 98	143	7.1	0.42	0.35	0.27	0.27	0.75	0.08	0.16	0.25	2.9	-1.6	-3.7	0.9
CN140	Omega Kral	17.8231	-20.1173	Mar 98	287	6.3	0.69	0.62	0.44	0.37	0.51	0.09	0.86	0.76	-2.1	-2.4	-3.4	1.0
CN142	Grenswag	17.9289	-20.2488	Mar 98	242	5.5	0.97	0.43	0.43	0.29	1.35	0.03	0.30	0.48	-0.8	-2.6	-3.7	9.3
CN144	Waterberg Flach	17.3538	-20.4119	Mar 98	289	7.3	1.96	0.18	0.66	0.11	2.68	0.14	0.07	0.07	-1.0	-0.3	-2.8	2.9
CN145	Okatjikona	17.3982	-20.3953	Mar 98	375	7.6	1.60	0.08	2.11	0.05	3.54	0.06	0.13	0.20	-1.3	0.1	-3.3	3.7
CN146	Leo	17.8328	-20.2323	Mar 98	117	6.6	0.27	0.18	0.56	0.15	0.75	0.07	0.09	0.30	-1.9	-2.3	-3.9	1.1
CN147	Diepwater	17.7219	-20.1952	Mar 98	151	6.5	0.47	0.26	0.42	0.25	0.76	0.06	0.08	0.52	-0.7	-2.2	-3.8	1.2
CN148	Tolnel	17.8846	-20.1404	Mar 98	117	6.6	0.28	0.23	0.20	0.25	0.69	0.02	0.07	0.18	-0.1	-2.3	-4.5	1.0
CN150	Hirschgrund	17.9721	-20.2122	Mar 98	258	5.6	0.62	0.34	0.89	0.49	2.04	0.01	0.11	0.20	-0.8	-2.6	-4.3	12.3
CN154	Kabare	18.0623	-20.0187	Mar 98	799	7.3	3.31	5.13	0.81	0.05	9.35	0.06	0.02	0.04	-0.9	0.4	-3.1	10.2
CN155	Oktrooi	18.0865	-19.9979	Mar 98	783	7.3	4.22	4.11	0.16	0.08	8.46	0.04	0.27	0.19	-2.2	0.5	-3.2	9.2
CN156	Schönau	18.1707	-19.9914	Mar 98	950	7.2	4.92	5.41	0.18	0.04	9.12	0.08	0.29	0.69	1.8	0.4	-2.9	10.2
CN157	Ongongoro	18.2461	-20.0549	Mar 98	1196	7.7	3.47	6.21	3.94	0.16	11.39	0.90	0.17	1.10	0.8	0.8	-2.0	11.8
CN158	Koblenz NW	18.1335	-20.0959	Mar 98	820	7.6	3.73	4.49	0.77	0.15	9.13	0.17	0.01	0.23	-2.1	0.8	-2.6	9.5
CN159	Koblenz SW	18.1677	-20.1081	Mar 98	984	7.2	4.21	4.53	2.17	0.15	10.32	0.04	0.07	0.44	0.9	0.5	-3.2	11.4
CN160	Koblenz S	18.2096	-20.1116	Mar 98	1002	7.2	5.69	2.54	2.68	0.25	9.72	0.75	0.11	0.88	-1.3	0.5	-1.8	10.9
CN161	Koblenz E	18.1958	-20.0915	Mar 98	1006	7.8	4.50	5.01	2.81	0.15	10.01	0.77	0.06	0.94	2.8	1.1	-1.9	10.3
CN164		18.2532	-20.2190	Mar 98	1480	7.0	8.24	4.51	4.47	0.28	13.49	1.25	0.06	3.05	-1.0	0.4	-1.0	15.7
CN165		18.1930	-20.2932	Mar 98	12540	6.9	18.18	12.59	98.30	1.74	7.71	18.95	0.93	108.32	-1.9	0.8	0.1	9.1
CN166		18.2619	-20.3982	Mar 98	1020	7.5	4.56	4.12	3.09	0.08	9.53	0.67	0.71	1.04	-0.5	0.6	-1.5	10.1

\* saturation index

### Comparison of samples taken in 1997 and in 1998

In order to get an overview of the stability of the hydrochemical data in time electric conductivity was surveyed as a proxy value during the sampling campaigns in 1997 and 1998. Temperature correction for 25 °C was made if necessary, using independent temperature measurements. Electric conductivity was continuously monitored during pumping and determined only after stabilization of the signal. The pairs of values are shown in Figure 4.26. The straight diagonal line indicates the line of perfect match, the dashed line delineating a 5 % error interval.

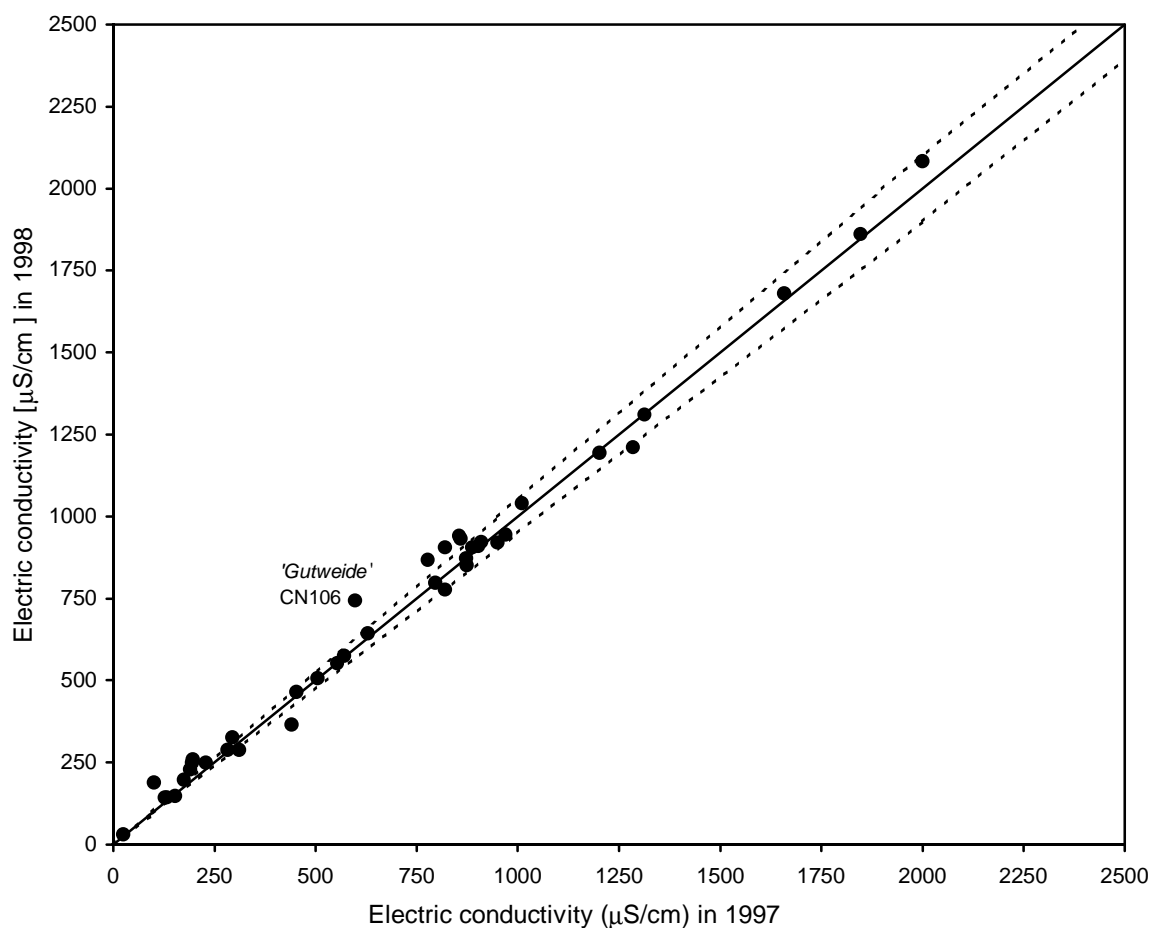


**Figure 4.26** Electric conductivity of groundwater from boreholes monitored in 1997 and 1998 in  $\mu\text{S}/\text{cm}$ .

In general, electric conductivity measured in June 1997 was well reproduced in early 1998. There is no detectable trend in the data. For one borehole, CN106 ‘Gutweide’, a large difference was observed (598 vs. 743  $\mu\text{S}/\text{cm}$ ). This borehole is located directly downstream of a dam, and the groundwater level is very shallow. The different electric conductivity is

probably caused by seepage from the dam. For some other boreholes the electric conductivity varied by 5 to 10 %. As long as sampling errors can be excluded, these minor differences may be caused by seasonal variations in response to groundwater recharge, or by varying intake areas of a pumped borehole. Field notes on the sampling locations indicate that boreholes showing variations in electric conductivity either have shallow groundwater levels (< 20 m depth to the groundwater table) or/and are located close to ephemeral rivers/pans.

The factors causing such variations in the hydrochemical composition were studied by a comparison of full hydrochemical analyses for selected boreholes (framed reference numbers in Figure 4.25: **CN017**, **CN021** and **CN081**).

The borehole 'Okambora', sample number **CN017**, is located between the Waterberg and the Omatako river and lies about 10 km south-west of Goblenz (see Figure 4.25). The groundwater is pumped from the Etjo sandstone aquifer covered by Kalahari sediments. **CN017** 'Okambora' is an example for stable hydrochemical conditions due to a thick unsaturated zone that attenuates the composition and flow rate of groundwater recharge. The intake area is the Etjo sandstone further to the west. In Figure 4.27 the major element profiles of the samples from June 1997 and March 1998 are juxtaposed.

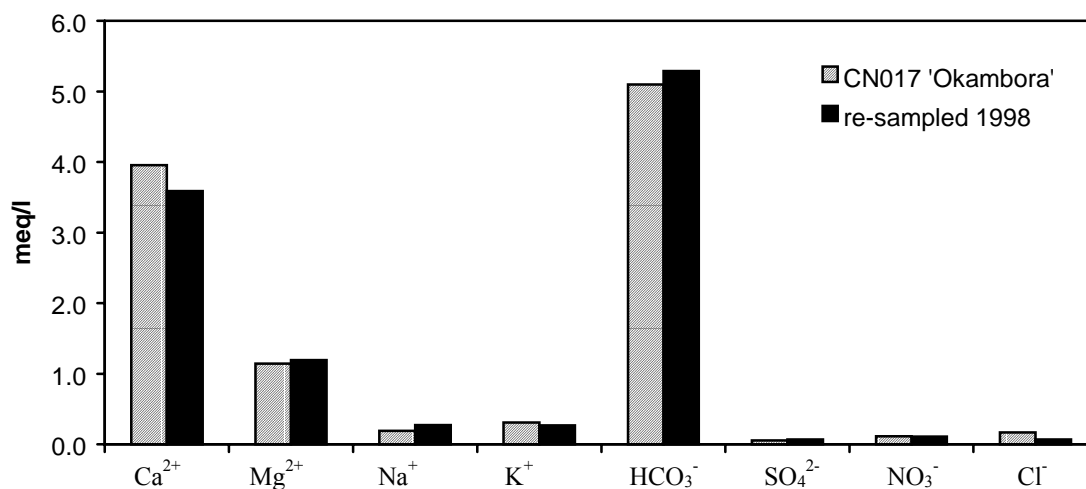


**Figure 4.27** Major element distribution of groundwater from borehole 'Okambora', sample number **CN017**, sampled in June 1997 and March 1998 (black).

The high relative differences in Na<sup>+</sup> and Cl<sup>-</sup> concentrations are caused by very low total concentrations (< 0.5 mg/l) at which level problems already arise with the analytical precision of the applied methods.

The groundwater table at **CN081** 'Omambonde Ost' is relatively shallow and close to the Omambonde ephemeral river. The major element profiles of samples taken in 1997 and 1998

are similar in their overall composition (Figure 4.28). For  $\text{Mg}^{2+}$ ,  $\text{Na}^+$  and  $\text{HCO}_3^-$  the differences are within the margin of analytical errors ( $< 5\%$ ).

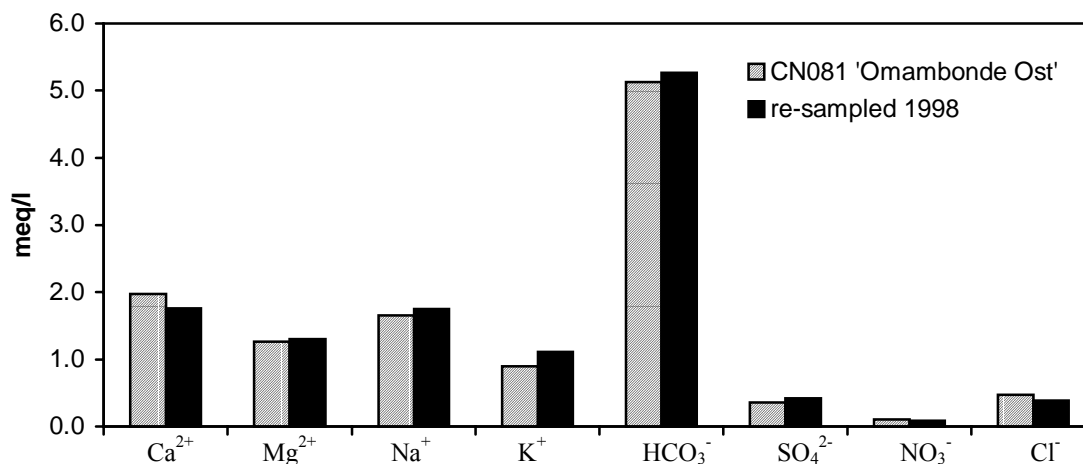


**Figure 4.28** Major element distribution of groundwater from borehole 'Omambonde Ost', sample number CN081, sampled in June 1997 and March 1998 (black).

The differences of measured concentrations for  $\text{Ca}^{2+}$  (11 %),  $\text{K}^+$  (20 %) and of  $\text{Cl}^-$  (19 %), however, are beyond the range of analytical error. Electric conductivity and chloride concentrations have slightly decreased by 1998. These changes are indicators of a 'freshening' that may have been caused by intense rainstorms and recharge in the 1997/1998 rainy season.

Sample CN021 is one of the few showing a strong variability in hydrochemical parameters (Figure 4.29). It is located within the Otavi Mountain Foreland. Despite of its name, 'Tiefwasser' (Engl. 'Deep water'), the water table is only between 10 to 15 m below the surface and thus relatively shallow as compared to other parts of the study area (such as Waterberg, Sandveld, and most of the Kalahari).

At CN021 Kalahari sediments (Tk) of 10 to 30 m cover metamorphic rocks of the Grootfontein metamorphic complex (Mgr). The Kalahari is composed of sand and calcareous formations with some embedded conglomerates. The hydrochemical composition of groundwater sample CN021 corresponds to that of group (b) and is characterized by dolomite dissolution and a typical  $\text{Ca}^{2+}:\text{Mg}^{2+}$  ratio close to 1.  $\text{Ca}^{2+}$  and  $\text{Mg}^{2+}$  are the dominant anions,  $\text{Na}^+$  and  $\text{K}^+$  concentrations are relatively small with  $\text{Na}^+ > \text{K}^+$ . The major ion is  $\text{HCO}_3^-$ , and the concentrations of  $\text{SO}_4^{2-}$  and  $\text{Cl}^-$  are smaller by almost one order of magnitude.

The comparison of the samples taken in 1997 and in 1998 shows an increase of  $\text{Ca}^{2+}$  and  $\text{HCO}_3^-$  in 1998 as compared to 1997. While the concentrations of  $\text{Mg}^{2+}$ ,  $\text{Na}^+$  and  $\text{NO}_3^-$  remain

more or less stable,  $\text{Cl}^-$  concentrations decrease significantly. The hydrochemical changes suggest an addition of  $\text{Ca}^{2+}$ - $\text{HCO}_3^-$  type water that also has low  $\text{Cl}^-$  concentrations.

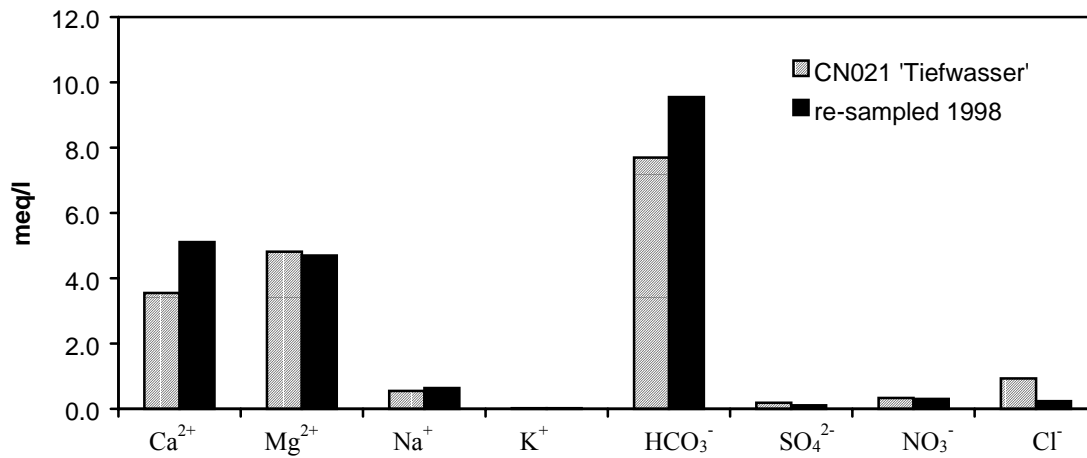


**Figure 4.29** Major element distribution of groundwater from borehole 'Tiefwasser', sample number CN021, sampled in June 1997 and March 1998 (black).

Due to the availability of calcite in the aquifer it is also possible that calcite dissolution takes place in situ resulting from the admixture of fresh groundwater. Due to the occurrence of heavy rainstorms and floods in the early rain season 1997/1998 (December 1997) these hydrochemical changes are probably caused by groundwater recharge.

In conclusion, few boreholes (CN106 'Gutweide', CN021 'Tiefwasser') that are located in the direct vicinity of ephemeral rivers and at the same time characterized by a shallow groundwater table show variations in hydrophysical and hydrochemical parameters. Recharge mainly affects  $\text{Ca}^{2+}$ ,  $\text{HCO}_3^-$  and  $\text{Cl}^-$  concentrations. Variations in  $\text{Na}^+$ ,  $\text{SO}_4^{2-}$  and  $\text{NO}_3^-$  where less pronounced, and  $\text{Mg}^{2+}$  proved to have a very low sensitivity. The assumption of long-term steady state conditions for the hydrochemical parameters of groundwater is approximately met when the unsaturated zone is thick enough to attenuate the hydrochemical variations caused by direct or indirect recharge from ephemeral rivers.

#### *Hydrochemical evolution along groundwater flow-paths*

Three hydrochemical profiles along groundwater head gradients have been selected for the characterization of the hydrochemical evolution and of mixing (see Figure 4.25). The interpretation of these profiles is based on notions of the distribution of hydrochemical groundwater types developed in an earlier chapter (Chapter 4.3.4). Profile AG extends along a groundwater flow line from outcrops of the Karibib Formation, belonging to the Damara Sequence, across the Waterberg thrust fault and the Etjo sandstone towards Goblenz.

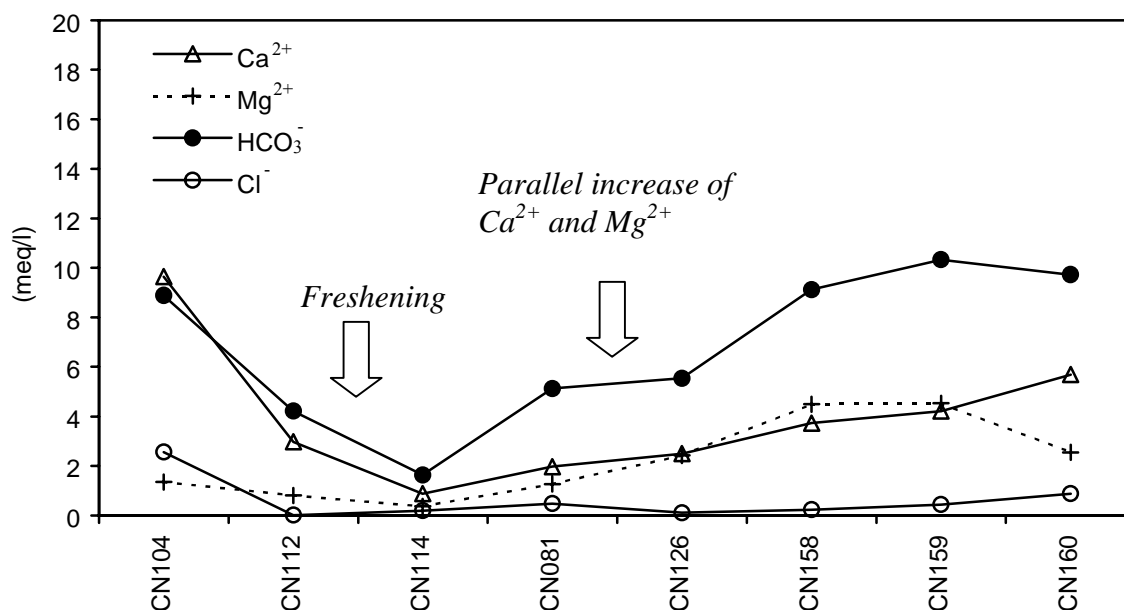


**Figure 4.30** Hydrochemical profile AG (location shown in Figure 4.25) from the outcrops of the Karibib Formation (marbles) towards Goblenz.

The first sample CN104 ‘*Harubib*’ was taken from a borehole directly within the marbles. Ca<sup>2+</sup> and HCO<sub>3</sub><sup>-</sup> are dominant, Mg<sup>2+</sup> reaches 1.4 meq/l, and the Cl<sup>-</sup> concentration is relatively high (2.6 meq/l). This sample belongs to hydrochemical group (a). The following samples, CN112 and CN114, along that flow line have decreasing Ca<sup>2+</sup> and HCO<sub>3</sub><sup>-</sup> concentrations; for Cl<sup>-</sup> the decrease is only observed at CN112. This decrease corresponds to a freshening of the groundwater by recharge along the Omambonde ephemeral river or by inflow from the Etjo sandstone. From CN114 through CN081, CN126 and CN158 there is again an increase of the concentration of the earth alkaline elements Ca<sup>2+</sup> and Mg<sup>2+</sup>. The cation ratio Ca<sup>2+</sup>: Mg<sup>2+</sup> is close to 1. The groundwater potentials in this area together with the hydrochemical changes strongly suggest an inflow of groundwater belonging to group (b) from the Otavi Mountains (dolomite). While samples CN158 and CN159 are similar except for a slight increase in Cl<sup>-</sup>, groundwater evolves towards a Ca<sup>2+</sup>-HCO<sub>3</sub><sup>-</sup> type at CN160.

In conclusion, two inflows can be identified along flow profile AG extending along the Omambonde ephemeral river: In its upper part there is evidence for inflow of fresh groundwater from the west (Etjo sandstone or groundwater recharge along the Omambonde), in the lower part the hydrochemical evolution points to an inflow of groundwater type (b).

Profile BG (Figure 4.31) reflects the hydrochemical evolution from the outcrops of the Tsumeb and Abenab subgroups down to the wells at Goblenz. The changes in concentration of Ca<sup>2+</sup>, Mg<sup>2+</sup>, HCO<sub>3</sub><sup>-</sup> and Cl<sup>-</sup> are relatively small and smooth. From borehole CN118 to borehole CN158 there is only a slight decrease of the concentrations of Mg<sup>2+</sup> and HCO<sub>3</sub><sup>-</sup>, with

increasing concentrations of  $\text{Ca}^{2+}$ . From borehole CN154 to Goblenz there is a steady increase of the chloride concentration.

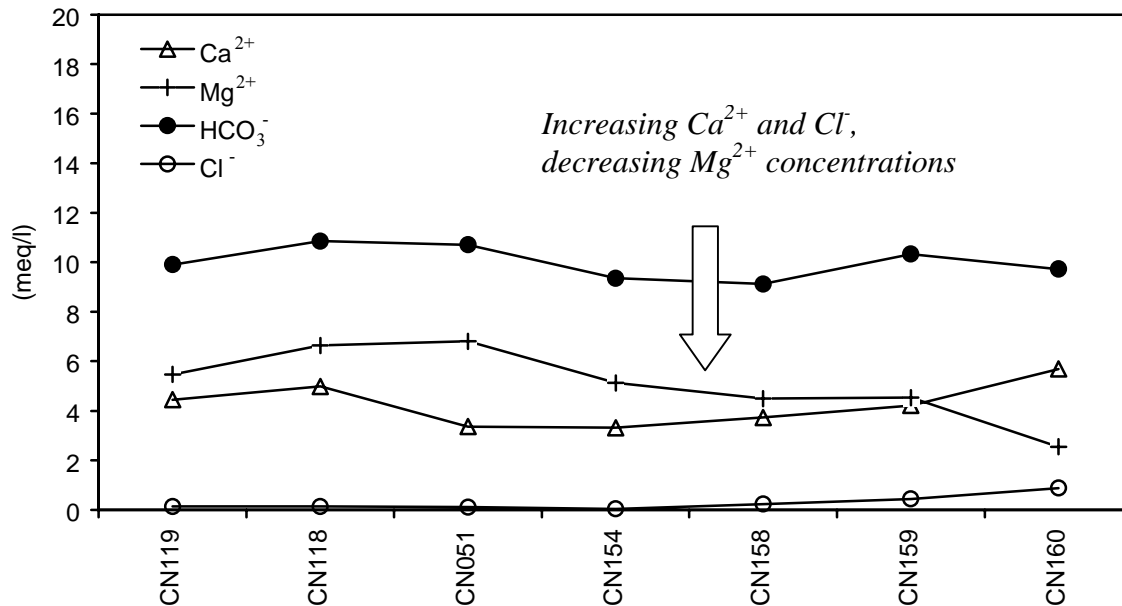


**Figure 4.31** Hydrochemical profile BG (location shown in Figure 4.25) from outcrops of the Tsumeb and Abenab subgroups (dolomite) towards Goblenz - western section.

The original composition with high  $\text{Mg}^{2+}$  concentrations is gradually changed by the additional contribution of groundwater with high  $\text{Ca}^{2+}$  concentrations and  $\text{HCO}_3^-$  that are lower than 10 meq/l. This pattern can be explained by mixing with groundwater types (a) from the Karibib marbles (high  $\text{Ca}^{2+}$  and similar  $\text{HCO}_3^-$ , slightly elevated  $\text{Cl}^-$  concentrations). This conceptual model explains only part of the increasing chloride concentrations. Therefore, the influence of a more saline end member, as identified in the cluster analysis (e) along this profile, is likely and should be accounted for in the mixing-cell model.

Profile EG represents a profile of samples through the Kalahari towards Goblenz. It should be noted that due to the higher content of dissolved solids the scale in Figure 4.32 had to be increased by a factor of six as compared to Figures 4.30 and 4.31. Between CN008 and CN165 there is a steady and parallel increase of the concentrations of  $\text{Na}^+$  and  $\text{Cl}^-$ . In this part of the boreholes tap the Lower Kalahari. The fact that the  $\text{Na}^+/\text{Cl}^-$  ratio evolves towards a characteristic value of about 1 strongly suggests mixing with a NaCl source in the Lower Kalahari. This must not necessarily be a solid phase of evaporates; NaCl may just as well be released from pore-water in clays or any formation water. As compared to the  $\text{Na}^+$  and  $\text{Cl}^-$  profiles, the concentrations of  $\text{Ca}^{2+}$ ,  $\text{Mg}^{2+}$  and  $\text{SO}_4^{2-}$  show only slight increases up to borehole CN165, while  $\text{HCO}_3^-$  remains more or less constant. Between CN165 and CN164 there is an abrupt change in the hydrochemical composition. CN164 and CN160 (Goblenz) are tapping the Middle Kalahari aquifer containing groundwater of good quality.



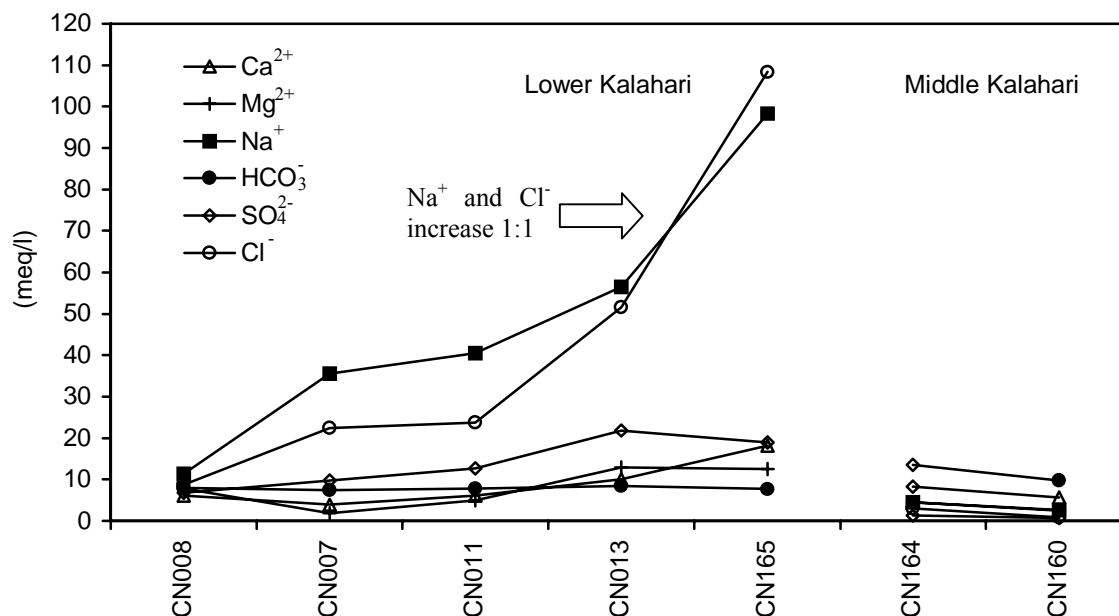


**Figure 4.32** Hydrochemical profile EG (location shown in Figure 4.25) from the western Kalahari towards Goblenz.

It needs to be checked by the quantitative mixing calculations whether or not this connection contributes to the water balance of the Middle Kalahari aquifer near Goblenz. In any case, due to the abrupt change along this profile the inflow from the Lower Kalahari can only be small, as compared to other groundwater flows towards Goblenz.

#### *Calcite and gypsum saturation indices in the vicinity of Goblenz*

Based on the theory outlined in Chapter 3.2, the saturation index of groundwater samples with respect to calcite has been calculated (Figure 4.33). These calculations help identify areas where the assumption of conservative behaviour as a prerequisite for the mixing-cell approach is not met due to possible dissolution/precipitation of calcite. As already pointed out in Chapter 3, the saturation index only indicates the direction of equilibrium reactions and does not imply that these reactions actually take place.

For the majority of samples the groundwater is super-saturated with respect to calcite. For these samples the saturation index indicates slight to pronounced super-saturation (0 and 0.6). Only in the Etjo sandstone the groundwater is clearly subsaturated for calcite.

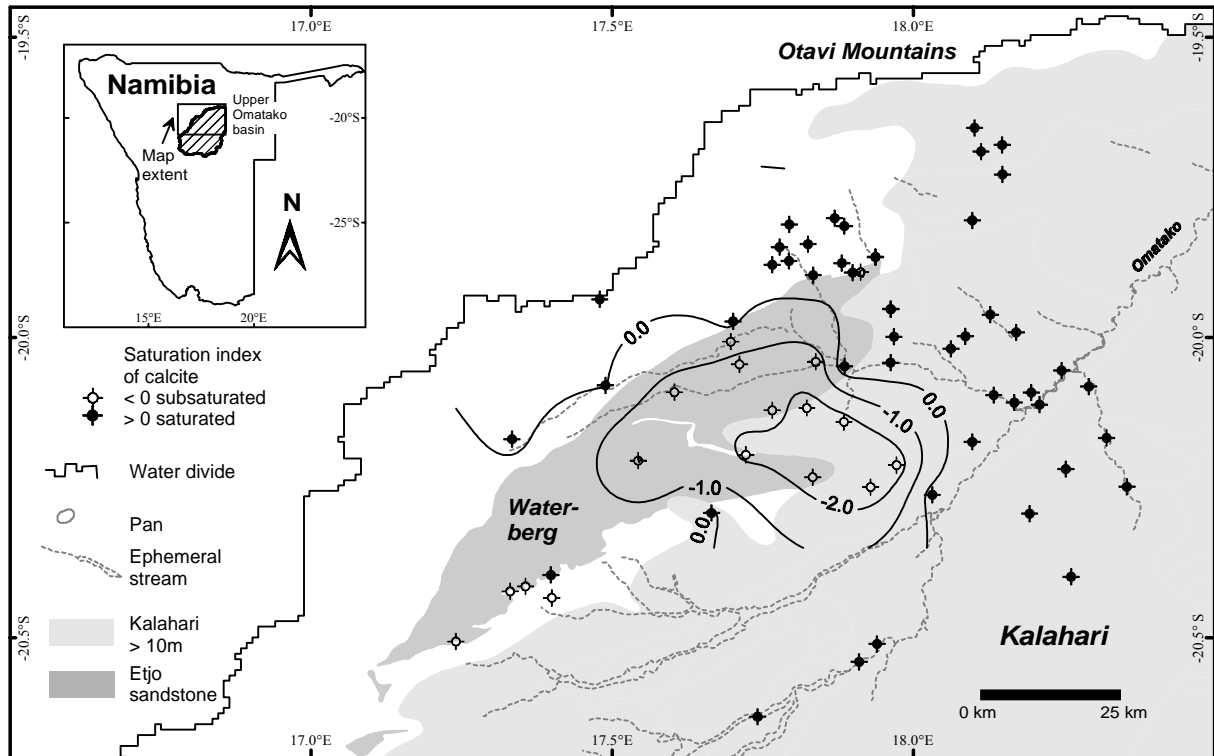


**Figure 4.33** Saturation indices of calcite calculated from groundwater samples taken in the vicinity of Goblenz. Negative values (open circles) indicate subsaturation. Values above zero (filled circles) indicate that calcite *precipitation* is possible.

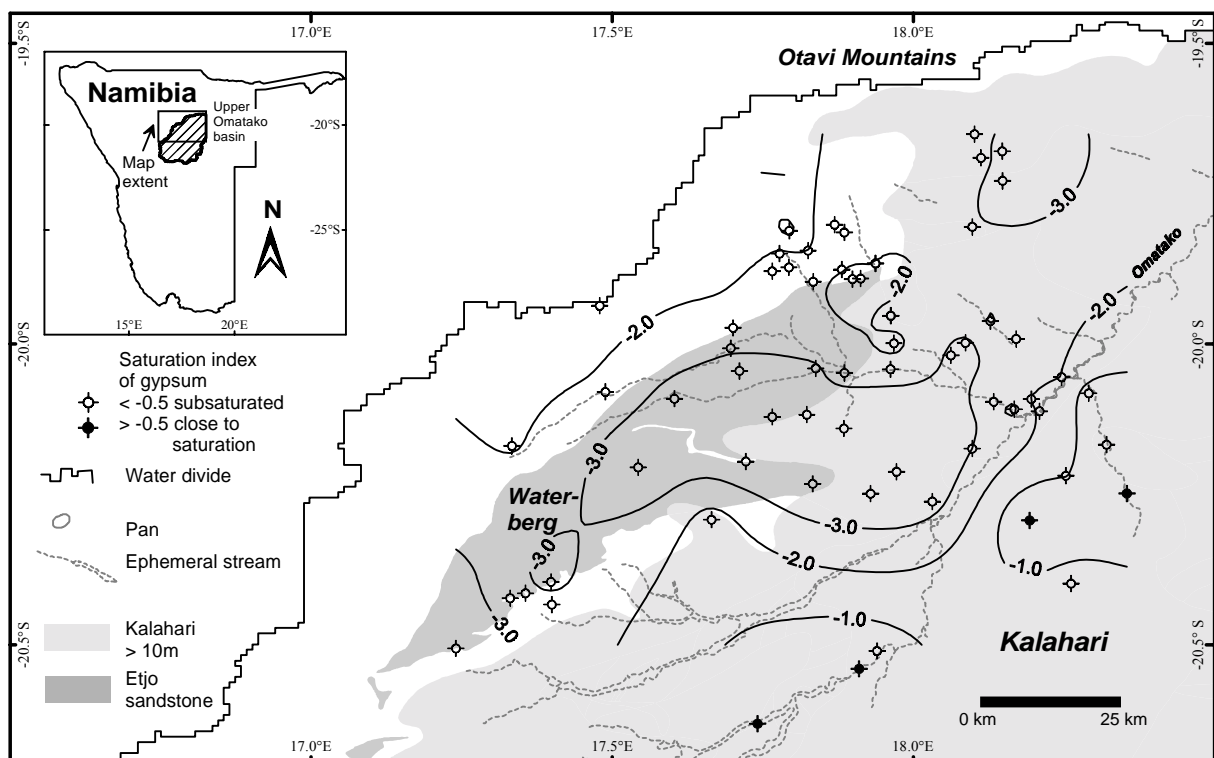


**Figure 4.34** Saturation indices of gypsum calculated from groundwater samples taken in the vicinity of Goblenz. Negative values (open circles) indicate subsaturation, i.e. gypsum *dissolution* is thermodynamically possible. Values above zero (filled circles) indicate that gypsum *precipitation* is thermodynamically possible.

The fact that the groundwater in the Etjo sandstone is so strongly subsaturated for calcite also provides information about the area and mechanism of recharge. Slow movement of soil water through a vegetated soil results in the equilibration of soil water with ambient  $\text{CO}_2$  partial pressures and calcite coatings or nodules in the soil. The reaction rates of calcite are known to be high enough to allow the establishment of full equilibrium. The extremely low contents of  $\text{Ca}^{2+}$ ,  $\text{HCO}_3^-$  show that for the Western Waterberg the contribution of recharge through the soil matrix is small as compared to the contribution from areas devoid of soil cover or characterized by significant macropore/fracture recharge.

Figure 4.34 shows that the groundwater is clearly subsaturated for gypsum in all samples except for 4 samples in the Kalahari with only slight subsaturation. This means that gypsum precipitation does not take place. Dissolution of gypsum is possible where gypsum exists in the aquifer. Since gypsum precipitation requires much higher concentration factors than calcite precipitation, gypsum will only be found in evaporite beds, for example in present or old groundwater discharge zones with strong evaporation. Gypsum dissolution is probably not relevant for the areas north of Goblenz, but it cannot be excluded for the Kalahari aquifers, especially the Lower Kalahari Formation. Therefore the mixing calculations including  $\text{Ca}^{2+}$ ,  $\text{HCO}_3^-$  and  $\text{SO}_4^{2-}$  should be restricted to the extent of the sandstone aquifer beneath the Kalahari directly north of Goblenz. The (more or less) calcite-free sandstone beneath the Kalahari provides an approximately ideal aquifer for mixing reactions, due to the absence of easily soluble mineral phases. Downstream of Goblenz problems arise with calcite and gypsum dissolution as well as with NaCl dissolution in the Lower Kalahari aquifer.

#### 4.4.2 Stable isotopes

Prior to the interpretation of stable isotope data in groundwater the input functions of  $^{18}\text{O}$  and  $^2\text{H}$  with respect to precipitation were studied. To that end, stable isotope data in precipitation collected in the framework of the *GNIP* program (*Global Network of Isotopes in Precipitation*) of the IAEA (International Atomic Energy Agency) were used. Within *GNIP* monthly data on  $\delta^{18}\text{O}$ ,  $\delta^2\text{H}$ , tritium and aggregated monthly meteorological parameters (monthly amount of precipitation, mean temperature and vapour pressure) have been collected and published as IAEA reports (IAEA, 1969-1994). In Namibia there is a single *GNIP* station at Windhoek (No. 6811000, altitude: 1,728 m a. s. l., latitude S 22.57°, longitude E 17.10°) with a record starting in January 1961. Since December 1980 the record is discontinuous. Figure 4.35 shows the isotopic time series between 1961 and 1980 and the associated meteorological parameters temperature, rainfall and vapour pressure.

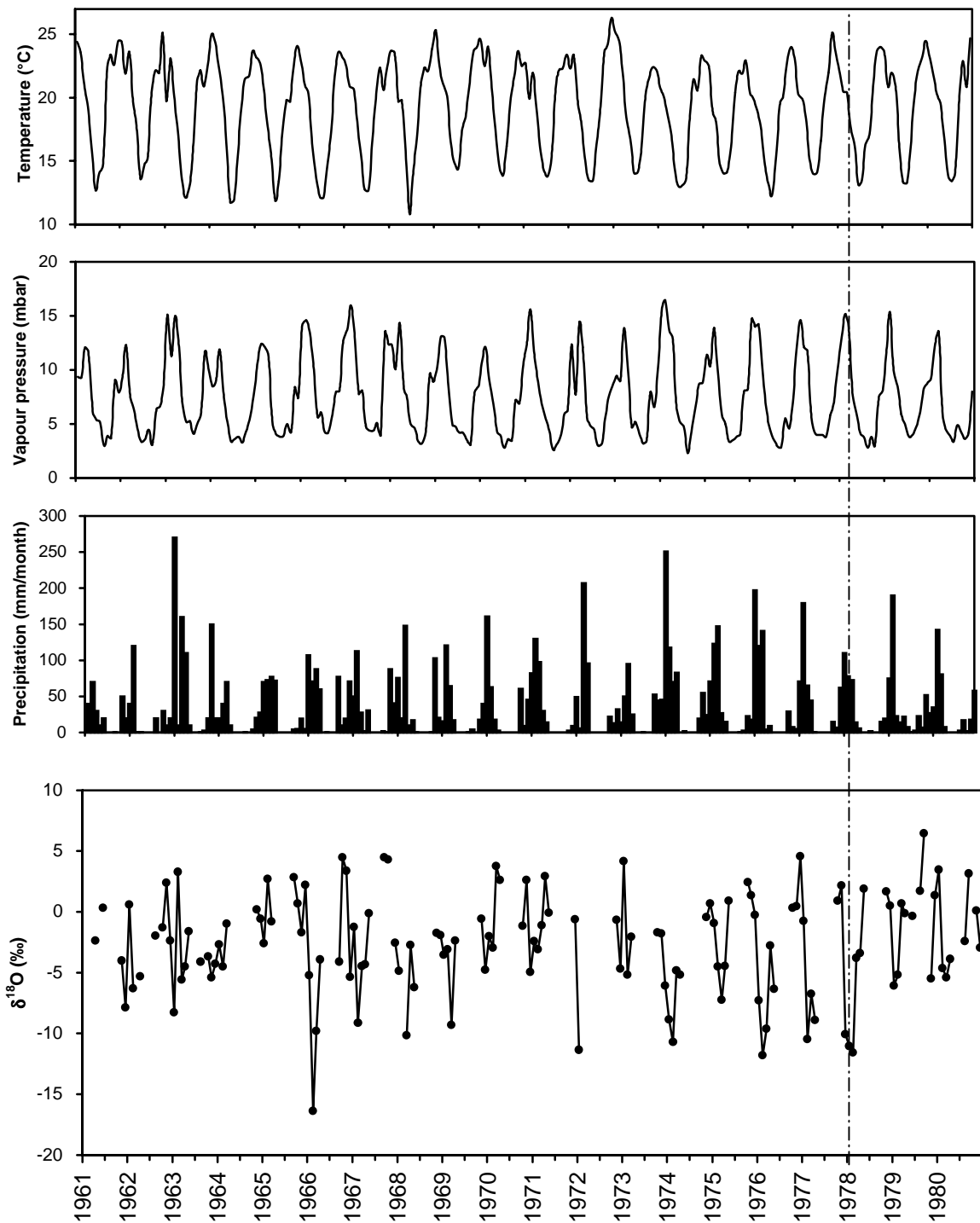


**Figure 4.35** Time series of temperature ( $^{\circ}$  C), vapour pressure (mbar), precipitation (mm/month) and  $\delta^{18}\text{O}$  (‰) at Windhoek between 1961 and 1980.

There is a strong seasonal variation in the parameters measured. Due to the summer solstice of the southern hemisphere (December, 21<sup>st</sup>) the months with the highest mean temperature are December and January. Approximately one month later the highest mean monthly vapour pressure (February) is reached (see the line through February 1978 in Figure 4.35) indicating the inflow of air masses with higher moisture contents. During the same month, the highest precipitation and the most depleted  $\delta^{18}\text{O}$ (‰) values are observed. On the average, these

variations result in a seasonal isotope effect, which has already been described by VOGEL & VAN URK (1975). In Figure 4.36 the seasonal distributions of the monthly averages of  $\delta^{18}\text{O}$  in precipitation and of the most depleted  $\delta^{18}\text{O}$  values has been plotted for each month. The monthly average of  $\delta^{18}\text{O}$  (‰) varies between 2 and -6 ‰. Rainfall at the beginning of the rainy season in November has a relatively heavy isotopic signature of around zero ‰  $\delta^{18}\text{O}$ . During the southern summer season (December to March), mean isotopic rainfall composition shifts towards more depleted values. For February an average value of -6 ‰  $\delta^{18}\text{O}$  was obtained, the most extreme value on record for this month being -16 ‰  $\delta^{18}\text{O}$  in 1966. Low  $\delta^{18}\text{O}$  values correlate with high monthly amounts of rainfall. At the end of the rainy season a general return to heavier (higher) values is observed. The precipitation-weighted average of  $\delta^{18}\text{O}$  at Windhoek is -4.3 ‰.

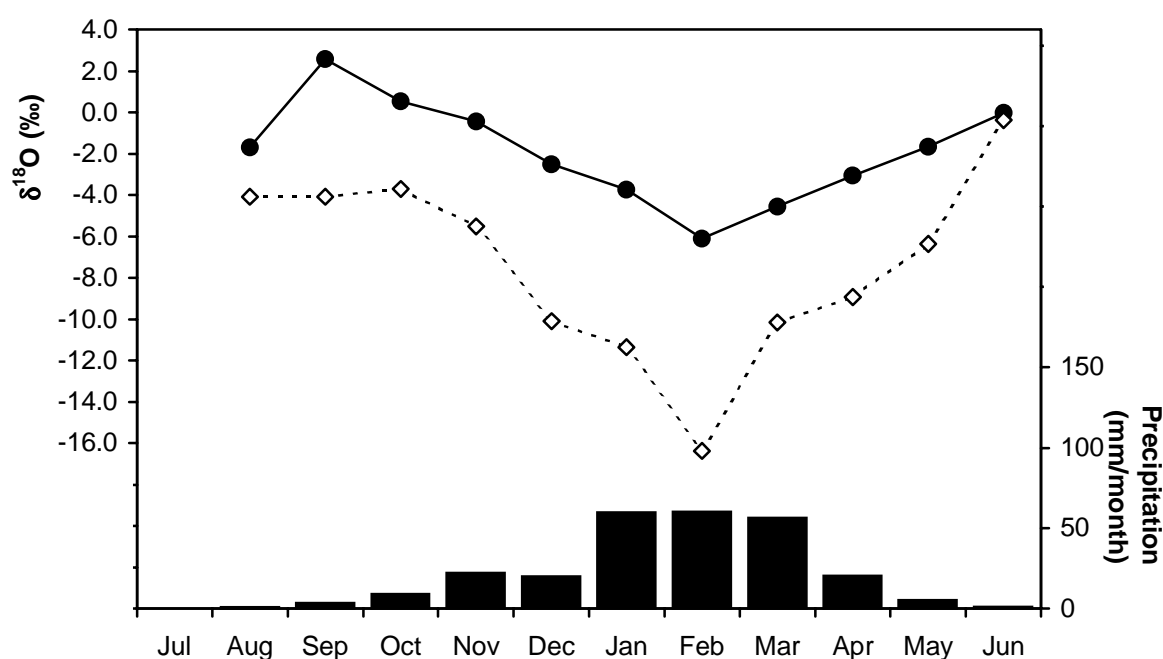


**Figure 4.36** The seasonal distribution of average  $\delta^{18}\text{O}$  measured in precipitation (monthly bulk samples) at Windhoek (continuous line with filled circles) and of the most depleted values of  $\delta^{18}\text{O}$  for each month recorded between 1961 and 1980 (dashed line). The bars indicate mean monthly amounts of precipitation scaled to the right y-axis.

The  $\delta^{18}\text{O}$  and  $\delta^2\text{H}$  values plot approximately along the Global Meteoric Water Line defined by  $\delta^2\text{H}=8*\delta^{18}\text{O}+10$  ‰ VSMOW. Samples of precipitation with heavier (higher)  $\delta^{18}\text{O}$  and  $\delta^2\text{H}$  values tend to fall below the Global Meteoric Water Line. Taking into account the climatic conditions at Windhoek during the rainy season (high temperatures) and the sampling method (bulk samples from several events), this effect is likely to be caused by evaporation in the atmosphere or during sampling, especially for small rainfall events. In view of these conditions, the match between the Global Meteoric Water Line and local precipitation at Windhoek was considered to be good enough so as not to define a local meteoric water line.

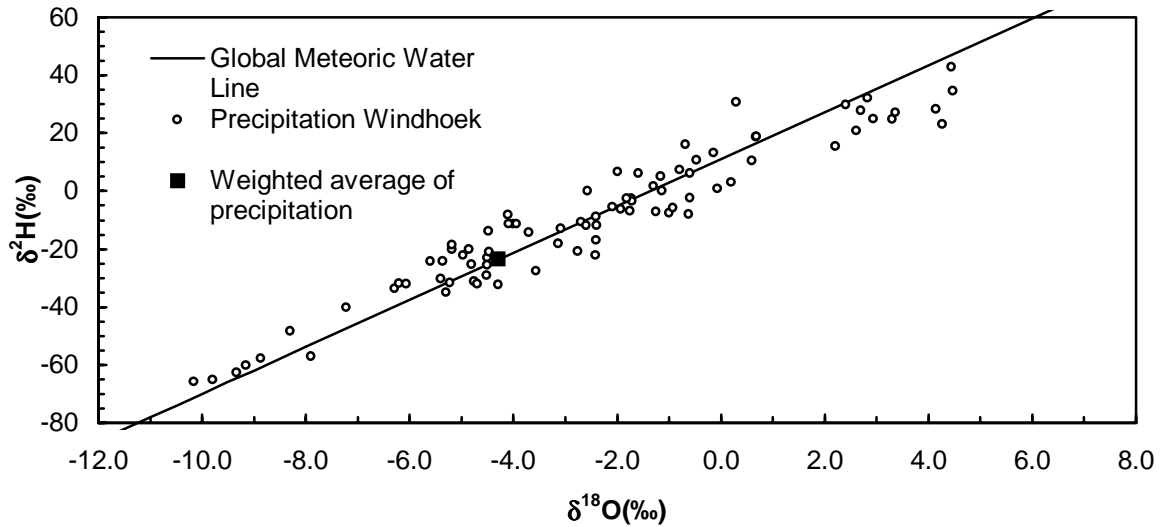


**Figure 4.37**  $\delta^{18}\text{O}$  -  $\delta^2\text{H}$  diagram of IAEA-GNIP data at Windhoek between 1961 and 1980.

No reference time series of stable isotopes in the study area 200 km north-east of Windhoek is available. It is assumed that the isotopic composition of precipitation at Windhoek has more or less similar characteristics as precipitation in the study area of the Omatako basin. The influence of winter rainfall may be more pronounced at Windhoek than in the study area further to the north-east. However, the altitude of the rainfall station at Windhoek (1,728 m) very well corresponds to the altitude of the assumed recharge areas within the study area - the Otavi Mountain and Waterberg ridges.

#### *Stable isotopes in the groundwater*

Altogether 132 samples were taken for analysis of the stable isotopes  $^{18}\text{O}$  and  $^2\text{H}$ . From these samples,  $\delta^{18}\text{O}$  and  $\delta^2\text{H}$  as compared to VSMOW standard were measured at the Niedersächsisches Landesamt für Bodenforschung, the state geological survey of Lower Saxony, at Hannover.

Altogether 86 groundwater boreholes or shallow wells and two pans with floodwater (filled for several weeks after a rainfall event) were sampled. In order to perform a check on the temporal stability of the isotopic data, 44 boreholes were sampled twice: the first sampling was made in July/August 1997 and the second one in March 1998 after a good rain season, with several small floods in the Omambonde river in 1997/1998. The location of the samples is documented in Figure 4.38; the data are listed in Table 4.3. The location of two profiles CG and DG, discussed in detail below, is also marked in Figure 4.38.

**Stable isotope samples**

- - 1997
  - ⊕ - 1998
  - ⊕ - 1997 and 1998
  - - Monthly time series 1997 - 1998
- 
- Water divide
  - Pan
  - Ephemeral stream
  - Kalahari > 10m
  - Etjo sandstone
  - Isotope profile

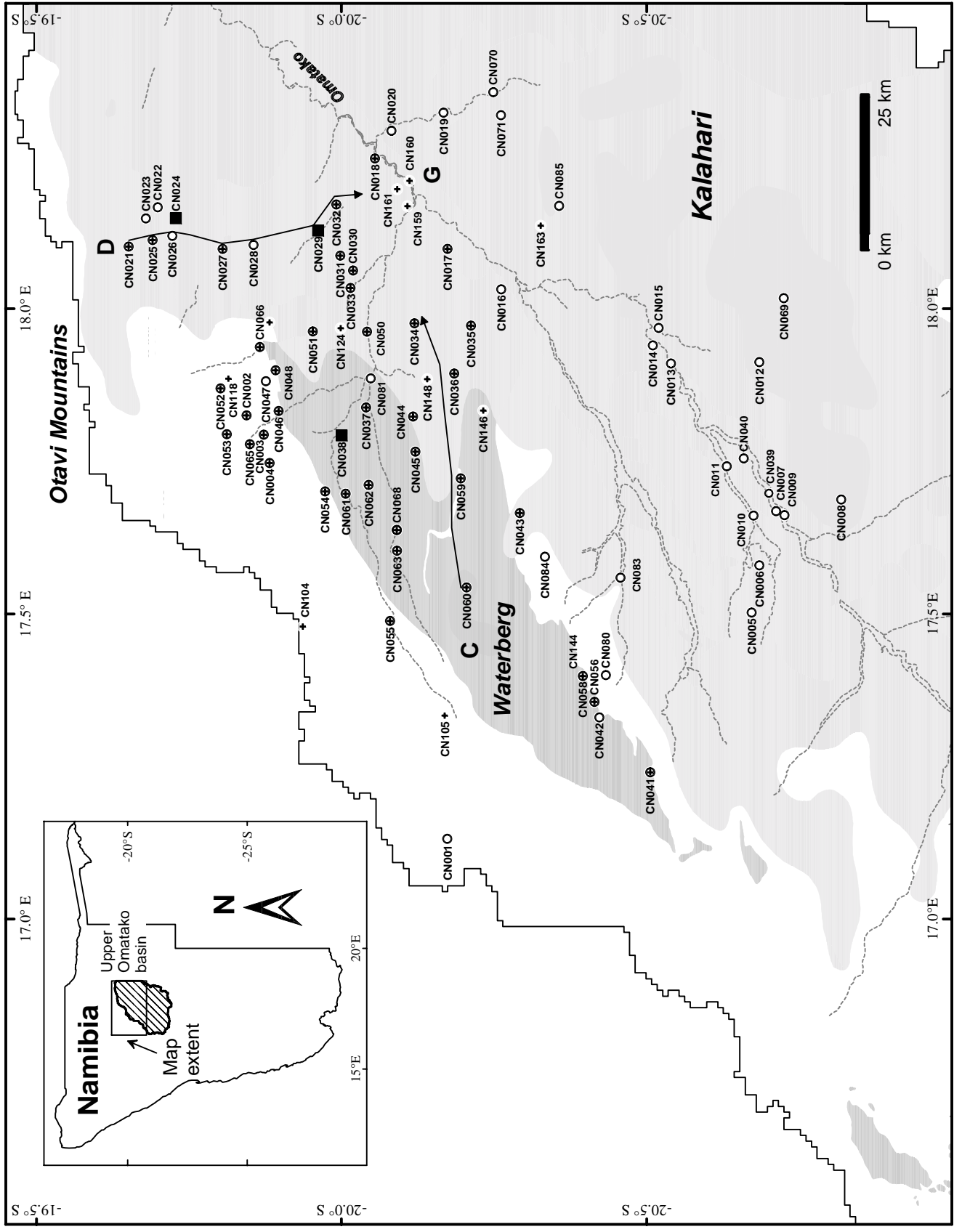


**Figure 4.38**

Location of samples for stable isotope analysis. Empty circles depict boreholes sampled in 1997; crosses represent boreholes sampled in early 1998. Boreholes with a circle and a cross were sampled twice. Stations with time series are shown as filled squares.

**Table 4.3** Stable isotope data of groundwater samples in the Omatako basin, 1997 and 1998

sample	name	date	longitude [°E]	latitude [°S]	elevation [m]	Temp. [°C]	ec [µS/cm]	pH	$\delta^{18}\text{O}$ [‰]	$\delta^2\text{H}$ [‰]
CN001	Oros	14-Jun-97	17.1312	-20.1733	1524	24.1	524	6.6	-8.9	-61.2
CN002	Schoenhausen	16-Jun-97	17.8250	-19.8445	1427	24.2	1285	6.9	-8.8	-62.0
CN003	Gai Kaisa 'West'	16-Jun-97	17.7933	-19.8725	1424	23.9	859	6.5	-8.6	-57.6
CN004	Osambusatjuru	16-Jun-97	17.7469	-19.8821	1449	25.0	472	6.6	-9.3	-63.3
CN005	Ompanda	17-Jun-97	17.5022	-20.6722	1329	26.9	1285	8.1	-9.0	-62.6
CN006	Ombu Yovakuru	17-Jun-97	17.5792	-20.6847	1311	26.4	3360	7.3	-9.0	-63.8
CN007	Okahitwa North	17-Jun-97	17.6682	-20.7119	1296	29.9	4740	7.4	-7.9	-58.2
CN008	Ovitatu	18-Jun-97	17.6873	-20.8187	1310	24.1	2460	7.5	-8.1	-59.2
CN009	Okahitwa South	18-Jun-97	17.6614	-20.7258	1296	23.9	1625	7.2	-7.0	-53.1
CN010	Ornatjetjeva	18-Jun-97	17.6607	-20.6749	1300	28.8	5570	7.3	-8.1	-59.4
CN011	Ornatanga	18-Jun-97	17.7414	-20.6312	1289	25.5	5290	7.3	-7.5	-55.5
CN012	Omanbandjou	18-Jun-97	17.9121	-20.6846	1281	26.0	5820	6.9	-8.0	-57.5
CN013	Ombujomenje	18-Jun-97	17.9100	-20.5398	1271	26.7	9040	7.2	-7.5	-56.7
CN014	Okajpe	18-Jun-97	17.9397	-20.5100	1269	20.0	294	7.8	-8.1	-62.5
CN015	Okaundja	18-Jun-97	17.9684	-20.5193	1265	25.8	5340	8.0	-6.6	-49.8
CN016	Otjituwa	19-Jun-97	18.0315	-20.2618	1255	26.6	749	7.5	-8.3	-61.8
CN017	Okambora	19-Jun-97	18.0978	-20.1738	1250	26.1	506	7.6	-9.7	-66.4
CN018	Ongongoro	20-Jun-97	18.2461	-20.0549	1242	22.2	1202	7.8	-7.8	-58.1
CN019	Omitjete	20-Jun-97	18.3208	-20.1671	1256	26.5	1255	7.5	-8.0	-57.9
CN020	Okomuparara	20-Jun-97	18.2913	-20.0817	1248	25.3	2460	7.1	-9.1	-64.3
CN021	Tiefwasser	21-Jun-97	18.1017	-19.6510	1402	24.1	935	7.5	-8.4	-59.9
CN022	Wilhelmsruh	21-Jun-97	18.1660	-19.6986	1356	23.4	737	7.9	-7.5	-52.6
CN023	Kikuyu	21-Jun-97	18.1475	-19.6794	1370	25.0	1022	7.6	-8.0	-59.7
CN024	Okamutombe Farm	21-Jun-97	18.1481	-19.7284	1353	24.8	950	7.4	-7.2	-54.8
CN025	Okamutombe Nord	21-Jun-97	18.1124	-19.6903	1383	22.2	820	7.5	-7.4	-56.0
CN026	Okamutombe West	21-Jun-97	18.1191	-19.7225	1370	18.5	1414	7.8	-7.8	-58.9
CN027	Havelberg	21-Jun-97	18.0978	-19.8050	1345	23.0	910	7.6	-6.6	-51.0
CN028	Harmonie	21-Jun-97	18.1041	-19.8560	1315	24.1	1923	7.8	-5.6	-47.8
CN029	Schwarzfelde	21-Jun-97	18.1278	-19.9618	1270	24.9	1312	6.8	-7.8	-58.7
CN030	Kabare	21-Jun-97	18.0623	-20.0187	1273	26.1	797	7.1	-8.4	-62.9
CN031	Oktrooi	21-Jun-97	18.0865	-19.9979	1268	25.1	820	7.3	-8.3	-61.5
CN032	Schoenau	22-Jun-97	18.1707	-19.9914	1253	24.8	969	7.2	-6.9	-53.8
CN033	Okshof	22-Jun-97	18.0337	-20.0149	1280	25.8	1010	6.8	-8.0	-60.6
CN034	Waagstuk	22-Jun-97	17.9761	-20.1192	1326	27.2	230	5.9	-8.6	-59.9
CN035	Hirschgrund	22-Jun-97	17.9721	-20.2122	1297	26.1	196	5.1	-8.3	-58.9
CN036	Duineveld	22-Jun-97	17.8935	-20.1847	1368	26.5	191	5.8	-8.6	-59.7
CN037	Omambonde West	22-Jun-97	17.8378	-20.0403	1296	24.4	197	6.3	-9.5	-66.5
CN038	Kameldorn	22-Jun-97	17.7921	-20.0002	1299	24.6	218	6.4	-9.4	-65.6
CN039	Okahitwa Pan (surface water)	17-Jun-97	17.6712	-20.7052	1295	16.9	223	8.6	6.1	14.0
CN040	Ornaihi Pan (surface water)	18-Jun-97	17.7547	-20.6588	1286	12.9	145	8.2	0.7	-9.1
CN041	Waterberg No 2	29-Jun-97	17.2404	-20.5059	1560	22.5	25	5.6	-10.1	-69.8
CN042	Okomumbonde	29-Jun-97	17.3303	-20.4224	1460	24.0	241	6.8	-9.6	-66.8
CN043	Bisiepan	29-Jun-97	17.6648	-20.2920	1376	25.9	630	7.3	-9.2	-65.3
CN044	Omega Kral	30-Jun-97	17.8231	-20.1173	1370	25.8	312	5.9	-9.3	-64.5



## (continued) Stable isotope data of groundwater samples in the Omatako basin, 1997 and 1998

sample	name	reference	date	longitude [°E]	latitude [°S]	elevation [m]	Temp. [°C]	ec [μS/cm]	pH	δ <sup>18</sup> O [‰]	δ <sup>2</sup> H [‰]
CN045	Omega Groote Pos		30-Jun-97	17.7656	-20.1210	1397	25.5	133	6.0	-9.5	-66.4
CN046	Gai Kaisa 'Farm'		30-Jun-97	17.8324	-19.8967	1400	18.5	872	6.7	-8.7	-62.1
CN047	Gunuchas Windmotor		01-Jul-97	17.8812	-19.8760	1396	23.9	1125	6.6	-7.0	-55.4
CN048	Gunuchas 'Haus'		01-Jul-97	17.8989	-19.8919	1378	23.8	2000	6.2	-8.9	-63.4
CN049	Gunuchas electric pump		01-Jul-97	17.9125	-19.8911	1375	25.7	1659	6.5	-8.9	-64.6
CN050	Omambondetal Farm		01-Jul-97	17.9621	-20.0417	1269	23.4	553	7.4	-8.4	-58.6
CN051	Omambondetal Nord		01-Jul-97	17.9625	-19.9529	1328	25.0	887	7.3	-8.3	-61.6
CN052	Hochkamp No. 14		01-Jul-97	17.8693	-19.8014	1470	25.0	874	7.2	-9.4	-66.0
CN053	Salzbrunnen Farm		24-Jul-97	17.7940	-19.8117	1465	26.8	1846	6.7	-9.0	-64.2
CN054	Breitenbach 'Farm'		02-Jul-97	17.7007	-19.9730	1402	23.7	854		-8.9	-63.3
CN055	Gutweide Farm		02-Jul-97	17.4885	-20.0796	1420	24.7	598		-5.5	-42.0
CN056	Waterberg Tief		08-Jul-97	17.3559	-20.4141	1500	25.2	296	7.4	-9.5	-66.7
CN057	Waterberg 'Flach'		08-Jul-97	17.3538	-20.4119	1520	24.2	284	7.5	-9.7	-67.1
CN058	Okatjikona		09-Jul-97	17.3982	-20.3953	1435	24.4	442	7.5	-9.8	-66.7
CN059	Diepwater		09-Jul-97	17.7219	-20.1952	1417	25.9	153	6.5	-9.4	-64.5
CN060	Panorama		09-Jul-97	17.5430	-20.2049	1492	25.9	128	6.8	-9.6	-66.8
CN061	Breitenbach 'Mittelposten'		10-Jul-97	17.6967	-20.0069	1331	24.6	454	7.1	-8.5	-62.8
CN062	Breitenbach 'Wilhelmsfeld'		10-Jul-97	17.7112	-20.0445	1372	26.0	175	6.8	-9.6	-67.8
CN063	Rimini 'Farm'		10-Jul-97	17.6032	-20.0908	1400	26.7	102	6.6	-9.7	-68.7
CN065	Gesundbrunnen		12-Jul-97	17.7778	-19.8495	1439	24.0	903	6.7	-8.9	-63.9
CN066	Hairbib		12-Jul-97	17.9371	-19.8660	1385	43.7	4970	6.6	-9.4	-66.1
CN067	Rimini		13-Jul-97	17.6372	-20.0906	1380	24.5	185	6.5	-9.9	-68.8
CN068	Rimini		13-Jul-97	17.6372	-20.0906	1380	24.5	185	6.5	-9.9	-68.7
CN069	Ohamuheke		14-Jul-97	18.0170	-20.7247	1320	26.5	1235	6.9	-8.0	-59.2
CN070	Otišepa		15-Jul-97	18.3545	-20.2484	1274	30.4	5860	6.1	-8.9	-62.7
CN071	Otišepa Pan		15-Jul-97	18.3166	-20.2614	1290	27.2	1120	6.9	-8.6	-62.9
CN080	Otišepa Pan		22-Jul-97	17.3995	-20.4331	1410	35.2	677	8.3	-8.5	-61.0
CN081	Omambonde Ost		23-Jul-97	17.8856	-20.0478	1275	23.9	571	7.2	-8.6	-60.9
CN083	Elandsweide		11-Aug-97	17.5591	-20.4569	1328	25.4	4290	7.4	-8.5	-62.4
CN084	Erindi Ura		11-Aug-97	17.5933	-20.3333	1360	30.7	2780	7.6	-9.4	-66.7
CN085	Okomutenja		12-Aug-97	18.1683	-20.3567	1281	27.3	3420	6.1	-8.7	-62.3
CN101	Waterberg 'No.2'	CN041	Mar-98	17.2404	-20.5059	1560	26.0	30	4.8	-10.1	-68.6
CN102	Kameeldorn	CN038	Mar-98	17.7921	-20.0002	1299				-9.4	-64.6
CN103	Gai Kaisa 'Farm' No. 2		Mar-98	17.8335	-19.8963	1403	25.0	1263	6.8	-8.8	-61.6
CN104	Harubib		Mar-98	17.4791	-19.9363	1551	25.3	1506	6.8	-8.8	-64.6
CN105	Oase		Mar-98	17.3334	-20.1692	1536	27.8	950	6.7	-9.0	-48.6
CN106	Gutweide 'Haus'	CN055	Mar-98	17.4885	-20.0796	1420	28.1	743	6.8	-6.7	-61.6
CN107	Gutweide 'Rivier'		Mar-98	17.3334	-20.1692	1420	30.1	773	6.8	-6.0	-48.3
CN108	Rimini 'Farm'	CN063	Mar-98	17.6032	-20.0908	1400	27.9	188	6.7	-9.7	-44.3
CN109	Panorama	CN060	Mar-98	17.5430	-20.2049	1492	26.7	141	6.4	-9.4	-66.1
CN110	Bisepan	CN043	Mar-98	17.6648	-20.2920	1376	27.7	643	7.5	-9.0	-65.4
CN111	Breitenbach 'Wilhelmsfeld'	CN062	Mar-98	17.7112	-20.0445	1372	26.7	197	6.5	-9.0	-63.8
CN112	Breitenbach 'Mittelposten'	CN061	Mar-98	17.6967	-20.0069	1331	25.1	464	7.0	-8.8	-66.4

(continued) Stable isotope data of groundwater samples in the Omatako basin, 1997 and 1998

sample	name	reference	date	longitude [°E]	latitude [°S]	elevation [m]	Temp. [°C]	ec [µS/cm]	pH	$\delta^{18}\text{O}$ [‰]	$\delta^2\text{H}$ [‰]
CN113	Breitenbach 'Farm'	CN054	Mar-98	17.7007	-19.9730	1402	26.0	941	6.7	-8.8	-61.8
CN114	Omambonde West	CN037	Mar-98	17.8378	-20.0403	1296	25.0	260	6.5	-9.6	-65.5
CN115	Gai Kaisa 'Farm'	CN046	Mar-98	17.8324	-19.8967	1400	25.1	872	6.8	-8.7	-60.8
CN116	Osambusatjuru	CN004	Mar-98	17.7656	-19.8789	1530	27.7	997	6.8	-8.9	-62.5
CN117	Gai Kaisa 'West'	CN003	Mar-98	17.7933	-19.8725	1424	28.9	932	6.8	-8.6	-60.5
CN118	Hochkamp 'Farm'		Mar-98	17.8853	-19.8144	1493	24.1	1049	7.0	-9.1	-64.4
CN119	Hochkamp 'No. 14'	CN052	Mar-98	17.8693	-19.8014	1470	24.6	850	7.1	-9.3	-64.9
CN120	Gunuchas 'Windmotor'	CN047	Mar-98	17.8812	-19.8760	1396	25.5	1099	6.8	-8.7	-60.8
CN121	Gunuchas 'Haus'	CN048	Mar-98	17.8989	-19.8919	1378	26.1	2082	6.2	-8.7	-62.0
CN122	Gunuchas 'E-Pumpe'	CN049	Mar-98	17.9125	-19.8911	1375	26.4	1679	6.5	-8.9	-63.2
CN123	Gesundbrunnen	CN065	Mar-98	17.7778	-19.8495	1439	24.8	910	6.6	-8.7	-62.7
CN124	Omambondetal 'Mittelposten'		Mar-98	17.9678	-19.9987	1479	28.0	1273	7.0	-8.6	-63.2
CN125	Omambondetal 'Nord'	CN051	Mar-98	17.9625	-19.9529	1328	26.3	905	7.4	-8.0	-60.5
CN126	Omambondetal 'Haus'	CN050	Mar-98	17.9621	-20.0417	1269	26.5	552	7.7	-8.2	-57.4
CN127	Omambonde Ost	CN081	Mar-98	17.8856	-20.0478	1275	25.1	574	7.6	-8.2	-59.3
CN128	Schönhausen	CN002	Mar-98	17.8250	-19.8445	1427	24.8	1212	7.2	-8.7	-61.8
CN129	Salzbrunnen Farm	CN053	Mar-98	17.7940	-19.8117	1465	28.2	1861	6.9	-8.8	-62.5
CN131	Hairbib 'Heiße Quelle'		Mar-98	17.9371	-19.8660	1385	42.7	4974	6.5	-9.2	-64.8
CN132	Hairbib Haus	CN066	Mar-98	17.9772	-19.8821	1385	27.8	1508	7.1	-8.9	-64.2
CN134	Tiefwasser	CN021	Mar-98	18.1017	-19.6510	1402	28.2	868	7.1	-8.3	-60.2
CN136	Okamutombe 'Farm'	CN024	Mar-98	18.1481	-19.7284	1353	25.9	921	7.1	-7.1	-57.4
CN137	Okamutombe 'Nord'	CN025	Mar-98	18.1124	-19.6903	1383	25.6	1148	7.0	-7.3	-59.0
CN138	Havelberg	CN027	Mar-98	18.0978	-19.8050	1345	24.8	923	7.0	-6.4	-51.4
CN139	Omega Groote Pos	CN045	Mar-98	17.7656	-20.1210	1397	27.0	143	7.1	-9.6	-66.2
CN140	Omega Kral	CN044	Mar-98	17.8231	-20.1173	1370	27.0	287	6.3	-9.3	-64.0
CN143	Waterberg 'Tief'	CN056	Mar-98	17.3559	-20.4141	1500	25.6	325	7.1	-9.3	-67.0
CN144	Waterberg 'Flach'	CN057	Mar-98	17.3538	-20.4119	1520	24.2	287	7.1	-9.5	-66.5
CN145	Okajjikona	CN058	Mar-98	17.3982	-20.3953	1435	27.0	365	7.7	-9.6	-65.7
CN146	Leo		Mar-98	17.8328	-20.2323	1429	27.6	117	6.9	-8.4	-59.7
CN147	Diepwater	CN059	Mar-98	17.7219	-20.1952	1417	27.2	147	6.4	-9.4	-64.1
CN148	Toinel		Mar-98	17.8846	-20.1404	1316	27.8	93	6.6	-9.0	-63.1
CN149	Duineveld		Mar-98	17.8935	-20.1847	1368	27.2	229	6.3	-8.5	-60.2
CN150	Hirschgrund	CN035	Mar-98	17.9721	-20.2122	1297	27.3	249	5.2	-8.2	-59.8
CN151	Waagstuk	CN034	Mar-98	17.9761	-20.1192	1326	28.0	249	6.4	-8.6	-60.2
CN152	Schwarzfelde	CN029	Mar-98	18.1278	-19.9618	1270	26.6	1310	6.9	-7.8	-58.1
CN153	Okshof	CN033	Mar-98	18.0337	-20.0149	1280	26.4	1041	7.0	-7.8	-60.4
CN154	Kabare	CN030	Mar-98	18.0623	-20.0187	1273	27.0	797	7.1	-8.2	-63.4
CN155	Oktrooi	CN031	Mar-98	18.0865	-19.9979	1268	26.2	776	7.0	-8.1	-62.2
CN156	Schönau	CN032	Mar-98	18.1707	-19.9914	1253	25.8	944	7.2	-6.8	-54.7
CN157	Ongongoro	CN018	Mar-98	18.2461	-20.0549	1242	27.7	1193	7.0	-7.6	-58.1
CN159	Koblentz SW		Mar-98	18.1677	-20.1081	1240	26.9	986	6.8	-8.1	-61.9
CN160	Koblentz S		Mar-98	18.2096	-20.1116	1230	27.0	1004	6.8	-8.1	-61.3
CN161	Koblentz E		Mar-98	18.1958	-20.0915	1235	27.1	1017	6.8	-8.2	-62.2
CN162	Okambora	CN017	Mar-98	18.0978	-20.1738	1250	27.2	506	6.8	-9.5	-67.5
CN163	Omakande		Mar-98	18.1357	-20.3263	7865	26.8		6.6	-8.4	-61.7

The  $\delta^{18}\text{O}$  -  $\delta^2\text{H}$  diagram of all samples is shown in Figure 4.39 (filled circles). For reference the weighted average of  $\delta^{18}\text{O}$  and  $\delta^2\text{H}$  of precipitation at Windhoek is also plotted (square).

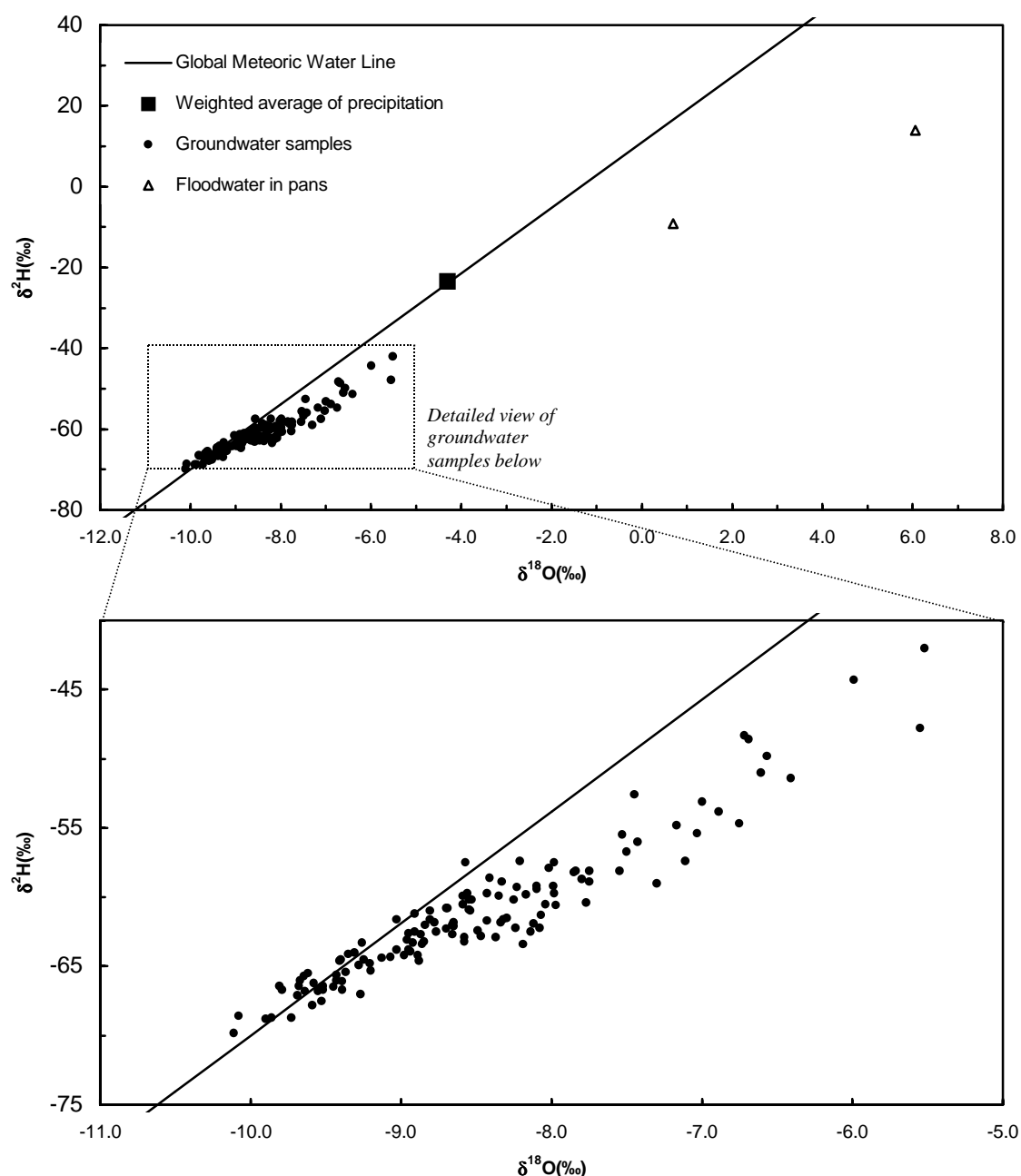


**Figure 4.39**  $^{18}\text{O}$  -  $^2\text{H}$  diagram of groundwater and two surface water samples taken in 1997 in the Goblenz area. The full line represents the Global Meteoric Water Line, given by  $\delta^2\text{H} = 8 * \delta^{18}\text{O} + 10$  ‰ VSMOW. A detailed view of groundwater samples only is given in the lower graph.

The groundwater samples have  $\delta^{18}\text{O}$  values that range between -10.1 ‰ at a spring at the Waterberg rest camp (CN041) and -5.5 ‰ (CN055 at Gutweide Farm). Two samples of surface water in pans are strongly enriched, with values of +0.7 ‰ and +6.6 ‰. In general, the groundwater has a light composition as compared to the weighted average of precipitation

at Windhoek which is -4.3 ‰. The difference is not due to the altitude effect because the altitude of Windhoek (1,728 m) is comparable to that of the highest mountain ranges and recharge areas in the Omatako basin (1,600 to 1,750 m in the Otavi Mountains and highest Waterberg sandstone outcrops). The observed bias is interpreted as a selective contribution of effective precipitation with low  $\delta^{18}\text{O}$  and  $\delta^2\text{H}$  values to groundwater recharge. A similar phenomenon was observed in the Negev (LEVIN ET AL., 1980) and in the Sonora deserts (ADAR & NEUMAN, 1988). This interpretation is consistent with the results of the water balance modelling showing that the majority of small rainfall events does not produce any recharge at all. It is only by intense, prolonged or consecutive events that the threshold for groundwater recharge is exceeded. The seasonal distribution of  $\delta^{18}\text{O}$  in precipitation (Figure 4.36) and the climatic water balance (Figure 4.7) both indicate that the highest likelihood of recharge and the months with the most depleted precipitation coincide in February.

The  $\delta^{18}\text{O}$  -  $\delta^2\text{H}$  diagram shows that there is an evaporative enrichment for some more enriched groundwater samples, while other samples plot close to the Global Meteoric Water Line. According to their  $\delta^{18}\text{O}$  -  $\delta^2\text{H}$  relationship, the later samples have not undergone detectable evaporative enrichment and have a typical spectrum of  $\delta^{18}\text{O}$  from -10 ‰ to -8.5 ‰ VSMOW (Figure 4.40).

Most of the samples in the area of Etjo sandstone outcrops without Kalahari cover belong to this type (i.e. CN041 'Waterberg No. 2'), as well as some samples from other areas without Kalahari cover (CN002 'Gai Kaisa West', CN052 'Hochkamp No. 14'). The recharge areas for these lie between 1,500 and 1,750 m a. s. l.

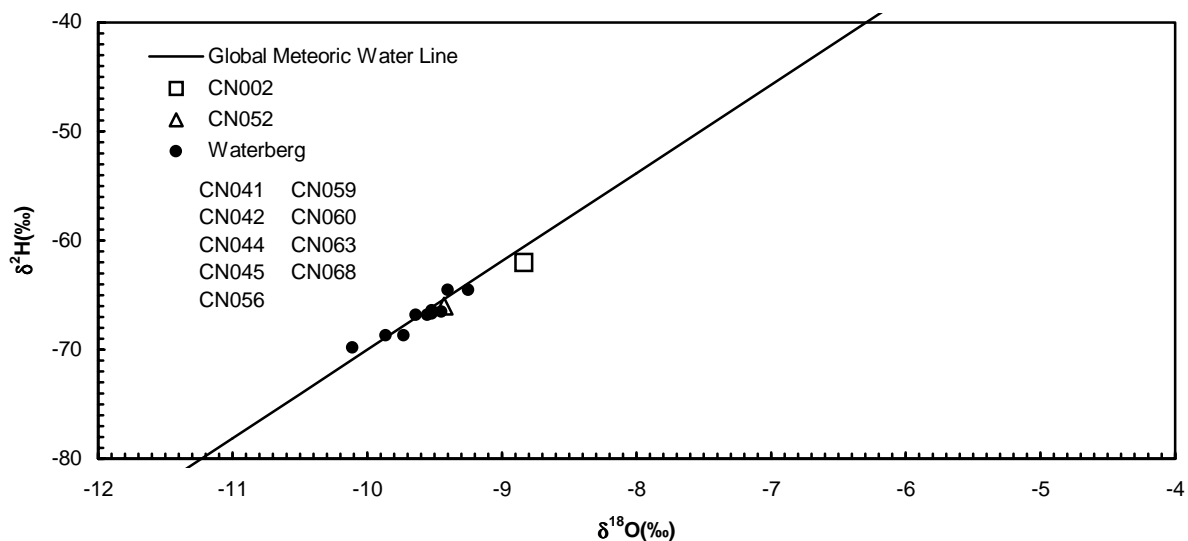


**Figure 4.40**  $^{18}\text{O}$  -  $^2\text{H}$  diagram with samples plotting close to the Global Meteoric Water Line: filled circles represent samples from the Waterberg area, the triangle and the square represent selected samples from other areas without Kalahari cover.

The  $\delta^{18}\text{O}$  values from groundwater samples from the Waterberg vary between  $-10.1\text{‰}$  and  $-9.3\text{‰}$ . The most depleted values are observed in the western part of the Waterberg close to the elevated recharge areas (CN041, CN042).

Other groundwater samples plot below the Global Meteoric Water Line and show signs of evaporative enrichment. The evaporative enrichment is pronounced for two samples of surface water. The latter, CN039 ‘Okahitwa Pan’ and CN040 ‘Omaihi Pan’, were taken from two pools of standing surface water in the Omatako river at about 1,290 m a. s. l. They had accumulated during the previous rainy season 1996/1997 and had been exposed to open surface evaporation for several weeks. Consequently they have become strongly enriched in the heavier isotopes  $^{18}\text{O}$  and  $^2\text{H}$ .

The determination of the slope of the evaporation line from all samples in Figure 4.39 is difficult. The samples were taken from different groundwater types having an original variability of their isotopic composition before evaporation. Consequently the evolution took place along parallel evaporation lines. In addition, some samples represent mixtures of different groundwater types. Therefore, the slope of the evaporation line has been determined only from boreholes that a) could be attributed to a specific original groundwater type and b) were not located in mixing zones.

These conditions exist along profile DG in Figure 4.38. The samples all belong to hydrochemical group (d) formed by groundwater recharged in the Otavi Mountains. Along this profile an evaporative enrichment is observed (see Figure 4.6 for comparison).

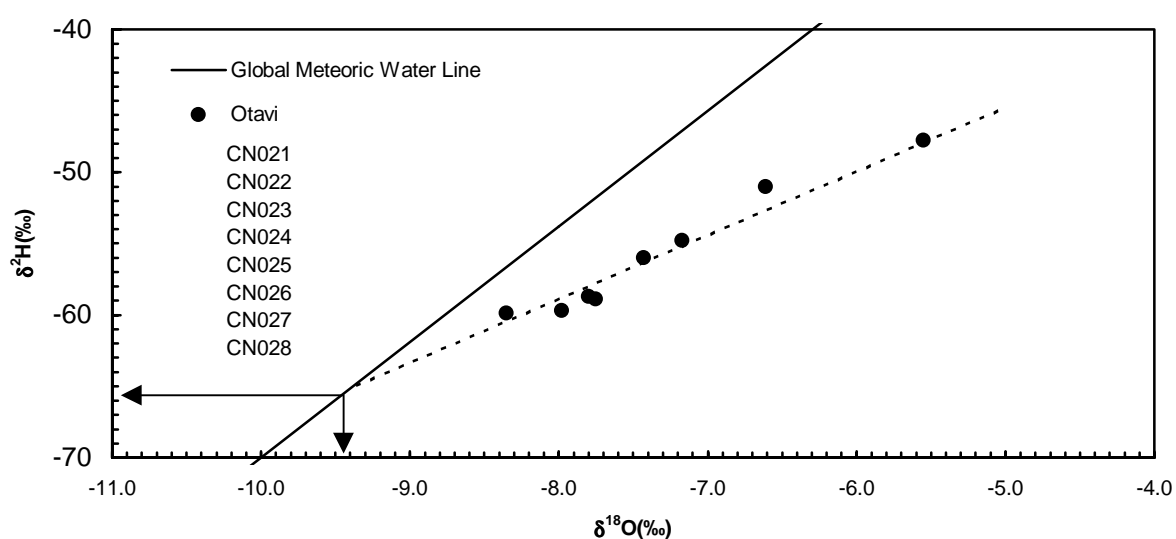


**Figure 4.41**  $^{18}\text{O}$  -  $^2\text{H}$  diagram of groundwater samples belonging to the same groundwater type and isotopically enriched along the flowline DG in Figure 4.38. The continuous line represents the Global Meteoric Water Line defined by  $\delta^2\text{H}=8.1*\delta^{18}\text{O}+10.8\text{‰}$  VSMOW. The dashed line represents the evaporation line fitted by linear regression.

If only the boreholes along this profile are plotted in a  $\delta^{18}\text{O}$  -  $\delta^2\text{H}$  diagram, they show an evaporative enrichment with much less scatter (Figure 4.41). The regression through all samples has a slope of 4.5 with  $R^2=0.96$ . The evaporation line intersects the Global Meteoric Water Line at  $\delta^{18}\text{O}=-9.5$  ‰ and  $\delta^2\text{H} = -66$  ‰, which represents the original isotopic composition prior to evaporative enrichment.

In the same way, an evaporation line was determined for groundwater samples taken from Kalahari aquifers (Figure 4.42). The list of samples used is given in the figure below.

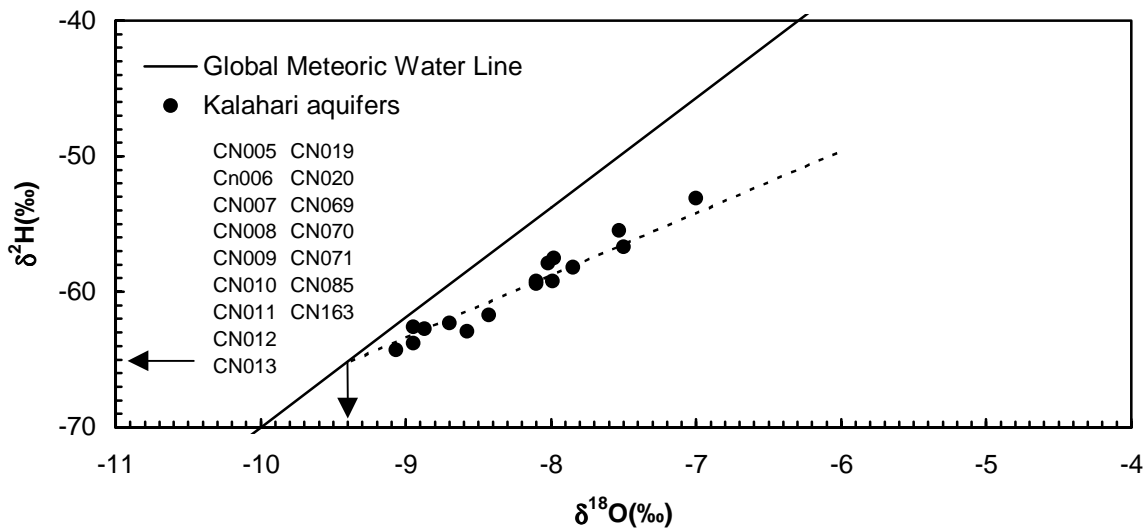


**Figure 4.42**  $\delta^{18}\text{O}$  -  $\delta^2\text{H}$  diagram of groundwater samples from the Kalahari along flowline CG in Figure 4.38. The continuous line represents the Global Meteoric Water Line, the dashed line the evaporation line fitted by linear regression.

A similar slope of 4.6 has been derived from these samples by linear regression with  $R^2=0.95$ . Similar to the previous analysis, the evaporation line intersects the Global Meteoric Water Line at  $\delta^{18}\text{O} = -9.4$  ‰ and  $\delta^2\text{H} = -65$  ‰. For further calculations it will therefore be assumed that the mean evaporation line has an average slope of 4.5.

There are only two permanent groundwater discharge areas in the whole study area where groundwater presently reaches the surface and is directly exposed to evaporation: the Rietfontein springs (close to Grootfontein, Figure 1.1) south of the Otavi Mountains, and the Waterberg springs at the base of the Etjo sandstone. The Rietfontein springs recently stopped flowing due to intensive groundwater extraction. Before the cessation of spring flow open surface evaporation and isotopic enrichment may have taken place in the groundwater discharge zone. The signal of isotopic enrichment could have been transferred to the groundwater in the Otavi Mountain Foreland by some re-infiltration of enriched surface water into the aquifer.

Still, such a mechanism can not explain the evaporative enrichment in the Kalahari where groundwater discharge zones are missing. Therefore, alternative concepts explaining the observed isotopic enrichment were considered.

A characteristic evaporative enrichment of groundwater below dunes was found in arid and semi-arid climate (DINÇER ET AL., 1974; ALLISON ET AL., 1985). The observed enrichment, with a small slope of about 2 in a  $\delta^{18}\text{O}$  -  $\delta^2\text{H}$  diagram, was seen as a result of vapour diffusion from soil moisture prior to recharge. In fact a large part of the Kalahari basin in the study area is covered with sand dunes. However, the isotopic composition of groundwater in the study area is not consistent with such a mechanism. The observed slope of the evaporation lines in the Kalahari and Otavi Foreland aquifers is about 4.6. Therefore it seems more likely that isotopic enrichment is caused by open surface evaporation during indirect recharge.

In the Kalahari and in the Otavi Foreland, there are numerous depressions (pans) and small artificial dams in ephemeral rivers that are sporadically flooded. Pools of standing water remain for several weeks after floods. Strong isotopic enrichment by open surface evaporation was observed in filled dams and pans as shown by samples CN039 and CN040. Seepage from dams and pans may then transfer the signal of isotopic enrichment to the groundwater.

In the Negev isotopic enrichment was also detected in surface runoff and river discharge (DODY ET AL., 1995; ADAR ET AL., 1998). It was proposed that runoff was partly trapped and enriched in on-surface depression storage before being flushed by subsequent spells of runoff. Therefore evaporative enrichment of flood water can also be transferred to the groundwater by streambed infiltration within the Kalahari.

In conclusion, the isotopic enrichment in the Kalahari and in the Otavi Mountain Foreland is probably caused by evaporation from surface depressions or pans/artificial dams during and after runoff events.

#### *Temporal variability of stable isotopes in groundwater*

Before an interpretation of the spatial distribution of stable isotope can be made in a meaningful way, the temporal variability of stable isotope data needs to be examined. Only if it is small as compared to spatial differences, a regional analysis will make sense.

In order to determine the importance of temporal variations for a large area, an economic sampling strategy had to be defined. Sampling for a multi-year time series with high resolution during the period of most likely recharge would have been the perfect solution.

This approach was logistically not feasible in the framework of this study. Therefore, target areas were chosen for a two-level sampling strategy:

- *re-sampling was made for as many boreholes as possible, and*
- *monthly time series were produced for selected boreholes.*

Temporal variations in the groundwater occur where the isotopic variations in the precipitation are not attenuated in the unsaturated zone and then once more in the saturated zone, in other words where the depth to the groundwater table is smaller than the depth of attenuation (Chapter 3.2.2). Variations in the isotopic composition of groundwater are most likely where depth to the groundwater table is small, reflecting isotopic variability in rainstorms and from ephemeral floods.

Using the regionalized map of depth to the groundwater table (Figure 4.6), the re-sampling focused on the area north of Goblenz. Altogether 44 boreholes were sampled twice in order to screen a relatively large area and to detect variations. The first sampling was made after a dry period in July 1997. The second sampling was carried out in March 1998. A few weeks earlier, in late December 1997, heavy rainfall events were recorded that also produced floods in some parts of the Omatoko basin. According to local farmers some areas between the Otavi Mountains and Goblenz were flooded for several days.

In Figure 4.43 the isotope data from samples taken in July 1997 and March 1998 are compared. The perfect match between both  $\delta^{18}\text{O}$  values (1997 on the x-axis, 1998 on the y-axis) would be given by the diagonal 1:1 line. An analytical error range of 0.1 ‰ for  $\delta^{18}\text{O}$  and of 1 ‰ for  $\delta^2\text{H}$  has been added to both sides of the original line - a relative difference of 0.2 ‰ for  $\delta^{18}\text{O}$  (2 ‰ for  $\delta^2\text{H}$ ) is considered to be the maximum deviation still within the error range.

In general, there is a good correlation between both samples. There seems to be a slight trend of enrichment for many samples but this trend is still within the margins of analytical error. Only three other samples out of 44 have more depleted values in 1998. For one sample, CN106 'Gutweide', there is a strong variation of -1.2 ‰ in  $\delta^{18}\text{O}$  between 1997 and 1998. The sample was taken north of the Waterberg. Sample CN106 is an outlier with deviations of -1.2 ‰ for  $\delta^{18}\text{O}$  and -6 ‰ for  $\delta^2\text{H}$ . The direction of this large deviation is opposed to the general trend.



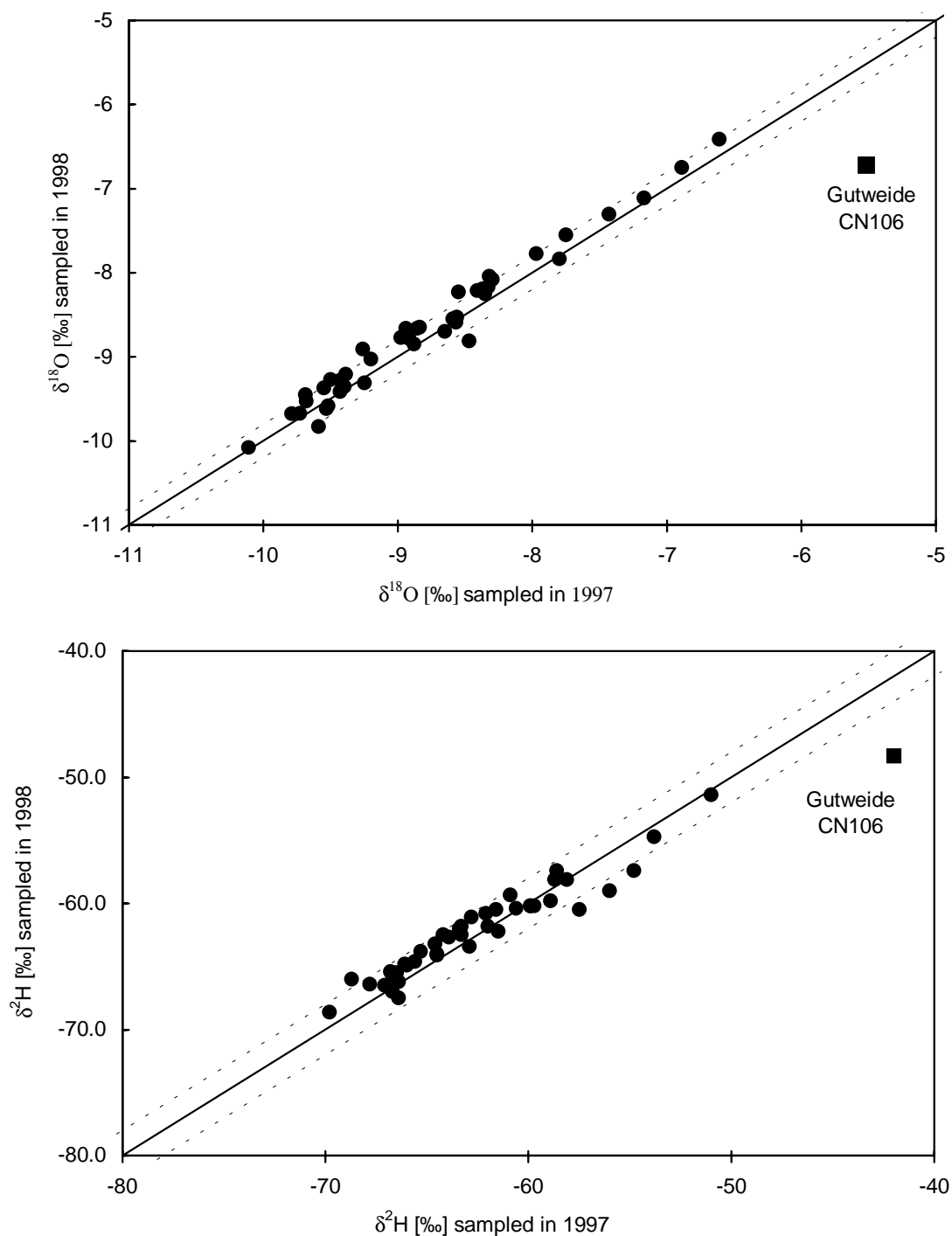


**Figure 4.43** Comparison of the stable isotope data of samples taken in 1997 and 1998.

If the frequency distributions of deviations between  $\delta^{18}\text{O}$  and  $\delta^2\text{H}$  values in 1997 and 1998 are considered in detail (Figure 4.44), a slight trend towards heavier values in 1998 becomes more evident. This trend is consistent for both  $\delta^{18}\text{O}$  and  $\delta^2\text{H}$ . The location of the frequency distributions suggests that an average shift of +0.2 ‰ for  $\delta^{18}\text{O}$  and +2 ‰ for  $\delta^2\text{H}$  occurred between July 1997 and March 1998.

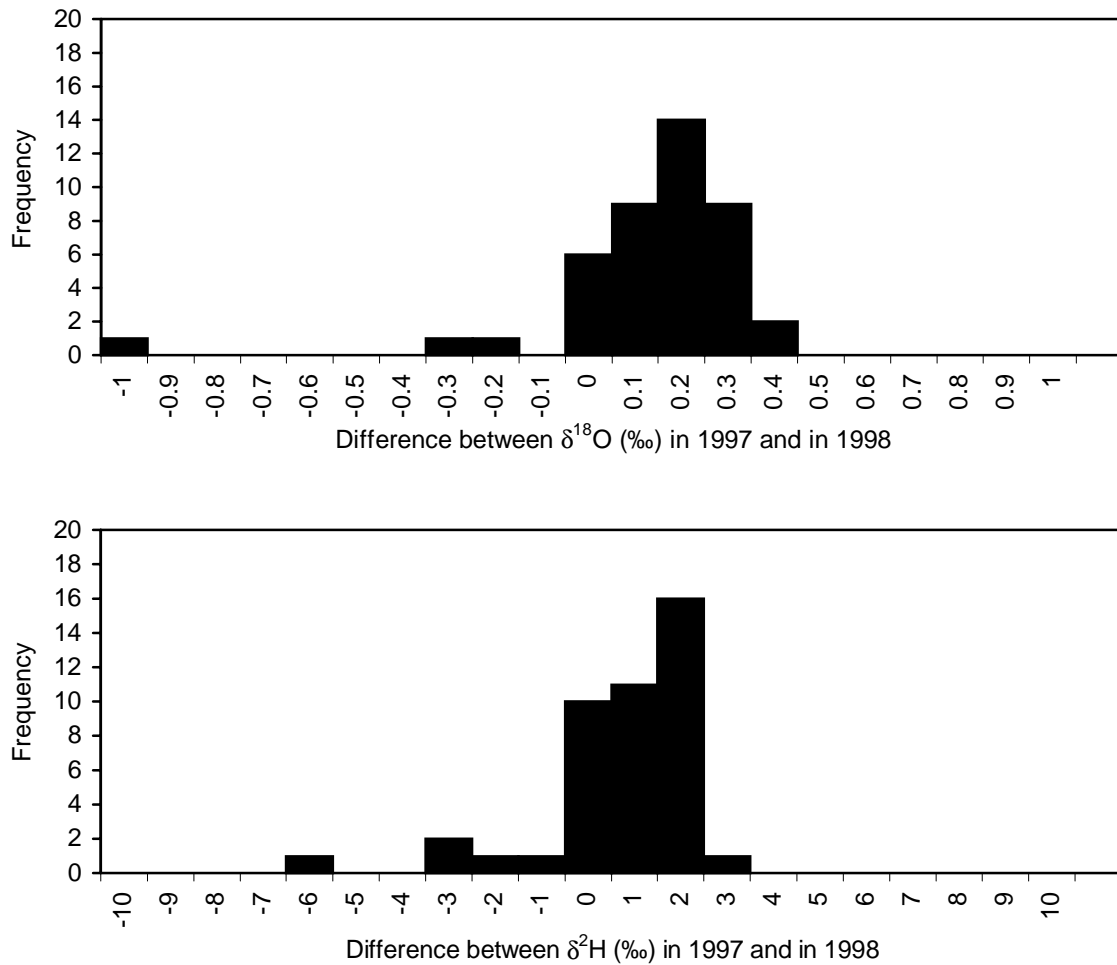


**Figure 4.44** Frequency distribution of deviations between  $\delta^{18}\text{O}$  and  $\delta^2\text{H}$  values (‰ VSMOW).

It is concluded that there is a consistent shift in both the  $\delta^{18}\text{O}$  and  $\delta^2\text{H}$  values between 1997 and 1998. The trend towards heavier values indicates that recharge in the rainy season 1997/1998, which probably caused these deviations, had a more positive signal than the groundwater sampled in 1997. More detailed information on the cause and timing of these variations was obtained from time series analysis of monthly groundwater samples.

Close to ephemeral rivers or sinkholes, where recharge was expected to possibly modify the isotopic composition of groundwater, sampling for monthly time series by local farmers was organized. The sampling period covered the time between November 1997 and March 1998. The list of analyses is given in Table 4.4. In Figure 4.45 the time series measured for  $\delta^{18}\text{O}$  at CN038 'Kameeldorn', CN029 'Schwarzfelde' and CN024 'Okamutombe' are shown.

In order to better characterize the source area a correction of  $\delta^{18}\text{O}$  for evaporative enrichment according to GEYH & PLOETHNER (1997) was applied. Corrected values indicate the isotopic

composition without enrichment by evaporation. As the corrected value marks the intersection of the evaporation line with the Global Meteoric Water Line, it is defined by:

$$\delta^{18}\text{O}_{\text{corrected}} = \frac{\delta^2\text{H}_{\text{measured}} - e * \delta^{18}\text{O}_{\text{measured}} - d}{8 - e} \quad (45)$$

where  $e$  corresponds to the slope of the evaporation line determined earlier as 4.5, and  $d$  is the deuterium excess of global precipitation, with  $d = +10$  ‰. In the study area the variability of corrected  $\delta^{18}\text{O}$  in groundwater is assumed to reflect mainly different recharge altitudes. An altitude effect of about +0.25‰ for the Otavi Mountains and the southern Foreland has been postulated by PLOETHNER ET AL. (1997). It was derived by attributing the altitude of assumed recharge areas to evaporation-corrected  $\delta^{18}\text{O}$  data.

**Table 4.4** Stable isotope time series data.

sample	longitude °E	latitude °S	depth [m]	level [m]	date	$\delta^{18}\text{O}$ [‰]	$\delta^2\text{H}$ [‰]	$\delta^{18}\text{O}_{\text{corrected}}$ [‰]
<b>Kameeldorn CN038</b>	17.7921	-20.0002	9.0	5.5	06-97	-9.4	-65.6	-9.5
					11-97	-9.3	-64.4	-9.3
					12-97	-8.5	-62.8	-9.8
					01-98	-8.9	-63.8	-9.7
					02-98	-9.4	-64.8	-9.3
					03-98	-9.4	-64.6	-9.2
<b>Schwarzfelde CN029</b>	18.1278	-19.9618	50.0	20.0	06-97	-7.8	-58.7	-9.6
					12-97	-7.8	-58.0	-9.4
					01-98	-7.9	-58.3	-9.4
					02-98	-7.6	-57.3	-9.4
					03-98	-7.8	-58.0	-9.4
<b>Okamutombe CN024</b>	18.14810	-19.72838	-	10.0	06-97	-7.2	-54.8	-9.3
					09-97	-7.2	-56.8	-9.9
					10-97	-7.1	-55.6	-9.6
					11-97	-7.1	-55.5	-9.6
					12-97	-7.2	-55.3	-9.4
					01-98	-7.1	-55.5	-9.6
					02-98	-7.1	-57.5	-10.2
					03-98	-7.1	-57.4	-10.1

The first sample was taken in July 1997. During the rainy season 1997/1998 monthly samples were taken between September/November to March. The sampling period included a flood event in late December 1997 observed by local farmers in the Omambonde ephemeral river and in the Otavi Foreland, where video shots show widespread sheet flows that lasted for several days. For all boreholes the groundwater table is between 5.5 and 20 m below the surface. At CN038 'Kameeldorn' the groundwater table is very shallow, approximately 5 to 6 m below the surface. The borehole is located directly on the bank of the Omambonde ephemeral river.

A pronounced variation in the isotopic composition is observed at CN038. In July 1997 and February, March 1998  $\delta^{18}\text{O}$  of groundwater samples at 'Kameeldorn' all had values of about -9.4 ‰;  $\delta^2\text{H}$  ranged between -65.6 ‰ and -64.6 ‰. In the sample from December 1997 taken just after the flood  $\delta^{18}\text{O}$  had increased to -8.5 ‰ and  $\delta^2\text{H}$  to -62.8 ‰. The sample from January 1998 is characterized by intermediate values. At the same time corrected  $\delta^{18}\text{O}$  in December 1997 and January 1998 became more depleted by about 0.3-0.4 ‰. The isotopic composition at CN038 'Kameeldorn' has probably been affected by the flood event in December 1997. However, the changes did not persist for more than two months. The isotopic composition returned to the initial values in February 1998.

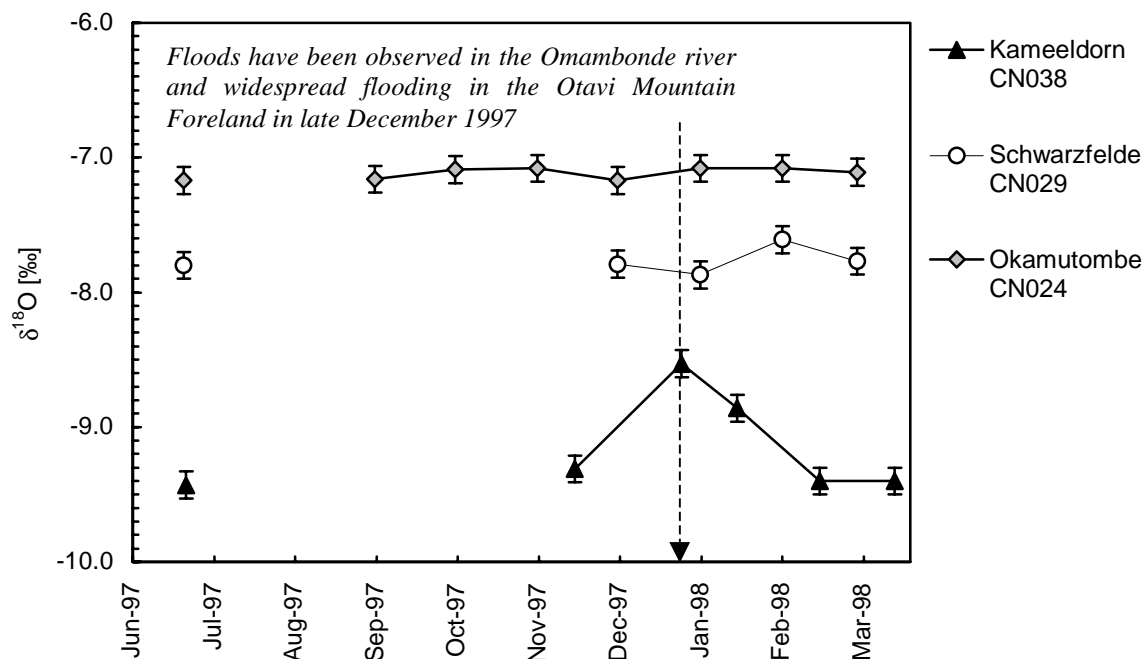


**Figure 4.45** Time series of  $\delta^{18}\text{O}$  between November 1997 and March 1998 at Okamutombe, Kameeldorn and Schwarzfelde. In Figure 4.38, the location of these boreholes is marked by black squares.

At CN029 'Schwarzfelde' there is a slight increase of  $\delta^{18}\text{O}$  and  $\delta^2\text{H}$  for February 1998. The samples of July and December 1997 and/or March 1998 all have  $\delta^{18}\text{O}$  values of -7.9 ‰ and -7.8 ‰;  $\delta^2\text{H}$  is between -58.7 ‰ and -58.0 ‰. For February  $\delta^{18}\text{O}$  indicates a slightly heavier isotopic composition with  $\delta^{18}\text{O} = -7.6$  ‰ and  $\delta^2\text{H} = -57.3$  ‰. The  $\delta^{18}\text{O}$  values at CN024 'Okamutombe' are stable. All values range between -7.1 ‰ and -7.2 ‰, which is within the analytical error of  $\pm 0.1$  ‰.

It is interesting to note that the observed variation has the same sign as the general shift towards a heavier isotopic composition (+0.2 ‰) observed from the 44 samples taken in July 1997 and March 1998.

Some constraints for the isotopic composition of the floodwater that caused these changes can be made. The flood in the Omambonde river at CN038 had  $\delta^{18}\text{O} > -8.5$  ‰. The mixtures with flood recharge in December 1997 and January 1998 point to an evaporated end member (Figure 4.46). This is very clear at CN038 ‘Kameeldorn’ where the samples of July 1997, November 1997, February and March 1998 all lie on the Global Meteoric Water Line. Samples from December 1997 and January 1998 clearly plot below the meteoric water line. A similar but much weaker effect is observed at CN029 ‘Schwarzfelde’ where the sample taken in February 1998 is slightly more enriched.

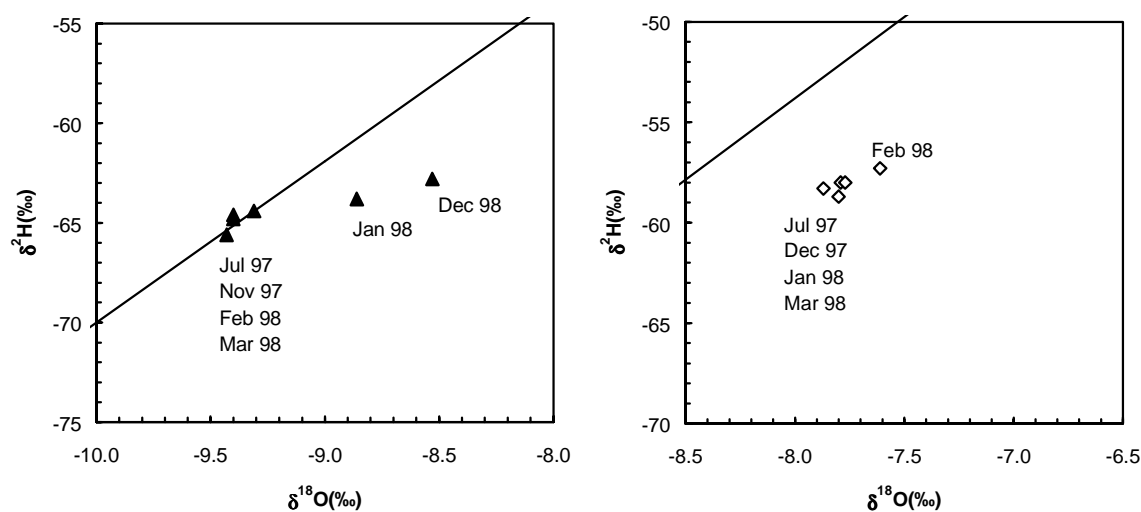


**Figure 4.46** Time series data at CN038 ‘Kameeldorn’ and at CN029 ‘Schwarzfelde’ plotted in a  $\delta^{18}\text{O}$ - $\delta^2\text{H}$  diagram.

For the corrected  $\delta^{18}\text{O}$  values the trend is reversed. Samples that were influenced by the flood event at CN038 have more depleted corrected  $\delta^{18}\text{O}$  values (Table 4.4).

For understanding the relative isotopic changes it is important to recall the hydrogeological context. A background isotopic composition without evaporative enrichment is observed before and after the impact of flood recharge at CN038. This composition reflects groundwater inflow from the Otavi Mountains to the north (Figure 4.1) characterized by  $\delta^{18}\text{O} = -9.5$  ‰ and  $\delta^2\text{H} = -66$  ‰ (Figure 4.41).

The documented occurrence of episodic floods and the existence of sinkholes in the Otavi Foreland suggest that the observed fluctuations of the isotopic composition are at least partly due to indirect recharge from floods. The hydrological data (Chapter 2.2) show that most of the runoff is generated in the more elevated mountainous rim of the Omatako basin which explains the observed relative depletion in *corrected*  $\delta^{18}\text{O}$ . A selective contribution of

intensive and depleted rainfall to surface runoff may enhance this effect (LEVIN ET AL., 1980). The evaporative enrichment observed in the response to the flood event at CN038 takes place during runoff formation (DODY ET AL., 1995) or after the runoff event by evaporation from pans.

### *Regional distribution of stable isotopes in groundwater*

For the following discussion it must be taken into account that the accuracy of spatial discrimination of isotopic signals in groundwater is reduced by the above mentioned temporal variations. The regional distribution of  $\delta^{18}\text{O}$  is shown in Figure 4.47. Samples that plot close to the meteoric water line and have a deuterium excess of  $d > +10$  ‰ are marked by open circles (○); samples that have undergone evaporative enrichment are represented by a black dot (●). All samples from the Kalahari (e) and most of the samples from the Otavi Foreland (d) are isotopically enriched by evaporation.

With a single exception in the Sandveld (marked with a frame, -9.7 ‰), all samples without evaporative enrichment belong to areas with less than 10 m of overlying Kalahari sediments. In bare rock areas, fractures offer direct recharge pathways through which rainfall can reach the groundwater with little or without any evaporative enrichment. Four subareas can be distinguished: In an area north of the Waterberg, where undifferentiated metamorphic rocks of the Damara Sequence and marbles of the Karibib Formation are exposed, two samples with -8.9 ‰ and -9.0 ‰ were taken (a), two samples with  $\delta^{18}\text{O}$  of -9.7 ‰ and -9.8 ‰ are from the Otavi Mountains (b). Further south and close to the Waterberg contact with the Etjo sandstone, two samples have -9.3 ‰ and -8.6 ‰, the later being located close to an ephemeral river.

The largest group of groundwater samples without evaporative enrichment in terms of sample numbers is found in the Waterberg area ( $c_1$  and  $c_2$ ). The range of  $\delta^{18}\text{O}$  for all groundwater samples in the Etjo sandstone is -10.1 ‰ to -9.3 ‰. A group of samples from the west ( $c_1$ ) were taken from springs or shallow boreholes along the southern slope of the Waterberg, with values between -10.1 ‰ and -9.6 ‰. An eastern group of samples ( $c_2$ ) was taken from boreholes within the Etjo sandstone. The large range of 0.8 ‰ in the groundwater can probably be explained as the combined effect of recharge at different altitudes and of temporal variations.

The samples with evaporative enrichment (●) have been corrected using Equation (45). A correction for evaporative enrichment gives an idea of the initial isotopic composition. If there

is an altitude effect in the isotopic composition of rainfall, the regional distribution of corrected  $\delta^{18}\text{O}$  in groundwater (Figure 4.48) provides information on the recharge altitude.

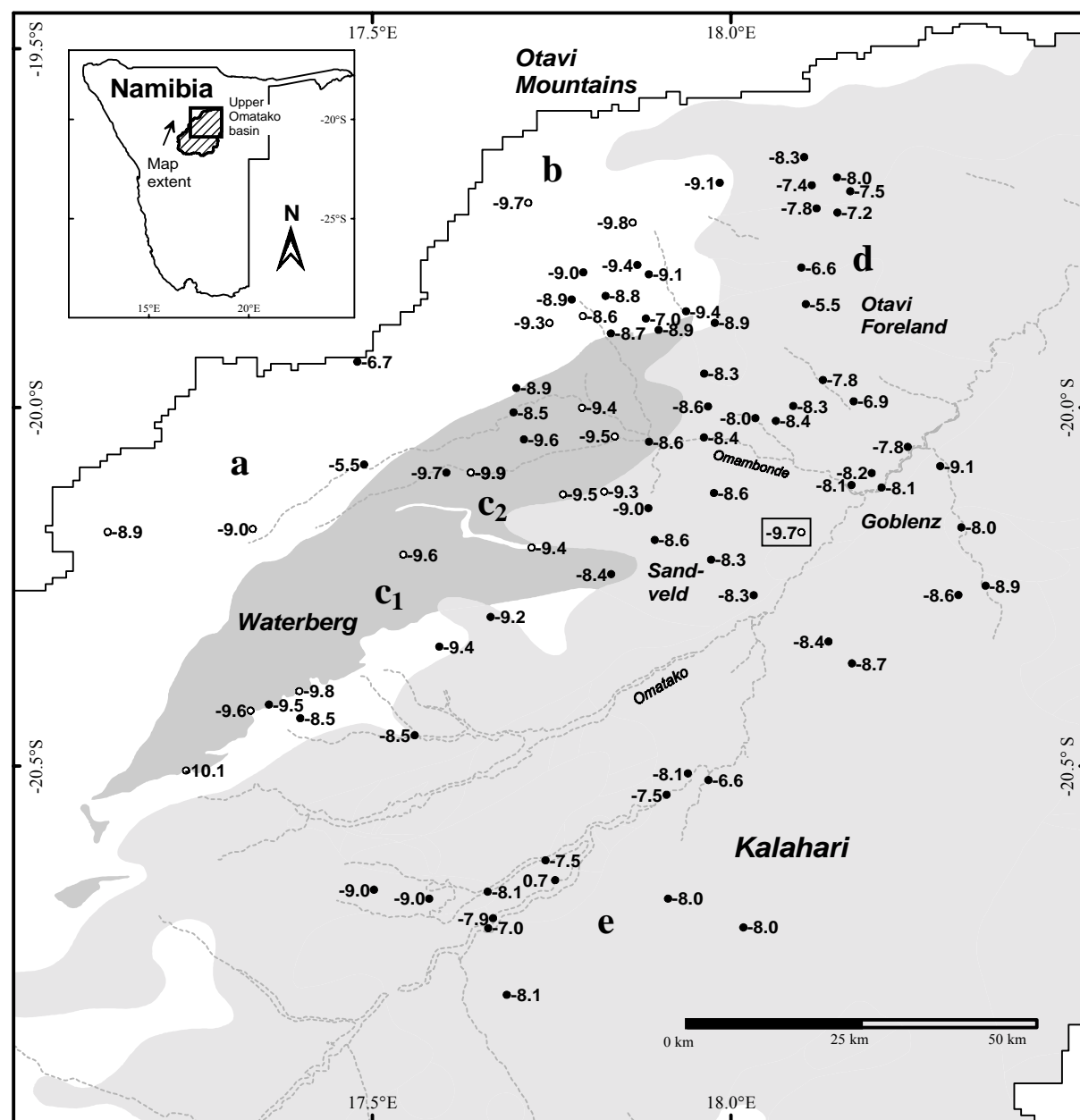


**Figure 4.47** Samples for stable isotopes from boreholes in the Omatako basin. The values indicate  $\delta^{18}\text{O}$  (‰ VSMOW).

In order to facilitate interpretation of the data, the expected mean  $\delta^{18}\text{O}$  of recharge at the local altitude is plotted as a greyscale background contour map. This map has been obtained by the following method:

- an observed value of -9.8 ‰ for the high recharge areas in the Otavi Mountains was taken as a reference,

- a map of the differences from this reference elevation was determined for every point in the catchment with the digital elevation model of the Omatako basin (this DEM is shown in Figure 1.1 and has a spatial resolution of 1 x 1 km).

Using this difference map, the expected composition at each point in the Omatako basin was calculated for an altitude effect of 0.25 ‰/100 m.

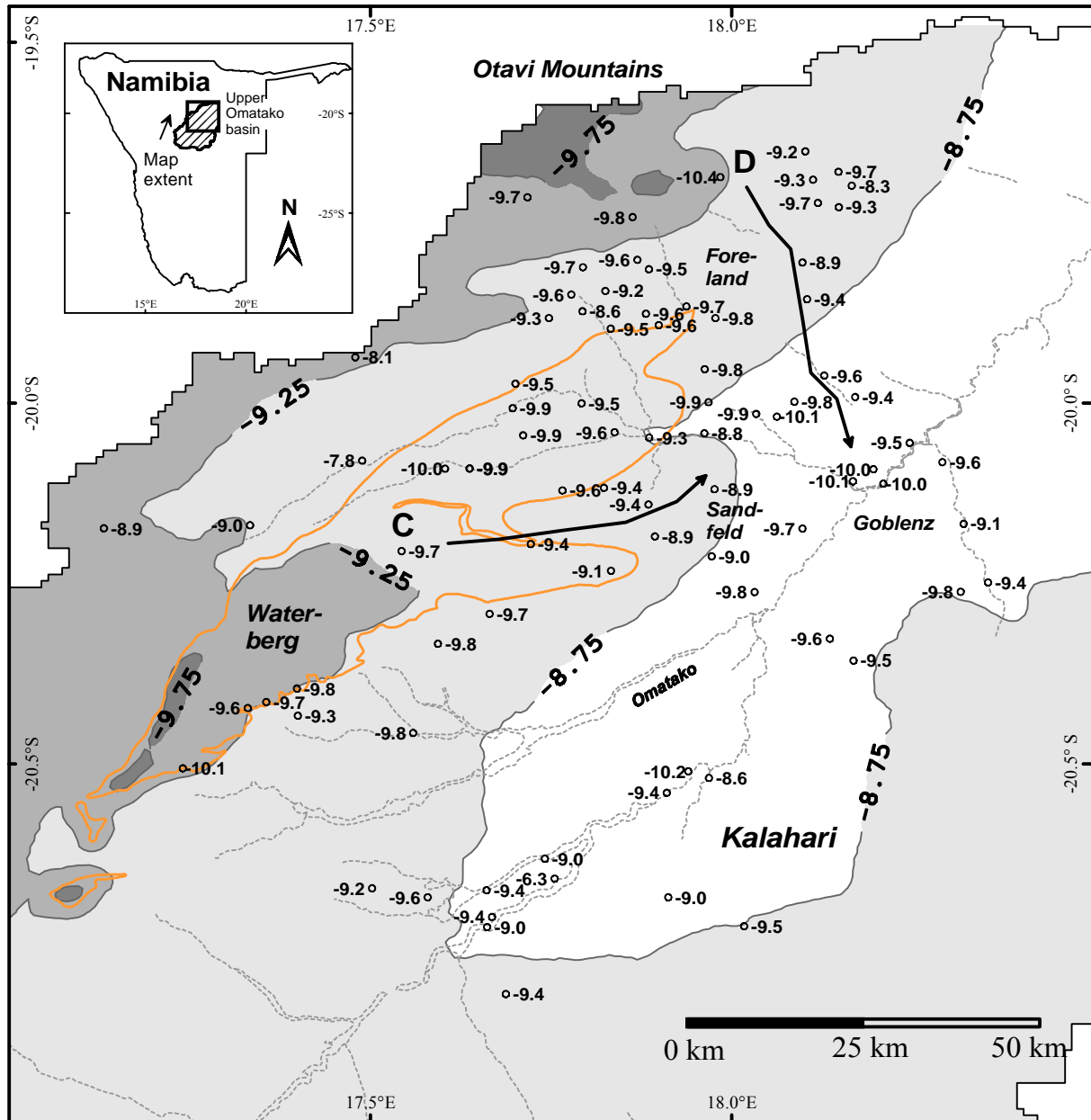


**Figure 4.48** Samples for stable isotopes taken in 1997 from boreholes in the Omatako basin. The values represent  $\delta^{18}\text{O}$  (‰) corrected for evaporative enrichment, assuming a slope of the evaporation line of 4.5. The background colour map displays the expected average isotopic composition of groundwater from local recharge with an altitude effect of 0.25 ‰/100 m (PLOETHNER ET AL., 1997). The orange line is the outline of the Etjo sandstone.



Based on the altitude effect, a difference of 1.25 ‰ in terms of corrected  $\delta^{18}\text{O}$  is expected between the highest recharge areas in the Waterberg and Otavi Mountains (~1,750 m) and recharge in the lower Otavi Foreland and Kalahari (~1250 m). The majority of boreholes in the Otavi Foreland, in the Sandveld and in the Kalahari has more depleted values of corrected  $\delta^{18}\text{O}$  as compared to the expected isotopic composition of local recharge. Therefore groundwater in these boreholes has probably been recharged at higher altitudes in the Otavi Mountains (Otavi Foreland) and in the outcrops of Etjo sandstone of the Waterberg (Sandveld).

The difference between corrected  $\delta^{18}\text{O}$  and the expected local composition is also pronounced for the Kalahari. While local recharge would have  $\delta^{18}\text{O}$  values of less than -8.75 ‰, most of the corrected values in the Kalahari are above -9.0 ‰ and reach up to -9.8 ‰. This composition points to an estimated altitude of about 1,500 m to 1,750 m, which is reached only in the outcrops around the Kalahari. Some boreholes in the Kalahari have corrected values deviating from the regional average towards a more enriched isotopic composition. Most of these sampling points are observed in areas with very shallow groundwater. Such deviations towards a heavier composition of corrected  $\delta^{18}\text{O}$  suggest that in some areas with thin Kalahari cover also direct recharge stemming from rainfall within the Kalahari occurs.

Two isotope profiles that are of major interest for the Goblenz area (CG in Figure 4.49 and DG in Figure 4.50) have been drawn to show the isotopic evolution along flow paths in more detail. Measured and evaporation-corrected values for  $\delta^{18}\text{O}$  (‰) have been plotted. The location of the profiles is shown in Figure 4.48. The first profile CG runs through the Waterberg area from the outcrops of Etjo sandstone into the Sandveld (Figure 4.49). The samples taken from boreholes in the Etjo sandstone without Kalahari cover (CN060, CN059, CN045), have measured  $\delta^{18}\text{O}$  values between -9.4 ‰ and -9.6 ‰. The groundwater has suffered almost no evaporation, consequently the corrected values differ by only 0.1 ‰.

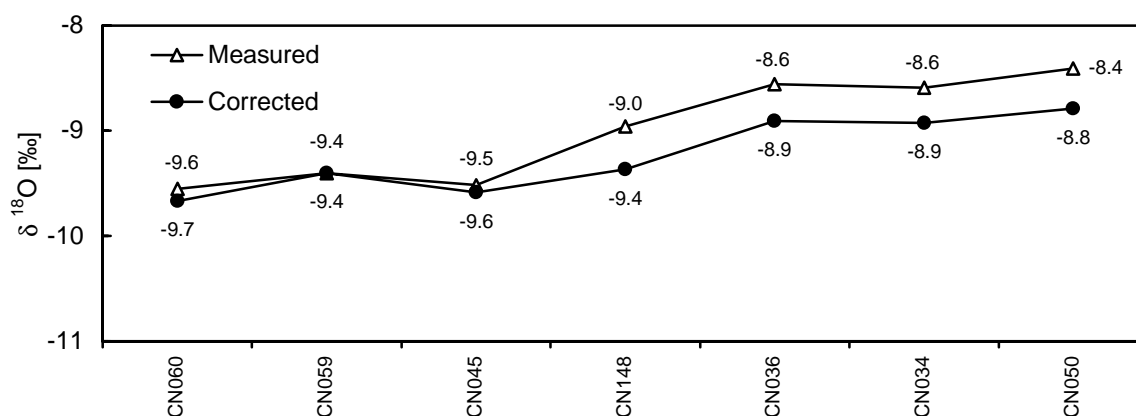


**Figure 4.49** Cross-section CG through the Waterberg from the outcrops of Etjo sandstone into the area covered by Kalahari sand.

With the transition to the Sandveld area, which is covered with Kalahari sediments, there is a change of isotopic composition. First, measured values increase to about -8.6 ‰. The comparison of corrected and measured values indicates an enrichment by evaporation. If the evaporative enrichment is removed, the corrected  $\delta^{18}\text{O}$  values increase to about -8.9 ‰. The corrected value significantly differs from the composition of the groundwater in the uncovered Etjo sandstone. It is therefore concluded that groundwater recharge takes place in the topographically lower Sandveld area. The corrected values correspond to the signal of direct recharge, if the altitude effect is accounted for (Figure 4.48). The last sample of profile CG is CN050 at 'Omambondetal Farm'. This borehole is located in the Omambonde valley. Profile CG and the spatial distribution in Figure 4.48 show that the corrected value at CN050 (-8.8 ‰) corresponds well to the isotopic signal of the Sandveld area. This confirms lateral flow from the Sandveld area to the Omambonde valley.

Profile DG runs through the Otavi Foreland where it follows a flow path towards Goblenz. The first sample G-049 is from PLOETHNER ET AL. (1997) and is the most depleted corrected sample along this flow line with -10.4 ‰. The following measured values steadily increase all the way to CN028, where  $\delta^{18}\text{O}$  reaches -5.6 ‰ and then irregularly drops towards Goblenz with -8.1 ‰. The boreholes in the Otavi Foreland have heavier corrected  $\delta^{18}\text{O}$  values than groundwater in the Otavi Mountains. The occurrence of heavier values in the Otavi Foreland as compared to the recharge in the Otavi Mountains indicates some degree of mixing between groundwater from the Otavi Mountains and local recharge in the Otavi Foreland.

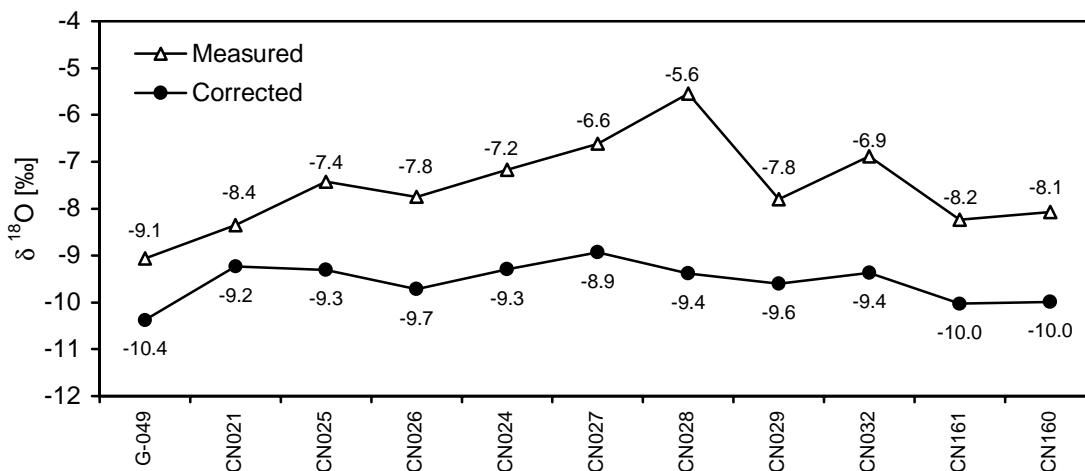


**Figure 4.50** Cross-section DG through the Otavi Foreland. Evaporation-corrected  $\delta^{18}\text{O}$  (‰) values are shown. The first sample (G-049) is from PLOETHNER ET AL. (1997).

From CN028 onwards, there is a decrease of the measured and corrected  $\delta^{18}\text{O}$  values towards Goblenz. This may be a result of a) emergence of deep groundwater discharge from the Otavi Mountains or b) indirect recharge from the Omambonde tributary draining an elevated sub-basin north of the Waterberg.

The observed fluctuations in the isotopic record at CN038 ‘*Kameeldorn*’ are in favour of the second alternative. Still both alternatives will be considered in the mixing-cell model (Chapter 4.5).

#### 4.4.3 Tritium, $^{13}\text{C}$ and $^{14}\text{C}$ analyses

Twelve samples for  $^{14}\text{C}$ ,  $^{13}\text{C}$  and  $^3\text{H}$  analysis have been taken in selected locations. For the  $^{14}\text{C}$  determination 60 litres samples of groundwater were taken. Sulphate was removed directly in the field by adding  $\text{BaCl}_2$  causing a quantitative precipitation of  $\text{BaSO}_4$ . The inorganic carbon was precipitated as  $\text{Ba}(\text{CO}_3)_2$  with  $\text{Ba}(\text{OH})_2$  solution. Care was taken not to contaminate the sample with recent  $^{14}\text{C}$  from atmospheric  $\text{CO}_2$  by using filters with granular  $\text{NaOH}$ .  $^3\text{H}$  analysis was made from 1 litre samples. Large volumes were taken in order to allow an enrichment of  $^3\text{H}$ .

Previous investigations had focused on sampling for  $^{14}\text{C}$  and  $^3\text{H}$  analysis in the Otavi Mountains and in the Kalahari. The results of these investigations are discussed in PLOETHNER ET AL. (1997). The additional analyses taken for this study focused on establishing a link between the two clusters of available  $^{14}\text{C}$  data in the Otavi Mountains and in the Kalahari. The data is listed in Table 4.5 together with stable isotope data and information on borehole depth and groundwater levels.

**Table 4.5**  $^{14}\text{C}$  (percent modern carbon),  $^3\text{H}$  (tritium units) and  $\delta^{13}\text{C}$  (‰) data from sampling campaigns.

sample name	date	alt. (m)	level m	depth m	$\delta^{18}\text{O}$ ‰	$\delta^2\text{H}$ ‰	$^3\text{H}$ TU	pmC	dev.	$^{14}\text{C}$ age	error	$\delta^{13}\text{C}$ ‰
CN008 Ovitatu	18.06.97	1310	61.0	85	-8.1	-59.2	1.8	63.2	0.6	3685	80	-8.7
CN016 Otjituwa	19.06.97	1255	48.8	91	-8.3	-61.8	0.1	64.9	0.7	3475	90	-9.6
CN019 Omitjete	20.06.97	1256	78.0	150	-8.0	-57.9	0.1	7.6	0.2	20625	260	-6.8
CN020 Okomuparara	20.06.97	1248	30.0	51	-9.1	-64.3		0.4	0.4	38840		-1.7
CN021 Tiefwasser	21.06.97	1402	35.0	70	-8.4	-59.9	1.3	80.9	0.7	1700	65	-8.8
CN029 Schwarzfelde	21.06.97	1270	20.0	50	-7.8	-58.7	0.3	80.8	0.5	1710	65	-8.4
CN053 Salzbrunnen	24.07.97	1465	25.0	70	-9.0	-64.2	1.5	72.7	0.8	2560	85	-9.0
CN056 Waterberg Tief	08.07.97	1500	25.0	100	-9.5	-66.7	0.3	63.1	1.2	3705	150	-15.7
CN060 Panorama	09.07.97	1492		215	-9.6	-66.8	0.1	81.2	0.7	1670	70	-15.1
CN066 Hairabib	12.07.97	1385	45.7	107	-9.4	-66.1	0.1	3.3	0.2	27460	515	-0.4
CN069 Ohamuheke	14.07.97	1320	40.0	75	-8.0	-59.2	1.8	56.3	0.6	4615	80	-10.9
CN070 Otjisepa	15.07.97	1274	61.5	174	-8.9	-62.7	1.8	0.4	0.1	43270	2175	-0.5

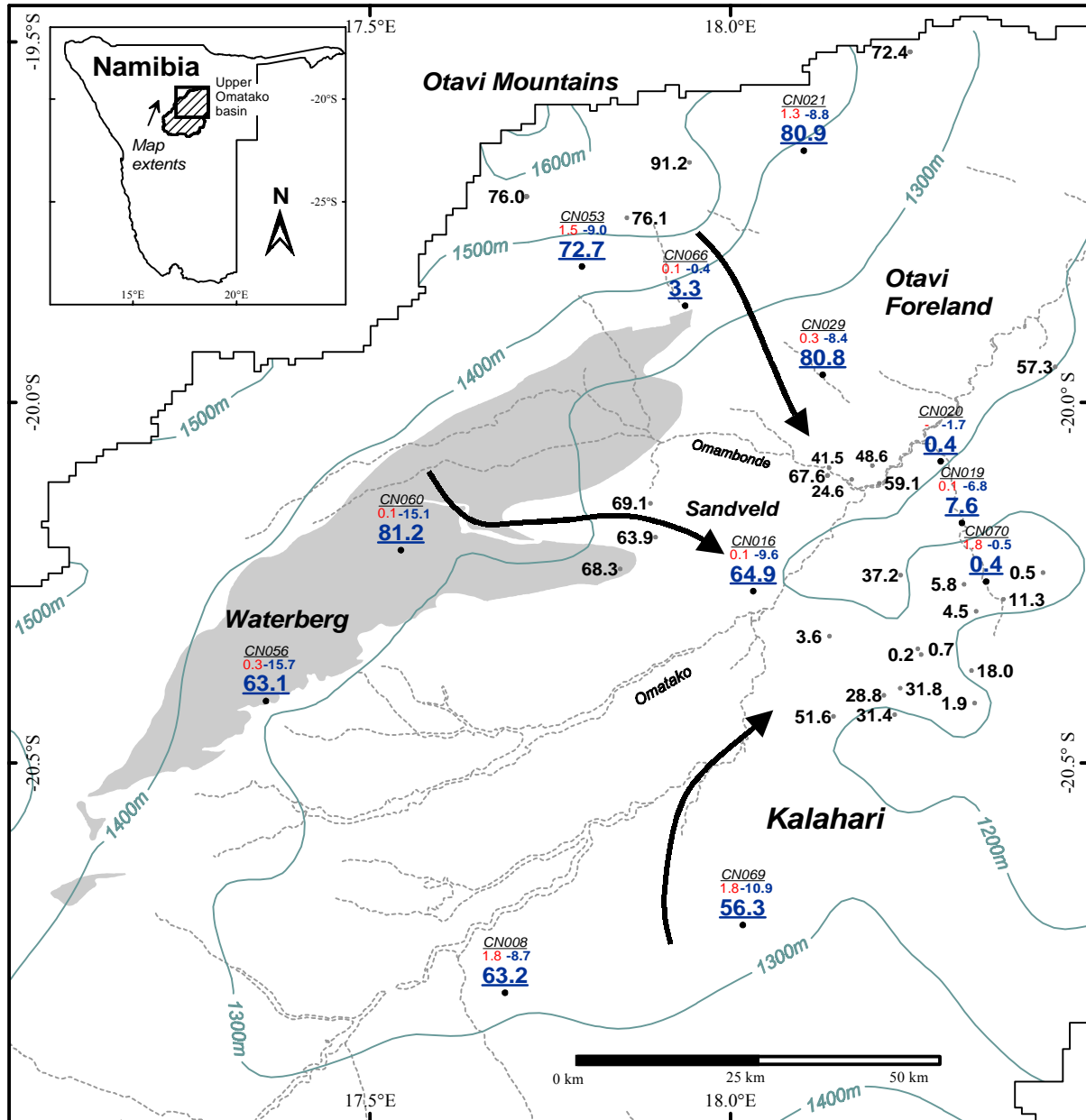


**Figure 4.51** Data from sampling campaigns (CN-#) are given with  $^{14}\text{C}$  (percent modern carbon) in blue and underlined,  $^3\text{H}$  (tritium units) in red, upper left and  $\delta^{13}\text{C}$  (‰) in blue upper right, additional  $^{14}\text{C}$  data from PLOETHNER ET AL. (1997) in pmC.

Figure 4.51 shows available analyses given in percent modern carbon from PLOETHNER ET AL. (1997). Samples taken for this study are plotted with sample number (black, italics), tritium activity in TU (red),  $\delta^{13}\text{C}$  (blue) and percent modern carbon (underlined). The groundwater flow pattern is indicated by groundwater contour lines.

From 12 samples five contained tritium above 1 TU. Two samples had slightly more than 0.1 TU and in four samples the level was below the detection limit of 0.1 TU. The samples CN053 and CN021 were taken within or close to the Otavi Mountains. Measurable tritium in these samples indicates that part of the groundwater was recharged after the early fifties of the

20<sup>th</sup> century. In the Etjo sandstone aquifer only sample CN056 has detectable tritium. CN056 is located at the southern slope of the Waterberg. The water level is about 25 m below ground. The other two tritium samples taken from the Etjo sandstone have levels below 0.1 TU. As indicated by the strong depletion in <sup>18</sup>O and <sup>2</sup>H the main recharge areas seem to be in the most elevated parts of the north-western Waterberg at some distance from CN056 and CN060 (Figure 1.1). In the Kalahari three samples with about 1.8 TU are found (CN008, CN069 and CN070), only one sample from the Kalahari has tritium less than 0.1 TU. Although samples were taken only after a stabilisation of physical parameters it is possible that these levels of tritium result from contamination with young groundwater in the borehole.

At first sight <sup>13</sup>C values exhibit strong variability. When data on <sup>13</sup>C is grouped according to hydrogeological units some patterns appear. Samples taken in the Waterberg area from the Etjo sandstone aquifer (CN056 and CN060) have  $\delta^{13}\text{C}$  values of -15.1 and -15.7 ‰. These values correspond closely to the expected composition of dissolved inorganic carbon originating from C3 plants and closed system carbonate dissolution in the aquifer. The soil CO<sub>2</sub> of C3 plants has a  $\delta^{13}\text{C}$  composition of about -23 ‰ (VOGEL, 1993). During the solution of CO<sub>2</sub> in water and dissociation of H<sub>2</sub>CO<sub>3</sub> to HCO<sub>3</sub><sup>-</sup> further enrichment increases the average composition to about -15 ‰. Studies on the thickness of the unsaturated zone (Figure 4.6) showed that groundwater levels are more than 60 m below the surface within the Waterberg area. Therefore closed system dissolution prevails and CO<sub>2</sub> is added during recharge only. Within the aquifer the dissolved inorganic carbon is ‘ageing’ as a result of radioactive decay only. Calcite saturation indices demonstrate that groundwater is strongly subsaturated for calcite in the Etjo sandstone aquifer. As a result calcite dissolution does not affect the dissolved inorganic carbon content. The Etjo sandstone aquifer provides good conditions for the application of the <sup>14</sup>C method.

This is not the case in the Otavi Mountain Foreland. In this area  $\delta^{13}\text{C}$  values vary between -9.0 at CN053 and -8.4 ‰ at CN029. The sample CN066 represents an outlier being strongly enriched in <sup>13</sup>C (-0.4 ‰). The cause for the shift in  $\delta^{13}\text{C}$  compared to the Etjo sandstone is a combination of several factors. The Otavi Mountains are one of the wettest spots in Namibia which may result in a higher percentage of C4 plants. Soil CO<sub>2</sub> of C4 plants is enriched in <sup>13</sup>C compared to that of C3 plants. Dissolved inorganic carbon in soil water percolating from the root zone of C4 plants will carry this fingerprint to the groundwater. In addition dolomite dissolution definitely takes place in the recharge area as indicated by Ca<sup>2+</sup>:Mg<sup>2+</sup> ratios close to 1. It produces a shift towards heavier  $\delta^{13}\text{C}$  values. Finally it has been shown earlier that groundwater levels are very shallow in this part of the Otavi Mountain Foreland. In some parts groundwater levels are less than 5 m below the surface. As a consequence carbonate equilibrium is established in an open system with respect to CO<sub>2</sub>. The addition of CO<sub>2</sub>

provides a continuous source of modern carbon. This explains the high values of percent modern carbon within most of the Otavi Foreland down to Goblenz.

The hydrogeological background information and the tritium and  $\delta^{13}\text{C}$  data now provide a conceptual framework for the interpretation of the  $^{14}\text{C}$  distribution in the study area. Due to different hydrochemical processes, it is necessary to treat the Waterberg area (Etjo sandstone), the Otavi Foreland and the Kalahari individually.

Along the groundwater flow-path from the Waterberg towards the Kalahari pmC values decrease from 81.2 (CN060) to 64.9 pmC (CN016) (Figure 4.51). Two of the previously taken samples fit into this evolution (68.3 and 69.1 pmC), one sample has a slightly higher value than CN016. The general decrease of pmC towards the east is in agreement with an observed hydraulic gradient. In terms of conventional ages there is an increase of about 1670 to 3475 years along a flow-path of 50 km. With an estimated effective porosity of 0.1 this results in a flow velocity of 2.8 m/year assuming a simplified piston flow situation. The gradient between CN060 and CN016 is about 4 ‰, hence, a hydraulic conductivity of  $2.2 \cdot 10^{-5}$  m/s is obtained (or a transmissivity of  $8.8 \cdot 10^{-4}$  m<sup>2</sup>/s for an assumed saturated thickness of 40 m). These values are in good agreement with estimates of MAINARDY (1999) and with data from pumping tests made by the DWA (DEPARTMENT OF WATER AFFAIRS, 1997).

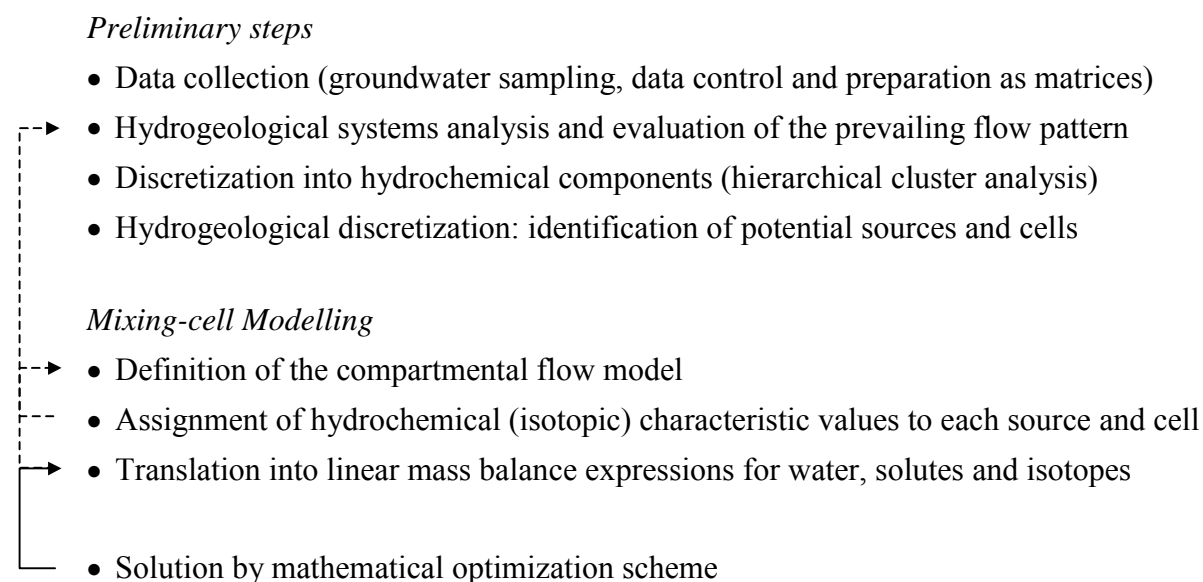
In the Otavi Mountain Foreland very shallow groundwater levels (Figure 4.6) probably cause open system conditions with respect to CO<sub>2</sub>. This means that groundwater is in contact with CO<sub>2</sub> sources (from deep roots) and that pCO<sub>2</sub> (containing  $^{14}\text{C}$ ) is supplied at a constant partial pressure. As a result  $^{14}\text{C}$  concentrations of samples remain high as for CN029 (Figure 4.51). One sample in the Otavi Foreland (CN066) has only 3.3 pmC and  $\delta^{13}\text{C} = -0.4$  ‰. This sample was taken from a deep borehole at Hairabib with a high temperature of about 40°C. The  $\delta^{13}\text{C}$  value indicates that carbonate dissolution has possibly diluted DIC. However, a correction based on  $\delta^{13}\text{C}$  remains speculative since neither initial  $\delta^{13}\text{C}$  of recharge nor  $\delta^{13}\text{C}$  of the carbonate source are known.

$^{14}\text{C}$  data from earlier studies in the Kalahari exhibit a high variability (PLOETHNER ET AL., 1997). Five additional samples were taken: CN008, CN019, CN020, CN069 and CN070. Groundwater from two boreholes within the Kalahari and south-west of Goblenz have 56 to 63 pmC. CN019, CN020 and CN070 taken within the Kalahari north-east and east of Goblenz contain between 0.4 and 7.6 pmC, corresponding to conventional ages of about 20,000 and > 38,000 years respectively. It is concluded that high pmC observed at CN008 and CN069 indicate groundwater flow from the southern recharge area within the hard-rock outcrops of the Damara Sequence.

Although there is a high variability of pmC a trend towards lower average pmC in groundwater east of Goblenz is observed. The extreme variability may result from mixing between regional groundwater inflow from the south and localized recharge in the pan belt east of Goblenz. As indicated by enrichment in  $^{13}\text{C}$  for some samples with low pmC values dissolution of carbonates contributes to the observed scattering in pmC.

## 4.5 Mixing-cell modelling

The process of mixing-cell modelling can be subdivided in several steps with three main stages:



In the previous chapters a detailed investigation of hydrogeological and physical constraints as well as hydrochemistry and isotopic composition has been carried out. These introductory steps already led to a qualitative understanding of the groundwater flow system components and their physical and chemical characteristics. The definition of the conceptual flow model and the mathematical solution of the mass balances are an interactive process as indicated by the arrows in the scheme above.

Depending on the success of the optimization, the system structure was adjusted if necessary and - in fact - optimized itself. The dashed arrows indicate that in some cases the results of the model optimization suggested a review of the definition of aquifers and of flow connections.

#### 4.5.1 Synthesis of the conceptual flow model

The interpretation of hydrochemical profiles and of the isotopic evolution has yielded further qualitative evidence of the mixing of different components, thereby permitting the identification of three major groundwater flow-paths:

- from the Otavi Mountains to the Goblenz area
- from the Otavi Mountains to the Otavi Foreland and to the Omambonde valley
- and from the Waterberg to the Omambonde valley

In a similar way, the spatial distribution of stable isotopes suggests mixing of shallow groundwater in the Otavi Foreland and with localized recharge. Evidence for recharge has also been found in the Sandveld area. Deeper groundwater flow components have been identified from depleted corrected values in the southern Otavi Foreland and near Goblenz. Finally, hydrochemical data have revealed the existence and possible mixing with deep and more saline groundwater in the Otavi Foreland. This information is summarised in Figure 4.52, which represents the fifth step in the scheme outlined above: the definition of the compartmental groundwater flow model.

The major objective of the study has been to elucidate the groundwater flow contributions to the groundwater resources on which the Goblenz state water scheme relies. The map of saturation of the Kalahari sediments confirms the existence of an extended trough of Kalahari sediments south of Goblenz, part of which is saturated with fresh groundwater. The extent of this aquifer is shown in Figure 4.52, where blue colours indicate a saturated thickness of 50 m and more.

In Figure 4.52, circles represent recharge end members, the *sources* for the mixing-cell model. As a result of the cluster analysis, five major source types (a, b, c, d and e), some with subgroups, have been distinguished. For every end member, the dominant geological source areas have been marked, where the water-rock interactions take place that produce the typical hydrochemical composition.

An important constraint for the application of steady-state the mixing-cell model is the conservative behaviour of tracers that are used for mixing calculations. The Etjo sandstone aquifer offers almost ideal conditions for conservative mixing, since readily soluble minerals (carbonates and gypsum) are absent. Therefore the distinction is introduced between an outer '*reaction zone*' and a '*conservative mixing zone*'. The mixing zone corresponds to the extent



of the Etjo sandstone which is partly covered by Kalahari sediments (orange border line). The application of the mixing-cell approach has to be restricted to the ‘*conservative mixing zone*’.

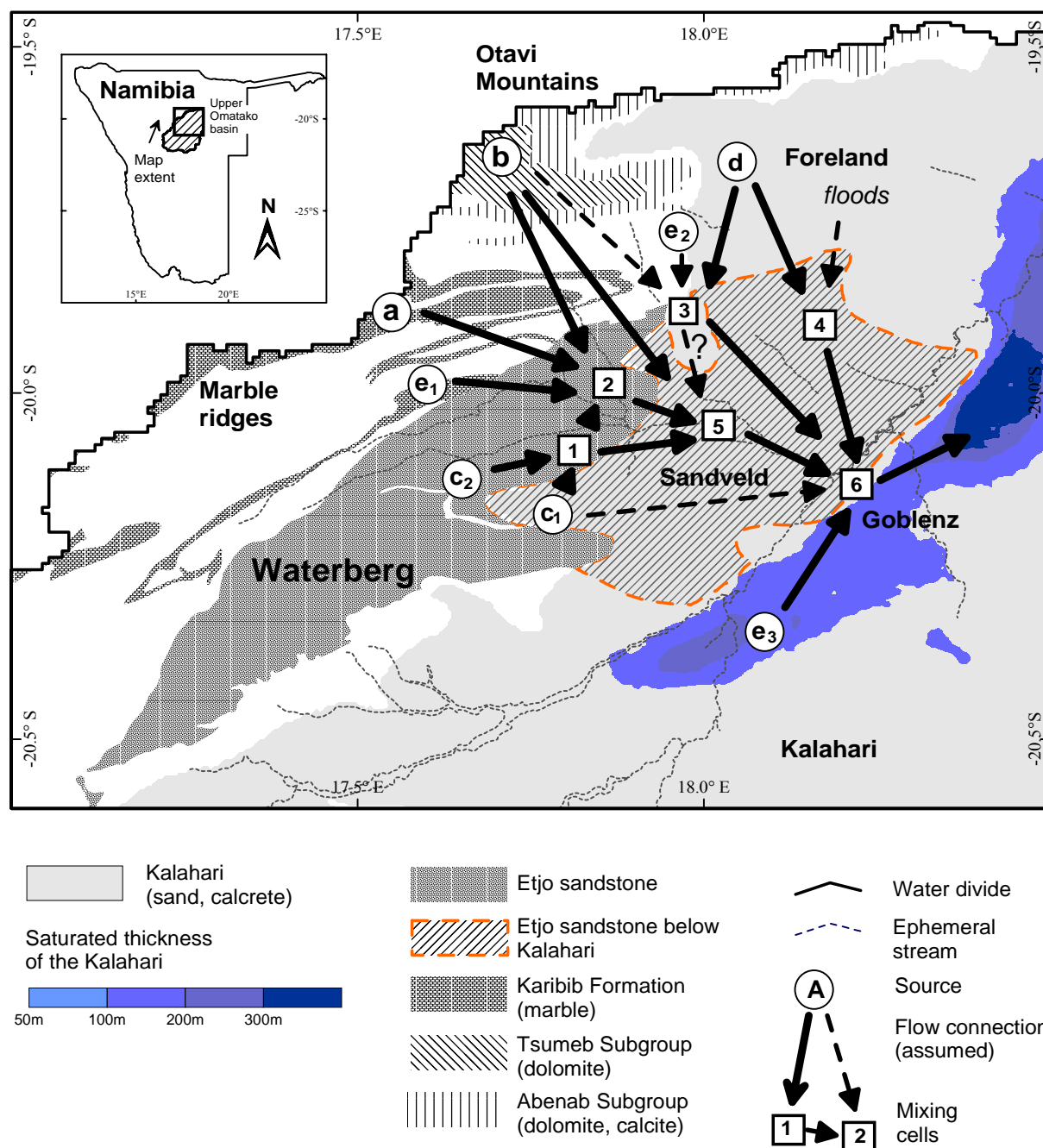


**Figure 4.52** Conceptual model of sources, flow connections and cells in the Goblenz area.

As described in the methodological chapter, the mixing-cell approach allows to mathematically derive groundwater flows from the inverse solution of the mass balances of water and solutes. The conceptual flow model of Figure 4.52 has been translated into mass balance equations for each individual cell making use of the available hydrochemical data.

In several areas, hydrochemical and isotope data provided evidence for recharge, especially in the Otavi Foreland and in the Sandveld. Therefore, floodwater has been sampled and introduced into the mixing model as a potential source of recharge. All cells have been integrated into a flow network corresponding to Figure 4.52 and groundwater flow rates have been determined from the optimized solution of the mass balance equations.

#### 4.5.2 Single-cell modelling with hydrochemical groups

First, the mixing-cell model was run with the *average cluster concentrations* identified in Chapter 4.3.4 and specified in Figure 4.24. An inverse estimation of inflows was performed for each single cell 1 to 6 (Figure 4.52, square frame). All potential sources and inflows were specified for each cell according to the results of the previous hydrogeological, hydrochemical and isotope studies. The mixing-cell model was then used to calculate the percentages of inflows from different sources. The results are summarized in Table 4.6.

**Table 4.6** Percentages of inflow from different sources to groundwater compartments or cells in the vicinity of Goblenz. The inflow percentage was calculated based on conservative mixing between hydrochemical groups with average concentrations of major ions. Zero indicates that no flow was attributed to the source by the mixing model, sources without connection to the cell are marked ‘-’.

	<i>Sources defined by average concentrations of hydrochemical groups</i>									<i>floodwater</i>
	a	b	c <sub>1</sub>	c <sub>2</sub>	d <sub>1</sub>	d <sub>2</sub>	e <sub>1</sub>	e <sub>2</sub>	e <sub>3</sub>	
<i>Cell 1</i>	0	-	8	92	-	-	0	-	-	0
<i>Cell 2</i>	75	16	-	-	-	-	0	0	-	9
<i>Cell 3</i>	-	0	-	-	74	26	-	0	-	0
<i>Cell 4</i>		94	-	-	0	0	-	0	-	6

	<i>Flows from cell to cell</i>						<i>Additional Sources</i>			
	<i>Cell 1</i>	<i>Cell 2</i>	<i>Cell 3</i>	<i>Cell 4</i>	<i>Cell 5</i>	<i>Cell 6</i>	e <sub>1</sub>			
<i>Cell 5</i>	70	18	10	-	-	-	2	-	-	0
<i>Cell 6</i>	4	-	6	87	3	-	-	-	-	0

##### *Cell 1 - Waterberg*

According to the conceptual model cell 1 receives inflow from the sources c<sub>1</sub> and c<sub>2</sub> (Figure 4.52). Inflow from the sources a and e<sub>1</sub> can not be excluded a priori. The inverse mixing model assigned zero % of total inflow to the sources a and e<sub>1</sub>, about 8 % to c<sub>1</sub> and 92 %

percent to  $c_2$ .  $C_1$  was already characterized as recharge within the outcrops of Kalkrand basalt. These outcrops cover only a relatively small area within the Sandveld as shown by the extent of Jk in the geological map in Figure 2.6. They still seem to be important for preferential recharge. The mixing calculations were performed for all major ions except for potassium and bicarbonate. In this case the inclusion of  $Ca^{2+}$  into the mixing calculations was justified because the aquifer matrix of the Etjo sandstone is almost carbonate free. Accordingly the total solute mass balance error was smaller than 5 %.

No contributions from floods were detected. However, the average major ion concentrations of  $c_1$  and floodwater are quite similar. Both end members are characterized by little exchange with soil  $CO_2$ , low concentrations of  $HCO_3^-$  and limited water-rock interactions. These two sources may therefore substitute each other in mixing calculations for cell 1.

#### *Cell 2 - Upper part of the Omambonde valley*

According to the conceptual flow model there is inflow to cell 2 from the sources a, b,  $e_1$  or  $e_2$ . Inflow from the Etjo sandstone and recharge from floods can not be excluded. The mixing-cell calculation for cell 2 identified three non-zero inflows coming from the sources a, b and from floods. Source a represents inflow from the marble ridges and yields 75 % of total inflow to cell 2. Source b represents groundwater from the Otavi Mountains and still contributes 16 % percent of total inflow to cell 2 or the upper reach of the Omambonde valley.

The hydrochemical evolution along profile AG (Figure 4.30) indicated already that concentrations of major ions decrease. Groundwater recharge from floods is possible along the ephemeral stream Omambonde and variations in the isotopic composition of groundwater have been observed in this area at CN038 'Kameeldorn'. Nevertheless, the sources  $c_1$  and floodwater have a similar hydrochemical composition and could substitute each other. Therefore the inflow of 9 % floodwater could also represent at least some inflow from the Etjo sandstone.

#### *Cells 3 and 4 - Otavi Mountain Foreland*

There are five potential inflows to cell 3, namely from the Otavi Mountains (group b), the Otavi Foreland (groups  $d_1$  and  $d_2$ ), saline water (group  $e_2$ ) and recharge. The other hydrochemical groups have no hydraulic connections to cell 3. As a result of the mixing

modelling, cell 3 receives about three quarters of its total inflow from  $d_1$  and the remaining quarter of inflow from the more saline group  $d_2$ .

$D_1$  and  $d_2$  represent outflow from the Otavi Mountains. They are still characterized by their dolomitic fingerprint but contain more  $Mg^{2+}$ ,  $Na^+$  and  $Cl^-$  than group b. This may result from mixing with groundwater from a deeper aquifer represented by the end member  $e_2$ . In the eastern part of the Otavi Foreland the influence of mixing with this saline end member decreases and the hydrochemical and isotopic composition shifts back to the original fingerprint of group b. Accordingly more than 90 % of the total inflow to cell 4 further east in the Otavi Foreland are attributed to groundwater from the Otavi Mountains (group b). A few percent of inflow stem from floodwater. This result is supported by the existence of sinkholes in this area providing shortcuts to the groundwater table. In this case no other source exists that could have been substituted by floodwater.

#### *Cell 5 - Lower part of the Omambonde valley*

Cell receives inflows from  $e_2$  and from the cells 1, 2 and 3. The largest part of total inflow to cell 5 (70 %) comes from the Etjo sandstone, cell 1. Cell 2 still contributes 18 % of the inflow to cell 5. About 10 % of the total inflow to cell 5 were assigned to cell 3 in the Otavi Foreland. A very small inflow of only 2 % from  $e_2$  was found. Despite of its small proportional flow rate, the source  $e_2$  could not be omitted from the mass balance without a consequent failure of the optimization algorithm. The inclusion of this source term contributing only a few percent of total inflow was necessary.

#### *Cell 6 - Goblenz*

Finally, cell 6 'Goblenz' gets about 87 % of its total inflow from the Otavi Foreland, cell 4. It was shown earlier that cell 4 contains mainly groundwater from the Otavi Mountains with small components of floodwater recharge. The remaining 13 % inflow to cell 6 'Goblenz' come from cell 1 (Etjo sandstone, 4 %), the cell 3 (Otavi Foreland, 6 %) and cell 5 (middle part of the Omambonde valley, 3 %). In the lower part of the Omambonde valley and close to Goblenz inflow from the Otavi Foreland becomes dominant and is most important for recharge of the Goblenz well-field.

### 4.5.3 Multi-cell modelling with specific boreholes

After the calculation of inflows into single cells as described above, a multi-cell flow model was developed solving inflow and flow rates for the whole network simultaneously. The optimization of such a combined flow model was not feasible based on average concentrations of hydrochemical groups. Apparently the variability within each of the 7 groups prohibited a precise solution of all mass balance equations at the same time. Therefore a detailed multi-cell model was developed based on hydrochemical data from individual boreholes. Figure 4.53 presents the most feasible flow pattern towards Goblenz and the results obtained for all flow connections. For this model run the mass balance for water fluxes and solutes is closed within an error margin of less than 5 % for the whole flow model.

In Figure 4.53 the single borehole numbers are indicated (for reference see the full table with all 1,531 analyses in Annex B). For each borehole the contribution to the next cell is specified in percent. In order to facilitate the comparison with the single cell modelling described above in Chapter 4.5.2 and data from Table 4.6, the hydrochemical groups are shown to which the boreholes were assigned by cluster analysis (Figure 4.53).

The absolute outflow at Goblenz is assumed to amount to about 1 Mm<sup>3</sup> per year (DWA, 1997). According to the multi-cell mixing modelling Goblenz receives most of its inflow, that is 740,000 m<sup>3</sup>/y, from a shallow aquifer with dolomite groundwater of the Otavi Mountains and their Foreland (cell 4, borehole 1486). Cell 4 in the Otavi Foreland receives most of its inflow (98 %) from dolomitic groundwater (group b, borehole 1182) and contains small components of floodwater (~2 %). Again, this result is supported by the discovery of dissolution features in secondary carbonates beneath a thin layer of Kalahari sand near borehole 1182. The mixing-cell modelling does not allow a quantification of floodwater recharge with such a precision. Nevertheless, there is strong evidence for indirect recharge in this area. Floodwater had to be included as a source term in order to solve the equations. A decrease of concentrations is observed in this area and can not be caused by inflow from other sources as in the Waterberg area.

Another 120,000 m<sup>3</sup>/y derive directly from the Waterberg sandstone aquifer to the south (source c<sub>1</sub>, borehole 596). The remaining 140,000 m<sup>3</sup>/y are formed by inflow of a mixed component which is composed of cell 5 (borehole 852, 11 %) and cell 3 (borehole 359, 3 %). Their individual composition could also be traced back to the different source areas. Cell 5 (borehole 852) receives almost two thirds of its inflow from the Waterberg (cell 1, borehole 623). Cell 3 is a mixture of inflows from several boreholes in the Otavi Foreland belonging to

three different hydrochemical groups,  $d_1$  (boreholes 1312, 1316),  $d_2$  (borehole 540) and  $e_2$  (borehole 289).

The main sources of cell 2 are boreholes within the Karibib Formation (group a, boreholes 314 and 870, together  $39 + 54 = 93\%$ ) and the Otavi Mountains (group b, borehole 1362,  $7\%$ ). An inflow from the saline source  $e_1$  was not detected.

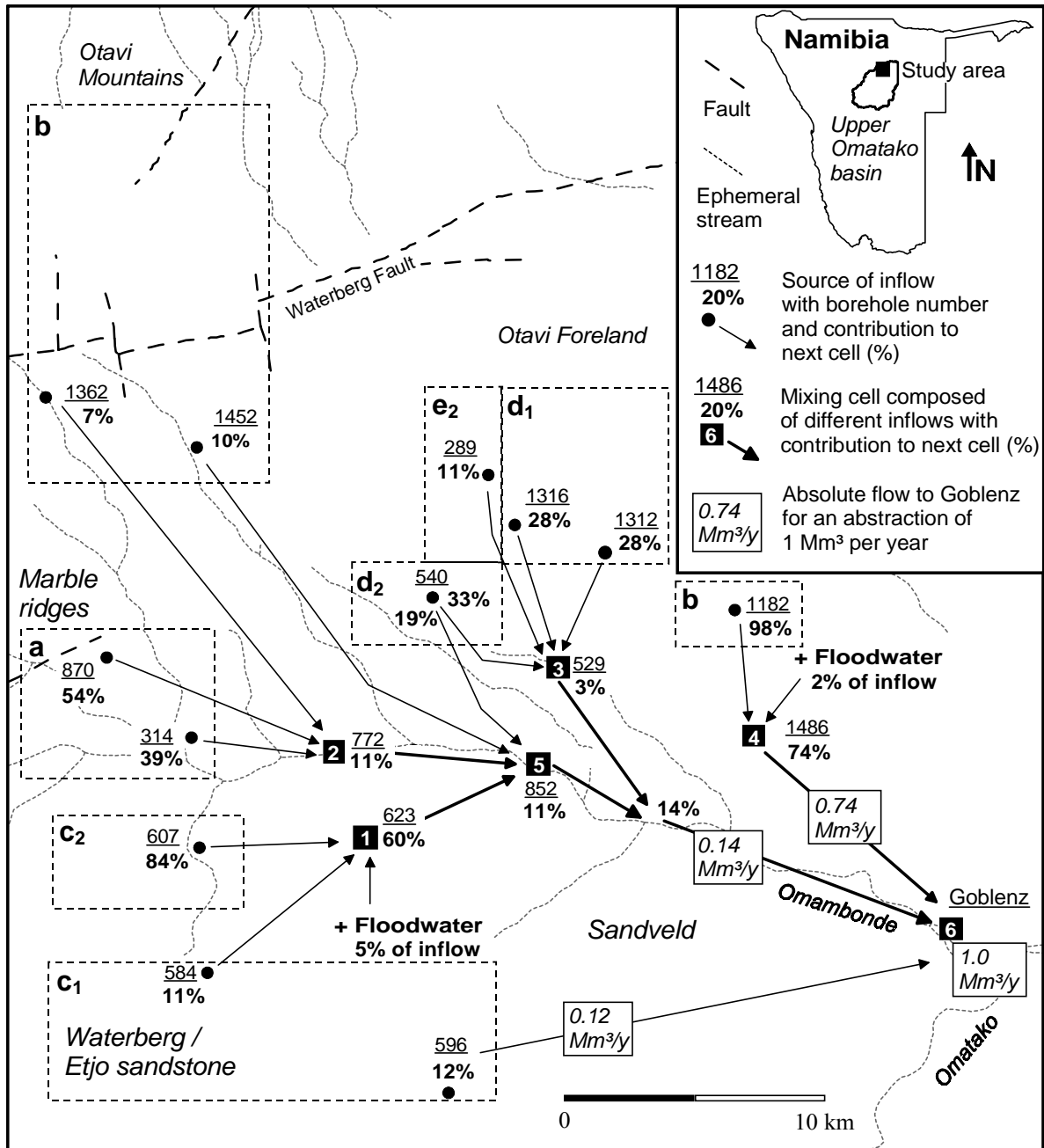


**Figure 4.53** Results of the mixing-cell model for the Goblenz area. Percentages indicate the relative contribution from different sources and cells to the *next* borehole. For direct flow contributions to the Goblenz area the absolute amounts are indicated in  $Mm^3/y$ .

---

Cell 1 integrates inflows from two different subgroups in the Waterberg area, namely  $c_1$  (borehole 584, 11 %) and  $c_2$  (borehole 607, 84 %). A floodwater contribution of about 5 % of the total inflow to cell 1 is estimated by the mixing-cell model. This figure is less reliable than that for floodwater recharge into cell 4 due to the similarity between floodwater and groundwater from the Etjo sandstone (sources  $c_1$  and  $c_2$ , boreholes 584 and 607).

The comparison of both model runs gives some insight into the precision of calculated flow rates. The general selection of source terms and their relative importance is the same in both model runs. In general deviations result from hydrochemical similarity in several constituents, for example in the case of floodwater and groundwater from the Etjo sandstone. Differences between flow rates calculated from average concentrations and analyses from individual boreholes correspond within a range of  $\pm 5$  to about 15 %. The precision is higher in areas with distinct hydrochemical groups and well defined sources or inflows.





## 5 Conclusions

The integration of hydrogeological, hydrophysical and hydrochemical methods has been an important aspect of this work. Each single method used in the previous chapters - water balances, hydrochemistry, stable isotope,  $^{14}\text{C}$  and  $^3\text{H}$  analyses as well as inverse mixing-cell modelling - gave specific insights into the hydrogeology of the Upper Omatako basin. The latter provided a quantitative estimation for the groundwater flows into the Kalahari for the Upper Omatako basin.

### 5.1 Methodological perspectives

The application of the mixing-cell model to this large area has shown that this method may represent a tool for validation that allows quantification of mixing relationships even in complex terrain. In this case, the Etjo sandstone provides an almost ideal aquifer for mixing due to limited water-rock interactions. The study has also demonstrated that extensive hydrochemical and stable isotope studies are needed prior to the application of the model itself. Preliminary studies are necessary to assure conservative behaviour and to identify possible flow connections.

In this study the delineation of a '*reaction zone*', in which the groundwater gets its fingerprint, and a '*mixing zone*', where the mixing-cell model is applied, has been introduced. Major ions were only used after the consideration of thermodynamic equilibrium (Figure 4.33, 4.34). Among major ions  $\text{Mg}^{2+}$ ,  $\text{Cl}^-$ ,  $\text{NO}_3^{2-}$ , and in some areas  $\text{SO}_4^{2-}$ , were considered to be reliable, largely conservative tracers within the mixing zone. The stable isotopes  $^{18}\text{O}$  and  $^2\text{H}$  did not provide additional information, due to similar isotopic signals. In order to extend the applicability of the model, new tracers (isotopes, industrial tracers) should be looked for. Their applicability in terms of conservative behaviour must be considered for each individual case.

### 5.2 Hydrogeotopes

The previous chapters have been arranged according to a systematic '*top-down*' approach. General studies yielding important constraints for additional and more detailed investigations were carried out first. Hence, preliminary hydrogeological investigations were followed by

hydrochemical studies which later were complemented by isotope investigations. Only then, based on all the integrated information, the mixing-cell modelling could be performed. In this, the final chapter, the results obtained by different methods will be combined and compared.

This discussion will be grouped by the major hydrogeological subdivisions of the Upper Omatako basin, for which the term '*hydrogeotopes*' is introduced. This term is proposed in analogy to the hydrological term '*hydrotope*' as used in a recent publication by BECKER & BRAUN (1999). It designates different parts of the hydrogeological system having similar hydrogeological properties. Such typical properties or trends result from specific processes (i. e. recharge, evaporation, mixing and water-rock interactions). A hydrogeotope should always be considered to be part of a hydrogeological system. Therefore, the identification of hydrogeotopes requires:

- a hydrogeological disaggregation
- an understanding of processes causing the typical physical and chemical properties, and
- a concept of its external links and its function within the system.

The distinction between the two major hydrogeotopes of the study area, the '*hardveld*' and the '*sandveld*', has been introduced already at the beginning of this study. The '*hardveld*' is characterized by hardrock outcrops along the rim of the Upper Omatako basin. The '*sandveld*' is the vast and extremely flat sedimentary basin with continental deposits belonging to the Kalahari Group.

The present study revealed the eminent importance of the mountainous rim for the water balance of the Kalahari, both in terms of surface and ground water. Most of the surface runoff is generated on hard-rock outcrops or exposures of less permeable Omingonde sediments outside the Kalahari basin (Figure 2.4, Table 2.1). The regional groundwater level contour map (Figure 4.1) shows that recharge in the mountainous hardrock rim drives the groundwater flow system of the Upper Omatako basin. Within the mountainous rim soil cover is thin or missing and direct rainfall recharge takes place. Mountain front recharge from these outcrops into the Kalahari is a major factor for the hydrogeology of the Upper Omatako basin.

The Otavi Mountain Foreland has more than 10 m of Kalahari cover and, by definition, belongs to the Kalahari basin ('*sandveld*'). However, it differs from the rest of the Kalahari basin due to its function as a conveyor of groundwater from the Otavi Mountains southward, and due to the existence of widespread carbonate crusts. It is therefore discussed separately (see Chapter 5.2.2).

### 5.2.1 The mountainous hardrock rim

Soil water balance modelling has confirmed that direct groundwater recharge in hardrock environments (Figure 3.3, A) tends to be higher than in areas covered with thick Kalahari sediments (Figure 3.3, B). In the Upper Omatako basin the highest recharge probability is found in February in the late rainfall season (Figure 4.7). At 'Grootfontein' (Figure 4.1), an area with thin sand cover, average recharge rates are between 0.1 and 2.5 % of mean annual rainfall (Figure 4.13). Inter-annual variability is controlled by the distribution of rainfall intensities and does almost not correlate with mean annual rainfall (Table 4.1). The water balance model also indicates that surface runoff is produced episodically, triggering indirect recharge processes (Figure 3.3, C; Figure 4.13, season 1983/1984). Recharge rates are higher where effective field capacity is reduced, as long as bedrock permeability is sufficient for allowing deep percolation. Reduced bedrock permeability results in the generation of inter-flow along hillslopes and may cause colluvial deep percolation (Figure 3.3, B). In some areas recharge may be constrained by low bedrock permeability and drop to 0.1 % of mean annual rainfall (MAINARDY, 1999).

The degree and type of carbonate dissolution/precipitation controls the major ion composition of groundwater (Figure 4.15) in the mountainous hardrock rim. The  $\text{Ca}^{2+}:\text{Mg}^{2+}$  ratio helps to distinguish between groundwater recharged in the Otavi Mountains' Tsumeb and Abenab Subgroups (dolomite) and marbles of the Karibib Formation (Damara Sequence), as shown in Figure 4.16. In addition the  $\log(\text{Sr}^{2+}/\text{Ca}^{2+})$  was found to be an excellent fingerprint for separating both groups and was used to trace the outflow of the Otavi Mountain groundwater into the Kalahari (Figure 4.17). A hydrochemical subdivision of water types in the 'hardveld' was derived from cluster analysis of groundwater chemical data (Figure 4.14). Such a geostatistical approach should only be used as a last resort when samples cannot be attributed to specific aquifers a priori. The western and south-western secondary aquifers within rocks of the Damara Sequence (Figure 4.19, group a), the Otavi Mountain karst aquifers of the Tsumeb and Abenab subgroups (Figure 4.20, group b) and the Waterberg Etjo sandstone aquifer (Figure 4.20, group c) represent the major hydrochemical end members of the mountainous rim in the Upper Omatako basin. Each group could be attributed to aquifers.

In the Otavi Mountains and in the western part of the Waterberg area almost no or only little isotopic enrichment by evaporation is observed (Figure 4.40). However, the isotopic composition of groundwater from the secondary aquifers in the Damara Sequence north of the Waterberg indicates some evaporative enrichment. This probably results from the spatial distribution of depth to the water table (Figure 4.6). North of the Waterberg shallow groundwater levels are observed (Figure 4.6, A), while the depth to the water table is larger in

the Otavi Mountains (Figure 4.6, B) and in the Waterberg (Figure 4.6, C). The initial isotopic composition of groundwater in the main recharge areas of the Otavi Mountains and the Waterberg were found to be quite similar (-9.7 to -10.1 ‰). Re-sampling indicated a weak seasonal variation of  $\pm 0.2$  ‰ for the majority of groundwater samples (Figure 4.44). Therefore the differences in the isotopic composition cannot be used for distinguishing between groundwater from the Otavi Mountains and the Etjo sandstone.  $^{14}\text{C}$  and tritium data confirm that the hardrock outcrops are areas of active recharge (Figure 4.51).

### 5.2.2 The Otavi Mountain Foreland

The Otavi Mountain Foreland represents a complex conveyor of groundwater from the Otavi Mountains towards Goblenz. Extensive carbonate crusts are found in this area (Figure 2.7, b). Carbonate crust formations are remnants of a hydrogeological regime characterized by the existence of an open groundwater discharge zone, possibly a swamp. The reduction of  $\text{CO}_2$  partial pressure at the contact with the atmosphere caused the precipitation of carbonate, now found as calcrete. Visual evidence for dissolution of these secondary carbonates under present conditions is displayed Figure 4.12 (a+b). Sinkhole development became possible only after a reduction of groundwater inflow from the Otavi Mountains and a subsequent decline of groundwater levels. The development of a vegetated, thin eolian sand cover favoured the re-dissolution of calcrete.

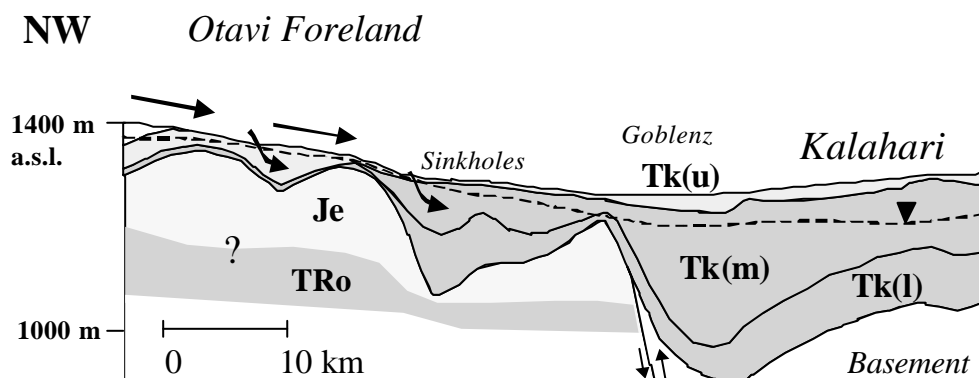


**Figure 5.1** Cross-section through the Otavi Mountain Foreland: (Je) Etjo sandstone, Tk(u) Upper Kalahari, Tk(m) Middle Kalahari, Tk(l) Lower Kalahari

Several cycles of crust formation and re-dissolution may have occurred in the past; hence care needs to be taken with respect to age interpretation of such carbonate crusts. It is likely that sinkholes occur also in other places within the Otavi Foreland with similar sedimentary successions and hydrogeological conditions. These sinkholes represent short-cuts to the groundwater table (Figure 5.1). Field investigations have revealed that episodic widespread

overland flow forms on the southern pediment of the Otavi Mountains. Video evidence shows that runoff may occur as sheet flow into the Otavi Mountain Foreland, inundating this area for days with several decimetres of water. Rapid infiltration through sinkholes causing periodic rises of the groundwater table has been observed by farmers. In the Otavi Foreland several percent of total inflow were attributed to floodwater according to the mixing-cell approach (see also below for more detail). It is recommended to monitor groundwater levels in the Otavi Mountain front area at least on a weekly basis in order to record the impact of flood events.

The hydrochemical composition of groundwater in the Otavi Foreland indicates its provenance from the Otavi Mountains: the groundwater is dolomitic (balanced  $\text{Ca}^{2+}:\text{Mg}^{2+}$  ratio) and plots close to groundwater from the Otavi Mountains in a Piper diagram (Figure 4.15). This is also supported by the spatial distribution of  $\text{Ca}^{2+}:\text{Mg}^{2+}$  (Figure 4.16) and  $\text{Sr}^{2+}:\text{Ca}^{2+}$  ratios (Figure 4.17). In both maps groups (b) and (d) have similar values. But hydrological and mixing processes in the Otavi Foreland modify the chemical and isotopic composition of groundwater. In the Otavi Foreland mixing with deeper, more saline, groundwater occurs. Simple mixing calculations allow to constrain this inflow to  $< 5\%$ . It causes an increase in  $\text{Mg}^{2+}$ ,  $\text{SO}_4^{2-}$  and  $\text{Cl}^-$  in the northern part of the Otavi Foreland. In this area, the shallow Kalahari aquifer, from which the samples were taken, is underlain by gneisses of the Grootfontein complex (Figure 2.6 and Figure 4.1). The saline end member probably represents groundwater from this fractured aquifer below the Kalahari.

The isotopic composition of groundwater in the Otavi Foreland is characterized by an evaporative enrichment with slope 4.5 (Figure 4.41). The  $\delta^{18}\text{O}$  and of  $\delta^2\text{H}$  values corrected for evaporation have a composition similar to the groundwater in the Otavi Mountains. The evaporative enrichment is probably caused by evaporation from flooded pans in the Otavi Foreland and infiltration of the non-evaporated part from pans. Flooding of pans is presently caused by ephemeral floods and thus indicates indirect recharge processes. This is clearly shown by the impact of a flood event on the isotopic composition of groundwater at CN038 'Kameeldorn' (Figure 4.45). It cannot be excluded that in former times higher groundwater levels may also have contributed to the seasonal or episodic filling of pans, and that this isotopic signal is still found in the groundwater.

### 5.2.3 The Kalahari basin

GIS-based analyses were used to visualize several troughs in the pre-Kalahari surface (Figure 4.2, B). In two major troughs thick successions of Kalahari sediments have accumulated (Figure 4.1). A map of saturated thickness of Kalahari sediments reveals that these major

troughs are partly saturated with groundwater (Figure 4.3, d+f). Two major aquifers are found in this trough: the Lower Kalahari aquifer containing groundwater of poor quality, and the Middle Kalahari aquifer with relatively fresh groundwater. In the main trough, extending from south-west to north-east (Figure 4.3, d), both aquifers are developed.

In general direct recharge rates are assumed to be well below 1 % where Kalahari sediments are thick (Figure 1.4). Exceptionally high values may be found in areas with exposed and karstified calcrete. The existence of calcrete crusts, especially when covered with thin and vegetated sand deposits, may provide good conditions for direct recharge. The extended pan area south of Goblenz exemplifies the characteristics of a preferential recharge area within the Kalahari: The hydrogeological configuration in this area requires increased local recharge rates sustaining the groundwater mound in this area (Figure 4.1). In the future, remote sensing may help to better identify and delineate such zones for the assessment of recharge distribution.

The analysis of hydrological data in the second chapter reveals that surface runoff generation is low in the Kalahari. Unit runoff in the Kalahari amounts to about 1 mm/m<sup>2</sup> (Table 2.1). It is by about one order of magnitude lower than in the mountainous rim (Figure 2.4). As a consequence,

- indirect recharge from ephemeral floods will be highest along the transition between mountainous rim and Kalahari,
- internal runoff generation and associated indirect recharge will be localized and sporadic.

Two 'islands' of pre-Kalahari Omingonde sediments (TRo, Figure 2.6) emerging from the Kalahari sand sea represent another hint as to how important the thickness of a Kalahari cover is for controlling mean annual recharge. The map of chloride concentrations shows a strong decrease downstream of these outcrops (Figure 4.18, g+h). Plumes of groundwater with low chloride concentrations indicate preferential recharge spots. In addition, runoff generation is enhanced due to the low permeability of the Omingonde Formation. Runoff triggers indirect recharge in ephemeral rivers and pans developed south of the exposures of Omingonde sediments (Figure 4.1).

Within the Kalahari basin hydrochemical processes are complicated and make cluster analysis and the interpretation of water-rock interactions difficult if not impossible. Saline end members in the Kalahari could be identified (Figure 2.23). However, their hydrochemical evaluation remains speculative.

The isotopic evolution of groundwater in the Kalahari shows clear signs of evaporative enrichment (Figure 4.42). There are no groundwater discharge areas in the Upper Omatako basin; therefore enrichment is probably caused by indirect recharge. Ephemeral floods accumulate in pans. Open surface evaporation from these pools takes place during the warm rainfall season and, finally, the partly evaporated water infiltrates resulting in deep percolation as *indirect* recharge. Removing the influence of evaporation points to an interesting observation: The groundwater of the Kalahari has a corrected initial isotopic composition corresponding to mountain/ mountain front recharge (Figure 4.48). This observation confirms the importance of the mountainous rim for the water balance of the Kalahari basin. Inflow to the Kalahari takes place either by surface runoff and indirect recharge, or by direct recharge in the outer mountain rim and subsequent lateral groundwater inflow. In both cases the isotopic signal of rainfall at higher altitudes is preserved in the Kalahari's groundwater.

### 5.3 The groundwater resources of Goblenz

The etymology of the name Goblenz reveals already something about the hydrological environment: The small town on the edge of the Kalahari was named after the German town Koblenz (from Lat., confluens – flowing together) which is located at the confluence of the rivers Rhine and Moselle. The Namibian town at the edge of the Kalahari marks the confluence of two *ephemeral* rivers: the Omatako and the Omingonde. These ephemeral rivers are only activated during floods lasting between a few days (Omingonde) up to a few weeks (Omatako). Most of the discharge of the Omatako is presently intercepted by the Omatako dam (Figure 2.1). Although the hydrological data for a more detailed statement do not exist (yet), the coincident activation of runoff in both rivers must be a rare event. Hydrologically, Goblenz hardly deserves its name. However, hydrogeologically it does!

The Middle Kalahari aquifer directly south of Goblenz receives groundwater inflows from all recharge areas in the Upper Omatako basin – it is a major zone of groundwater confluence (Figure 4.1). This is also the main explanation for the availability of fresh groundwater in that area. The Goblenz state water scheme taps the Middle Kalahari aquifer along a major trough shown in Figure 4.3 (d). This aquifer receives most of its inflow from mountain front recharge. The respective percentages of inflow from different source areas were determined by a mixing-cell approach (Figure 4.54). According to the inverse mixing model, Goblenz receives about 74 % (up to 87 % for cluster modelling, Table 4.6) from the Otavi Mountains and the Otavi Mountain Foreland. Another 12 % (4 % for cluster modelling) derive from the Waterberg sandstone aquifer. Altogether about 14% (8 % for cluster modelling) are formed by inflow of a mixed component from the western part of the study area, mainly the Karibib Formation.

In conclusion, the aquifer that is tapped by the water scheme at Goblenz heavily depends on inflow from mountain front recharge. The major contribution comes from the Otavi Mountains. In the long run groundwater abstraction at Goblenz will thus be affected by any measures that heavily influence groundwater inflow from the Otavi Mountains, the Waterberg, and the fractured aquifer north of the Waterberg. With regard to vulnerability, the southern Otavi Foreland and the lower Omingonde valley may be critical areas due to shallow groundwater levels and fast flow connections. Pollution in these areas would also affect the water quality at Goblenz. The key to the availability and protection of groundwater at Goblenz is given by its name – it is sustained by the *confluence* of groundwater mainly from mountain front recharge.



## References

- ABDULRAZZAK M. J. & MOREL-SEYTOUX (1983): Recharge from an ephemeral stream following wetting front arrival to water table. *Water Resources Research*, **19** (1): 194-200
- ADAR E. M. (1984): Quantification of aquifer recharge distribution using environmental isotopes and regional hydrochemistry. *Doctoral thesis*, Univ. of Arizona, Tucson, United States, 269 p.
- ADAR E. M. (1996): Quantitative evaluation of flow systems, groundwater recharge and transmissivities using environmental tracers. *IAEA TECDOC*, **910**: 113-154
- ADAR E. M. & NEUMAN S. P. (1988): Estimation of spatial recharge distribution using environmental isotopes and hydrochemical data. II, Application to Aravaipa Valley in southern Arizona, U. S. A. *J. Hydrol.*, **97**(1-4): 279-302
- ADAR E. M. & SOREK S. (1990): Numerical method for aquifer parameter estimation utilizing environmental tracers in transient flow system. In: *ModelCARE 1990 - calibration and reliability in groundwater modelling* (ed. by Karel Kovar). *IAHS-AISH Publ.*, **195**: 135-148
- ADAR E. M., NEUMAN S. P. & WOOLHISER D. A. (1988): Estimation of spatial recharge distribution using environmental isotopes and hydrochemical data. I, Mathematical model and application to synthetic data. *J. Hydrol.*, **97** (1-4): 251-277
- ADAR E. M., ISSAR A. S., SOREK S. & GEV I. (1992): Modelling of flow pattern in a shallow aquifer affected by reservoirs. I, Evaluation of the flow system by environmental tracers. In: *Transport in Porous Media* (D. Reidel Publishing Company. Dordrecht, International) **8**: 1-20
- ADAR E. M., DODY A., GEYH M. A., YAIR A., YAKIREVICH A. & ISSAR A. S. (1998): Distribution of stable isotopes in arid storms. 1. Relation between the distribution of isotopic composition in rainfall and in the consequent runoff. *Hydrogeology Journal*, **6**: 50-65
- AGNEW C. & ANDERSON E. (1992): *Water Resources in the Arid Realm*. Routledge, 329 p.
- ALLISON G. B. (1989): A review of some of the physical, chemical and isotopic techniques available for estimating groundwater recharge. In: *I. Simmers (ed. ) Estimation of Natural Groundwater Recharge*. *NATO Advanced Sciences Institutes Series C*: 49-72
- ALLISON G. B. & HUGHES M. W. (1983): The use of natural tracers as indicators of soil water movements in a temperate semi-arid region. *J. Hydrol.*, **60**: 157-173
- ALLISON G. B., STONE W. J. & HUGHES M. W. (1985): Recharge in karst and dune elements of a semi-arid landscape as indicated by natural isotopes and chloride. *J. Hydrol.*, **76**: 1-25
- ALLISON G. B., GEE G. W. & TYLER S. W. (1994): Recharge in arid and semi-arid regions. . *Soil Science Society of America Journal*, Vol **58** (Proc. Symp. 30. Oct. 1991, Denver, CO).
- APPELO C. A. J. & POSTMA D. (1996): *Geochemistry, groundwater and pollution*. Balkema, Rotterdam, (third corrected print, bound), 536 p.
- BAERTSCHI P. (1976): Absolute  $^{18}\text{O}$  content of Standard Mean Ocean Water. *Earth and Planetary Science Letters*, **31**: 341-344
- BAHRENBURG G., GIESE E. & NIPPER J. (1992): *Statistische Methoden in der Geographie 2*. Teubner Studienbücher Geographie, Stuttgart, 412 p.
- BALEK J. (1988): Groundwater recharge concepts. In: *I. Simmers (ed. ) Estimation of Natural Groundwater Recharge*. *NATO Advanced Sciences Institutes Series C*: 3-9
- BARD E., HAMELIN B., FAIRBANKS R. G. & ZINDLER A. (1990): Calibration of the  $^{14}\text{C}$  time scale over the past 30,000 years using mass spectrometric U-Th ages from Barbados corals. *Nature*, **345**: 405

- BEAR J. (1972): Dynamics of Fluids in Porous Media. New York, American Elsevier Publishing Company
- BEAUMONT P. (1989): Drylands - Environmental Management and Development. *Routledge*, 536 p.
- BECKER A. & BRAUN P. (1999): Disaggregation, aggregation and spatial scaling in hydrological modelling. *J. Hydrol.*, **217**: 239-252
- BESBES M. & DE MARSILY G. (1984): From infiltration to recharge: use of a parametric transfer function. *J. Hydrol.*, **74**: 271-292
- BESBES M., DELHOMME J. P. & DE MARSILY G. (1978): Estimating recharge from ephemeral streams in arid regions, a case study at Kairouan, Tunisia. *Water Resources Research*, **14**(2): 281-290
- BEVEN K. & GERMANN P. (1982): Macropores and Water Flow in Soils. *Water Resources Research*, **Vol. 18**: 1311-1325
- BLÜMEL W. D. (1982): Calcretes in Namibia and SE-Spain, relations to substratum, soil formation and geomorphic factors. Yaalon D. H. (ed. ) Aridic Soils and Geomorphic Processes. *Catena Suppl.*, **1**, Braunschweig: 67-82
- BOOCCOCK C. & VAN STRATEN (1962): Notes on the geology and hydrology of the central Kalahari region. Bechuanaland Protectorate. *Trans. Geol. Soc. S. Afr.*, **65**: 125-171
- BOUGHTON W. C. & STONE J. J. (1985): Variation of runoff with watershed area in a semi-arid location. *J. Arid Environments*, **9** (1): 13-25
- BREDENKAMP D. B., VAN RENSBURG H. J., VAN TONDER G. J. & BOTHA L. J. (1995): Manual on Quantitative Estimation of Groundwater Recharge Based on Practical Hydro-Logical Methods. *Water Research Commission, Pretoria*, 363 p.
- BROOK G. A., FOLKOFF M. E. & BOX E. O. (1983): A world model of soil carbon dioxide. *Earth Surf. Proc.*, **8**: 79-88
- BROWN C. E. (1998): Applied Multivariate Statistics in Geohydrology and Related Sciences. Springer Verlag, 248 p.
- BUCKINGHAM E. (1907): Studies on the Movement of Soil Moisture. *USDA Bur. Soil Bull.*, **38**
- BUNDESANSTALT FÜR GEOWISSENSCHAFTEN UND ROHSTOFFE - BGR (1997): German-Namibian Groundwater Exploration Project. Reports on Hydrogeological and Isotope Hydrological Investigations. Technical Cooperation Project No. 89.2034.0, Hannover
- BUSCHE D. & ERBE W. (1987): Silicate karst landforms of the southern Sahara (north-eastern Niger and southern Libya). In: Laterites; some aspects of current research. *Zeitschrift f. Geomorphologie. Supplementband*, **64**, 55-72
- BUSCHE D. & SPONHOLZ B. (1990): Silikatkarst in der südlichen Sahara; Einflußgröße für das Grundwasser? (Siliceous karst in the southern Sahara; major influence for ground water?). *Zentralblatt für Geologie und Palaeontologie*, Teil I: Allgemeine, Angewandte, Regionale und Historische Geologie, **4**, Schweizerbart'sche Verlagsbuchhandlung. Stuttgart, Federal Republic of Germany, 425 p.
- CAMPANA M. E. & SIMPSON E. S. (1984): Groundwater residence times and recharge rates using a discrete-state compartment model and <sup>14</sup>C data. *J. Hydrol.*, **72**: 171-185
- CLARK I. & FRITZ P. (1997): Environmental Isotopes in Hydrology. *CRC Press*, 328 p.
- CRAIG H. (1961): Isotopic variations in meteoric waters. *Science*, **113**: 1702-1703
- CRERAR S., FRY R. G., SLATER P. M., VAN LANGENHAVE G. & WHEELER D. (1988): An unexpected factor affecting recharge from ephemeral river flows in SWA/Namibia. I. Simmers (ed. ) *Estimation of Natural Groundwater Recharge*, D. Reidel Publ.: 11-28

- DACHROTH W. & SONNTAG C. (1983): Grundwasserneubildung und Isotopendatierung in Südwestafrica/Namibia. *Z. dt. geol. Ges.*, **134**: 1013-1041
- DARCY H. (1856): Les Fontaines Publiques de la Ville de Dijon. Paris: Victor Dalmont.
- DE BEER J. H. & BLUME J. (1983): Geophysical and Hydrogeological Investigations of the Ground Water Resources of Hereroland SWA/Namibia. Geophysics Division, National Physical Research Laboratory, Council of Scientific and Industrial Research, Pretoria, South Africa, 31 p.
- DE BEER J. H. & BLUME J. (1985): Geophysical and hydrogeological investigations of the ground water resources of western Hereroland, South West Africa/Namibia. *Trans. Geol. Soc. S. Afr.*, **88**: 483-493
- DEPARTMENT OF WATER AFFAIRS - DWA (1988): Evaporation Map for Namibia. *Rep. of Namibia, Ministry of Agriculture, Water and Rural Development. Hydrology Division*, Report No: 11/1/8/1/H1
- DEPARTMENT OF WATER AFFAIRS - DWA (1992a): Updated Isohyetal Rainfall Map for Namibia. *Rep. of Namibia, Ministry of Agriculture, Water and Rural Development, Compiled by Hydrology Division*, Report 11/1/8/H5, File 11/1/8/1
- DEPARTMENT OF WATER AFFAIRS - DWA (1992b): Unit Runoff Map for Namibia. *Rep. of Namibia, Ministry of Agriculture, Water and Rural Development. Hydrology Division*, File 11/1/5/1, Report 11/1/5/1/H2
- DEPARTMENT OF WATER AFFAIRS - DWA (1993): Reconnaissance Report on Water Supply to Settlements along the Omuramba Omatako between Goblenz - Okakarara and Okakarara - Central Reservoir Pipelines. *Rep. of Namibia, Ministry of Agriculture, Water and Rural Development. Geohydrology Division*, File 13/5/1/2, Report 2530/5/1/2/P3
- DEPARTMENT OF WATER AFFAIRS - DWA (1997): Goblenz State Water Scheme. Memorandum on Drilling and Test Pumping. *Rep. of Namibia, Ministry of Agriculture, Water and Rural Development. Internal Report*, File 12/8/1/1
- DE VRIES H. H. & VAN HOYER M. (1988): Groundwater Studies in semi-arid Botswana - a review. In: I. Simmers (ed. ) *Estimation of Natural Groundwater Recharge*. NATO Advanced Sciences Institutes Series C: 339-348
- DINÇER T., AL-MUGRIN A. & ZIMMERMANN U. (1974): Study of the infiltration and recharge through the sand dunes in arid zones with special reference to the stable isotopes and thermonuclear Tritium. *J. Hydrol.*, **23**:79-109
- DODY A., ADAR E. M., YAKIREVICH A., GEYH M. A. & YAIR A. (1995): Evaluation of depression storage in an arid rocky basin using stable isotopes of oxygen and hydrogen. *IAHS-AISH Publ.* **232**: 417-427
- DREVER J. I. (1988): The geochemistry of natural waters. 2<sup>nd</sup> ed. Prentice-Hall, 437 pp.
- EICHINGER L., MERKEL B., NEMETH G., SALVAMOSER J. & STICHLER W. (1984): Seepage and velocity determinations in unsaturated quaternary gravel. In: *Recent investigations in the Zone of Aeration*, Proc. Munich, Oct. 1984: 303-313
- FONTES J. CH. & GARNIER J. M. (1979): Determination of the initial <sup>14</sup>C activity of total dissolved carbon: A review of existing models and a new approach. *Water Resources Research*, **15**: 399-413
- FOSTER S. S. D, BATH A. H., FARR J. L. & LEWIS W. J. (1982): The likelihood of active groundwater recharge in the Botswana Kalahari. *J. Hydrol.*, **55**: 113-136
- FROMMURZE H. F. (1953): Hydrological research in arid and semi-arid areas in the Union of South Africa and Angola. *Rev. Res., Arid Zone Hydrol., U. N. E. S. C. O., Paris*: 58-77

- GANSSEN R. (1963): Südwest-Afrika, Böden und Bodenkultur - Versuch einer Klimapedologie warmer Trockengebiete. Verlag von Dietrich Reimer, Berlin, 160 p.
- GAT Y. (1995): The relationship between the isotopic composition of precipitation, surface runoff and groundwater for semi-arid and arid zones. *IAHS Publ.* No. **232** (Application of Tracers in Arid Zone Hydrology, Proc. of the Vienna Symposium, August 1994, ed. by E. Adar & C. Leibundgut): 409-416
- GAT J. R. & GONFIANTINI R. (1981): Stable isotope hydrology. Deuterium and Oxygen-18 in the Water Cycle. A monograph prepared under the aegis of the IAEA/UNESCO working group on nuclear techniques in hydrology of the International Hydrological Programme (IHP). *Technical Reports Series*, **210**, Vienna, 337 p.
- GEE G. W. & HILLEL D. (1988): Groundwater Recharge in Arid Regions: Review and Critique of Estimation Methods. *Hydrological Processes*, **2**: 255-266
- GEHRELS J. C. & VAN DER LEE J. (1990): Rainfall and recharge a critical analysis of the atmosphere-soil-groundwater relationship in Kanye, semi-arid Botswana. M. Sc. Thesis, Free Univ. Amsterdam.
- GEYH M. A. (1995): Geochronologische Aspekte Paläohydrologischer und Paläoklimatischer Befunde in Namibia. *Geomethodica* (Basel, Veröff. = 20 BGC), **20**: 75-99
- GEYH M. A. & SCHLEICHER H. (1990): Absolute age determination; physical and chemical dating methods and their application. Springer Verlag, Berlin, Federal Republic of Germany, 503 p.
- GEYH M. A. & PLOETHNER D. (1997): Isotope Hydrological Study in Eastern Owambo, Etosha Pan, Otavi Mountain Land and Central Omatoko catchment including Waterberg Plateau. *German-Namibian Groundwater Exploration Project. Technical Cooperation Project No. 89. 2034. 0.*, Follow-up report, **Vol. 2**, Hannover, 34 p.
- GIESKE A. (1992): Dynamics of groundwater recharge. A case study in semi-arid Botswana. Freie Univ. Amsterdam, 289 S., Enschede.
- GIESKE A., SELAULO E. & MCMULLAN S. (1990): Groundwater recharge through the unsaturated zone of southeastern Botswana: a study on chlorides and environmental isotopes. *Regionalization in Hydrology (Proc. of the Ljubijana Symposium, April 1990)*. *IAHS Publ.*, **191**: 33-44
- GONFIANTINI R. (1986): Environmental isotopes in lake studies. In: *Handbook of Environmental Isotope Geochemistry* (ed. by P. Fritz and J. Ch. Fontes), Vol. **2**, The Terrestrial Environment, B. Elsevier, Amsterdam, The Netherlands: 113-168
- GUNTHORPE R. J. (1983): Coal exploration project - Progress Report (Geological Survey Files).
- GUNTHORPE R. J. (1987): Coal exploration project - Final Report (Geological Survey Files).
- HAGEMAN R., NIEF G. & ROTH E. (1970): Absolute isotopic scale for deuterium analysis in natural waters. Absolute D/H ratio for SMOW. *Tellus*, **22**: 712-715
- HAUDE W. (1954): Zur praktischen Bestimmung der aktuellen und potentiellen Evaporation und Evapotranspiration. *Mitteilungen des deutschen Wetterdienstes*, **8**, Bad Kissingen, 22 S.
- HENDRICKX J. M. H. & WALKER G. R. (1997): Recharge from precipitation. In: *Recharge of Phreatic Aquifers in (Semi-) Arid Areas* (ed. Ian Simmers): 19-111
- HEYNS P. (1996): Water Resources Management in Namibia. Department of Water Affairs, Namibia, *Internal Memorandum*, 15 p.
- HOHELLA M. F. & WHITE A. F. (1990): Mineral-water interface geochemistry. *Reviews in Mineralogy*, **23**, Mineral Soc. Am., 603 p.
- HOEFS J. (1997): Stable Isotope Geochemistry. Springer (4<sup>th</sup> ed. ), 201 p.

- HORTON R. E. (1940): An Approach toward a Physical Interpretation of Infiltration-Capacity. *Soil Sci. Soc. Am. J.*, **5**: 399-417
- HUBER B. (1992): Der Einfluß des Trenngefüges auf die Grundwasserströmung in Klufftgrundwasserleitern. *Hydrogeologie und Umwelt*, **5**, Univ. Würzburg/Germany, 293 p.
- HUYSER D. J. (1979a): 'N intensiewe opname van waterbronne in die res van die distrik Otjiwarongo. 47ste Veradering van die Loodskomitee vir Waternavorsing in Suidwes-Afrika. SWA Streeklaboratorium, Nasionale Instituut vir Waternavorsing, Wetenskaplike en Nywerheidsnavoringsgraad. Windhoek, 1979.
- HUYSER D. J. (1979b): 'N intensiewe opname van waterbronne in die res van die distrik Grootfontein. 47ste Veradering van die Loodskomitee vir Waternavorsing in Suidwes-Afrika. SWA Streeklaboratorium, Nasionale Instituut vir Waternavorsing, Wetenskaplike en Nywerheidsnavoringsgraad. Windhoek, 1979.
- IAEA - INTERNATIONAL ATOMIC ENERGY AGENCY (1969-1994): Environmental Isotope Data World Survey of Isotope Concentration in Precipitation:
- No. 1 (STI/DOC/10/96) 1953-1963, 421 pages, published in 1969  
 No. 2 (STI/DOC/10/117) 1964-1965, 404 pages, published in 1970  
 No. 3 (STI/DOC/10/129) 1966-1967, 421 pages, published in 1971  
 No. 4 (STI/DOC/10/147) 1968-1969, 404 pages, published in 1973  
 No. 5 (STI/DOC/10/165) 1970-1971, 421 pages, published in 1975  
 No. 6 (STI/DOC/10/192) 1972-1975, 404 pages, published in 1979  
 No. 7 (STI/DOC/10/226) 1976-1979, 421 pages, published in 1983  
 No. 8 (STI/DOC/10/264) 1980-1983, 404 pages, published in 1986  
 No. 9 (STI/DOC/10/311) 1984-1987, 188 pages, published in 1990  
 No. 10 (STI/DOC/10/371) 1988-1991, 214 pages, published in 1994
- IAEA - INTERNATIONAL ATOMIC ENERGY AGENCY (1996): Manual on Mathematical Models in Isotope Hydrogeology. *IAEA TECDOC*, **910**, 207 p.
- JONES C. R. (1982): The Kalahari of Southern Africa. In: The Geological Story of the World's Deserts (ed. by T. L. Smiley). *Striae*, **17**: 20-34
- KAUFMANN S. & LIBBY W. F. (1954): The natural distribution of tritium. *Physical Review*, **93**: 1337-1344
- KELLER S. & VAN HOYER M. (1992): Erkundung und Bewirtschaftung von präkambrischen Karstaquiferen im südlichen Afrika. *Z. dt. geol. Ges.*, **143**: 277-290
- KÜLLS C., LEIBUNDGUT C., SCHWARZ U. & SCHICK A. (1994): Channel infiltration study using dye tracers. *IAHS Publ.*, No. **232**: 429-436
- KÜLLS C., CONSTANTINOU C. & UDLUFT, P. (2000): Dynamics of groundwater recharge in natural environments and mining areas: Case studies from Cyprus. (*Conf. Min. Wealth Athens*, in print)
- KÜLLS C. & UDLUFT P. (2000): Mapping the availability and dynamics of groundwater recharge Part II: Case studies (*Congress Regional Geological Cartography and Information Systems, München*, in print)
- LERNER D. N., ISSAR A. S. & SIMMERS I. (1990): Groundwater Recharge - A Guide to Understanding and Estimating Natural Recharge. *IAH, International Contributions to Hydrogeology*, **Vol. 8**
- LEVIN M., GAT J. R. & ISSAR A. (1980): Precipitation, flood and groundwaters of the Negev Highlands: an isotopic study of desert hydrology. *Arid Zone Hydrology: Investigations with isotope techniques*. Proc. Adv. Group Meeting, Vienna, IAEA: 3-22
- LLOYD J. W. (1986): A Review of Aridity and Groundwater. *Hydrological Processes*, **Vol. 1**: 63-78

- MAIDMENT D. R. (1992): Handbook of Hydrology. MacGraw-Hill
- MAINARDY H. (1999): Grundwasserneubildung in der Übergangszone zwischen Festgesteinsrücken und Kalahari-Lockersedimentüberdeckung (Namibia). *Hydrogeologie und Umwelt*, **17**, 145 p. (PhD, Univ. Würzburg)
- MAJOUBE M. (1971): Fractionnement en oxygène-18 et en deutérium entre l'eau et sa vapeur. *J. Chim. Phys.*, **197**: 1423
- MARTIN H. (1961): Hydrology and water balance of some regions covered by Kalahari sands in South West Africa. *Proc. Inter-African Conference on Hydrology, Nairobi 1960*
- MAZOR E. (1982): Rain recharge in the Kalahari - A note on some approaches to the problem. *J. Hydrol.*, **55**: 137-144
- MAZOR E., BIELSKY M., VERHAGEN B. TH., SELLSCHOP J. P. F., HUTTON L. & JONES M. T. (1980): Chemical composition of groundwaters in the vast Kalahari flatland. *J. Hydrol.*, **48**: 147-165
- MILLER R. MCG. (ED. ) (1983): Evolution of the Damara Orogen of SW Africa/Namibia. *Special Publ. of the Geological Society of South Africa*, No. **11**, 515 p.
- MOORSOM R., FRANZ J. & MUPOTOLA M. (1995): Coping with Aridity - Drought Impact and Preparedness in Namibia - Experiences from 1992/93. Brandes & Apsel Verl., 250 p.
- MORSE J. W. & MACKENZIE F. J. (1990): Geochemistry of sedimentary carbonates. Elsevier, Amsterdam.
- MÜNNICH K. O. (1968): Isotopendatierung von Grundwasser. *Naturwissenschaften*, **55**: 158-163
- PARKHURST D. L., THORSTENSON D. C. & PLUMMER L. N. (1990): PHREEQE - A computer program for geochemical calculations. *US Geol. Surv. Water Res. Inv.*, 80-96
- PASSARGE S. (1904): Die Kalahari. Reimer, Berlin: 823 p.
- PEARSON F. J. (1965): Use of 13-C/12-C ratios to correct radiocarbon ages of material initially diluted by limestone. In: Proc. 6<sup>th</sup> Intern. Conf. Radiocarbon and Tritium, Pulman, Washington: 357
- PLOETHNER D., SCHMIDT G. A., KEHRBERG S. & GEYH M. A. (1997): Hydrogeology and Isotope Hydrology of the Otavi Mountain Land and its Surroundings (KARST\_01 and KARST\_02). Bundesanstalt für Geowissenschaften und Rohstoffe. *German-Namibian Groundwater Exploration Project (Technical Cooperation No. 89. 2034. 0). Reports on hydrogeological and isotope hydrological investigations*, **Vol. D-III**: 65 p.
- PLUMMER L. N., VACHER H. L., MACKENZIE F. T., BRICKER O. P. & LAND L. S. (1976): Hydrogeochemistry of Bermuda: a case history of groundwater diagenesis of biocalcarenes. *Geol. Soc. Am. Bull.*, **87**: 1301-1316
- PRIESTLEY C. H. B. & TAYLOR R. J. (1972): On the assessment of surface heat flux and evaporation using large scale parameters. *Mon Weather Rev*, **100**: 81-92
- ROSENTHAL E., ADAR E., ISSAR A. S. & BATELAAN O. (1990): Definition of groundwater flow patterns by environmental tracers in the multiple aquifer system of southern Arava Valley, Israel. *J. Hydrol.*, **117** (1-4): 339-368
- ROZANSKI K., ARAGUÁS-ARAGUÁS L. & GONFIANTINI R. (1993): Isotopic patterns in modern global precipitation. In: *Continental Isotope Indicators of Climate*. American Geophysical Union Monograph.
- RUSHTON K. R. (1988): Numerical and conceptual models for recharge estimation in arid and semi-arid zones. In: I. Simmers (ed. ) Estimation of Natural Groundwater Recharge. *NATO Advanced Sciences Institutes Series C*: 223-238
- SAMI K. & HUGHES D. A. (1996): A comparison of recharge estimates to a fractured sedimentary aquifer in South Africa from a chloride mass balance and an integrated surface-subsurface model. *J. Hydrol.*, **179**:111-136

- SACS - SOUTH AFRICAN COMMITTEE FOR STRATIGRAPHY) (1980): Stratigraphy of South Africa, Part 1. Lithostratigraphy of the Republic of South Africa, SWA/Namibia and the Republics of Boputhatswana, Transkei and Venda. *Handbook of the Geological Survey of South Africa*, **8**.
- SCHMIDT G. A. (1997a): Otavi Mountain Land: Data Base Evaluation and Conceptual Modelling KARST\_01 & KARST\_02. Bundesanstalt für Geowissenschaften und Rohstoffe, *German-Namibian Groundwater Exploration Project (Technical Cooperation No. 89. 2034. 0). Reports on hydrogeological and isotope hydrological investigations*, **Vol. E-II**
- SCHMIDT G. A. (1997b): Otavi Mountain Land: Groundwater Modelling Part 1 and Part 2. Bundesanstalt für Geowissenschaften und Rohstoffe, *German-Namibian Groundwater Exploration Project (Technical Cooperation No. 89. 2034. 0). Reports on hydrogeological and isotope hydrological investigations*, **Vol. E-III**
- SCHNEIDER M. B. (1989): Leitlinien der wasserwirtschaftlichen Wasserversorgung. *Frankfurter Wirtschafts- und Sozialgeogr. Schriften*, **Heft 53**: 212-228
- SEEGER K. G. (1990): An Evaluation of the Groundwater Resources of the Grootfontein Karst Area. *DWA unpubl. Report, Windhoek*, **No. 12/5/G2**: 187 p.
- SEIMONS & VAN TONDER (1993): Geohydrological characterisation and modelling of the Otjiwarongo marble aquifer in Namibia. *Afr. Geosci. Rev.*, **1**: 71-79
- SEUFFERT O., BUSCHE D. & LOWE P. (1999): Rainfall structure - rainfall erosivity: New concepts to solve old problems. *Petermanns Geographische Mitteilungen*, **143**(5-6): 475-490
- SHARMA M. L. (1986): Measurement and Prediction of Natural Groundwater Recharge - An Overview. *J. Hydrol. (N. Z.)*, **25**(1): 49-57
- SHAW P. A. & THOMAS D. S. G. (1996): The quaternary paleoenvironmental history of the Kalahari, Southern Africa. *J. arid environm.*, **32**: 9-22
- SIMMERS I. (1987): Estimation of Natural Groundwater Recharge. *NATO ASI SERIES C, Mathematical and Physical Sciences*, Vol. **222**, Reidel Publ. Comp., 510 p.
- SIMMERS I., HENDRICKX J. M. H., KRUSEMAN G. P. & RUSHTON K. R. (1997): Recharge of Phreatic Aquifers in (Semi-) Arid Areas (ed. by I. Simmers). *Intern. Assoc. of Hydrogeologists*, **19**., Balkema, 277 p.
- SIMPSON E. S. & DUCKSTEIN L. (1976): Finite state mixing-cell models. In: *Karst Hydrology and Water Resources* (ed. by V. Yevjevich), Water Resources Publications, **Vol. 2**: 489-508, Fort Collins, Colorado.
- STUIVER M. & REIMER J. (1993): Extended <sup>14</sup>C data base and revised CALIB 3.0 <sup>14</sup>C age calibration program. *Radiocarbon*, **35**(1): Tucson: 215-230
- STUIVER M. & KRA R. (EDS.) (1986): Calibration issue. *Radiocarbon*, **28**(2B) Tucson: 805-1030
- STUMM W. & MORGAN J. J. (1995): Aquatic Chemistry. 3<sup>rd</sup> ed. Wiley & Sons, New York, 1022 p.
- SZAPIRO S. & STECKEL F. (1967): Physical properties of heavy oxygen water. 2. Vapour pressure. *Transactions Faraday Society*, **63**: 883
- THOMAS D. S. G. (1986): The nature and depositional setting of arid and semi-arid Kalahari sediments, Southern Africa. *J. Arid Environments*, **14**: 17-26
- THOMAS D. S. G. & SHAW P. A. (1990): The Deposition and Development of the Kalahari Group Sediments, Central Southern Africa. *J. African Earth Sci.*, **10**(1/2): 187-197
- THOMAS D. S. G. & SHAW P. A. (1992): *The Kalahari Environment*. Cambridge University Press.
- UBELL K. (1977): Hydraulische Methoden zur Bestimmung der Fließvorgänge in klüftigen Gesteinen. *Ber. Bundesanst. Gewässerk.*, p. 105, Koblenz/Germany

- UDLUFT P. & BLASY L. (1975): Ermittlung des unterirdischen Abflusses und der nutzbaren Porosität mit Hilfe der Trockenwetter-Auslaufkurve. *Z. dt. geol. Ges.*, **126** (1975): 325-336
- UDLUFT P. & SALAMEH E. (1976): Berechnung des Grundwasserabflusses und der Gebietsdurchlässigkeit mit der Wasseranalyse. (Computing Groundwater Runoff and Permeability by Water Analyses). *Wasserwirtschaft*, **66**: 316-319
- UDLUFT P. & ZAGANA E. (1994): Computer-aided water budget of the Venetikos catchment area. *Proc. of the 7<sup>th</sup> Congress of the Geol. Soc. Of Greece*, **XXX/4**:267-274
- UDLUFT P. & KÜLLS C. (2000): Mapping the availability and dynamics of groundwater recharge Part I: Modelling techniques. (*Congress Regional Geological Cartography and Information Systems, München 2000*)
- UREY H. C. (1947): The thermodynamic properties of isotopic substances. *J. Chemical Soc.*: 562-581
- VAN GENUCHTEN M. TH. (1980): A Closed-form equation for Predicting the Hydraulic Conductivity of Unsaturated Soils. *Soil Sci. Soc. Am. J.*, **44**: 892-898
- VAN TONDER G. J. & KIRCHER J. (1990): Estimation of natural groundwater recharge in the Karoo aquifers of South Africa. *J. Hydrol.*, **121**: 395-419
- VEGTER J. R. (1985): Dolomitic water supplies with special reference to southern and western Transvaal. *Workshop on groundwater drilling in the Republic of South Africa, Johannesburg*.
- VERHAGEN B. TH. (1985): Isotope geohydrology; some hydrochemical and water supply insights into the Kalahari. *The proceedings of a seminar on the Mineral exploration of the Kalahari*(ed. by D. Hutchins & A. P. Lynam): 278-293
- VERHAGEN B. TH. (1990): Isotope Hydrology of the Kalahari: Recharge or no Recharge? Univ. Natal, Dep. Geol., Durban, South Africa. *Palaeoecology of Africa and of the Surrounding Islands*, **21**: 143-158
- VERHAGEN B. TH. (1992): Detailed geohydrology with environmental isotopes: a case study at Serowe, Botswana. In: *Isotope techniques in water resources development 1991*. Proc. symposium, Vienna, 1991 (IAEA): 345-362.
- VERHAGEN B. TH., MAZOR E. & SELLSHOP J. P. F. (1975): Radiocarbon and tritium evidence for direct rain recharge to groundwaters in the Northern Kalahari. *Nature*, **249**: 203-234
- VERHAGEN B. TH., SMITH P. E. & MCGEORGE I. (1979): Tritium profiles in the Kalahari sands as a measure of rain-water recharge. Proc. Isotope Hydrology, Vienna, 1978 (IAEA): 733-751
- VERHAGEN B. TH., GEYH M., FRÖHLICH K. & WITH K. (1991): Isotope Hydrological Methods for the Quantitative Evaluation of Ground Water Resources in Arid and Semi-arid Areas - Development of a Methodology. *Research reports of the Ministry for economic cooperation of the Fed. Rep. of Germany*, 164 p.
- VERHAGEN B. TH. (1999): Recharge Quantification with Radiocarbon: Independent Corroboration in Three Karoo Aquifer Studies in Botswana. Internat. Symp. In: *Isotope Techniques in Water Resources Development and Management*, Vienna, May 1999: 2-12
- VOGEL J. C. (1970): Carbon-14 dating of groundwater. In: *Isotope Hydrology 1970*, IAEA Symposium 129, March 1970, Vienna: 225-239
- VOGEL J. C. (1993): Variability of carbon isotope fractionation during photosynthesis. In: *Stable Isotopes and Plant Carbon - Water Relations* (ed. by J. R. Ehleringer, A. E. Hall & G. D. Farquhar), Academic Press, San Diego, Ca: 28-39
- VOGEL J. C. & VAN URK H. (1975): Isotopic composition of groundwater in semi-arid regions of southern Africa. *J. Hydrol.*, **25**: 23-36
- VOGEL J. C., THILO L. & VAN DIJKEN M. (1974): Determination of groundwater recharge with tritium. *J. Hydrol.*, **23**: 131-140



- 
- WHEELER D., CRERAR S., SLATER P. & VAN LANGENHOVE G. (1987): Investigation of Recharge Processes to Alluvium in Ephemeral Rivers. In: *Proc. of the 1987 Hydrological Sciences Symp., Rhodes Univ., Grahamstown, South Africa*. Int. Assoc. Hydrol. Sci., **Vol. 2**: 395-417
- WILLIAMS R. E. (1982): Statistical identification of hydraulic connections between the surface of a mountain and internal mineralized sources. *Ground Water*, **20**(4): 466-478
- WOOLHISER D. A., GARDNER H. R. & OLSEN S. R. (1982): Estimation of multiple inflows to a stream reach using water chemistry data. *Trans. Am. Soc. Agric. Eng.*, **25**(3): 616-622
- WOOLHISER D. A., EMMERICH W. E., & SHIRLEY E. D. (1985): Identification of water sources using normalized chemical ion balances: a laboratory test. *J. Hydrol.*, **65**: 205-301
- WORTHINGTON P. F. (1976): Geophysical investigations of groundwater potential in Hereroland, South West Africa. Geophysical Division, National Physical Research Laboratory, CSIR, Pretoria, South Africa, Ref: *Kon/Gf/73/1*, 43 p.
- WORTHINGTON P. F. (1979): A Preliminary Appraisal of the Groundwater Resources of Hereroland, South West Africa. Geophysical Division, National Physical Research Laboratory, CSIR, Pretoria, South Africa, 43 p.
- WRABEL J. (1999): Ermittlung der Grundwasserneubildung im semi-ariden Bereich Namibias mittels der Chlorid-Bilanz-Methode. *Hydrogeologie und Umwelt*, **16**, Diss., Univ. Würzburg, 155 p.
- YAIR A. (1992): The control of headwater area on channel runoff in a small arid watershed. *Overland flow - hydraulics and erosion mechanics* (ed. Parsons A. J. & Abrahams A. D. ): 53-68
- YAIR A. & SHACHAK M. (1987): Studies in watershed ecology of an arid area. In: *Progress in Desert Research* (ed. Berkofsky L. & Wurtele M. G. ): 145-193
- YAKIREVICH A., DODY A., ADAR E. M., BORISOV V., GEYH M. A. & YAIR A. (1998): Distribution of stable isotopes in arid storms. II, A double-component model of kinematic wave flow and transport. *Hydrogeology Journal*, **6**: 66-76
- ZAGANA E. & UDLUFT P. (1999): Wasserhaushalt im Aliakmonas Einzugsgebiet, Bilanzierung und Modellierung. *Hydrogeologie und Umwelt*, **18**, 31 p.
- ZIMMERMANN U., MÜNNICH K. O. & ROETHER W. (1967): Downward movement of soil moisture traced by means of hydrogen isotopes. In: *Isotope techniques in the Hydrologic Cycle, Geophysical Monograph Series*, **11**, American Geophysical Union.



**Manual for MIG – a Mixing-Cell Input Generator for  
Steady Flow Mixing Calculations**

## Preface

The following computer code is restricted to a steady flow and steady hydrochemical system. The code for the non-steady hydrological system is yet heavily dependent on external optimization libraries such as the NAG<sup>®</sup> Library. Therefore, a stand-alone “friendly” code or solver for the non-steady system is yet to be compiled. Those of the readers that are looking for the possibility to implement the mixing-cell approach in a non-steady hydrological flow system are encouraged to contact the author.

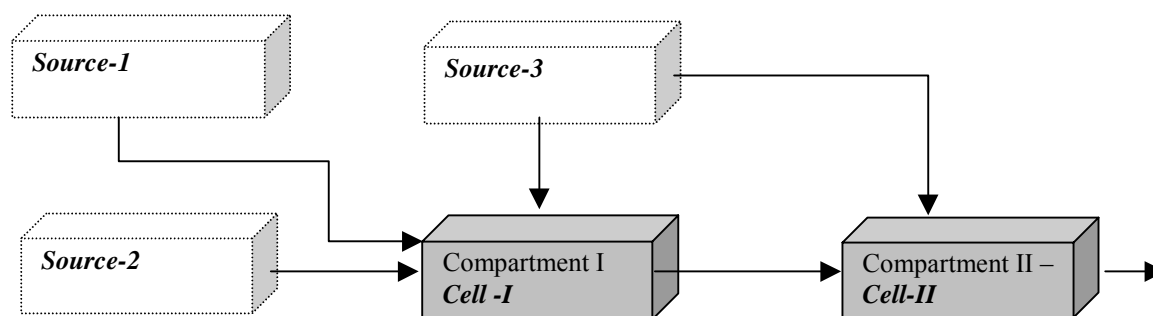
In order to simplify the procedure of preparing the data and running the Mixing-Cell Model for steady flow system ( $MCM_{sf}$ ) a special Mixing Input Generator (MIG) has been programmed. MIG is a Visual Basic Microsoft<sup>®</sup> application that runs within Excel 5.0 (and with more advanced versions such as Office 2000) on Windows95 environment and newer versions. The program has been tested and used successfully on Windows NT, Windows 95 and Windows 98 together with Excel 5.0, 7.0 & 2000. The development of the stand alone Version  $MIG_{SA}$  that runs on Windows systems without needing Microsoft Excel is under way. Section 1 provides some clarifications of terms that are used both in  $MCM_{sf}$  and MIG, whereas Section 2 shortly reviews the mathematical algorithm. For elaboration on the basic assumptions and for further mathematical description the user is referred to the text on mixing cell modelling in chapter 3.

## 1 Basic Terminology

A *source* term is any flow component that contributes water and mass of dissolved constituents to any cell within the modelled aquifer. A source is used to represent external inputs into the flow system (for example: sources of groundwater recharge or any genuine contribution from outside of the modelled aquifer). It is considered as a potential end-member with a constant chemical and isotopic composition. A source can also be used to simplify part of the modelled system such that a complex subsystem can be introduced as a source of inflow into the modelled area.

The modelled aquifer is discretized into homogeneous compartments within which all the considered parameters such as hydraulic heads, isotopic composition and the ionic concentrations are assumed to be constant. Mixing and dilution of contributors such as upstream compartments and external sources control the characteristic chemicals and the isotopic compositions of each compartment. Every well-mixed or homogeneous aquifer

section (or compartment) that is characterised by a unique representative chemical and/or isotopic composition and receives input fluxes is referred to as a *cell*.



A cell must have input and output fluxes either as outflux into a downstream cell or withdrawal of water by pumping. It can have a number of sources and can contribute water to downstream cell(s). In the above example, cell I receives *inflows* from sources 1, 2 and 3 and contributes flux into cell II. Cell II receives inflow from source 3 and from cell I. Any connection between two components has a unique flow direction. Fluxes into and out of cells are proposed along the downstream gradients. Possible hydraulic connections among cells are proposed prior to the optimization process based on groundwater heads' gradients, i.e. the assigned flow vector can not change its direction during the optimization. As a result of the optimization process a flow rate ( $\geq 0$ ) is attributed to each potential flow component. Some flow considered fluxes might end up with an effective flow rate that equals 0. It means that this specific flow component does not really exist. However, the model will assign any flux values to missing flow components that were not identified or introduced into the model.

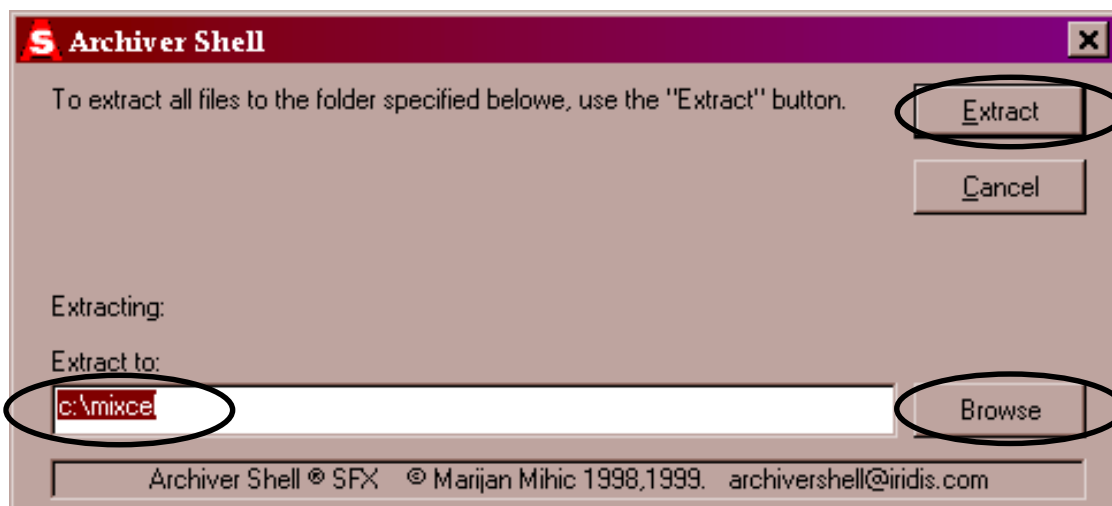
## 2 MIG Program installation and execution

### 2.1 System requirements

A PC with a Windows version from Windows 95 or newer versions is needed. MIG itself is an Excel file that contains a number of "Macro" routines for processing other Excel files. Therefore, Excel 5.0 or newer versions such as Excel2000 with the installed Visual Basic application is required. Whether or not the Visual Basic component is installed on the system can be checked by running the Microsoft Office or Excel installer. To install the Visual Basic open the Control Panel under Settings and open Add/Remove Programs Properties. Select (e.g.) Microsoft Office 2000 Professional for installation. The language of the system (English, German, International versions) does not seem to make any difference to the program execution. All the comments and commands of MIG, however, are in English.

## 2.2 Installation of MIG

The installation file **setup.exe** contains the necessary software. Go to the Windows Explorer, choose the appropriate installation drive and activate (double-click) **setup.exe**. A window with the caption 'Archiver shell' will appear and prompt for the selection of a program directory into which the software will be installed.



The suggested directory is `c:\mixcel`. Please confirm or choose an alternative directory using the 'Browse' button. Pushing the 'Extract' button will start the extraction of three files into the program directory (here for the default directory). In this directory you will find the following files:

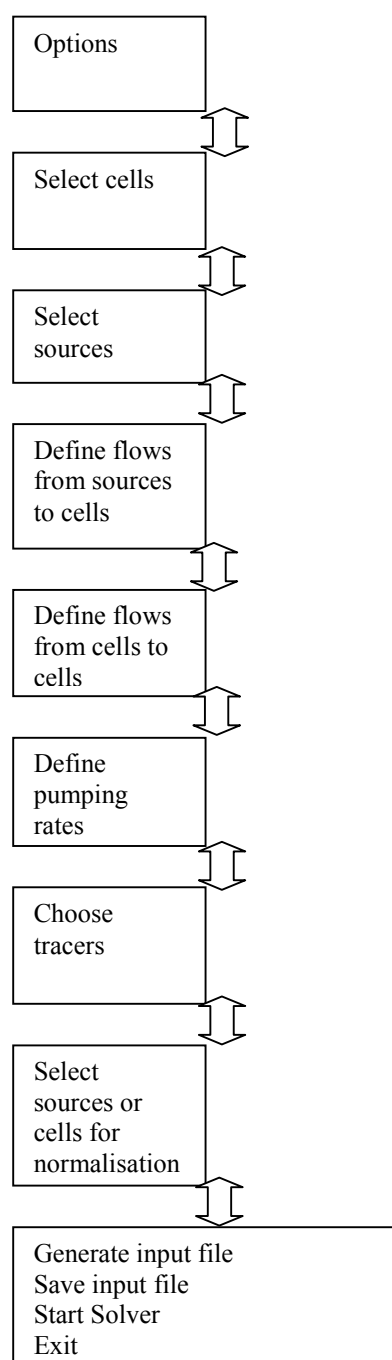
```
c:\mixcel\Mig.xls  
c:\mixcel\Multi.exe  
c:\mixcel\Data.xls
```

The file **Mig.xls** is the Excel file that contains the Visual Basic code. The file **Multi.exe** is the optimizer, an executable Fortran file that can be called by MIG. Finally, **Data.xls** is an example file with some chemical data. After the extraction of these three files, MIG can be operated under the Excel environment.

**Tip:** If MIG is used regularly it might be useful to copy the program `Mig.xls` into the Excel start-up folder. Every time, Excel is executed, the program checks the start-up folder and loads all the \*.xls files (and add-ins) that are contained in this folder. As a consequence, MIG will always be loaded and present on your system. In order to do this, please locate the folder `...\Microsoft Office\Office\XlStart\XlStart`. The beginning of the path depends on where you chose to install your Microsoft Office program. The default location is in `C:\Program Files\Microsoft Office\Office\XlStart\`.

## 2.3 MIG menu structure

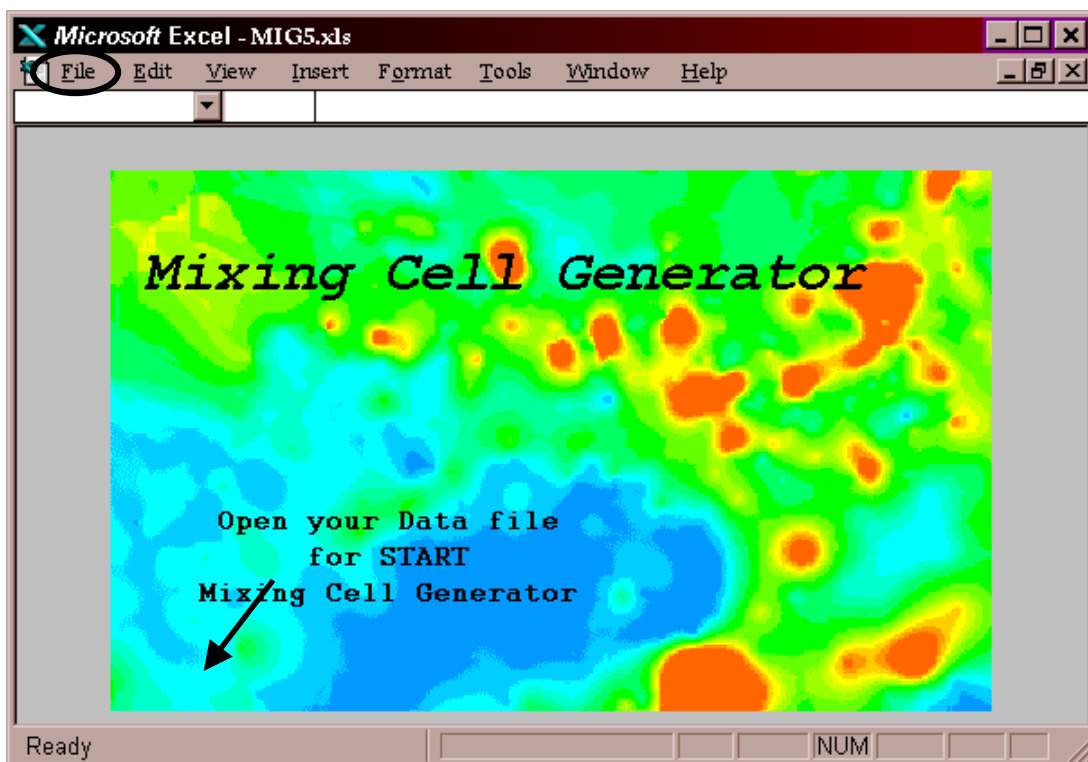
MIG is a tool for preparing the data in an appropriate format and for producing input files for a solver that contains the structure of linear equations. In order to guide the user through the procedure of defining the mixing cell model a certain structure has been followed, which is described below. After defining some straight forward program options, first the cells, then the sources are selected. As described in the terminology, any compartment (flow component), that has no inflows from other components, is called a *source*. Any compartment (flow component), that gets an input from or is receiving at least another inflow, is called a *cell*.



In the next menu the user is asked to define the flows from sources to cells, followed by a menu where the user can define the flow between cells. After this menu the user can enter or modify pumping/discharge rates – these are fluxes that are extracted from the system by pumping or natural discharge. Next, the tracers are selected and the weights (of conservancy) are modified. Finally, the user is asked whether the data should be normalised or not. At this stage, the user can generate input files for the Solver, save them and activate the solver directly from the MIG program. Detailed descriptions for each step are given below with the description of the single forms.

## 2.4 Loading and running MIG

In order to use MIG two files are always required. First, one needs to open and load **c:\mixcel\Mig.xls** with the Excel program. Please start Excel, go to the 'File/open' menu and open the file **Mig.xls** from the directory that you have selected during the installation. The program is loaded and you should see the image below.



**Tip:** Your system might have a warning system switched on that informs you that you are about to open a file containing macros – this is an additional safety against Macro-Viruses. Choose the option 'Activate Macros'. If you will use MIG regularly you might wish to switch this warning off.



In order to activate the program you have now to open the *data file*. As also indicated by the message, the mixing cell generator is a macro file – **always the user needs to open a data file to work with MIG**.

Go to ‘File/Open’ and select the file with hydrochemical and/or isotope data. Some instructions and limitations about the format of the data file are given below:

- The data file should be an Excel file format 5.0 (or newer version). Of course one may use imported dBase, Lotus or other files as well.

<i>Column with sample names</i>				<i>Matrix with chemical data</i>							
NAME	LONG	MLAT	GWL	Cammol	Mqmmol	Nammol	Kmmol	Hmmol	Smmol	Nmmol	Cimmol
CN007	17.66820	-20.71190		4.000	1.958	35.494	0.235	7.490	9.733	0.050	22.424
CN008	17.68733	-20.81865		3.039	3.962	11.353	0.486	7.998	3.435	1.193	8.744
CN010	17.66067	-20.67492		5.519	1.481	46.543	0.263	6.490	12.231	0.310	27.360
CN011	17.74138	-20.63117		6.121	4.962	40.453	0.384	7.801	12.679	4.435	23.694
CN013	17.91003	-20.53983		10.005	13.001	56.547	0.895	8.391	21.808	0.642	51.618
CN014	17.93970	-20.51003		0.821	0.239	0.178	0.176	2.344	0.041	0.008	0.085
CN017	18.09777	-20.17375		1.979	0.572	0.191	0.307	5.097	0.028	0.115	0.169
CN021	18.10167	-19.65100		1.779	2.411	0.557	0.015	7.703	0.097	0.329	0.931

- The uppermost row in every data column should contain the *column names*. The samples which characterise each cell and source should be arranged in rows. Columns representing the properties (sample name, co-ordinates, heads, chemical concentrations etc.). It does not matter in which column the sample names are found exactly and where the first column with the chemical data starts. The location of the sample name column and the location of the first column with chemical data can be specified and later introduced into the MIG data processor (see ‘Program settings’). However, it is useful (set default) to have the column names in the first column and to have the *sub-matrix with chemical data* in one block (sub-matrix) that is not interrupted by other descriptive information not used for the modelling.
- The data file should contain one *column with sample names*. The sample names should be shorter than 16 characters (this limitation is caused by a limitation of the sample name length in the Fortran solver: **Multi.exe**). If these sample names contain more than 16 characters you will be warned during program execution to shorten them.
- The *matrix with chemical data* should be complete and should not contain null values, strings or empty cells. Please, remove any row or samples that do not contain a full complete analysis. However, MIG checks also whether the chemical data-set is complete and only offers samples for selection as cells or sources that contain meaning values: zero (real zero values) and above.

- It can be useful to include groundwater levels – if these are available. MIG performs an automatic check of flow directions being consistent with water levels. The location of the column with water levels can be configured within MIG.

In order to get an idea of how the data file should look like, an example file, called **data.xls** is installed in the MIG directory (see Figure above). This example file contains only the sample names, the x – y co-ordinates and the chemical data for the major elements (in mmol/l).

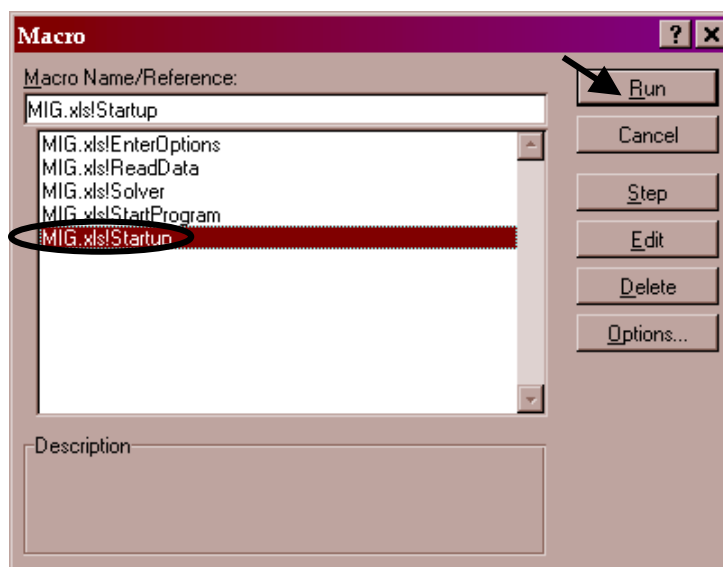
The screenshot shows a Microsoft Excel window titled 'Microsoft Excel - data.xls'. The spreadsheet has columns labeled A through J. Column A contains sample names, B and C contain coordinates (LONG and MLAT), D contains GWL, E contains Cammol, and F through J contain Mgmol values. A 'Windows' menu is open, showing two files: '1 data.xls' and '2 MIG.xls'. The 'Windows' menu also includes options like 'New Window', 'Arrange...', 'Hide', 'Unhide...', 'Split', and 'Freeze Panes'.

	A	B	C	D	E	F	G	H	I	J
1	NAME	LONG	MLAT	GWL	Cammol	Mgmol				
2	Rain				0.047	0.0			0.105	0.028
3	Storm				0.030	0.0			0.080	0.006
4	Soil				1.328	0.0			2.614	0.024
5	Calcrete				0.630	0.0			1.198	0.026
6	Dolomite				0.389	0.3			1.449	0.028
7	Spring				0.794	0.3			1.290	0.886
8	Sandstone				0.060	0.0			0.220	0.011
9	Flood				0.821	0.2			2.344	0.041
10	CN007	17.66820	-20.71190		4.000	1.958	35.494	0.235	7.490	9.733
11	CN008	17.68733	-20.81865		3.039	3.962	11.353	0.486	7.998	3.435
12	CN010	17.66067	-20.67492		5.519	1.481	46.543	0.263	6.490	12.231
13	CN011	17.74138	-20.63117		6.121	4.962	40.453	0.384	7.801	12.679
14	CN013	17.91003	-20.53983		10.005	13.001	56.547	0.895	8.391	21.808
15	CN014	17.93970	-20.51003		0.821	0.239	0.178	0.176	2.344	0.041
16	CN017	18.09777	-20.17375		1.979	0.572	0.191	0.307	5.097	0.028
17	CN021	18.10167	-19.65100		1.779	2.411	0.557	0.015	7.703	0.097
18	CN041	17.24038	-20.50590		0.060	0.091	0.074	0.059	0.220	0.011
19	CN042	17.33030	-20.42237		0.851	0.148	0.609	0.084	1.950	0.256

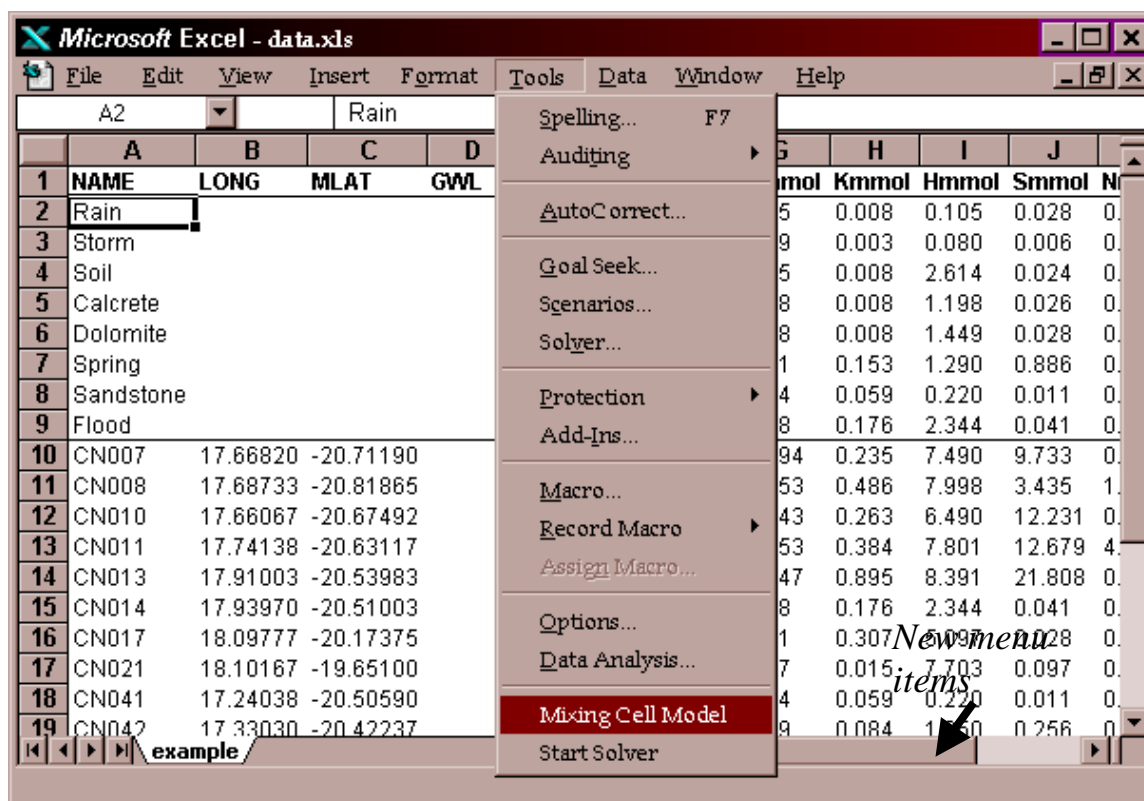
After opening and selecting the data file, in the menu 'File/Open' two files should be already loaded and listed in the menu 'Windows': **data.xls** and **Mig.xls** (see circle on the figure below). **Mig.xls** is loaded in the background.

### Adding menu items

In order to simplify the use of MIG, the program contains a macro that adds two menu elements to your Excel program. This step has to be executed only during the first use of MIG and after any re-installation of MIG or of Excel. In order to add the menu items press ALT+F8, select the macro **MIG.XLS!Startup** (circle) and press the button 'Run' (arrow).



In a case where the key combination ALT+F8 fails for any reason, the user may also reach this window by going to 'Tools/Macro/Macros'. After executing the macro, the user should see two extra menu items in the menu 'Tools'. These are 'Mixing cell model' and 'Start Solver'.



**Important:** When using MIG for the very first time, please define the path to the Solver as described below in the section 'Program settings' before pressing the button 'Start Solver'.

### Starting the MIG operation

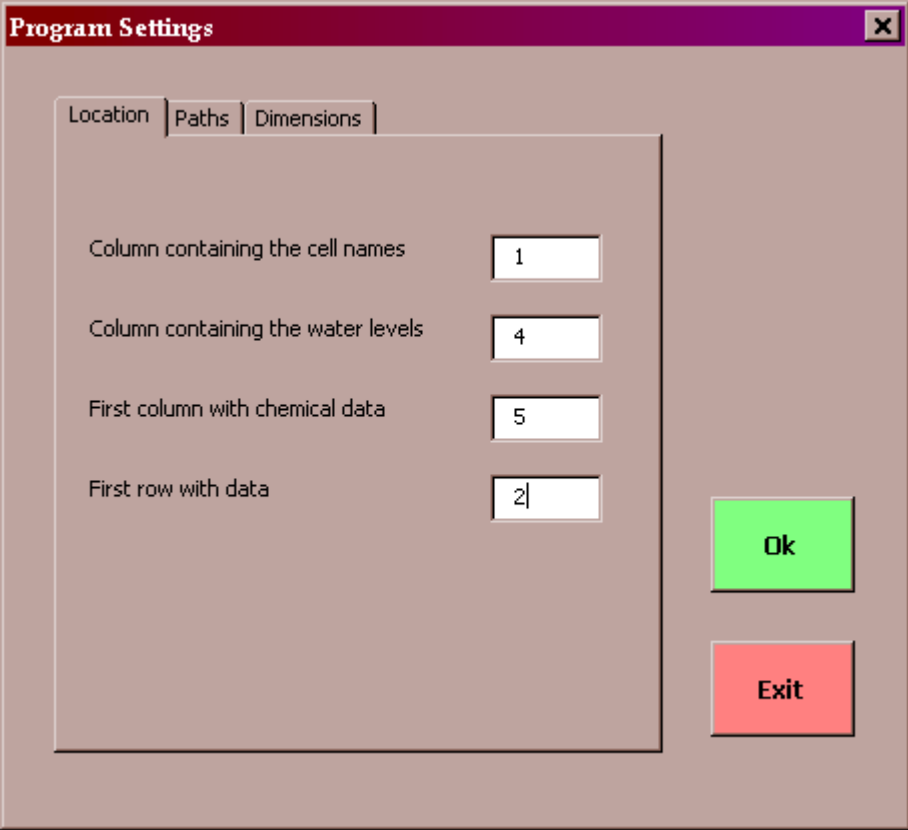
Now, the user can start MIG by clicking on 'Tools/Mixing Cell Model'. After clicking on this menu element, a window should appear with the caption 'Program settings'.

**Problems:** If you do not see the menu item 'Mixing Cell Model' in the 'Tools' menu than you need to go back to the point [Adding menu items](#) (see above) and execute the described steps. Alternatively, the user simply left out the data file, or the path to the data file has not properly established. In this case the user has to go back to the menu 'Window' select the desired data file or re-open it in case it has been closed. If a message indicating that another instance of mig.xls is already open, then re-execute the procedure described in [Add menu items](#) (ALT+F8, execute MIG.XLS!Startup).

### Program Settings

The first window, 'Program Settings', allows you to configure MIG and to define default values. It contains the option sheets 'Locations', 'Dimensions' and 'Paths'.

Please note that any changes that one makes in the program settings are kept and are made permanent if you save MIG at the end of the session.



The screenshot shows a 'Program Settings' dialog box with a title bar containing a close button. The dialog has three tabs: 'Location', 'Paths', and 'Dimensions'. The 'Location' tab is selected. Below the tabs are four input fields with labels: 'Column containing the cell names' (value: 1), 'Column containing the water levels' (value: 4), 'First column with chemical data' (value: 5), and 'First row with data' (value: 2). To the right of the input fields are two buttons: 'Ok' (green) and 'Exit' (red).

### *Locations*

In the sheet 'Locations' the structure of the data file is defined. The '*column containing the cell names*' (default = 1) option specifies in which column the well names are listed. These names are later used to identify the samples in the following configuration of the mixing cell

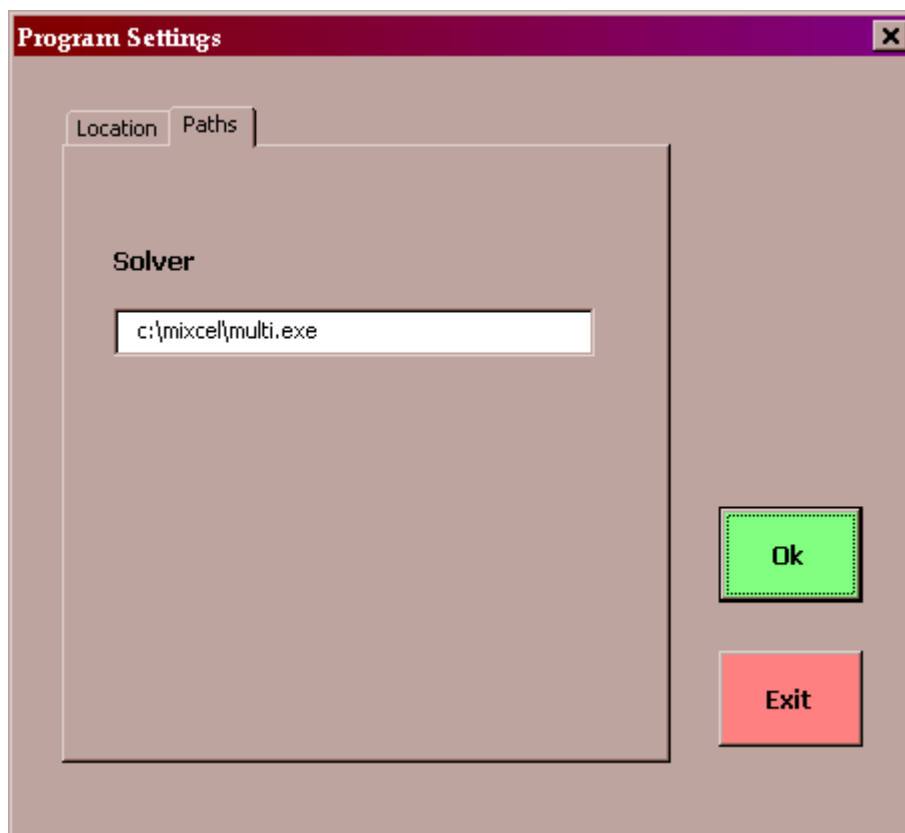
model structure. The '*column containing the water levels*' shows in which column the water levels are written. If this column is set to a column containing real water levels, an automatic check will be made during the selection of flow pattern (cell's connections), whether this flow connection is hydraulically possible. If both elements have real values for water levels (not null values) flows will only be allowed downward head gradients. If one or both of the elements do not contain water level data, this check will not be performed.

**Tip:** If you do not have water level data or if water levels are not reliable, select a column number of a column that is completely empty (for example 256 – Excel sheets have a maximum of 256 columns). This will not activate the water level checking routine.

The '*first column with chemical data*' indicates in which column the chemical data starts in the data file. The '*first row with data*' is the number of the first row containing chemical data beneath the column names. The default is 2.

### Paths

This option sheet contains the path name for the locations of the FORTRAN solver `Multi.exe`. If this path is not set correctly, the solver will not be called successfully by MIG. Please, check whether this path is set correctly. The default is `c:\mixcel\multi.exe`

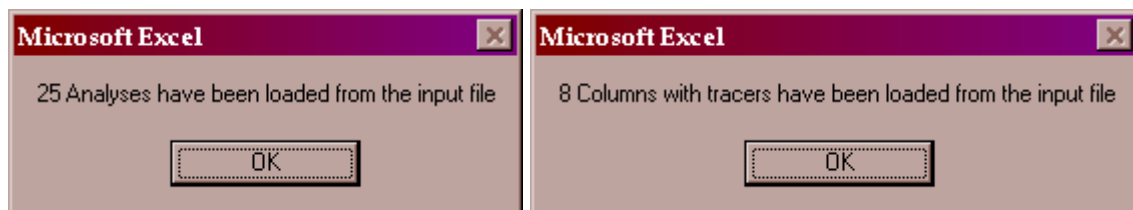


### *Dimensions*

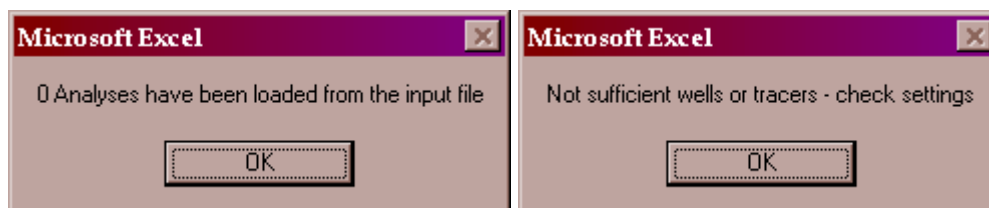
The third sheet with options in the ‘Program settings’ is hidden. Here, the maximum number of samples (default = 1024), tracers (default = 128), sources (default = 512) and inflows (default = 512) are selected. The default values are more than sufficient for natural and solvable problems. If you need to increase these values, the user should consult the programmer.

After all these settings have been completed the user can proceed by clicking ‘OK’. With ‘Exit’ you leave MIG (for re-start, just go to ‘Tools/Mixing Cell Model’). Now, a message appears indicating the number of loaded analyses and tracers. If everything is Ok, 25 analyses and 8 tracers from the example file should have been loaded. If the number of loaded analyses is zero, or if the number of loaded tracers is zero, MIG will inform the user that the number of cells and/or tracers is not sufficient and will abort. In this case start MIG again (‘Tools/Mixing Cell Model’) and check the settings in ‘Program settings/Location’ carefully.

*Program has loaded the analyses successfully.*



*In case of a problem the following messages will prompt. In this case the MIG program failed to load analyses or tracers and asks the user to check the settings in ‘Program settings/Locations’.*



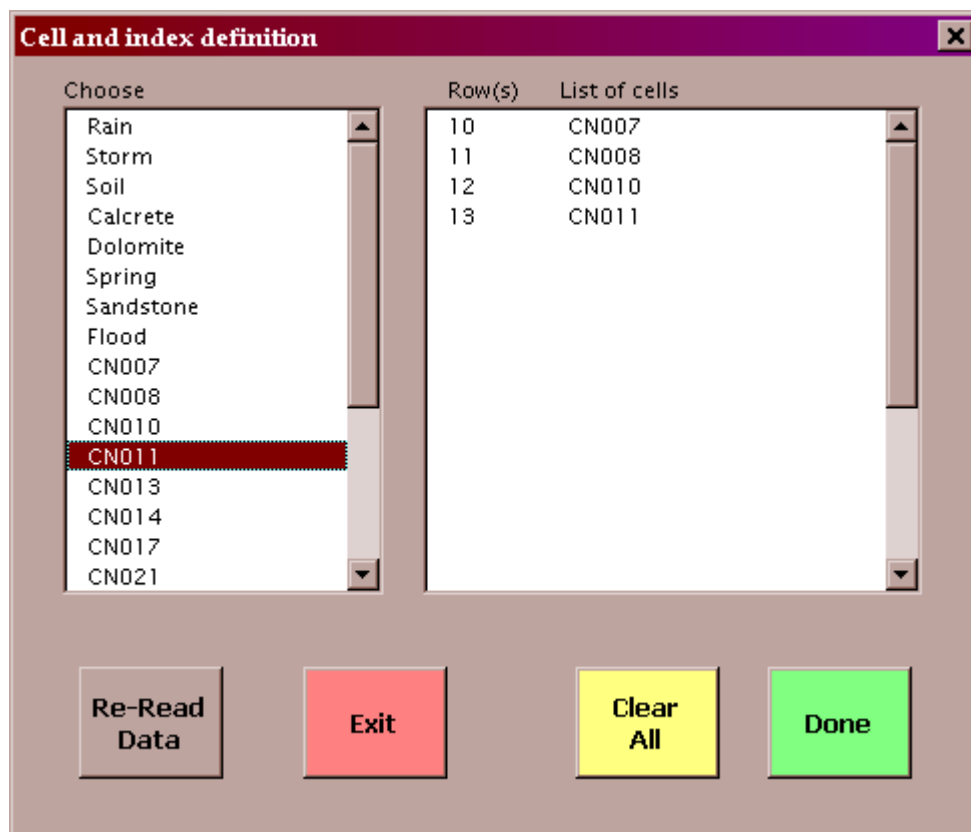
**Possible problems:** The program stops reading data as soon as it encounters an empty row. If this is the case, check the data file and delete the row with empty (not defined) concentration. If the loading still fails, try the standard format exactly as in the example file `data.xls`: Column names in the first row, sample names in the first column and tracers starting from column 5. Then use the default values:

<i>Column containing the well names</i>	<i>1</i>
<i>Column containing the water levels</i>	<i>4</i>
<i>First column with chemical data:</i>	<i>5</i>
<i>First row with data</i>	<i>2</i>

### Selection of cells

The next form that appears now is called '*cell and index definition*'. In this menu the user selects the cells that are used for the mixing cell model – sources will be selected in the next step. The list in the left window contains the sample names from the sample name column that was defined previously. By double-clicking on these sample names in the list, the collection of cells can be completed. It is recommended to prepare a schematic cell configuration for the flow pattern and than to choose the cells from upstream to downstream and to select the lowest cell as the last one. The 'Clear All' button can be used to completely clear the list of selections. With 'Re-Read Data' the user can go back to the form 'Parameter settings' and re-read the data. With 'Exit' bottom the 'MIG' is terminated. As you can see in the 'Window' list the file **mig.xls** is still loaded and MIG can easily be re-started by going to '**Tools/Mixing Cell Model**'. With '**Done**' this form is closed, all the selections are kept and saved and the next form is loaded.

In the following example as presented bellow, cells CN007, CN008, CN0010 and CN0011 were selected (right window).

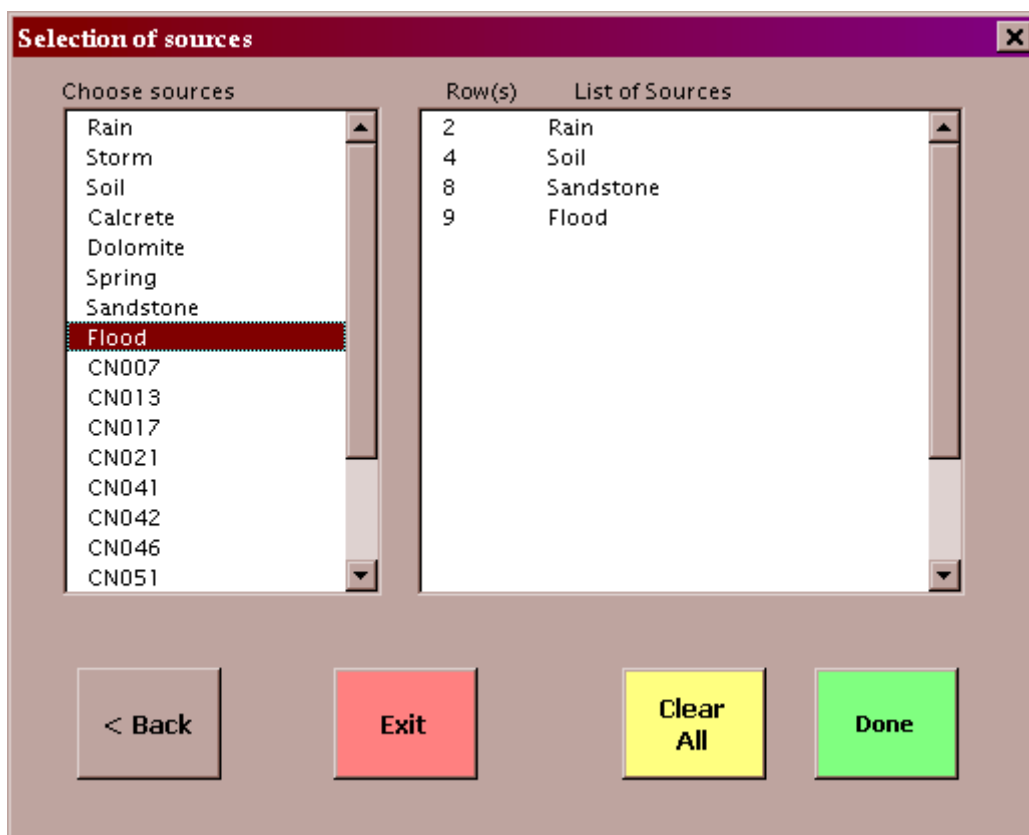


To the right hand a new list of selected cells is shown. It is composed of two columns. The first column lists the row number - this is the number of the row as in the data file. The

second column contains the sample name. A small message appears after pressing the 'Done' button, which indicates the number of selected cells.

### Select sources

The next menu is used for the selection of sources. As defined above, sources are flow components (clusters or single bore holes) that do not receive any other potential inflow but contribute to specific cell or cells. A source can be used as a potential contributor to more than one cell if hydrologically and hydrochemically justified. Sources can also be used to represent sub-systems for a simplification of the model. In the list to the left, cells that have been selected previously will not be listed again. From this list, all the sources that will be used for the definition of the mixing cell model structure must be selected. Choosing more sources than cells does not pose a problem. Sources can be omitted during the following definition of inflows. Again, the '**Clear All**' button can be used to completely clear the list of selected sources. With '<**Back**' the user can go back to the form '*cell and index definition*'. With '**Exit**' the 'Mixing cell model' is terminated. With '**Done**' this form is closed and all the selections are kept and saved and the next form is loaded. Again, a small message box indicates the number of selected sources.



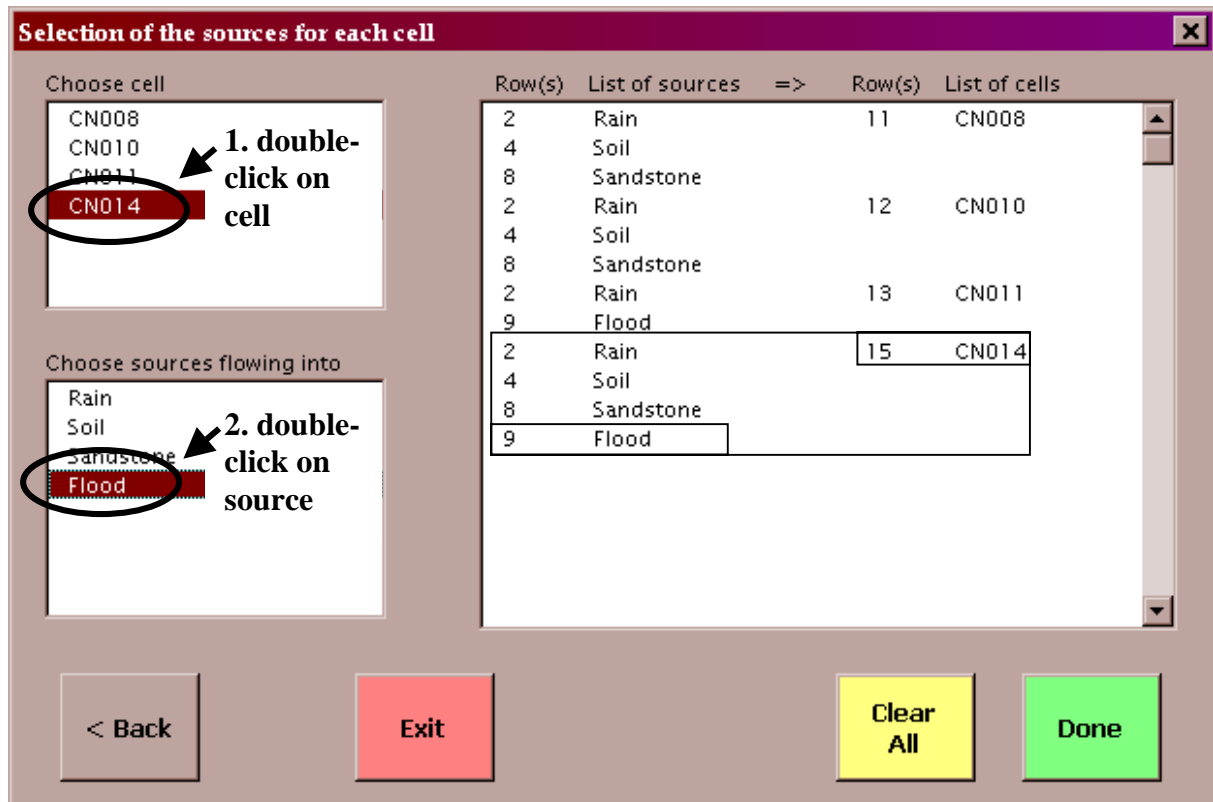
Choose sources	Row(s)	List of Sources
Rain	2	Rain
Storm	4	Soil
Soil	8	Sandstone
Calcrete	9	Flood
Dolomite		
Spring		
Sandstone		
<b>Flood</b>		
CN007		
CN013		
CN017		
CN021		
CN041		
CN042		
CN046		
CN051		

< Back      Exit      Clear All      Done



### Assigning inflows from sources to each cell

Now the user reaches the form on which the sources for each cell are defined and selected. For each cell the potential inflows are selected. This is done by “double-clicking” on a certain cell in the window to the upper left first. Then the user double-click on the source that feeds this cell in the window to the lower left. As a result, this flow connection will appear in the large result window to the right.



The right window displays four columns, two columns for the sources and two columns for the cells. For both the sources and cells, the row index (from the data file) and the sample name are listed. Of course several sources can be selected for one cell. Therefore, this procedure is repeated until all the required inflows from sources for a certain cell are listed. Now, the user proceeds to the next cell by double-click on the desired cell and then selecting the respective inflows from sources.

If a certain connection between source and cell exists already, the connection will not be accepted and a warning appears. Also, if the user has specified a column with water levels for sources and for cells and if both contain contradicting data, a warning might appear if this connection is hydraulically impossible. For avoiding this, go back to ‘Program settings’ and

specify an empty row for the column with water level data. However, this constraint might be very helpful for avoiding hydraulically impossible models!

Again, the ‘**Clear All**’ button can be used to completely clear the list of selected inflows. With ‘<**Back**’ the user can go back to the form ‘*selection of sources*’. With ‘**Exit**’ the ‘Mixing cell model’ is terminated. With ‘**Done**’ this form is closed, all the selections are kept and saved and the next form is loaded. A small message box indicates the number of flows from sources to cells.

### Select flows from cells to cells

In the next form the user is asked to specify the flows between cells. It is helpful and recommended for avoiding confusion (although not necessary for the correct solution of the problem) to choose the flow connections from the highest to the lowest potential.

**Definition of flows between cells**

Choose discharging cell

- CN008
- CN010
- CN011
- CN014

1. double-click on cell

Choose receiving cell

- CN008
- CN010
- CN011
- CN014

2. double-click on cell

Row(s)	Discharging	=>	Row(s)	Receiving cell
11	CN008		12	CN010
			13	CN011
			15	CN014

< Back      Exit      Clear All      Done

A warning will appear:

- if a connection is re-entered that exists already
- if a connection is entered that exists already in the opposite sense
- if water level data has been specified and does not allow this connection

As in the previous form for each cell the flows to other cells are selected. This is done by double-clicking on the discharging cell in the window to the upper left first. Then the user

double-clicks on the receiving cell in the window to the lower left. As a result, this flow connection will appear in the large result window to the right. For both cells, the row index (from the data file) and the sample name are listed. Therefore, this procedure is repeated until all the required flows between cells are listed.

The '**Clear All**' button can be used to completely clear the list of selected flows. With '<**Back**' the user can go to the previous form. With '**Exit**' the 'Mixing cell model' is terminated. With '**Done**' this form is closed, all the selections are kept and saved and the next form is loaded. A small message box indicates the number of flows from cells to cells. At this stage the flow connections have been defined, hence the structure of the model is ready.

### Abstraction rates

In the next form, the user can enter the abstraction rates of water (e.g. pumping rates). These can be pumping rates by which groundwater is abstracted from each cell before flowing into other cells according to its flow connections. For the last cell the abstraction rate corresponds to the total outflow of the system (the user is urged to use the same units for rate of pumping as for the rates of discharge).

Cellindex	Cellname	Abstraction/outflow
10	CN007	0
11	CN008	0
12	CN010	0.1
13	CN011	1

Change Rate: 0.1

Buttons: < Back, Exit, Done, Clear All

**Comment:** By default, the abstraction rates are set to 0 for all cells except for the last cell. The last cell has a default outflow rate of 1. These are normalised abstraction rates. Later, the normalisation is made by dividing the abstraction rate of each cell by the sum over all cells.

The default abstraction rates can be changed in this form. The user needs to click on the cell for which he wants to make the modification first. Then, he clicks on the text-field '**Change Rate**' and enters a new value. When the **ENTER** key is pressed, the new value will appear in the list to the left. The total sum of abstraction/outflow is now calculated automatically. Here, the previous remark is re-iterated that the cells should be arranged according to the cascade of flows from higher water levels to lower. The outflow rate of the lowest cell corresponds to the output of the system. It needs to be larger than zero otherwise the whole system has no outflow and – due to a simple mass balance – all flows will be zero as well.

With '<**Back**' the user can go back to the previous form. With '**Exit**' the 'Mixing cell model' is terminated. With '**Done**' this form is closed, all the selections are kept and saved and the next form is loaded. Now the form for the selection of tracers is shown.

### Selection of tracers

The tracers that are found in the matrix starting from the 'first column with chemical data' are displayed in the left window. The tracers that should be used for the mixing cell model can be selected by double-clicking on the names (these are the same names of constituents as appears in the first row of the data set).

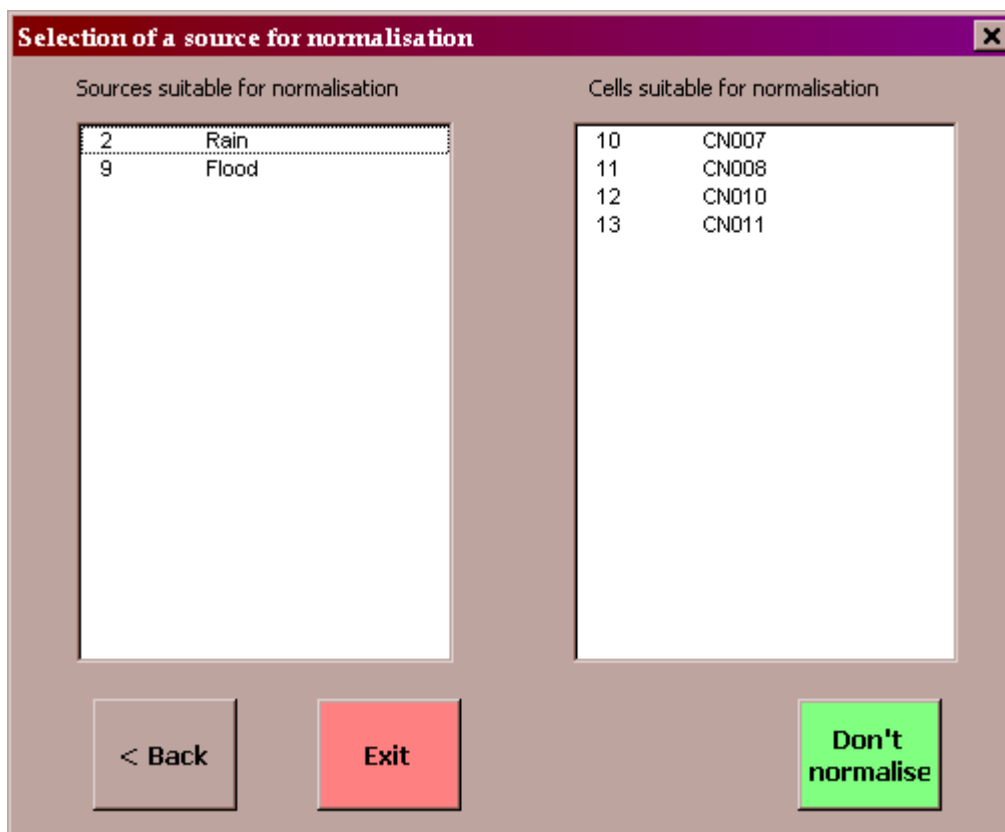
The dialog box titled "Selection of tracers" contains the following elements:

- Available Tracers:** A list box containing Cammol, Mgmmol, **Nammol** (highlighted), Kmmol, Hmmol, Smmol, Nmmol, and Clmmol.
- Selected Tracers Table:**

Index	Tracer	Weight
5	Cammol	1
6	Mgmmol	1
7	Nammol	1
- Buttons:** "< Back" (grey), "Exit" (red), "Clear All" (yellow), and "Done" (green).

The program automatically prevents the user from choosing one tracer twice. In the right result window the selected tracers are shown with the index, the name and the default weight. At the moment the default weight (given for the assigned level of conservancy) can not be modified here. With the '**Clear All**' function the list of selected tracers can be reset. After the selection is made, the next window can be called with the '**Done**' button. At least one tracer needs to be selected here, otherwise the user can not proceed. A small message window indicates the number of selections.

The next and last form allows the selection of a source or a cell for the normalisation of the chemical data. The program checks automatically, which sources and cells are suitable for normalisation and those are listed in the following window.



Sources suitable for normalisation		Cells suitable for normalisation	
2	Rain	10	CN007
9	Flood	11	CN008
		12	CN010
		13	CN011

If the user wants to normalise, a double-click on the selected source/cell is needed. A prompt will appear, asking for confirmation. If the user does not want any normalisation to be performed he can select 'Don't normalise'.

Finally, the last toolbar before running appears with several buttons: With '< **Back**' you can go back to the previous form for changes.



With ‘**Build Input for Wolff**’ an input file is generated using all the settings that were made in the previous forms. Before the file is produced, the user is asked to enter a descriptive name for the model. Now, the input file is generated and formatted as an Excel table. It is helpful, however, to adjust the table name to the description of the run by double-clicking on the table name tag (circle) and entering a table name.

	A	B	C	D	E	F	G	H	I
1	Namibia								
2	5/28/99								
3		6	7	2	1				
4		4	2						
5		1	1						
6		-2							
7		1							
8		100							
9	Pumpage		0	100					
10	Weights		1	1	1	1	1	1	1
11	Name	Cammol	Mgmmol	Nammol	Kmmol	Hmmol	Smmol	Clmmol	
12		314	2.04824	2.42791	3.56692	1.81595	7.15443	1.14509	4.62597
13		583	0.52954	0.2298	0.47849	0.17904	1.47885	0.04164	0.56414
14		870	1.76848	0.26977	0.47849	0.23019	3.29743	0.16656	0.70518
15		1362	2.91749	2.46788	0.73948	0.07673	10.11213	0.38517	0.59235
16		623	0.14987	0.07993	0.2175	0.25577	0.59953	0.04164	0.16924
17		1452	2.24807	3.08734	0.65249	0.07673	10.55179	0.18738	0.25386
18		772	2.22808	1.06908	3.65392	0.81846	6.59487	0.73911	3.13099
19		852	1.24893	1.2789	1.52247	0.17904	5.6556	0.23943	0.31028
20	NORMAL								

The next step is to save this input file by pressing the button ‘**Save Input File**’. You need to enter a name for this run. This operation can not be cancelled – a name needs to be given. This operation causes an ASCII file to be written that can now be used with the solver **Multi.exe**. If the path to the solver is set correctly, the solver can now be started by pressing the button ‘**Run Wolff Algorithm**’.

**Potential problem:** The program might not execute the solver – probably the path is not correct. Identify the location of the file **multi.exe**. It should be contained in **c:\mixcel** (or in the alternative directory that the user have specified when installing the program). Restart the ‘**Mixing Cell Model**’ and adjust the path on the second sheet of ‘**Program settings/Path**’.

The solver now prompts for the name of an input file and for the name of an output file – If the set up of the flow pattern is backed also by water and chemical balance it will also produce a result.

## **2.5 Terminating MIG**

Before leaving save mig.xls if you want to keep the program settings for further attempts and alternative flow configurations. Be careful when saving the data file. The name needs to be reset to the original name and the file type specified as Excel file. Choose ‘File/Save as...’ and select ‘Excel file’, specify a name and save the file.





Annex B

B-1

name	No	dec. longitude	E	dec. latitude	S	Temp.	depth	level	error	pH	ec	← mmol/l			→						log Sr <sup>2+</sup> :Ca <sup>2+</sup>			
												Ca <sup>2+</sup>	Mg <sup>2+</sup>	Na <sup>+</sup>	K <sup>+</sup>	HCO <sub>3</sub> <sup>-</sup>	SO <sub>4</sub> <sup>2-</sup>	NO <sub>3</sub> <sup>-</sup>	Cl <sup>-</sup>	Si		F	Sp <sup>2+</sup>	Ca <sup>2+</sup> :Mg <sup>2+</sup>
W41Y800	1	18.05044		-20.21176			114	63	2.0	7.1	25640	29.2	4.7	234.9	2.8	5.6	17.2	0.0	253.9	0.47	0.09	0.31	6.2	-2.0
W7Y821	2	17.74200		-20.41991			110	33	1.3	7.3	19110	15.2	7.0	157.5	2.4	6.5	13.0	0.0	167.0	0.18	0.15	0.25	2.2	-1.8
W12Y865	3	18.30456		-20.82443			86	30	-1.9	6.9	18210	23.2	7.1	127.9	1.8	3.6	9.4	0.0	176.0	0.30	0.12	0.41	3.3	-1.8
W4Y801	4	18.15907		-20.27421			59	37	-0.7	7.2	15040	14.7	3.4	119.6	3.3	3.6	11.5	0.1	135.4	0.15	0.06	0.41	4.4	-1.6
W4Y802	5	18.19302		-20.29321			90	63	-1.9	6.9	12540	9.1	6.3	98.3	1.7	7.7	9.5	0.9	108.3	0.37	0.03	0.18	1.4	-1.7
W12Y863	6	18.18235		-20.88326			112	19	2.1	7.5	13690	16.7	1.4	106.6	1.7	1.8	9.8	0.0	117.3	0.37	0.15	0.25	11.6	-1.8
W5Y805	7	17.83511		-20.36471			44	0.4	0.4	7.0	6730	3.1	4.8	69.6	1.5	62.2	2.3	0.3	19.2	0.32	0.06	0.04	0.6	-1.9
W5Y810	8	17.90204		-20.32036			87	48	0.8	7.8	7640	0.3	7.8	93.1	2.9	88.8	3.9	0.0	13.8	0.10	0.04	0.00	0.0	-2.4
W4Y797	9	17.93792		-20.31041			113	24	-1.1	7.0	11810	6.2	17.1	80.9	2.3	31.0	9.8	0.2	82.4	0.53	0.01	0.29	0.4	-1.3
W11Y856	10	18.12221		-20.11765			56	41	1.9	8.3	8850	4.5	7.7	69.6	1.4	15.2	5.8	0.7	64.3	0.11	0.07	0.11	0.6	-1.6
W11Y857	11	18.06305		-20.90679			10		-1.6	7.4	10600	3.8	8.1	87.9	0.6	5.9	22.9	0.0	64.3	0.17	0.03	0.11	0.5	-1.5
D423Y686	12	18.16489		-20.82805			99	37	-1.4	7.3	7840	1.5	6.1	69.6	0.5	10.9	16.2	0.0	44.6	0.23	0.04	0.04	0.3	-1.6
W10Y854	13	17.57486		-20.80163			64	58	1.8	7.3	8560	2.6	6.7	68.5	2.5	15.5	10.0	2.9	48.0	0.38	0.03	0.08	0.4	-1.5
W10Y855	14	17.68828		-20.80905			84	27	2.2	7.1	8500	8.6	11.7	59.2	1.1	8.6	18.7	0.5	50.2	0.63	0.05	0.17	0.7	-1.7
B987Y3389	15	18.64971		-19.54801					0.7	7.3	7420	4.4	7.4	52.6	0.7	9.7	11.5	0.2	42.9	0.52	0.06	0.04	0.6	-2.1
D338Y2956	16	17.56814		-20.46377			76		-1.2	7.2	7730	18.7	4.7	27.4	0.6	3.4	4.5	2.4	62.1	0.45	0.02	0.08	4.0	-2.4
D219W1872	17	17.26296		-21.10054				40	-0.9	7.0	7500	11.8	18.2	33.8	1.4	3.6	14.3	1.4	63.4	1.10	0.01	0.19	0.6	-1.8
D218W1886	18	17.30038		-21.05525			29	9	-1.9	7.5	6800	8.3	16.2	35.4	1.9	6.8	16.1	1.9	48.7	1.55	0.02	0.11	0.5	-1.9
W10Y853	19	17.73521		-20.81629			67	18	-0.6	6.9	11040	20.1	17.7	42.2	0.9	6.1	6.0	1.7	100.7	0.35	0.04	0.36	1.1	-1.7
B973Y3284	20	18.33560		-20.88054					0.8	7.0	10160	15.4	11.3	58.9	0.8	4.8	9.4	0.0	88.0	0.55	0.09	0.20	1.4	-1.9
B973Y3283	21	17.74376		-20.38496					1.2	7.8	8750	12.2	1.7	64.9	1.6	2.0	5.1	0.0	79.8	0.70	0.15	0.03	7.0	-2.6
B972Y3283	22	17.67370		-20.38768					0.4	7.6	10000	13.1	1.7	69.5	1.6	1.9	5.7	0.0	86.6	0.77	0.14	0.04	7.6	-2.6
W7Y822	23	17.73812		-20.46335					-2.3	6.4	3790	10.4	10.1	5.7	0.6	13.4	3.9	0.1	28.2	0.58	0.07	0.08	1.0	-2.1
B805Y4659	24	17.64012		-19.64855			165	24	1.5	7.0	5350	13.0	14.8	4.1	0.0	11.9	1.6	20.3	22.6	0.28	0.02	0.00	0.9	-3.5
B199Y3061	25	18.25240		-19.76812					1.7	7.3	5520	8.2	17.3	9.9	1.0	11.7	2.4	28.6	14.7	0.48	0.04	0.01	0.5	-2.7
B199Y3059	26	18.24952		-19.76359					0.8	7.6	5080	6.9	12.7	10.5	4.3	9.6	2.9	23.1	14.7	0.50	0.03	0.01	0.5	-2.8
B198Y3336	27	18.26008		-19.69656			25		-0.1	7.1	3820	3.4	13.8	6.2	0.0	13.5	0.4	8.1	18.3	0.52	0.02	0.01	0.2	-2.4
B198Y3335	28	18.25720		-19.70109			25		1.8	7.8	4290	3.0	14.6	10.2	0.1	13.5	0.6	10.6	18.6	0.83	0.02	0.01	0.2	-2.3
W9Y844	29	17.93501		-20.50688			87	40	-2.4	7.9	5300	8.7	9.3	20.4	0.1	1.8	11.2	1.9	33.0	0.65	0.05	0.05	0.9	-2.2
D227Y1110	30	17.59789		-21.20471			67	41	1.4	7.4	4160	8.0	10.3	7.4	0.8	6.1	2.9	0.4	31.3	1.12	0.03	0.07	0.8	-2.1
D216W3592	31	17.33301		-20.98007			91	82	-1.4	7.0	5800	9.5	12.0	13.0	0.6	6.6	7.2	0.7	36.8	1.63	0.03	0.12	0.8	-1.9
B198Y3337	32	18.28871		-19.71920			25		0.1	7.3	5560	3.6	18.3	3.0	0.0	14.7	0.6	9.4	31.6	0.43	0.03	0.02	0.2	-2.3
B1973Y3429	33	18.21689		-19.67029			30	18	0.0	7.2	5650	6.7	13.8	18.5	0.8	11.0	4.4	14.3	26.2	0.37	0.02	0.01	0.5	-2.7
D256Y1142	34	17.68138		-21.11232			43	21	0.4	7.5	5550	8.4	10.3	16.5	0.5	5.9	3.3	16.0	25.4	1.05	0.04	0.06	0.8	-2.2
B179Y3074	35	18.11228		-19.84420					1.0	7.7	5080	5.5	11.1	16.3	2.8	8.0	3.1	11.1	26.0	0.33	0.03	0.01	0.5	-2.7
W5Y806	36	18.03298		-20.37647			73	31	0.2	6.9	6070	6.6	8.4	42.2	1.1	38.8	2.9	0.2	28.0	0.77	0.02	0.05	0.8	-2.1
D393Y671	37	17.47409		-20.81612					2.2	8.3	6420	0.4	0.7	64.4	0.2	23.6	6.8	0.5	26.0	0.53	0.15	0.01	0.6	-1.8
D423Y680	38	17.49136		-20.74094			150	61	-1.5	7.8	6100	3.0	2.9	49.0	0.5	18.0	3.9	0.1	37.2	0.62	0.15	0.04	1.0	-1.8
D423Y682	39	17.49520		-20.79710			116	40	1.4	7.3	5670	3.5	4.2	47.4	0.3	15.6	12.0	0.2	21.4	1.07	0.03	0.03	0.9	-2.1
W13Y871	40	18.35694		-21.06968			44	30	1.7	7.1	5520	3.3	3.6	42.6	0.4	7.7	10.8	0.3	25.3	0.48	0.10	0.05	0.9	-1.8
W13Y870	41	18.32493		-21.03258			39	15	-0.3	7.8	5520	3.0	1.8	46.8	0.3	7.5	9.4	0.2	30.5	0.45	0.17	0.04	1.6	-1.9
D423Y679	42	17.45969		-20.74004			148	67	1.7	7.5	5250	2.0	4.5	40.5	0.5	11.7	5.7	0.2	28.8	0.58	0.09	0.08	0.4	-1.4
D238Y695	43	17.50576		-20.88225					-1.1	7.5	5030	1.7	4.4	38.5	0.7	8.8	6.6	2.6	27.9	0.48	0.04	0.06	0.4	-1.4
W7Y823	44	17.65082		-20.48597			96	78	2.3	8.0	2490	0.2	0.5	25.2	0.2	14.5	1.1	0.3	8.5	0.28	0.16	0.01	0.5	-1.5
W6Y816	45	18.62367		-19.96380			134	87	-0.4	7.8	2610	0.4	0.7	24.4	1.0	13.6	4.0	1.3	4.9	0.25	0.04	0.01	0.7	-1.8
J240W2023	46	16.92802		-21.33786			24	1.4	8.6	6.6	2870	0.7	1.8	24.6	0.8	12.0	5.2	0.2	6.9	1.05	0.11	0.01	0.4	-2.0
D423Y684	47	17.49712		-20.80254			30	15	1.6	8.3	3060	0.8	0.9	27.0	0.1	17.6	4.2	0.0	3.5	1.03	0.06	0.01	0.8	-2.0
D103W2306	48	16.64587		-21.05797			101	64	-1.2	8.1	2510	0.5	0.7	26.5	0.9	20.9	1.8	1.3	4.5	1.07	0.27	0.01	0.7	-1.7
W2Y782	49	18.55674		-19.67240			260	17	1.3	6.9	3080	1.4	1.5	28.9	1.4	22.6	0.9	0.1	10.7	0.30	0.03	0.01	1.0	-2.1
W7Y824	50	17.64016		-20.47511			71	41	0.6	8.2	3360	0.8	1.0	31.8	0.2	16.6	3.7	0.2	10.7	0.38	0.21	0.01	0.9	-1.8
W1Y768	51	18.66149		-19.55385			45	5	0.8	7.3	4070	1.6	3.5	34.4	0.2	17.1	7.3	0.5	11.8	0.70	0.02	0.02	0.5	-2.0
D386W3599	52	17.37812		-20.92391					0.7	7.6	3900	1.8	3.6	33.5	0.6	22.4	5.6	0.5	10.2	0.47	0.07	0.02	0.5	-2.0
D196W1837	53	16.94722		-21.25272			91	30	0.0	7.9	3800	0.9	1.8	43.3	0.4	18.8	7.3	0.9	14.8	0.57	0.11	0.01	0.5	-1.9
B233Y3376	54	18.52783		-19.62681			76	20	2.3	7.5	4860	1.3	2.5	42.6	0.1	20.0	2.7	14.3	8.2	0.73	0.10	0.01	0.5	-2.2
W6Y812	55	18.30747		-20.29864			109	78	-0.9	6.7	5560	8.4	9.5	27.0	0.7	20.4	4.6	0.1	35.0	1.15	0.02	0.08	0.9	-2.0
W5Y807	56	18.03298		-20.38190					37	-0.1	6.7	4530	7.2	5.7	23.9	0.5	13.2	4.7	0.1	27.6	0.65	0.01	0.3	-2.5
B174Y3322	57	18.00864		-19.83786			91	41	1.6	7.1	5180	6.2	10.3	23.9	1.1	17.1	3.9	11.7	19.7	0.52	0.04	0.03	0.6	-2.3
B163Y3003	58	17.																						

name	No	dec. longitude	E	dec. latitude	S	Temp.	depth	level	error	pH	ec	←		→													log
												Ca <sup>2+</sup>	Mg <sup>2+</sup>	Na <sup>+</sup>	K <sup>+</sup>	HCO <sub>3</sub> <sup>-</sup>	SO <sub>4</sub> <sup>2-</sup>	NO <sub>3</sub> <sup>-</sup>	Cl <sup>-</sup>	Si	F	SP <sup>2+</sup>	Ca <sup>2+</sup> :Mg <sup>2+</sup>	SP <sup>2+</sup> :Ca <sup>2+</sup>			
D336Y2954	61	17.49136		-20.45290			85		0.6	7.9	4420	6.4	1.0	28.7	0.4	2.4	3.5	0.1	33.8	0.37	0.06	0.08	0.08	6.4	-1.9		
W12/Y864	62	18.25994		-20.83348			91	36	-1.1	7.8	4640	5.8	0.7	33.5	0.9	8.0	2.5	0.0	35.5	0.90	0.07	0.08	0.08	8.3	-1.8		
D202/W1858	63	17.09117		-21.24366			79	34	1.1	7.2	4150	4.0	5.2	30.4	1.2	8.2	4.9	0.4	30.5	0.82	0.01	0.05	0.05	0.8	-1.9		
B149/Y5504	64	17.64395		-19.93659					0.4	7.7	4490	3.8	3.4	28.7	0.4	8.2	0.4	0.6	33.8	0.50	0.02	0.10	0.10	1.1	-1.6		
D437/Y710	65	17.68714		-20.95199			37	9	-1.5	7.4	4100	3.9	7.3	25.4	0.7	9.1	8.5	0.8	22.8	0.00	0.06	0.05	0.05	0.5	-1.9		
D438/Y720	66	17.83301		-20.89874					0.2	7.5	4100	4.5	7.2	23.3	0.7	5.8	9.4	0.2	22.6	0.83	0.05	0.05	0.05	0.6	-2.0		
D435/Y705	67	17.65355		-20.87591					-1.8	7.7	3890	3.7	8.1	21.5	0.6	8.1	11.2	2.1	20.0	1.02	0.08	0.05	0.05	0.5	-1.8		
D434/Y700	69	17.67274		-20.85145			76		1.0	8.0	4710	4.1	7.4	29.8	0.9	8.1	11.2	2.1	20.0	1.02	0.08	0.05	0.05	0.6	-1.8		
J243/1/W2020	70	16.85029		-21.28623		29.0			1.8	7.8	4300	0.9	3.4	35.1	0.7	8.8	6.5	0.3	20.5	1.08	0.25	0.02	0.03	0.3	-1.7		
D264/Y651	71	17.81958		-21.08062			27	9	2.1	7.5	4790	2.4	4.8	37.0	0.8	8.9	9.5	1.2	20.9	1.36	0.21	0.04	0.05	0.5	-1.8		
D192/W1833	72	16.86564		-21.26359		40.0			1.6	7.8	3150	1.3	0.4	33.5	1.2	6.9	5.7	0.1	18.1	0.92	0.39	0.01	2.9	-2.1			
B972/Y3282	73	17.67466		-20.36141			165		1.4	7.9	2700	4.2	2.1	18.6	0.4	5.0	2.0	0.0	21.7	0.87	0.08	0.05	1.9	-1.9			
D336Y2953	74	17.46633		-20.51721					0.2	7.6	2760	2.4	0.4	20.2	0.3	1.4	2.9	0.0	18.9	0.37	0.15	0.03	5.4	-1.9			
B345/Y2960	75	17.60653		-20.33152					1.9	8.0	3200	1.6	0.5	23.9	0.2	2.1	2.2	0.1	20.6	0.25	0.15	0.03	2.9	-1.7			
W12/Y868	76	18.24345		-21.02262					-0.5	7.3	3200	1.5	1.6	26.8	0.3	8.7	3.0	0.1	18.6	0.50	0.21	0.03	1.0	-1.6			
D264/Y653	77	17.81958		-21.09420			65	15	1.3	7.5	4070	2.0	3.2	29.6	0.7	9.4	6.5	1.7	15.5	1.12	0.22	0.03	0.6	-1.9			
D423/Y683	78	17.51536		-20.78533			107	67	2.0	7.4	3210	2.3	2.9	24.4	0.2	10.3	4.7	0.6	13.3	0.70	0.02	0.02	0.8	-2.0			
D264/Y652	79	17.83205		-21.08786			51	9	2.0	7.5	3350	1.9	2.6	25.2	0.6	8.5	5.8	0.5	12.7	0.97	0.21	0.02	0.7	-1.9			
B980/Y3286	80	17.81574		-20.32246					1.7	7.9	2700	1.7	1.9	23.1	0.5	11.2	1.7	0.5	14.6	0.53	0.05	0.03	0.9	-1.8			
B139/Y3775	81	17.40307		-20.03170			63		-1.7	7.4	3190	3.7	2.0	21.7	0.5	10.8	2.6	0.0	18.9	0.60	0.13	0.06	1.9	-1.8			
W12/Y867	82	18.25218		-20.98914			52	7	-0.9	7.7	1990	1.7	1.3	14.8	0.3	9.1	1.3	0.2	9.3	0.90	0.25	0.04	1.3	-1.7			
W11/Y855	83	17.86645		-20.84163			37	23	1.6	7.4	2100	1.3	2.2	15.1	0.3	9.5	2.3	0.2	7.3	1.03	0.12	0.02	0.6	-1.8			
J137/Y1163	84	17.74184		-21.37319					0.6	-0.9	8.3	2580	0.9	3.6	15.9	0.8	9.4	2.2	3.5	8.7	1.17	0.15	0.02	0.3	-1.7		
D391/Y677	85	17.40307		-20.71014			125	70	-2.1	8.4	1820	0.4	0.5	15.8	0.2	9.5	1.5	0.0	6.1	0.25	0.08	0.01	0.8	-1.7			
D383/W1663	86	17.21305		-20.72736					-0.4	-0.6	8.1	1530	0.4	0.5	15.3	0.2	7.8	0.7	0.4	7.6	0.85	0.21	0.01	0.7	-1.8		
D390/W3609	87	17.32246		-20.68841					-0.4	7.9	1750	1.2	0.9	13.0	0.3	7.0	1.2	0.1	7.9	0.85	0.32	0.01	1.3	-2.1			
D383/W1662	88	17.21401		-20.75272					1.4	7.3	1800	1.9	1.4	13.4	0.4	8.5	1.9	0.0	7.3	0.67	0.28	0.02	1.3	-2.0			
D375/W2183	89	17.84069		-21.21105			33	5	0.9	8.2	2020	1.5	2.0	13.7	0.7	7.8	2.6	0.7	7.4	0.92	0.08	0.01	0.7	-2.1			
W13/Y869	90	17.85605		-21.30072					1.2	7.9	2250	1.5	1.9	15.7	1.0	7.4	4.2	0.4	6.4	1.12	0.19	0.02	0.8	-2.0			
D436/Y717	91	18.30359		-20.99276			78	14	0.3	7.9	2150	2.7	2.3	12.9	0.3	9.3	3.3	0.1	6.9	0.58	0.06	0.03	1.2	-2.0			
D436/Y717	92	17.78407		-20.88043					1.8	7.6	2100	1.9	2.7	14.0	0.5	8.6	3.1	0.5	7.6	1.12	0.11	0.02	0.4	-1.8			
W8/Y835	94	17.77401		-20.63439			132		2.0	7.3	2480	1.7	4.5	15.8	0.7	13.0	3.0	0.6	7.9	0.85	0.11	0.03	0.4	-1.8			
W11/Y775	95	18.61591		-19.57014					0.7	7.3	2750	3.1	3.1	17.0	0.1	12.0	1.0	10.3	4.5	1.00	0.05	0.01	1.0	-2.4			
D377/Y1030	96	17.47601		-20.90580					-0.3	7.8	2070	0.8	1.6	17.7	0.5	10.4	3.2	0.7	5.6	0.78	0.09	0.02	0.5	-1.6			
D3761/W2173	97	17.91939		-21.19475			24	3	0.5	8.2	2600	1.9	1.7	18.2	1.4	9.1	3.5	0.7	9.3	1.68	0.27	0.02	1.1	-2.0			
D216/W3593	98	17.33973		-20.99728			47	21	-2.1	7.5	2850	0.9	1.7	18.7	0.5	10.1	3.6	0.0	8.0	1.08	0.11	0.01	0.5	-2.0			
D201/W1855	99	17.10940		-21.17210			85	24	-0.1	7.3	1950	0.9	0.4	20.0	0.2	1.7	8.4	0.0	4.3	0.43	0.07	0.01	2.2	-2.1			
W11/Y858	100	18.10572		-20.82896			110	24	-0.6	7.1	3090	3.1	3.0	21.3	0.4	10.9	5.5	0.6	11.6	0.72	0.07	0.04	1.0	-1.9			
J239/Y2146	101	16.94242		-21.46105			68	57	1.5	7.7	3280	1.9	6.4	20.0	0.5	12.1	7.0	0.1	9.6	1.03	0.05	0.03	0.3	-1.8			
D443/Y684	102	17.84165		-20.93297			61	24	0.4	7.4	2720	2.7	3.4	16.5	0.5	7.2	4.4	0.3	12.8	0.98	0.06	0.03	0.8	-2.0			
D438/Y721	103	17.85317		-20.90036					0.1	7.9	2870	2.9	4.5	16.3	0.5	6.6	5.5	0.2	13.8	0.83	0.05	0.03	0.6	-1.9			
D435/Y703	104	17.70154		-20.87681					-1.1	7.9	2510	2.5	3.9	14.9	0.5	7.6	4.9	0.8	10.7	1.07	0.08	0.03	0.6	-1.9			
D435/Y701	105	17.65067		-20.88134					1.3	8.1	2780	2.4	4.9	16.1	0.5	7.8	4.7	0.9	12.1	1.00	0.08	0.04	0.5	-1.8			
D437/Y711	106	17.69578		-20.95652					0.4	7.5	2770	2.7	5.1	14.8	0.6	7.2	5.2	0.5	12.7	1.05	0.08	0.04	0.5	-1.9			
D261/Y725	107	17.66891		-20.97826			61	23	1.0	7.6	2660	2.8	4.8	15.0	0.5	7.8	4.9	0.5	11.8	1.18	0.06	0.04	0.6	-1.9			
D267/Y622	108	17.89635		-21.13949			61	12	0.3	7.4	2660	2.5	2.7	19.4	0.7	7.8	4.8	0.4	12.4	1.30	0.12	0.02	1.0	-2.0			
W4/Y799	109	18.09505		-20.20452			131	61	1.0	7.4	2620	2.4	3.0	18.2	0.5	7.4	5.0	0.0	11.6	1.07	0.04	0.03	0.8	-1.9			
D253/Y1147	110	17.71305		-21.24638					-1.8	7.8	2890	2.1	2.4	18.1	0.3	7.4	4.4	0.5	11.8	1.13	0.08	0.01	0.9	-2.2			
D194/W1602	111	16.89155		-21.10960			73	60	0.1	7.7	2400	1.7	1.6	19.6	0.8	6.4	4.2	0.2	11.6	1.15	0.32	0.01	1.1	-2.1			
W7/Y826	112	17.70441		-20.54389			125	85	-0.7	7.4	2430	2.2	3.5	15.1	0.5	8.0	4.7	1.0	9.2	0.92	0.07	0.03	0.6	-1.9			
D437/Y712	113	17.70441		-20.93388			37	9	1.6	7.7	2300	2.0	3.6	15.1	0.6	8.5	4.4	0.6	8.2	1.05	0.11	0.02	0.6	-1.9			
D437/Y706	114	17.70729		-20.91938			31	9	1.9	7.9	2560	2.2	3.9	17.4	0.4	6.6	5.5	0.5	9.2	1.05	0.10	0.03	0.6	-1.9			
D194/W1601	115	16.91651		-21.12772			108	60	1.6	7.5	2050	1.3	0.8	17.6	0.2	4.2	3.6	0.1	9.6	0.60	0.33	0.01	1.5	-2.0			
D267/Y628	116	17.82534		-21.12138			61	18	-0.1	7.8	2370	1.6	2.2	17.3	0.4	8.0	3.1	2.1	8.7	1.30	0.16	0.02	0.7	-2.0			
D264/Y648	117	17.79846		-21.07246			46	9	2.1	7.7	2460	1.9	2.3	17.5	0.5	7.7	4.2	0.5	8.7	1.03	0.07	0.02	0.9	-2.0			
D207/W1866	118	17.23033		-21.19928			61	18	-0.9	7.7	1950	1.1	1.3	17.3	0.7	7.6	2.8	0.7	9.4	1.15	0.02	0.01	0.9	-2.0			
D267/Y621	120	17.91459		-21.15217			61	9	0.7	7.4	2370	1.9	2.0	16.3	0.7	6.9	3.7	0.5	9.3								

name	No	dec. longitude	E	dec. latitude	S	Temp.	depth	level	error	pH	ec	← Ca <sup>2+</sup> , Mg <sup>2+</sup> , Na <sup>+</sup> , K <sup>+</sup> , HCO <sub>3</sub> <sup>-</sup> , SO <sub>4</sub> <sup>2-</sup> , NO <sub>3</sub> <sup>-</sup> , Cl <sup>-</sup> , Si		F	Sr <sup>2+</sup>	Ca <sup>2+</sup> :Mg <sup>2+</sup>	log Sr <sup>2+</sup> :Ca <sup>2+</sup>					
												(m)	(%)					(μS/cm)	mmol/l			
D437Y707	123	17.70825	-20.92935	37	12	-1.2	7.8	3380	3.9	7.4	16.5	0.8	8.1	8.1	1.2	15.5	0.98	0.05	0.5	-1.9		
D253Y1148	124	17.68234	-21.22192	49	21	-1.9	7.9	4980	6.0	8.1	18.7	0.4	8.4	3.7	16.6	16.9	1.23	0.07	0.05	0.7	-2.1	
D435Y704	125	17.71785	-20.86504			1.6	7.5	3070	5.2	5.9	14.5	0.6	6.4	4.8	1.0	19.2	1.02	0.05	0.04	0.9	-2.1	
D214W1882	126	17.24280	-21.07790	31	49	-1.4	7.6	2950	4.4	4.1	16.9	0.6	6.9	4.5	0.6	19.0	1.31	0.03	0.05	1.1	-1.9	
D280Y370	127	18.19386	-21.05707	226	17	0.5	7.1	4240	7.1	7.0	14.4	0.1	8.9	1.2	16.3	14.7	0.85	0.03	0.03	1.1	-2.4	
D280Y369	128	18.21017	-21.08424	50	27	-1.0	7.0	4290	7.5	8.0	12.8	0.3	8.2	1.2	14.3	20.0	1.05	0.04	0.03	0.9	-2.4	
B184Y3085	129	18.16123	-19.78533			1.8	7.2	3310	6.2	4.7	12.8	0.9	8.7	3.3	0.5	17.8	0.33	0.02	1.3	-3.2		
D240Y1046	131	17.64971	-20.93207	30	13	2.1	8.1	2340	2.5	4.9	10.5	0.4	6.5	3.3	0.5	11.0	1.00	0.03	0.5	-1.9		
D239Y1043	132	17.57294	-20.95199	30	12	0.0	7.3	2720	3.2	5.7	12.3	0.5	7.8	4.7	2.9	10.6	1.20	0.06	0.04	0.6	-1.9	
W7Y828	133	17.43065	-20.55023	115	70	-2.0	7.2	2760	3.4	5.1	12.4	0.4	6.1	5.1	0.6	14.1	1.15	0.04	0.7	-2.0		
D214W1883	135	17.23992	-21.07337	64	49	-1.5	7.8	2280	4.0	3.5	10.9	0.5	6.8	2.6	0.5	14.6	1.55	0.02	0.05	1.2	-1.9	
D206W1867	136	17.18330	-21.14221	59	40	0.6	7.4	2150	4.0	3.9	9.6	0.4	5.7	2.8	0.7	13.5	1.07	0.03	0.04	1.0	-2.0	
D338Y2955	137	17.53071	-20.47192	122	11	7.4	7.4	2760	5.6	0.8	12.4	0.3	1.8	2.2	0.0	18.6	0.58	0.03	7.2	-2.3		
D304Y2951	138	17.50672	-20.39312	189	18	1.2	7.9	1710	3.4	0.9	6.1	0.2	1.5	0.2	0.1	12.7	0.43	0.04	4.0	-1.9		
B158Y13304	139	17.81190	-19.99004	18	15	0.5	7.8	2700	7.9	2.2	6.2	0.8	2.2	2.7	8.0	11.3	0.55	0.02	0.01	3.5	-2.7	
D423Y667	140	17.50996	-20.80797	101	7	1.1	7.9	2140	0.5	0.7	20.2	0.1	15.9	1.9	0.0	2.4	0.57	0.14	0.01	0.8	-2.0	
D423Y1681	141	17.45873	-20.70833	85	61	1.0	8.5	2030	0.4	1.1	18.7	0.2	14.3	0.6	0.3	5.6	0.63	0.09	0.02	0.4	-1.3	
W6Y813	142	18.36857	-20.32217	236	117	-2.0	8.0	1770	0.6	0.6	15.9	1.4	13.2	1.1	0.4	4.7	0.37	0.04	0.01	0.9	-2.1	
D386Y1W3601	143	17.33493	-20.90036			0.4	8.0	1750	0.4	0.4	17.7	0.1	14.4	1.2	0.1	2.1	0.27	0.20	0.01	0.9	-1.7	
J82Y2030	144	17.38868	-20.89946	152	52	1.6	7.9	1620	0.2	0.4	17.2	0.6	13.0	1.0	0.4	3.0	0.55	0.07	0.00	0.6	-1.9	
D163W1640	145	17.07006	-20.88949	106	69	2.2	7.4	1760	0.8	0.4	17.4	0.2	12.7	1.6	0.0	3.1	0.17	0.18	0.01	1.8	-2.0	
W6Y811	146	18.31426	-20.34208	185	120	0.3	7.4	2090	2.0	1.5	14.0	1.8	11.0	4.5	0.4	2.4	0.57	0.04	0.02	1.3	-2.1	
D269Y667	147	17.78311	-21.12138	37	8	1.7	7.5	1770	0.8	1.5	14.4	0.2	9.6	2.2	0.3	4.1	1.13	0.16	0.01	0.6	-1.9	
W6Y817	148	18.54413	-20.06516	133	114	1.6	7.8	1650	0.5	0.7	14.8	0.7	11.8	1.0	0.7	2.9	0.23	0.06	0.01	0.7	-1.9	
D238Y696	149	17.52591	-20.88134			0.2	8.5	1580	0.1	0.9	14.1	0.6	12.3	1.0	0.0	2.0	0.53	0.12	0.00	0.1	-1.3	
D216W3594	150	17.27639	-20.89946	156	113	-0.7	8.3	1500	0.0	0.1	15.2	0.1	11.8	0.5	0.8	2.0	0.17	0.25	0.00	0.6	-1.9	
J256W2083	151	16.70058	-21.24004	116	61	0.0	8.3	1150	0.5	0.1	12.0	0.1	10.6	0.5	0.0	1.6	0.32	0.15	0.01	3.3	-1.5	
D423Y685	152	17.51536	-20.79801	82	27	2.0	8.0	1350	0.8	0.7	11.7	0.1	11.4	0.6	0.3	1.6	1.17	0.04	0.01	1.3	-2.1	
D174W1611	153	16.95010	-21.02083	73	55	-0.9	7.5	1460	1.1	0.6	12.1	0.4	11.4	0.7	0.7	2.5	1.05	0.25	0.01	1.9	-2.1	
D100W2310	154	16.61324	-21.14764	62	46	1.2	7.8	1440	0.7	0.4	12.4	0.8	10.8	0.6	0.0	2.5	0.45	0.36	0.01	1.5	-1.8	
J248W3530	156	16.78311	-21.37953			0.2	8.5	1660	1.2	2.1	9.4	0.4	12.0	1.1	0.1	2.4	1.17	0.05	0.01	0.6	-2.2	
W2Y777	157	18.64403	-19.62896	122	28	1.0	7.5	1530	1.2	2.1	10.9	0.1	13.3	0.8	0.6	1.7	0.83	0.06	0.01	0.6	-2.0	
J244W4429	158	16.81958	-21.43478	76	46	-0.7	7.5	1540	0.9	2.5	10.4	0.3	13.5	0.9	0.5	2.0	1.23	0.07	0.01	0.4	-2.2	
J114Y1680	159	18.01344	-21.48188	99	9	-1.5	8.0	1960	1.7	2.3	12.4	0.4	10.8	1.7	5.4	3.7	1.20	0.21	0.01	0.7	-2.2	
J83Y2031	160	17.36276	-21.69746	91	67	-2.0	7.6	1580	1.4	1.2	12.2	0.3	12.5	1.7	0.0	2.4	0.95	0.06	0.00	1.1	-2.4	
B220Y3349	161	18.47793	-19.79801	91	67	2.4	7.5	1910	2.0	2.0	11.5	0.1	12.8	0.5	1.3	3.8	1.05	0.07	0.01	1.0	-2.5	
W3Y791	162	18.35597	-20.11584	151	78	-0.2	7.6	1280	0.6	0.8	11.9	0.6	14.5	0.1	0.1	0.5	0.67	0.05	0.01	0.7	-2.1	
W4Y796	163	18.21435	-20.05430	78	37	1.8	7.8	1640	1.9	1.5	13.3	0.6	15.4	0.5	0.2	3.3	0.67	0.03	0.01	1.3	-2.4	
D201W1851	164	17.08637	-21.12953	67	30	-4.3	7.8	1420	1.2	2.1	11.5	0.4	16.1	0.4	0.0	2.2	1.56	1.22	0.02	0.6	-1.7	
D189W2080	165	16.70250	-21.15489	96	55	-1.4	7.9	1800	1.0	2.3	12.2	0.3	15.2	0.7	1.5	1.4	0.72	0.06	0.02	0.4	-1.7	
B494Y3794	166	17.44242	-19.86957			0.5	7.2	1810	1.4	3.0	11.5	0.3	15.4	0.4	1.1	3.0	0.42	0.06	0.02	0.5	-1.9	
B215Y3363	167	18.40691	-19.63587			-1.1	7.3	1690	1.1	2.3	10.9	0.0	14.5	0.5	0.0	2.7	0.58	0.03	0.00	0.5	-2.5	
W2Y786	168	18.47721	-19.97919			2.0	7.1	2520	3.1	4.1	12.6	1.2	16.9	0.2	0.1	9.7	0.85	0.02	0.02	0.8	-2.2	
W2Y785	169	18.48594	-19.89140	73	27	-1.2	7.0	2630	2.4	4.0	14.4	1.4	19.8	0.5	0.1	8.3	0.45	0.02	0.03	0.6	-1.9	
W2Y784	170	18.54510	-19.79819	91	55	0.5	7.8	2480	3.3	3.7	10.4	1.0	18.1	0.6	0.5	6.6	0.85	0.03	0.03	0.9	-2.1	
J98Y2006	171	17.67658	-21.87703	69	18	2.0	7.2	2850	1.7	2.9	19.6	0.2	21.3	0.5	0.9	5.3	0.93	0.24	0.01	0.6	-2.2	
B248Y1Y3812	172	18.58622	-19.50453			1.3	8.4	1940	0.7	3.1	12.4	0.1	18.7	0.2	0.0	0.2	0.83	0.13	0.01	0.2	-1.9	
B243Y3384	173	18.55950	-19.54438			2.1	7.4	2870	8.0	5.3	10.0	0.9	4.8	12.5	0.0	6.2	0.37	0.03	0.06	1.5	-2.1	
B214Y3445	174	18.31382	-19.61775			1.9	7.7	1650	0.7	3.1	12.4	0.1	18.7	0.6	0.1	1.7	0.40	0.06	0.00	0.2	-2.4	
W6Y818	175	18.37342	-20.20814	171	53	2.1	7.4	2670	8.0	5.3	10.0	0.9	4.8	12.5	0.0	6.2	0.37	0.03	0.06	1.5	-2.1	
B344Y4662	177	17.72649	-19.78804			1.3	8.4	1940	0.7	3.1	12.4	0.1	18.7	0.6	0.1	1.7	0.40	0.06	0.00	0.2	-2.4	
D192W1835	178	16.87044	-21.19293	137	47	-2.4	7.7	1020	0.3	0.3	10.2	0.1	3.6	1.2	1.3	4.4	0.77	0.27	0.00	1.0	-2.2	
D382W1667	179	17.06622	-20.76178	174	76	0.0	7.9	1120	0.8	0.1	9.8	0.3	4.8	0.8	1.0	4.1	0.92	0.46	0.01	6.3	-1.9	
D382W1668	180	17.09885	-20.77264	174	76	-2.0	7.9	1070	0.5	0.0	10.0	0.2	4.5	0.9	0.0	4.7	0.82	0.65	0.01	49.0	-1.9	
D173W1614	181	16.91171	-21.01288	125	43	-1.2	7.2	1220	0.6	0.0	10.2	0.3	4.5	1.1	0.2	4.5	0.33	0.53	0.00	12.0	-2.5	
D382W1669	182	17.12860	-20.75453	137	61	-1.3	8.0	1160	0.5	0.0	10.4	0.3	3.8	1.1	0.0	5.3	0.95	0.72	0.01	11.5	-1.7	
D161W1673	183	17.03647	-20.78533	27.0	159	61	1.3	7.9	1180	0.8	0.5	10.4	0.2	4.6	1.1	0.0	5.6	0.77	0.47	0.01	1.5	-1.9
D183W1625	184	16.95681	-21.09330	28.4	95	40	0.1	7.7	1800	1.3	0.2	14.6	0.3	6.0	2.3	0.0	6.9	0.68	0.27	0.01	7.0	-2.1
D173W1615	185	16.92226	-21.00634	34.0	73	24	-0.9	7.8	1580	0.6	0.1	13.6	0.5	5.6	2.1	0.0	5.5	1.61	0.53	0.01	9.0	-2.0
D389W2035	186	17.26296	-20.79801	134	46	-0.9	8.0	1500	0.5	0.5	12.4	0.2	6.3	1.3	0.5	5.4	0.40	0.17	0.01	1.1	-1.7	

**Annex B**

**B-4**

name	No	dec. longitude	E	dec. latitude	S	Temp. (°C)	depth (m)	level (m)	error (%)	pH	ec (µS/cm)	mmol/l			NO <sub>3</sub> <sup>-</sup>	Cl <sup>-</sup>	Si	F	Sr <sup>2+</sup>	Ca <sup>2+</sup> ·Mg <sup>2+</sup>	log Sr <sup>2+</sup> ·Ca <sup>2+</sup>			
												Ca <sup>2+</sup>	Mg <sup>2+</sup>	Na <sup>+</sup>										
D287/W2040	187	17.26775	-20.66757	17.26775	-20.66757		226	85	-2.2	7.9	1520	0.7	1.0	12.0	0.2	8.2	0.9	0.4	5.8	0.32	0.06	0.02	0.7	-1.6
D174/W1612	188	16.94914	-21.02536	16.94914	-21.02536		122	71	-1.6	8.0	1650	0.8	0.4	13.9	0.3	8.0	1.6	0.5	5.1	0.37	0.26	0.01	2.2	-2.0
D285/W3618	189	17.37620	-20.61141	17.37620	-20.61141		116	91	-0.9	7.8	1240	0.3	0.4	10.9	0.2	7.1	0.8	0.4	3.4	0.30	0.16	0.01	0.7	-1.6
D172/W1605	190	16.82246	-21.07880	16.82246	-21.07880		94	52	-0.5	7.9	1420	0.4	0.2	11.3	0.2	7.6	0.9	0.0	3.5	0.37	0.26	0.00	2.2	-2.0
J256/W2082	191	16.68618	-21.24547	16.68618	-21.24547		94	52	-0.5	7.9	1420	1.1	1.2	10.7	0.3	9.1	1.1	0.2	4.2	0.77	0.13	0.01	0.9	-2.0
J247/W2018	192	16.81862	-21.26268	16.81862	-21.26268	29.6	123	70	0.1	7.8	1540	1.1	1.8	10.8	0.4	9.5	1.1	0.1	4.9	0.62	0.14	0.02	0.6	-1.8
D392/Y674	193	17.38868	-20.75543	17.38868	-20.75543		194	31	-0.5	7.6	1910	1.6	2.2	11.5	0.8	10.0	0.6	0.4	4.7	0.42	0.13	0.02	0.7	-1.6
W7/Y819	194	17.81862	-20.39729	17.81862	-20.39729		144	31	-0.5	7.6	1910	1.6	2.2	11.5	0.8	10.0	0.6	0.4	4.7	0.42	0.13	0.02	0.7	-1.6
D3661/W3600	195	17.35893	-20.89130	17.35893	-20.89130		70	39	2.3	8.0	2000	1.8	3.1	11.7	0.3	11.1	2.5	0.5	4.9	0.82	0.07	0.04	0.6	-1.7
W7/Y827	196	17.42774	-20.56109	17.42774	-20.56109		70	39	2.3	8.0	1620	1.3	1.9	10.7	0.3	8.5	1.9	0.9	3.5	1.17	0.08	0.02	0.7	-1.8
D437/Y714	197	17.73800	-20.95199	17.73800	-20.95199		37	9	0.4	8.0	1590	1.1	1.8	11.3	0.4	8.4	2.4	0.4	3.7	1.02	0.13	0.01	0.6	-1.9
D437/Y713	198	17.73512	-20.94565	17.73512	-20.94565		31	9	1.3	7.6	1690	1.3	1.9	12.1	0.4	8.8	2.6	0.4	4.0	1.07	0.10	0.01	0.7	-2.0
D374/W2110	199	17.82726	-21.23460	17.82726	-21.23460		28	6	-0.5	7.8	1800	1.3	1.7	11.1	0.7	6.9	2.9	0.9	4.5	1.46	0.12	0.02	0.8	-1.9
J138/W2171	200	17.76679	-21.41033	17.76679	-21.41033		30	9	1.0	8.1	1780	1.1	1.7	12.3	0.7	8.2	2.1	0.2	5.4	1.53	0.16	0.01	0.6	-2.0
D438/Y722	201	17.88004	-20.92120	17.88004	-20.92120		201	85	0.8	8.3	1890	1.8	2.1	12.0	1.2	7.8	2.6	0.4	7.1	1.21	0.09	0.02	0.8	-2.0
D3771/W2133	202	17.92035	-21.25362	17.92035	-21.25362		49	24	-0.3	8.0	2000	1.4	2.0	12.5	0.7	7.6	2.6	0.7	6.3	1.48	0.02	0.7	1.4	-1.9
D437/Y715	203	17.75432	-20.92844	17.75432	-20.92844		31	9	0.7	8.2	1890	1.9	2.6	11.6	0.4	7.4	3.5	0.5	5.9	1.15	0.07	0.02	0.7	-2.0
D436/Y718	204	17.73800	-20.89130	17.73800	-20.89130		204	85	0.7	8.1	1890	2.1	2.9	11.5	0.5	7.2	4.1	0.4	5.9	1.03	0.07	0.02	0.7	-2.0
B136/Y3769	205	17.39827	-20.08424	17.39827	-20.08424		205	85	-2.1	7.5	1820	1.0	2.8	10.9	0.3	7.6	3.0	0.4	5.5	0.38	0.11	0.04	0.3	-1.4
D432/Y689	207	17.56622	-20.86504	17.56622	-20.86504		207	85	-2.1	7.5	1820	1.0	2.8	10.9	0.3	7.6	3.0	0.4	5.5	0.38	0.11	0.04	0.3	-1.4
J22/W4556	208	16.61516	-21.58605	16.61516	-21.58605		85	24	1.7	7.4	1530	1.7	2.7	6.5	0.3	7.2	0.8	2.1	4.1	0.57	0.03	0.01	0.6	-2.1
D271/Y757	209	17.79079	-21.21649	17.79079	-21.21649		209	85	-0.2	7.6	1640	2.3	2.7	7.1	0.4	7.4	0.9	3.8	4.4	1.12	0.08	0.02	0.9	-2.1
D273/Y1181	211	17.75240	-21.31703	17.75240	-21.31703		27	16	-2.2	7.6	1400	1.3	1.4	8.1	0.3	7.3	1.4	0.3	3.9	1.30	0.06	0.01	0.9	-2.2
D374/W2116	212	17.82917	-21.29167	17.82917	-21.29167		40	6	-0.4	7.9	1410	1.6	1.5	7.5	0.4	6.5	1.7	1.2	2.9	1.30	0.08	0.01	1.0	-2.1
D264/Y654	213	17.78023	-21.09601	17.78023	-21.09601		30	9	0.0	7.7	1290	1.5	1.6	7.2	0.3	6.6	1.5	0.6	3.5	1.15	0.08	0.01	1.0	-2.2
D215/W2029	214	17.25048	-20.98822	17.25048	-20.98822	24.8	79	24	-0.5	7.6	1480	2.8	1.6	5.3	0.3	5.9	0.6	0.8	6.5	1.35	0.05	0.02	1.8	-2.1
D381/W1658	215	17.09981	-20.81250	17.09981	-20.81250		73	51	1.5	7.1	1410	3.6	1.2	6.1	0.2	7.4	0.9	0.9	5.2	1.02	0.32	0.03	2.9	-2.1
D213/W1878	216	17.20250	-20.98279	17.20250	-20.98279		67	27	0.2	8.3	1200	2.1	1.5	7.0	0.4	6.6	0.7	0.3	5.4	1.26	0.02	0.02	1.6	-2.0
D327/W3622	218	17.33205	-20.82264	17.33205	-20.82264		82	73	-0.1	7.5	1400	1.8	0.8	8.9	0.2	7.1	1.0	0.1	5.1	0.75	0.16	0.01	2.2	-2.3
D265/W3619	219	17.40115	-20.65851	17.40115	-20.65851		219	85	-1.0	7.9	1260	0.8	0.9	9.3	0.3	7.4	0.7	0.2	3.9	0.27	0.11	0.01	0.9	-1.9
D2741/W2136	220	17.86948	-21.23732	17.86948	-21.23732		91	24	0.0	7.6	1740	1.8	1.8	9.4	0.6	6.3	1.7	1.6	5.6	1.40	0.08	0.02	1.0	-2.1
D272/Y766	221	17.73129	-21.27989	17.73129	-21.27989		45	9	-1.0	7.9	1740	2.0	1.8	9.6	0.2	6.7	0.9	4.8	4.5	1.20	0.07	0.01	1.1	-2.3
D264/Y655	222	17.77927	-21.05978	17.77927	-21.05978		37	9	0.6	7.6	1560	1.6	1.6	9.7	0.3	6.7	1.6	1.5	4.4	1.12	0.08	0.01	1.0	-2.1
W9/Y846	223	18.09602	-20.48145	18.09602	-20.48145		124	46	0.2	7.2	2040	3.5	2.5	8.5	0.3	7.3	0.5	9.1	3.4	0.70	0.06	0.02	1.4	-2.2
W1/Y776	224	18.62658	-19.56923	18.62658	-19.56923		62	6	-1.0	8.3	2580	3.9	4.2	9.5	0.1	7.7	1.0	13.1	3.7	0.68	0.04	0.01	0.9	-2.4
J154/Y2332	225	17.32054	-21.48007	17.32054	-21.48007		56	4	-0.3	7.8	1950	2.4	2.8	8.6	0.5	6.8	1.0	0.6	5.2	1.05	0.03	0.02	0.8	-2.2
D279/Y421	226	18.11516	-21.23913	18.11516	-21.23913		20	8	-0.4	7.5	1850	2.4	2.4	8.8	0.4	8.4	0.8	4.6	5.4	1.18	0.04	0.02	0.8	-2.1
W6/Y836	227	17.73133	-20.60995	17.73133	-20.60995		76	64	1.6	7.4	1520	1.5	2.5	8.8	0.3	8.4	1.9	0.4	3.8	0.62	0.06	0.01	0.6	-2.0
D223/Y1203	228	17.39251	-21.28804	17.39251	-21.28804		65	19	-0.8	8.3	1740	1.1	2.8	9.5	0.4	8.4	1.8	0.7	5.2	1.13	0.06	0.01	0.6	-1.8
D214/W1885	229	17.21209	-21.02899	17.21209	-21.02899		67	49	0.2	7.7	1510	2.2	2.7	8.7	0.3	8.7	1.8	0.6	5.8	1.35	0.03	0.02	0.8	-1.8
W6/Y834	230	17.74782	-20.69955	17.74782	-20.69955		61	12	-0.1	7.8	1990	3.2	3.2	9.4	0.4	8.6	3.2	1.9	5.2	0.47	0.05	0.02	1.0	-2.2
B7995/Y4987	232	17.40403	-19.59149	17.40403	-19.59149		61	12	-0.1	7.3	2250	3.2	4.3	9.8	0.0	12.1	3.2	1.6	4.9	0.72	0.05	0.02	0.8	-2.3
W11/Y859	233	18.19593	-20.71855	18.19593	-20.71855		43	10	0.2	7.0	2430	4.6	2.2	10.9	0.3	8.9	0.5	7.4	7.5	0.82	0.04	0.02	2.1	-2.0
W10/Y852	234	17.92435	-20.66697	17.92435	-20.66697		37	18	-1.1	7.6	1880	2.0	1.6	11.1	0.3	7.2	0.7	0.3	10.3	0.47	0.07	0.02	1.2	-2.1
D264/Y657	235	17.77831	-21.06612	17.77831	-21.06612		30	9	2.0	7.3	2630	3.6	3.3	12.2	0.4	6.6	2.3	5.4	8.7	1.67	0.04	0.02	1.1	-2.2
J143/Y1369	236	17.78503	-21.48822	17.78503	-21.48822		24	10	0.7	8.4	2100	2.7	2.8	11.4	0.5	5.3	2.4	4.2	8.2	0.77	0.06	0.00	1.0	-2.8
D264/Y656	237	17.77351	-21.06341	17.77351	-21.06341		37	9	2.2	7.6	2400	3.3	3.3	10.9	0.4	6.2	2.1	5.7	7.3	1.13	0.05	0.02	1.0	-2.2
D436/Y719	238	17.76486	-20.91757	17.76486	-20.91757		30	9	0.7	7.6	2100	2.0	3.0	12.1	0.6	7.4	2.9	1.7	7.3	1.13	0.11	0.02	0.7	-2.0
D261/Y724	239	17.68426	-20.99275	17.68426	-20.99275		91	23	1.2	7.6	2250	2.4	4.1	11.7	0.5	7.5	3.2	2.5	8.2	1.03	0.07	0.03	0.6	-1.9
D239/Y1042	241	17.56662	-20.91757	17.56662	-20.91757		30	12	0.1	8.0	1850	2.6	4.9	6.4	0.5	7.0	4.2	1.3	5.1	1.23	0.06	0.04	0.5	-1.9
D437/Y708	242	17.67754	-20.92844	17.67754	-20.92844		31	9	1.7	8.3	1890	1.9	2.7	9.8	0.4	6.8	1.8	1.7	6.5	0.62	0.06	0.02	0.7	-2.0
D391/Y678	243	17.40115	-20.70833	17.40115	-20.70833		111	49	-0.5	8.0	1590	2.2	1.8	8.6	0.3	6.9	1.3	0.1	7.5	0.70	0.08	0.02	1.2	-2.0
D391/Y675	244	17.38964	-20.69112	17.38964																				

name	No	dec. longitude	E	dec. latitude	S	Temp. (°C)	depth (m)	level (m)	error (%)	pH	ec (µS/cm)	Ca <sup>2+</sup>	Mg <sup>2+</sup>	Na <sup>+</sup>	K <sup>+</sup>	HCO <sub>3</sub> <sup>-</sup>	SO <sub>4</sub> <sup>2-</sup>	NO <sub>3</sub> <sup>-</sup>	Cl <sup>-</sup>	Si	F	Sr <sup>2+</sup>	Ca <sup>2+</sup> :Mg <sup>2+</sup>	log Sr <sup>2+</sup> :Ca <sup>2+</sup>
D233Y1073	252	17.46353	-21.10054			6	4	1.2	8.3	2250	3.6	3.5	7.3	1.6	9.1	1.2	3.7	7.3	1.15	0.05	0.02	1.0	-2.2	
B139Y3774	253	17.39347	-20.05254			46	27	0.8	6.9	1730	3.4	1.8	7.7	0.2	9.1	0.8	0.2	7.2	0.62	0.03	0.03	1.8	-2.0	
B139Y3773	254	17.41939	-20.03804			50	27	0.7	6.9	1820	4.0	1.8	7.7	0.2	8.9	0.8	0.4	8.3	0.63	0.03	0.03	2.2	-2.1	
B136Y3768	255	17.47409	-20.04620			52	51	-0.6	7.2	2090	5.0	2.8	6.5	0.2	7.8	2.2	3.7	6.6	0.57	0.05	0.04	1.8	-2.1	
J27W4523	256	16.66891	-21.72101			73	15	1.4	7.7	3930	7.9	10.1	5.2	0.4	9.1	2.4	16.1	13.5	1.03	0.07	0.02	0.8	-2.6	
J104Y1764	257	17.89060	-21.73460			46	10	2.3	7.1	3340	8.7	6.2	5.7	0.5	6.7	1.1	12.6	13.5	0.78	0.05	0.03	1.4	-2.5	
D277Y411	258	18.06142	-21.27899			46	10	2.3	7.1	3810	8.2	8.4	6.5	0.5	6.2	1.9	14.6	14.1	1.00	0.03	0.04	1.1	-2.3	
D253Y1149	259	17.68618	-21.22554			58	27	-1.9	7.5	4580	9.7	8.7	5.4	0.3	5.5	2.6	16.6	16.9	1.20	0.04	0.05	1.1	-2.3	
B344/Y4469	260	17.79655	-19.75815			30	9	-1.2	7.1	3360	6.6	10.9	2.1	0.0	8.6	1.6	8.0	18.3	0.43	0.01	0.00	0.6	-3.2	
D225Y1112	261	17.55374	-21.25362			65	43	1.3	8.1	3640	8.9	7.3	6.7	1.4	8.1	2.3	17.1	9.6	0.95	0.04	0.03	1.2	-2.5	
B215Y3364	262	18.37140	-19.65399			76	6	2.0	7.1	3590	7.2	5.8	7.1	2.1	8.3	0.7	14.0	10.2	0.43	0.01	0.13	1.3	-3.0	
J27W4524	263	16.65931	-21.72283			95	43	1.4	6.9	3190	6.5	6.4	7.9	0.7	8.1	1.9	8.9	12.4	0.93	0.06	0.02	1.0	-2.6	
B178Y3080	264	18.06814	-19.79076			152	27	1.7	7.5	2870	6.2	4.9	7.4	0.0	10.3	0.4	4.9	14.1	0.80	0.02	0.01	1.3	-2.9	
D254/Y1121	265	17.65835	-21.20109			61	26	1.4	7.5	3530	12.7	3.7	4.6	0.9	6.0	3.1	17.1	7.8	0.82	0.03	0.02	3.4	-2.9	
B99/2/W3512	266	17.20441	-20.26993			49	22	2.2	7.4	6400	12.6	2.7	1.4	0.2	4.6	1.1	17.5	6.5	0.30	0.02	0.06	4.6	-2.3	
D275Y641	267	17.94626	-21.16938			46	9	2.0	7.9	2520	5.9	4.8	4.0	0.5	5.6	2.0	5.0	10.2	1.12	0.06	0.03	1.2	-2.2	
D254/Y1118	268	17.65931	-21.17391			61	26	1.4	8.2	2810	8.5	3.9	4.4	0.3	5.7	0.7	10.3	11.3	1.28	0.03	0.04	2.2	-2.4	
D254/Y1120	269	17.65259	-21.19565			61	21	2.2	7.6	2600	9.2	4.1	1.3	0.2	6.4	0.9	13.7	5.2	1.07	0.04	0.03	2.2	-2.4	
D446/Y659	270	18.02879	-21.02446			44	21	-1.1	7.4	2650	7.6	4.5	2.6	0.2	7.4	0.3	11.4	8.2	1.05	0.03	0.00	1.7	-3.3	
B177Y3332	271	18.01922	-19.75091			49	27	-0.8	7.2	2550	8.0	2.5	0.8	0.0	6.9	0.3	7.3	7.3	0.40	0.01	0.00	3.2	-3.4	
B197/3/Y3430	272	18.21977	-19.67301			30	18	-1.9	7.2	3180	2.9	8.8	9.7	0.3	11.3	2.0	6.9	12.4	0.30	0.03	0.01	0.3	-2.6	
B212Y3340	273	18.30806	-19.67663			25	7.3	7.6	3130	2.5	7.0	12.6	0.0	14.8	0.6	5.6	9.0	0.50	0.03	0.01	0.4	-2.6		
B197/2/Y3435	274	18.23992	-19.66033			61	49	-1.2	8.5	1840	0.3	4.0	11.6	0.8	13.0	1.7	8.1	7.8	0.58	0.03	0.01	0.2	-2.5	
J187/Y2381	275	17.21689	-21.75815			27	49	-1.2	8.5	1840	0.3	4.0	11.6	0.8	13.0	1.7	8.1	7.8	0.58	0.03	0.01	0.2	-2.5	
B212Y3339	276	18.30710	-19.68116			29	5.1	10.7	0.3	11.6	0.8	4.9	7.9	0.3	11.6	0.8	4.9	7.9	0.37	0.04	0.01	0.6	-2.7	
B199Y3056	277	18.29079	-19.72464			61	1	-1.3	7.2	2920	2.8	4.5	9.5	0.1	12.3	1.1	0.1	9.9	0.47	0.03	0.01	0.6	-2.4	
B179Y3075	278	18.08349	-19.85960			28	4.5	9.5	0.1	12.3	1.1	0.1	9.9	0.3	10.8	0.6	10.9	8.7	0.60	0.03	0.01	0.5	-2.6	
B228Y4530	279	18.35413	-19.52083			44	9.3	3.7	0.1	10.8	0.6	9.6	10.9	8.7	10.8	0.6	10.9	8.7	0.60	0.03	0.01	0.5	-2.6	
B199Y3058	280	18.25816	-19.76540			30	3.0	7.6	4.3	2920	4.4	9.3	3.7	0.1	12.0	0.6	9.6	10.9	0.42	0.04	0.01	0.4	-2.7	
B505/Y4524	281	17.43186	-19.76540			30	3.0	7.6	4.3	2920	4.4	9.3	3.7	0.1	12.0	0.6	9.6	10.9	0.42	0.04	0.01	0.4	-2.7	
B201Y3063	282	18.34357	-19.83062			33	3	-0.6	7.4	2320	2.9	7.0	4.7	0.2	11.4	0.5	5.0	7.3	0.37	0.02	0.00	0.4	-2.8	
B186Y3090	283	18.12092	-19.71739			25	1.5	8.5	6.2	2490	1.5	8.5	6.2	0.0	13.9	0.1	3.4	7.9	0.65	0.02	0.01	0.2	-2.3	
B198Y3334	284	18.26296	-19.70290			25	1.5	8.5	6.2	2490	1.5	8.5	6.2	0.0	13.9	0.1	3.4	7.9	0.65	0.02	0.01	0.2	-2.3	
B193Y3062	285	18.21497	-19.80707			61	30	0.2	8.8	1660	0.5	7.8	3.6	0.0	14.3	0.1	0.2	5.4	0.20	0.03	0.00	0.1	-2.2	
B593/2/Y4753	286	18.10269	-19.81250			91	9	-1.3	7.5	1880	1.8	6.2	3.7	0.0	12.3	0.1	0.6	6.9	0.48	0.03	0.01	0.3	-2.4	
B178Y3077	287	18.14299	-19.83786			48	18	1.6	7.5	2210	2.3	6.8	4.6	0.6	12.8	0.4	3.4	5.6	0.53	0.06	0.02	0.3	-2.1	
B164/Y3014	288	18.24088	-19.45199			61	30	0.2	8.8	1660	0.5	7.8	3.6	0.0	14.3	0.1	0.2	5.4	0.20	0.03	0.00	0.1	-2.2	
B179/Y1Y3073	289	18.14299	-19.83786			91	9	-1.3	7.5	1880	1.8	6.2	3.7	0.0	12.3	0.1	0.6	6.9	0.48	0.03	0.01	0.3	-2.4	
B213/Y3439	290	18.24376	-19.59692			152	56	-0.2	7.8	1930	2.1	7.0	2.6	0.1	13.5	0.5	0.1	6.2	0.45	0.01	0.03	0.3	-2.3	
B163Y3004	291	17.97985	-19.87500			52	2	-0.2	7.0	2710	5.2	7.8	1.8	0.0	10.5	0.2	7.1	10.2	0.62	0.03	0.00	0.2	-2.5	
B44/Y4475	292	17.90595	-19.73822			30	3	-0.3	7.6	3100	3.2	10.9	4.0	0.4	11.9	1.6	6.6	11.3	0.43	0.01	0.00	0.3	-3.1	
B212/Y3341	293	18.28695	-19.67644			52	2	-0.2	7.0	2550	1.4	9.1	4.9	0.0	11.3	0.2	3.0	10.7	0.58	0.03	0.00	0.2	-2.5	
B182Y3029	294	18.22841	-19.98370			45	37	1.0	6.6	2630	6.9	6.6	3.8	0.1	9.1	1.1	7.6	11.6	0.65	0.04	0.09	1.0	-1.9	
B583Y3093	295	17.34933	-19.75000			74	5	-0.1	7.3	2980	4.5	7.8	4.7	0.0	10.0	0.7	5.0	13.0	0.45	0.03	0.01	0.6	-2.5	
B163Y3001	296	18.01248	-19.92935			34	30	-0.2	7.8	2260	2.9	4.7	5.9	2.3	12.2	0.1	1.2	9.9	0.27	0.03	0.01	0.6	-2.7	
B216Y3348	297	18.40211	-19.69565			43	14	0.6	7.7	2010	4.4	5.3	1.5	0.5	6.7	0.2	6.6	7.3	1.17	0.09	0.02	0.8	-2.3	
B191/Y3042	298	18.30134	-19.91757			30	6	-1.3	7.5	1850	3.2	5.1	1.7	0.1	6.1	0.2	3.5	8.9	0.65	0.02	0.00	0.6	-2.2	
J113/Y1737	299	18.02207	-21.57689			43	14	0.6	7.7	2010	4.4	5.3	1.5	0.5	6.7	0.2	6.6	7.3	1.17	0.09	0.02	0.8	-2.3	
B503Y4520	300	17.47601	-19.79076			30	6	-1.3	7.5	1850	3.2	5.1	1.7	0.1	6.1	0.2	3.5	8.9	0.65	0.02	0.00	0.6	-2.2	
W7/Y820	301	17.81280	-20.40181			244	40	-1.5	7.6	1910	3.9	3.5	4.4	0.4	11.4	0.2	0.6	7.8	0.62	0.04	0.02	1.1	-2.2	
B186Y3089	302	18.14875	-19.71649			37	16	-2.1	7.2	2040	4.0	4.7	3.0	0.0	9.3	0.6	3.9	6.8	0.38	0.02	0.00	0.8	-3.0	
B175Y3327	303	17.79635	-19.60254			37	27	2.1	7.3	2260	5.0	4.9	4.1	0.2	8.4	0.6	5.0	8.5	0.50	0.03	0.01	1.0	-3.1	
B517/Y4635	304	17.57582	-19.63859			43	24	0.2	7.3	1910	5.2	2.8	3.2	0.0	9.7	0.2	0.2	6.6	0.73	0.02	0.00	0.8	-2.3	
B175Y3325	305	17.98464	-19.76902			91	34	-0.8	7.1	2110	3.4	4.5	3.0	0.6	7.2	0.3	6.2	5.6	1.20	0.10	0.00	1.9	-3.4	
J103/Y204	306	17.68522	-21.70471			61	21	-1.2	7.6	1680	3.0	3.6	4.8	0.4	7.1	0.6	5.9	4.9	1.13	0.05	0.02	0.8	-2.3	
D398/Y384	307	18.09789	-21.13678			44	18	-1.8	7.6	1740	3.3	3.3	4.3	0.1	8.0	0.3	3.8	5.9	1.07	0.04	0.03	1.0	-2.4	
J122/Y1677	308	18.01631	-21.42120			44	18	-1.8	7.6	1740	3.3	3.3	4.3	0.1	8.0	0.3	3.8	5.9	1.07	0.04	0.03	1.0	-2.4	
D260/Y5367	309	18.20441	-21.10054			160	58	1.8	7.0															



name	No	dec. longitude °E	dec. latitude °S	Temp. (°C)	depth (m)	level (m)	error (%)	pH	ec (µS/cm)	Ca <sup>2+</sup>	Mg <sup>2+</sup>	Na <sup>+</sup>	K <sup>+</sup>	HCO <sub>3</sub> <sup>-</sup>	SO <sub>4</sub> <sup>2-</sup>	NO <sub>3</sub> <sup>-</sup>	Cl <sup>-</sup>	Si	F	Sr <sup>2+</sup>	Ca <sup>2+</sup> ·Mg <sup>2+</sup>	log Sr <sup>2+</sup> ·Ca <sup>2+</sup>
D202/W1861	376	17.13532	-21.21739		92	35	-1.9	7.6	1080	1.1	1.7	7.3	0.5	9.9	1.3	0.1	1.5	0.88	0.05	0.01	0.7	-2.0
D386/W3598	377	17.35125	-20.93116				2.0	7.5	1440	1.9	2.5	7.0	0.3	9.1	1.5	0.0	3.4	0.60	0.03	0.03	0.8	-1.8
D241/Y1036	378	17.56238	-21.01540		30	13	0.6	7.4	1460	2.0	2.5	7.6	0.4	9.8	2.0	0.3	2.6	1.41	0.03	0.02	0.8	-2.1
B144/Y3763	379	17.49520	-20.02627		46	37	1.6	7.2	1540	2.6	2.5	7.3	0.2	10.5	2.0	0.0	2.8	0.38	0.03	0.03	1.1	-1.9
D270/Y754	380	17.75240	-21.17301		31	8	-0.5	8.0	960	1.0	1.4	5.4	0.3	7.2	0.6	0.5	1.6	1.43	0.09	0.01	0.7	-2.0
D267/Y627	381	17.81094	-21.13949		15	3	0.3	7.9	1020	1.2	1.3	5.4	0.3	6.9	0.6	0.6	2.0	1.28	0.07	0.01	0.9	-2.1
D3751/W2178	382	17.81286	-21.20924		23	4	-1.3	7.7	1090	1.0	1.3	6.1	0.5	6.5	1.1	0.6	2.1	1.51	0.08	0.01	0.8	-2.0
D272/Y767	383	17.73704	-21.25634		37	6	0.2	7.7	1030	1.1	1.2	6.2	0.2	7.0	0.7	0.4	2.3	1.12	0.05	0.01	1.0	-2.2
D200/W1845	384	17.05086	-21.21105			18	0.3	7.4	880	1.1	1.2	6.3	0.2	7.1	0.9	0.3	1.9	0.88	0.04	0.01	0.9	-1.9
D200/W1843	385	17.04702	-21.20562		58	24	-0.5	7.8	930	1.3	1.3	6.1	0.2	7.3	0.9	0.4	2.1	0.90	0.04	0.01	0.9	-2.0
J224/Y2312	386	17.39347	-21.55797		91	55	-2.3	7.9	1370	1.9	2.9	4.7	0.5	7.8	0.4	4.3	2.5	1.08	0.05	0.02	0.7	-2.1
D432/Y688	387	17.56622	-20.84873		67	30	0.1	8.0	1220	1.1	2.5	5.0	0.4	8.1	0.6	0.6	2.7	1.36	0.09	0.02	0.4	-1.7
D3751/W2182	388	17.80806	-21.17844		30	12	-0.1	8.1	1180	1.4	2.3	5.2	0.5	7.0	1.4	0.6	2.7	1.43	0.07	0.01	0.6	-2.0
D275/Y642	389	17.95106	-21.18116		61	12	0.3	7.7	1250	2.1	1.7	5.4	0.4	7.2	1.4	0.6	2.8	1.28	0.08	0.01	1.6	-2.2
D244/Y1066	390	17.54031	-21.05888		31	11	-0.8	7.7	1090	1.7	1.9	5.0	0.3	7.0	1.8	0.4	1.7	1.28	0.04	0.01	0.9	-2.1
D179/W1642	391	17.17658	-21.06612		98	57	-0.7	7.9	1080	1.4	1.6	5.3	0.3	6.8	0.7	0.1	3.4	0.80	0.04	0.01	0.9	-2.1
D163/W1641	392	17.06238	-20.91757	26.6	128	44	-1.6	7.2	1250	2.7	1.0	5.2	0.3	7.2	0.6	1.6	3.2	1.12	0.10	0.02	2.7	-2.2
J225/Y248	393	17.35797	-21.56522		76	27	0.7	7.5	1140	0.7	2.6	5.1	0.6	8.5	0.6	1.2	1.4	1.12	0.07	0.01	0.3	-1.7
D209/W3564	394	17.32054	-21.29076		47	6	-0.7	7.5	1020	0.8	1.9	5.2	0.8	9.0	0.5	0.5	1.1	1.48	0.07	0.01	0.4	-1.9
D218/W1888	395	17.33109	-21.09873		67	18	1.6	7.6	890	0.9	1.8	5.7	0.4	8.2	0.8	0.4	0.8	1.66	0.03	0.01	0.5	-2.1
D210/W3561	396	17.29750	-21.23188		47	12	0.6	7.6	960	0.9	1.5	6.0	0.3	8.4	0.7	0.3	0.9	1.38	0.06	0.01	0.6	-2.1
J215/Y1221	397	17.58253	-21.29891		56	18	-1.9	7.6	1030	1.0	1.4	5.9	0.3	7.7	0.8	0.7	1.2	1.18	0.06	0.01	0.7	-2.1
D2571/Y738	398	17.76296	-21.11322		21	9	0.8	7.8	980	0.8	1.6	5.7	0.4	7.4	0.6	0.7	1.2	1.25	0.12	0.01	0.5	-1.9
J163/Y2107	399	17.30806	-21.40670		43	9	1.2	8.0	880	0.9	1.1	5.5	0.4	7.4	0.1	1.0	1.0	1.10	0.08	0.01	0.8	-2.1
D209/W3565	400	17.30038	-21.28623		47	9	-1.0	7.6	860	0.7	1.2	5.4	0.3	7.7	0.5	0.3	0.8	1.38	0.06	0.01	0.6	-2.1
D203/W3569	401	17.17274	-21.26902		47	11	-2.0	7.8	900	0.7	1.5	5.0	0.4	7.7	0.6	0.4	0.9	1.20	0.08	0.01	0.4	-1.9
D216/W3590	403	17.31094	-20.94384		107	47	0.6	7.6	1100	1.0	1.0	7.2	0.3	8.0	0.7	0.1	1.9	1.30	0.07	0.01	1.0	-2.1
D204/W1846	404	17.20441	-21.21649		46	14	-0.7	7.6	950	1.0	1.7	7.0	0.4	8.2	0.9	0.4	1.9	1.23	0.04	0.01	0.7	-2.0
D209/W3566	406	17.28215	-21.27808		61	9	-0.9	7.9	960	0.6	1.3	6.7	0.3	8.2	0.6	0.4	1.2	1.21	0.07	0.01	0.5	-1.9
D201/W1852	407	17.06910	-21.13496		79	39	-1.1	7.5	790	1.0	0.8	6.3	0.2	8.3	0.4	0.3	0.8	1.10	0.10	0.01	1.2	-2.0
D202/W1863	408	17.12572	-21.20562		24	9	0.2	7.5	960	1.3	1.6	6.9	0.4	9.1	1.2	0.4	1.0	1.05	0.03	0.01	0.8	-2.1
D202/W1862	409	17.13340	-21.19837		91	21	-0.4	7.6	920	0.9	1.3	7.5	0.4	9.5	1.1	0.1	0.5	0.95	0.03	0.01	0.7	-2.1
D223/Y1207	410	17.35988	-21.27899		45	12	-0.6	8.0	950	0.6	1.1	6.7	0.4	9.0	0.3	0.5	0.5	1.12	0.08	0.01	0.5	-1.9
D223/Y1205	411	17.36084	-21.28261		33	12	0.4	8.2	990	0.8	1.3	6.6	0.3	9.1	0.4	0.6	0.5	0.97	0.08	0.01	0.6	-2.0
D125/W1609	412	16.67658	-21.01721		183	32	-1.0	8.2	810	1.1	0.5	6.1	0.2	8.7	0.2	0.0	0.4	0.43	0.12	0.01	2.3	-2.0
D393/Y672	413	17.39923	-20.81612				2.6	7.4	1110	1.5	1.9	5.0	0.3	9.4	0.2	0.4	1.4	1.00	0.04	0.03	0.8	-1.7
D387/Y670	414	17.38004	-20.83333		133	49	1.7	7.9	1050	1.7	1.8	4.4	0.2	9.4	0.1	0.4	1.1	1.03	0.07	0.02	1.0	-1.9
J224/Y2307	415	17.43858	-21.50725		101	64	-2.3	7.8	1110	1.7	1.9	5.0	0.3	10.0	0.7	0.8	1.2	1.10	0.05	0.01	0.9	-2.2
D388/W3607	416	17.29750	-20.81341				2.0	7.9	960	1.4	1.7	4.8	0.2	9.6	0.2	0.1	0.6	1.23	0.05	0.01	0.8	-2.0
D381/W1659	417	17.14395	-20.78533		73	49	0.3	7.4	960	1.6	1.5	5.3	0.3	9.8	0.3	0.4	0.8	1.12	0.13	0.02	1.1	-1.8
D383/W1665	418	17.19194	-20.75453		213		0.5	7.5	860	1.3	1.2	5.0	0.2	9.0	0.1	0.3	0.6	1.21	0.10	0.02	1.1	-1.9
D383/W1666	419	17.18810	-20.74547		170	85	1.5	7.4	920	1.4	1.3	5.6	0.2	9.0	0.2	0.5	0.9	1.13	0.11	0.02	1.0	-1.9
D383/W1664	420	17.17083	-20.75815	25.8	168	73	0.5	7.5	870	1.2	1.1	5.7	0.2	9.0	0.2	0.3	0.6	0.93	0.10	0.02	1.1	-1.8
W10/Y851	421	18.03589	-20.71312		81	44	-0.5	7.6	1100	1.7	1.4	5.2	0.5	8.9	0.6	0.7	1.4	0.77	0.06	0.02	1.2	-2.0
D170/W1901	422	16.75912	-20.99099		95	53	-1.4	7.6	840	1.4	0.9	5.8	0.3	8.8	0.3	0.0	1.4	0.33	0.09	0.01	1.6	-2.1
D175/W1650	423	17.04990	-20.94293		91	60	0.6	7.6	1000	2.0	1.3	4.8	0.3	8.2	0.5	0.3	2.0	0.93	0.04	0.01	1.5	-2.1
D227/Y1109	424	17.61132	-21.19475		66	41	2.0	7.8	1100	1.9	1.8	5.1	0.3	8.3	0.9	0.3	1.7	0.53	0.02	0.02	1.1	-2.1
D100/W2309	425	16.58445	-21.18841		137	91	0.3	7.9	1010	1.4	1.7	4.6	0.3	8.1	0.6	0.6	1.7	0.43	0.05	0.02	0.8	-1.9
W13/Y872	426	18.38118	-20.96742		100	55	0.0	7.3	1100	1.8	2.0	4.5	0.3	9.1	1.0	0.2	1.0	0.53	0.04	0.02	0.9	-2.0
D280/Y2348	427	18.26967	-21.14946		31	9	-1.3	7.5	1040	1.2	2.3	4.4	0.2	9.0	0.2	0.2	1.0	1.05	0.07	0.01	0.5	-2.0
W6/Y815	429	18.66537	-20.15656		161	116	1.4	7.4	820	1.3	0.9	4.3	0.4	8.0	0.1	0.2	0.5	0.68	0.06	0.01	1.5	-2.3
Y106/Y1749	430	18.01536	-21.72373		46	24	1.9	8.0	800	1.1	1.3	4.2	0.4	8.5	0.1	0.1	0.2	0.77	0.09	0.01	0.9	-2.3
D380/W1655	431	17.15643	-20.87228		91	70	0.2	7.5	840	1.3	1.2	4.7	0.3	8.5	0.2	0.3	0.6	0.87	0.06	0.01	1.1	-2.1
D171/W1607	432	16.73608	-21.04076		45		-2.0	7.7	890	1.7	0.6	4.8	0.3	8.4	0.3	0.2	0.9	0.75	0.14	0.01	2.9	-2.2
D384/W1661	433	17.22361	-20.80888	26.0			0.6	7.4	820	1.5	1.2	4.2	0.2	8.8	0.1	0.3	0.4	1.43	0.06	0.01	1.2	-2.1
D180/W1636	434	17.06046	-21.06975	26.4	94	55	-1.5	7.3	900	1.5	1.2	4.1	0.3	9.0	0.2	0.2	0.6	1.12	0.04	0.01	1.3	-2.1
D286/W3613	435	17.31286	-20.63315		107	61	0.9	7.3	900	1.9	1.3	4.2	0.2	9.6	0.2	0.1	0.3	1.10	0.03	0.02	1.5	-2.1
D167/W1685	436	16.91075	-20.89946		154	55	-0.2	7.5	840	1.5	1.4	4.2	0.3	9.4	0.2	0.0	0.5	0.85	0.07	0.02	1.1	-1.8

name	No	dec. longitude	E	dec. latitude	S	Temp. (°C)	depth (m)	level (m)	error (%)	pH	ec (µS/cm)	Ca <sup>2+</sup>	Mg <sup>2+</sup>	Na <sup>+</sup>	K <sup>+</sup>	HCO <sub>3</sub> <sup>-</sup>	SO <sub>4</sub> <sup>2-</sup>	NO <sub>3</sub> <sup>-</sup>	Cl <sup>-</sup>	Si	F	Sr <sup>2+</sup>	Ca <sup>2+</sup> :Mg <sup>2+</sup>	log Sr <sup>2+</sup> :Ca <sup>2+</sup>	
																									mmol/l
B344/5/Y4661	438	17.71977		-19.76902			91	0	0.2	7.2	2040	5.0	4.1	5.7	0.3	11.4	5.5	0.0	1.7	1.03	0.17	0.03	1.2	-2.2	
B793/Y2607	439	17.38580		-19.69746					0.5	6.9	1560	3.5	3.2	4.7	0.1	10.7	2.3	0.6	2.2	0.38	0.03	0.03	0.01	1.1	-2.4
B794/5/Y4626	440	17.39827		-19.68569					1.2	7.3	1460	3.2	3.0	4.8	0.2	11.6	1.9	0.0	1.6	0.38	0.02	0.01	1.1	-2.4	
B793/Y2605	441	17.38580		-19.69746					-0.4	7.0	1370	3.1	2.7	4.3	0.1	11.2	1.8	0.2	1.3	0.38	0.03	0.01	1.2	-2.4	
J102/Y1938	442	17.77543		-21.72645			91	61	-1.8	7.8	1260	2.6	2.0	5.0	0.4	10.2	1.7	0.1	1.5	0.85	0.03	0.01	1.3	-2.5	
J101/Y1767	443	17.82054		-21.74275			64	37	-1.5	7.5	1530	3.5	2.3	4.3	0.4	9.5	2.5	0.1	2.3	0.90	0.02	0.02	1.5	-2.4	
B509/Y4514	444	17.43090		-19.69475					7.8	1300	1.6	3.1	5.0	0.2	8.9	1.9	0.0	1.7	0.52	0.01	0.00	0.5	-2.5		
J30/W4514	445	16.77543		-21.69384			148	105	-0.6	7.1	1210	2.7	3.3	3.1	0.2	10.6	1.8	0.2	1.0	0.77	0.02	0.01	0.8	-2.3	
B793/Y2606	446	17.37332		-19.69022			61	29	1.0	6.9	1330	3.2	3.1	3.5	0.1	11.5	1.6	0.1	1.2	0.37	0.03	0.01	1.0	-2.4	
B504/Y4492	447	17.55758		-19.77446					0.7	7.8	1230	2.4	3.2	3.1	0.4	11.5	1.5	0.0	0.1	0.43	0.02	0.01	0.7	-2.2	
B805/Y4657	448	17.63052		-19.67844			84	36	1.7	7.3	1280	1.9	3.7	3.9	0.0	9.6	2.3	0.2	0.2	0.63	0.03	0.00	0.5	-2.7	
B327/W780	449	17.22457		-19.79710			77	77	0.8	7.6	1290	1.9	4.2	4.1	0.3	10.8	2.2	0.3	0.8	0.42	0.03	0.01	0.5	-2.5	
J82/Y2029	450	17.39347		-21.69746			91	49	-1.6	7.4	1030	1.2	1.7	5.3	0.5	10.6	0.3	0.4	0.4	0.78	0.04	0.01	0.7	-2.1	
D388/W3608	451	17.33589		-20.79529					1.3	7.7	1040	1.5	1.9	5.0	0.3	10.4	0.2	0.3	0.7	1.46	0.04	0.02	0.8	-2.0	
D189/W2081	452	16.73129		-21.15399			137	30	0.1	8.0	950	1.2	1.5	6.0	0.1	11.0	0.1	0.0	0.0	0.60	0.07	0.02	0.8	-1.9	
W9/Y838	453	18.25994		-20.34842			117	80	-2.0	7.3	1060	1.7	2.1	4.3	0.2	10.5	0.6	0.2	0.8	0.77	0.02	0.01	0.8	-2.3	
W9/Y837	454	18.25509		-20.36561			123	73	-2.3	7.6	1060	1.4	2.4	4.0	0.2	10.3	0.5	0.3	0.8	0.73	0.10	0.01	0.6	-2.0	
D190/W1830	455	16.81094		-21.11232			92	37	-0.4	7.5	890	1.4	2.3	4.4	0.3	10.8	0.2	0.2	0.8	0.80	0.05	0.02	0.6	-1.9	
W3/Y789	456	18.28807		-19.99005			87	24	0.3	7.2	1100	2.4	2.0	3.6	0.2	10.8	0.4	0.1	0.7	0.57	0.02	0.01	1.2	-2.6	
W5/Y804	457	17.86033		-20.35294			72	30	-2.2	7.6	1000	1.5	1.4	4.3	0.6	10.2	0.2	0.2	0.6	0.73	0.05	0.01	1.1	-2.4	
D159/W1907	458	16.82054		-20.88406			81	75	-0.9	7.8	860	2.0	1.4	4.0	0.3	10.4	0.1	0.1	0.6	1.05	0.02	0.01	1.4	-2.3	
W3/Y787	459	18.40155		-19.98281			176	80	-1.0	7.1	1250	2.0	2.1	4.7	0.5	10.6	0.1	0.2	2.7	0.67	0.01	0.01	1.0	-2.2	
B231/Y3379	461	18.46353		-19.66576			59	3	-2.4	7.6	1480	2.5	2.6	4.5	0.0	11.2	0.4	1.4	2.1	0.87	0.04	0.01	1.0	-2.6	
W9/Y843	462	17.88458		-20.52489			73	44	-1.5	7.6	1210	2.3	2.5	3.8	0.2	9.8	0.6	1.3	1.8	0.77	0.04	0.01	0.9	-2.3	
W5/Y809	463	18.05626		-20.27240			123	22	0.1	7.2	1230	2.1	2.8	4.1	0.1	9.9	0.5	1.7	1.3	1.57	0.03	0.01	0.8	-2.6	
B202/Y3036	464	16.84357		-21.47101			49	40	1.5	7.3	1290	1.5	3.4	3.9	0.2	9.4	0.2	2.1	1.5	0.25	0.02	0.01	0.5	-2.3	
W3/Y788	465	18.35797		-19.90127			170	79	-1.0	7.7	1200	1.3	4.1	3.8	0.0	9.9	0.2	2.6	1.9	0.93	0.03	0.01	0.3	-2.3	
B566/JY4491	466	18.40058		-20.06425					0.0	7.9	1350	1.6	2.9	4.6	0.1	11.2	0.5	0.1	1.5	0.48	0.04	0.01	0.6	-2.4	
W2/Y781	467	18.58868		-19.67964					-2.3	8.3	1340	1.6	3.0	4.7	0.3	10.8	0.2	2.4	1.4	1.05	0.04	0.01	0.5	-2.4	
B190/Y3041	468	17.56814		-19.76993					-0.2	7.9	1190	1.3	3.2	4.3	0.2	10.2	0.9	0.5	1.0	0.63	0.04	0.00	0.4	-2.6	
J254/W3528	469	18.34069		-19.93478					-0.7	8.5	1060	0.4	3.3	4.8	0.1	10.1	0.4	0.1	1.4	0.83	0.04	0.00	0.1	-2.4	
J254/W3527	470	16.67179		-21.35236		27.0	104	34	0.1	8.0	1220	1.5	3.0	3.4	0.2	10.2	0.1	1.2	0.8	0.30	0.03	0.01	0.5	-2.3	
J254/W3527	471	16.64107		-21.34511			101	27	0.4	7.8	1200	1.3	3.0	3.5	0.4	10.7	0.2	0.9	0.5	0.77	0.06	0.02	0.4	-1.8	
J253/W4448	472	16.67630		-21.43659		26.2	101	55	-0.7	7.2	1190	2.0	3.0	2.9	0.3	10.9	0.7	0.2	0.8	0.85	0.03	0.01	0.7	-2.3	
W2/Y778	473	18.60427		-19.61629			56	5	-1.9	7.4	1130	1.7	2.5	3.4	0.1	10.6	0.2	0.4	1.1	0.68	0.04	0.01	0.7	-2.4	
B230/Y3368	474	18.44338		-19.59783					0.4	7.4	1230	1.9	2.8	3.3	0.0	10.9	0.1	0.4	1.3	0.55	0.04	0.00	0.7	-2.7	
J189/Y2376	475	17.14779		-21.73007			73	52	-1.6	7.9	1110	1.3	2.9	3.4	0.4	10.8	0.1	0.3	1.5	0.87	0.06	0.01	0.5	-2.1	
B183/Y3066	476	18.21497		-19.87862					-0.7	7.8	1130	1.6	3.2	3.2	0.0	11.1	0.0	0.0	1.7	0.70	0.02	0.00	0.5	-2.6	
B987/Y3388	477	18.64107		-19.57790					-0.1	7.5	940	1.1	2.9	2.8	0.0	9.6	0.5	0.0	0.2	0.67	0.08	0.01	0.4	-2.1	
B189/Y3030	479	18.28887		-20.00181			35	27	1.7	9.0	830	0.2	2.8	3.9	0.5	9.3	0.3	0.0	0.2	0.40	0.04	0.00	0.1	-2.3	
J85/Y173	480	17.49232		-21.61685			107	70	2.2	8.2	1070	1.3	2.7	3.5	0.5	9.8	0.4	0.1	0.8	0.80	0.02	0.00	0.5	-2.5	
J187/2/Y2330	481	17.28023		-21.64493			165	79	-1.8	7.8	980	1.4	2.4	3.4	0.4	10.0	0.4	0.4	0.5	0.88	0.03	0.01	0.6	-2.3	
D172/W1618	482	16.86180		-20.99004			73	31	0.0	7.5	930	1.4	2.1	3.7	0.3	10.0	0.1	0.4	0.3	0.88	0.10	0.01	0.7	-2.1	
J118/W9923	483	18.17562		-21.42572			91	61	-1.1	7.5	980	1.7	1.8	3.7	0.3	9.3	0.4	0.4	0.7	1.08	0.04	0.01	0.9	-2.2	
D402/Y366	484	18.23992		-21.15670			41	11	-1.5	7.3	910	1.2	2.1	3.4	0.3	9.1	0.3	0.0	0.7	0.88	0.07	0.01	0.6	-2.0	
B1777/Y3329	485	18.06334		-19.77264			85	64	1.3	8.0	1040	1.8	2.2	3.3	0.2	9.3	0.7	0.0	0.5	0.42	0.02	0.00	0.8	-2.9	
W8/Y829	486	17.47333		-20.64796			123	69	-0.1	7.6	1300	2.5	2.6	2.7	0.9	9.3	0.4	2.5	1.3	1.25	0.05	0.01	1.0	-2.4	
W9/Y842	487	17.81183		-20.56837			81	52	-1.5	7.4	1170	2.3	2.6	2.8	0.1	9.8	0.2	1.9	1.0	0.87	0.04	0.01	0.9	-2.4	
W9/Y840	488	18.26186		-20.39819			138	104	-0.6	7.5	1020	2.3	2.1	3.1	0.1	9.5	0.3	0.7	1.0	0.92	0.04	0.01	1.1	-2.4	
D402/Y360	489	18.29367		-21.17301			39	9	1.0	7.9	970	2.1	2.1	3.2	0.1	9.6	0.4	0.2	0.7	1.00	0.06	0.01	1.0	-2.3	
J87/W174	490	17.50000		-21.72917			61	27	1.8	7.2	970	1.8	2.0	2.9	0.3	9.2	0.2	0.2	0.5	0.92	0.04	0.00	0.9	-2.7	
W3/Y792	491	18.26770		-20.18914			121	19	-1.1	7.0	870	1.9	1.8	2.4	0.2	9.8	0.1	0.1	0.4	1.05	0.01	0.01	1.1	-2.2	
D380/W1654	492	17.13724		-20.87953		26.6	91	70	1.4	7.4	870	2.0	1.8	2.7	0.3	9.6	0.1	0.2	0.3	1.15	0.05	0.02	1.1	-2.1	
D131/W2072	493	16.67562		-20.81793			34	25	-1.4	8.0	850	2.3	0.8	3.3	0.2	9.4	0.1	0.1	0.3	0.58	0.17	0.01	2.9	-2.7	
B800/Y4481	494	17.62764		-19.86322					-1.6	7.4	980	2.6	1.4	2.3	0.1	10.1	0.1	0.3	0.4	0.63	0.02	0.00	1.8	-2.4	
B486/W760	495	17.19002		-19.89221			64	40	-1.9	7.6	1090	3.3	1.4	3.2	0.2	8.6	1.1	1.1	1.3	0.58	0.02	0.00	2.4	-2.4	
B802/Y4480	496	17.64012		-19.84601			61	24	-1.9	7.6	990	3.7	1.6	3.3	0.1	9.4	0.6	2.5	1.5	0.50	0.03	0			



name	No	dec. longitude	E	dec. latitude	S	Temp. (°C)	depth (m)	level (m)	error (%)	pH	ec (µS/cm)	mmol/l													log Sr <sup>2+</sup> :Ca <sup>2+</sup>
												Ca <sup>2+</sup>	Mg <sup>2+</sup>	Na <sup>+</sup>	K <sup>+</sup>	HCO <sub>3</sub> <sup>-</sup>	SO <sub>4</sub> <sup>2-</sup>	NO <sub>3</sub> <sup>-</sup>	Cl <sup>-</sup>	Si	F	Sr <sup>2+</sup>	Ca <sup>2+</sup> :Mg <sup>2+</sup>		
D387Y669	500	17.36084		-20.85779			122	49	1.4	7.8	1350	1.7	2.2	7.1	0.3	11.6	0.6	0.3	1.7	0.97	0.07	0.03	0.01	0.8	-1.8
J248W3529	501	16.75432		-21.35326			114	55	-0.1	8.1	1600	1.4	3.3	7.0	0.3	11.5	0.9	0.8	2.8	0.95	0.04	0.01	0.1	0.4	-2.2
B248Y3818	502	18.60461		-19.46014			44	14	1.2	7.3	1430	0.9	3.6	7.2	0.1	11.9	0.5	1.4	1.7	0.82	0.03	0.01	0.3	0.3	-2.0
B218Y3345	503	18.45681		-19.70290			34	30	1.7	7.9	1580	2.3	3.1	6.5	0.1	11.4	0.5	0.8	3.4	0.52	0.04	0.01	0.7	2.7	-2.8
B188Y3034	504	18.23129		-19.90761			64	12	-0.2	7.9	1280	2.2	2.2	6.0	0.0	12.5	0.1	0.0	2.3	0.38	0.03	0.00	1.0	0.0	-2.8
B183Y3068	505	18.18714		-19.89493					-0.6	7.1	1880	2.7	3.3	8.1	0.0	14.0	0.5	1.4	3.8	0.62	0.03	0.01	0.8	0.8	-2.5
B242Y3375	506	18.50672		-19.54257			76	6	1.6	7.7	2260	1.8	5.6	8.0	0.0	13.5	0.4	5.1	4.2	0.85	0.06	0.02	0.3	0.2	-2.0
B172Y3007	507	18.07102		-19.94203			65	4	0.2	8.0	2210	2.0	5.3	7.5	1.2	15.1	0.7	1.3	5.4	0.93	0.03	0.01	0.4	0.4	-2.2
B248Y3383	508	18.58157		-19.50725			55	15	0.6	8.3	1240	0.6	3.2	7.6	0.1	14.8	0.1	0.0	0.1	0.37	0.06	0.01	0.2	0.2	-2.0
B987Y3390	509	18.64491		-19.51178					1.5	8.4	1200	0.3	3.3	7.4	0.1	13.3	0.3	0.0	0.3	0.67	0.08	0.00	0.1	0.1	-2.1
B246Y3385	510	18.60461		-19.52717					1.0	8.4	1250	0.6	3.5	7.0	0.1	14.0	0.2	0.0	0.1	0.87	0.14	0.01	0.2	0.2	-1.9
B246Y3386	511	18.64299		-19.50091			67	27	2.0	8.1	1440	0.8	3.5	8.7	0.0	14.2	0.7	0.1	1.0	0.80	0.11	0.01	0.2	0.2	-1.9
B212Y3342	512	18.31670		-19.64764					0.8	8.4	1510	0.2	4.1	8.7	0.0	15.8	0.3	0.0	0.8	0.77	0.09	0.01	0.2	0.1	-2.4
B987Y3391	513	18.64683		-19.51359					1.8	7.4	1370	0.9	3.8	6.6	0.1	13.2	0.4	0.1	1.4	0.87	0.03	0.00	0.1	0.2	-2.0
B248Y33815	514	18.51727		-19.48822			82	12	1.9	7.1	1280	1.4	3.8	5.7	0.1	13.7	0.4	0.2	0.7	0.67	0.03	0.01	0.4	0.4	-2.4
B230Y3367	515	18.42610		-19.61232					-0.8	8.1	1460	0.7	4.1	6.2	0.1	14.2	0.5	0.0	1.1	0.73	0.04	0.00	0.2	0.2	-2.5
B163Y3002	516	17.96449		-19.90489			86	55	-0.6	7.7	1570	1.3	3.9	6.5	0.3	16.0	0.1	0.6	0.9	0.50	0.03	0.01	0.3	0.2	-2.1
B3442Y4463	517	17.79175		-19.78080			85	67	0.1	6.6	2480	6.2	8.4	2.6	0.1	25.2	3.2	0.0	0.5	0.37	0.02	0.02	0.7	0.7	-2.5
B200Y3052	519	18.30518		-19.77264			43	1	-0.7	7.5	1820	1.8	5.8	3.7	2.6	18.6	0.7	0.6	1.1	0.50	0.03	0.01	0.3	0.3	-2.5
B200Y3051	520	18.30230		-19.77717			8	1	-0.5	7.3	2210	1.6	6.6	6.1	2.6	19.3	0.8	1.9	2.5	0.48	0.03	0.01	0.3	0.3	-2.5
B162Y2983	521	17.89923		-19.89221			41	24	0.3	6.8	2210	5.7	4.5	4.4	0.3	19.9	0.8	1.5	2.2	0.60	0.04	0.03	1.3	2.4	-2.4
B748Y3362	522	18.34741		-19.71739					-0.3	7.2	1300	2.4	3.0	2.8	0.0	12.6	0.1	0.1	1.0	0.46	0.05	0.02	0.0	0.8	-2.8
B242Y3373	523	18.52879		-19.52808			44	9	-1.8	8.0	1090	1.3	3.1	3.3	0.1	12.0	0.1	0.0	0.1	0.58	0.05	0.01	0.4	0.4	-2.1
B227Y4526	524	18.35509		-19.56612			43	29	-1.6	7.9	1120	1.5	3.1	3.3	0.1	12.0	0.1	0.5	0.5	0.58	0.03	0.00	0.5	0.5	-2.6
B801Y4479	525	17.63436		-19.76993					-1.3	7.2	1360	1.7	3.5	4.3	0.3	12.2	0.8	0.7	1.0	0.93	0.04	0.00	0.5	0.6	-2.6
J179W4604	526	16.78407		-21.65217			116	73	1.9	6.9	1310	2.2	3.9	3.0	0.1	12.1	0.5	0.6	1.1	0.95	0.02	0.01	0.6	0.6	-2.4
J259W4503	527	16.76104		-21.58967			61	1.3	7.9	1280	2.2	3.7	3.6	0.2	11.6	0.6	0.4	1.8	0.88	0.02	0.01	0.6	0.6	-2.4	
J259W4504	528	16.78791		-21.57065			73	49	1.5	7.3	1220	1.6	4.2	3.5	0.2	11.9	0.4	0.7	1.5	0.80	0.02	0.01	0.4	0.4	-2.3
B168Y3013	529	18.03551		-20.04710					-0.9	7.9	1210	1.5	3.5	3.3	0.2	11.6	0.4	0.0	1.2	0.65	0.03	0.01	0.4	0.4	-2.4
W3/Y793	530	18.25315		-20.21900			121	71	-0.8	7.0	1480	4.1	2.3	4.5	0.3	13.5	0.6	0.1	3.0	0.80	0.01	0.01	1.8	2.5	-2.5
B220Y3350	531	18.45969		-19.78623					-1.7	7.2	1740	1.7	5.8	5.0	0.1	13.2	1.0	3.1	2.2	0.80	0.07	0.01	0.3	0.3	-2.1
B180Y3021	532	18.09885		-19.91757					1.9	7.7	1440	2.2	4.3	4.0	0.1	13.7	0.4	0.0	2.0	0.88	0.04	0.01	0.5	0.5	-2.4
B215Y3366	533	18.34069		-19.62138			36	11	-1.0	7.3	1510	1.8	4.1	4.3	0.0	12.9	0.4	0.9	1.8	0.50	0.03	0.00	0.4	0.4	-2.7
B166Y2983	534	17.97793		-19.97011			152	61	-0.1	7.7	1460	1.8	4.1	4.1	0.3	13.3	0.4	0.0	2.2	0.25	0.03	0.01	0.4	0.4	-2.3
B248Y33811	535	18.54127		-19.45924			60	30	-1.5	7.2	1080	1.1	4.1	3.2	0.0	13.0	0.3	0.0	0.5	0.80	0.03	0.01	0.3	0.2	-2.1
J246Y2153	536	16.82726		-21.56975			108	70	-1.4	7.5	1040	1.4	4.1	2.0	0.2	12.4	0.1	0.5	0.5	0.83	0.02	0.01	0.4	0.4	-2.3
B227Y4529	537	18.37236		-19.58062			25	6	-1.2	7.3	1120	1.3	4.1	2.1	0.0	12.9	0.1	0.0	0.2	0.68	0.04	0.01	0.3	0.3	-2.3
B216Y3347	538	18.39827		-19.68388			34	30	-1.5	7.5	1390	1.5	4.7	2.6	0.1	13.0	0.1	0.5	1.7	0.68	0.05	0.01	0.3	0.3	-2.3
B167Y3016	539	18.01440		-20.02899					1.8	7.6	1410	1.9	4.7	3.0	0.2	12.9	1.0	0.1	1.0	0.32	0.03	0.01	0.4	0.4	-2.3
B166Y2982	540	17.97889		-19.98913			73	53	-1.9	7.6	1410	1.7	4.5	2.9	0.2	13.1	0.9	0.0	1.2	0.32	0.03	0.01	0.4	0.4	-2.2
B3443Y4468	541	17.71881		-19.82156					-0.2	7.2	1490	2.2	4.9	2.9	0.2	14.0	1.3	0.4	0.5	0.50	0.02	0.01	0.5	0.5	-2.3
B3443Y4467	542	17.75240		-19.82428					0.1	7.3	1610	2.6	5.3	2.8	0.1	13.9	1.8	0.6	0.7	0.57	0.02	0.01	0.5	0.5	-2.3
B3443Y4466	543	17.74952		-19.81703					1.9	7.1	1540	2.6	4.9	2.6	0.0	13.4	1.7	0.0	0.4	0.55	0.02	0.01	0.5	0.5	-2.3
B5663Y4488	544	17.60269		-19.75543					-0.1	7.4	1140	2.3	3.6	2.0	0.1	13.4	0.2	0.0	0.4	0.48	0.02	0.00	0.6	0.6	-2.8
B508Y4495	545	17.52207		-19.75272					-0.7	7.3	1230	2.5	3.6	2.1	0.2	12.9	0.8	0.0	0.1	0.60	0.02	0.01	0.7	0.7	-2.4
B801Y4477	546	17.70058		-19.79891			91	55	-0.7	7.3	1230	2.5	3.6	2.1	0.2	12.9	0.8	0.0	0.1	0.60	0.02	0.01	0.7	0.7	-2.4
B3441Y3316	547	17.83589		-19.83243			46	29	0.8	7.9	1150	2.3	4.7	1.5	0.1	13.0	0.8	0.2	0.7	0.48	0.03	0.01	0.5	0.5	-2.3
B192Y3049	548	18.25816		-19.81522			79	4	-1.8	7.2	1210	2.2	4.1	1.5	0.0	14.1	0.1	0.0	0.5	0.60	0.02	0.00	0.5	0.5	-2.9
B161Y3000	549	17.91267		-19.83696					-0.7	7.6	1410	2.0	4.9	2.0	0.1	14.0	0.9	0.1	0.4	0.42	0.03	0.01	0.4	0.4	-2.4
B202Y3037	550	18.36468		-19.89764					0.6	7.5	1660	1.9	5.3	3.6	0.1	11.2	0.1	3.7	3.0	0.97	0.03	0.01	0.4	0.4	-2.4
B228Y4531	551	18.34741		-19.55525					1.3	7.3	1640	2.1	4.7	3.9	0.0	11.5	0.8	0.2	3.8	0.42	0.03	0.00	0.4	0.4	-2.7
B195Y3431	552	18.16507		-19.67029			85	43	-1.2	7.2	1550	1.9	4.9	3.0	0.0	12.1	0.1	0.7	4.2	0.63	0.02	0.00	0.4	0.4	-2.8
B182Y3028	553	18.21017		-19.94293			67	1	-0.5	7.8	1820	1.9	5.8	4.1	0.9	11.9	1.2	2.2	4.2	0.83	0.03	0.00	0.3	0.3	-2.6
B227Y4527	554	18.35701		-19.56975			46	9	1.3	7.6	1440	2.0	5.1	2.4	0.1	11.5	0.0	2.6	2.3	0.68	0.03	0.01	0.4	0.4	-2.5
B195Y3433	555	18.17658		-19.69475			61	46	1.3	7.7	1440	1.8	5.3	2.0	0.0	11.7	0.2	1.0	3.0	0.37	0.02	0.00	0.3	0.3	

Annex B

B-10

name	No	dec. longitude	E	dec. latitude	S	Temp.	depth	level	error	pH	ec	Ca <sup>2+</sup>	Mg <sup>2+</sup>	Na <sup>+</sup>	K <sup>+</sup>	HCO <sub>3</sub> <sup>-</sup>	SO <sub>4</sub> <sup>2-</sup>	NO <sub>3</sub> <sup>-</sup>	Cl <sup>-</sup>	Si	F	Sr <sup>2+</sup>	Ca <sup>2+</sup> :Mg <sup>2+</sup>	log Sr <sup>2+</sup> :Ca <sup>2+</sup>
B174/Y4677	561	17.90595		-19.62228		46	9	-0.6	7.4	1550	2.6	4.9	2.5	0.0	13.3	0.2	1.0	3.1	0.35	0.03	0.00	0.5	-3.0	
B989/Y3357	562	18.40403		-19.76268		76	43	-1.1	7.1	1460	2.1	4.9	2.9	0.1	15.2	0.9	0.1	0.3	0.57	0.02	0.01	0.4	-2.5	
B344/ZY4462	563	17.83397		-19.79257		61	46	0.7	7.4	1370	2.3	4.9	2.0	0.0	15.1	0.4	0.4	0.7	0.52	0.03	0.00	0.5	-2.7	
B199/Y3060	564	18.25240		-19.78080		67	34	2.4	7.5	1770	2.3	6.2	4.4	0.1	15.5	2.0	0.0	1.0	0.42	0.05	0.01	0.4	-2.4	
B195/Y3432	565	18.17658		-19.68931		61	37	-0.1	7.4	1370	1.6	6.0	1.3	0.2	15.8	0.1	0.2	0.5	0.67	0.03	0.00	0.3	-2.4	
B162/Y2994	566	17.91363		-19.88496		61	36	-0.7	7.9	200	0.5	0.1	1.1	0.1	1.3	0.0	0.0	1.2	0.13	0.02	0.00	4.9	-2.8	
B316/Y4501	568	17.64491		-19.47428		571	17.75624	-0.25906	7.8	230	0.5	0.2	1.3	0.2	2.0	0.0	0.0	0.8	0.20	0.03	0.00	2.9	-2.5	
B111/Y4736	569	18.14107		-19.48279		572	17.73033	-0.22736	8.1	240	2.13	183	-0.1	8.1	2.0	2.0	0.0	0.6	0.22	0.04	0.00	2.0	-2.3	
B977/Y3302	570	17.74952		-20.02717		573	17.93858	-0.20199	6.7	310	0.1	0.2	0.9	0.5	1.2	0.2	0.0	0.4	0.32	0.02	0.00	0.9	-2.2	
B974/Y3288	571	17.76624		-20.25906		574	17.76775	-0.30888	7.7	250	0.4	0.3	1.0	0.2	1.2	0.6	0.0	0.3	0.18	0.04	0.00	1.3	-2.5	
B974/Y3287	572	17.73033		-20.22736		575	17.63148	-0.11685	6.8	190	0.6	0.1	0.2	0.1	1.6	0.1	0.0	0.1	0.33	0.01	0.00	5.0	-2.9	
B986/Y2972	573	17.93858		-20.20199		576	17.71977	-0.205707	7.5	190	0.5	0.2	0.4	0.2	1.6	0.1	0.0	0.2	0.25	0.01	0.00	3.4	-2.6	
B973/Y3285	574	17.76775		-20.30888		577	18.29079	-0.1989402	7.1	190	0.7	0.1	0.0	0.0	1.6	0.1	0.0	0.0	0.02	0.02	0.00	6.3	-2.5	
B111/Y4736	569	18.14107		-19.48279		578	17.94338	-0.24909	6.8	220	0.4	0.2	0.4	0.3	1.5	1.8	0.0	0.4	0.75	0.03	0.00	1.8	-2.3	
B977/Y3303	579	17.73800		-20.06703		579	17.73800	-0.206703	7.9	220	0.8	0.1	0.6	0.2	1.7	0.0	0.1	0.6	0.23	0.02	0.00	8.8	-2.8	
B977/Y3301	580	17.77927		-20.06793		580	17.77927	-0.206793	8.0	200	0.6	0.4	0.3	0.2	1.7	0.0	0.0	0.6	0.28	0.02	0.00	1.6	-2.6	
B156/Y3294	581	17.84357		-20.02174		581	17.84357	-0.202174	7.8	230	0.6	0.3	0.6	0.2	1.7	0.1	0.1	0.6	0.35	0.02	0.00	2.0	-2.7	
B977/Y3300	582	17.80614		-20.05888		582	17.80614	-0.205888	7.4	160	0.5	0.1	0.5	0.2	1.4	0.0	0.0	0.5	0.15	0.02	0.00	4.3	-2.8	
B157/Y3289	583	17.84549		-20.06703		583	17.84549	-0.206703	7.8	190	0.5	0.2	0.5	0.2	1.5	0.0	0.0	0.6	0.20	0.03	0.00	2.3	-2.7	
B157/Y3291	584	17.89731		-20.12500		584	17.89731	-0.2012500	7.9	250	0.9	0.3	0.3	0.2	2.2	2.2	0.0	0.7	0.25	0.02	0.00	3.7	-2.9	
B158/Y3295	585	17.84741		-20.02083		585	17.84741	-0.202083	7.5	240	0.9	0.1	0.4	0.2	2.4	0.0	0.2	0.7	0.18	0.02	0.00	3.6	-2.6	
B158/Y3305	586	17.81382		-19.99457		586	17.81382	-0.1999457	7.8	280	1.1	0.3	0.4	0.2	2.4	0.0	0.0	0.7	0.28	0.02	0.00	3.6	-2.6	
B157/Y3291	587	17.81958		-20.03442		587	17.81958	-0.203442	7.9	260	1.0	0.2	0.5	0.3	2.3	2.3	0.0	0.7	0.18	0.02	0.00	4.3	-3.0	
D335/Y2491	588	17.41747		-20.37319		588	17.41747	-0.37319	7.3	270	0.9	0.1	0.6	0.1	2.4	0.0	0.1	0.1	0.60	0.01	0.00	11.6	-2.5	
D334/Y2489	589	17.39347		-20.39040		589	17.39347	-0.39040	7.0	70	0.8	0.1	0.7	0.1	2.6	0.1	0.1	0.1	0.48	0.01	0.00	7.1	-2.4	
B986/Y2973	590	17.97697		-20.21286		590	17.97697	-0.21286	6.9	250	0.3	0.2	0.9	0.5	2.2	2.2	0.0	0.1	0.3	0.65	0.00	1.7	-2.3	
D332/W3625	591	17.34741		-20.41576		60	21	-0.6	6.9	210	0.6	0.3	0.3	0.1	2.1	2.1	0.0	0.1	0.50	0.01	0.00	1.9	-2.4	
D332/W3624	592	17.34453		-20.41395		60	21	-0.6	7.5	210	0.8	0.1	0.4	0.1	2.1	2.1	0.0	0.2	0.57	0.02	0.00	5.6	-2.5	
B983/Y3293	593	17.33877		-20.42301		60	21	-1.3	7.0	210	0.7	0.1	0.4	0.1	1.9	1.9	0.0	0.2	0.53	0.04	0.00	5.3	-2.6	
B968/Y2959	594	17.60365		-20.26540		594	17.60365	-0.26540	7.5	230	0.5	0.2	0.6	0.3	2.1	2.1	0.0	0.2	0.22	0.02	0.00	2.4	-2.4	
B155/Y4454	595	17.75144		-20.00000		122	91	-0.7	7.5	210	0.6	0.2	0.3	0.2	2.1	2.1	0.0	0.2	0.17	0.01	0.00	2.5	-2.6	
B986/Y2975	596	17.98464		-20.16848		137	67	0.4	6.5	190	0.2	0.1	0.3	0.5	0.9	0.9	0.0	0.3	0.77	0.01	0.00	2.4	-2.6	
B980/ZY2978	597	17.89347		-20.25453		137	67	2.0	6.8	100	0.1	0.1	0.3	0.2	0.5	0.0	0.0	0.3	0.65	0.03	0.00	1.9	-2.1	
B980/ZY2977	598	17.85605		-20.25634		137	67	-2.0	7.2	140	0.1	0.1	0.7	0.2	0.9	0.1	0.0	0.4	0.38	0.03	0.00	1.9	-2.3	
B979/Y2964	599	17.83877		-20.23822		152	116	-1.3	7.0	140	0.1	0.1	0.5	0.2	0.7	0.1	0.0	0.2	0.43	0.02	0.00	1.3	-2.2	
B982/Y2970	600	17.85701		-20.18025		122	91	1.9	7.6	130	0.1	0.1	0.4	0.2	0.6	0.6	0.0	0.3	0.30	0.02	0.00	1.3	-2.2	
B975/Y2962	601	17.70537		-20.15851		152	119	0.7	7.0	160	0.2	0.1	0.4	0.3	0.8	0.8	0.1	0.1	0.32	0.02	0.00	1.7	-2.4	
B983/Y3292	602	17.87716		-20.14946		116	100	-1.0	7.1	170	0.3	0.5	0.2	0.2	1.2	1.2	0.0	0.6	0.23	0.02	0.00	0.5	-2.4	
B978/Y2967	603	17.83493		-20.11957		274	73	0.5	7.0	220	0.4	0.3	0.4	0.3	0.9	0.9	0.1	0.5	0.28	0.02	0.00	1.2	-2.3	
B979/Y2965	604	17.79367		-20.19203		152	116	-0.6	7.1	180	0.2	0.2	0.2	0.3	0.9	0.9	0.1	0.0	0.13	0.02	0.00	0.8	-2.2	
B978/Y2966	605	17.81190		-20.15217		137	97	-0.7	6.8	160	0.3	0.1	0.3	0.3	1.0	1.0	0.0	0.3	0.33	0.02	0.00	2.8	-2.4	
B986/Y2974	606	17.93378		-20.16938		137	97	0.7	6.8	160	0.3	0.1	0.3	0.3	0.9	0.9	0.1	0.0	0.25	0.04	0.00	2.1	-2.6	
B984/Y2989	607	17.89443		-20.07971		30	21	-1.8	7.0	150	0.2	0.1	0.3	0.3	0.9	0.9	0.1	0.0	0.17	0.01	0.00	1.9	-2.2	
B970/Y3756	608	17.66987		-20.19022		145	123	-0.3	6.7	150	0.2	0.1	0.3	0.3	0.8	0.8	0.1	0.0	0.02	0.02	0.00	3.8	-2.6	
B975/Y2963	609	17.72745		-20.19565		152	122	-1.3	7.3	110	0.1	0.0	0.4	0.3	0.8	0.8	0.0	0.1	0.02	0.02	0.00	0.0	-2.2	
B970/Y3755	610	17.62284		-20.16667		153	125	-0.6	6.7	130	0.2	0.1	0.2	0.2	0.8	0.8	0.0	0.1	0.08	0.01	0.00	1.9	-2.2	
B967/Y3754	611	17.58637		-20.19656		611	6.8	140	6.8	140	0.2	0.1	0.1	0.1	0.8	0.8	0.0	0.1	0.08	0.01	0.00	1.7	-2.2	
D332/W3626	612	17.33973		-20.41395		612	17.33973	-0.41395	7.7	100	0.4	0.1	0.1	0.1	1.0	1.0	0.0	0.1	0.28	0.01	0.00	3.2	-2.3	
B976/Y3760	613	17.68810		-20.08877		613	6.8	130	6.8	130	0.2	0.1	0.3	0.2	1.0	1.0	0.0	0.1	0.23	0.01	0.00	2.1	-2.3	
B976/Y3759	614	17.70345		-20.13859		614	6.6	130	6.6	130	0.2	0.2	0.2	0.2	1.0	1.0	0.0	0.1	0.20	0.01	0.00	1.0	-2.2	
B969/Y3758	615	17.60845		-20.07971		615	7.4	150	7.4	150	0.3	0.1	0.3	0.2	1.0	1.0	0.0	0.1	0.13	0.01	0.00	2.5	-2.3	
B967/Y3753	616	17.53935		-20.19837		616	6.8	160	6.8	160	0.3	0.1	0.3	0.2	1.1	1.1	0.0	0.0	0.08	0.01	0.00	2.5	-2.2	
B985/Y2979	617	17.93762		-20.13587		617	6.7	90	6.7	90	0.1	0.1	0.3	0.2	0.4	0.4	0.0	0.3	0.10	0.03	0.00	1.0	-2.4	
B982/Y2969	618	17.87332		-20.22373		220	99	-1.4	6.8	130	0.1	0.1	0.4	0.2	0.5	0.5	0.1	0.1	0.17	0.02	0.00	1.1	-2.2	
D327/W3621	619	17.28311		-20.47283		619	6.1	50	6.1	50	0.0	0.1	0.1	0.1	0.3	0.3	0.0	0.0	0.23	0.01	0.00	0.5	-1.9	
D291/Y2957	620	17.48464		-20.31612		620	6.9	70	6.9	70	0.0	0.0	0.0	0.2	0.2	0.2	0.0	0.1	0.28	0.03	0.00	1.3	-1.9	
D304/Y2952	621	17.49136		-20.36141		621	5.9																	

## Annex B

## B-11

name	No	dec. longitude	E	dec. latitude	S	Temp.	depth	level	error	pH	ec	mmol/l										log Sr <sup>2+</sup> :Ca <sup>2+</sup>			
												Ca <sup>2+</sup>	Mg <sup>2+</sup>	Na <sup>+</sup>	K <sup>+</sup>	HCO <sub>3</sub> <sup>-</sup>	SO <sub>4</sub> <sup>2-</sup>	NO <sub>3</sub> <sup>-</sup>	Cl <sup>-</sup>	Si	F		SP <sup>2+</sup>	Ca <sup>2+</sup> :Mg <sup>2+</sup>	
B985Y2981	622	17.96389		-20.12591			244	85	0.8	6.9	100	0.1	0.0	0.2	0.3	0.4	0.1	0.1	0.1	0.33	0.01	0.00	0.00	2.5	-2.3
B985Y2980	623	17.95585		-20.07699			110	104	0.4	6.6	100	0.1	0.1	0.2	0.3	0.6	0.0	0.0	0.2	0.30	0.03	0.00	0.00	1.9	-2.3
B978Y2968	624	17.76775		-20.12138			113	91	0.9	6.9	120	0.1	0.1	0.2	0.2	0.5	0.1	0.0	0.1	0.17	0.01	0.00	0.00	1.3	-2.0
B964Y3752	625	17.47313		-20.20199				6.6	-1.4	6.7	90	0.1	0.1	0.1	0.2	0.5	0.0	0.1	0.1	0.12	0.01	0.00	0.00	1.9	-2.4
B133W3750	626	17.38484		-20.21830				7.0	0.0	6.7	90	0.1	0.1	0.1	0.2	0.7	0.0	0.1	0.17	0.01	0.00	0.00	1.3	-2.2	
B982Y2971	627	17.82917		-20.18659			91	76	1.9	6.8	2210	2.0	1.8	4.4	5.8	2.5	0.9	7.1	5.6	0.50	0.02	0.01	0.1	1.1	-2.4
D334Y1Y2490	628	17.40403		-20.34478				6.8	0.3	8.2	730	0.6	0.1	4.7	0.1	1.5	0.1	0.2	0.46	0.04	0.01	0.00	7.9	-1.9	
D240Y1045	629	17.09981		-21.20380				7.6	-0.2	7.6	530	0.2	0.0	5.3	0.2	2.4	0.1	0.1	3.2	0.03	0.01	0.00	7.3	-2.0	
D190W1832	630	16.78023		-21.20652			152	37	-0.5	8.3	640	0.3	0.1	6.6	0.1	3.9	0.4	0.2	2.5	0.28	0.15	0.00	2.8	-2.0	
D287W2041	634	17.25432		-20.61141			91	61	0.2	7.2	800	1.2	0.3	5.0	0.2	5.3	0.8	0.0	1.9	0.50	0.10	0.01	4.0	-2.1	
J138W2168	635	17.79175		-21.41667			30	9	0.5	8.3	980	0.9	0.8	6.3	0.4	5.6	0.8	0.9	1.1	1.51	0.11	0.01	1.1	-2.2	
D100W2308	636	16.58829		-21.14221			75	49	-1.6	8.1	730	0.5	0.3	6.0	0.3	6.2	0.5	0.0	0.5	0.77	0.48	0.01	1.5	-2.0	
B971Y2961	639	17.66891		-20.30163				8.0	1.2	8.0	610	1.3	0.1	2.8	0.1	3.6	0.7	0.2	0.6	0.97	0.05	0.00	10.8	-1.3	
J229Y1Y219	640	17.56334		-21.49909				7.9	1.2	7.9	820	0.8	1.9	2.8	0.4	7.2	0.4	0.1	0.2	0.38	0.03	0.00	0.4	-2.3	
J147Y185	641	17.75048		-21.56793				7.5	-0.1	7.5	740	0.9	1.5	2.6	0.2	7.0	0.2	0.1	0.2	0.85	0.04	0.00	0.6	-2.4	
D240Y1045	642	17.61036		-20.93569			46	20	-0.1	7.5	770	1.1	1.5	2.6	0.2	6.3	0.3	0.5	0.7	1.38	0.06	0.01	0.7	-1.9	
D240Y1048	643	17.60777		-20.96286			30	13	0.2	7.9	800	1.3	1.8	2.5	0.3	7.0	0.3	0.6	0.8	1.26	0.08	0.01	0.7	-2.0	
D235Y1027	644	17.45489		-20.94746			49	24	-1.2	7.7	750	1.2	1.7	2.4	0.3	6.9	0.4	0.3	0.6	1.21	0.06	0.01	0.7	-2.0	
J245W4427	645	16.78311		-21.46920			146	67	-3.1	7.4	750	1.1	1.4	2.7	0.1	6.5	0.2	0.2	0.8	0.85	0.05	0.01	0.8	-2.2	
J126Y443	647	17.96161		-21.30616			30	6	-0.5	7.5	790	1.0	1.5	2.9	0.4	6.4	0.4	0.5	0.7	1.26	0.08	0.01	0.7	-2.1	
D231W3585	648	17.36564		-21.09783			30	14	-0.7	7.7	760	1.1	1.5	2.6	0.2	6.3	0.3	0.5	0.7	1.38	0.06	0.01	0.7	-2.2	
D234Y1084	649	17.45681		-21.03633			30	8	1.0	7.7	840	1.4	1.5	2.9	0.4	6.7	0.3	0.6	0.9	1.25	0.06	0.01	0.9	-2.0	
D232Y1081	650	17.40691		-21.12138			34	8	1.2	8.5	780	1.6	1.3	2.7	0.2	6.5	0.3	0.5	0.9	1.18	0.04	0.01	1.3	-2.3	
D229Y1089	651	17.43282		-21.17029			61	16	1.7	7.8	790	1.5	1.4	2.8	0.2	6.4	0.4	0.7	0.6	1.21	0.05	0.01	1.0	-2.2	
J122Y1672	652	18.07965		-21.41848			26	10	-2.0	7.6	750	1.3	1.4	1.9	0.3	7.2	0.1	0.2	0.3	1.28	0.06	0.01	0.9	-2.3	
J112Y1432	653	17.96161		-21.62319			57	18	-1.8	8.0	690	1.3	1.5	1.6	0.3	6.8	0.1	0.5	0.3	1.20	0.05	0.01	0.9	-2.3	
D227Y1108	654	17.55950		-21.17844			41	40	1.8	8.5	740	1.0	2.1	2.1	0.4	6.6	0.2	0.7	0.6	1.31	0.05	0.01	0.5	-2.0	
J128W2163	655	17.92898		-21.36594			24	4	0.2	8.0	710	1.1	1.4	2.3	0.4	6.5	0.2	0.4	0.5	1.50	0.08	0.01	0.8	-2.1	
J125Y431	656	18.01631		-21.33877			31	8	0.0	7.8	730	1.2	1.5	2.3	0.3	6.6	0.2	0.6	0.4	1.25	0.07	0.01	0.8	-2.2	
D216W3589	657	17.26967		-20.95743			61	61	1.9	7.6	820	1.5	1.6	2.2	0.2	6.8	0.2	0.5	0.6	1.55	0.06	0.01	0.9	-2.1	
D385W3604	658	17.26296		-20.86866				7.9	2.1	7.9	670	1.3	1.3	2.6	0.2	6.8	0.1	0.3	0.3	1.45	0.05	0.01	1.1	-2.2	
D385W3603	659	17.26296		-20.86413				8.0	1.2	8.0	650	1.3	1.3	2.4	0.2	6.7	0.2	0.3	0.3	1.45	0.06	0.01	1.1	-2.3	
D179W1645	660	17.13436		-21.07121			102	46	-1.3	7.5	610	1.3	1.0	2.3	0.2	6.4	0.2	0.2	0.2	1.07	0.05	0.01	1.4	-2.1	
J131Y1404	663	17.84933		-21.48007			10	1	0.0	7.6	990	1.6	1.6	3.2	0.9	6.7	0.4	1.4	1.6	1.07	0.05	0.01	1.1	-2.3	
D167W1684	664	16.94722		-20.94475			85	55	1.0	7.2	840	2.0	1.2	2.6	0.4	6.7	0.2	0.5	1.5	1.50	0.08	0.01	1.6	-2.4	
J35Y2358	665	17.06910		-21.63587			77	49	-0.5	8.4	700	0.8	1.5	2.4	0.3	5.3	0.1	0.8	1.3	1.13	0.04	0.00	0.6	-2.3	
J133W2152	666	17.83877		-21.38315			30	5	-1.0	8.1	620	0.8	1.3	1.9	0.3	5.3	0.1	0.3	0.5	1.46	0.06	0.01	0.6	-2.0	
J132W2156	667	17.88292		-21.40761			29	5	-1.0	8.1	650	0.8	1.4	2.0	0.4	5.8	0.1	0.3	0.5	1.43	0.06	0.01	0.6	-2.0	
D274W2119	668	17.88676		-21.27083			39	11	0.9	8.2	710	0.7	1.9	1.9	0.4	5.5	0.2	0.5	1.0	1.55	0.05	0.01	0.4	-1.9	
J148Y1774	669	17.81094		-21.68750			61	30	-2.1	7.4	750	1.5	1.4	1.7	0.3	6.4	0.1	1.0	0.5	1.05	0.05	0.01	1.0	-2.2	
J131Y1395	670	17.86564		-21.52899			37	12	-1.9	8.0	650	1.4	1.2	1.7	0.3	6.2	0.1	0.6	0.6	0.98	0.03	0.00	1.2	-2.5	
J239Y2143	671	17.01536		-21.43116			56	20	-1.7	7.9	590	1.2	1.2	1.4	0.2	5.7	0.1	0.4	0.3	1.08	0.03	0.01	1.0	-2.2	
J122Y1674	672	18.03455		-21.42029			26	10	-0.4	7.8	620	1.3	1.3	1.3	0.2	5.8	0.1	0.6	0.3	1.25	0.04	0.01	1.0	-2.4	
D279Y425	673	18.11708		-21.26359			33	6	-2.2	7.5	620	1.3	1.1	1.5	0.3	5.7	0.1	0.3	0.5	1.13	0.04	0.01	1.2	-2.3	
J169Y2088	674	17.09693		-21.46467			43	20	1.7	9.0	610	1.1	1.4	2.1	0.1	5.7	0.1	0.6	0.3	1.03	0.05	0.01	0.8	-2.3	
J163Y2106	675	17.27351		-21.40851			37	9	1.6	8.8	660	1.2	1.1	2.0	0.3	5.5	0.1	0.7	0.3	1.15	0.06	0.01	1.0	-2.3	
J229Y1Y218	676	17.59117		-21.51630			76	8	0.6	7.8	770	1.2	1.4	2.3	0.3	6.0	0.4	0.7	0.4	1.13	0.04	0.01	0.9	-2.3	
J230Y236	677	17.66411		-21.46467			49	24	-1.7	7.7	730	1.2	1.3	2.0	0.3	6.2	0.1	0.7	0.5	1.18	0.05	0.01	1.0	-2.3	
D249Y1122	678	17.62956		-21.15761			61	26	2.1	8.1	610	1.2	1.1	2.0	0.3	5.9	0.1	0.2	0.4	1.21	0.04	0.01	1.1	-2.2	
J230Y234	681	17.63532		-21.51087			61	12	-0.4	8.1	710	0.9	1.3	2.4	0.4	6.1	0.1	0.6	0.4	1.13	0.06	0.01	0.7	-2.3	
J158Y2122	682	17.14875		-21.51449			77	30	-0.8	8.4	640	1.0	1.2	2.3	0.3	6.1	0.0	0.5	0.4	1.02	0.04	0.01	0.8	-2.3	
J159Y2116	683	17.13532		-21.38406			59	9	-1.2	8.4	640	0.8	1.3	2.7	0.3	6.1	0.2	0.4	0.3	1.17	0.05	0.01	0.6	-2.0	
D256Y1145	684	17.65259		-21.15217			55	23	1.8	7.7	740	1.2	1.3	2.6	0.2	6.3	0.1	0.8	0.3	1.17	0.06	0.01	0.9	-2.2	
J168Y2080	685	17.05662		-21.39402			30	20	1.8	8.4	660	0.9	1.5	2.4	0.2	6.3	0.2	0.3	0.2	0.85	0.04	0.01	0.6	-2.1	
D229Y1094	686	17.44722		-21.18659			61	16	2.3	8.1	660	1.3	1.4	2.3	0.2	6.4	0.3	0.2	0.3	0.95	0.05	0.01	0.9	-2.2	
D286W3615	687	17.33685		-20.61594			61	30	-0.5	7.6	540	1.1	0.6	2.4	0.1	5.3	0.2	0.2	0.1	1.35	0.03	0.01	1.9	-2.1	
D286W3614	688	17.33301		-20.61594			61	30	-0.2	7.6	550	1.2	0.7	2.6	0.2	5.7	0.2	0.2	0.2	1.43	0.03	0.01	1.7	-2.2	

name	No	dec. longitude	E	dec. latitude	S	Temp. (°C)	depth (m)	level (m)	error (%)	pH	ec (µS/cm)	Ca <sup>2+</sup>	Mg <sup>2+</sup>	Na <sup>+</sup>	K <sup>+</sup>	HCO <sub>3</sub> <sup>-</sup>	SO <sub>4</sub> <sup>2-</sup>	NO <sub>3</sub> <sup>-</sup>	Cl <sup>-</sup>	Si	F	SP <sup>2+</sup>	Ca <sup>2+</sup> :Mg <sup>2+</sup>	log Sr <sup>2+</sup> :Ca <sup>2+</sup>
D162W1671	691	17.01344		-20.82337		27	213	1.5	7.6	600	1.2	1.0	2.6	0.2	6.0	0.1	0.1	0.2	0.4	1.41	0.14	0.01	1.2	-2.0
D149W2044	692	17.23321		-20.57880		55	117	-0.8	7.9	580	0.8	0.9	2.4	0.3	5.8	0.1	0.0	0.1	0.1	0.87	0.02	0.01	0.9	-1.9
D443Y568	694	17.91651		-21.02536		27	46	-0.1	7.5	670	1.7	0.7	2.2	0.1	5.2	0.1	0.5	1.3	1.33	0.03	0.03	0.00	2.4	-2.6
D233Y1069	696	17.48389		-20.97618		9	30	2.0	7.6	690	1.7	0.8	2.3	0.2	5.7	0.3	0.3	0.6	1.13	0.05	0.01	2.1	-2.4	
D106W2272	697	16.44050		-20.97373		34	55	0.5	7.6	710	1.6	1.2	2.2	0.1	5.5	0.9	0.0	0.4	0.58	0.03	0.01	1.4	-2.5	
D404Y691	698	17.54415		-20.87047				-0.6	7.9	960	0.9	1.4	4.6	0.4	6.2	0.4	0.6	1.9	1.20	0.07	0.01	0.7	-1.9	
D243Y1075	699	17.56238		-21.10507		15	46	0.6	8.3	860	0.9	1.4	4.4	0.3	6.6	0.3	0.5	1.5	0.95	0.04	0.01	0.7	-2.3	
D241Y1037	700	17.58637		-21.00725		30	13	-1.2	8.2	830	0.9	1.4	4.3	0.3	7.0	0.5	0.3	1.3	1.21	0.05	0.01	0.6	-2.0	
J135W2144	701	17.81382		-21.31703		31	12	0.0	8.0	1100	1.3	1.8	4.2	0.5	6.1	0.4	1.3	2.6	1.43	0.07	0.01	0.7	-2.0	
D219W1874	702	17.30230		-21.12319		29	61	0.4	8.2	910	1.0	2.1	4.4	0.4	6.8	0.8	0.6	2.0	1.46	0.03	0.01	0.5	-1.9	
D273Y1180	703	17.77543		-21.30344		20	12	-0.7	7.9	800	1.1	1.1	3.7	0.3	6.4	0.4	0.3	1.2	1.23	0.05	0.01	1.0	-2.3	
D244Y1061	704	17.58829		-21.04167		31	11	-0.4	8.3	840	1.0	1.6	3.7	0.3	6.5	0.6	0.2	1.5	1.26	0.04	0.01	0.7	-2.1	
J228Y1208	705	17.55470		-21.53261		82	9	-0.2	7.5	930	1.2	1.8	3.0	0.3	6.9	0.3	0.7	1.3	1.08	0.04	0.01	0.6	-2.1	
J111Y1423	706	17.95106		-21.56159		40	15	-0.4	7.7	840	1.0	1.7	3.3	0.5	7.0	0.2	0.5	1.2	1.20	0.08	0.01	0.6	-2.1	
J133W2151	707	17.88100		-21.36322		31	5	-1.9	8.1	840	0.9	1.6	3.1	0.4	6.4	0.2	0.7	1.3	1.41	0.06	0.01	0.6	-2.0	
D235Y1025	708	17.38868		-20.99366		18	0.8	8.3	7.6	760	0.8	1.6	3.5	0.2	6.6	0.2	0.4	1.0	1.17	0.11	0.01	0.5	-1.9	
J127Y1212	709	17.93378		-21.28351		43	10	2.0	8.0	970	1.1	2.0	3.9	0.5	7.1	0.5	0.7	1.2	1.56	0.11	0.01	0.5	-1.9	
D231W3587	710	17.36756		-21.12862		61	14	0.9	7.8	980	1.2	1.9	3.7	0.3	6.9	0.5	1.2	0.9	1.38	0.07	0.01	0.7	-2.2	
D203W3568	711	17.19674		-21.26812		47	11	1.8	7.6	840	1.2	1.7	3.7	0.3	7.5	0.5	0.3	0.7	1.46	0.05	0.01	0.7	-2.2	
D257Y1737	712	17.76296		-21.10870		55	9	1.4	7.9	860	1.0	1.1	5.1	0.3	6.9	0.5	0.6	0.8	1.23	0.13	0.01	1.0	-2.0	
D243Y1077	713	17.54798		-21.08786		46	15	2.3	8.4	880	1.4	1.2	4.7	0.3	7.0	1.0	0.1	0.7	0.92	0.04	0.01	1.1	-2.1	
D207W1864	714	17.18906		-21.15761		46	15	0.0	7.6	780	1.2	1.3	4.8	0.3	7.0	0.7	0.8	1.0	1.15	0.03	0.01	0.9	-2.1	
D256Y1143	715	17.64875		-21.10145		43	20	-1.5	7.7	850	1.1	0.9	4.8	0.3	7.5	0.4	0.4	0.6	1.21	0.04	0.01	1.3	-2.2	
D205W1869	716	17.11036		-21.11504		74	55	0.9	7.8	860	1.0	1.0	4.3	0.2	7.3	0.3	0.3	0.3	1.53	0.05	0.01	1.1	-2.1	
D232Y1080	717	17.41651		-21.09058		35	8	0.4	7.8	880	1.4	1.4	3.7	0.2	6.9	0.6	0.5	0.9	1.28	0.05	0.01	1.0	-2.1	
D234Y1028	718	17.45393		-20.99728		34	11	0.0	7.9	820	1.2	1.3	4.2	0.2	7.0	0.5	0.5	0.8	1.25	0.05	0.01	0.9	-2.1	
D201W1854	719	17.09117		-21.16395		73	37	-0.5	7.6	720	1.3	1.2	4.3	0.2	7.2	0.7	0.2	0.7	1.17	0.06	0.01	1.1	-2.0	
J161Y12091	720	17.15739		-21.34239		35	12	1.2	8.0	810	0.8	1.5	3.8	0.4	6.7	0.3	0.6	0.7	0.97	0.07	0.01	0.6	-2.0	
D192W1834	721	16.88196		-21.21105		107	43	-0.5	7.9	700	0.8	1.4	4.1	0.2	6.4	0.3	1.2	0.6	1.18	0.06	0.01	0.6	-1.8	
D206W1868	722	17.14107		-21.08424		60	43	0.2	7.8	660	1.1	0.9	4.1	0.2	6.7	0.5	0.2	0.6	1.28	0.03	0.01	1.2	-2.2	
D204W1847	723	17.20250		-21.23188		67	14	-0.1	7.6	650	1.0	1.0	3.9	0.4	6.6	0.3	0.4	0.7	1.25	0.07	0.01	0.9	-2.1	
D179W1644	724	17.17466		-21.01178		37	39	-2.2	7.6	740	1.1	1.0	3.9	0.3	6.6	0.4	0.5	0.9	1.26	0.03	0.01	1.0	-2.0	
J255W3526	725	16.70729		-21.29348		111	49	-1.5	7.8	1020	0.9	1.6	4.8	0.2	7.3	0.5	0.4	1.6	1.02	0.06	0.01	0.6	-2.3	
D404Y693	726	17.57006		-20.89221				1.7	7.6	1030	1.2	2.0	4.5	0.3	7.5	0.7	0.5	1.4	1.28	0.05	0.02	0.6	-2.3	
D237Y1031	727	17.49520		-20.96920				-0.2	7.6	910	0.9	1.8	4.6	0.3	7.8	0.4	0.9	0.8	1.36	0.06	0.01	0.5	-1.9	
D249Y1126	728	17.56718		-21.13496		46	23	1.5	8.3	960	1.2	1.4	5.1	0.5	7.9	0.3	0.6	1.3	1.35	0.06	0.01	0.9	-2.2	
D233Y1070	729	17.45777		-21.06431		30	9	1.7	7.8	1030	1.5	1.5	4.6	0.7	8.2	0.5	0.7	1.0	1.20	0.04	0.01	1.0	-2.0	
W10Y850	730	18.06208		-20.63620		84	55	0.4	7.8	970	1.4	1.4	3.9	1.0	7.4	0.2	0.5	2.1	0.83	0.04	0.01	1.1	-2.0	
D256Y1144	731	17.65259		-21.13768		34	15	-0.1	7.9	950	1.2	1.4	4.2	0.3	7.4	0.2	0.7	1.1	1.07	0.05	0.01	0.8	-2.1	
D180W1635	732	17.10173		-21.07246		86	40	0.6	7.6	960	1.6	1.2	4.3	0.3	7.4	0.4	0.3	1.4	1.17	0.05	0.01	1.3	-2.2	
D179W1643	733	17.16987		-21.04620		65	47	-0.8	8.2	900	1.5	1.3	4.2	0.3	7.6	0.5	0.1	1.5	1.23	0.04	0.01	1.2	-2.1	
D198W1838	734	17.00000		-21.23822		37	15	-1.0	7.5	840	1.6	1.5	4.0	0.2	7.9	0.3	0.4	1.7	1.03	0.03	0.01	1.0	-2.2	
D103W2307	735	16.61516		-21.10417		49	37	-1.1	7.8	890	1.6	1.5	3.9	0.1	7.2	0.3	0.8	1.5	0.80	0.06	0.02	1.1	-1.9	
J218Y1358	736	17.61708		-21.48370		33	9	1.2	8.3	700	1.0	1.6	2.9	0.3	5.9	0.4	0.4	1.0	0.63	0.06	0.00	0.7	-2.9	
J131Y1400	737	17.90403		-21.46558		37	9	0.8	8.2	710	1.0	1.4	3.0	0.3	6.0	0.2	0.7	0.9	1.08	0.05	0.01	0.8	-2.2	
J131Y1394	738	17.85797		-21.49728		34	9	-0.1	8.0	600	0.5	1.2	3.3	0.4	5.7	0.2	0.2	0.6	0.63	0.05	0.00	0.4	-2.1	
J163Y12105	739	17.27447		-21.39130		37	9	1.7	8.7	790	0.9	1.4	3.6	0.4	6.3	0.2	0.9	0.6	1.28	0.06	0.01	0.7	-2.1	
D216W3591	740	17.29559		-20.92754		98	76	-0.1	7.6	720	0.8	1.1	3.4	0.2	6.1	0.3	0.0	0.8	0.83	0.05	0.00	0.7	-2.4	
J231Y1231	741	17.61420		-21.58062		27	15	1.3	8.7	900	0.5	1.5	3.2	0.3	6.5	0.2	0.2	0.2	1.10	0.05	0.00	0.7	-2.4	
D216W3588	742	17.30230		-21.00091		76	15	-0.1	7.6	720	0.8	1.2	3.3	0.3	6.6	0.2	0.0	0.5	1.36	0.04	0.01	1.0	-2.0	
D291Y2958	743	17.56622		-20.33062		95	76	0.1	8.1	600	1.0	0.3	3.3	0.1	5.5	0.1	0.0	0.4	0.55	0.03	0.01	3.6	-1.9	
B99W3515	744	17.26008		-20.32246		47	17	7.6	7.6	720	0.9	0.7	3.9	0.2	6.1	0.1	0.1	0.7	0.85	0.03	0.01	1.4	-2.0	
D201W1853	746	17.07486		-21.15761		95	37	-0.6	7.4	590	1.2	0.6	3.3	0.3	6.7	0.1	0.0	0.5	0.65	0.05	0.01	1.9	-2.1	
J161Y12103	747	17.20729		-21.37500		37	24	1.5	8.7	750	1.0	1.5	3.3	0.3	7.3	0.2	0.4	0.5	0.95	0.07	0.01	0.7	-2.1	
D180W1637	749	17.11996		-21.03804		95	24	0.6	7.3	770	1.3	1.1	3.7	0.2	7.2	0.3	0.2	0.6	0.83	0.03	0.01	1.2	-2.1	
D166W1675	750	16.96257		-20.91757		85	67	-0.9	7.3	740	1.7	0.6	3.8	0.2	7.2	0.2	0.1	0.8	0.97	0.11	0.00	3.0	-2.6	
D380W1656	751	17.21209		-20.88134		26.4	91	52	-1.2	7.4	700	1.5	0.9	3.4	0.2	7.4	0.2	0.2	0.5	1.43	0.04	0.01	1.6	-2.3
D162W1670	752	17.02687		-20.81793		92	27	-0.8	7.6	620	1.1	0.8	3.1	0.2	7.0	0.1	0.1	0.0	1.85	0.22	0.01	1.4	-2.0	
J38Y2368	755	16.90499		-21.69656		208	6																	

name	No	dec. longitude	E	dec. latitude	S	Temp.	depth	level	error	pH	ec	Ca <sup>2+</sup>	Mg <sup>2+</sup>	Na <sup>+</sup>	K <sup>+</sup>	HCO <sub>3</sub> <sup>-</sup>	SO <sub>4</sub> <sup>2-</sup>	NO <sub>3</sub> <sup>-</sup>	Cl <sup>-</sup>	Si	F	Sr <sup>2+</sup>	Ca <sup>2+</sup> :Mg <sup>2+</sup>	log Sr <sup>2+</sup> :Ca <sup>2+</sup>
W3/Y794	757	18.26188		-20.12760		148	70	0.3	7.8	790	1.4	0.8	4.2	0.2	6.6	0.2	0.3	0.3	1.6	0.92	0.02	0.01	1.7	-2.3
B345/Y3281	759	17.64299		-20.36232		52	12	-0.4	8.0	1120	2.2	2.2	3.3	0.2	7.3	1.4	0.5	2.0	2.0	1.03	0.05	0.01	1.0	-2.2
D279/Y422	760	18.15067		-21.24094		91	30	-1.0	7.8	1080	2.0	2.2	3.3	0.1	7.3	0.5	1.6	2.1	0.88	1.00	0.03	0.01	1.1	-2.3
W9/Y841	761	17.80116		-20.57285		42	18	-0.5	7.8	1160	2.0	2.4	3.1	0.4	6.8	0.4	2.5	2.3	1.15	1.00	0.03	0.01	0.9	-2.4
J150/Y178	762	17.59789		-21.62500		59	18	-0.5	7.8	1160	2.0	2.4	3.1	0.4	6.8	0.4	2.5	2.3	1.15	1.00	0.03	0.01	0.8	-2.2
J122/Y1675	763	18.00480		-21.42754		61	21	-1.3	7.6	1150	1.6	2.3	3.5	0.5	7.2	0.5	1.8	2.1	1.12	1.00	0.06	0.01	0.7	-2.2
J231/Y225	764	17.64971		-21.54529		61	15	0.6	7.7	1130	1.9	2.3	3.5	0.3	7.2	0.2	2.4	2.1	1.26	0.08	0.01	0.1	0.8	-2.3
D267/Y620	765	17.93378		-21.11775		85	46	1.6	7.3	1210	2.6	2.0	4.3	0.2	8.5	0.6	1.6	2.0	0.65	0.05	0.01	1.3	-2.3	
W9/Y845	766	18.09408		-20.48688		58	45	1.6	7.1	1280	2.5	2.8	4.0	0.2	8.9	1.2	0.5	2.4	0.98	0.04	0.01	1.1	-2.8	
J28/W4509	767	16.69674		-21.61051		46	6	-1.0	7.1	1330	2.9	2.5	3.1	0.1	8.3	0.3	2.9	2.6	0.95	0.03	0.00	1.1	-2.8	
D280/Y376	768	18.09693		-20.99457		61	34	2.1	7.5	1540	2.6	3.7	4.1	0.6	8.7	0.6	3.1	3.4	1.33	0.06	0.02	0.7	-2.1	
D225/Y114	769	17.54798		-21.22645		125	12	0.1	7.2	1040	3.0	0.9	2.5	0.2	6.4	0.4	0.4	2.9	1.03	0.07	0.01	3.3	-2.4	
W11/Y860	770	18.19981		-20.71131		107	49	-0.8	7.5	1160	2.9	1.5	3.2	0.3	6.6	0.5	1.6	3.2	1.08	0.07	0.01	2.0	-2.4	
D183/W1617	771	16.92131		-21.04076		18	6	-1.5	7.7	1190	2.2	1.1	3.7	0.8	6.6	0.7	0.2	3.1	0.42	0.04	0.01	2.1	-2.6	
B984/Y2986	772	17.94242		-20.04529		39	12	-0.7	7.0	1270	3.9	1.1	2.6	0.2	7.8	0.2	0.8	3.9	0.57	0.04	0.02	3.6	-2.2	
B139/Y3776	773	17.40979		-19.98460		46	8	1.2	7.6	1480	2.9	4.1	0.9	0.4	6.1	0.6	0.8	1.9	1.28	0.05	0.01	0.8	-2.3	
D395/Y383	774	18.03839		-21.14040		179	53	0.6	7.2	1630	3.5	3.5	2.5	0.1	6.6	0.2	7.1	2.3	0.88	0.04	0.01	1.0	-2.5	
W10/Y849	775	18.14549		-20.61991		61	49	0.9	7.3	1390	2.5	2.9	2.6	0.3	6.6	0.3	3.9	2.3	1.18	0.03	0.01	0.9	-2.3	
J85/Y171	776	17.44050		-21.62138		30	14	-1.7	7.9	1040	2.2	2.2	1.6	0.3	5.8	0.1	1.8	3.1	1.26	0.04	0.01	1.0	-2.4	
D227/Y1107	777	18.00960		-21.39855		61	34	1.8	7.8	1290	2.6	3.5	1.4	0.4	6.2	0.2	4.2	2.7	1.28	0.05	0.02	0.7	-2.1	
D227/Y1106	778	17.54127		-21.19565		46	34	1.7	7.7	1080	2.1	2.9	1.4	0.4	6.2	0.1	3.1	1.9	1.18	0.05	0.02	0.7	-2.1	
D227/Y1107	779	17.54415		-21.19928		62	9	-1.4	8.0	970	1.9	2.5	1.0	0.2	7.4	0.5	0.0	0.8	1.18	0.03	0.01	0.8	-2.3	
J218/Y1360	781	17.67083		-21.41395		30	9	1.1	8.3	950	2.0	2.3	1.7	0.2	4.2	0.3	1.9	3.6	0.68	0.03	0.01	0.9	-2.4	
B156/Y3309	782	17.79846		-19.99275		26	15	-0.9	8.0	1100	3.5	1.0	1.8	0.5	3.0	0.4	4.0	3.4	0.63	0.02	0.01	3.6	-2.7	
W8/Y833	783	17.66149		-20.64706		168	18	-0.9	7.6	860	1.7	1.5	2.3	0.5	6.8	0.2	1.1	1.1	0.87	0.05	0.01	1.1	-2.3	
J84/Y1439	784	17.34549		-21.67663		69	18	0.0	7.1	820	1.6	1.7	2.0	0.5	7.0	0.2	0.7	1.1	0.93	0.02	0.01	0.9	-2.4	
J228/Y207	785	17.56046		-21.53533		98	27	1.5	7.2	990	1.8	2.1	2.2	0.2	7.4	0.1	1.1	1.0	1.08	0.04	0.01	0.9	-2.4	
J147/Y191	786	17.78311		-21.64130		76	73	0.0	7.3	880	1.7	1.8	1.8	0.2	7.6	0.5	0.0	0.8	0.90	0.02	0.00	0.9	-2.7	
J111/Y1428	787	17.97697		-21.56431		23	13	-2.0	7.3	910	1.6	1.9	2.4	0.3	7.4	0.1	0.6	1.9	1.15	0.04	0.01	0.9	-2.4	
J148/Y1776	788	17.83493		-21.67391		61	30	-1.5	8.1	940	1.9	1.9	2.3	0.3	7.0	0.7	0.8	1.5	1.03	0.05	0.01	1.0	-2.3	
D385/W3605	789	17.26967		-20.86866		47	38	2.4	7.6	980	2.1	2.1	2.2	0.2	7.2	0.2	1.1	1.6	1.63	0.06	0.01	1.0	-2.2	
J84/Y1437	790	17.38292		-21.65761		64	43	-1.4	7.3	1190	2.0	2.8	1.8	0.5	7.4	0.1	2.8	1.8	1.10	0.03	0.01	0.6	-2.2	
J103/Y206	791	17.67946		-21.70924		49	18	-1.3	7.6	1070	1.6	2.6	1.3	0.5	6.9	0.1	2.1	1.3	1.20	0.09	0.01	0.6	-2.2	
D280/Y17373	792	18.12476		-21.04620		46	20	-2.1	7.3	1110	2.3	1.8	1.3	0.3	7.2	0.5	1.7	1.3	1.00	0.03	0.00	1.3	-2.7	
D156/W1892	793	16.98081		-20.75091		91	67	-0.4	7.5	840	2.7	1.1	2.4	0.2	7.2	0.1	1.5	1.4	1.33	0.02	0.01	2.5	-2.3	
B99/W3516	794	17.25624		-20.31884		75	57	1.0	7.5	940	2.6	1.0	2.0	0.2	7.4	0.4	0.1	1.0	0.67	0.02	0.02	2.5	-2.2	
D395/Y381	796	18.06430		-21.12591		79	49	-1.9	7.5	970	2.4	1.9	1.4	0.1	8.1	0.1	0.4	2.0	1.25	0.02	0.00	1.2	-2.7	
J172/Y2128	797	17.03935		-21.55978		21	20	-0.3	7.6	1080	2.9	1.5	2.3	0.3	6.3	0.2	2.7	2.1	1.28	0.04	0.01	1.9	-2.5	
D256/Y1146	798	17.66219		-21.15308		43	17	0.0	8.0	1100	2.6	1.7	2.3	0.2	6.8	0.2	1.4	2.3	1.28	0.06	0.01	1.5	-2.3	
W10/Y847	799	18.12415		-20.49955		108	55	-0.4	7.3	1020	2.3	1.8	2.1	0.2	7.3	0.1	1.1	2.0	0.70	0.02	0.01	1.3	-2.3	
B188/Y3035	800	18.24568		-19.92482		47	9	-1.9	7.3	1040	2.2	1.6	1.8	0.8	6.6	0.3	1.6	1.9	0.43	0.02	0.00	1.3	-3.0	
D277/Y417	806	18.04127		-21.27083		24	11	-1.5	7.6	920	1.7	1.6	2.4	0.3	5.8	0.4	1.1	1.9	1.08	0.04	0.01	1.0	-2.2	
D243/Y1078	807	17.50960		-21.09601		30	11	0.3	7.9	900	1.8	1.7	2.1	0.2	5.7	0.3	1.4	1.7	1.17	0.04	0.01	1.0	-2.2	
J105/Y1753	808	17.94818		-21.73279		73	24	0.0	7.7	880	2.0	1.8	1.5	0.3	6.0	0.2	1.5	1.4	0.90	0.07	0.01	1.1	-2.2	
J131/Y1399	809	17.87620		-21.47283		38	3	-1.0	7.5	780	1.9	1.4	1.8	0.2	5.8	0.1	1.3	1.4	1.17	0.04	0.01	1.4	-2.4	
D243/Y1079	810	17.50096		-21.11322		30	11	0.3	8.3	770	1.9	1.2	1.7	0.2	5.8	0.1	0.8	1.2	1.36	0.04	0.01	1.5	-2.3	
D233/Y1072	811	17.43762		-21.11413		46	9	1.8	7.9	840	1.8	1.4	2.2	0.2	6.1	0.2	0.7	1.4	1.28	0.04	0.01	1.3	-2.3	
D398/Y385	812	18.10173		-21.10960		46	30	2.4	7.8	940	2.7	2.1	0.9	0.1	5.9	0.1	2.7	1.3	1.25	0.02	0.00	1.3	-2.9	
D280/Y17374	813	18.11900		-21.04167		64	20	-2.0	7.3	1040	2.4	2.2	1.3	0.1	6.6	0.2	2.8	1.3	0.97	0.03	0.01	1.1	-2.7	
B121/W3498	814	17.33493		-20.01540		55	43	-1.8	7.4	790	1.5	2.2	0.4	0.4	5.0	0.3	1.1	1.4	0.72	0.03	0.02	2.2	-2.1	
J187/W2329	815	17.30998		-21.66123		37	9	0.9	7.8	680	1.2	2.1	1.4	0.2	4.8	0.9	0.0	1.4	0.52	0.03	0.00	0.6	-3.3	
J144/Y1386	816	17.78119		-21.57246		31	0	1.3	9.6	310	0.1	1.5	0.5	0.0	3.3	0.0	0.0	0.2	0.02	0.01	0.00	0.1	-2.5	
B593/Y3442	817	18.26296		-19.54620		46	30	-1.9	7.6	500	0.8	1.7	0.2	0.0	5.0	0.1	0.1	0.2	0.27	0.08	0.00	0.5	-2.8	
B41/Y14808	818	18.02687		-19.63949		46	9	-2.1	8.4	400	0.3	1.8	0.7	0.0	4.6	0.1	0.0	0.4	0.42	0.02	0.00	0.2	-2.5	
B752/Y4824	819	17.53071		-19.58333		46	37	-0.5	7.6	700	1.3	0.6	1.7	0.1	5.0	0.1	0.3	0.3	1.07	0.02	0.01	1.9	-2.3	
B192/Y173048	820	18.26488		-19.83062		64	37	-0.5	7.6	700	1.3	0.6	1.7	0.1	5.0	0.1	0.3	0.3	1.07	0.02	0.01	1.9	-2.3	
D287/W2039	826	17.25048		-20.63225		47	30	-0.4	7.8	490	1.1	0.6	1.9	0.2	4.9	0.1	0.1	0.1	1.38	0.03	0.03	0.01	1.7	-2.2
D286/W3616	827	17.33973		-20.61594		47	30	-0.4	7.8	490	1.1													

name	No	dec. longitude	E	dec. latitude	S	Temp. (°C)	depth (m)	level (m)	error (%)	pH	ec (µS/cm)	Ca <sup>2+</sup>	Mg <sup>2+</sup>	Na <sup>+</sup>	K <sup>+</sup>	HCO <sub>3</sub> <sup>-</sup>	SO <sub>4</sub> <sup>2-</sup>	NO <sub>3</sub> <sup>-</sup>	Cl <sup>-</sup>	Si	F	Sr <sup>2+</sup>	Ca <sup>2+</sup> :Mg <sup>2+</sup>	log Sr <sup>2+</sup> :Ca <sup>2+</sup>
J115/Y1699	831	18.09117		-21.503623			33	13	2.3	7.6	590	1.9	0.7	1.3	0.1	4.9	0.1	0.7	0.5	1.28	0.02	0.00	2.8	-2.7
D234/Y1085	833	17.41171		-21.03623			30	8	1.5	7.9	650	1.8	1.0	1.3	0.1	5.6	0.1	0.5	0.6	1.31	0.06	0.01	1.8	-2.2
J169/Y2090	834	17.05182		-21.46105			49	10	0.7	8.6	560	1.1	1.3	1.3	0.2	5.3	0.1	0.5	0.2	1.13	0.05	0.01	0.8	-2.3
J169/Y2095	835	17.04990		-21.43297			31	13	0.8	8.3	570	1.0	1.2	1.5	0.2	5.2	0.1	0.5	0.2	1.13	0.04	0.01	0.9	-2.3
J159/Y2120	836	17.14012		-21.44112			49	15	-1.3	8.4	540	0.8	1.2	1.6	0.2	5.2	0.1	0.5	0.3	1.07	0.04	0.01	0.7	-2.1
J131/Y1402	838	17.85509		-21.46196			37	5	-0.7	7.4	590	1.2	1.0	1.6	0.3	5.3	0.1	0.7	0.4	1.13	0.05	0.01	1.2	-2.2
J121/Y1694	839	18.02591		-21.44475			37	9	-1.9	7.8	570	1.3	1.1	1.0	0.2	5.2	0.0	0.7	0.3	1.21	0.03	0.01	1.2	-2.3
J121/Y1691	840	18.05566		-21.45833			36	18	-0.4	8.0	490	1.1	1.1	0.8	0.3	5.2	0.0	0.2	0.2	1.13	0.02	0.00	1.0	-2.4
D215/W2027	841	17.30134		-21.04438			17	14	-1.5	7.8	500	0.9	1.1	0.7	0.3	4.6	0.2	0.1	0.0	1.20	0.08	0.01	0.9	-1.9
J144/Y1381	842	17.73992		-21.55888			37	9	-0.2	8.0	460	0.4	1.5	1.5	0.2	4.2	0.3	0.0	0.7	0.55	0.04	0.00	0.3	-2.8
D99/W2578	843	16.56910		-21.14040			20	2	0.4	8.2	420	0.7	1.0	1.0	0.1	4.1	0.1	0.1	0.0	0.88	0.03	0.01	0.7	-2.0
J144/Y1385	845	17.77447		-21.55435			37	9	0.4	8.1	600	1.1	1.5	1.3	0.2	4.8	0.3	0.4	0.8	0.63	0.04	0.00	0.7	-3.0
B984/Y2988	846	17.89347		-20.04529			15	6	-1.2	7.6	620	0.9	0.8	1.4	1.0	4.9	0.2	0.3	0.3	0.48	0.05	0.00	1.1	-2.5
B514/Y4646	847	17.50576		-19.62953			46	24	-2.3	7.4	480	0.8	1.0	1.6	0.4	5.3	0.1	0.0	0.0	0.48	0.02	0.00	0.8	-2.7
B798/Y4632	848	17.44818		-19.62953					-1.2	7.6	510	0.8	1.3	1.7	0.0	5.6	0.1	0.0	0.2	0.43	0.03	0.00	0.6	-2.5
J146/Y4737	849	17.46737		-19.62591			91	46	0.2	7.8	500	0.8	1.1	1.9	0.0	5.5	0.1	0.0	0.0	0.43	0.02	0.00	0.7	-2.5
D149/W2047	852	17.97217		-20.04438			44	27	-1.1	8.2	660	1.2	1.3	1.5	0.2	5.7	0.2	0.4	0.3	0.42	0.04	0.00	1.0	-2.4
B166/Y2985	854	18.61397		-20.95475			134	105	-0.4	8.3	480	0.9	0.8	1.1	0.1	3.2	0.1	0.7	0.8	0.93	0.01	0.00	1.1	-2.4
W13/Y876	855	16.57965		-21.56884			104	1	0.0	7.6	460	0.9	0.7	1.4	0.4	3.7	0.1	0.1	1.1	0.30	0.01	0.00	1.1	-2.4
J22/W4557	857	17.02591		-20.98007			98	79	-0.3	7.4	1170	2.5	1.0	0.7	0.1	3.8	0.2	1.9	1.7	0.83	0.03	0.02	2.6	-2.2
D124/W2247	858	16.58253		-20.98007			75	40	2.0	7.8	550	1.9	0.4	1.2	0.1	3.4	0.1	0.9	1.1	0.75	0.05	0.00	4.3	-2.6
W13/Y874	864	18.60815		-21.15023			67	13	-0.6	7.3	460	1.3	0.6	1.2	0.1	4.5	0.1	0.1	0.4	1.13	0.02	0.00	2.3	-2.6
D123/W2257	866	16.57294		-20.91667			37	30	2.5	7.3	510	1.6	0.5	1.0	0.2	4.5	0.1	0.2	0.1	0.70	0.03	0.00	3.2	-2.6
D106/W2269	867	16.50576		-20.98551			30	18	0.8	7.6	480	1.5	0.6	0.8	0.1	4.2	0.0	0.0	0.7	0.60	0.12	0.01	2.4	-2.4
B166/Y3308	868	17.78407		-19.97645			26	15	1.1	8.0	390	1.6	0.4	0.9	0.2	4.2	0.0	0.0	0.2	0.33	0.02	0.00	3.6	-2.5
B158/Y3297	869	17.86084		-20.01902			3		0.1	7.4	380	1.5	0.4	0.6	0.2	2.8	0.1	0.3	1.1	0.32	0.02	0.00	4.3	-2.7
B158/Y3296	870	17.86084		-20.01087					0.7	7.5	400	1.8	0.3	0.5	0.2	3.3	0.2	0.4	0.7	0.38	0.03	0.00	6.6	-2.8
B157/Y3290	871	17.84261		-20.03633			37	20	0.3	7.6	400	1.6	0.3	0.6	0.2	3.5	0.7	0.1	0.6	0.25	0.03	0.00	5.6	-2.7
D160/W1681	872	16.87044		-20.81522			50	42	2.1	7.1	350	1.3	0.5	0.2	0.1	3.6	0.0	0.1	0.0	0.95	0.03	0.00	2.7	-2.8
D160/W1680	873	16.87236		-20.81975			75	38	-0.4	7.2	290	1.3	0.2	0.2	0.1	3.2	0.0	0.1	0.0	0.85	0.03	0.00	5.3	-3.3
D971/W2581	874	16.46353		-21.16214			13	6	1.0	7.6	380	1.5	0.2	0.2	0.1	3.0	0.1	0.2	0.3	0.42	0.03	0.01	6.2	-2.3
D123/W2256	875	16.57390		-20.96105			8	7	0.1	7.3	380	1.3	0.3	0.1	0.4	3.2	0.2	0.0	0.0	0.25	0.02	0.00	4.8	-2.7
D131/W2073	876	16.67658		-20.82246			11	3	-1.2	7.8	350	1.2	0.3	0.7	0.1	3.3	0.1	0.2	0.0	0.52	0.13	0.00	3.7	-2.5
D334/Y2488	877	17.39251		-20.39402			8		-0.6	7.3	400	1.5	0.2	0.7	0.1	3.9	0.1	0.1	0.1	0.53	0.02	0.01	9.3	-2.4
D128/W2074	878	16.64779		-20.85507			128	119	-0.1	8.1	370	1.3	0.2	0.7	0.2	3.7	0.1	0.0	0.0	0.50	0.01	0.00	5.5	-2.6
J22/W4552	879	16.58349		-21.55888			4	1	-1.7	7.0	390	1.2	0.4	0.2	0.4	3.8	0.1	0.0	0.2	0.50	0.01	0.00	2.8	-2.5
D149/W2049	880	17.10269		-20.57699					1.3	7.4	430	1.4	0.5	0.4	0.2	3.9	0.1	0.1	0.2	0.42	0.02	0.00	2.6	-2.7
B327/W781	881	17.29079		-19.79710			12	8	2.0	7.8	360	1.3	0.6	0.3	0.1	3.5	0.1	0.1	0.3	0.28	0.02	0.01	2.2	-1.9
B150/Y4445	882	17.61228		-19.98641					2.5	7.5	420	1.7	0.4	0.2	0.1	3.9	0.0	0.0	0.2	0.15	0.02	0.01	4.6	-2.1
B112/W3503	883	17.32917		-20.16486					-1.7	7.8	540	1.6	0.5	0.5	0.1	4.0	0.2	0.1	0.3	0.62	0.03	0.02	3.5	-1.8
B757/Y4988	884	17.74952		-19.66123					-1.5	7.8	550	1.7	1.3	0.1	0.1	6.0	0.1	0.1	0.0	0.23	0.02	0.00	1.3	-3.2
B46/Y4977	885	17.75528		-19.59149			68	55	-2.1	7.6	560	1.6	1.4	0.2	0.0	6.1	0.0	0.2	0.2	0.22	0.02	0.00	1.2	-3.5
B561/W778	886	17.27255		-19.75362			68	20	1.0	7.5	560	1.5	1.2	0.4	0.1	5.6	0.0	0.0	0.1	0.45	0.02	0.01	1.2	-2.4
B46/Y4978	887	17.70921		-19.59058			15	3	-1.4	7.6	510	1.5	1.2	0.2	0.0	5.6	0.1	0.0	0.1	0.17	0.02	0.00	1.2	-3.1
B46/Y4976	888	17.76104		-19.59420			117	49	-0.7	7.7	550	1.5	1.4	0.2	0.0	5.7	0.1	0.1	0.2	0.22	0.05	0.00	1.1	-3.7
B984/Y2990	889	17.91651		-20.02446			18	6	-1.2	7.8	620	1.0	1.5	1.0	0.1	5.9	0.1	0.0	0.2	0.47	0.05	0.00	0.7	-2.4
J98/Y2005	890	17.71401		-21.79801			71	55	-1.4	7.9	630	1.4	1.3	1.2	0.5	6.2	0.1	0.4	0.3	0.95	0.07	0.01	1.1	-2.3
J104/Y1765	891	17.86372		-21.70652			70	18	-0.2	7.9	620	1.4	1.4	1.1	0.3	6.4	0.1	0.4	0.2	0.90	0.06	0.01	1.0	-2.3
B579/W770	892	17.25432		-19.85326			61	46	1.2	7.7	560	1.4	1.3	1.1	0.3	6.4	0.1	0.0	0.2	0.53	0.01	0.01	1.0	-2.0
B600/Y4733	894	18.08061		-19.61775			61		-2.0	7.6	650	1.3	1.9	0.6	0.0	6.5	0.0	0.4	0.5	0.22	0.03	0.00	0.7	-3.1
B485/W3492	895	17.28407		-19.96286					0.1	7.8	740	1.5	1.1	0.8	0.7	6.6	0.1	0.0	0.1	0.28	0.02	0.01	1.4	-2.0
D394/Y613	896	17.95681		-21.13678			40	12	-0.4	8.3	750	1.4	2.1	0.7	0.5	6.3	0.1	1.4	0.4	1.30	0.06	0.01	0.6	-2.2
B202/Y3038	897	18.35693		-19.89674					0.1	7.5	840	1.3	2.6	0.8	0.3	6.5	0.1	1.6	0.6	0.80	0.02	0.00	0.5	-2.4
B171/Y3009	899	18.12476		-20.01359			91	43	-1.5	8.2	550	1.0	1.9	0.2	0.1	6.0	0.1	0.1	0.1	0.80	0.01	0.00	0.5	-2.4
J148/Y1771	900	17.82054		-21.66395			61	21	-1.9	7.8	860	1.8	1.7	1.4	0.4	6.7	0.1	1.7	0.5	1.07	0.06	0.01	1.0	-2.2
J103/Y203	901	17.68810		-21.67844			56	37	1.2	7.2	780	2.0	1.3	1.5	0.2	6.9	0.3	0.1	0.5	0.92	0.03	0.00	1.6	-3.0
D280/Y1378	902	18.16507		-21.01540			79	5	-1.2	8.0	810	2.0	1.6	1.3	0.1	6.8	0.2	1.0	0.6	0.82	0.03	0.00	1.2	-2.7
D280/Y1375	904	18.11324		-2																				

name	No	dec. longitude	E	dec. latitude	S	Temp.	depth	level	error	pH	ec	mmol/l					F	log Sr <sup>2+</sup> :Ca <sup>2+</sup>						
												Ca <sup>2+</sup>	Mg <sup>2+</sup>	Na <sup>+</sup>	K <sup>+</sup>	HCO <sub>3</sub> <sup>-</sup>			SO <sub>4</sub> <sup>2-</sup>	NO <sub>3</sub> <sup>-</sup>	Cl <sup>-</sup>	Si		
J148/Y1770	906	17.81862	-21.65942				50	20	-1.2	7.9	690	1.4	1.6	1.1	0.4	6.7	0.1	0.6	0.2	1.13	0.07	0.01	0.9	-2.0
J107/Y1741	907	17.95681	-21.63496				55	33	-1.0	7.9	660	1.6	1.4	1.3	0.3	6.8	0.2	0.1	0.2	1.07	0.08	0.01	1.2	-2.2
J107/Y1740	908	17.96393	-21.63859				76	37	-1.7	7.7	630	1.6	1.3	1.0	0.3	6.9	0.1	0.2	0.2	1.10	0.08	0.01	1.3	-2.3
D167/W1687	85	16.89060	-20.93478				85	55	0.7	7.3	640	1.8	1.4	0.6	0.5	7.3	0.0	0.1	0.0	1.21	0.06	0.01	1.3	-2.2
D178/W1647	911	17.13340	-20.98822				91	49	-1.6	7.6	600	1.4	0.8	2.0	0.3	6.0	0.1	0.5	0.2	1.50	0.08	0.01	1.7	-2.2
D178/W1646	912	17.14683	-20.95924			26.4	79	55	-0.9	7.5	610	1.7	0.8	1.8	0.2	6.2	0.1	0.3	0.3	1.17	0.03	0.01	2.1	-2.3
D288/W2037	913	17.20154	-20.63315				61	44	0.9	7.9	620	1.8	0.3	2.1	0.2	6.0	0.1	0.1	0.0	0.93	0.03	0.01	5.7	-2.5
D164/W1653	914	17.03071	-20.89221				71	37	-0.9	7.3	580	1.9	0.5	1.9	0.2	6.2	0.1	0.1	0.2	0.98	0.12	0.00	4.1	-2.6
J108/Y1746	915	17.89060	-21.68841				79	43	-0.5	8.0	630	1.8	0.9	1.7	0.3	6.7	0.1	0.2	0.2	0.82	0.04	0.01	2.1	-2.5
D131/W2070	916	16.70154	-20.78714				61	21	-1.9	7.7	660	2.0	0.6	1.9	0.2	7.1	0.2	0.0	0.0	0.88	0.02	0.01	3.4	-2.4
D157/W1695	917	16.89443	-20.76540				91	37	1.0	7.6	550	1.6	0.7	1.5	0.3	6.1	0.0	0.0	0.1	0.08	0.08	0.01	2.2	-2.1
B145/Y3785	918	17.57774	-20.05797				101	37	-0.7	7.7	600	1.9	0.6	1.7	0.1	6.5	0.1	0.0	0.3	0.27	0.02	0.01	3.1	-2.3
B46/Y4981	919	17.73033	-19.57065				101	37	-0.7	7.7	590	1.8	1.6	0.1	0.0	6.9	0.0	0.0	0.0	0.13	0.04	0.00	1.2	-3.1
B46/Y4979	920	17.70633	-19.59330				91	55	-1.3	7.4	630	2.2	1.3	0.1	0.0	7.1	0.0	0.0	0.1	0.17	0.03	0.00	1.7	-3.3
B488/W3484	921	17.37332	-19.81341				21	77	0.1	7.4	700	2.6	0.8	0.3	0.1	6.8	0.1	0.0	0.1	0.38	0.02	0.03	3.1	-2.0
B46/Y4980	922	17.70633	-19.58605				77	30	-1.8	7.3	610	2.4	0.9	0.1	0.0	6.9	0.0	0.0	0.1	0.17	0.04	0.00	2.7	-3.0
B46/Y4975	923	17.74376	-19.61232				95	24	-0.9	7.4	600	2.4	0.9	0.1	0.0	6.8	0.0	0.0	0.1	0.13	0.02	0.00	2.7	-3.0
B497/W774	925	17.31478	-19.82880				91	20	-1.9	7.4	730	2.3	1.5	0.7	0.2	6.7	0.8	0.0	0.5	0.53	0.01	0.01	1.5	-2.3
D166/W1674	926	16.97025	-20.86504				56	53	-0.1	7.4	580	2.3	0.8	0.4	0.2	6.7	0.0	0.1	0.1	1.15	0.07	0.01	2.9	-2.5
B578/W766	927	17.24472	-19.88859				32	18	0.6	7.5	600	2.1	1.0	0.7	0.1	6.6	0.1	0.1	0.2	0.52	0.01	0.01	2.2	-2.4
D163/W791	928	16.84165	-20.71467				70	18	0.7	7.5	600	2.4	1.0	0.7	0.1	6.8	0.1	0.2	0.5	0.67	0.04	0.01	2.4	-2.3
B485/W3495	929	17.33685	-19.97101				55	30	-0.9	7.2	880	2.5	0.9	0.8	0.2	6.6	0.2	0.4	0.7	0.82	0.02	0.02	2.6	-2.1
D324/W354	930	16.92706	-20.57609				70	15	0.4	8.0	710	1.9	0.9	1.1	0.1	6.4	0.1	0.2	0.1	0.75	0.07	0.01	2.1	-2.5
B158/Y3298	931	16.98848	-20.50725				70	15	0.4	7.2	700	2.0	1.2	1.3	0.1	6.5	0.1	0.6	0.4	0.40	0.08	0.00	1.7	-2.8
D149/W2045	932	17.87332	-19.98188				91	67	0.1	7.7	560	1.9	1.4	0.7	0.1	6.3	0.3	0.0	0.6	0.50	0.03	0.01	1.4	-2.5
D132/W2253	933	17.00960	-20.63225				49	12	-0.8	8.0	620	2.0	0.5	1.1	0.1	5.9	0.1	0.1	0.0	0.58	0.04	0.01	3.7	-2.4
B485/W3494	934	16.62380	-20.82790			40.0	61	30	1.2	7.6	610	2.0	0.5	1.4	0.1	6.2	0.0	0.0	0.0	0.77	0.11	0.00	4.1	-2.6
D361/W3522	935	17.29175	-19.97554				88	91	-0.7	7.7	600	1.8	0.8	1.3	0.2	6.0	0.6	0.0	0.0	0.52	0.02	0.02	2.5	-2.1
B117/W3500	936	17.24952	-20.05797				113	52	2.2	7.7	750	2.3	0.7	0.8	0.2	5.9	0.3	0.0	0.1	0.82	0.06	0.01	3.0	-2.5
D149/W2048	938	17.06334	-20.51721				37	30	-1.0	7.6	620	2.6	0.2	0.3	0.2	5.0	0.0	0.5	0.4	0.37	0.02	0.00	13.0	-2.8
B489/Y3784	940	17.48081	-19.93297				70	44	-1.4	7.1	540	1.7	0.6	0.4	0.3	5.3	0.0	0.1	0.1	0.97	0.03	0.00	2.8	-2.2
W3/Y790	941	16.32299	-20.01991				30	44	-1.4	7.1	540	1.7	0.6	0.4	0.3	5.3	0.0	0.1	0.1	0.97	0.03	0.00	2.8	-2.2
D215/W2028	942	17.29655	-21.01087				18	14	1.1	7.5	470	1.9	0.3	0.7	0.3	5.0	0.1	0.0	0.0	1.08	0.06	0.00	6.1	-2.6
D169/W1899	943	16.77735	-20.90851				70	43	1.1	7.7	490	2.1	0.5	0.7	0.2	5.1	0.1	0.2	0.4	0.70	0.02	0.01	4.3	-2.5
B336/W3506	944	17.16507	-20.02627				43	20	-1.6	7.3	630	2.0	0.3	0.4	0.3	5.2	0.1	0.0	0.1	0.58	0.02	0.00	6.1	-2.9
D160/W1678	945	16.88676	-20.82337				98	41	0.7	7.4	410	1.7	0.5	0.3	0.2	4.6	0.0	0.0	0.0	0.17	0.03	0.00	3.7	-3.0
B152/Y4447	946	17.69962	-20.00181				91	61	-1.8	7.3	480	1.6	0.4	0.4	0.2	4.7	0.1	0.1	0.0	0.33	0.01	0.01	3.6	-2.4
B151/Y4453	947	17.66027	-19.96558				107	46	0.0	7.3	510	1.7	0.6	0.3	0.1	4.8	0.1	0.0	0.0	0.33	0.02	0.01	2.7	-2.4
B798/I/Y4630	948	17.44818	-19.62862						-1.6	7.8	420	1.1	0.9	0.4	0.0	4.5	0.1	0.1	0.0	0.22	0.02	0.00	1.2	-3.2
B581/W776	949	17.28023	-19.78442				23	6	-0.2	7.6	450	1.4	1.1	0.3	0.1	4.9	0.1	0.1	0.2	0.60	0.02	0.01	1.3	-2.0
B155/Y4455	950	17.76967	-19.95833						-2.2	7.4	500	1.2	1.1	0.5	0.1	5.3	0.1	0.0	0.0	0.47	0.02	0.01	1.2	-2.0
B107/W2695	951	17.12860	-20.11866						-2.2	7.4	490	1.5	0.7	0.5	0.2	5.1	0.1	0.1	0.1	0.55	0.01	0.01	2.0	-2.3
D166/W1676	952	16.91843	-20.86141				61	49	1.8	7.1	580	2.7	0.4	0.4	0.2	6.2	0.0	0.2	0.0	0.98	0.03	0.00	6.9	-3.0
D129/W1688	953	16.73608	-20.88134				76	30	1.8	7.1	560	2.6	0.3	0.5	0.2	5.8	0.0	0.4	0.0	0.90	0.03	0.01	9.4	-2.6
B575/W761	954	17.18042	-19.95924				90	40	0.0	7.3	500	2.6	0.4	0.1	0.1	5.9	0.0	0.0	0.2	0.37	0.02	0.01	6.7	-2.4
B504/Y4983	955	17.53647	-19.80072						-1.0	7.5	590	2.4	0.7	0.3	0.1	5.9	0.1	0.5	0.2	0.55	0.02	0.01	3.5	-2.5
B99/Z/W3511	956	17.19674	-20.26993				98		-1.6	7.4	770	2.6	0.8	0.4	0.1	5.7	0.1	0.1	0.6	0.57	0.03	0.02	3.1	-2.1
B576/W655	957	17.18810	-19.93478						-0.7	7.2	750	3.0	0.8	0.3	0.1	5.7	0.2	0.8	1.1	0.28	0.02	0.01	3.9	-2.7
B159/Y3312	958	17.80518	-19.86685						0.5	7.8	500	2.9	0.2	0.1	0.0	5.6	0.0	0.0	0.5	0.48	0.03	0.01	18.3	-2.6
B138/Y3772	959	17.32917	-20.15580						0.9	7.2	860	3.5	0.3	0.3	0.1	5.5	0.2	1.4	0.6	0.57	0.03	0.02	13.4	-2.2
B114/W3501	960	17.48273	-19.99094						0.4	7.0	750	3.3	0.2	0.6	0.4	6.2	0.2	1.1	0.2	0.25	0.02	0.01	17.3	-2.8
D154/W1894	961	16.82630	-20.72645				44	23	2.1	8.2	670	3.1	0.6	0.4	0.2	6.2	0.1	0.6	0.7	0.67	0.02	0.01	4.8	-2.5
B106/W469	962	17.19194	-20.19384				40		-0.3	7.4	660	3.0	0.2	0.6	0.3	6.2	0.1	0.3	0.7	0.42	0.03	0.02	13.3	-2.1
B344/I/Y3315	964	17.78215	-19.84601				60	32	0.4	8.0	1500	5.8	2.1	1.1	0.1	8.4	1.1	3.7	2.6	0.48	0.02	0.01	2.8	-2.6
B344/I/Y3314	965	17.8023	-19.83696				46	30	0.3	7.9	1040	4.8	1.7	0.3	0.1	9.2	0.4	0.9	2.3	0.43	0.02	0.01	2.8	-2.6
B98/W472	966	17.07198	-20.18931				82	59	1.2	7.1	1170	5.9	0.6	0.5	0.1	8.4	0.3	2.4	2.0	0.33	0.03	0.02	10.2	-2.3
B336/W3505	967	17.15163	-20.05435				89	52	-1.7	7.4	1450	5.8	0.3	1.3	0.1	8.6	0.4	2.2	2.7	0.48	0.03	0.02	16.7	-2.4
B145/Y3787	968	17.56622	-20.02536						0.8	6.8	176													

name	No	dec. longitude	E	dec. latitude	S	Temp. (°C)	depth (m)	level (m)	error (%)	pH	ec (µS/cm)	mmol/l					F	SI	Ca <sup>2+</sup> ·Mg <sup>2+</sup>	Ca <sup>2+</sup> ·Mg <sup>2+</sup>	log Sr <sup>2+</sup> :Ca <sup>2+</sup>			
												Ca <sup>2+</sup>	Mg <sup>2+</sup>	Na <sup>+</sup>	K <sup>+</sup>	HCO <sub>3</sub> <sup>-</sup>						SO <sub>4</sub> <sup>2-</sup>	NO <sub>3</sub> <sup>-</sup>	Cl <sup>-</sup>
B489Y3783	969	17.47985		-19.93025					0.8	7.2	1180	4.6	0.7	2.2	0.3	9.0	0.5	0.6	2.3	0.20	0.01	0.02	7.0	-2.5
B152Y4448	970	17.70250		-19.96014			37	15	-1.9	7.2	1260	4.6	1.2	1.4	0.1	8.8	0.3	3.2	1.2	0.37	0.03	0.05	3.7	-2.0
B572W892	971	17.11996		-20.03442			30	30	-1.4	7.1	950	4.5	0.5	0.6	1.0	9.1	0.3	0.7	1.4	0.30	0.02	0.01	9.3	-2.5
B586Y4831	972	17.49616		-19.51178			70	20	-0.2	6.8	980	4.5	0.4	0.2	0.0	8.6	0.1	0.6	0.8	0.32	0.02	0.02	10.0	-2.5
B586Y4830	973	17.49844		-19.50815			70	20	1.8	6.8	1000	4.7	0.4	0.3	0.0	8.6	0.1	0.7	0.9	0.32	0.02	0.01	10.6	-2.5
B993W3513	974	17.29942		-20.25091					1.7	7.2	1300	5.0	0.7	0.8	0.2	8.4	0.3	1.7	1.4	0.77	0.03	0.02	6.6	-2.4
B94W468	975	17.04990		-20.15580			73	64	-0.7	7.0	970	5.1	0.5	0.5	0.2	8.9	0.2	1.7	1.2	0.43	0.03	0.01	9.4	-2.6
B144Y3762	976	17.53359		-20.06341			24	6	1.8	6.8	1040	5.0	0.6	0.5	0.1	8.9	0.3	0.5	1.5	0.42	0.03	0.03	8.1	-2.3
B758Y4639	977	17.50768		-19.64312			37	27	1.9	7.8	1100	4.0	1.7	0.6	0.0	7.7	0.1	1.2	2.6	0.27	0.01	0.00	2.4	-3.3
B99W459	978	17.24472		-20.21467			117	76	-0.9	6.9	900	4.0	0.8	0.8	0.1	7.6	0.2	0.8	2.0	0.37	0.03	0.04	4.9	-2.0
B151Y4451	979	17.65259		-20.02264			61	1	-0.7	7.6	1140	4.2	1.1	1.2	0.1	7.6	0.3	2.1	1.9	0.37	0.04	0.05	3.8	-1.9
B571W890	980	17.11132		-20.05163			40	30	-1.3	7.3	950	4.7	0.6	0.8	0.1	8.4	0.2	0.6	2.4	0.17	0.02	0.01	7.7	-2.5
B571W889	981	17.11036		-20.04710			37	37	-1.2	7.1	970	4.6	0.8	0.6	0.1	7.9	0.2	1.6	1.9	0.28	0.02	0.01	5.5	-2.5
B108W464	982	17.11719		-20.09239			52	35	-1.5	7.1	920	5.1	0.4	0.4	0.1	7.8	0.2	1.4	2.3	0.37	0.02	0.01	11.6	-2.7
D160W1677	983	16.93570		-20.81522			122	73	0.3	7.3	1080	3.6	1.6	1.2	0.3	6.2	0.1	3.6	1.8	1.26	0.04	0.01	2.3	-2.5
B993W3514	984	17.29655		-20.25453					-0.9	7.1	1320	4.4	0.7	1.0	0.3	5.6	0.3	3.6	1.9	0.80	0.03	0.02	6.3	-2.3
B580W783	985	17.28407		-19.83605			47	01	0.1	7.3	1020	3.5	1.2	1.0	0.2	5.5	0.1	1.5	3.3	0.37	0.02	0.01	3.0	-2.4
B135Y3764	986	17.48848		-20.06975			37	12	1.3	7.0	1330	5.2	0.8	1.8	0.1	5.9	0.9	3.2	2.7	0.72	0.04	0.02	6.7	-2.4
B144Y3761	987	17.52015		-20.06522			47	18	0.6	7.2	860	2.6	2.2	0.3	0.0	6.8	0.3	2.0	2.0	0.45	0.03	0.03	6.6	-2.2
B127W3502	988	17.35413		-20.15399			107	107	-1.2	7.2	1250	4.4	0.7	0.7	0.1	6.9	0.3	2.0	2.0	0.70	0.03	0.03	11.5	-2.2
B107W466	989	17.10461		-20.09149					-0.6	7.0	980	4.8	0.3	1.2	0.2	6.7	0.2	2.1	2.8	0.33	0.01	0.01	15.6	-2.6
W9Y839	990	18.26188		-20.35204			166	88	-0.4	7.3	970	3.4	1.6	0.7	0.1	8.3	0.1	1.4	0.9	0.93	0.04	0.01	2.1	-2.5
D254Y1116	991	17.65931		-21.19475			91	27	-0.3	7.3	1000	3.6	1.4	1.0	0.2	9.0	0.1	1.0	1.1	1.20	0.04	0.01	2.6	-2.4
D254Y1115	992	17.66411		-21.19565			91	27	1.9	7.5	1100	3.7	1.9	1.3	0.1	8.7	0.1	2.0	1.4	1.23	0.04	0.02	2.0	-2.4
B189Y3031	994	18.29750		-19.97373			47	18	2.3	7.3	1040	2.7	3.0	0.2	0.1	8.1	0.1	1.1	1.9	0.50	0.02	0.00	0.9	-2.8
B600Y4731	995	18.05182		-19.63496			73	18	0.6	7.2	860	2.6	2.2	0.3	0.0	8.7	0.0	0.4	0.6	0.50	0.03	0.00	1.2	-3.5
B317Y4865	996	17.74280		-19.51178			204	122	-2.1	7.2	960	2.8	2.2	0.3	0.0	8.7	0.1	0.9	1.1	0.20	0.03	0.01	1.3	-2.7
B181Y3024	997	18.19386		-20.00000			32	26	1.5	7.5	990	2.7	2.9	0.4	0.1	8.9	0.1	1.2	0.9	0.45	0.03	0.01	0.9	-2.7
B175Y3324	999	18.08349		-19.62138			61	18	0.2	7.5	900	2.6	2.1	0.7	0.0	8.2	0.0	1.0	0.7	0.42	0.03	0.00	1.3	-3.2
B175Y3324	1000	18.01248		-19.80435			55	30	0.0	7.4	920	2.8	1.8	0.8	0.0	8.9	0.1	0.0	0.8	0.25	0.01	0.00	1.6	-3.1
D324W355	1001	16.99520		-20.51178			52	9	2.1	7.1	800	3.0	1.0	1.2	0.2	8.3	0.1	0.2	0.2	0.68	0.09	0.01	2.9	-2.5
B49Y4848	1002	17.54607		-19.46558			61		-0.8	7.2	840	2.8	1.2	1.0	0.2	8.1	0.3	0.3	0.5	0.12	0.04	0.01	2.4	-2.4
B485W3496	1003	17.33877		-19.95652					-0.7	7.5	820	2.6	0.9	1.0	0.3	7.8	0.1	0.3	0.1	0.53	0.02	0.01	3.1	-2.4
B485W3493	1004	17.29846		-19.96105					0.1	7.5	820	2.3	1.3	1.0	0.3	8.1	0.2	0.0	0.0	0.50	0.02	0.01	1.8	-2.3
J189Y2377	1005	17.15547		-21.77717			61	12	-1.7	7.9	770	2.7	1.1	0.7	0.2	8.5	0.0	0.2	0.1	0.65	0.04	0.01	2.4	-2.7
B3447Y4675	1006	17.87908		-19.63043			45	24	-0.5	7.4	760	2.8	1.1	0.5	0.0	8.2	0.0	0.1	0.2	0.40	0.02	0.00	2.5	-3.4
B3447Y4674	1007	17.86180		-19.64040			42	32	-1.8	7.5	740	2.7	1.2	0.5	0.0	8.3	0.1	0.0	0.2	0.43	0.02	0.00	2.2	-3.2
B335W3490	1008	17.37908		-19.97464			62	34	0.5	7.5	800	3.0	0.9	0.5	0.3	8.2	0.1	0.0	0.1	0.47	0.02	0.02	3.3	-2.2
D365W3518	1009	17.19674		-20.32246			91	168	1.7	7.2	950	3.3	1.0	0.8	0.1	8.5	0.1	0.4	0.3	1.08	0.03	0.02	3.3	-2.3
B145Y3786	1011	17.56430		-20.03261			168	116	2.1	7.1	920	3.7	0.7	0.7	0.1	8.5	0.2	0.1	0.2	1.08	0.02	0.01	5.0	-2.5
W9Y832	1012	17.71775		-20.67240			139	59	-1.3	8.4	930	3.4	0.6	1.7	0.1	8.8	0.2	0.0	0.3	0.42	0.04	0.01	1.2	-2.3
J38Y2370	1013	16.95585		-19.70018			115	90	-1.5	7.5	860	2.3	1.6	1.7	0.2	8.9	0.1	0.3	0.7	0.87	0.04	0.01	1.5	-2.4
J106Y1750	1014	18.00960		-21.69928			100	30	-0.8	7.9	760	2.4	1.6	1.0	0.3	9.0	0.1	0.0	0.3	0.80	0.04	0.01	1.6	-2.3
D482W3507	1015	17.17946		-20.00815			74	46	-0.3	7.5	920	2.7	1.4	1.2	0.3	8.8	0.2	0.1	0.4	0.60	0.03	0.01	1.9	-2.5
B231Y3378	1016	18.43762		-19.64040			61	2	-1.9	7.4	920	2.3	1.7	1.2	0.0	9.0	0.1	0.0	0.5	0.50	0.04	0.00	1.4	-2.8
B138Y3771	1017	17.43186		-19.98732			95	61	-0.6	7.0	780	2.6	1.1	2.0	0.2	8.7	0.3	0.3	0.3	0.53	0.02	0.02	2.3	-2.2
B109W461	1018	17.24952		-20.13859			95	61	-0.6	7.0	780	2.3	1.4	1.7	0.2	8.7	0.1	0.2	0.3	0.37	0.07	0.04	1.6	-1.7
B108W462	1019	17.21785		-20.08786			112	76	-1.4	6.9	720	2.5	1.2	1.5	0.2	8.5	0.3	0.0	0.2	0.33	0.03	0.02	2.1	-2.1
D153W792	1020	16.82342		-20.67482			101	18	1.4	7.2	760	3.6	0.9	0.5	0.1	7.2	0.1	0.7	1.2	0.48	0.02	0.01	3.8	-2.4
B488Y3781	1021	17.42514		-19.94656			41	52	1.3	7.4	980	4.0	0.8	1.0	0.1	7.3	0.2	1.7	1.2	0.40	0.01	0.02	4.9	-2.4
B486W758	1022	17.21785		-19.95199			140		-0.9	7.5	970	3.9	1.1	0.7	0.0	8.1	0.1	1.0	1.0	0.47	0.02	0.00	3.6	-3.6
B45Y4672	1023	17.84069		-19.64855					-0.9	7.9	890	3.4	1.4	0.3	0.1	7.8	0.2	0.5	1.4	0.28	0.02	0.01	2.5	-2.7
B576W656	1024	17.19482		-19.93931					-0.9	7.5	890	3.4	1.4	0.3	0.1	7.8	0.2	0.5	1.4	0.28	0.02	0.00	3.6	-3.6
B148Y4815	1025	17.54702		-19.93025					-1.8	6.9	1070	3.5	1.3	1.3	0.3	7.9	0.1	1.5	1.4	0.40	0.06	0.02	2.7	-2.2
B496Y3801	1026	17.52015		-19.85598					-0.8	7.3	820	3.5	0.7	0.3	0.2	7.2	0.1	0.7	0.9	0.25	0.02	0.02	5.3	-2.2
B569W639	1027	17.06046		-20.08696			37	27	0.5	7.0	810	3.4	0.8	0.3	0.0	7.5	0.1	0.4	0.5	0.38	0.02	0.01	4.3	-2.6
B492W772	1028	17.31574		-19.88315			134	73	-0.7	7.0	770	3.5	0.8	0.3	0.1	7.3	0.2	0.6	0.7	0.30	0.02	0.00	4.6	-2.6
D																								



name	No	dec. longitude	E	dec. latitude	S	Temp. (°C)	depth (m)	level (m)	error (%)	pH	ec (µS/cm)	Ca <sup>2+</sup>	Mg <sup>2+</sup>	Na <sup>+</sup>	K <sup>+</sup>	HCO <sub>3</sub> <sup>-</sup>	SO <sub>4</sub> <sup>2-</sup>	NO <sub>3</sub> <sup>-</sup>	Cl <sup>-</sup>	Si	F	Sr <sup>2+</sup>	Ca <sup>2+</sup> ·Mg <sup>2+</sup>	log Sr <sup>2+</sup> :Ca <sup>2+</sup>	
																									91
B146Y3789	1030	17.51823	-19.97654																						-2.5
B569W640	1031	17.08925	-20.07609				50	29	-1.2	7.0	700	3.0	0.6	0.2	0.1	7.1	0.0	0.1	0.3	0.40	0.02	0.01	0.01	5.0	-2.5
B575W763	1032	17.15067	-19.94112				58	22	2.1	7.4	640	3.1	0.6	0.3	0.1	6.8	0.1	0.2	0.3	0.48	0.01	0.01	0.01	5.4	-2.4
B489Y3782	1033	17.46161	-19.94565						-0.9	7.0	670	3.0	0.4	0.4	0.1	6.9	0.0	0.2	0.3	0.43	0.02	0.01	0.01	6.7	-2.5
B488Y3779	1034	17.40403	-19.95924				52	34	-0.1	7.0	6320	2.6	0.6	0.7	0.1	7.1	0.1	0.0	0.0	0.3	0.02	0.01	0.01	4.2	-2.3
B486W759	1035	17.22361	-19.94656				182	55	-0.5	7.2	710	3.0	0.9	0.3	0.0	6.6	0.1	0.8	0.7	0.38	0.02	0.01	0.01	3.2	-2.5
D427W3519	1036	17.23321	-20.34783						-1.5	7.5	930	3.4	0.5	0.6	0.1	6.9	0.2	0.8	0.5	0.95	0.04	0.02	0.01	7.1	-2.2
B135Y3765	1037	17.48560	-20.07609				23		1.8	6.9	780	3.4	0.5	0.7	0.1	7.1	0.3	0.2	0.5	0.55	0.05	0.02	0.01	7.0	-2.3
B130W3767	1038	17.42131	-20.11141						0.9	7.0	830	3.3	0.5	1.1	0.2	6.6	0.4	0.7	0.8	0.48	0.03	0.01	0.01	6.1	-2.5
B498W3486	1039	17.37716	-19.81341				52		0.7	7.6	780	3.0	0.9	0.3	0.1	7.7	0.1	0.0	0.1	0.17	0.02	0.02	0.01	3.5	-2.1
B799Z/Y4973	1040	17.38964	-19.59783				68		1.4	7.1	810	3.3	1.1	0.3	0.0	8.0	0.1	0.7	0.2	0.33	0.02	0.01	0.01	3.0	-2.6
B571W888	1041	17.05950	-20.02717				27		-1.5	7.4	650	3.3	0.6	0.2	0.1	8.1	0.1	0.0	0.2	0.22	0.02	0.01	0.01	5.0	-2.5
B498W3485	1042	17.36948	-19.92428				40		0.1	7.2	800	3.2	0.8	0.2	0.1	7.9	0.1	0.1	0.1	0.37	0.02	0.02	0.01	4.2	-2.2
B573W886	1044	17.11036	-19.96649				28		-0.2	7.4	630	3.3	0.6	0.2	0.1	7.4	0.1	0.2	0.3	0.22	0.02	0.01	0.01	5.8	-2.4
B569W638	1045	17.06430	-20.09058				38	29	-0.6	7.0	720	3.2	0.6	0.2	0.0	7.5	0.0	0.1	0.2	0.40	0.02	0.01	0.01	5.6	-2.6
B488Y3780	1046	17.40403	-19.93388				234	74	2.2	7.2	680	3.4	0.6	0.1	0.0	7.5	0.1	0.0	0.1	0.13	0.01	0.01	0.01	5.8	-2.7
B787Y4839	1047	17.62188	-19.49457						-0.4	7.5	730	2.7	1.2	0.5	0.1	7.7	0.3	0.0	0.1	0.30	0.05	0.01	0.01	2.3	-2.6
B758Y4640	1048	17.53263	-19.63315				37	12	0.6	7.7	800	3.2	1.0	0.6	0.0	7.6	0.0	0.6	0.6	0.20	0.01	0.00	0.00	3.2	-3.5
B45Y4671	1049	17.84453	-19.64946				1049		0.4	7.4	770	2.9	1.1	0.5	0.0	7.5	0.1	0.5	0.5	0.37	0.02	0.00	0.00	2.8	-3.6
D362W401	1050	16.96257	-20.36775				40		0.7	7.3	640	3.1	0.7	0.6	0.2	7.7	0.1	0.1	0.4	0.72	0.02	0.01	0.01	4.5	-2.5
D154W1895	1051	16.82821	-20.73551				79	21	1.1	7.5	620	3.2	0.5	0.4	0.1	7.4	0.0	0.2	0.2	1.00	0.02	0.01	0.01	6.0	-2.5
B121W3497	1052	17.34453	-20.02899				46		1.2	7.4	850	3.1	0.7	0.9	0.1	7.5	0.3	0.2	0.2	0.68	0.03	0.01	0.01	4.5	-2.3
B117W3499	1053	17.27351	-20.02446				96	58	0.0	7.3	830	3.0	0.6	1.1	0.2	7.7	0.3	0.1	0.2	0.80	0.02	0.02	0.02	5.2	-2.3
B569W2912	1054	17.04319	-20.06522				55	32	-0.9	7.8	690	4.0	0.6	0.2	0.1	9.5	0.1	0.0	0.1	0.33	0.02	0.01	0.01	6.5	-2.8
B493W3488	1055	17.37428	-19.87228						-1.2	7.2	910	4.0	0.6	0.1	0.0	9.4	0.1	0.1	0.1	0.22	0.02	0.01	0.01	6.4	-2.6
B493W3487	1056	17.36084	-19.91304				186		1.4	7.2	940	4.2	0.7	0.1	0.0	9.4	0.1	0.0	0.1	0.27	0.02	0.01	0.01	6.3	-2.5
B150Y4446	1057	17.61612	-19.97464						-1.9	7.1	830	3.7	0.6	0.3	0.1	9.3	0.0	0.0	0.0	0.25	0.02	0.01	0.01	6.5	-2.5
B585Y4827	1058	17.51248	-19.53442						1.0	6.8	910	4.4	0.5	0.2	0.0	9.5	0.0	0.0	0.1	0.32	0.02	0.01	0.01	8.9	-2.5
B482W3508	1059	17.20825	-20.00000				55	24	0.3	7.2	980	4.6	0.3	0.2	0.1	9.4	0.1	0.4	0.2	0.42	0.03	0.02	0.02	14.3	-2.3
B150Y4444	1060	17.60845	-20.01449						1.0	6.9	910	4.7	0.3	0.2	0.1	9.9	0.1	0.0	0.2	0.30	0.03	0.02	0.02	16.4	-2.4
B492W773	1061	17.31190	-19.87953				157	80	0.5	7.3	900	3.6	1.6	0.3	0.1	9.0	0.2	0.5	0.8	0.32	0.01	0.01	0.01	2.3	-2.4
D368W388	1062	17.01248	-20.25362						2.4	7.1	810	3.7	1.0	0.3	0.1	8.4	0.1	0.4	0.6	0.43	0.03	0.02	0.02	3.6	-2.3
B148Y4814	1063	17.54511	-19.89583						-0.6	6.7	910	3.3	1.1	0.5	0.2	8.5	0.1	0.3	0.7	0.33	0.06	0.01	0.01	3.0	-2.4
B499Y3796	1064	17.45489	-19.84420				37	18	-0.4	7.0	790	3.4	0.9	0.1	0.0	8.6	0.1	0.1	0.1	0.25	0.03	0.02	0.02	3.6	-2.4
B98W475	1065	17.13244	-20.23007				40	34	1.3	7.0	670	3.4	1.1	0.3	0.1	8.6	0.1	0.2	0.3	0.15	0.04	0.02	0.02	3.0	-2.2
B98W474	1066	17.12572	-20.20471				49	14	1.2	6.8	670	3.5	1.0	0.3	0.1	8.6	0.1	0.2	0.3	0.10	0.04	0.02	0.02	3.4	-2.2
B334W454	1067	17.00384	-20.08696				24		1.2	7.0	690	3.4	1.0	0.3	0.1	8.5	0.0	0.1	0.3	0.27	0.03	0.00	0.00	3.4	-4.5
B581W779	1068	17.31286	-19.79076				36	9	-1.5	7.3	790	3.4	0.9	0.3	0.1	9.1	0.1	0.0	0.1	0.33	0.02	0.01	0.01	3.6	-2.3
B147Y3791	1069	17.52975	-19.90580						0.3	7.4	820	3.5	1.1	0.1	0.0	8.9	0.1	0.2	0.1	0.32	0.02	0.01	0.01	3.2	-2.4
B148Y4813	1070	17.54223	-19.89946						-1.5	7.2	940	3.4	1.1	0.4	0.1	8.9	0.1	0.3	0.5	0.37	0.05	0.02	0.02	3.2	-2.4
B147Y3790	1071	17.52207	-19.90851						0.1	7.2	870	3.5	1.3	0.2	0.1	8.9	0.1	0.3	0.5	0.42	0.02	0.01	0.01	2.7	-2.5
B495Y3793	1072	17.45489	-19.90670						-0.5	7.1	770	3.7	0.6	0.1	0.0	8.5	0.1	0.0	0.2	0.22	0.02	0.02	0.00	6.0	-3.0
B493W3489	1073	17.38004	-19.88406				113	78	0.4	7.4	900	3.8	0.7	0.1	0.0	8.5	0.1	0.4	0.1	0.20	0.02	0.01	0.01	5.2	-2.5
B581W777	1074	17.27927	-19.77808				30	12	-1.0	7.3	700	3.6	0.6	0.3	0.1	8.5	0.1	0.1	0.2	0.32	0.02	0.01	0.01	6.4	-2.4
B98W473	1075	17.10653	-20.17663				137	107	-1.7	8.3	730	3.6	0.6	0.3	0.1	8.6	0.1	0.1	0.2	0.28	0.02	0.01	0.01	6.5	-2.4
B334W455	1076	16.98177	-20.12138						1.7	6.9	840	3.9	0.9	0.1	0.1	9.1	0.1	0.0	0.3	0.32	0.03	0.02	0.02	4.1	-2.3
B502Y3798	1077	17.40883	-19.81703				3		0.4	7.2	680	3.9	0.6	0.2	0.0	9.0	0.0	0.1	0.1	0.33	0.02	0.01	0.01	6.1	-2.6
B573W2911	1078	17.11612	-19.97283						-1.3	7.0	820	3.9	0.5	0.0	0.0	8.8	0.1	0.0	0.2	0.32	0.03	0.00	0.00	7.2	-3.2
B495Y3792	1079	17.44722	-19.90761				23	3	-0.5	6.9	810	3.6	0.9	0.1	0.1	8.7	0.1	0.1	0.3	0.27	0.03	0.02	0.02	4.2	-2.3
B502Y3799	1080	17.43762	-19.80797				30	15	-0.1	7.0	790	3.6	0.8	0.4	0.2	8.9	0.1	0.0	0.2	0.20	0.03	0.02	0.02	4.2	-2.3
B502Y3797	1081	17.41075	-19.82246				36	15	0.8	7.3	720	3.6	0.9	0.1	0.0	8.9	0.1	0.0	0.2	0.20	0.03	0.02	0.02	4.7	-2.5
B334W457	1083	17.01248	-20.11051				37	9	-0.3	7.1	710	3.7	0.8	0.3	0.0	8.9	0.0	0.1	0.3	0.30	0.02	0.01	0.01	4.5	-2.6
B334W453	1084	16.98608	-20.09058						0.9	6.9	720	3.8	0.8	0.3	0.1	9.0	0.0	0.1	0.3	0.27	0.02	0.01	0.01	4.7	-2.2
B528W891	1085	17.01056	-20.24728				52		1.9	7.1	780	4.2	0.6	0.4	0.1	8.5	0.1	0.5	0.6	0.40	0.02	0.02	0.02	6.6	-2.4
B585Y4828	1086	17.48944	-19.51630						-1.3	6.8	930	3.9	0.7	0.4	0.0	8.6	0.1								

name	No	dec. longitude	E	dec. latitude	S	Temp. (°C)	depth (m)	level (m)	error (%)	pH	ec (µS/cm)	mmol/l				F	Si	Ca <sup>2+</sup>	Mg <sup>2+</sup>	Na <sup>+</sup>	K <sup>+</sup>	HCO <sub>3</sub> <sup>-</sup>	SO <sub>4</sub> <sup>2-</sup>	NO <sub>3</sub> <sup>-</sup>	Cl <sup>-</sup>	Sr <sup>2+</sup>	Ca <sup>2+</sup> ·Mg <sup>2+</sup>	log Sr <sup>2+</sup> :Ca <sup>2+</sup>
												Ca <sup>2+</sup>	Mg <sup>2+</sup>	Na <sup>+</sup>	K <sup>+</sup>													
B135Y3766	1090	17.44146		-20.10326			213		-1.0	6.8	860	3.9	0.4	0.4	0.1	8.9	0.3	0.0	0.1	0.42	0.03	0.02	0.00	0.00	8.8	-2.4		
B569W641	1091	17.03743		-20.06703			37	21	-0.1	7.5	800	4.2	0.1	0.1	0.0	8.3	0.1	0.2	0.2	0.33	0.01	0.00	0.00	0.00	29.9	-3.0		
D364W394	1092	17.09021		-20.26178			60	58	-1.0	7.1	700	3.6	0.4	0.4	0.1	8.1	0.1	0.0	0.3	0.43	0.03	0.02	0.00	0.00	9.2	-2.2		
B483W3504	1093	17.23225		-20.02325			37	37	-1.7	7.4	860	3.9	0.3	0.3	0.1	8.2	0.1	0.1	0.2	0.38	0.02	0.01	0.00	0.00	12.2	-2.6		
D358W339	1094	17.06046		-20.22192			76	55	1.4	6.9	730	3.9	0.5	0.3	0.1	8.4	0.1	0.1	0.3	0.38	0.03	0.02	0.00	0.00	7.7	-2.3		
B575W762	1095	17.13052		-19.92210			61	24	0.9	7.6	720	3.8	0.5	0.2	0.1	8.2	0.1	0.1	0.1	0.53	0.01	0.01	0.00	0.00	7.7	-2.9		
B482W3509	1096	17.22841		-19.97645			122	91	1.0	7.0	830	3.8	0.3	0.3	0.1	8.2	0.1	0.0	0.1	0.67	0.03	0.04	0.00	0.00	10.8	-2.0		
B500Y3800	1097	17.50672		-19.82246			30	30	0.2	7.3	860	3.7	0.7	0.4	0.1	8.1	0.2	0.6	0.4	0.32	0.03	0.02	0.00	0.00	5.1	-2.3		
B106W471	1098	17.17946		-20.19928			27	12	1.7	7.2	720	3.6	0.8	0.7	0.1	8.1	0.1	0.4	0.5	0.50	0.03	0.04	0.00	0.00	4.5	-1.9		
D358W390	1099	17.02111		-20.19475	27.0		101	40	-1.7	7.4	720	3.3	0.7	0.3	0.1	8.2	0.0	0.1	0.3	0.47	0.03	0.01	0.00	0.00	4.5	-2.4		
B99W460	1100	17.28023		-20.21649			92	49	-1.8	6.9	720	3.4	0.6	0.5	0.1	8.2	0.1	0.3	0.5	0.40	0.03	0.02	0.00	0.00	5.3	-2.2		
B335W3491	1101	17.38196		-19.98188			47	40	0.9	7.2	830	3.3	0.6	0.6	0.1	8.1	0.1	0.0	0.1	0.52	0.02	0.02	0.00	0.00	5.3	-2.3		
B992W3510	1102	17.15451		-20.23460			33	33	-1.0	7.3	850	3.5	0.6	0.3	0.1	8.0	0.1	0.3	0.3	0.58	0.03	0.03	0.00	0.00	5.9	-2.3		
B105W458	1103	17.19578		-20.18025			12	9	-1.7	7.0	660	3.4	0.5	0.4	0.1	8.0	0.1	0.1	0.3	0.53	0.03	0.01	0.00	0.00	6.5	-2.4		
J269Y2158	1104	16.85509		-21.52446			122	61	-2.3	7.7	790	1.3	2.4	1.1	0.1	8.4	0.1	0.3	0.3	1.15	0.02	0.00	0.00	0.00	0.6	-2.6		
J166W3541	1105	17.13340		-21.30525			30	24	-1.7	7.5	900	1.1	2.3	1.7	0.3	8.1	0.2	0.3	0.4	1.05	0.03	0.01	0.00	0.00	0.5	-2.0		
D362W399	1106	16.97505		-20.34783			60	46	1.8	7.3	620	0.8	2.4	2.0	0.4	8.2	0.0	0.1	0.2	0.27	0.10	0.01	0.00	0.00	0.3	-1.9		
B5661Y4484	1108	17.60269		-19.82156			107	67	0.1	7.4	1010	1.8	3.0	1.7	0.3	8.6	1.0	0.7	0.3	0.58	0.05	0.01	0.00	0.00	0.6	-2.1		
J102Y1993	1109	17.77351		-21.68569			107	67	-1.5	8.4	860	0.0	3.2	2.4	0.6	7.2	0.7	0.6	0.5	0.32	0.02	0.00	0.00	0.00	0.0	-1.1		
D161W1840	1110	18.43282		-19.68931			34	21	-1.4	7.7	830	0.4	2.8	2.2	0.1	7.3	0.1	0.0	1.2	0.42	0.03	0.00	0.00	0.00	0.1	-2.4		
J84Y1438	1111	17.37908		-21.62047			57	24	-1.7	7.6	1020	1.0	3.0	2.3	0.6	8.4	0.1	1.6	1.1	1.05	0.05	0.01	0.00	0.00	0.4	-1.9		
J1181W9921	1112	18.14875		-21.39583			61	15	0.5	7.6	1140	1.4	3.5	2.3	0.6	9.1	0.2	1.5	1.5	1.21	0.04	0.02	0.00	0.00	0.4	-1.9		
J221W4588	1113	16.57869		-21.54167			46	37	2.3	7.3	1040	1.9	2.6	2.7	0.0	8.2	0.2	0.9	1.6	0.43	0.05	0.01	0.00	0.00	0.7	-2.5		
J1662Y2321	1114	17.29271		-21.56884			55	50	-1.3	8.1	1000	1.6	2.4	3.0	0.4	8.4	0.2	1.7	1.3	1.05	0.06	0.01	0.00	0.00	0.7	-2.1		
D198W1840	1115	16.96257		-21.28714			67	30	-0.7	7.5	900	1.1	2.0	3.0	0.3	8.5	0.3	0.6	0.6	0.88	0.02	0.01	0.00	0.00	0.8	-2.2		
D279Y420	1116	18.08445		-21.21196			57	47	-2.1	7.7	800	1.1	1.8	3.6	0.3	8.2	0.4	0.3	1.4	0.98	0.02	0.01	0.00	0.00	0.6	-2.2		
B183Y3069	1117	18.19674		-19.88225			91	70	-1.5	7.8	710	1.6	1.3	2.4	0.2	8.0	0.1	0.2	0.3	1.25	0.03	0.01	0.00	0.00	1.2	-2.2		
D380W1657	1118	17.18042		-20.86866			91	70	-1.7	7.7	820	1.6	1.2	2.5	0.2	7.6	0.1	0.0	0.4	1.03	0.09	0.01	0.00	0.00	1.4	-2.1		
D367W3521	1119	17.08541		-20.47373			305	51	0.0	7.8	820	1.6	1.2	2.5	0.2	7.6	0.1	0.0	0.4	1.03	0.09	0.01	0.00	0.00	1.4	-2.1		
D285W3620	1120	17.34357		-20.60598			104	66	-0.9	7.3	760	2.1	1.2	2.3	0.2	8.0	0.2	0.0	0.3	1.23	0.03	0.01	0.00	0.00	1.7	-2.2		
D175W1651	1121	17.00672		-20.97594	27.2		104	66	-0.9	7.3	780	2.0	0.9	3.0	0.3	8.0	0.2	0.2	0.6	1.07	0.02	0.01	0.00	0.00	2.3	-2.5		
D163W1638	1122	17.12188		-20.91395			101	44	1.6	7.3	790	1.8	1.1	3.0	0.3	7.6	0.1	0.3	0.5	0.97	0.02	0.01	0.00	0.00	1.7	-2.3		
D286W3612	1123	17.30710		-20.60236			69	61	-0.1	7.2	940	2.2	1.4	3.2	0.3	9.1	0.3	0.1	0.8	1.38	0.02	0.01	0.00	0.00	1.6	-2.2		
D285W3617	1124	17.34837		-20.61051			124	60	0.3	7.5	880	2.2	1.4	2.7	0.2	8.8	0.2	0.5	0.5	1.17	0.03	0.02	0.00	0.00	1.6	-2.0		
D127W1906	1125	17.00288		-20.05888			108	46	-1.5	7.5	730	2.5	0.7	2.3	0.3	8.4	0.1	0.3	0.3	1.38	0.05	0.03	0.00	0.00	3.5	-1.9		
J98Y2004	1126	16.67850		-20.91214			82	43	-2.1	7.4	840	1.7	1.6	2.2	0.5	8.7	0.3	0.1	0.4	1.10	0.06	0.01	0.00	0.00	1.1	-2.3		
J102Y1997	1128	17.75528		-21.73460			82	43	-2.1	7.4	840	1.7	1.6	2.2	0.5	8.7	0.3	0.1	0.4	1.10	0.06	0.01	0.00	0.00	1.1	-2.5		
J255W3525	1129	16.64683		-21.31703			65	58	-0.4	7.9	960	1.6	2.0	2.3	0.3	8.8	0.1	0.6	0.4	1.35	0.06	0.01	0.00	0.00	0.8	-2.1		
D225Y1111	1130	17.58733		-21.22826			63	41	4.5	8.0	890	1.9	2.2	2.3	0.3	9.0	0.2	0.5	0.1	1.10	0.03	0.01	0.00	0.00	0.8	-2.1		
D170W1900	1131	16.78215		-20.98641			91	79	-0.2	7.9	740	1.9	2.0	2.0	0.2	9.2	0.1	0.0	0.3	0.93	0.01	0.01	0.00	0.00	0.9	-2.2		
D167W1686	1132	16.88580		-20.93931			76	55	0.1	7.3	800	1.9	1.8	1.9	0.3	8.8	0.1	0.2	0.4	0.93	0.08	0.02	0.00	0.00	1.0	-1.9		
B5661Y4483	1133	17.60173		-19.87138			110	52	-1.2	7.5	870	1.9	1.7	2.0	0.2	8.9	0.1	0.2	0.3	0.88	0.03	0.01	0.00	0.00	1.1	-2.3		
D427W3520	1135	17.22073		-20.35507			73	49	0.5	7.3	720	1.7	1.8	1.8	0.3	8.4	0.1	0.2	0.2	0.50	0.12	0.01	0.00	0.00	1.2	-2.2		
D362W403	1136	17.00576		-20.34692			61	52	0.9	7.5	810	1.7	1.6	2.6	0.2	8.7	0.1	0.1	0.2	0.35	0.04	0.01	0.00	0.00	0.9	-2.4		
D171W1608	1138	16.78695		-21.02385			110	43	-0.5	7.5	830	1.4	1.7	3.0	0.1	8.5	0.2	0.5	0.2	0.70	0.04	0.01	0.00	0.00	1.1	-2.1		
B508Y4494	1139	17.54127		-19.75091			61	43	-1.4	7.8	730	1.8	1.2	2.3	0.2	7.5	0.3	0.0	0.6	0.97	0.05	0.01	0.00	0.00	1.5	-2.2		
B520Y4645	1140	17.60749		-19.66576			122	30	0.9	7.7	650	1.4	1.5	2.0	0.3	7.4	0.1	0.0	0.3	0.53	0.01	0.00	0.00	0.00	0.9	-2.7		
B491W771	1141	17.29079		-19.94746			122	30	0.9	7.7	650	1.4	1.5	2.0	0.3	7.4	0.1	0.0	0.3	0.53	0.01	0.00	0.00	0.00	0.9	-2.7		
J114Y1688	1144	18.04702		-21.53533			49	19	-1.3	8.3	690	1.6	1.1	2.3	0.2	7.4	0.2	0.0	0.5	0.77	0.06	0.01	0.00	0.00	1.4	-2.6		
J30W4516	1145	16.82150		-21.77989			91	43	-1.4	7.8	730	1.8	1.2	2.3	0.2	7.5	0.3	0.0	0.6	0.97	0.05	0.01	0.00	0.00	1.5	-2.2		
D132W2254	1147	16.59885		-20.82085			148	122	0.7	7.5	790	1.8	0.9	3.0	0.1	7.4	0.0	0.2	0.6	0.55	0.04	0.00	0.00	0.00	1.9	-2.6		
D126W1948	1148	16.64395		-20.94746			55	30	-0.1	7.7	650	1.9	0.7	2.7	0.2	7.3	0.2	0.0	0.5	0.77								

## Annex B

## B-19

name	No	dec. longitude	E	dec. latitude	S	Temp.	depth	level	error	pH	ec	mmol/l							F	Si	NO <sub>3</sub> <sup>-</sup>	Cl <sup>-</sup>	SO <sub>4</sub> <sup>2-</sup>	HCO <sub>3</sub> <sup>-</sup>	SO <sub>4</sub> <sup>2-</sup>	NO <sub>3</sub> <sup>-</sup>	Cl <sup>-</sup>	Si	F	Si <sup>2+</sup>	Ca <sup>2+</sup> ·Mg <sup>2+</sup>	log	Sr <sup>2+</sup> ·Ca <sup>2+</sup>
												Ca <sup>2+</sup>	Mg <sup>2+</sup>	Na <sup>+</sup>	K <sup>+</sup>	HCO <sub>3</sub> <sup>-</sup>	SO <sub>4</sub> <sup>2-</sup>	NO <sub>3</sub> <sup>-</sup>															
J82/Y2027	1156	17.39731	-21.74909	94	8	-1.9	7.7	680	1.5	1.5	1.5	0.1	7.3	0.1	0.4	0.1	1.00	0.07	0.01	0.01	0.01	0.01	0.01	0.01	0.01	0.01	0.01	0.01	1.0	-2.2			
J43/Y2391	1157	17.04319	-21.79438	86	27	-1.5	7.8	700	1.7	1.3	1.6	0.2	7.6	0.0	0.0	0.1	0.2	0.68	0.03	0.00	0.00	0.00	0.00	0.00	0.00	0.00	0.00	0.00	1.3	-2.6			
J148/Y1778	1158	17.86084	-21.65489	75	43	-2.0	7.5	750	1.9	1.5	1.3	0.3	7.6	0.1	0.6	0.2	1.18	0.05	0.01	0.01	0.01	0.01	0.01	0.01	0.01	0.01	0.01	1.3	-2.4				
J148/Y1773	1159	17.80134	-21.65127	44	30	-0.2	8.1	800	2.1	1.7	1.3	0.2	7.8	0.2	0.6	0.3	0.67	0.04	0.00	0.00	0.00	0.00	0.00	0.00	0.00	0.00	0.00	1.2	-2.7				
B572/W2910	1161	17.08157	-19.99728	46	37	-0.1	7.6	620	2.5	0.9	1.3	0.2	7.3	0.2	0.3	0.3	0.67	0.02	0.01	0.01	0.01	0.01	0.01	0.01	0.01	0.01	0.01	2.6	-2.5				
D163/W790	1162	16.81670	-20.69475	64	21	-0.6	7.6	630	2.3	0.9	1.4	0.2	7.9	0.0	0.0	0.1	0.52	0.05	0.01	0.01	0.01	0.01	0.01	0.01	0.01	0.01	0.01	2.4	-2.5				
B139/Y3778	1163	17.37140	-20.00091	179	58	2.6	7.0	680	2.4	0.8	1.7	0.1	7.5	0.1	0.0	0.1	1.05	0.02	0.03	0.03	0.03	0.03	0.03	0.03	0.03	0.03	0.03	3.1	-1.9				
D288/W2038	1164	17.21017	-20.59692	73	52	-0.5	7.5	770	2.3	0.9	1.6	0.2	7.9	0.1	0.0	0.1	1.47	0.04	0.01	0.01	0.01	0.01	0.01	0.01	0.01	0.01	0.01	2.6	-2.3				
D129/W1689	1165	16.78215	-20.87228	91	84	1.2	7.3	720	2.3	0.9	2.0	0.2	7.8	0.1	0.0	0.4	0.98	0.06	0.01	0.01	0.01	0.01	0.01	0.01	0.01	0.01	0.01	2.6	-2.5				
B133/Y3751	1166	17.40979	-20.17029	20	10	0.5	8.0	620	1.7	2.3	0.9	0.1	7.8	0.1	0.2	0.4	0.77	0.01	0.02	0.02	0.02	0.02	0.02	0.02	0.02	0.02	0.02	2.3	-2.0				
B794/Y2604	1169	17.40307	-19.64764	17	40	-0.8	7.0	750	2.1	0.9	1.9	0.1	7.8	0.1	0.1	0.2	0.77	0.01	0.02	0.02	0.02	0.02	0.02	0.02	0.02	0.02	0.02	0.7	-2.2				
B452/Y4673	1171	17.82821	-19.61775	17	40	-0.8	7.0	750	2.1	0.9	1.9	0.1	7.8	0.1	0.1	0.2	0.77	0.01	0.02	0.02	0.02	0.02	0.02	0.02	0.02	0.02	0.02	0.7	-2.2				
B317/Y4866	1174	17.80038	-19.48641	98	61	-1.8	7.7	620	1.5	2.2	0.3	0.0	7.4	0.1	0.0	0.4	0.25	0.02	0.00	0.00	0.00	0.00	0.00	0.00	0.00	0.00	0.00	0.7	-3.2				
J43/Y2392	1175	17.10077	-21.76268	69	33	-2.0	7.7	720	1.7	1.9	0.5	0.3	7.9	0.0	0.2	0.1	1.15	0.09	0.01	0.01	0.01	0.01	0.01	0.01	0.01	0.01	0.01	0.9	-2.5				
D254/Y1117	1176	17.68330	-21.76486	46	27	1.9	8.0	730	1.5	2.3	0.4	0.4	7.2	0.1	0.5	0.3	1.30	0.11	0.02	0.02	0.02	0.02	0.02	0.02	0.02	0.02	0.02	0.6	-2.0				
B579/W769	1178	17.23033	-19.83424	61	40	-0.2	7.6	780	1.8	2.4	0.7	0.3	7.2	0.0	1.3	0.7	0.45	0.03	0.01	0.01	0.01	0.01	0.01	0.01	0.01	0.01	0.01	0.7	-2.4				
B183/Y3067	1179	18.20154	-19.86413	79	43	-1.4	8.0	680	1.2	2.2	0.7	0.0	7.3	0.0	0.0	0.4	0.67	0.02	0.00	0.00	0.00	0.00	0.00	0.00	0.00	0.00	0.00	0.6	-2.8				
B171/Y3008	1180	18.14203	-20.02174	99	43	-1.5	8.2	830	1.3	2.6	0.6	0.1	7.2	0.1	0.4	0.9	0.80	0.03	0.01	0.01	0.01	0.01	0.01	0.01	0.01	0.01	0.01	0.5	-2.3				
B317/Y4864	1181	17.78695	-19.54710	232	122	-1.8	7.3	710	2.1	1.6	0.1	0.0	7.6	0.1	0.1	0.2	0.17	0.03	0.00	0.00	0.00	0.00	0.00	0.00	0.00	0.00	0.00	1.3	-3.2				
B171/Y3010	1182	18.08829	-19.99366	91	40	-2.1	7.9	810	2.1	1.8	0.3	0.2	7.6	0.1	0.5	0.4	0.43	0.02	0.00	0.00	0.00	0.00	0.00	0.00	0.00	0.00	0.00	1.2	-2.8				
B316/Y4504	1184	17.58733	-19.70109	184	29	-2.0	7.5	650	1.7	1.7	0.6	0.1	7.6	0.1	0.1	0.0	0.43	0.02	0.00	0.00	0.00	0.00	0.00	0.00	0.00	0.00	0.00	1.0	-2.7				
B149/Y5502	1185	17.61804	-19.88587	115	17	-1.1	7.3	710	2.2	1.8	0.3	0.1	8.1	0.1	0.0	0.3	0.25	0.01	0.01	0.01	0.01	0.01	0.01	0.01	0.01	0.01	0.01	1.3	-2.4				
B580/W782	1186	17.22937	-19.79710	41	25	1.1	7.7	700	2.1	1.8	0.7	0.1	8.0	0.1	0.1	0.1	0.37	0.02	0.01	0.01	0.01	0.01	0.01	0.01	0.01	0.01	0.01	1.1	-2.1				
B147/Y4676	1187	17.90883	-19.62591	33	5	-2.2	7.6	730	1.8	1.8	0.7	0.0	8.2	0.1	0.0	0.1	0.33	0.03	0.00	0.00	0.00	0.00	0.00	0.00	0.00	0.00	0.00	1.0	-2.9				
B5662/Y4485	1188	17.60461	-19.80254	17	40	-0.5	7.8	820	1.3	2.8	0.8	0.2	8.1	0.0	0.8	0.4	0.55	0.03	0.00	0.00	0.00	0.00	0.00	0.00	0.00	0.00	0.00	0.5	-2.9				
B188/Y3033	1189	18.27255	-19.95652	49	18	1.5	7.7	820	1.4	3.0	0.7	0.1	8.3	0.1	0.3	0.5	0.62	0.03	0.00	0.00	0.00	0.00	0.00	0.00	0.00	0.00	0.00	0.5	-2.6				
B91/Y4718	1190	17.99136	-19.46014	37	1	-0.6	7.8	700	1.0	3.0	0.1	0.0	8.0	0.0	0.0	0.0	0.23	0.05	0.00	0.00	0.00	0.00	0.00	0.00	0.00	0.00	0.4	-2.8					
B593/Y14750	1191	18.27159	-19.46558	16	24	-0.1	7.8	710	1.6	2.4	0.1	0.0	7.9	0.0	0.0	0.2	0.25	0.01	0.00	0.00	0.00	0.00	0.00	0.00	0.00	0.00	0.7	-3.4					
B591/Y4869	1193	17.96929	-19.46649	122	30	-1.6	7.7	730	1.5	2.3	0.4	0.1	7.8	0.1	0.1	0.3	0.23	0.05	0.00	0.00	0.00	0.00	0.00	0.00	0.00	0.00	0.7	-2.8					
B172/Y3006	1195	18.07486	-19.97645	85	34	-1.9	8.2	720	1.1	2.5	0.4	0.1	7.8	0.1	0.0	0.1	0.47	0.02	0.00	0.00	0.00	0.00	0.00	0.00	0.00	0.00	0.5	-2.6					
B752/Y4819	1196	17.61516	-19.55616	16	23	-1.1	7.6	760	1.6	2.3	0.5	0.0	8.4	0.0	0.0	0.1	0.75	0.07	0.00	0.00	0.00	0.00	0.00	0.00	0.00	0.00	0.7	-2.9					
B511/Y4505	1197	17.56662	-19.69293	52	37	1.7	7.3	770	1.7	2.3	0.7	0.1	8.2	0.1	0.0	0.0	0.30	0.03	0.00	0.00	0.00	0.00	0.00	0.00	0.00	0.00	0.8	-2.6					
B5663/Y4490	1200	17.57774	-19.74728	1	55	-0.2	7.5	770	1.7	2.6	0.3	0.1	8.7	0.1	0.0	0.2	0.40	0.01	0.00	0.00	0.00	0.00	0.00	0.00	0.00	0.00	0.6	-3.1					
B316/Y4497	1201	17.57678	-19.74185	91	55	-0.2	7.5	770	1.6	2.6	0.1	0.1	8.6	0.1	0.0	0.1	0.27	0.01	0.00	0.00	0.00	0.00	0.00	0.00	0.00	0.00	0.6	-3.4					
B752/Y4823	1202	17.53071	-19.57609	91	30	-0.1	7.0	770	1.7	2.5	0.2	0.0	8.1	0.0	0.2	0.1	0.30	0.08	0.00	0.00	0.00	0.00	0.00	0.00	0.00	0.00	0.7	-2.9					
B322/Y4699	1203	17.94818	-19.55254	17	40	1.5	7.9	720	1.7	2.6	0.0	0.0	8.2	0.0	0.1	0.1	0.20	0.02	0.00	0.00	0.00	0.00	0.00	0.00	0.00	0.00	0.7	-3.3					
B656/Y4651	1207	17.70250	-19.69475	17	40	0.0	8.0	730	1.7	2.5	0.2	0.0	7.8	0.3	0.1	0.2	0.23	0.02	0.00	0.00	0.00	0.00	0.00	0.00	0.00	0.00	0.7	-3.1					
B593/Y3443	1208	18.24856	-19.51087	17	40	-0.3	7.7	800	1.9	2.3	0.2	0.0	7.7	0.4	0.2	0.1	0.23	0.01	0.00	0.00	0.00	0.00	0.00	0.00	0.00	0.00	0.8	-3.0					
B794/Y2603	1209	17.39731	-19.65670	17	40	-2.4	7.8	710	1.9	2.2	0.1	0.1	8.2	0.1	0.1	0.1	0.20	0.02	0.00	0.00	0.00	0.00	0.00	0.00	0.00	0.00	0.8	-3.1					
B591/Y4873	1210	17.92131	-19.49547	37	9	-1.6	7.4	730	1.9	2.2	0.0	0.0	8.3	0.1	0.1	0.1	0.15	0.03	0.00	0.00	0.00	0.00	0.00	0.00	0.00	0.00	0.9	-2.6					
B12/Y4700	1211	18.01536	-19.54438	37	9	1.6	7.6	720	2.0	2.3	0.1	0.0	8.2	0.0	0.0	0.0	0.18	0.02	0.00	0.00	0.00	0.00	0.00	0.00	0.00	0.00	0.9	-3.4					
B10/Y4712	1213	18.04894	-19.48913	27	27	-0.3	7.5	700	1.8	2.1	0.1	0.0	7.9	0.0	0.0	0.0	0.22	0.03	0.00	0.00	0.00	0.00	0.00	0.00	0.00	0.00	0.9	-3.1					
B792/Y2609	1214	17.30710	-19.68025	46	46	-0.3	7.5	1370	3.0	4.1	1.0	0.1	11.0	0.4	2.0	1.5	0.38	0.02	0.01	0.01	0.01	0.01	0.01	0.01	0.01	0.01	0.7	-2.7					
B44/3/Y2996	1215	17.86388	-19.80435	30	14	0.3	7.4	1390	2.9	4.5	0.6	0.0	11.4	0.2	1.4	2.1	0.32	0.03	0.00	0.00	0.00	0.											

name	No	dec. longitude	E	dec. latitude	S	Temp. (°C)	depth (m)	level (m)	error (%)	pH	ec (µS/cm)	Ca <sup>2+</sup>	Mg <sup>2+</sup>	Na <sup>+</sup>	K <sup>+</sup>	HCO <sub>3</sub> <sup>-</sup>	SO <sub>4</sub> <sup>2-</sup>	NO <sub>3</sub> <sup>-</sup>	Cl <sup>-</sup>	Si	F	SP <sup>2+</sup>	Ca <sup>2+</sup> ·Mg <sup>2+</sup>	log Sr <sup>2+</sup> ·Ca <sup>2+</sup>
B1777Y3328	1233	18.03839		-19.78895			24	9	0.5	7.4	1390	3.1	3.2	2.3	0.0	10.3	0.6	0.9	2.3	0.53	0.02	0.00	1.0	-2.9
B174Y3321	1234	18.04319		-19.85598			38		0.5	7.8	1340	2.6	2.5	2.4	0.1	10.5	0.1	0.3	1.6	0.45	0.02	0.01	1.1	-2.6
B178Y3078	1235	18.07678		-19.84330			91	4	1.5	7.1	1330	3.1	3.0	2.9	0.3	11.6	0.4	0.5	2.0	0.47	0.02	0.01	1.0	-2.7
B174Y3319	1236	18.03263		-19.86594			49	14	0.5	7.8	1200	3.0	3.1	2.9	0.2	11.6	0.7	0.3	1.7	0.48	0.03	0.01	1.0	-2.7
B507Y4509	1237	17.46833		-19.72917			55		-0.9	7.3	1460	3.7	3.8	1.4	0.1	10.4	2.3	0.7	1.1	0.37	0.02	0.01	1.0	-2.6
B3442Y4461	1238	17.79942		-19.80435			64	34	-0.5	7.2	1690	2.8	6.0	1.8	0.1	10.7	3.3	1.2	1.2	0.42	0.02	0.01	0.5	-2.4
B243Y3383	1239	18.54031		-19.57609					-1.6	7.4	1740	2.7	4.9	1.9	0.2	9.6	0.3	4.9	2.8	0.70	0.05	0.01	0.6	-2.4
B242Y3370	1241	18.47025		-19.55978			46	9	-1.2	7.3	1390	2.5	4.1	1.0	0.0	10.2	0.1	1.5	2.8	0.75	0.03	0.01	0.6	-2.5
B177Y3331	1242	17.99232		-19.74909			49	37	1.2	7.3	1740	4.5	4.5	1.1	0.0	9.8	0.1	5.9	2.7	0.42	0.01	0.00	1.0	-3.2
B178Y3317	1244	17.87812		-19.84058			26	21	0.5	7.8	1600	3.8	4.9	1.9	0.1	9.9	1.7	2.5	3.4	0.50	0.03	0.02	0.8	-2.3
J104Y1763	1245	17.89347		-21.73641			73	12	-0.2	7.9	1530	3.3	2.8	1.5	2.1	8.7	0.6	3.5	2.5	1.08	0.05	0.02	1.2	-2.3
W11Y861	1246	18.26576		-20.66968			122	27	-0.1	7.1	1150	3.0	2.3	1.5	0.3	9.1	0.4	0.1	2.5	0.83	0.04	0.03	1.3	-2.0
J189Y2379	1247	17.12572		-21.76721			82	73	-2.2	7.4	1250	3.0	2.8	1.7	0.3	9.7	0.3	1.7	2.3	0.92	0.04	0.01	1.1	-2.5
B181Y3027	1248	18.16123		-19.88641			85	17	0.1	7.4	1130	3.1	2.6	1.1	0.1	9.2	0.3	1.1	1.6	0.38	0.02	0.00	1.2	-3.0
B179Y1Y3071	1249	18.14491		-19.86232			55	9	1.2	7.6	1210	2.7	2.8	1.7	0.0	8.7	0.1	1.5	2.2	0.43	0.02	0.00	1.0	-2.8
B179Y3076	1250	18.10940		-19.88315					-2.0	7.5	1170	3.4	1.8	2.0	0.0	9.9	0.2	0.1	2.5	0.37	0.02	0.00	1.9	-3.1
B172Y3005	1251	18.05758		-19.96196			70	34	-1.9	7.4	1280	3.3	1.4	2.0	1.1	9.4	0.4	1.1	1.8	0.33	0.01	0.00	2.4	-3.0
B175Y3326	1252	17.95585		-19.80344			30	12	1.3	7.3	1620	4.2	3.3	2.1	0.5	10.4	0.3	1.6	4.5	0.37	0.01	0.00	1.3	-3.1
B177Y3330	1253	18.01344		-19.76268			20	6	-2.2	7.5	1740	4.7	2.7	2.7	0.0	9.3	0.6	4.5	3.4	0.33	0.01	0.00	1.8	-3.3
B149Y5503	1254	17.64587		-19.88859					-1.5	7.3	1530	5.2	2.0	2.4	0.0	8.5	0.9	3.7	3.3	0.18	0.02	0.00	2.7	-3.1
W7Y825	1255	17.59263		-20.50860					-0.6	7.8	1320	3.5	2.6	1.8	0.4	8.3	1.2	0.2	3.6	0.65	0.07	0.02	1.3	-2.2
B159Y3313	1256	17.83013		-19.88678					0.1	8.0	1250	4.1	2.9	1.7	0.1	9.2	0.8	1.9	3.3	0.47	0.03	0.02	1.4	-2.4
B146Y3788	1257	17.55086		-19.98279			91	34	0.8	7.0	1360	4.2	2.6	1.5	0.2	9.6	0.1	2.4	2.8	0.47	0.03	0.05	1.6	-2.0
B47Y4860	1258	17.79367		-19.46014			4	0	-1.6	7.0	1330	5.0	2.5	0.3	0.0	15.7	0.1	0.0	0.0	0.43	0.06	0.02	2.0	-2.5
B47Y4859	1259	17.79750		-19.45562			8	3	-0.5	7.2	1170	4.2	2.5	0.4	0.1	13.7	0.1	0.0	0.1	0.45	0.06	0.02	1.7	-2.4
B47Y4856	1260	17.78599		-19.47554			50	43	0.3	7.0	1200	4.7	2.1	0.5	0.1	13.5	0.2	0.1	0.1	0.33	0.06	0.01	2.2	-2.6
B47Y4855	1261	17.74952		-19.45743			40	10	-0.6	6.9	1220	4.6	2.3	0.4	0.1	14.2	0.2	0.0	0.1	0.43	0.05	0.02	2.0	-2.3
B47Y4854	1262	17.74568		-19.45562					-0.3	7.5	1220	4.9	2.3	0.3	0.0	14.6	0.1	0.0	0.0	0.35	0.05	0.02	2.1	-2.4
B748Y3361	1263	18.34357		-19.75996			20	3	-0.5	8.5	730	0.3	3.2	1.1	0.0	8.1	0.0	0.0	0.0	0.30	0.02	0.00	0.1	-2.6
B44Y4Y4476	1265	17.90307		-19.70471					-2.0	8.5	790	0.2	4.3	0.3	0.1	9.4	0.1	0.0	0.3	0.35	0.01	0.00	0.1	-2.7
B214Y3447	1266	18.29367		-19.58424					0.8	8.6	860	0.1	4.1	1.2	0.6	9.4	0.2	0.0	0.4	0.57	0.02	0.00	0.0	-2.3
B5662Y4486	1267	17.59405		-19.80254					0.3	7.5	1230	0.5	5.8	0.7	0.5	10.3	0.2	2.0	1.0	0.40	0.03	0.01	0.1	-2.0
B214Y3446	1268	18.27255		-19.57880					1.9	8.5	1130	0.5	5.6	1.6	0.0	10.0	0.2	0.9	2.0	0.60	0.02	0.00	0.1	-2.6
B241Y4540	1269	18.45393		-19.50362			52	20	-1.7	7.4	1230	1.5	4.7	1.0	0.1	10.7	0.1	1.9	1.4	0.50	0.02	0.01	0.3	-2.5
B241Y4538	1270	18.43282		-19.47826			49	32	1.2	7.8	1210	1.6	4.9	1.0	0.0	10.6	0.2	1.5	1.5	0.50	0.02	0.01	0.3	-2.5
B201Y3054	1271	18.30806		-19.83333					-0.2	8.4	1100	0.7	4.9	1.8	0.3	11.9	0.1	0.0	1.4	0.55	0.04	0.00	0.1	-2.3
B3442Y4460	1272	17.80422		-19.80254			105	18	0.1	8.0	1220	1.1	4.5	2.6	0.1	9.8	1.4	0.5	0.8	0.60	0.03	0.01	0.2	-2.3
B203Y3351	1273	18.40499		-19.85960					1.5	7.5	1180	1.2	4.1	2.3	0.0	10.0	0.1	1.1	1.4	0.77	0.05	0.01	0.3	-2.1
B193Y3063	1274	18.21977		-19.81522					2.1	8.8	970	0.2	4.5	2.6	0.0	9.7	0.1	0.0	1.7	0.60	0.03	0.00	0.1	-2.3
B808Y4939	1275	18.12380		-19.48732					-0.5	7.8	880	1.3	4.3	0.2	0.0	11.2	0.0	0.0	0.3	0.38	0.04	0.00	0.3	-2.9
B44Y2Y4772	1278	17.87236		-19.71014			73	20	-2.2	7.8	930	1.8	3.4	0.2	0.1	11.0	0.0	0.0	0.2	0.23	0.01	0.00	0.5	-3.4
B752Y4826	1279	17.50480		-19.58877					1.0	7.2	1200	2.5	4.1	0.6	0.0	11.8	0.1	0.6	1.0	0.38	0.08	0.00	0.6	-3.0
B316Y4500	1280	17.69482		-19.75815			61	30	-1.7	7.2	1230	2.6	4.0	0.6	0.1	11.4	0.4	1.0	1.0	0.52	0.03	0.00	0.6	-2.9
B186Y3091	1282	18.07965		-19.69565			62	45	-2.1	7.2	1170	1.8	4.2	0.6	0.1	12.0	0.1	0.2	0.9	0.40	0.02	0.00	0.4	-2.8
B794Y1Y4517	1283	17.42418		-19.67935			69	16	0.5	7.3	1030	2.5	3.5	0.4	0.1	12.0	0.0	0.1	0.1	0.37	0.01	0.00	0.7	-3.0
B794Y1Y4516	1284	17.42035		-19.68297			61	15	0.9	7.1	1030	2.7	3.3	0.3	0.0	12.0	0.1	0.0	0.0	0.35	0.01	0.00	0.8	-3.4
B316Y4502	1289	17.61228		-19.74275			58	40	-1.7	7.4	1050	2.8	3.2	0.3	0.0	12.6	0.1	0.0	0.1	0.35	0.01	0.00	0.9	-3.1
B159Y3310	1290	17.85988		-19.89674					0.4	8.1	1070	3.4	3.5	0.8	0.1	12.3	0.7	0.1	0.8	0.35	0.02	0.00	1.0	-2.2
B213Y3438	1291	18.26104		-19.63949					1.9	7.3	1150	1.8	4.1	1.4	0.4	12.4	0.2	0.1	0.3	0.53	0.03	0.02	1.0	-2.8
B202Y3040	1292	18.35797		-19.87409			25		-1.0	7.4	1130	1.6	4.3	1.4	0.0	12.8	0.1	0.1	0.5	0.58	0.03	0.01	0.4	-2.5
B198Y3338	1293	18.25528		-19.74185					2.0	7.4	1140	1.6	4.5	1.0	0.0	12.5	0.1	0.0	0.2	0.37	0.03	0.00	0.4	-2.7
B184Y3086	1294	18.13532		-19.74094					-1.3	7.7	1060	1.6	4.1	0.8	0.0	12.2	0.1	0.0	0.3	0.38	0.02	0.00	0.4	-2.8
B199Y3057	1295	18.29942		-19.76178					0.4	7.2	1130	2.5	3.7	1.1	0.0	13.1	0.1	0.0	0.3	0.40	0.04	0.00	0.7	-2.9
B215Y3365	1296	18.34837		-19.66848			37	11	-2.1	7.2	1180	2.3	3.3	1.3	0.0	12.6	0.0	0.0	0.5	0.42	0.03	0.00	0.7	-2.8
B162Y2995	1297	17.87716		-19.86594			57	24	-0.6	7.5	1190	2.3	3.5	1.5	0.1	12.4	0.3	0.0	0.4	0.43	0.05	0.02	0.6	-2.1
B566Y1Y4482	1298	17.57869		-19.85236			78		-1.5	7.2	1090	2.1	3.4	1.0	0.2	12.3	0.1	0.0	0.0	0.80	0.02	0.00	0.6	-2.8
B155Y4456	1299	17.76583		-19.94112					-1.3	7.3	1040	2.1	3.0	1.5	0.1	11.9	0.1	0.0	0.2	0.55	0.02	0.00	0.4	-1.8
J245W4426	1300	16.80998		-21.50000																				

**Annex B**

**B-21**

name	No	dec. longitude	E	dec. latitude	S	Temp. (°C)	depth (m)	level (m)	error (%)	pH	ec (µS/cm)	Ca <sup>2+</sup>	Mg <sup>2+</sup>	Na <sup>+</sup>	K <sup>+</sup>	HCO <sub>3</sub> <sup>-</sup>	SO <sub>4</sub> <sup>2-</sup>	NO <sub>3</sub> <sup>-</sup>	Cl <sup>-</sup>	Si	F	SP <sup>2+</sup>	Ca <sup>2+</sup> ·Mg <sup>2+</sup>	log Sr <sup>2+</sup> ·Ca <sup>2+</sup>		
B204/Y3353	1302	18.38772		-19.80888					1.5	7.9	970	1.0	3.6	2.0	0.0	10.7	0.1	0.0	0.1	0.70	0.04	0.00	0.00	0.3	-2.4	
B241/Y4539	1303	18.42802		-19.47645			76	29	-1.4	7.6	990	1.0	3.2	2.8	0.0	10.8	0.1	0.0	0.5	0.52	0.03	0.01	0.01	0.3	-2.3	
B203/Y3352	1304	18.42706		-19.83152					1.5	7.3	1020	0.8	3.5	3.0	0.0	10.8	0.1	0.1	0.2	0.95	0.07	0.01	0.01	0.2	-2.0	
B989/Y3356	1305	18.40595		-19.77717			63		0.8	8.2	970	1.4	3.5	1.3	0.0	10.7	0.1	0.0	0.1	0.63	0.05	0.01	0.01	0.4	-2.4	
B801/Y4478	1306	17.64971		-19.79620					-1.2	7.3	970	1.6	3.2	1.2	0.3	10.8	0.1	0.2	0.0	0.72	0.03	0.01	0.01	0.5	-2.1	
B566/2/Y4487	1307	17.56910		-19.79982					0.3	7.7	1010	1.6	3.7	0.9	0.4	10.7	0.5	0.0	0.1	0.62	0.03	0.01	0.01	0.4	-2.5	
B748/Y3360	1308	18.38292		-19.74004					-1.2	7.1	1040	2.1	2.5	1.3	0.0	10.6	0.0	0.0	0.3	0.43	0.03	0.00	0.00	0.8	-2.8	
B586/Y4833	1309	17.48560		-19.47373			30	8	0.2	7.1	1000	2.1	2.9	1.7	0.1	10.5	0.5	0.0	0.2	0.37	0.02	0.00	0.02	0.7	-2.1	
B243/Y3382	1310	18.52879		-19.59964					-1.2	7.4	1000	1.5	2.9	1.7	0.0	10.3	0.1	0.0	0.3	0.62	0.07	0.01	0.01	0.5	-2.3	
B204/Y3354	1311	18.37140		-19.78804					1.4	7.3	970	1.3	3.3	1.7	0.0	10.3	0.1	0.1	0.2	0.55	0.04	0.00	0.00	0.4	-2.5	
B167/Y3017	1312	18.04031		-20.00362					-1.6	7.9	970	1.2	3.1	1.8	0.2	10.2	0.2	0.0	0.5	0.47	0.03	0.00	0.00	0.4	-2.5	
J179/W4606	1313	16.82726		-21.64764			46	30	-1.2	7.4	1090	1.6	3.7	1.5	0.0	10.6	0.1	0.9	0.8	1.08	0.01	0.02	0.04	0.4	-2.0	
B246/Y3387	1314	18.58925		-19.55435					0.6	7.7	1180	1.6	4.3	1.9	0.1	11.1	0.4	0.3	1.0	0.87	0.10	0.01	0.01	0.4	-2.2	
B184/Y3083	1315	18.11036		-19.79710					-0.9	7.2	1100	2.1	3.3	1.6	0.1	11.4	0.1	0.1	1.0	0.42	0.02	0.00	0.00	0.4	-2.8	
B167/Y3015	1316	18.00864		-19.96286					-0.6	7.7	1100	2.0	3.2	2.0	0.0	11.4	0.2	0.4	0.5	0.47	0.04	0.01	0.01	0.6	-2.4	
W2/Y780	1317	18.55674		-19.68597			171	9	-2.1	7.3	1030	1.8	3.2	1.3	0.0	11.2	0.1	0.2	0.4	0.85	0.07	0.01	0.01	0.6	-2.4	
J28/W4511	1318	16.75144		-21.65851			114	67	0.2	7.8	1000	1.9	3.7	1.4	0.2	11.4	0.3	0.4	0.3	0.77	0.05	0.01	0.01	0.5	-2.5	
B989/Y3355	1319	18.41075		-19.80707					1.4	8.0	1040	1.4	3.9	1.5	0.0	11.5	0.1	0.0	0.1	0.53	0.04	0.01	0.01	0.4	-2.4	
B166/Y2984	1320	17.96065		-19.45018					0.0	7.5	930	1.9	3.5	0.8	0.1	11.3	0.1	0.0	0.1	0.45	0.03	0.00	0.00	0.5	-2.3	
B808/Y4937	1321	18.11132		-19.45018					2.0	8.4	900	2.1	3.7	1.0	0.1	11.3	0.2	0.0	0.7	0.45	0.03	0.01	0.01	0.6	-2.2	
B159/Y3311	1322	17.40403		-19.59601			25		-2.2	7.3	1040	2.5	3.1	0.7	0.0	11.7	0.2	0.1	0.4	0.32	0.04	0.01	0.01	0.8	-2.5	
B799/4/Y4986	1323	17.53743		-19.73551			91	55	-0.9	7.4	1030	2.7	3.0	0.6	0.1	11.5	0.3	0.0	0.2	0.35	0.01	0.00	0.00	0.9	-3.0	
B508/Y4486	1324	17.51248		-19.70018					-0.7	7.5	1080	2.6	3.0	1.2	0.1	11.6	0.4	0.2	0.3	0.47	0.02	0.01	0.01	0.9	-2.7	
B511/Y4508	1325	17.50000		-19.69928			61	24	-1.8	7.7	1030	2.2	3.2	1.1	0.1	11.6	0.4	0.0	0.1	0.55	0.02	0.00	0.00	0.7	-2.8	
B510/Y4510	1326	17.62188		-19.71558			76	46	-0.7	7.2	1100	2.4	3.3	1.2	0.1	11.6	0.6	0.4	0.2	0.72	0.02	0.01	0.01	0.7	-2.6	
B316/Y4498	1327	18.28407		-19.79529					1.1	-1.2	7.3	970	2.2	3.1	0.6	0.0	11.1	0.0	0.0	0.1	0.55	0.03	0.00	0.00	0.7	-2.8
B200/Y3050	1328	18.19194		-19.74275			14	10	-1.9	7.1	1020	2.3	2.8	0.7	0.3	11.1	0.1	0.0	0.4	0.35	0.02	0.00	0.00	0.8	-3.0	
B194/Y3065	1329	18.10365		-19.79529					-2.0	7.4	990	2.3	2.9	0.9	0.0	11.2	0.1	0.0	0.4	0.35	0.03	0.00	0.00	0.8	-3.0	
B184/Y3084	1330	18.10365		-19.74275					2.7	7.2	1080	2.7	2.6	1.2	0.0	10.9	0.1	0.7	0.6	0.55	0.03	0.00	0.00	1.1	-2.8	
B316/Y4503	1332	17.40403		-19.74457			76	55	-2.2	7.2	1080	2.8	2.9	1.3	0.1	11.4	0.6	0.4	0.3	0.50	0.03	0.02	0.02	1.0	-2.2	
B505/Y4522	1333	17.40499		-19.74275			52	31	-1.5	7.9	1100	2.8	3.0	1.3	0.1	11.3	0.6	0.3	0.2	0.48	0.03	0.02	0.02	1.0	-2.2	
B173/2/Y3318	1334	18.05182		-19.89946			40	29	0.8	7.9	950	2.8	3.0	1.4	0.1	11.0	0.5	0.0	0.9	0.45	0.03	0.01	0.01	0.9	-2.6	
B521/Y4641	1336	17.58541		-19.66303					-1.0	7.4	1040	2.7	2.5	1.9	0.0	12.3	0.1	0.0	0.0	0.52	0.02	0.00	0.00	1.1	-2.8	
B798/8/Y4631	1337	17.44146		-19.63949					0.8	7.7	970	2.4	3.0	1.3	0.0	11.3	0.6	0.3	0.0	0.35	0.02	0.00	0.00	1.1	-3.1	
B794/4/Y4625	1338	17.41171		-19.66304					0.1	7.2	1040	2.5	2.8	1.7	0.1	11.3	0.3	0.3	0.3	0.33	0.02	0.01	0.01	0.9	-2.7	
B794/3/Y4624	1339	17.41939		-19.65308			55		0.2	7.3	1040	2.6	3.0	1.6	0.1	11.3	0.2	0.6	0.4	0.10	0.02	0.00	0.00	0.9	-2.8	
W5/Y808	1340	18.06887		-20.40452			32	21	-1.2	7.0	970	2.2	2.5	1.7	0.0	11.1	0.1	0.0	0.2	0.60	0.03	0.00	0.00	0.9	-2.7	
B518/Y4643	1341	17.59021		-19.64764					-0.3	7.6	990	2.4	2.7	1.6	0.0	11.4	0.1	0.1	0.2	0.52	0.02	0.00	0.00	0.9	-3.2	
B155/Y4457	1342	17.74856		-19.95199					-1.7	7.1	1020	2.4	2.5	1.7	0.1	11.7	0.1	0.0	0.2	0.50	0.03	0.02	0.02	1.0	-2.0	
B792/Y2608	1343	17.34261		-19.70199					0.8	7.1	1200	3.0	2.9	2.4	0.1	11.1	1.1	0.0	0.7	0.37	0.03	0.01	0.01	1.0	-2.4	
B506/Y4519	1344	17.44338		-19.73732			30	9	-0.9	7.5	1140	3.0	2.5	1.7	0.1	10.4	1.0	0.3	0.5	0.45	0.02	0.01	0.01	1.2	-2.6	
B344/2/Y4464	1345	17.76296		-19.77717			125	79	-1.9	7.3	1120	2.5	2.9	1.7	0.1	10.6	1.2	0.0	0.0	0.50	0.03	0.01	0.01	0.9	-2.3	
B582/Y2612	1346	17.31766		-19.76359					-1.8	7.0	1050	2.4	2.5	2.2	0.1	10.9	0.5	0.5	0.5	0.47	0.03	0.03	0.03	1.0	-1.9	
B799/1/Y4972	1347	17.39251		-19.60326					0.6	7.9	960	2.3	2.5	2.0	0.1	10.7	0.3	0.0	0.2	0.45	0.01	0.01	0.01	0.9	-2.2	
B519/Y4647	1348	17.60557		-19.65580					0.3	7.4	950	2.2	2.3	2.4	0.0	10.8	0.2	0.2	0.0	0.47	0.02	0.00	0.00	1.0	-3.0	
B233/Y3377	1349	17.60749		-19.66304					1.4	7.4	990	2.4	2.3	2.8	0.0	11.3	0.2	0.2	0.0	0.43	0.02	0.00	0.00	1.1	-2.8	
J80/Y2025	1350	18.48848		-19.69928			91	6	-1.2	7.3	1090	1.8	2.4	2.9	0.1	10.9	0.2	0.1	0.2	0.63	0.06	0.01	0.01	0.7	-2.5	
J30/W4517	1352	16.83877		-21.82337			104	43	0.9	7.5	1030	3.7	1.3	2.5	0.2	11.0	0.2	0.4	1.0	0.87	0.04	0.01	0.01	2.9	-2.5	
B108/W463	1353	16.83877		-21.78444			107	58	-1.7	7.3	1090	3.1	1.8	2.7	0.2	11.0	0.4	0.4	1.0	0.82	0.02	0.01	0.01	1.7	-2.5	
B787/Y4835	1354	17.20921		-20.07428			91		0.8	7.1	910	3.1	1.6	2.0	0.4	11.3	0.0	0.0	0.2	0.37	0.02	0.02	0.02	2.0	-2.1	
B787/Y4834	1355	17.62284		-19.477645					-1.2	7.1	1350	3.5	2.7	1.8	0.1	9.6	1.0	2.1	0.8	0.45	0.04	0.01	0.01	1.3	-2.6	
B486/W2906	1356	17.62188		-19.47283			73	41	1.9	7.0	1390	3.3	2.7	2.4	0.1	9.4	1.2	1.6	0.5	0.38	0.03	0.01	0.01	1.2	-2.6	
B787/Y4836	1357	17.19194		-19.88859					0.5	7.4	1060	3.3	2.4	2.4	0.2	9.4	2.0	0.2	0.3	0.60	0.02	0.02	0.02	1.4	-2.2	
B787/Y4838	1358	17.61228		-19.51540					-0.8	7.0	1170	3.4	2.0	1.1	0.1	9.9	0.8	0.0	0.1	0.33	0.06	0.01	0.01	1.7	-2.7	
B509/Y4515	1360	17.62572		-19.46467					-0.3	7.8	1050	2.9	2.9	0.9	0.1	9.8	1.2	0.2	0.2	0.40	0.01	0.01	0.01	1.0	-2.6	
B158/Y3299																										

name	No	dec. longitude °E	dec. latitude °S	Temp. (°C)	depth (m)	level (m)	error (%)	pH	ec (µS/cm)	Ca <sup>2+</sup>	Mg <sup>2+</sup>	Na <sup>+</sup>	K <sup>+</sup>	HCO <sub>3</sub> <sup>-</sup>	SO <sub>4</sub> <sup>2-</sup>	NO <sub>3</sub> <sup>-</sup>	Cl <sup>-</sup>	Si	F	SP <sup>2+</sup>	Ca <sup>2+</sup> :Mg <sup>2+</sup>	log Sr <sup>2+</sup> :Ca <sup>2+</sup>	
																							mmol/l
B344/5/Y4663	1366	17.76536	-19.74547		91	24	0.1	7.2	1080	3.8	1.7	0.7	0.2	10.1	0.2	0.4	0.9	0.30	0.02	0.00	0.00	2.3	-2.9
J80/Y2024	1367	17.48177	-21.81522		73	21	0.2	7.4	900	3.7	1.2	0.8	0.3	9.8	0.3	0.3	0.1	0.4	0.47	0.04	0.01	3.2	-2.7
B582/Y2611	1368	17.28119	-19.75453				-1.3	7.1	940	3.5	1.2	0.8	0.0	9.6	0.2	0.2	0.5	0.47	0.03	0.02	0.02	3.0	-2.2
B486/W2907	1369	17.24664	-19.93297		104	78	-0.5	7.4	840	4.1	1.0	0.4	0.1	10.3	0.1	0.1	0.3	0.32	0.01	0.01	0.01	4.8	-2.9
B154/Y4459	1370	17.73512	-19.87319				-1.4	7.2	950	3.7	1.3	0.3	0.1	10.4	0.1	0.2	0.2	0.32	0.02	0.02	0.02	2.8	-2.3
B499/Y3795	1371	17.43474	-19.83333		30	12	-0.9	6.8	910	3.2	1.1	0.1	0.1	9.6	0.1	0.0	0.1	0.40	0.03	0.02	0.02	2.9	-2.2
B578/W764	1374	17.20633	-19.85870		54	35	0.5	7.7	830	3.1	1.6	0.7	0.1	9.4	0.1	0.3	0.4	0.58	0.02	0.01	0.01	1.9	-2.7
B49/Y4853	1375	17.53071	-19.45380		91	12	7.5	860	3.2	1.6	0.7	0.1	0.1	9.4	0.3	0.0	0.1	0.28	0.04	0.01	0.01	2.1	-2.4
B49/Y4847	1376	17.53465	-19.49094		91	16	7.0	860	2.9	1.6	0.7	0.1	0.1	9.4	0.3	0.0	0.1	0.33	0.03	0.01	0.01	1.8	-2.3
B153/Y4450	1377	17.68138	-19.88768		37	15	-0.2	7.1	890	3.3	1.5	0.4	0.1	11.8	0.1	0.1	0.1	0.32	0.02	0.02	0.02	2.3	-2.3
B752/Y4822	1378	17.57102	-19.49819		98	88	0.9	6.8	1070	3.3	2.8	0.1	0.0	11.8	0.0	0.0	0.1	0.33	0.08	0.00	0.00	1.2	-3.0
B509/Y4513	1380	17.45585	-19.66395				1.0	7.4	940	2.8	2.8	0.2	0.0	11.1	0.1	0.0	0.0	0.25	0.01	0.00	0.00	1.0	-3.4
B47/Y4858	1384	17.71305	-19.46105		110	46	-1.2	7.1	980	3.3	2.2	0.4	0.1	11.2	0.2	0.0	0.1	0.32	0.06	0.01	0.01	1.5	-2.6
B47/Y4857	1385	17.73992	-19.46920		140	55	-1.8	7.1	1040	3.4	2.2	0.6	0.1	11.2	0.2	0.1	0.5	0.33	0.06	0.01	0.01	1.6	-2.5
B578/W765	1392	17.21497	-19.86775		58	33	-1.6	7.7	850	2.9	2.0	0.8	0.2	10.9	0.1	0.0	0.1	0.57	0.02	0.02	0.02	1.4	-2.3
B192/Y1Y3046	1393	18.23608	-19.83786		37	4	-2.2	7.0	950	2.7	2.2	0.7	0.0	10.8	0.1	0.0	0.2	0.48	0.02	0.00	0.00	1.2	-3.2
B583/Y3092	1394	17.34453	-19.75543		40	24	-1.0	7.1	930	2.3	2.3	0.9	0.1	10.0	0.1	0.2	0.2	0.57	0.04	0.03	0.03	1.0	-1.8
B579/W767	1395	17.20633	-19.84420		61	40	1.9	7.2	850	2.7	2.3	0.7	0.2	10.0	0.1	0.0	0.1	0.62	0.03	0.00	0.00	1.1	-3.2
B242/Y3374	1396	18.52399	-19.50000		49	12	-1.9	7.1	970	2.5	2.2	0.6	0.0	10.3	0.1	0.0	0.1	0.62	0.03	0.01	0.01	1.1	-2.6
B583/Y3094	1397	17.32342	-19.73188		43	28	-0.2	7.0	1040	2.7	2.6	0.9	0.1	10.4	0.4	0.3	0.2	0.57	0.03	0.03	0.03	1.0	-1.9
B505/Y4523	1398	17.40403	-19.71739		79	55	-0.1	7.7	990	2.5	2.8	0.9	0.1	10.5	0.5	0.0	0.2	0.28	0.02	0.00	0.00	0.9	-2.9
B758/Y4637	1399	17.56142	-19.65127		37	27	-0.5	7.3	930	2.5	2.6	0.7	0.0	10.3	0.1	0.5	0.1	0.42	0.02	0.00	0.00	1.0	-3.1
B758/Y4636	1400	17.56910	-19.65761		37	37	0.3	7.9	880	2.4	2.6	0.6	0.0	10.4	0.1	0.2	0.0	0.48	0.02	0.00	0.00	0.9	-3.2
B799/Y4974	1401	17.40019	-19.60145		43	24	1.2	7.2	970	2.6	2.5	0.5	0.0	10.6	0.1	0.3	0.1	0.30	0.02	0.00	0.00	1.1	-2.8
B1777/Y3333	1402	18.03359	-19.74185		63	24	1.2	7.2	970	2.8	2.6	0.2	0.0	10.4	0.1	0.0	0.2	0.40	0.01	0.00	0.00	1.1	-3.2
B794/Y2Y4622	1403	17.42035	-19.64674		61	17	-1.4	7.4	880	2.7	2.5	0.0	0.0	10.6	0.1	0.0	0.2	0.08	0.01	0.00	0.00	1.1	-3.1
B744/Y4867	1404	17.86852	-19.50634		67	20	-1.6	7.5	910	2.8	2.4	0.0	0.0	10.4	0.1	0.1	0.1	0.20	0.04	0.00	0.00	1.2	-3.0
B510/Y4511	1405	17.48273	-19.66757		55	37	-0.2	7.5	880	2.7	2.4	0.0	0.0	10.5	0.0	0.0	0.0	0.20	0.01	0.00	0.00	1.2	-3.2
B794/Y2Y4623	1409	17.42226	-19.64855		37	27	-0.2	7.5	870	2.7	2.5	0.0	0.0	10.1	0.2	0.2	0.2	0.08	0.01	0.00	0.00	1.1	-3.3
B511/Y4507	1410	17.53935	-19.67572		66	30	-0.2	7.2	870	2.5	2.3	0.2	0.0	9.8	0.1	0.0	0.1	0.25	0.01	0.00	0.00	1.1	-3.2
B317/Y4862	1411	17.83109	-19.49819		66	30	-0.2	7.2	870	2.7	2.3	0.0	0.0	10.0	0.1	0.1	0.0	0.18	0.06	0.00	0.00	1.1	-3.0
B175/Y3323	1416	17.99328	-19.81793		55	37	-0.4	7.8	930	2.8	2.3	0.3	0.0	10.2	0.1	0.0	0.2	0.45	0.01	0.00	0.00	1.2	-3.1
B10/Y4713	1419	18.02015	-19.49275				0.0	7.7	880	2.2	2.9	0.1	0.0	10.1	0.0	0.0	0.2	0.25	0.03	0.00	0.00	0.8	-3.2
B380/Y4882	1420	17.90307	-19.64764				-0.2	7.8	990	1.3	3.9	0.4	0.0	9.2	0.1	0.4	1.2	0.13	0.03	0.00	0.00	0.3	-2.7
B181/Y3026	1421	18.16795	-20.01359		65	17	1.6	7.3	1020	2.2	3.3	0.7	0.1	9.3	0.1	0.3	1.6	0.43	0.02	0.00	0.00	0.7	-2.7
B178/Y3081	1422	18.05086	-19.81703		36	23	-0.3	7.8	880	2.3	3.7	0.8	0.1	9.6	0.1	1.7	1.0	0.62	0.02	0.00	0.00	0.6	-2.7
B583/Y3095	1423	17.27447	-19.73460		55	18	-1.0	8.0	900	1.8	3.1	1.1	0.1	9.4	0.3	0.0	0.1	0.40	0.03	0.02	0.02	0.4	-1.8
B510/Y4512	1424	17.47313	-19.71196		60	22	-0.7	7.3	810	1.5	2.9	0.7	0.0	9.5	0.1	0.0	0.0	0.47	0.04	0.01	0.01	0.5	-2.3
B229/Y4536	1425	18.41843	-19.54076		70	21	1.2	7.0	860	1.7	3.0	0.6	0.0	9.7	0.1	0.0	0.0	0.63	0.03	0.01	0.01	0.6	-2.5
B44/Y4474	1426	17.89731	-19.73188		61	46	0.2	7.9	740	1.4	3.2	0.6	0.0	9.4	0.0	0.1	0.3	0.25	0.01	0.00	0.00	0.6	-2.8
B195/Y3434	1427	18.17370	-19.68478		52	24	0.9	7.7	840	1.4	3.3	0.1	0.0	9.2	0.1	0.0	0.1	0.17	0.08	0.00	0.00	0.4	-3.0
B752/Y4825	1428	17.52111	-19.59420				-1.6	7.6	770	1.5	2.9	0.2	0.0	9.0	0.0	0.0	0.2	0.25	0.04	0.00	0.00	0.5	-3.2
B808/Y4938	1429	18.08157	-19.47736		47	18	1.4	7.5	810	1.6	3.0	0.4	0.1	9.2	0.1	0.0	0.1	0.50	0.05	0.01	0.01	0.6	-2.5
B189/Y3032	1430	18.26871	-19.99638		60	22	-0.7	7.3	810	1.5	2.9	0.7	0.0	9.5	0.1	0.0	0.0	0.47	0.04	0.01	0.01	0.5	-2.3
B248/Y3820	1431	18.58637	-19.47917		70	21	1.2	7.0	860	1.7	3.0	0.6	0.0	9.7	0.1	0.0	0.0	0.63	0.03	0.01	0.01	0.6	-2.4
B248/Y3816	1432	18.58733	-19.48551		59	2	-2.3	7.2	900	1.7	2.6	0.8	0.0	9.5	0.1	0.0	0.1	0.67	0.05	0.01	0.01	0.6	-2.5
B201/Y3055	1435	18.34837	-19.86141		67	30	0.2	7.4	850	2.0	2.7	0.6	0.0	9.9	0.1	0.0	0.1	0.47	0.04	0.00	0.00	0.8	-2.8
B758/Y4638	1436	17.56142	-19.64855				0.5	7.5	910	2.3	2.3	0.7	0.0	9.8	0.1	0.0	0.0	0.40	0.02	0.00	0.00	1.0	-3.1
B501/W3483	1438	17.36948	-19.79438		46	6	-0.4	7.2	890	2.1	2.5	0.6	0.0	9.5	0.1	0.0	0.1	0.50	0.02	0.00	0.00	0.8	-1.9
B242/Y3372	1439	18.50576	-19.56069				2.5	7.6	900	2.1	2.6	0.7	0.2	9.5	0.1	0.0	0.1	0.50	0.02	0.00	0.00	0.8	-2.6
B168/Y3011	1440	18.06622	-20.01902				-2.4	7.5	860	1.9	2.5	0.4	0.1	9.6	0.0	0.0	0.0	0.37	0.02	0.01	0.01	0.8	-2.5
B784/Y4816	1441	17.45873	-19.57156		53	24	0.2	6.9	1090	2.8	3.1	0.4	0.0	10.8	0.1	1.2	0.5	0.48	0.06	0.00	0.00	0.9	-2.8
B656/Y4650	1442	17.68138	-19.70743		82	2	0.1	7.4	1020	2.6	3.3	0.2	0.0	10.0	0.1	1.0	1.1	0.73	0.07	0.02	0.02	0.8	-3.2
W2/Y783	1443	18.50242	-19.64163		200	18	-2.2	7.0	1100	2.6	2.8	0.8	0.6	10.5	0.1	1.1	0.5	0.73	0.02	0.01	0.01	0.8	-2.1
B442/Y4471	1444	17.86372	-19.72373		49	12	-2.1	7.4	980	2.1	3.1	0.4	0.0	10.7	0.1	0.2	0.4	0.33	0.01	0.00	0.00	0.7	-3.3
B166/Y3087	1445	18.14779	-19.72645		28		-1.4	7.4	970	2.1	3.1	0.5	0.0	10.6	0.1	0.1	0.5	0.42	0.02	0.00	0.00	0.7	-2.9
B752/Y4821	1446	17.51440	-19.57337		46	24	0.8	7.0	980	2.0	3.1</												

name	No	dec. longitude	E	dec. latitude	S	Temp.	depth	level	error	pH	ec	mmol/l											log Sr <sup>2+</sup> :Ca <sup>2+</sup>
												Ca <sup>2+</sup>	Mg <sup>2+</sup>	Na <sup>+</sup>	K <sup>+</sup>	HCO <sub>3</sub> <sup>-</sup>	SO <sub>4</sub> <sup>2-</sup>	NO <sub>3</sub> <sup>-</sup>	Cl <sup>-</sup>	Si	F	Sr <sup>2+</sup>	
B248/1/Y3814	1448	18.55662	-19.48460	76	24	2.4	7.5	920	0.1	0.1	0.2	0.2	0.2	0.73	0.02	0.00	0.00	0.8	-2.7				
B316/Y4499	1449	17.65835	-19.71196	67	52	2.1	7.3	920	10.5	0.1	10.5	0.1	0.1	0.33	0.01	0.00	0.00	0.7	-2.7				
B197/2/Y3437	1450	18.21689	-19.64130	33	18	2.4	7.4	970	10.6	0.1	10.6	0.1	0.0	0.45	0.02	0.00	0.00	0.8	-3.0				
B197/3/Y3428	1451	18.20250	-19.64946	46	33	2.1	7.1	940	10.5	0.1	10.5	0.1	0.0	0.45	0.02	0.00	0.00	0.7	-2.9				
B164/Y2991	1452	17.89347	-19.93478	46	46	2.2	7.6	990	10.6	0.2	10.6	0.2	0.4	0.47	0.03	0.01	0.07	0.7	-2.4				
B44/3/Y2997	1455	17.87044	-19.79167	42	10	2.0	7.8	950	10.0	0.0	10.0	0.0	0.0	0.17	0.03	0.00	0.00	0.7	-3.1				
B216/1/Y3343	1456	18.41171	-19.66486	34	21	1.8	7.4	1020	10.2	0.1	10.2	0.1	0.4	0.58	0.04	0.01	0.06	0.6	-2.5				
B181/Y3025	1457	18.19866	-20.00725	85	19	2.3	8.0	910	10.2	0.1	10.2	0.1	0.1	0.4	0.04	0.01	0.5	-2.4					
B164/Y2992	1459	17.90403	-19.95562	46	6	2.0	7.6	1170	10.3	0.1	10.3	0.1	0.4	0.45	0.04	0.01	0.5	-2.4					
B161/Y2998	1460	17.80230	-19.80797	43	6	2.0	7.7	1080	10.4	0.2	10.4	0.2	0.7	0.32	0.00	0.00	0.6	-2.9					
B505/Y4525	1462	17.39060	-19.76268	44	23	2.4	7.5	960	10.1	0.2	10.1	0.2	0.0	0.60	0.03	0.00	1.1	-2.0					
B49/Y4851	1463	17.49328	-19.45652	46	46	2.5	7.2	890	9.7	0.3	9.7	0.3	0.0	0.30	0.04	0.01	1.2	-2.3					
B180/Y3022	1465	18.13532	-19.91214	110	79	1.8	7.4	990	9.9	0.1	9.9	0.1	0.0	0.32	0.03	0.00	1.6	-3.0					
J44/Y2132	1466	16.90499	-21.59873	98	37	2.4	7.2	910	10.0	0.2	10.0	0.2	0.4	0.95	0.02	0.01	0.7	-2.4					
J269/Y2156	1467	16.82534	-21.53633	122	82	1.7	8.0	920	10.3	0.1	10.3	0.1	0.2	1.03	0.02	0.00	0.7	-2.7					
J22/W4553	1468	16.61612	-21.54529	98	40	2.2	7.7	1110	9.6	0.1	9.6	0.1	0.4	0.77	0.02	0.01	0.9	-2.5					
J189/Y2378	1469	17.12956	-21.77899	49	40	2.2	7.7	1110	9.7	0.1	9.7	0.1	0.8	0.97	0.04	0.01	0.9	-2.5					
B178/Y3079	1470	18.07006	-19.78351	40	5	1.9	7.5	930	9.5	1.7	9.5	1.7	0.0	0.17	0.02	0.00	0.8	-2.8					
B566/3/Y4489	1471	17.59981	-19.76993	46	30	2.0	7.4	940	8.7	0.2	8.7	0.2	1.1	0.57	0.03	0.00	0.8	-2.9					
B231/Y3381	1472	18.47025	-19.62319	30	12	1.8	7.5	950	8.9	0.1	8.9	0.1	0.6	0.58	0.05	0.01	0.8	-2.5					
B344/2/Y4465	1473	17.77927	-19.78170	91	49	1.9	6.9	840	8.8	0.6	8.8	0.6	0.6	0.17	0.02	0.01	0.9	-2.4					
B174/Y3320	1475	18.02399	-19.87319	18	9	2.3	7.5	750	8.5	2.0	8.5	2.0	0.5	0.40	0.03	0.01	1.2	-2.6					
B787/Y4837	1476	17.58733	-19.45199	76	65	2.0	7.9	820	9.1	0.2	9.1	0.2	0.0	0.03	0.03	0.02	1.3	-2.2					
W2/Y779	1477	18.57711	-19.64434	70	46	2.1	7.3	780	9.0	0.1	9.0	0.1	0.0	0.42	0.04	0.01	1.0	-2.6					
B589/Y4845	1478	17.68810	-19.46014	46	30	2.2	7.0	800	9.1	0.1	9.1	0.1	0.0	0.38	0.03	0.01	1.1	-2.5					
B586/Y4832	1480	17.48464	-19.47101	30	12	2.0	7.5	940	9.6	0.3	9.6	0.3	0.0	0.1	0.33	0.02	0.01	0.9	-2.2				
B49/Y4846	1481	17.52591	-19.47373	46	46	2.4	7.2	910	9.3	0.2	9.3	0.2	0.4	0.33	0.03	0.01	1.1	-2.3					
B784/Y4817	1482	17.43666	-19.56612	76	65	2.1	6.9	860	9.2	0.1	9.2	0.1	0.0	0.35	0.07	0.01	0.9	-2.4					
B518/Y4642	1483	17.59117	-19.64493	2.0	2.1	2.3	7.5	780	9.0	0.0	9.0	0.1	0.2	0.33	0.02	0.00	1.0	-3.1					
B180/Y3020	1484	18.09213	-19.90761	70	46	2.1	7.8	880	9.3	0.1	9.3	0.1	0.0	0.3	0.62	0.03	0.01	0.9	-2.5				
J244/W4434	1485	16.77927	-21.42391	2.3	2.0	2.0	7.0	900	9.1	0.1	9.1	0.1	0.7	0.2	1.63	0.02	0.00	1.1	-3.6				
B589/Y4845	1486	18.09405	-20.03895	2.0	2.3	2.0	7.5	830	9.0	0.1	9.0	0.1	0.0	0.2	1.08	0.01	0.01	0.9	-2.5				
B764/1/Y4809	1489	18.13340	-19.61413	2.6	2.5	2.5	7.4	940	9.7	0.1	9.7	0.1	0.1	0.4	0.58	0.05	0.00	1.0	-2.9				
B798/Y4627	1491	17.42322	-19.63768	13	13	2.6	7.4	810	9.5	0.1	9.5	0.1	0.1	0.17	0.02	0.00	1.1	-3.2					
B798/2/Y4629	1492	17.43858	-19.62862	83	55	2.6	7.4	810	9.3	0.1	9.3	0.1	0.0	0.17	0.02	0.00	1.2	-3.0					
B762/Y4820	1493	17.62092	-19.57337	83	55	2.6	7.0	860	9.3	0.0	9.3	0.0	0.0	0.18	0.07	0.00	1.2	-3.2					
B754/1/Y4810	1494	18.09981	-19.56793	73	55	2.4	7.2	840	9.1	0.0	9.1	0.0	0.0	0.20	0.05	0.00	1.1	-3.1					
B744/Y4868	1495	17.92226	-19.50725	73	55	2.4	7.3	790	8.9	0.1	8.9	0.1	0.0	0.1	0.22	0.05	0.00	1.1	-3.1				
B511/Y4506	1496	17.54607	-19.67572	73	55	2.5	7.4	790	9.0	0.1	9.0	0.1	0.1	0.20	0.01	0.00	1.2	-3.4					
B754/1/Y4811	1497	18.10461	-19.56612	73	55	2.1	7.4	790	9.5	0.0	9.5	0.0	0.0	0.25	0.05	0.00	0.8	-3.1					
B732/Y4740	1498	18.20729	-19.50272	73	850	2.2	7.3	850	9.5	0.2	9.5	0.2	0.0	0.3	0.25	0.00	0.8	-3.1					
B41/1/Y4807	1499	17.98273	-19.65761	73	18	2.4	7.0	890	9.6	0.0	9.6	0.0	0.1	0.1	0.22	0.04	0.00	0.9	-3.5				
B376/Y4726	1500	18.10557	-19.64221	61	43	2.2	7.3	840	9.3	0.0	9.3	0.0	0.2	0.1	0.38	0.02	0.00	0.9	-3.1				
B376/Y4725	1501	18.10461	-19.64764	61	43	2.3	7.8	840	9.3	0.0	9.3	0.0	0.2	0.1	0.38	0.02	0.00	1.0	-3.0				
B656/Y4649	1502	17.68426	-19.70471	20	3	2.4	7.3	830	9.3	0.1	9.3	0.1	0.0	0.30	0.02	0.00	1.0	-3.2					
B11/Y4875	1504	18.01919	-19.51902	20	3	2.2	7.5	820	9.4	0.0	9.4	0.0	0.0	0.17	0.02	0.00	1.0	-3.3					
B656/1/Y4648	1506	17.67850	-19.68841	2.3	2.1	2.3	7.4	760	8.7	0.1	8.7	0.1	0.0	0.22	0.02	0.00	1.1	-3.3					
B44/Y4621	1507	17.86276	-19.73822	2.2	2.1	2.2	7.4	720	8.5	0.0	8.5	0.0	0.0	0.13	0.01	0.00	1.0	-3.5					
B517/Y4634	1508	17.57582	-19.63587	108	2	2.2	7.7	740	8.5	0.0	8.5	0.0	0.0	0.13	0.01	0.00	1.0	-3.1					
B42/Y4668	1509	17.98081	-19.70562	198	198	2.1	7.4	730	8.3	0.0	8.3	0.0	0.0	0.17	0.01	0.00	1.0	-3.3					
B317/Y4863	1510	17.86276	-19.53804	33	33	2.1	7.3	740	8.4	0.0	8.4	0.0	0.1	0.17	0.03	0.00	1.0	-3.3					
B317/Y4861	1511	17.83109	-19.49366	33	33	2.3	7.8	800	8.5	0.1	8.5	0.1	0.3	0.22	0.06	0.01	1.1	-2.6					
B322/Y4698	1515	17.93186	-19.56069	30	30	2.0	7.1	780	8.8	0.0	8.8	0.0	0.1	0.18	0.03	0.00	0.8	-3.3					
B12/Y4701	1516	17.98848	-19.54257	30	6	2.5	7.7	750	8.8	0.0	8.8	0.0	0.0	0.17	0.03	0.00	0.8	-3.3					
B344/4/Y4470	1517	17.83589	-19.74909	18	6	2.1	7.3	810	8.9	0.0	8.9	0.0	0.0	0.20	0.01	0.00	1.0	-3.8					
B11/Y4874	1518	18.02495	-19.51630	20	3	2.2	7.5	780	8.9	0.1	8.9	0.1	0.1	0.17	0.01	0.00	1.0	-3.0					
B805/Y4658	1520	17.67562	-19.63678	198	58	2.1	7.5	760	8.8	0.0	8.8	0.0	0.0	0.10	0.02	0.00	0.9	-3.5					
B11/Y4739	1521	18.16042	-19.49638	1522	18.10940	2.2	7.4	780	8.8	0.0	8.8	0.0	0.0	0.18	0.02	0.00	1.0	-3.2					
B754/1/Y4812	1522	18.10940	-19.56431	2.1	2.5	2.1	7.3	840	9.1	0.0	9.1	0.0	0.0	0.23	0.05	0.00	0.8	-3.1					
B593/Y3441	1523	18.28023	-19.54076	2.1	2.5	2.1	7.2	860	9.0	0.1	9.0	0.1	0.1	0.2	0.38	0.02	0.00	0.9	-2.7				

## Annex B

## B-24

name	No	dec. longitude °E	dec. latitude °S	Temp. (°C)	depth (m)	level (m)	error (%)	pH	ec (µS/cm)	mmol/l										log Sr <sup>2+</sup> :Ca <sup>2+</sup>			
										Ca <sup>2+</sup>	Mg <sup>2+</sup>	Na <sup>+</sup>	K <sup>+</sup>	HCO <sub>3</sub> <sup>-</sup>	SO <sub>4</sub> <sup>2-</sup>	NO <sub>3</sub> <sup>-</sup>	Cl <sup>-</sup>	Si	F		Sr <sup>2+</sup>	Ca <sup>2+</sup> :Mg <sup>2+</sup>	
B786/1/Y4628	1524	17.41651	-19.63315		18	8	0.4	7.7	770	2.2	2.4	0.1	0.0	8.9	0.1	0.1	0.1	0.1	0.22	0.02	0.00	0.9	-3.2
B593/2/Y4751	1525	18.25720	-19.46558		61	30	-0.5	7.5	790	2.1	2.4	0.1	0.0	8.9	0.1	0.1	0.1	0.1	0.25	0.02	0.00	0.9	-3.0
B593/1/Y4748	1527	18.29175	-19.46467				-1.6	7.2	800	2.1	2.3	0.2	0.0	9.0	0.0	0.1	0.2	0.23	0.01	0.00	0.9	-3.1	
B44/Y4620	1528	17.86564	-19.73913		21	1	-1.1	7.5	750	2.2	2.3	0.0	0.0	9.2	0.1	0.0	0.0	0.22	0.01	0.00	1.0	-3.2	
B41/Y3448	1529	17.99232	-19.68207				-1.8	7.4	750	2.1	2.3	0.0	0.0	9.2	0.0	0.1	0.1	0.20	0.01	0.00	0.9	-3.2	
B1/Y4738	1530	18.17946	-19.50181		37	8	-1.0	7.3	800	2.2	2.4	0.1	0.0	9.2	0.0	0.0	0.1	0.20	0.02	0.00	0.9	-3.2	



## Curriculum vitae

---

geboren am 11.01. 1966  
in Mölln/Hzgt. Lauenburg  
ledig

### Schulbildung

1976 – 1982 Gymnasium Ratzeburg  
1982 –1983 Austauschschüler am  
Collège Jean XXIII Brüssel  
1983 – 1986 Gymnasium Ratzeburg, Abitur

### Universität

1988 – 1990 Grundstudium Hydrologie mit Nebenfach Physik und Chemie  
1990 – 1994 Hauptstudium Hydrologie mit Nebenfach Bodenkunde und  
Meteorologie  
Dez. 1994 Diplom in Hydrologie zum Thema ‚*Transmission losses in  
Nahal Zin, Israel*‘

Dez. 1994 – Feb. 1996 Wissenschaftl. Mitarbeiter am Institut für Hydrologie, Freiburg  
(u.a. Machbarkeitsstudie für das ‚*Zin Floodwater Project*‘)  
Mrz. 1996 – Aug. 1997 Promotionsstipendium der DFG im Rahmen des Graduierten-  
kollegs ‚*Geowissenschaftl. Gemeinschaftsforschung in Afrika*‘  
Okt. 1998 – Jun. 1999 Forschungsaufenthalt am Jakob-Blaustein International Centre  
Sde Boker/Israel  
Sept. 1997 –Sept. 2000 Mitarbeit im internationalen Forschungsprojekt ‚*GREM -  
Groundwater Recharge in the Eastern Mediterranean*‘  
(Israel, Griechenland, Zypern, Jordanien, Deutschland)

### Fortbildungen

Sept. 1997 ‚*Geochemisch-thermodynamische Interpretation von  
Wasseranalysen*‘  
Okt. 1997 ‚*3-D Grundwassermodellierung mit Modflow*‘  
Sept. 1998 ‚*Paleohydrological Methods in Groundwater and Waste  
Management (<sup>14</sup>C, Isotopes)*‘ EU Advanced Study Course

### Mitarbeit/Organisationen

nationaler Ansprechpartner für IHP/OHP-FRIEND  
Arbeitsgruppe III ‚*Large scale variations*‘

### Sprachen

Englisch und Französisch in Schrift und Sprache fließend,  
Grundkenntnisse in Hebräisch

## **Publikationen**

---

### **Artikel**

- KÜLLS C., LEIBUNDGUT C. SCHWARZ U. & SCHICK A. (1994): Channel infiltration study using dye tracers. Application of Tracers in Arid Zone Hydrology. *IAHS Publ.*, **232** (ed. by E. Adar & C. Leibundgut): 429-436
- KÜLLS C., ZAGANA E. & UDLUFT P. (1998): Integrated evaluation of quantitative and qualitative groundwater potential in the Eastern Mediterranean Region. In: *Groundwater Sustainable Solutions* (ed. by T. R. Weaver & C. R. Lawrence): 683-688
- KÜLLS C., ADAR E. M. & UDLUFT P. (2000): Resolving patterns of groundwater flow by inverse hydro-chemical modelling in a semi-arid Kalahari basin. *IAHS Publ.* no. **262**, (Tram2000, Liège): 447-451
- KÜLLS C. & SCHWARZ O. (2000): Grundwasseranreicherung in den Waldbeständen der Teninger Allmend bei Freiburg im Breisgau. *Frankfurter Geowissenschaftliche Arbeiten, Serie D, Physische Geographie*: 67-78
- KÜLLS C., CONSTANTINOU C. & UDLUFT P. (2000): Dynamics of groundwater recharge in natural environments and mining areas: Case studies from Cyprus. *Conf. Min. Wealth Athens*, Juli 2000: in print
- KÜLLS C. & UDLUFT P. (2000): Mapping the availability and dynamics of groundwater recharge. Part II: Case studies. *Congress Regional Geological Cartography and Information Systems, München 2000*: in print
- KÜLLS C. & SALAMEH E. & UDLUFT P. (2000): Assessing water supplies for irrigation – availability of natural resources and sustainability indices. *Tropentag Hohenheim, 11./12. Oct. 2000. Conf. Proceedings*: in print

### **Mitautorenschaft bei Artikeln**

- DEMUTH S. & KÜLLS C. (1997): Probability Analysis and regional aspects of droughts. *Sustainability of Water Resources under Increasing Uncertainty* (ed. by D. Rosbjerg et al.), *IAHS Publ.*, **240**: 97-104
- UDLUFT P. & KÜLLS C. (2000): Mapping the availability and dynamics of groundwater recharge. Part I: Modelling techniques. *Congress Regional Geological Cartography and Information Systems, München 2000*: in print
- ZAGANA E., KÜLLS C. & UDLUFT P. (1999): Hydrochemie und Wasserhaushalt des Aliakmonas, Nordgriechenland. *Vom Wasser*, **94**: 29-39

### **Abstracts**

- KÜLLS C., WRABEL J., MAINARDY H. & UDLUFT P. (1997): Regionalization of Groundwater Recharge in the Northwestern Kalahari, Namibia. In: *Landschaftsökologie und Umweltforschung*, **25**: 137-141
- KÜLLS C., ADAR E. M., GEYH M. & UDLUFT P. (1999): Identification of Subsurface Fluxes into the North-Western Kalahari Basin Using Environmental Tracers. EUG 10, Strasbourg, *J. Conf. Abstr.*, 4(1): 584

### **Einladungsvorträge & Kolloquien**

- KÜLLS C. & ADAR E. M. (1999): Hydrochemical Perspectives on Groundwater Recharge Processes in Semi-Arid and Arid Regions (keynote). *Unsaturated Zone Workshop*, Sde Boker, Juni 1999 (K.P. Seiler & Y. Gat).
- KÜLLS C. (2000): Separierung von Abflüssen mit Isotopenmethoden. *Isotopenanwendungen in der Hydrogeologie*, Mai 2000, München.